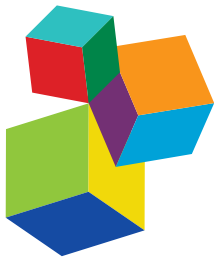


PLANCTOMYCETES-VERRUCOMICROBIA- CHLAMYDIAE BACTERIAL SUPERPHYLUM: NEW MODEL ORGANISMS FOR EVOLUTIONARY CELL BIOLOGY, 2nd Edition

EDITED BY: Laura van Niftrik and Damien P. Devos

PUBLISHED IN: Frontiers in Microbiology



Frontiers Copyright Statement

© Copyright 2007-2019 Frontiers Media SA. All rights reserved.

All content included on this site, such as text, graphics, logos, button icons, images, video/audio clips, downloads, data compilations and software, is the property of or is licensed to Frontiers Media SA ("Frontiers") or its licensees and/or subcontractors. The copyright in the text of individual articles is the property of their respective authors, subject to a license granted to Frontiers.

The compilation of articles constituting this e-book, wherever published, as well as the compilation of all other content on this site, is the exclusive property of Frontiers. For the conditions for downloading and copying of e-books from Frontiers' website, please see the Terms for Website Use. If purchasing Frontiers e-books from other websites or sources, the conditions of the website concerned apply.

Images and graphics not forming part of user-contributed materials may not be downloaded or copied without permission.

Individual articles may be downloaded and reproduced in accordance with the principles of the CC-BY licence subject to any copyright or other notices. They may not be re-sold as an e-book.

As author or other contributor you grant a CC-BY licence to others to reproduce your articles, including any graphics and third-party materials supplied by you, in accordance with the Conditions for Website Use and subject to any copyright notices which you include in connection with your articles and materials.

All copyright, and all rights therein, are protected by national and international copyright laws.

The above represents a summary only. For the full conditions see the Conditions for Authors and the Conditions for Website Use.

ISSN 1664-8714
ISBN 978-2-88945-974-2
DOI 10.3389/978-2-88945-974-2

About Frontiers

Frontiers is more than just an open-access publisher of scholarly articles: it is a pioneering approach to the world of academia, radically improving the way scholarly research is managed. The grand vision of Frontiers is a world where all people have an equal opportunity to seek, share and generate knowledge. Frontiers provides immediate and permanent online open access to all its publications, but this alone is not enough to realize our grand goals.

Frontiers Journal Series

The Frontiers Journal Series is a multi-tier and interdisciplinary set of open-access, online journals, promising a paradigm shift from the current review, selection and dissemination processes in academic publishing. All Frontiers journals are driven by researchers for researchers; therefore, they constitute a service to the scholarly community. At the same time, the Frontiers Journal Series operates on a revolutionary invention, the tiered publishing system, initially addressing specific communities of scholars, and gradually climbing up to broader public understanding, thus serving the interests of the lay society, too.

Dedication to Quality

Each Frontiers article is a landmark of the highest quality, thanks to genuinely collaborative interactions between authors and review editors, who include some of the world's best academicians. Research must be certified by peers before entering a stream of knowledge that may eventually reach the public - and shape society; therefore, Frontiers only applies the most rigorous and unbiased reviews.

Frontiers revolutionizes research publishing by freely delivering the most outstanding research, evaluated with no bias from both the academic and social point of view. By applying the most advanced information technologies, Frontiers is catapulting scholarly publishing into a new generation.

What are Frontiers Research Topics?

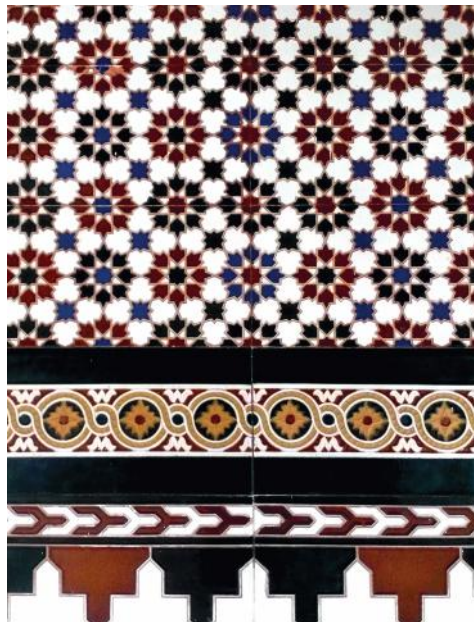
Frontiers Research Topics are very popular trademarks of the Frontiers Journals Series: they are collections of at least ten articles, all centered on a particular subject. With their unique mix of varied contributions from Original Research to Review Articles, Frontiers Research Topics unify the most influential researchers, the latest key findings and historical advances in a hot research area! Find out more on how to host your own Frontiers Research Topic or contribute to one as an author by contacting the Frontiers Editorial Office: researchtopics@frontiersin.org

PLANCTOMYCETES-VERRUCOMICROBIA-CHLAMYDIAE BACTERIAL SUPERPHYLUM: NEW MODEL ORGANISMS FOR EVOLUTIONARY CELL BIOLOGY, 2nd Edition

Topic Editors:

Laura van Niftrik, Radboud University, Netherlands

Damien P. Devos, Centro Andaluz de Biología del Desarrollo (CSIC), Universidad Pablo de Olavide, Spain



Traditional tiles from Seville, Spain (Azulejos, Seville, Spain) from Damien P. Devos

The Planctomycetes, Verrucomicrobia, Chlamydiae (PVC) and related phyla have recently emerged as fascinating subjects for research in evolutionary cell biology, ecology, biotechnology, evolution and human health. This interest is prompted by particular characteristics observed in the PVC superphylum that are otherwise rarely observed in bacteria but are however still poorly described or understood, such as the presence of a complex endomembrane system, or compacted DNA throughout most of the cell cycle. Therefore, the members of the PVC superphylum represent an excellent example of the value of studying bacteria other than 'classical' models.

Publisher's note: In this 2nd edition, the following article has been updated: Kohn T, Heuer A, Jogler M, Vollmers J, Boedecker C, Bunk B, Rast P, Borchert D, Glöckner I, Freese HM, Klenk H-P, Overmann J, Kaster A-K, Rohde M, Wiegand S and Jogler C (2016) *Fuerstia marisgermanicae* gen. nov., sp. nov., an Unusual Member of the Phylum Planctomycetes from the German Wadden Sea. *Front. Microbiol.* 7:2079. doi: 10.3389/fmicb.2016.02079

Citation: van Niftrik, L., Devos, D. P., eds. (2019). Planctomycetes-Verrucomicrobia-Chlamydiae Bacterial Superphylum: New Model Organisms for Evolutionary Cell Biology, 2nd Edition. Lausanne: Frontiers Media. doi: 10.3389/978-2-88945-974-2

Table of Contents

- 05 Editorial: Planctomycetes-Verrucomicrobia-Chlamydiae Bacterial Superphylum: New Model Organisms for Evolutionary Cell Biology**
Laura van Niftrik and Damien P. Devos

BIOACTIVE COMPOUNDS

- 08 Untangling Genomes of Novel Planctomycetal and Verrucomicrobial Species From Monterey Bay Kelp Forest Metagenomes by Refined Binning**
John Vollmers, Martinique Frentrup, Patrick Rast, Christian Jogler and Anne-Kristin Kaster
- 23 Developing Techniques for the Utilization of Planctomycetes as Producers of Bioactive Molecules**
Olga Jeske, Frank Surup, Marcel Ketteniß, Patrick Rast, Birthe Förster, Mareike Jogler, Joachim Wink and Christian Jogler
- 37 Planctomycetes as Novel Source of Bioactive Molecules**
Ana P. Graça, Rita Calisto and Olga M. Lage

CELL BIOLOGY

- 53 Identification and Partial Characterization of a Novel UDP-N-Acetylenolpyruvoylglucosamine Reductase/UDP-N-Acetyl muramate:L-Alanine Ligase Fusion Enzyme From Verrucomicrobium spinosum DSM 4136^T**
Kubra F. Naqvi, Delphine Patin, Matthew S. Wheatley, Michael A. Savka, Renwick C. J. Dobson, Han Ming Gan, Hélène Barreteau, Didier Blanot, Dominique Mengin-Lecreulx and André O. Hudson
- 66 Three Novel Species With Peptidoglycan Cell Walls Form the New Genus Lacunisphaera gen. nov. in the Family Opitutaceae of the Verrucomicrobial Subdivision 4**
Patrick Rast, Ines Glöckner, Christian Boedeker, Olga Jeske, Sandra Wiegand, Richard Reinhardt, Peter Schumann, Manfred Rohde, Stefan Spring, Frank O. Glöckner, Christian Jogler and Mareike Jogler
- 84 Characterization of Outer Membrane Proteome of Akkermansia muciniphila Reveals Sets of Novel Proteins Exposed to the Human Intestine**
Noora Ottman, Laura Huuskonen, Justus Reunanen, Sjef Boeren, Judith Klievink, Hauke Smidt, Clara Belzer and Willem M. de Vos
- 97 The S-Layer Protein of the Anammox Bacterium Kuenenia stuttgartiensis is Heavily O-Glycosylated**
Muriel C. F. van Teeseling, Daniel Maresch, Cornelia B. Rath, Rudolf Figl, Friedrich Altmann, Mike S. M. Jetten, Paul Messner, Christina Schäffer and Laura van Niftrik
- 107 Evolutionary Cell Biology of Division Mode in the Bacterial Planctomycetes-Verrucomicrobia-Chlamydiae Superphylum**
Elena Rivas-Marín, Inés Canosa and Damien P. Devos

CHLAMYDIAE

- 118 A Zebrafish Model for Chlamydia Infection With the Obligate Intracellular Pathogen *Waddlia chondrophila***

Alexander G. J. Fehr, Maja Ruetten, Helena M. B. Seth-Smith, Lisbeth Nufer, Andrea Voegtlin, Angelika Lehner, Gilbert Greub, Philip S. Crosier, Stephan C. F. Neuhauss and Lloyd Vaughan

- 133 *Ca. Similichlamydia* in *Epitheliocystis* Co-infection of Gilthead Seabream Gills: Unique Morphological Features of a Deep Branching Chlamydial Family**

Helena M. B. Seth-Smith, Pantelis Katharios, Nancy Dourala, José M. Mateos, Alexander G. J. Fehr, Lisbeth Nufer, Maja Ruetten, Maricruz Guevara Soto and Lloyd Vaughan

NEW GENERA AND SPECIES

- 142 *Fuerstia marisgermanicae* gen. nov., sp. nov., an Unusual Member of the Phylum Planctomycetes From the German Wadden Sea**

Timo Kohn, Anja Heuer, Mareike Jogler, John Vollmers, Christian Boedeker, Boyke Bunk, Patrick Rast, Daniela Borchert, Ines Glöckner, Heike M. Freese, Hans-Peter Klenk, Jörg Overmann, Anne-Kristin Kaster, Manfred Rohde, Sandra Wiegand and Christian Jogler

- 157 Corrigendum: *Fuerstia marisgermanicae* gen. nov., sp. nov., an Unusual Member of the Phylum Planctomycetes From the German Wadden Sea**

Timo Kohn, Anja Heuer, Mareike Jogler, John Vollmers, Christian Boedeker, Boyke Bunk, Patrick Rast, Daniela Borchert, Ines Glöckner, Heike M. Freese, Hans-Peter Klenk, Jörg Overmann, Anne-Kristin Kaster, Manfred Rohde, Sandra Wiegand and Christian Jogler

GENETIC TOOLS

- 159 Development of Genetic Tools for the Manipulation of the Planctomycetes**

Elena Rivas-Marín, Inés Canosa, Eduardo Santero and Damien P. Devos



Editorial: Planctomycetes-Verrucomicrobia-Chlamydiae Bacterial Superphylum: New Model Organisms for Evolutionary Cell Biology

Laura van Niftrik^{1*} and Damien P. Devos²

¹ Microbiology, Faculty of Science, Institute for Water and Wetland Research, Radboud University, Nijmegen, Netherlands

² Centro Andaluz de Biología del Desarrollo-CSIC, Universidad Pablo de Olavide, Seville, Spain

Keywords: PVC bacteria, bioactive compounds, peptidoglycan, cell surface, genetic tools, cell biology and cell division

Editorial on the Research Topic

Planctomycetes-Verrucomicrobia-Chlamydiae Bacterial Superphylum: New Model Organisms for Evolutionary Cell Biology

OPEN ACCESS

Edited by:

Frank T. Robb,
University of Maryland, Baltimore,
United States

Reviewed by:

Matthew Stott,
GNS Science, New Zealand

*Correspondence:

Laura van Niftrik
l.vanniftrik@science.ru.nl

Specialty section:

This article was submitted to
Evolutionary and Genomic
Microbiology,
a section of the journal
Frontiers in Microbiology

Received: 22 June 2017

Accepted: 20 July 2017

Published: 02 August 2017

Citation:

van Niftrik L and Devos DP (2017)
Editorial: Planctomycetes-Verrucomicrobia-Chlamydiae Bacterial Superphylum: New Model Organisms for Evolutionary Cell Biology.
Front. Microbiol. 8:1458.
doi: 10.3389/fmicb.2017.01458

HISTORICAL CONTROVERSIES IN PLANCTOMYCETES-VERRUCOMICROBIA-CHLAMYDIAE (PVC) RESEARCH

The PVC superphylum bacteria have managed to intrigue and inspire researchers from the very start. Especially morphological and cell biological features of many PVC members puzzled, and in some cases, even misguided us researchers. This is illustrated by the initial misidentification of *Chlamydia trachomatis* as a virus (von Prowazek and Halberstadter, 1907), and the confusing etymology of Planctomycetes, meaning “floating fungus” (Gimesi, 1924). Toward the end of the last century, the controversy became even greater. The status of superphylum, the common ancestry of these bacteria with diverse genotypes, phenotypes, and life styles, was not yet recognized. In addition, the cell wall structure and apparent intracellular compartmentalization ran contrary to the classical bacterial dogma. Planctomycetes and Chlamydia were proposed to be devoid of peptidoglycan, an otherwise ubiquitous bacterial cell wall polymer (König et al., 1984; Liesack et al., 1986; McCoy and Maurelli, 2006; Cayrou et al., 2010). Planctomycetes were hypothesized to have a “third cell plan,” neither Gram-negative nor Gram-positive, and this was exemplified by *Gemmata obscuriglobus*, which was considered “the nucleated bacterium” (Fuerst, 2005). Further adding to the confusion was the observation that the Planctomycete undertaking anaerobic ammonium oxidation (anammox) did so by employing a specific intracellular anammoxosome compartment to support this process (Strous et al., 1999). The report of endocytosis-like protein uptake (previously only observed in eukaryotes) in *G. obscuriglobus* (Lonhienne et al., 2010) added more controversy and eventually it obtained the status of the “Platypus of microbiology” (Devos, 2013).

Only at the start of the present century, light began to dawn on this conundrum. First, commonalities of characters and phylogenies converged to the recognition of the PVC superphylum (Wagner and Horn, 2006). Then, the hypothesis that they represent variations of, but no exception to, the Gram-negative cell plan was percolating most research and discussions

(Devos, 2014). This eventually culminated with the discovery of peptidoglycan in almost all PVC members investigated (Pilhofer et al., 2013; Liechti et al., 2014; Jeske et al., 2015; van Teeseling et al., 2015; and this Research topic).

Since then, the PVC research community began to catch momentum and genome data and publication rate have increased exponentially. With the superphylum status now amply accepted, it is clear that PVC bacteria are fascinating new model organisms for bacterial and evolutionary cell biology. PVC bacteria are relevant to the environment (they are found in most sampled environments and are important contributors to major biogeochemical cycles), biotechnology (they are potential producers of bioactive compounds and used in bioremediation as well as responsible for the anammox process which is applied in wastewater treatment), evolutionary cell biology (they have features that separate them from other bacteria, such as extensive bacterial endomembrane systems and atypical modes of cell division) and human health (their presence has been linked to various conditions, from obesity to developmental disorders; Devos and Ward, 2014). The articles presented in this Research topic are a reflection of this diversity of research on PVC bacteria.

BIOACTIVE COMPOUNDS

Marine environments are a source of bioactive compounds. Many of these bioactive compounds are derived from sponges and macroalgae and their associated microbiome. Interestingly, some of the microbiomes have been reported to contain a high number of the slow-growing Planctomycetes. Therefore, there is currently a high interest in the potential of Planctomycetes as sources of bioactive compounds and antibiotics. Vollmers et al. investigated a brown macroalgae biofilm (*Macrocystis pyrifera*) from Monterey Bay for Planctomycetes and Verrucomicrobia using metagenomic shotgun and amplicon sequencing. Novel species were found and all contained secondary metabolite-related gene clusters. Jeske et al. developed a pipeline to cultivate and screen Planctomycetes for the production of antimicrobial compounds and showed antimicrobial activity of extracts from three Planctomycete species. Graça et al. isolated 40 Planctomycetes from macroalgae from the Portuguese coast and screened them for the production of antimicrobial compounds using molecular analysis (non-ribosomal peptide synthase and polyketide synthase genes) and bioactivity assays. The majority of the screened Planctomycetes (95%) contained one or both classes of secondary metabolite genes. In addition, approximately half of the Planctomycete extracts had antifungal (against *Candida albicans*, 43%) and antibacterial (against *Bacillus subtilis*, 54%) activity.

NEW PVC GENERA AND SPECIES NEEDED

Despite their relevance in global nutrient cycles, industrial applications, human health and evolution, the Planctomycetes, and Verrucomicrobia phyla are still largely undersampled. Kohn

et al. isolated a novel Planctomycete strain from the Wadden Sea (Germany) that is phylogenetically distant from other Planctomycetes and represents a novel genus. The isolate has an exceptionally large genome (9 Mb) including 45 “giant-genes.” They named the new Planctomycete after one of the Planctomycete research pioneers: Prof. John Fuerst (*Fuerstia marisgermaniae*).

CELL BIOLOGY

As described earlier, the PVC cell wall was a controversial topic for quite some years. Recent work has refuted the absence of peptidoglycan for both Chlamydia and Planctomycetes and in this Research topic, the lack of peptidoglycan is also challenged for Verrucomicrobia. Naqvi et al. show through genome analysis that *Verrucomicrobium spinosum* contains a novel open reading frame which is predicted to encode a fusion of the peptidoglycan synthesis enzymes MurB and MurC. The fusion gene was able to complement *Escherichia coli murB* and *murC* mutants and could be identified in specific lineages of the Verrucomicrobium phylum. Rast et al. describe three novel strains belonging to a novel genus of Verrucomicrobia subdivision 4 (*Lacunisphaera* gen. nov.) and detect peptidoglycan in their cell walls.

The cell surface can play an important role in the interaction with the environment and other (host) cells. Ottman et al. investigated the outer membrane proteome of Verrucomicrobia *Akkermansia muciniphila*. This is a beneficial member of the human gut microbiome as decreased levels have been associated with diseases. Because surface-exposed molecules play an important role in colonization and communication with the host and other microorganisms, the authors analyzed the outer membrane proteome. They found that the most abundant outer membrane protein PilQ most likely functions as a type IV pili secretin in *A. muciniphila*. van Teeseling et al. characterized the glycosylation of the S-layer which forms the outermost layer of the anammox Planctomycete cell wall. The S-layer is heavily glycosylated with an O-linked oligosaccharide which is additionally modified by methylation.

Finally, the Planctomycetes have various atypical modes of cell division; from FtsZ-less binary fission to FtsZ-less budding. Rivas-Marín et al. review the lack and presence of peptidoglycan in PVC bacteria and its involvement in chlamydial cell division. They also hypothesize about the possible evolution of the different modes of PVC cell division.

CHLAMYDIAE

Obligate intracellular Chlamydia are important pathogens of terrestrial and marine vertebrates. However, pathogenesis and host specificity are still largely unknown. Fehr et al. developed the first larval zebrafish model for chlamydial infections with *Waddlia chondrophila*. *Waddliacea* can infect and replicate in epithelia and macrophages. They demonstrate

that *W. chondrophila* is taken up and replicates in phagocytic cells (neutrophils) as well as macrophages and that myeloid differentiation factor 88 (My88) mediated signaling plays a role in the innate immune reaction to *W. chondrophila*. Seth-Smith et al. analyse genomes and ultrastructure of as-of-yet uncultivated chlamydial pathogens (Ca. Similichlamydiaceae) that cause epitheliocystis directly from tissue of gilthead seabream (*Sparus aurata*). They show that infection by chlamydial inclusions develops in a perinuclear location and follows a developmental cycle of replicating bodies and elementary bodies.

GENETIC TOOLS

For a long time Planctomycete research was hampered by the lack of genetic tools. However, recently the first genetic tools were developed for the Planctomycete *Planctopirus limnophila* (Jogler et al., 2011; Schreier et al., 2012; Erbilgin et al., 2014). Here, Rivas-Marín et al. developed genetic tools (mutagenesis by homologous recombination) for *P. limnophila* and three other Planctomycetes: *G. obscuriglobus*, *Gimesia maris*, and *Blastopirellula marina*.

REFERENCES

- Cayrou, C., Raoult, D., and Drancourt, M. (2010). Broad-spectrum antibiotic resistance of Planctomycetes organisms determined by Etest. *J. Antimicrob. Chemother.* 65, 2119–2122. doi: 10.1093/jac/dkq290
- Devos, D. P. (2013). *Gemmata obscuriglobus*. *Curr. Biol.* 23, R705–R707. doi: 10.1016/j.cub.2013.07.013
- Devos, D. P. (2014). PVC bacteria: variation of, but not exception to, the Gram-negative cell plan. *Trends Microbiol.* 22, 14–20. doi: 10.1016/j.tim.2013.10.008
- Devos, D. P., and Ward, N. L. (2014). Mind the PVCs. *Environ. Microbiol.* 16, 1217–1221. doi: 10.1111/1462-2920.12349
- Erbilgin, O., McDonald, K. L., and Kerfeld, C. A. (2014). Characterization of a planctomycetal organelle: a novel bacterial microcompartment for the aerobic degradation of plant saccharides. *Appl. Environ. Microbiol.* 80, 2193–2205. doi: 10.1128/AEM.03887-13
- Fuerst, J. A. (2005). Intracellular compartmentation in Planctomycetes. *Annu. Rev. Microbiol.* 59, 299–328. doi: 10.1146/annurev.micro.59.030804.121258
- Gimesi, N. (1924). Hydrobiologiai Tanulmanyok (Hydrobiologische Studien). I: *Planctomyces bekefi* gim. nov. gen. et sp. Kiadja a Magyar Ciszterci Rend. Budapest. 1–8.
- Jeske, O., Schüler, M., Schumann, P., Schneider, A., Boedeker, C., Jogler, M., et al. (2015). Planctomycetes do possess a peptidoglycan cell wall. *Nat. Commun.* 6:7116. doi: 10.1038/ncomms8116
- Jogler, C., Glöckner, F. O., and Kolter, R. (2011). Characterization of *Planctomyces limnophilus* and development of genetic tools for its manipulation establish it as a model species for the phylum Planctomycetes. *Appl. Environ. Microbiol.* 77, 5826–5829. doi: 10.1128/AEM.05132-11
- König, E., Schlesner, H., and Hirsch, P. (1984). Cell wall studies on budding bacteria of the Planctomyces/Pasteuria group and on a *Prosthecomicrobium* sp. *Arch. Microbiol.* 138, 200–205. doi: 10.1007/BF00402120
- Liechti, G., Kuru, E., Hall, E., Kalinda, A., Brun, Y. V., VanNieuwenhze, M. S., et al. (2014). A new metabolic cell wall labeling method reveals peptidoglycan in *Chlamydia trachomatis*. *Nature* 506, 507–510. doi: 10.1038/nature12892
- Liesack, W., König, H., Schlesner, H., and Hirsch, P. (1986). Chemical composition of the peptidoglycan-free cell envelopes of budding bacteria of the Pirella/Planctomycetes group. *Arch. Microbiol.* 145, 361–366. doi: 10.1007/BF00470872
- Lonhienne, T. G. A., Sagulenko, E., Webb, R. I., Lee, K.-C., Franke, J., Devos, D. P., et al. (2010). Endocytosis-like protein uptake in the bacterium *Gemmata obscuriglobus*. *Proc. Natl. Acad. Sci. U.S.A.* 107, 12883–12888. doi: 10.1073/pnas.1001085107
- McCoy, A. J., and Maurelli, A. T. (2006). Building the invisible wall: updating the chlamydial peptidoglycan anomaly. *Trends Microbiol.* 14, 70–77. doi: 10.1016/j.tim.2005.12.004
- Pilhofer, M., Aistleitner, K., Biboy, J., Gray, J., Kuru, E., Hall, E., et al. (2013). Discovery of chlamydial peptidoglycan reveals bacteria with murein saccule but without FtsZ. *Nat. Commun.* 4:2856. doi: 10.1038/ncomms3856
- Schreier, H. J., Dejtsakdi, W., Escalante, J. O., and Brailo, M. (2012). Transposon mutagenesis of *Planctomyces limnophilus* and analysis of a pckA mutant. *Appl. Environ. Microbiol.* 78, 7120–7123. doi: 10.1128/AEM.01794-12
- Strous, M., Fuerst, J. A., Kramer, E. H. M., Logemann, S., Muyzer, G., van de Pas-Schoonen, K. T., et al. (1999). Missing lithotroph identified as new planctomycete. *Nature* 400, 446–449. doi: 10.1038/22749
- van Teeseling, M. C. F., Mesman, R. J., Kuru, E., Espaillat, A., Cava, F., Brun, Y. V., et al. (2015). Anammox planctomycetes have a peptidoglycan cell wall. *Nat. Commun.* 6:6878. doi: 10.1038/ncomms7878
- von Prowazek, S., and Halberstadter, L. (1907). Zur Aetiologie des Trachoms. *Dtsch. Med. Wochenschr.* 33, 1285–1287. doi: 10.1055/s-0029-1188920
- Wagner, M., and Horn, M. (2006). The Planctomycetes, Verrucomicrobia, Chlamydiae and sister phyla comprise a superphylum with biotechnological and medical relevance. *Curr. Opin. Biotechnol.* 17, 241–249. doi: 10.1016/j.copbio.2006.05.005

FUTURE DIRECTIONS

The future directions for PVC research will most likely include important topics like; understanding their environmental significance, exploring the impact on and potential in human health and biotechnology, interaction with hosts, and other (micro)organisms, developing more genetic tools in more species, understanding their unusual cell division and in some cases life cycles and finally re-evaluate the PVC phylogeny and classification.

AUTHOR CONTRIBUTIONS

All authors listed have made a substantial, direct, and intellectual contribution to the work, and approved it for publication.

ACKNOWLEDGMENTS

The authors thank Christian Jogler for feedback on the editorial. DD was supported by the Spanish Ministry of Economy and Competitiveness (Grant BFU2013-40866-P) and the Junta de Andalucía (CEIC Grant C2A program to DD).

Conflict of Interest Statement: The authors declare that the research was conducted in the absence of any commercial or financial relationships that could be construed as a potential conflict of interest.

Copyright © 2017 van Niftrik and Devos. This is an open-access article distributed under the terms of the Creative Commons Attribution License (CC BY). The use, distribution or reproduction in other forums is permitted, provided the original author(s) or licensor are credited and that the original publication in this journal is cited, in accordance with accepted academic practice. No use, distribution or reproduction is permitted which does not comply with these terms.



Untangling Genomes of Novel *Planctomycetal* and *Verrucomicrobial* Species from Monterey Bay Kelp Forest Metagenomes by Refined Binning

John Vollmers¹, Martinique Frentrup¹, Patrick Rast¹, Christian Jogler^{1,2} and Anne-Kristin Kaster^{1*}

¹ Leibniz Institute DSMZ—German Collection of Microorganisms and Cell Cultures, Braunschweig, Germany, ² Department of Microbiology, Institute for Water and Wetland Research, Faculty of Science, Radboud University, Nijmegen, Netherlands

OPEN ACCESS

Edited by:

Damien Paul Devos,
University Pablo Olavide, Spain

Reviewed by:

Peter Dunfield,
University of Calgary, Canada
Jorge L. M. Rodrigues,
University of California, Davis, USA

*Correspondence:

Anne-Kristin Kaster
a.kaster@dsmz.de

Specialty section:

This article was submitted to
Evolutionary and Genomic
Microbiology,
a section of the journal
Frontiers in Microbiology

Received: 08 October 2016

Accepted: 07 March 2017

Published: 29 March 2017

Citation:

Vollmers J, Frentrup M, Rast P, Jogler C and Kaster A-K (2017)
Untangling Genomes of Novel *Planctomycetal* and *Verrucomicrobial* Species from Monterey Bay Kelp Forest Metagenomes by Refined Binning. *Front. Microbiol.* 8:472.
doi: 10.3389/fmicb.2017.00472

The kelp forest of the Pacific temperate rocky marine coastline of Monterey Bay in California is a dominant habitat for large brown macro-algae in the order of *Laminariales*. It is probably one of the most species-rich, structurally complex and productive ecosystems in temperate waters and well-studied in terms of trophic ecology. However, still little is known about the microorganisms thriving in this habitat. A growing body of evidence suggests that bacteria associated with macro-algae represent a huge and largely untapped resource of natural products with chemical structures that have been optimized by evolution for biological and ecological purposes. Those microorganisms are most likely attracted by algae through secretion of specific carbohydrates and proteins that trigger them to attach to the algal surface and to form biofilms. The algae might then employ those bacteria as biofouling control, using their antimicrobial secondary metabolites to defeat other bacteria or eukaryotes. We here analyzed biofilm samples from the brown macro-algae *Macrocystis pyrifera* sampled in November 2014 in the kelp forest of Monterey Bay by a metagenomic shotgun and amplicon sequencing approach, focusing on *Planctomycetes* and *Verrucomicrobia* from the PVC superphylum. Although not very abundant, we were able to find novel *Planctomycetal* and *Verrucomicrobial* species by an innovative binning approach. All identified species harbor secondary metabolite related gene clusters, contributing to our hypothesis that through inter-species interaction, microorganisms might have a substantial effect on kelp forest wellbeing and/or disease-development.

Keywords: algal biofilms, syntrophic interactions, biofouling control, natural product producers, genome binning

INTRODUCTION

Submarine kelp forests are one of the most species-rich, structurally complex, and productive ecosystems in temperate waters. They are extremely well studied in terms of trophic ecology (Dayton and Tegner, 1984; Steneck et al., 2002; Estes et al., 2004; Graham, 2004) and provide habitat and nutrition to diverse communities extending from microorganisms to mammals. Kelp forests are highly diverse at the phylum level (Steneck et al., 2002; Graham, 2004) and—like tropical rain

forests—important habitats and hot spots of biological diversity. Given that individual kelp algae can grow up to 50 cm in length every day, kelp forests are also major players in CO₂ fixation in temperate waters (Foster et al., 2012). The so-called giant kelp, *Macrocystis pyrifera*, dominates these ecosystems along the temperate west coasts of North America (Dayton, 1985; Foster and Schiel, 1985; Delille and Perret, 1991; Graham et al., 2007). Along the central coast of California the kelp forest is of tremendous importance for coastal biodiversity, productivity, and the human economy and kelp-surface-associated bacteria are believed to be important players in carbon and nitrogen turnover in this food web (Linley and Field, 1982; Graham, 2004). While this habitat has been intensively researched for decades, still little is known about the microorganisms associated and interacting with the kelp, as only recently molecular techniques have become available to study biofilm species composition and abundance (Bengtsson et al., 2010, 2011, 2012; Hollants et al., 2013; Michelou et al., 2013).

Bacteria-algae interactions include symbiotic and parasitic relationships and mainly depend on environmental parameters, such as the availability of inorganic nutrients and organic matter. In eutrophic coastal marine systems like the Monterey Bay kelp forest rapid bacterial biofilm colonization takes place. Heterotrophic microorganisms are most likely attracted by the macro-algae through secretion of specific carbohydrates and proteins that trigger them to attach to their surface and to form biofilms, while degrading complex algal polysaccharides (Bengtsson et al., 2011, 2012; Jeske et al., 2013; Wegner et al., 2013). Kelp exudates may shape bacterial community composition, and create communities that are kelp-specific rather than randomly assembled from the surrounding seawater (Taylor et al., 2004; Longford et al., 2007; Reis et al., 2009). A study by Michelou et al. (2013) with samples taken from Monterey Bay in the months March and May in 2010 using 454-tag pyrosequencing of 16S rRNA genes showed that bacterial community structure and membership correlated with the kelp surface serving as host, and varied over time. *M. pyrifera* surface was enriched with *Rhodobacteraceae*, *Sphingomonadaceae* (*Alphaproteobacteria*), *Flavobacteraceae*, *Sapspiraceae* (*Bacteroidetes*) families and unclassified *Gammaproteobacteria*. Interestingly, sequences from the phyla *Verrucomicrobia* and *Planctomycetes* were detected, although not in high abundance. Several taxa were highly similar to other bacteria known to either prevent the colonization of eukaryotic larvae or exhibit antibacterial activities, which holds true for *Verrucomicrobia* and *Planctomycetes* (Wagner and Horn, 2006; Rao et al., 2007).

Studies of biofilms from the kelp algae *Laminaria hyperborea* collected along the west coast of Norway showed *Verrucomicrobia* and *Planctomycetes* to be even among the most frequently detected lineages (Bengtsson and Øvreås, 2010). However, biofilm composition was subject to seasonal variations (Bengtsson et al., 2010) and due to the dominance of few abundant Operational Taxonomic Units (OTUs), the kelp surface was characterized as low-diversity habitat (Bengtsson et al., 2012). Given the slow growth of *Planctomycetal* species (Fuerst, 2013) their abundance in such habitats, that are packed with carbon sources in contrast to the largely

oligotrophic surrounding water, appears counter intuitive (Lage and Bondoso, 2014). Most other heterotrophs that dwell in such ecological niches divide much faster (for example 1.2–6.3 h for *Roseobacter* species (Christie-Oleza et al., 2012; Hahnke et al., 2013) and should generally outcompete slowly growing competitors. However, the interactions with the algae might involve the production of various secondary metabolites that are antimicrobial (defense against other, faster growing, heterotrophic bacteria) or algicidal (to destroy other eukaryotes like algae, diatoms or cyanobacteria for scavenging), and algae use those prokaryotic species as biofouling control (Zheng et al., 2005; Goecke et al., 2010). Those inter-species interactions of algae and bacteria and their resulting natural products are however not well understood (Estes et al., 2004).

We here analyzed for the first time a biofilm sample from *M. pyrifera* of the Monterey Bay kelp forest by a metagenomic shotgun and amplicon sequencing approach with a focus on the PVC superphylum (Figure 1). This study reports an in-depth description of the diversity and phylogenetic association of the microbial communities associated with *M. pyrifera*. Through inter-species interactions *Planctomycetes* and *Verrucomicrobia* might have a substantial effect on kelp forest wellbeing or disease-development, providing a foundation for understanding the microbial ecology of kelp forests.

MATERIALS AND METHODS

Sampling

Macrocystis pyrifera was collected in 6 m water depth at a temperature of 12°C from the kelp forest near the Monterey Bay Aquarium, California, USA (lat. 36.619; long. -121.901) in November 2014 (Figure 1). Samples were stored in sterile Artificial Sea Water (ASW; 0.8 M NaCl, 0.06 M Na₂SO₄, 0.1 M MgCl₂ × 6 H₂O, 19.5 mM CaCl₂ × 2 H₂O, 4.6 mM NaHCO₃, 18.5 mM KCl, 1.6 mM KBr, 0.08 mM SrCl₂ × 6 H₂O and 0.14 mM NaF) and shipped on ice to Germany the same day. Upon arrival, the algae were cut into several 5 cm² pieces and its biofilm was partially scraped off into 20 ml fresh ASW using a sterile scalpel, in order to achieve a partial enrichment of biofilm associated bacteria and to circumvent extracting eukaryotic cell material. However, since the biofilm was found to be thin and not always clearly visible, original kelp pieces were also retained for subsequent DNA extractions. Kelp pieces and scraped-off biofilm were stored separately in fresh ASW at -20°C until further processing.

DNA Extraction

In order to ensure a comprehensive representation of the kelp biofilm community, while minimizing eukaryotic DNA contamination from the algae itself and to enable a differential coverage binning approach, two different extraction methods were used to obtain DNA from kelp biofilm, resulting in DNA extracts A and B, respectively. Both extracts originated from the same kelp stipe, but from different blades. (Extract A) Sub-segments of one 5 cm² kelp piece and 1.5 ml of scraped-off biofilm suspension were combined and subjected to pulse vortexing as well as 5 min of vigorous shaking in order to

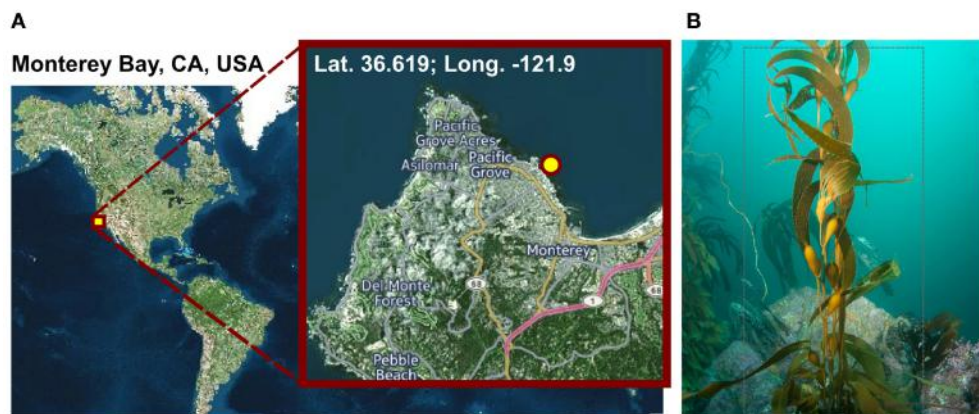


FIGURE 1 | Sampling. **(A)** Geographic position of the sampling site. Visualization was done with cartoDB (<https://www.carto.com>). **(B)** *Macrocystis pyrifera* (kelp) specimen photographed at the sampling location during sampling in November 2014 at a water depth of 6 m and a water temperature of 12°C.

detach and capture tenacious biofilm community members which may not have been efficiently scraped off. Eukaryotic cells were then removed from the suspension via gravity flow filtration using a polycarbonate filter with 10 μm pore size (Celltrics filter, Partec, Münster, Germany). **(Extract B)** In order to minimize carry-over of eukaryotic cell fragments and to protect sensitive community members from shearing forces, 2 ml of undisturbed scraped-off biofilm suspension were carefully transferred to a new microcentrifuge tube without including the precipitate of residual algae fragments which formed by natural sedimentation. Subsequently, all DNA extraction steps were identical for both approaches, beginning with a two-step protocol adopted from Ferrera et al. (2010). Microbial cells were harvested by centrifugation (40 min, 16,000 g, 4°C) and re-suspended in 950 μl lysis buffer (40 mM EDTA, 50 mM Tris-HCl, 0.75 M sucrose). The cell suspensions were enzymatically lysed under slight shaking for 45 min at 37°C using 1 mg/ml lysozyme (final conc.), followed by chemical lysis under slight shaking for 60 min at 55°C using 1 mg/ml SDS and 0.2 mg/ml proteinase K (final conc., respectively). Two rounds of phenol:chloroform:isopentanol [25:24:1; v:v:v] extractions and two rounds of chloroform:isopentanol [24:1; v:v] extractions were performed. DNA of each sample was precipitated for 12 h at -20°C, using 0.3 M sodium acetate (final conc.) and 1 volume of ice-cold isopropanol, washed twice with 70% ethanol and re-suspended in 20 μl of nuclease free water. DNA purity was verified photometrically using a Nanodrop 2,000 Spectrometer (Thermo Fischer Scientific, Wilmington, USA), while DNA yield was determined using a Qubit® 1.0 Fluorometer with an dsDNA HS Assay Kit (Life Technologies, Darmstadt, Germany).

Metagenomic Shotgun Library Preparation

Separate shotgun libraries, KelpA and KelpB, were produced for DNA extracts A and B, respectively. DNA was sheared using a Covaris® S220 sonication device (Covaris Inc; Massachusetts, USA; 55.5 μl shearing volume, 175 W Peak Incident Power, 5% Duty factor, 200 burst cycles, 55 s treatment time). Sequencing libraries were prepared using the NEBnext® Ultra™ DNA

Library Preparation Kit for Illumina® (New England Biolabs, Frankfurt, Germany) as per the manufacturer's instructions. Due to a high concentration of inhibitory contaminants, such as algal osmolytes released during sample treatment, extract A had to be diluted prior to library preparation, limiting the respective amount of input DNA to 5 ng. Therefore, 12 cycles of enrichment PCR were performed during the preparation of library KelpA. Since extract B was free of such contaminants, the full DNA yield of 105 ng could be utilized for preparation of library KelpB, necessitating only 6 cycles of enrichment PCR.

Amplicon Library Preparation

An aliquot of DNA extract A was diluted to 1 ng/ μl with PCR-grade water and subjected to Whole Genome Amplification (WGA) using the illustra™ GenomiPhi™ V2 DNA amplification Kit (GE Healthcare) and a Veriti 96-Well thermal cycler (Applied Biosystems). In order to reduce stochastic amplification bias, 10 independent amplification reactions were performed, using 1 μl of diluted DNA in a 20 μl reaction volume each, and subsequently pooled. WGA products were quantified using a Qubit® 3.0 Fluorometer with the Qubit® dsDNA BR Assay Kit (Life Technologies, Darmstadt, Germany). The V3 region of the 16S rRNA gene was amplified from the pooled WGA products via two subsequent PCR steps. Both reactions were performed in 50 μl reaction volumes consisting of 0.02 U/ μl Q5® High-Fidelity DNA Polymerase (New England Biolabs, Ipswich, MA, USA), 1 \times Q5 high GC enhancer, 1 \times Q5 reaction buffer and 200 μM dNTPs. While the applied temperatures varied, both PCR programs consisted of 10 amplification cycles, with 1 min each for denaturing, annealing and elongation, as well as a preliminary denaturing step and a final elongation step of 5 min each. Reactions were performed in triplicates, which were subsequently pooled in order to reduce stochastic amplification bias. The first pre-amplification step was performed using 0.1 μM each of the V3 region specific forward primer 341f (5'- CCT ACG GGW GGC WGC AG-3') and the universal reverse primer uni515r (5'- CCG CGG CTG CTG GCA C-3') modified from 341f and 518r by Muyzer et al. (1993), respectively. Three hundred

nano grams of WGA product was used as template. Cycling temperatures were 94°C for denaturing, 63°C for annealing and 72°C for elongation. Illumina® sequencing adapters and barcodes were added during the second amplification step following the pooling and purification of the pre-amplification products. For this step, 0.2 μM each of the extended V3 region primers “V3 fwd” (5'- AAT GAT ACG GCG ACC ACC GAG ATC TAC ACT CTT TCC CTA CAC GCT CTT CCG ATC TCC TAC GGG WGG CWG CAG -3') and “index 34 V3 rev” (5'- CAA GCA GAA GAC GGC ATA CGA GAT TAT TCG GTG ACT GGA GTT CAG ACG TGT GCT CTT CCG ATC TCC GCG GCT GCT GGC AC -3') were used, both of which were modified from Bartram et al. (2011). Fifteen microliters of pre-amplification product was used as template. Denaturing, annealing and elongation temperatures were 98, 65, and 72°C, respectively. PCR products were separated by electrophoresis using 2% agarose gels in 1 × Tris-Acetate-EDTA (TAE) buffer. The gel was stained with SYBR® gold (Thermo Fisher) for 1 h and inspected under UV light. Amplicon bands (~300 bp sized fragments) were excised and extracted using a spin column based approach (NucleoSpin Gel and PCR Clean-up; Macherey-Nagel).

Sequencing and Read Processing

All libraries were sequenced on an Illumina® MiSeq using v3 chemistry, 301 cycles per read and paired end settings. Raw sequences were subjected to adapter clipping and quality trimming using Trimmomatic v.0.36 (Bolger et al., 2014) with the following arguments: “LEADING:3 TRAILING:3 SLIDINGWINDOW:4:15 MINLEN:105.” For preliminary metagenome assemblies, only the resulting read pairs were used, excluding orphans. For subsequent mapping and reassembly steps, as well as amplicon analyses, overlapping read pairs were identified and merged using FLASH v.1.2.11 (Magoc and Salzberg, 2011). Due to the short length of the amplicon inserts, amplicon read pairs overlapped in their entire sequence length. Therefore, merging resulted in high confidence consensus sequences which minimized the influence of random sequencing errors. Merged amplicon reads were furthermore analyzed and filtered based on the presence of the employed V3 region specific forward and reverse primer sequences, which were subsequently clipped from the reads.

Metagenome Shotgun Assembly

Processed reads were pooled into a combined dataset KelpAB and assembled using IDBA-UD v.1.1.1 (Peng et al., 2012). For reference, additional individual assemblies were performed for each dataset, separately. In order to take optimal advantage of the longer MiSeq sequencing read lengths for correctly resolving repetitive regions, the source code was slightly altered to allow k-mer lengths of up to 251 bp, according to guidelines provided by the developers (<https://github.com/loneknightpy/idba>). For the preliminary metagenome shotgun assemblies, only paired reads were used, as IDBA_UD is not optimized for unpaired or merged reads.

Binning and Reassembly

Initial binning was performed using Maxbin v.2.1.1 (Wu et al., 2016) yielding 136 bins (Supplementary Table 1). After analysis and classification of these preliminary bins using CheckM v.1.0.4 (Parks et al., 2015), 8 *Planctomyceta* bins and 2 *Verrucomicrobial* bins were selected for further processing, in order to improve the assembly and remove residual contaminating genome fragments (Table 1). Putative contaminants were identified by taxonomically classifying the scaffolds of each bin using the Least Common Ancestor (LCA) approach implemented in MEGAN5 (Huson and Weber, 2013). Classifications were based on blastx and blastn comparisons against the NCBI nt and nr databases respectively, using an evalue cutoff of 1e-20. Only scaffolds that could be unambiguously assigned to any other phyla than the expected Planctomycetes or *Verrucomicrobia* were removed as putative contaminants. Subsequently, the average read coverage of each metagenomic scaffold was determined by mapping the sequencing datasets KelpA and KelpB individually against the combined assembly (KelpAB) using bowtie2 (Langmead and Salzberg, 2012). This information was used to analyze the coverage distribution within each of the selected bins. All outliers, consisting of scaffolds with coverage values larger than three-fold the median of the respective dataset and bin, were removed. Furthermore, bins were examined for sets of scaffolds displaying inverse relative coverage profiles when comparing KelpA and KelpB (e.g., displaying high abundance in KelpA but low abundance in KelpB or vice versa) and divided into appropriate sub-bins if applicable. In order to enable a targeted re-assembly, the corresponding sequencing reads were extracted from datasets KelpA and KelpB based on bowtie2 mappings for each of the hereby pre-filtered bins. To maximize sequence information and coverage, orphaned reads and merged read pairs were included in the analyses. To ensure high specificity, the “end-to-end” setting of bowtie2 was employed accepting only reads aligning in the entirety of their length. Furthermore, read pairs were only accepted if both reads mapped to the respective bin. The resulting read subsets were individually reassembled using SPAdes v.3.7.1 (Bankevich et al., 2012) and utilizing the scaffolds of the respective purified preliminary bin as “untrusted reference.” For final purification, new coverage profiles were calculated based on bowtie2 mappings and analyzed in order to identify scaffolds displaying differential coverage between datasets KelpA and KelpB, indicating putative contaminating genome fragments in each bin. To this end, the coverage values for each bin and dataset were converted into z-scores representing the respective deviation from the mean coverage of each analyzed bin. Putative contaminants were identified as scaffolds displaying differences above a specified cutoff between the z-scores for datasets KelpA and KelpB. Z-scores were recalculated for the remaining scaffolds, each time a putatively contaminating scaffold was removed. This process was performed iteratively beginning at a z-score cutoff of 4, decreasing the cutoff by 1 each time no further contaminants could be identified, until a final cutoff value of 2 was reached (corresponding to a coverage difference of 2 x the standard deviation for each dataset). The final, processed bins were re-examined using CheckM with appropriate phylum

TABLE 1 | General statistics of Planctomyces and Verrucomicrobia bins.

| Bin | IMG/M analysis project ID | Completeness & Contamination | | | | Assembly statistics | | | | | | Relative abundance compared to total bacterial population for individual bins and grouped bins, respectively [KelpA/KelpB/KelpAB] | |
|------------------------|---------------------------|---|-----------|-----------------------|------------|---------------------|-------------|----------|-------------------------|---------------------|--------|---|--|
| | | based on CheckM using phylum-specific markers | | | | based on tRNAs | | | | | | | |
| | | Compl. [%] | Cont. [%] | Strain heterogen. [%] | Compl. [%] | Genome size [bp] | No. contigs | N50 [bp] | Mean contig length [bp] | Longest contig [bp] | GC [%] | | |
| Planctomyces bin 1 | Gad136817 | 84.11 | 2.28 | 44.44 | >99 | 4,642,202 | 422 | 21,658 | 11,000 | 66,126 | 52.33 | 0.37%/ 0.65%/ 0.55% | |
| Planctomyces bin 2 | Gad136818 | 55.92 | 18.95 | 6.02 | 50 | 3,449,631 | 1,946 | 1,836 | 11,772,772 | 8,106 | 52.33 | 0.01%/ 0.05%/ 0.04% | |
| Planctomyces bin 3 | Gad136832 | 48.51 | 11.02 | 6.67 | 70 | 2,487,561 | 1,428 | 1,767 | 1,741 | 7,729 | 50.8 | 0.17%/ 0.1%/ 0.11% | |
| Planctomyces bin 4 | Gad136833 | 37.69 | 7.88 | 0 | 15 | 2,331,893 | 1,507 | 1,503 | 1,547 | 8,668 | 53.1 | 0.06%/ 0.1%/ 0.09% | |
| Planctomyces bin 5 | Gad136834 | 39.31 | 8.4 | 17.14 | 55 | 2,181,529 | 1,181 | 1,942 | 1,847 | 7,171 | 52.3 | 0.02%/ 0.01%/ 0.01% | |
| Planctomyces bin 6 | Gad136835 | 13.82 | 3.52 | 21.05 | 85 | 1,947,306 | 1,261 | 1,492 | 1,544 | 7,283 | 48.5 | 0.04%/ 0.11%/ 0.1% | |
| Planctomyces bin 7 | Gad136836 | 9.23 | 0.8 | 0 | 10 | 1,142,748 | 715 | 1,539 | 1,598 | 9,254 | 48.3 | 0.1%/ 0.12%/ 0.12% | |
| Planctomyces bin 8 | Gad136837 | 8.5 | 0 | 0 | 30 | 880,382 | 612 | 1,380 | 1,438 | 4,317 | 54 | 0.37%/ 0.04%/ 0.11% | |
| Verrucomicrobium bin 1 | Gad136838 | 47.77 | 0.41 | 0 | 45 | 1,639,567 | 806 | 2,209 | 2,034 | 9,554 | 47.8 | 0.84%/ 0%/ 0.17% | |
| Verrucomicrobium bin 2 | Gad136839 | 23.01 | 0.41 | 0 | 20 | 643,037 | 438 | 1,433 | 1,468 | 4,804 | 47.2 | 0.03%/ 0.09%/ 0.08% | |

Detailed completeness and contamination estimations were based on CheckM v1.0.4 (Parks et al., 2015) results using phylum-specific marker sets. "Contamination" values indicate the percentage of phylum-specific marker genes which were found in multiple copy number and do not necessarily reflect actual contamination. Similarly, "Strain heterogeneity" values indicate the percentage of multi-copy marker genes with more than 90% sequence identity and may not reflect actual heterogeneity. Bins were sorted and numbered, based on estimated completeness. Planctomyces bins are marked in shades of green, Verrucomicrobium bins are marked in shades of violet. Bins with completeness values lower than 20% are marked in gray, while completeness values above 20% are marked by bold lettering. Additional rough estimations of genome completeness, based on distinct rRNA species, are included for reference. Relative abundances were based on the average read coverage of each bin after mapping the unassembled reads to the combined metagenome assembly. Combined abundance values for different combinations of planctomyces and verrucomicrobial bins are shown in light green for Planctomyces bins and in light violet for Verrucomicrobes bins. The relative abundances of Planctomyces and Verrucomicrobial bins were found to be in accordance with estimations based on unassembled reads (Figure 2) as well as reconstructed 16S rRNA genes (Supplementary Table 5).

specific marker sets for Planctomycetes or *Verrucomicrobia* (**Table 1**).

Annotation and Functional Analyses

Gene calling and annotation was performed for processed bins using the Prokka pipeline v.1.12 (Seemann, 2014). Additionally, genes were annotated with SEED categories, based on blastp alignments against the NCBI nr database and subsequent LCA analyses using MEGAN5. AntiSMASH v.3.0 was employed to identify putative secondary metabolite gene clusters (Weber et al., 2015).

Analyses of Shotgun Metagenomic 16S rRNA Genes

RNAmmer v.1.2 was used to identify almost full-length (>1,100 bp) 16S rRNA gene sequences in the assembled metagenomes (Lagesen et al., 2007). However, due to the highly conserved nature of 16S rRNA genes, such sequences are likely to represent chimeras of different related strains when obtained by metagenome assembly. Therefore, the dedicated software tool EMIRGE (Miller et al., 2011) for reconstructing 16S rRNA genes from short read metagenomic data, was additionally employed for verification purposes. The resulting 16S rRNA sequences were aligned to the SILVA reference database and taxonomically classified using SINA (Pruesse et al., 2012; Quast et al., 2013; Yilmaz et al., 2014). Additionally, the sequences were phylogenetically clustered using a neighbor joining approach with 1,000 bootstrap iterations as implemented in ARB v.6.0.2 (Ludwig et al., 2004). A combination of phylogenetic, Multi Locus Sequence Analyses (MLSA) and coverage analyses was used to identify unambiguous connections between metagenomic bins and 16S rRNA gene sequences. Classification and relative abundances were visualized using the software tool Krona (Ondov et al., 2011).

Analyses of 16S rRNA Amplicon Sequences

The low sequence length and high throughput of the amplicon sequencing data required a slightly different analyses pipeline than the almost full-length sequences reconstructed from the shotgun metagenome datasets. However, the same reference database as well as general taxonomic classification framework was used. Classification of processed amplicon reads was performed using the SILVAngs service platform and associated analysis pipeline (Quast et al., 2013; Yilmaz et al., 2014). Reads were uploaded as suggested in the SILVAngs user-guide and processed by the SILVAngs software according to the recommended protocol, including sequence alignment with the SINA aligner (Pruesse et al., 2012). During the process, a de-replication step, eliminating 100% identical reads, as well as OTU definition and clustering was performed. OTUs were classified by a local BLAST search using blastn with default parameters in accordance to the non-redundant version of the SILVA SSU Ref database. Classification and relative abundance of defined OTUs was visualized using the implemented software tool Krona (Ondov et al., 2011).

Multi Locus Sequence Analyses (MLSA)

Proteinortho5 (Lechner et al., 2011) was used to detect groups of orthologous genes shared between selected reference genomes and processed metagenomic bins. Reference genomes were obtained from NCBI and IMG/M. For each set of bins and comparison genomes, the respective “unique core genome” was determined as the list of gene products universally present in single copy. The size and composition of the resulting unique core genome set is strongly dependent on the reference genomes and the completeness of the analyzed bins. Therefore, separate analyses were performed for each processed metagenomic bin as well as combinations of bins associated with the same phylum. The resulting unique core genome gene products were individually aligned using MUSCLE v.3.8.31 (Edgar, 2004) and subsequently concatenated. Regions that could not be aligned were filtered from the alignments using Gblocks v.0.91b (Castresana, 2000). The filtered alignments were clustered using the neighbor joining algorithm with 1,000 bootstrap permutations, in order to reliably place each bin into a phylogenetic context.

Accession Numbers

Metagenome data and sequences of the 8 *Planctomycetal* and 2 *Verrucomicrobial* bins were deposited with the Integrated Microbial Genomes (IMG) database. KelpAB (coassembly): Ga0136809, KelpA (single assembly): Ga0136854, KelpB (single assembly): Ga0136855; *Planctomycetal* bin 1: Ga0136817, *Planctomycetal* bin 2: Ga0136818, *Planctomycetal* bin 3: Ga0136832, *Planctomycetal* bin 4: Ga0136833, *Planctomycetal* bin 5: Ga0136834, *Planctomycetal* bin 6: Ga0136835, *Planctomycetal* bin 7: Ga0136836, *Planctomycetal* bin 8: Ga0136837; *Verrucomicrobial* bin 1: Ga0136838, *Verrucomicrobial* bin 2: Ga0136839.

RESULTS AND DISCUSSION

We here analyzed the biofilm community of *M. pyrifera* sampled from Monterey Bay kelp forest in November 2014 on multiple levels: Amplicon sequences, unassembled metagenomic shotgun reads, and assembled metagenome (**Figure 2**, Supplementary Figures 1, 2). Amplicon library sequencing yielded in 660.000 high quality reads in overlapping pairs, which could be merged into 330.000 consensus reads (Supplementary Figure 1A). Metagenomic shotgun sequencing yielded 36 mio raw reads per sequencing library. After quality trimming, 28 mio high quality reads were retained for library of KelpA and 34 mio reads for KelpB. In both cases, a large fraction of ~23 mio reads formed overlapping read pairs, which could be merged into longer consensus sequences prior to assembly (Supplementary Figure 1B). The amplicon library based approach indicated a bacterial biofilm community comprised predominantly of Proteobacteria and Bacteroidetes, with Planctomycetes and *Verrucomicrobia* representing lower but nonetheless substantial community fractions of 4% each (**Figure 2A**). This observation is in concurrence with a previous amplicon based analysis of *M. pyrifera* associated communities sampled during spring 2010. The overall trend of this community profile was furthermore

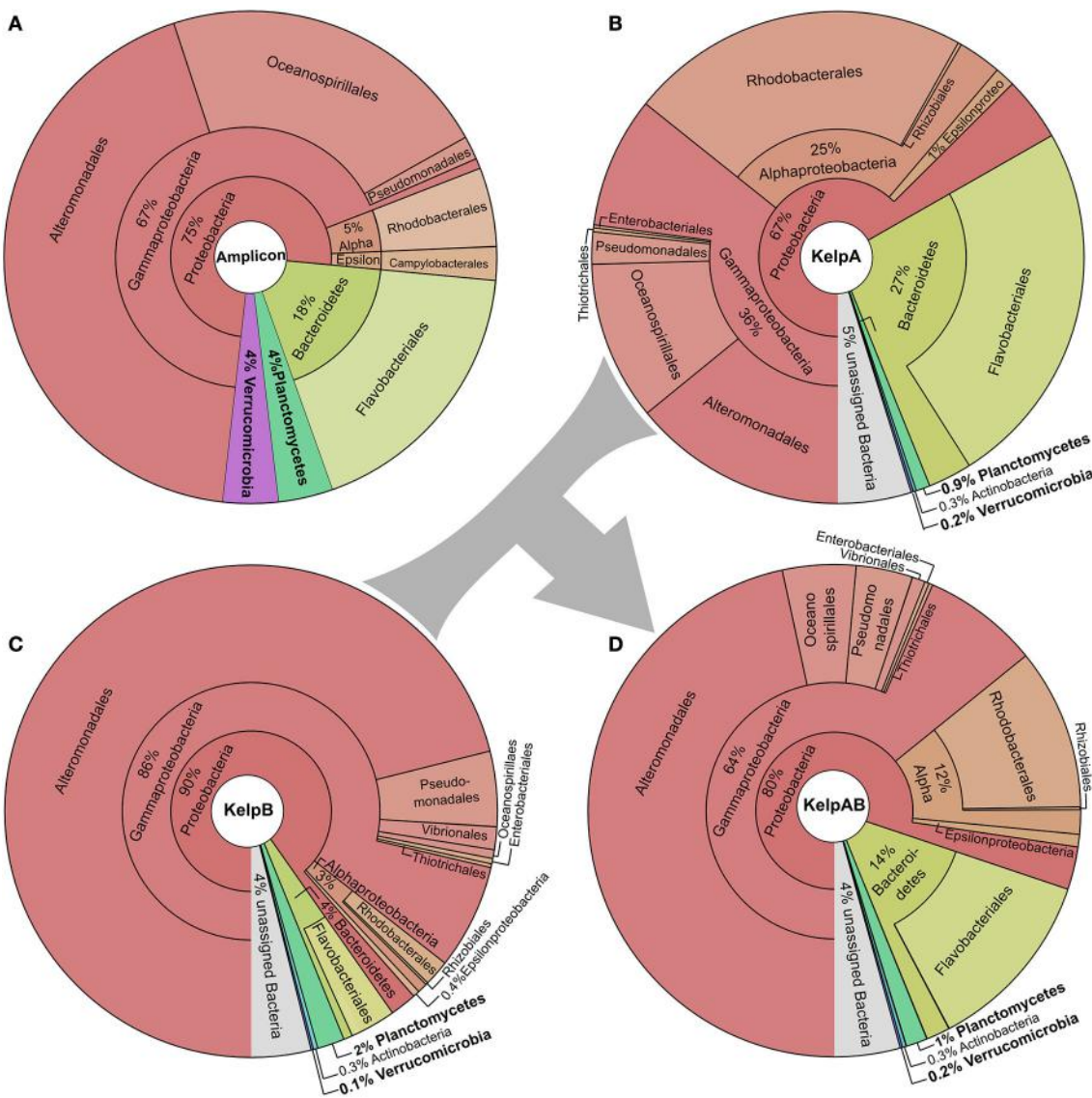


FIGURE 2 | Taxonomic composition of the kelp biofilm community. Pie charts showing the relative abundances of sequences associated with bacterial taxa within each sequencing dataset down to order level. Visualizations were done using KRONA (Ondov et al., 2011). **(A)** 16S rRNA amplicon dataset. Relative abundances were determined using the SILVA NGS pipeline (Quast et al., 2013; Yilmaz et al., 2014). **(B,C)** Metagenomic shotgun libraries of KelpA & KelpB, respectively. KelpA **(B)** was derived from the same sample as the amplicon library, while KelpB **(C)** was derived from a separate sample obtained from a different leaf of the same Kelp specimen, using a slightly modified DNA extraction protocol. Relative abundances were determined based on sequencing read classifications obtained by using the Least Common Ancestor (LCA) approach implemented in MEGAN5 (Huson and Weber, 2013). In order to maximize coverage for low abundant community members, both datasets were treated as a composite dataset KelpAB **(D)** for assembly.

confirmed by the Least Common Ancestor (LCA) taxonomic classification of a metagenomic shotgun sequencing dataset (KelpA) obtained from the same sample (**Figure 2B**), albeit with pronounced differences in the exact proportions of each bacterial fraction. Among the most noteworthy differences between the amplicon and the shotgun sequencing approach are the considerably lower fractions of Planctomycetes and *Verrucomicrobia* in the latter, comprising only 0.9 and 0.2% of the bacterial community, respectively. A cause for these discrepancies might be the bias introduced by the Phi29

based Whole Genome Amplification (Lasken, 2009) used in the preparation of the amplicon, but not the metagenomic shotgun library. However, since correct classification of short shotgun reads is highly dependent on the presence of closely related genome sequences within public databases, this divergence probably reflects the low representation of the PVC superphylum within currently sequenced genomes as well as the uniqueness of the Planctomycetes and *Verrucomicrobia* strains present in the here sampled habitat. The latter assumption is partially supported by the fact that relative abundances of

the PVC superphylum diverge by a factor of 4.4–20% between amplicon and metagenomic shotgun data sets, while most other phyla and classes diverge only by a factor of 1.5–5%. The underrepresentation of PVC-classified reads, caused by the generally high variability of protein coding genes in combination with the low number of currently available PVC reference genomes also increases the likelihood of PVC-associated reads being classified as “unassigned bacteria.”

In the past, PVC community members have been often reported to be highly abundant and sometimes even dominant in kelp biofilm communities (Bengtsson and Øvreås, 2010; Michelou et al., 2013). However, the dominance of specific species or OTUs is often only temporary (Bengtsson et al., 2012; Michelou et al., 2013), e.g., in form of seasonal blooms. Metagenomics data are therefore likely not generally representative for the respective environment but only for the specific set of conditions during sampling. In addition, virus infections might change a microbial community within hours. Therefore, crucial members of communities may only be found in low abundance most of the time, in some cases even always (K-strategists). Such organisms may be much harder to isolate and analyze, but represent a huge hidden genomic potential, which still remains to be discovered. Unfortunately, whether trying to obtain isolates from environmental samples, or trying to reconstruct genomes from metagenomes (Albertsen et al., 2013; Sangwan et al., 2016) the focus is most often laid on the most abundant community members. As a result, low abundant and/or slowly growing species are likely to be underrepresented in public databases. With our innovative binning approach we here provide insights into the genomes of some low abundance but ubiquitous *Planctomycetal* and *Verrucomicrobial* species on algae and were able to generate a good draft genome of a novel Planctomycete which cannot be assigned to any of the known genera with cultured representatives.

Since binning efficiency is significantly improved by employing multiple related datasets, two metagenomic shotgun libraries were produced using slightly altered extraction protocols and different blade sections of the same kelp specimen, resulting in the datasets KelpA and KelpB. Similar to KelpA, KelpB was dominated by Proteobacteria, particularly Gammaproteobacteria, and contained only relatively small fractions of Planctomycetes and *Verrucomicrobia* (Figure 2C). However, both datasets differed in the exact proportions of the individual observed taxa, caused by a combination of community variability within kelp specimens as well as differences in extraction protocols. Differences include a lower relative abundance of Planctomycetes in KelpA compared to KelpB, while the opposite seems to be true for *Verrucomicrobia*, indicating that coverage differences between these datasets may be utilized to improve subsequent binning steps. The most pronounced differences were observed for the class Alphaproteobacteria and the phylum Bacteroidetes, which are present in considerably lower abundance in KelpB compared to KelpA by factors of ~8 and ~7, respectively. This indicates that intra-host variation and differences in extraction methods may greatly influence the community structure observed by metagenomic analyses, but can be utilized for differential

coverage binning approaches. While both libraries confirm the dominance of Proteobacteria observed in the amplicon library, the observed fraction of Planctomycetes and *Verrucomicrobia* is considerably lower, representing only 0.1–2% of the bacterial community. In order to maximize sequencing coverage for low abundant community members present in both sequencing datasets, KelpA and KelpB were pooled into the combined dataset KelpAB (Figure 2D) and re-assembled, prior to binning.

Unfortunately, the preliminary bins obtained using Maxbin v.2.0 were of mixed quality, with a large degree of fragmentation as well as contamination in most bins (Supplementary Table 1). In order to obtain the most reliable and representative portrayal of contained PVC superphylum members, selected bins were rigorously filtered and processed using a stringent custom pipeline (for details please see Materials and Methods). This resulted in one almost complete and seven partial *Planctomycetal* and two partial *Verrucomicrobial* bins (Table 1). However, the final processed bins did not include 16S rRNA sequences, since those were predominantly encoded on small genome fragments, which did not include any additional markers. Due to the conserved nature of 16S rRNA genes, such fragments could therefore not be unambiguously binned based on sequence composition.

Instead, two complementary methods were employed to obtain 16S rRNA sequences from the original metagenomic datasets: Direct extraction of 16S rRNA gene sequences using the hidden Markov model approach of RNAmmer, and the mapping based reconstruction approach implemented by EMIRGE. However, since the resulting genes do not represent clonal sequences they should be regarded as consensus sequences, analog to so-called Operational Taxonomic Units (OTUs). After checking for potential chimeras using DECIPHER (Wright et al., 2012), taxonomic classification using the LCA-approach of SINA, and screening for PVC-associated genes, at least two distinct sequences, representing separate organisms, were identified for each, *Verrucomicrobia* and Planctomycetes. Neither of those sequences could be assigned to a currently cultivated species (Figures 3A,C) and were therefore considered novel. An overview of the total extracted and reconstructed 16S rRNA sequences, as well as their taxonomic annotation and relative abundances, is given in Supplementary Table 2.

In order to enable a similar phylogenetic placement of the processed metagenomic bins, a Multi Locus Sequence Analysis (MLSA) approach was employed (Figures 3B,D, Supplementary Figure 3). The unique core genome used for MLSA of different combinations of genomes can be deduced from the results of the ortholog detection given in Supplementary Tables 3, 4. Since the MLSA- and 16S rRNA based phylogenies were fully coherent with each other, the resulting phylogenetic information was used in combination with the respective abundance profiles to link 16S rRNA sequences with the most likely corresponding bins (Supplementary Table 5). The two obtained partial *Verrucomicrobial* bins, cluster within the *Verrucomicrobiales*, with bin 1 being more or less directly associated with the family *Rubritaleaceae* (closest sequenced relative: *Rubritalea marina* DSM 17716 with an MLSA identity of 79%), and bin 2 being positioned between the *Rubritaleaceae* and

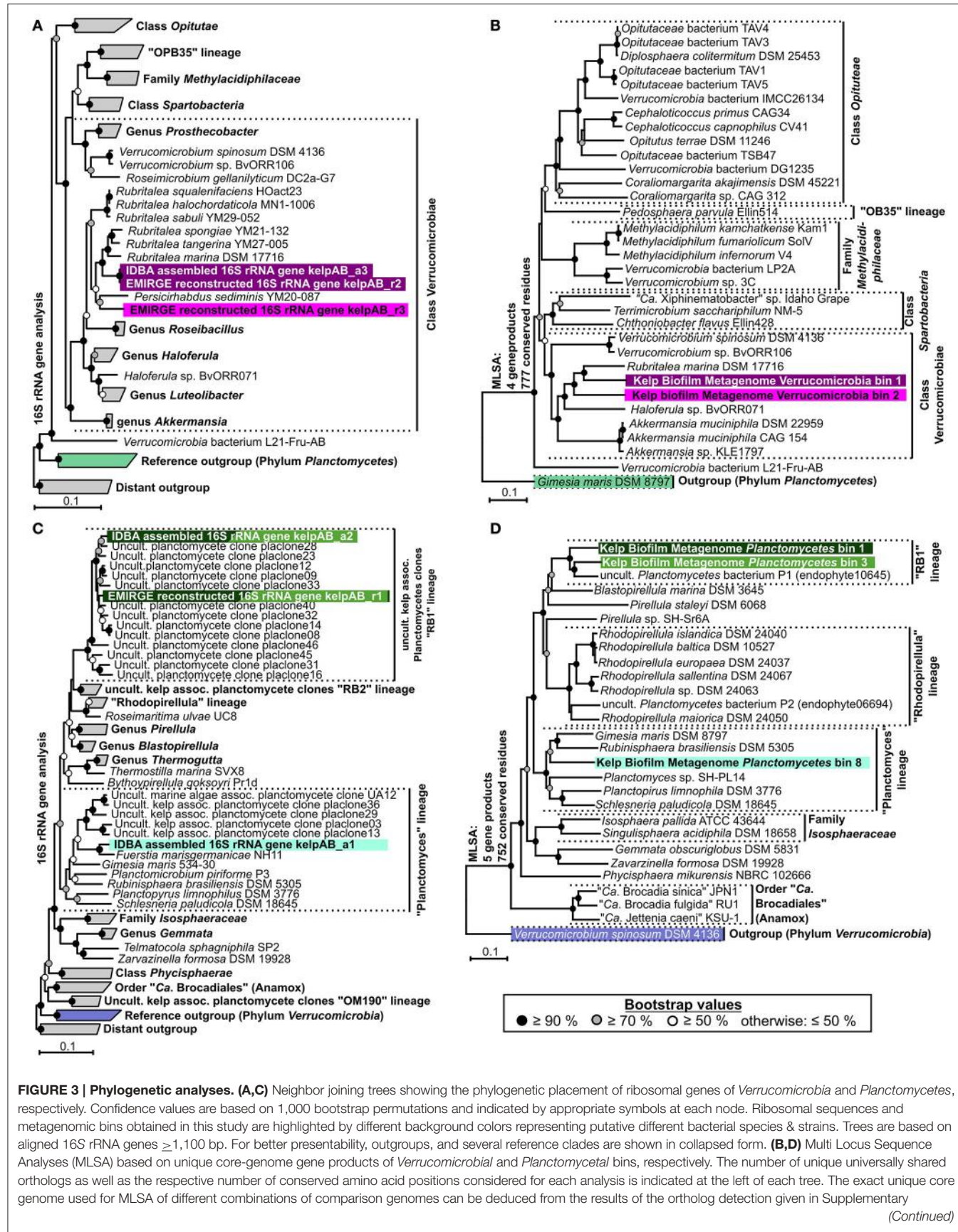


FIGURE 3 | Continued

Tables 3, 4. Due to the fragmented and incomplete nature of most metagenomic bins, relatively few universal orthologs could be considered in order to allow the simultaneous depiction of multiple representative bins. Higher phylogenetic resolutions can be found in the individual MLSA based phylogenies determined for each bin given in Supplementary Figure 3, which support the topologies depicted here. The MLSA results are in accordance with the observed 16S rRNA based phylogenies. Even though, due to strict binning parameters, none of the 16S rRNA genes depicted in (A,C) were included in any of the processed bins, each bin can be associated to a 16S rRNA gene based on phylogenetic placement as well as differential coverage information (Supplementary Table 5), as indicated by the respective background coloring (pink and purple = *Verrucomicrobia*, shades of green = *Planctomycetes*). Reference outgroups are marked in light violet (*Verrucomicrobia*) and light green (*Planctomycetes*)

the *Verrucomicrobiaceae* (closest sequenced relatives: *Rubritalea marina* DSM 17716 and *Haloferula* sp. BvORR071 with MLSA identities of 76 and 69%, respectively; **Figure 3B**). A highly similar topology is shown for the respective 16S phylogenies (**Figure 3A**), with the identical sequences KelpAB_r2 and KelpAB_a3 corresponding to bin 1 (closest relative: *Rubritalea marina* DSM 17716 with 95% identity) and KelpAB_r3 corresponding to bin 2 (closest relative *Persicirhabdus sediminis* YM20-087 with 93% identity, situated between *Rubritaleaceae* and *Verrucomicrobiaceae*).

The *Planctomycetal* bins 1–7 show on MLSA level the closest similarity to an uncultured Planctomycete genome P1 (MLSA identity values ranging from 73 to 79%), which was reconstructed from a red algae endophyte metagenome and is not to be confused with the *Rhodopirellula* sp. P1 (Bengtsson and Øvreås, 2010). Despite their relation, the observed phylogenetic distances imply that the here presented bins and the published uncultured endophyte Planctomycete genome P1 represent different taxa, at least on species and likely on genus level. This is supported by Average Nucleotide Identity (ANI) values of <90%, as determined using the Pyani package (<https://github.com/widdowquinn/pyani>), a value well below the commonly used species thresholds. Interestingly, the uncultured endophyte genome P1 contains a 195 bp long 16S rRNA gene fragment. While this fragment is unfortunately too short to be included in a comprehensive 16S rRNA based phylogenetic tree, BLAST comparisons revealed ~95% sequence identity to the kelp biofilm sequences KelpAB_r1 and KelpAB_a2, which are directly associated with the uncultured kelp associated “RB1” lineage. Therefore, and because of the similar tree topologies of MLSA and 16S rRNA based approaches (**Figures 3 C,D**), the aforementioned bins and the endophyte genome P1 could be unambiguously assigned to the “RB1” lineage, which has not previously been associated with genomic sequences to this day. This interesting lineage was previously shown to be the most abundant *Planctomycetal* group within biofilm communities on the surface of the kelp *Laminaria hyperborea*. Its members are highly diverse as indicated by the large number of closely related but distinct 16S rRNA gene sequences found in the respective clone libraries (**Figure 3C**). Assuming a similar presence of multiple closely related strains of the “RB1” lineage within the biofilm community of *M. pyrifera* would explain the high number and fragmented nature of the respective obtained *Planctomycetal* bins. Furthermore, this would explain the divergence between the “RB1” associated 16S rRNA genes obtained by the mapping based reconstruction approach (KelpAB_r1) and by direct assembly (KelpAB_a2). Such a divergence was not observed

for *Verrucomicrobia*, where the 16S rRNA gene sequence obtained by direct assembly (KelpAB_a3) was identical to its respective counterpart obtained by the mapping based approach (KelpAB_r2). As a consequence, all attempts to reconstruct further genomes of the “RB1” lineage or to obtain respective isolates should take potential strain heterogeneity into account and justifying the strict bin processing approach employed in this study (please see Materials and Methods).

To this day, no genomic sequence fragments or isolate cultures have been directly associated with the “RB1” lineage. The here presented *Planctomycetal* bins 1–7 represent multiple closely related strains of this lineage in various degrees of fragmentation and completeness (**Table 1**), providing an interesting glimpse into the “RB1” pan-genome. Of these bins, *Planctomycetal* bin 1 possessed the highest quality, with a presumed completeness of up to 84.11% or even >99% based on marker gene and tRNA counts, respectively. The degree of putative contamination, determined using standard checkM quality analyses workflows with Planctomycetes specific marker sets was ~2%. This is far below the average value for other published *Planctomycetal* bins, since equivalent analyses of Planctomycetes genomes frequently yield “contamination” values of more than 3% and up to 7% (Supplementary Table 6). That is why this bin can be considered “pure” to the greatest possible extent. A linear visualization of *Planctomycetal* bin 1 shows that the contained scaffolds possess orthologs to reference isolate Planctomycetes throughout the binned genome (Supplementary Figure 4), with the most orthologs found in the uncultured endophyte reference genome P1, confirming a low, if any, degree of contamination. Nonetheless, distinct genomic islands are also recognizable as short stretches with relatively few orthologs in reference genomes, illustrating the large potential for new genomic features of this lineage.

The presence of a “RB1” associated OTU was also confirmed by a similar, but different, sequence obtained by the mapping based 16S rRNA reconstruction approach (kelpAB_r1), showing 97% identity to KelpAB_a2 and 98% identity to RB1 associated clone “placlone40.” Members of the “RB1”-lineage have been previously shown to be abundant and highly diverse within plasmid clone libraries of kelp-associated communities (Bengtsson and Øvreås, 2010). This diversity may be reflected in the observed distinct clustering of the two “RB1”-associated 16S rRNA gene sequences (kelpAB_a2 & kelpAB_r1) obtained in this study using separate methods, indicating that they may actually be consensus sequences representing multiple diverse but closely related strains. Interestingly sequence kelpAB_a1 clusters more closely to

Fuerstia marisgermanicae NH11 (96% identity), a recently discovered novel *Planctomycetal* species, than to related plasmid clones obtained from other kelp-associated communities (Kohn et al., 2016).

In addition to the “RB1” associated bins, the low abundant and highly fragmented bin 8 as well as the corresponding 16S rRNA sequence KelpAB_a1, could be associated with the “planctomyces lineage.” This lineage contains a deep branching sub-group which clusters relatively close to, but nonetheless distinctly apart from several planctomycetes strains such as *Gimesia maris*. Interestingly, this deep-branching sub-group was also observed by Bengtsson and Øvreås (2010) to co-occur with the “RB1” lineage within kelp biofilm communities of *L. hyperborea* in relatively low abundance. However, the insights into the genomic potential of this sub-group are limited by the small size and low completeness of Planctomycete bin 8 (Table 1). Fortunately, the recently isolated strain *Fuerstera marisgermanica* (Kohn et al., 2016) proved to be not only associated with the aforementioned sub-group, but also most closely related to the here presented bin 8. Genome analyses of this species may provide more detailed insights into the potential role of this sub-group within marine biofilm communities.

All plancomycetal bins, with the exception of bin 8, contained genes encoding for flagellum synthesis. No such genes were identified in the *Verrucomicrobia* bins, which is in concordance with the non-motile lifestyle of their most closely related cultured representatives *Rubritalea marina* and *Persicirhabdus sediminis* (Scheuermayer et al., 2006; Yoon et al., 2008). Additional specifically noteworthy features identified in the PVC bins are listed in Supplementary Table 7.

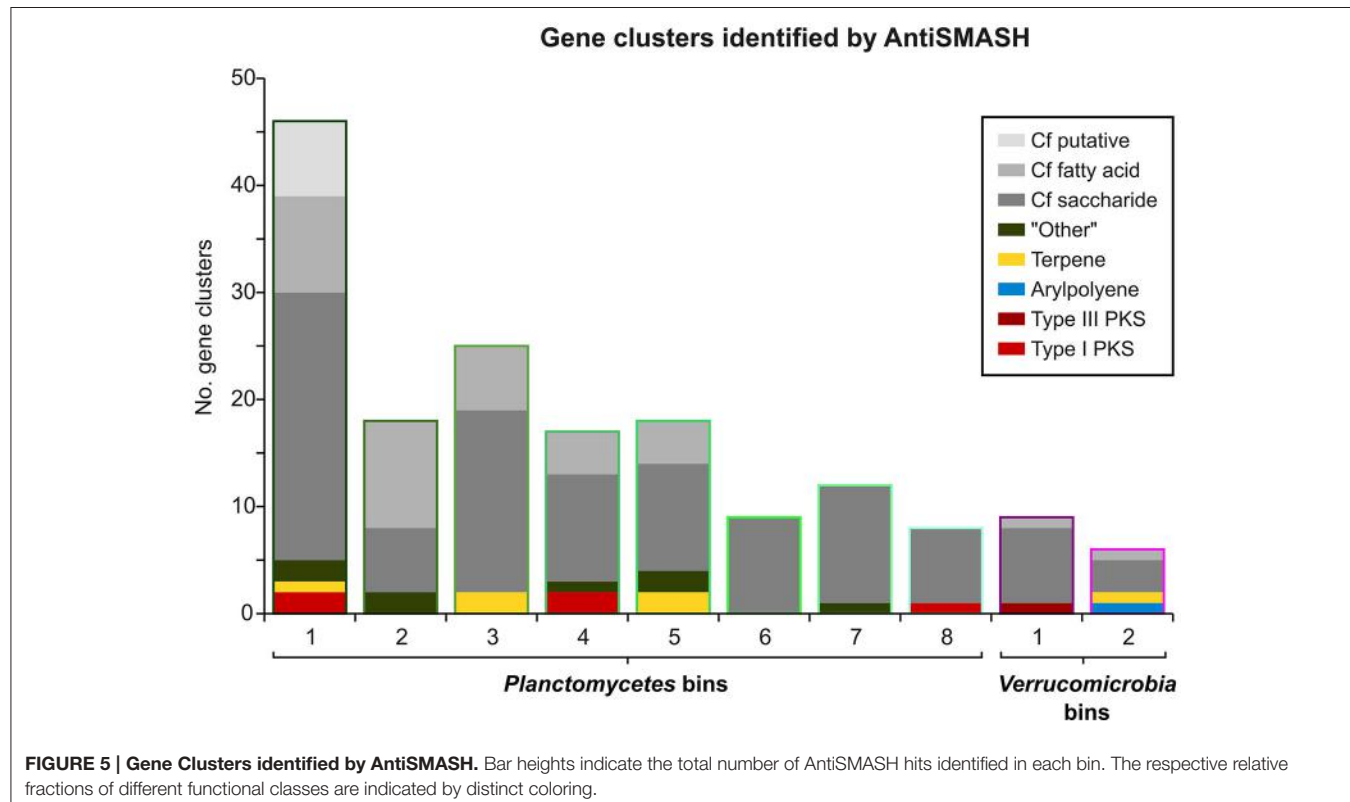
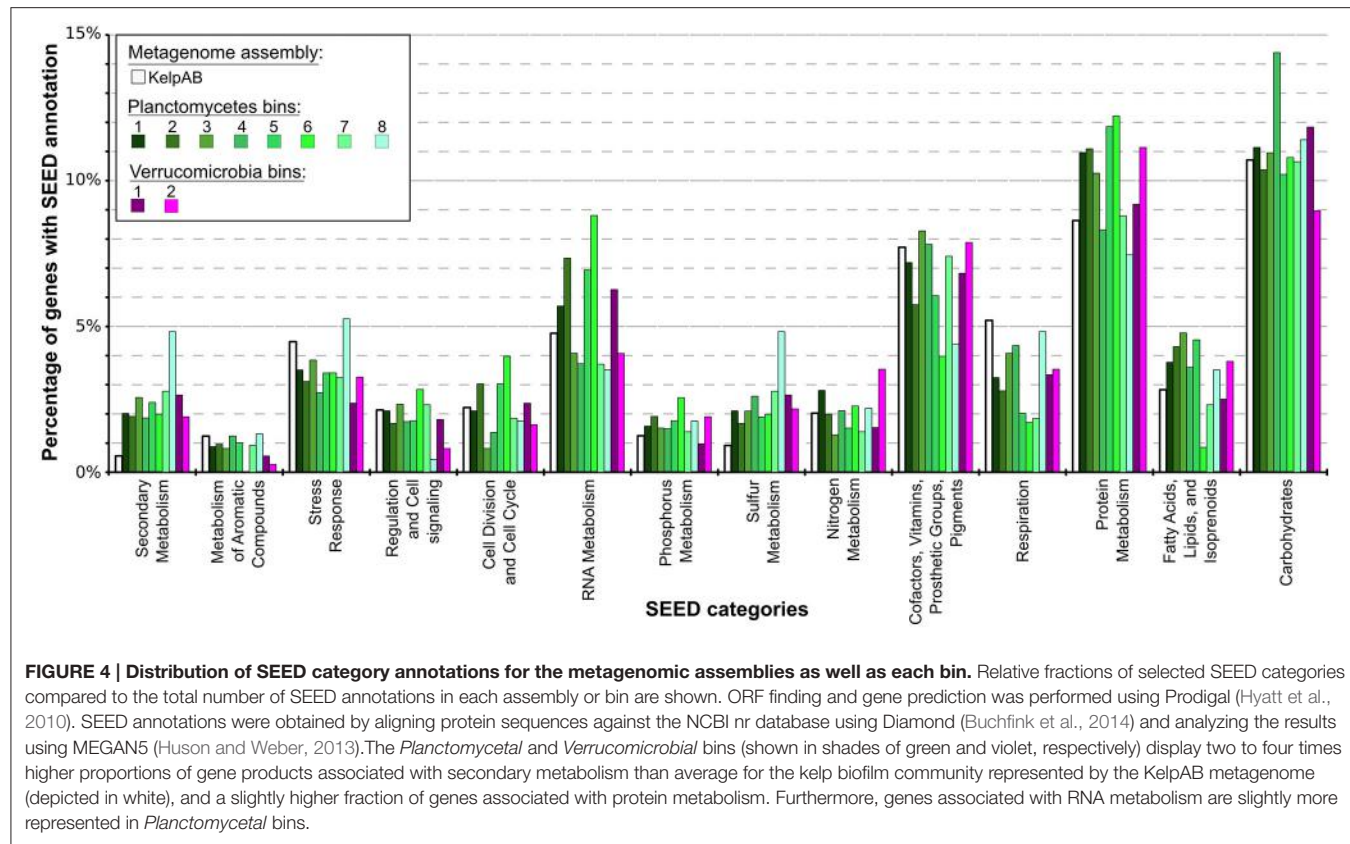
According to SEED annotations obtained via MEGAN5 analyses, a relatively high proportion of sulfur metabolism related genes was found in the *Planctomycetal* and *Verrucomicrobial* bins, which comprise a ~2–5 times higher fraction of the total SEED annotated genes compared to the total biofilm community (Figure 4; Supplementary Table 8). This observation is true for all of the processed PVC bins, including the almost-complete Planctomycetes bin 1, indicating that this is a general feature of the respective genomes and not biased by partial genome representation. The PVC-superphylum members might therefore represent the primary metabolizers of organic sulfur compounds within the kelp biofilm community. Such compounds are commonly produced in a large variety by marine macro algae (Sunda et al., 2002; Lage and Bondoso, 2014; Michel et al., 2006), and may therefore constitute key factors for the successful colonialization of, and adaptation to, algal surfaces. A high propensity for the utilization of sulfated glycopolymers has also been reported for several *Planctomycetes* and *Verrucomicrobia* cultures (Lage and Bondoso, 2011, 2012; Wegner et al., 2013; Spring et al., 2016). Furthermore, sulfated polysaccharides were the predominantly hydrolyzed glycopolymers during an unusual population spike of *Verrucomicrobia* observed at a Svalbard Fjord in 2008 (Cardman et al., 2014).

Other examples of nutrient scavenging which have been observed in different macroalgal associates include phosphorous

and nitrogen utilization (Egan et al., 2013). Although a slight increase of genes encoding for these categories can be observed for several bins, including the almost complete Planctomycetes bin 1, this increase far less distinct compared to the aforementioned sulfur metabolism and not coherent for all PVC bins. The same holds true for genes involved in fatty acid, lipid and isoprenoid metabolism, which may be relevant for host-microbe interactions due to the production of polyunsaturated fatty acids (PUFAs) and terpenes frequently observed in marine macroalgae (Potin et al., 2002). Therefore, while it may be hypothesized that the PVC-superphylum members are also involved in the metabolism of said nutrients and compounds in the kelp biofilm community, it is not conclusive whether they play a dominant role in this regard.

Genes encoding for respiration were found to be underrepresented in all of the PVC bins, indicating a relatively low metabolic activity. This might be contrasted by the comparatively high fraction of RNA metabolism related genes in several bins, which could be indicative for a complex regulatory network. These observations however do support the assumption that these genomes represent slow growing organisms, as frequently observed for PVC superphylum members.

Interestingly, an outstanding large relative fraction of the respective encoding genes in all of the processed bins are associated with secondary metabolism (Figure 4; Supplementary Table 8). This fraction is ~4–9 times higher in the *Planctomycetal* and *Verrucomicrobial* bins compared to the total kelp biofilm community and found evidence for a relatively high potential for secondary metabolite production in those species. Putative gene clusters were identified by AntiSMASH v.3 in all of the processed bins, including several potential Polyketide Synthase (PKS) clusters (Figure 5). PKSs are enzyme complexes or multi-domain enzymes which perform a stepwise biosynthesis of complex organic compounds, so-called polyketides, with varying pharmaceutical properties such as antibiotic activity (Jenke-Kodama et al., 2005). Nutrient rich habitats like kelp forests attract other –more rapidly- growing- heterotrophic bacteria that should be able to outcompete slow-growers. As *Verrucomicrobia* and *Planctomycetes* are both known to be relatively slowly growing organisms, secondary metabolites may likely serve as inhibitory agents against more rapidly growing competitors within the biofilm community. This would help explain the persistence and even frequent dominance of PVC superphylum members in kelp-associated communities, despite the constant danger of being out-competed by rapidly growing Proteobacteria. We therefore hypothesize that *Verrucomicrobia* and *Planctomycetes* are attracted by kelp through secretion of specific carbohydrates that trigger them to attach to the algal surface and to form biofilms. The kelp might then employ them as biofouling control, using their antimicrobial secondary metabolites to defeat other bacteria or eukaryotes. This would be in accordance with the low abundance but ubiquitous distribution of these species on marine algae, and shows that these phyla are very interesting for natural products production/pharmaceuticals. Only recently, *Planctomycetes* were demonstrated to produce small molecules with bioactivity



and their antibiotic effects were recently demonstrated (Jeske et al., 2013).

Although several studies have reported the discovery of new bioactive compounds from marine organisms and more than 15,000 structurally diverse bioactive compounds were isolated during the past 30 years (Hu et al., 2015), only two new classes of antibiotics have been brought to market during this period of time (Coates et al., 2011). In the post-genomic era one has come to realize that naturally occurring reservoirs of genetic diversity contain vast, untapped potential for production of biologically active chemical compounds that needs to be made available for society with the emerge of new technologies. The PVC superphylum is known for its biotechnological and medical relevance (Wagner and Horn, 2006) and a promising resource for natural products, however due to the relatively low representation of these phyla in public sequencing databases there are still may gaps to fill by e.g., specific isolation attempts or combinations of single cell (Rinke et al., 2013; Kaster et al., 2014) and metagenomics. Our study provides a first glimpse into this microbial dark matter by using an innovative binning approach to reconstruct genomes of low abundant species, shedding light

on Planctomycetes and *Verrucomicrobia* from biofilms of kelp algae.

AUTHOR CONTRIBUTIONS

AK and JV designed the experiments, performed the data analyses and wrote the paper. MF and PR performed the experiments. CJ collected the samples by scuba diving.

ACKNOWLEDGMENTS

We would like to thank Professor Alfred Spormann (Stanford University) and the staff of Hopkins Marine Station, especially Judy Thompson, for their generous help with the collection and shipment of the samples.

SUPPLEMENTARY MATERIAL

The Supplementary Material for this article can be found online at: <http://journal.frontiersin.org/article/10.3389/fmcb.2017.00472/full#supplementary-material>

REFERENCES

- Albertsen, M., Hugenholtz, P., Skarszewski, A., Nielsen, K. L., Tyson, G. W., and Nielsen, P. H. (2013). Genome sequences of rare, uncultured bacteria obtained by differential coverage binning of multiple metagenomes. *Nat. Biotechnol.* 31, 533–538. doi: 10.1038/nbt.2579
- Bankevich, A., Nurk, S., Antipov, D., Gurevich, A. A., Dvorkin, M., Kulikov, A. S., et al. (2012). SPAdes: a new genome assembly algorithm and its applications to single-cell sequencing. *J. Comput. Biol.* 19, 455–477. doi: 10.1089/cmb.2012.0021
- Bartram, A. K., Lynch, M. D., Stearns, J. C., Moreno-Hagelsieb, G., and Neufeld, J. D. (2011). Generation of multimillion-sequence 16S rRNA gene libraries from complex microbial communities by assembling paired-end illumina reads. *Appl. Environ. Microbiol.* 77, 3846–3852. doi: 10.1128/AEM.02772-10
- Bengtsson, M. M., and Øvreås, L. (2010). Planctomycetes dominate biofilms on surfaces of the kelp *Laminaria hyperborea*. *BMC Microbiol.* 10:261. doi: 10.1186/1471-2180-10-261
- Bengtsson, M. M., Sjøtun, K., and Øvreås, L. (2010). Seasonal dynamics of bacterial biofilms on the kelp *Laminaria hyperborea*. *Aquat. Microb. Ecol.* 60, 71–83. doi: 10.3354/ame01409
- Bengtsson, M. M., Sjøtun, K., Lanzén, A., and Øvreås, L. (2012). Bacterial diversity in relation to secondary production and succession on surfaces of the kelp *Laminaria hyperborea*. *ISME J.* 6, 2188–2198. doi: 10.1038/ismej.2012.67
- Bengtsson, M. M., Sjøtun, K., Storesund, J. E., and Øvreås, J. (2011). Utilization of kelp-derived carbon sources by kelp surface-associated bacteria. *Aquat. Microb. Ecol.* 62, 191–199. doi: 10.3354/ame01477
- Bolger, A. M., Lohse, M., and Usadel, B. (2014). Trimmomatic: a flexible trimmer for Illumina sequence data. *Bioinformatics* 30, 2114–2120. doi: 10.1093/bioinformatics/btu170
- Buchfink, B., Xie, C., and Huson, D. H. (2014). Fast and sensitive protein alignment using DIAMOND. *Nat. Methods* 12, 59–60. doi: 10.1038/nmeth.3176
- Cardman, Z., Arnosti, C., Durbin, A., Zier vogel, K., Cox, C., Steen, A., et al. (2014). *Verrucomicrobia* are candidates for polysaccharide-degrading bacterioplankton in an arctic fjord of Svalbard. *Appl. Environ. Microbiol.* 80, 3749–3756. doi: 10.1128/AEM.00899-14
- Castresana, J. (2000). Selection of conserved blocks from multiple alignments for their use in phylogenetic analysis. *Mol. Biol. Evol.* 17, 540–552. doi: 10.1093/oxfordjournals.molbev.a026334
- Christie-Oleza, J. A., Pi-a-Villalonga, J. M., Bosch, R., Nogales, B., and Armengaud, J. (2012). Comparative proteogenomics of twelve Roseobacter exoproteomes reveals different adaptive strategies among these marine bacteria. *Mol. Cell. Proteomics* 11:M111.013110. doi: 10.1074/mcp.M111.013110
- Coates, A. R., Halls, G., and Hu, Y. (2011). Novel classes of antibiotics or more of the same? *Br. J. Pharmacol.* 163, 184–194. doi: 10.1111/j.1476-5381.2011.01250.x
- Dayton, P. K. (1985). Ecology of kelp communities. *Annu. Rev. Ecol. Syst.* 16, 215–245. doi: 10.1146/annurev.es.16.110185.001243
- Dayton, P. K., and Tegner, M. J. (1984). Catastrophic storms, el nino, and patch stability in a southern California kelp community. *Science* 224, 283–285.
- Delille, D., and Perret, E. (1991). The influence of giant kelp *Macrocystis pyrifera* on the growth of subantarctic marine bacteria. *J. Exp. Mar. Biol. Ecol.* 153, 227–239. doi: 10.1016/0022-0981(91)90227-N
- Edgar, R. C. (2004). MUSCLE: multiple sequence alignment with high accuracy and high throughput. *Nucleic Acids Res.* 32, 1792–1797. doi: 10.1093/nar/gkh340
- Egan, S., Harder, T., Burke, C., Steinberg, P., Kjelleberg, S., and Thomas, T. (2013). The seaweed holobiont: understanding seaweed-bacteria interactions. *FEMS Microbiol. Rev.* 37, 462–476. doi: 10.1111/1574-6976.12011
- Estes, J. A., Danner, E. M., Doak, D. F., Konar, B., Springer, A. M., Steinberg, P. D., et al. (2004). Complex trophic interactions in kelp forest ecosystems. *Bull. Mar. Sci.* 74, 621–638.
- Ferrera, I., Massana, R., Balague, V., Pedros-Alio, C., Sanchez, O., and Mas, J. (2010). Evaluation of DNA extraction methods from complex phototrophic biofilms. *Biofouling* 26, 349–357. doi: 10.1080/08927011003605870
- Foster, M. S., Reed, D. C., Carr, M. H., Dayton, P. K., Malone, D. P., Pearse, J. S., et al. (2012). Kelp forests in California. *Smithson. Contrib. Mar. Sci.* 39, 115–132.
- Foster, M. S., and Schiel, D. R. (1985). *Ecology of Giant Kelp Forests in California: A Community Profile*. Moss Landing, CA: San Jose State University, Moss Landing Marine Labs.
- Fuerst, J. A. (ed.). (2013). *Planctomycetes: Cell Structure, Origins and Biology*. Totowa, NJ: Humana.
- Goedecke, F., Labes, A., Wiese, J., and Imhoff, J. F. (2010). Chemical interactions between marine macroalgae and bacteria. *Mar. Ecol. Prog. Ser.* 409, 267–299. doi: 10.3354/meps08607

- Graham, M. H. (2004). Effects of local deforestation on the diversity and structure of Southern California giant kelp forest food webs. *Ecosystems* 7, 341–357. doi: 10.1007/s10021-003-0245-6
- Graham, M. H., Kinlan, B. P., Druehl, L. D., Garske, L. E., and Banks, S. (2007). Deep-water kelp refugia as potential hotspots of tropical marine diversity and productivity. *Proc. Natl. Acad. Sci. U.S.A.* 104, 16576–16580. doi: 10.1073/pnas.0704778104
- Hahnke, S., Tindall, B. J., Schumann, P., Simon, M., and Brinkhoff, T. (2013). *Pelagimonas varians* gen. nov., sp. nov., isolated from the southern North Sea. *Int. J. Syst. Evol. Microbiol.* 63, 835–843. doi: 10.1099/ijss.0.040675-0
- Hollants, J., Leliaert, F., De Clerck, O., and Willems, A. (2013). What we can learn from sushi: a review on seaweed-bacterial associations. *FEMS Microbiol. Ecol.* 83, 1–16. doi: 10.1111/j.1574-6941.2012.01446.x
- Hu, Y., Chen, J., Hu, G., Yu, J., Zhu, X., Lin, Y., et al. (2015). Statistical research on the bioactivity of new marine natural products discovered during the 28 years from 1985 to 2012. *Mar. Drugs* 13, 202–221. doi: 10.3390/md13010202
- Huson, D. H., and Weber, N. (2013). Microbial community analysis using MEGAN. *Methods Enzymol.* 531, 465–485. doi: 10.1016/B978-0-12-407863-5.00021-6
- Hyatt, D., Chen, G.-L., Locascio, P. F., Land, M. L., Larimer, F. W., and Hauser, L. J. (2010). Prodigal: prokaryotic gene recognition and translation initiation site identification. *BMC Bioinformatics* 11:119. doi: 10.1186/1471-2105-11-119
- Jenke-Kodama, H., Sandmann, A., Müller, R., and Dittmann, E. (2005). Evolutionary Implications of bacterial polyketide synthases. *Mol. Biol. Evol.* 22, 2027–2039. doi: 10.1093/molbev/msi193
- Jeske, O., Jogler, M., Petersen, J., Sikorski, J., and Jogler, C. (2013). From genome mining to phenotypic microarrays: planctomycetes as source for novel bioactive molecules. *Antonie van Leeuwenhoek* 104, 551–567. doi: 10.1007/s10482-013-0007-1
- Kaster, A. K., Mayer-Blackwell, K., Pasarelli, B., and Spormann, A. M. (2014). Single cell genomic study of Dehalococcoidetes species from deep-sea sediments of the Peruvian Margin. *ISME J.* 8, 1831–1842. doi: 10.1038/ismej.2014.24
- Kohn, T., Heuer, A., Jogler, M., Vollmers, J., Boedeker, C., Bunk, B., et al. (2016). *Fuerstia marisgermaniae* gen. nov., sp. nov., an Unusual Member of the Phylum Planctomycetes from the German Wadden Sea. *Front. Microbiol.* 7:2079. doi: 10.3389/fmicb.2016.02079
- Lage, O. M., and Bondoso, J. (2011). Planctomycetes diversity associated with macroalgae. *FEMS Microbiol. Ecol.* 78, 366–375. doi: 10.1111/j.1574-6941.2011.01168.x
- Lage, O. M., and Bondoso, J. (2012). Bringing Planctomycetes into pure culture. *Front. Microbiol.* 3:405. doi: 10.3389/fmicb.2012.00405
- Lage, O. M., and Bondoso, J. (2014). Planctomycetes and macroalgae, a striking association. *Front. Microbiol.* 5:267. doi: 10.3389/fmicb.2014.00267
- Lagesen, K., Hallin, P., Rodland, E. A., Staerfeldt, H. H., Rognes, T., and Ussery, D. W. (2007). RNAmmer: consistent and rapid annotation of ribosomal RNA genes. *Nucleic Acids Res.* 35, 3100–3108. doi: 10.1093/nar/gkm160
- Langmead, B., and Salzberg, S. L. (2012). Fast gapped-read alignment with Bowtie 2. *Nat. Methods* 9, 357–359. doi: 10.1038/nmeth.1923
- Lasken, R. S. (2009). Genomic DNA amplification by the multiple displacement amplification (MDA) method. *Biochem. Soc. Trans.* 37, 450–453. doi: 10.1042/BST0370450
- Lechner, M., Fineiss, S., Steiner, L., Marz, M., Stadler, P. F., and Prohaska, S. J. (2011). Proteinortho: detection of (co-)orthologs in large-scale analysis. *BMC Bioinformatics* 12, 124–124. doi: 10.1186/1471-2105-12-124
- Linley, E. A. S., and Field, J. G. (1982). The nature and ecological significance of bacterial aggregation in a nearshore upwelling ecosystem. *Estuarine Coastal Shelf Sci.* 14, 1–11. doi: 10.1016/S0302-3524(82)80063-7
- Longford, S. R., Tujula, N. A., Crocetti, G. R., Holmes, A. J., Holmstrom, C., Kjelleberg, S., et al. (2007). Comparisons of diversity of bacterial communities associated with three sessile marine eukaryotes. *Aquat. Microb. Ecol.* 48, 217–229. doi: 10.3354/ame048217
- Ludwig, W., Strunk, O., Westram, R., Richter, L., Meier, H., Yadukumar, et al. (2004). ARB: a software environment for sequence data. *Nucleic Acids Res.* 32, 1363–1371. doi: 10.1093/nar/gkh293
- Magoč, T., and Salzberg, S. L. (2011). FLASH: fast length adjustment of short reads to improve genome assemblies. *Bioinformatics* 27, 2957–2963. doi: 10.1093/bioinformatics/btr507
- Michel, G., Nyval-Collen, P., Barbeyron, T., Czjzek, M., and Helbert, W. (2006). Bioconversion of red seaweed galactans: a focus on bacterial agarases and carrageenases. *Appl. Microbiol. Biotechnol.* 71, 23–33. doi: 10.1007/s00253-006-0377-7
- Michelou, V. K., Caporaso, J. G., Knight, R., and Palumbi, S. R. (2013). The ecology of microbial communities associated with *Macrocystis pyrifera*. *PLoS ONE* 8:e67480. doi: 10.1371/annotation/48e29578-a073-42e7-bca4-2f96a5998374
- Miller, C. S., Baker, B. J., Thomas, B. C., Singer, S. W., Banfield, J. F., Pace, N. R., et al. (2011). EMIRGE: reconstruction of full-length ribosomal genes from microbial community short read sequencing data. *Genome Biol.* 12:R44. doi: 10.1186/gb-2011-12-5-r44
- Muyzer, G., de Waal, E. C., and Uitterlinden, A. G. (1993). Profiling of complex microbial populations by denaturing gradient gel electrophoresis analysis of polymerase chain reaction-amplified genes coding for 16S rRNA. *Appl. Environ. Microbiol.* 59, 695–700.
- Ondov, B. D., Bergman, N. H., and Phillippy, A. M. (2011). Interactive metagenomic visualization in a Web browser. *BMC Bioinformatics* 12, 385–385. doi: 10.1186/1471-2105-12-385
- Parks, D. H., Imelfort, M., Skennerton, C. T., Hugenholz, P., and Tyson, G. W. (2015). CheckM: assessing the quality of microbial genomes recovered from isolates, single cells, and metagenomes. *Genome Res.* 25, 1043–1055. doi: 10.1101/gr.186072.114
- Peng, Y., Leung, H. C. M., Yiu, S. M., and Chin, F. Y. L. (2012). IDBA-UD: a de novo assembler for single-cell and metagenomic sequencing data with highly uneven depth. *Bioinformatics* 28, 1420–1428. doi: 10.1093/bioinformatics/bts174
- Potin, P., Bouarab, K., Salaün, J.-P., Pohnert, G., and Kloareg, B. (2002). Biotic interactions of marine algae. *Curr. Opin. Plant Biol.* 5, 308–317. doi: 10.1016/S1369-5266(02)00273-X
- Pruess, E., Peplies, J., and Glöckner, F. O. (2012). SINA: accurate high-throughput multiple sequence alignment of ribosomal RNA genes. *Bioinformatics* 28, 1823–1829. doi: 10.1093/bioinformatics/bts252
- Quast, C., Pruesse, E., Yilmaz, P., Gerken, J., Schweer, T., Yarza, P., et al. (2013). The SILVA ribosomal RNA gene database project: improved data processing and web-based tools. *Nucleic Acids Res.* 41, D590–D596. doi: 10.1093/nar/gks1219
- Rao, D., Webb, J. S., Holmstrom, C., Case, R., Low, A., Steinberg, P., et al. (2007). Low densities of epiphytic bacteria from the marine alga *Ulva australis* inhibit settlement of fouling organisms. *Appl. Environ. Microbiol.* 73, 7844–7852. doi: 10.1128/AEM.01543-07
- Reis, A. M. M., Araújo S. D. Jr., Moura, R. L., Francini-Filho, R. B., Pappas G. Jr., Coelho, A. M. A., et al. (2009). Bacterial diversity associated with the Brazilian endemic reef coral *Mussismilia brasiliensis*. *J. Appl. Microbiol.* 106, 1378–1387. doi: 10.1111/j.1365-2672.2008.04106.x
- Rinke, C., Schwientek, P., Sczyrba, A., Ivanova, N. N., Anderson, I. J., Cheng, J.-F., et al. (2013). Insights into the phylogeny and coding potential of microbial dark matter. *Nature* 499, 431–437. doi: 10.1038/nature12352
- Sangwan, N., Xia, F., Gilbert, J. A., Ramette, A., Tiedje, J. M., Tyson, G. W., et al. (2016). Recovering complete and draft population genomes from metagenome datasets. *Microbiome* 4:8. doi: 10.1186/s40168-016-0154-5
- Scheuermayer, M., Gulder, T. A. M., Bringmann, G., and Hentschel, U. (2006). *Rubritalea marina* gen. nov., sp. nov., a marine representative of the phylum “Verrucomicrobia,” isolated from a sponge (Porifera). *Int. J. Syst. Evol. Microbiol.* 56, 2119–2124. doi: 10.1007/ijss.0.64360-0
- Seemann, T. (2014). Prokka: rapid prokaryotic genome annotation. *Bioinformatics* 30, 2068–2069. doi: 10.1093/bioinformatics/btu153
- Spring, S., Bunk, B., Spröer, C., Schumann, P., Rohde, M., Tindall, B. J., et al. (2016). Characterization of the first cultured representative of *Verrucomicrobia* subdivision 5 indicates the proposal of a novel phylum. *ISME J.* 10, 2801–2816. doi: 10.1038/ismej.2016.204
- Steneck, R., Graham, M. H., Bourque, B. J., Corbett, D., Erlanson, J. M., Estes, J. A., et al. (2002). Kelp forest ecosystems: biodiversity, stability, resilience and future. *Environ. Conserv.* 29, 436–459 doi: 10.1017/s0376892902000322
- Sunda, W., Kieber, D. J., Kiene, R. P., and Huntsman, S. (2002). An antioxidant function for DMSP and DMS in marine algae. *Nature* 418, 317–320. doi: 10.1038/nature00851
- Taylor, M. W., Schupp, P. J., Dahllöf, I., Kjelleberg, S., and Steinberg, P. D. (2004). Host specificity in marine sponge-associated bacteria, and potential implications for marine microbial diversity. *Environ. Microbiol.* 6, 121–130. doi: 10.1046/j.1462-2920.2003.00545.x

- Wagner, M., and Horn, M. (2006). The Planctomycetes, *Verrucomicrobia*, Chlamydiae and sister phyla comprise a superphylum with biotechnological and medical relevance. *Curr. Opin. Biotechnol.* 17, 241–249. doi: 10.1016/j.copbio.2006.05.005
- Weber, T., Blin, K., Duddela, S., Krug, D., Kim, H. U., Brucolieri, R., et al. (2015). antiSMASH 3.0—a comprehensive resource for the genome mining of biosynthetic gene clusters. *Nucleic Acids Res.* 43, W237–W243. doi: 10.1093/nar/gkv437
- Wegner, C. E., Richter-Heitmann, T., Klindworth, A., Klockow, C., Richter, M., Achstetter, T., et al. (2013). Expression of sulfatases in *Rhodopirellula baltica* and the diversity of sulfatases in the genus Rhodopirellula. *Mar. Genomics* 9, 51–61. doi: 10.1016/j.margen.2012.12.001
- Wright, E. S., Yilmaz, L. S., and Noguera, D. R. (2012). DECIPHER, a search-based approach to chimera identification for 16S rRNA sequences. *Appl. Environ. Microbiol.* 78, 717–725. doi: 10.1128/AEM.06516-11
- Wu, Y. W., Simmons, B. A., and Singer, S. W. (2016). MaxBin 2.0: an automated binning algorithm to recover genomes from multiple metagenomic datasets. *Bioinformatics* 32, 605–607. doi: 10.1093/bioinformatics/btv638
- Yilmaz, P., Parfrey, L. W., Yarza, P., Gerken, J., Pruesse, E., Quast, C., et al. (2014). The SILVA and “All-species Living Tree Project (LTP)” taxonomic frameworks. *Nucleic Acids Res.* 42, D643–D648. doi: 10.1093/nar/gkt1209
- Yoon, J., Matsuo, Y., Adachi, K., Nozawa, M., Matsuda, S., Kasai, H., et al. (2008). Description of *Persicirhabdus sediminis* gen. nov., sp. nov., *Roseibacillus ishitakijimensis* gen. nov., sp. nov., *Roseibacillus ponti* sp. nov., *Roseibacillus persicus* sp. nov., *Luteolibacter pohnpeiensis* gen. nov., sp. nov. and *Luteolibacter algaee* sp. no. *Int. J. Syst. Evol. Microbiol.* 58, 998–1007. doi: 10.1099/ijss.0.65520-0
- Zheng, L., Han, X., Chen, H., Lin, W., and Yan, X. (2005). Marine bacteria associated with marine macroorganisms: the potential antimicrobial resources. *Ann. Microbiol.* 55, 119–124.

Conflict of Interest Statement: The authors declare that the research was conducted in the absence of any commercial or financial relationships that could be construed as a potential conflict of interest.

Copyright © 2017 Vollmers, Frentrup, Rast, Jogler and Kaster. This is an open-access article distributed under the terms of the Creative Commons Attribution License (CC BY). The use, distribution or reproduction in other forums is permitted, provided the original author(s) or licensor are credited and that the original publication in this journal is cited, in accordance with accepted academic practice. No use, distribution or reproduction is permitted which does not comply with these terms.



Developing Techniques for the Utilization of Planctomycetes As Producers of Bioactive Molecules

Olga Jeske¹, Frank Surup^{2,3}, Marcel Ketteni β ¹, Patrick Rast¹, Birthe Förster^{2,3}, Mareike Jogler¹, Joachim Wink² and Christian Jogler^{1*}

¹ Department of Microbial Cell Biology and Genetics, Leibniz Institute DSMZ, Braunschweig, Germany, ² Department of Microbial Drugs, Helmholtz Centre for Infection Research, Braunschweig, Germany, ³ German Centre for Infection Research Association, Partner Site Hannover-Braunschweig, Braunschweig, Germany

OPEN ACCESS

Edited by:

Damien Paul Devos,
Centro Andaluz de Biología del Desarrollo and University of Pablo Olavide, Sevilla, Spain

Reviewed by:

Marc Strous,
University of Calgary, Canada
Olga Lage,
University of Porto, Portugal

*Correspondence:

Christian Jogler
christian@jogler.de

Specialty section:

This article was submitted to
Evolutionary and Genomic Microbiology,
a section of the journal
Frontiers in Microbiology

Received: 20 April 2016

Accepted: 26 July 2016

Published: 19 August 2016

Citation:

Jeske O, Surup F, Ketteni β M, Rast P, Förster B, Jogler M, Wink J and Jogler C (2016) Developing Techniques for the Utilization of Planctomycetes As Producers of Bioactive Molecules. *Front. Microbiol.* 7:1242.
doi: 10.3389/fmicb.2016.01242

Planctomycetes are conspicuous, ubiquitous, environmentally important bacteria. They can attach to various surfaces in aquatic habitats and form biofilms. Their unique FtsZ-independent budding cell division mechanism is associated with slow growth and doubling times from 6 h up to 1 month. Despite this putative disadvantage in the struggle to colonize surfaces, Planctomycetes are frequently associated with aquatic phototrophic organisms such as diatoms, cyanobacteria or kelp, whereby Planctomycetes can account for up to 50% of the biofilm-forming bacterial population. Consequently, Planctomycetes were postulated to play an important role in carbon utilization, for example as scavengers after phototrophic blooms. However, given their observed slow growth, such findings are surprising since other faster-growing heterotrophs tend to colonize similar ecological niches. Accordingly, Planctomycetes were suspected to produce antibiotics for habitat protection in response to the attachment on phototrophs. Recently, we demonstrated their genomic potential to produce non-ribosomal peptides, polyketides, bacteriocins, and terpenoids that might have antibiotic activities. In this study, we describe the development of a pipeline that consists of tools and procedures to cultivate Planctomycetes for the production of antimicrobial compounds in a chemically defined medium and a procedure to chemically mimic their interaction with other organisms such as for example cyanobacteria. We evaluated and adjusted screening assays to enable the hunt for planctomycetal antibiotics. As proof of principle, we demonstrate antimicrobial activities of planctomycetal extracts from *Planctopirus limnophila* DSM 3776, *Rhodopirellula baltica* DSM 10527, and the recently isolated strain Pan216. By combining UV/Vis and high resolution mass spectrometry data from high-performance liquid chromatography fractionations with growth inhibition of indicator strains, we were able to assign the antibiotic activity to candidate peaks related to planctomycetal antimicrobial compounds. The MS analysis points toward the production of novel bioactive molecules with novel structures. Consequently, we developed a large scale cultivation procedure to allow future structural elucidation of such compounds. Our findings might have implications for the discovery of novel antibiotics as Planctomycetes represent a yet untapped resource that could be developed by employing the tools and methods described in this study.

Keywords: Planctomycetes, secondary metabolites, screening, antibiotics, natural products, *Planctopirus limnophila*, *Rhodopirellula baltica*

INTRODUCTION

Antibiotics are mostly small molecules with antimicrobial activity produced by nearly all sorts of living things. They revolutionized treatment of infectious diseases, saving countless lives. The ability to produce such active molecules – mostly as secondary metabolites – is unevenly distributed among different species (Berdy, 2005). In the kingdom of bacteria, Actinomycetes are the best studied producers, followed by Myxobacteria, Cyanobacteria and certain *Bacillus*- and *Pseudomonas* strains. In total about 13,800 ‘active’ compounds of bacterial origin are known (Berdy, 2005). However, these ‘usual suspects’ in terms of antibiotic production have been heavily screened in the past and the discovery of novel lead structures decreased, while rediscovery rates of known compounds increased (Cooper and Shlaes, 2011). Consequently, only four new classes of antibiotics have been brought to market in the past four decades (Cooper and Shlaes, 2011). This falls far short of demand and only 74 years after the first treatment with ‘natural’ antibiotics, we again face the specter of incurable bacterial infections, now due to multidrug resistant pathogens (Cooper and Shlaes, 2011). To prevent the post-antibiotic era from coming true, the discovery of novel antibiotic structures is key (Fowler et al., 2014). The chances to discover such structures correlate among other factors directly with the phylogenetic distance between the microorganism under study and the already known producers (Müller and Wink, 2014). Thus, phylogenetically distinct bacterial lineages might represent a valuable source for novel secondary metabolites. For instance, the candidate phylum ‘Tectomicrobia’ that dwells in association with a marine sponge was recently found to comprise a distinct and promising metabolic repertoire (Wilson et al., 2014). Besides such phylogenetic aspects, most potent antibiotic producers are characterized by large genomes with often more than 8 MB and complex life styles, involving for example differentiation processes (Müller and Wink, 2014). Employing these criteria, entire bacteria phyla could be judged as putative ‘talented’ producers if basic knowledge about their ecology, cell biology and genomic architecture is available.

Thus, we screened the literature with a focus on little studied ‘conspicuous’ bacterial phyla that might represent putative ‘talented’ producers and identified Planctomycetes as candidates. Firstly, these ubiquitous and environmentally important bacteria possess large genomes (Glöckner et al., 2003; Jeske et al., 2013). Secondly, the planctomycetal cell biology is remarkable and was speculated to parallel eukaryotic cells in some aspects (Fuerst and Sagulenko, 2011). While some of these findings, such as the lack of peptidoglycan cell walls have been recently challenged (Jeske et al., 2015; van Teeseling et al., 2015), other traits like their lifestyle switch after cell division, makes them unique among bacteria. Planctomycetes divide mostly through polar budding rather than binary fission, without employing the otherwise universal bacterial division protein FtsZ (Tekniepe et al., 1981; Pilhofer et al., 2008; Lee et al., 2009; Jogler et al., 2012). In the model organism *Planctopirus limnophila* for example, cell division is further coupled to a lifestyle switch, since only sessile stalked mother cells can divide. Flagellated, planktonic daughter cells need to develop into stalked, sessile

cells prior to division (Gade et al., 2005; Jogler et al., 2011; Jogler and Jogler, 2013). Attached Planctomycetes can form dense biofilms, preferably on the surface of blooming diatoms (Morris et al., 2006; Pizzetti et al., 2011a) and they represent up to 50% of the bacterial community on *Laminaria hyperborea* (Bengtsson and Øvreås, 2010). Given the slow growth of Planctomycetes under favorable laboratory conditions, some species have doubling times of up to 1 month (Strous et al., 1998), their abundance in such embattled carbon rich habitats in nature, in contrast to the largely oligotrophic surrounding water, appears counterintuitive (Lage and Bondoso, 2014). Most other heterotrophs that dwell in such ecological niches divide much faster (for example 1.2–6.3 h for *Roseobacter* sp., Christie-Oleza et al., 2012) and should outcompete Planctomycetes. However, the phototroph–planctomycetal allelopathic interactions might involve the production of various secondary metabolites that might exhibit antimicrobial activity (defense against other, faster growing, heterotrophic bacteria) or algicidal (to destroy algae, diatoms or cyanobacteria for scavenging). The latter is supported by a positive correlation of planctomycetal abundance with chlorophyll a concentrations, pointing toward remineralization of algal biomass after blooming events through Planctomycetes (Pizzetti et al., 2011b).

Planctomycetes were found to possess secondary metabolite gene clusters employing genome mining, targeting non-ribosomal peptide synthetases (NRPSs) and polyketide synthases (PKSs) encoding genes (Donadio et al., 2007). In the same year, planctomycetal type I polyketide keto-synthase domains were identified in two coastal Antarctic sediments (Zhao et al., 2008). Only recently, we followed a holistic approach and combined comprehensive genome mining with physiological studies to improve our understanding of the planctomycetal potential to degrade algal polysaccharides and to produce secondary metabolites (Jeske et al., 2013). We further supported the hypothesis of allelopathic interactions between Planctomycetes and phototrophs and found, from a genomic perspective, Planctomycetes to be ‘talented’ producers.

In this study we employed chemical assays with planctomycetal crude extracts and biological screening methods for live visualization to prove the planctomycetal production of molecules with antibiotic activity. We further developed the entire set of tools ranging from cultivating marine and limnic Planctomycetes in chemical defined media within process-controlled bioreactors, to the preparation of planctomycetal extracts, their chromatographic separation, fractionation and biological screening. Here, we provide the starting point for the in depth investigation of novel planctomycetal antibiotics.

MATERIALS AND METHODS

General Cultivation of Microorganisms

In this study, the novel chemically defined Maintain Medium 1 (MM1) was developed for *P. limnophila* DSM 3776. MM1 consists of artificial freshwater (10 µM NH₄Cl, 10 µM KH₂PO₄, 100 µM KNO₃, 200 µM MgSO₄ 7 H₂O, 100 µM CaCl₂ 2 H₂O, 250 µM CaCO₃, and 300 µM NaHCO₃), that was supplemented

with 20 ml/l mineral salts solution and 5 ml/l vitamin solution (double concentrated) and buffered with either 10 mM HEPES or 100 mM sodium phosphate buffer at pH 7.2. While HEPES was added before autoclaving, the sodium phosphate buffer ingredients (200 mM Na₂HPO₄ 7 H₂O; 200 mM Na₂HPO₄ 7 H₂O) were separately autoclaved and added afterward (28 ml/l of mono salt solution and 72 ml/l di-salt solution). Mineral salt solution and vitamin solution were prepared according to DSMZ medium 621¹. The metal salts for the mineral salt solution consisted of 250 mg/l Na-EDTA, 1095 mg/l ZnSO₄ 7 H₂O, 500 mg/l FeSO₄ 7 H₂O, 154 mg/l MnSO₄ H₂O, 39.5 mg/l CuSO₄ 7 H₂O, 20.3 mg/l CoCl₂ 6 H₂O, 17.7 mg/l Na₂B₄O₇ 10 H₂O of which 50 ml were added per liter of mineral salt solution. To allow growth in MM1, 10 ml/l sterile filtered carbon source (2.5% glucose solution or 5% N-acetyl-D-glucosamine (NAG) solution) was added.

For *Rhodopirellula baltica* SH1 DSM 10527, the chemically defined Maintain Medium 2 (MM2) was developed in this study. MM2 is composed of 250 ml/l 2x artificial sea water (46.94 g/l NaCl, 7.84 g/l Na₂SO₄, 21.28 g/l MgCl₂ 6 H₂O, 2.86 g/l CaCl₂ 2 H₂O, 0.384 g/l NaHCO₃, 1.384 g/l KCl, 0.192 g/l KBr, 0.052 g/l H₃BO₃, 0.08 g/l SrCl₂ 6 H₂O, and 0.006 g/l NaF) supplemented with 5 ml/l 1 M Tris/HCl pH 7.5, 20 and 5 ml/l vitamin solution (double concentrated, added after autoclaving) while buffered at pH 7.5. To allow growth in MM2, 40 ml/l sterile filtered carbon source (2.5% glucose solution or 5% NAG) was added.

For strain Pan216 the novel M1H NAG ASW culture broth was developed in this study. It is composed of 250 ml/l 2x artificial sea water (46.94 g/l NaCl, 7.84 g/l Na₂SO₄, 21.28 g/l MgCl₂ 6 H₂O, 2.86 g/l CaCl₂ 2 H₂O, 0.384 g/l NaHCO₃, 1.384 g/l KCl, 0.192 g/l KBr, 0.052 g/l H₃BO₃, 0.08 g/l SrCl₂ 6 H₂O, and 0.006 g/l NaF), supplemented with 0.25 g/l peptone, 0.25 g/l yeast extract, 20 ml/l mineral salts solution, 20 ml/l 5% (w/v) NAG solution, 10 ml/l 2.5% (w/v) glucose and 5 ml/l vitamin solution (double concentrated), 1 ml/l trace element solution [1500 mg/l N(CH₂COONa)₃ H₂O, 500 mg/l MnSO₄ H₂O, 100 mg/l FeSO₄ 7H₂O, 100 mg/l Co(NO₃)₂ 6H₂O, 100 mg/l ZnCl₂, 50 mg/l NiCl₂ 6H₂O, 50 mg/l H₂SeO₃, 10 mg/l CuSO₄ 5H₂O, 10 mg/l AlK(SO₄)₂ 12H₂O, 10 mg/l H₃Bo₃, 10 mg/l NaMoO₄ 2H₂O, 10 mg/l Na₂WO₄ 2H₂O] and buffered with 10 mM HEPES at pH 8.0.

All strains were cultivated at 28°C in their respective culture broth with slight agitation (80 rpm).

Indicator strains were cultured according to DSMZ cultivation recommendations².

Phylogeny of Strain Pan216

Pan216 was identified by 16S rRNA gene sequencing after amplification with the modified universal primers 8f (5'-AGA GTT TGA TCM TGG CTC AG-3') and 1492r (5'-GGY TAC CTT GTT ACG ACT T-3'; Lane, 1991). PCR reactions were performed directly on single colonies or liquid cultures using the *Taq* DNA Polymerase (Qiagen) with one reaction of 25 µl containing 11 µl PCR-grade H₂O, 2.5 µl 10x CoralLoad buffer, 2.5 µl Q-Solution,

0.5 µl dNTPs (10 mM each), 1 µl sterile bovine serum albumin solution (20 mg/ml), 0.5 µl MgCl₂ solution (25 mM), 0.125 µl *Taq*-Polymerase (1 U/µl) and 1 µl of each primer (10 pmol). The employed protocol consisted of two steps, the first step with an initial denaturation at 94°C, 5 min, 10 cycles of denaturation at 94°C, 30 s, annealing at 59°C, 30 s, elongation at 72°C, 1 min, followed by the second step with 20 cycles denaturation at 94°C, 30 s, annealing at 54°C, 30 s, elongation at 72°C, 1 min, and a final elongation step at 72°C, 7 min. All PCRs were carried out in an Applied Biosystems® Veriti® thermal cycler (Thermo Fisher Scientific) and PCR products were stored at 4°C until Sanger-sequencing.

Near full length 16S sequences were generated by assembly of the resulting sequences with the ContigExpress application of the Vector NTI® Advance 10 software (Thermo Fisher Scientific).

Alignments of near full length 16S rRNA sequences were performed using the SINA web aligner (Pruesse et al., 2012), corrected manually and used for phylogenetic tree reconstruction (**Supplementary Figure S1**). Tree reconstruction was performed with the ARB software package (Ludwig et al., 2004) using the Maximum likelihood RAxML module and rate distribution model GTR GAMMA running the rapid bootstrap analysis algorithm, the Neighbor Joining tool with Felsenstein correction for DNA and Maximum Parsimony method employing the Phylib DNAPARS module. Bootstrap values for all three methods were computed with 1,000 resamplings including the *Escherichia coli* 16S rRNA gene positions 101-1438. The analysis involved a total of 37 nucleotide sequences of described type strains and outgroup strains (gray box; compare Supplementary Table S2).

Growth Measurement of Planctomycetes

To measure growth of *P. limnophila* in the different cultivation media (**Figure 1A**), 250 ml baffled flasks with 70 ml respective growth medium were inoculated with 10 ml pre-culture, which were washed twice with MM1 prior inoculation. Likewise, *R. baltica* and Pan216 were incubated with different carbon sources (**Figures 1B,C**) and inoculated with a pre-culture washed twice with MM2. Afterward, the respective carbon source was supplemented (4 ml of 2.5% glucose, 4 ml of 2.5% dextran, or 2 ml of 5% NAG). As control *P. limnophila* was grown in M1 and *R. baltica* in M2 medium (Jeske et al., 2013) while Pan216 was grown in M1H NAG ASW medium. Individual growth conditions were analyzed in three biological replicates. The optical density of the culture was measured every 8 and 16 h at 600 nm with a spectrophotometer.

Cultivation of Planctomycetes in a Bioreactor

The respective growth medium was autoclaved in a 368 l chamber autoclave (BeliMed) within the 10 l culture vessel of the bioreactor (UniVessel, Sartorius). After sterile supplementation of the respective vitamins and carbon source the reactor was incubated for 2 days to exclude contaminations. For sterile inoculation, a planctomycetal pre-culture (0.1 volume) was transferred via a culture bottle into the 10 l culture vessel of the BIOSTAT®B system.

¹<https://www.dsmz.de/>

²<https://www.dsmz.de/catalogues/dzif-sammlung-der-dsmz/indikatorstaemme-fuer-wirkstoffforschung.html>.

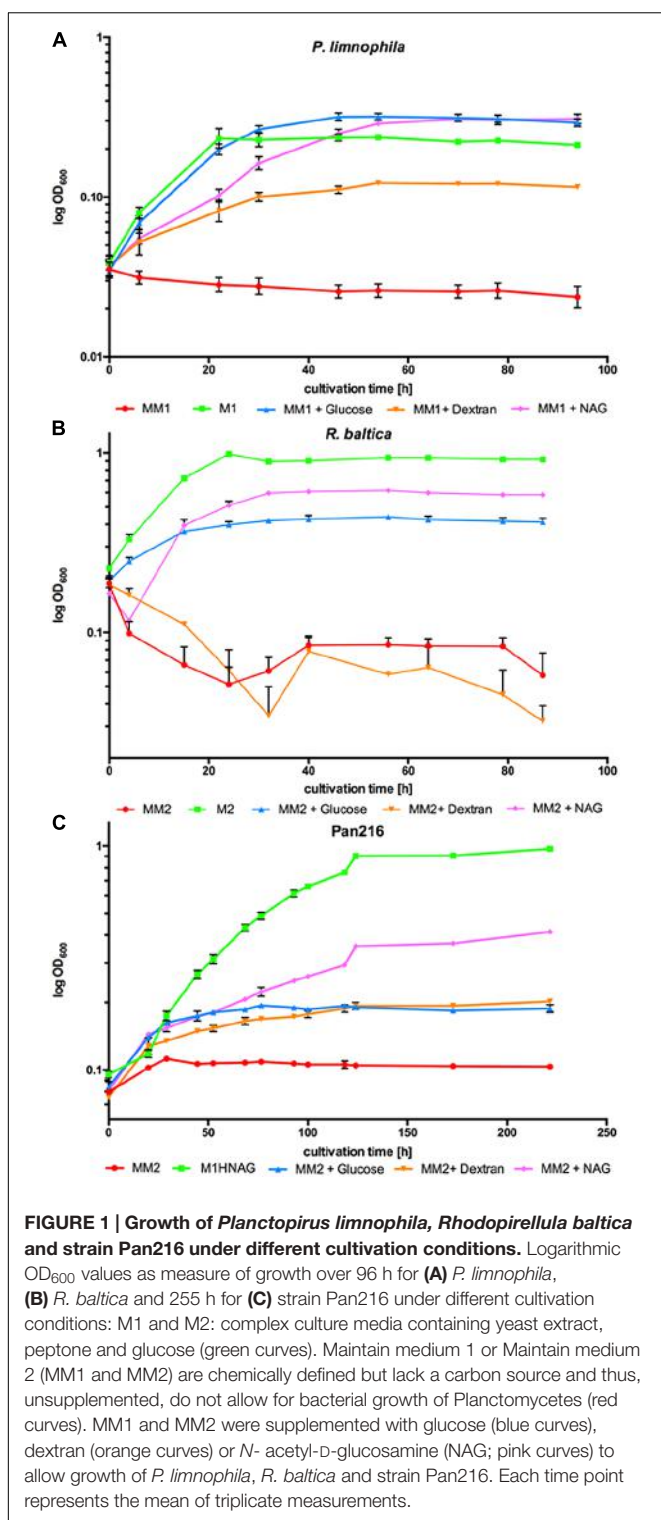


FIGURE 1 | Growth of *Planctopirpus limnophila*, *Rhodopirellula baltica* and strain Pan216 under different cultivation conditions. Logarithmic OD₆₀₀ values as measure of growth over 96 h for (A) *P. limnophila*, (B) *R. baltica* and 255 h for (C) strain Pan216 under different cultivation conditions: M1 and M2: complex culture media containing yeast extract, peptone and glucose (green curves). Maintain medium 1 or Maintain medium 2 (MM1 and MM2) are chemically defined but lack a carbon source and thus, unsupplemented, do not allow for bacterial growth of Planctomycetes (red curves). MM1 and MM2 were supplemented with glucose (blue curves), dextran (orange curves) or N-acetyl-D-glucosamine (NAG; pink curves) to allow growth of *P. limnophila*, *R. baltica* and strain Pan216. Each time point represents the mean of triplicate measurements.

Planctopirpus limnophila was cultured at 28°C in MM1 supplemented with glucose with a constant pH of 7.2 at 100 rpm agitation and a constant air supply (0.5 bar, 0.85 l/min). Samples for glucose consumption, OD₆₀₀ and biomass determination were taken every 24 h (Figure 3A).

In contrast, *R. baltica* was cultured in MM2 supplemented with glucose at pH 7.5 with otherwise identical parameters (Figure 3B).

For fed-batch cultivation the *P. limnophila* culture was spiked after 7 days with 25 ml NAG and 10 ml vitamin solution and cultured for 10 more days (Supplementary Figure S3).

Extraction of Secondary Metabolites from Planctomycetes

For crude extract preparation, 600 ml of a *P. limnophila* culture were incubated with 2% (v/v) of purified adsorbent resin XAD-16N (Rohm and Haas) at 28°C with 80 rpm agitation in a baffled flask for 3 days. The XAD-16N was collected by filtration through an analysis sieve and transferred into an extraction flask. 200 ml acetone were added and incubated in darkness for 1 h at room temperature. To remove the XAD resin the eluate was filtered (Macherey and Nagel 615 1/4, pore size 4–12 µm) after incubation. In parallel, cells were harvested by centrifugation and suspended in 200 ml acetone for 1 h in darkness at room temperature, followed by filtration. Employing a rotary evaporator (Hei VAP-Precision Heidolph) the acetone was removed to yield a solid residue (36°C; at 130 rpm; 1 mbar). The obtained residues were dissolved in 1 ml methanol (pA) and stored at –20°C. Extracts for *R. baltica* and Pan216 were prepared in the same manner. Cultures of Pan216 and XAD were harvested after 5 days of incubation due to their slower growth.

Measurement of Biomass Production and Glucose Consumption

To determine the dry weight of the planctomycetal cells at the given time points, 25 ml of the respective culture were filtered through two superimposed filters with a pore size of 2.5 µm each (Whatman Grade 5 Qualitative Filter Paper) employing a vacuum pump operating at 800 mbar. The filters were subsequently dried for 60 min at 80°C. Comparison of filter weight before and after filtration gave the bacterial dry mass. The glucose concentration was determined with a test strip (MQuantTM) according to the manufacturer's description.

Minimum Inhibitory Concentration Assay

To examine the minimum inhibitory concentrations (MICs) of planctomycetal crude extracts, 26–56 µl of indicator bacteria (for detailed information see Supplementary Table S1) were added to 20 ml of their respective culture medium and mixed well. The indicator strain stocks contained each 1 ml bacteria suspension with an OD₆₀₀ of 3.54 for *E. coli* DSM 1116, 4.05 for *E. coli* TolC, 7.7 *Micrococcus luteus* DSM 1790, 3.69 for *Bacillus subtilis* DSM 10 and 3.86 for *Staphylococcus aureus* DSM 346. Subsequent aliquots were stored at –80°C until usage. 150 µl of the diluted culture was dispensed into each well of a 96-well microtiter plate (initial OD₆₀₀ for the indicator bacteria was 0.01). An additional 130 µl of diluted indicator culture was added to the first row. 20 µl of the planctomycetal crude extracts were added to the first row. A serial dilution of the extract (1:1) was made by transferring 150 µl from one well to the next, this was done from row A to H. For negative and positive

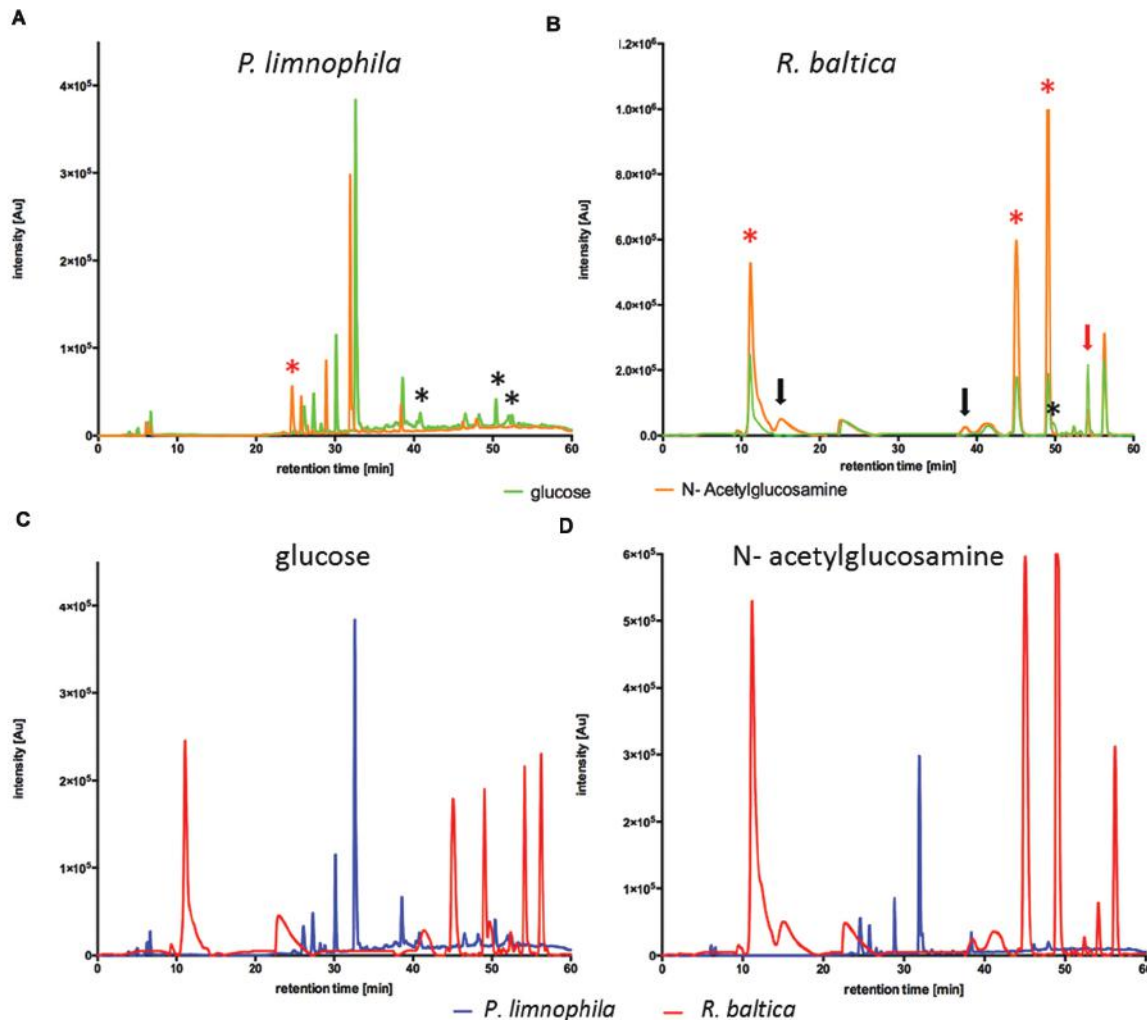


FIGURE 2 | High performance liquid chromatography (HPLC) analysis of *R. baltica* and *P. limnophila* extracts. (A) HPLC-analysis of extracts generated from *P. limnophila* cultivated in MM1 supplemented with glucose (green curve) and NAG (orange curve). Feeding glucose resulted in higher major peaks than NAG. Three minor peaks were exclusively produced if glucose was added (black asterisk), while one major peak was unique to NAG cultivation (red asterisk). **(B)** HPLC-analysis of extracts generated from *R. baltica* cultivated in MM2 supplemented with glucose (green curve) or NAG (orange curve). The intensity of the secondary metabolite peaks was higher in extracts from *R. baltica* cultivated with NAG as carbon source compared to extracts from cultivation with glucose. Extracts from glucose cultivation showed five peaks after 12 and 40–56 min with intensity only up to 2.2×10^5 Au, while same signal peaks from extracts from NAG cultivation showed intensity up to 10^6 Au. Three of the major peaks were significantly higher (red asterisk), while one showed less signal intensity (red arrow). The HPLC spectrum contains two additional minor peaks (black arrows) while one minor peak vanished (black asterisk). **(C)** Comparison of HPLC-chromatograms of XAD extracts from *P. limnophila* cultivated in MM1 (blue curve) and *R. baltica* in MM2 (red curve) supplemented with glucose as sole carbon source. Secondary metabolites signals from *P. limnophila* extracts were detected after a retention time of 7 and 26–38 min with an intensity of 5×10^4 up to 3.8×10^5 Au, while for *R. baltica* a signal was detected after 10 min with an intensity of 2.5×10^5 Au and additional signals were detected after 44–57 min with an intensity of 1.8×10^5 up to 2.4×10^5 Au. **(D)** Comparison of HPLC-chromatograms of XAD extracts from *P. limnophila* cultivated in MM1 (blue curve) and *R. baltica* in MM2 (red curve) supplemented with NAG as sole carbon source. Secondary metabolite signals from *P. limnophila* were detected with intensity up to 3×10^5 Au after a retention time of 25–38 min while secondary metabolite peaks from *R. baltica* extracts after 12 and 40–56 min with intensity up to 10^6 Au.

controls either 20 μ l methanol or 20 μ l of the respective culture medium were added instead of planctomycetal crude extracts. Subsequently, the microtiter plates were incubated for 24 h under constant agitation (150 rpm) at 30 or 37°C. After incubation, the growth of the indicator strains was reviewed visually. No turbidity of the media in a well showed an inhibition of the indicator strain.

Agar Plate Diffusion Assay

To determine antibiotic activity, filter disks (5 mm diameter, pore size 4–7 μ m; Whatman No 597) were coated with 90 μ l of planctomycetal crude extracts, while methanol (pA) coated disks served as negative control. The treated disks were placed on soft-agar plates inoculated with *B. subtilis* cells and incubated over night at 28°C. Soft-agar plates consisted of a 10 ml 1.5%

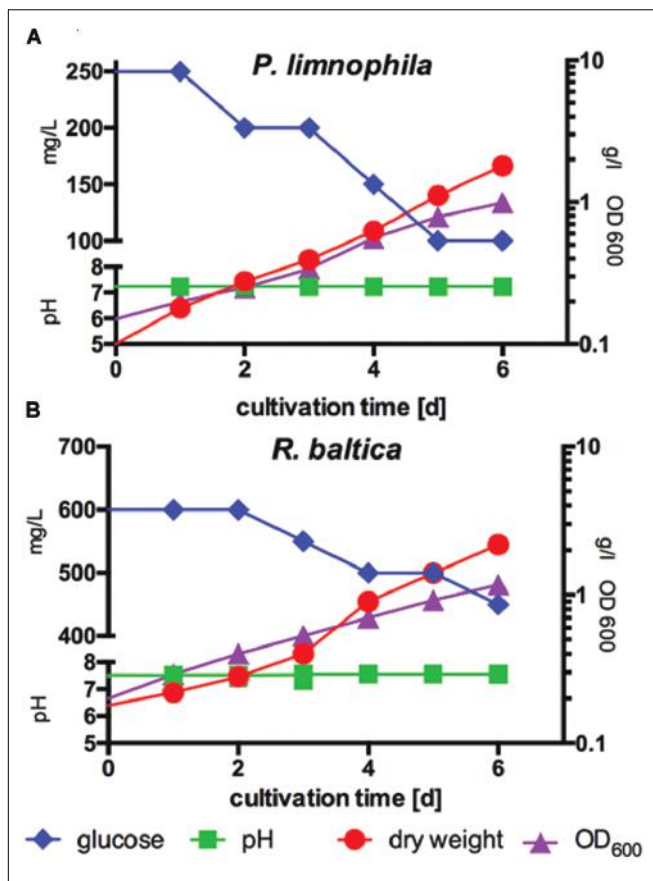


FIGURE 3 | Measurement of biomass production compared to optical density and glucose consumption of *P. limnophila* and *R. baltica* at constant pH. **(A)** Biomass production of *P. limnophila* compared to optical density at 600 nm (OD_{600}) and glucose consumption at constant pH over 6 days in MM1 supplemented with glucose in a 10 l fermenter. Glucose concentration decreased from 250 to 100 mg/l (blue curve), while the OD_{600} increased from 0.15 up to 0.99 (purple curve) and correlating with the OD_{600} also the dry weight increased from 0.1 g/l up to 1.8 g/l (red curve) during cultivation. The pH was 7.2 (green curve). **(B)** Biomass production of *R. baltica* compared to, OD_{600} -value and glucose consumption at constant pH over 6 days in MM2 supplemented with glucose in a 10 l fermenter. Glucose concentration decreased from 600 to 450 mg/l (blue curve), while the OD_{600} increased from 0.2 to 1.170 (purple curve) and correlating with the OD_{600} also the dry weight increased from 0.18 g/l and to 2.18 g/l (red curve) during cultivation. The pH was stabilized at 7.5 (green curve).

LB agar layer covered with a second layer of 10 ml 0.7% LB agar inoculated with 100 μl of a *B. subtilis* DSM10 overnight culture.

Dual Culture Assay

Dual culture assays were performed on M2 1.5% agar plates with *R. baltica* producer and *E. coli* DSM 1116 as indicator strain. Given the different doubling times of both species, *R. baltica* was inoculated first and incubated for 2 days at 28°C. Afterward, *E. coli* was inoculated on the same plate and the agar dishes were incubated for three more days at 28°C. To investigate if growth-altering effects appear in a distance-dependent manner,

respective bacteria were plated at different defined distances from each other (2, 10, and 15 mm respectively).

HPLC-Analysis of Planctomycetal Extracts

High performance liquid chromatography (HPLC) analysis was performed with a Prominence HPLC (Shimadzu) equipped with a Macherey and Nagel, CC 250/4.6 NUCLEODUR 100-5 C18 column (pore size 100 Å, particle size 5 μm) coupled to a SPD-M20A photo diode array (PDA) detector (Shimadzu). The PDA detector recorded all emitted wavelengths, while the wavelength with the highest signal intensities (254 nm) was used for further discrimination of the extracts. 15 μl of the investigated extracts were injected and eluted with a modified methanol-water gradient [solvent A: H_2O ; solvent B: methanol, gradient: 5% B for 10 min increasing to 100% B in 15 min, maintaining 100% B for 30 min, flow rate (FR) 0.6 ml/min]. Prior to the analysis of the extracts, the column was equilibrated with pure methanol. Results were analyzed using the LCsolution Shimadzu Software.

HPLC Fractionation

An Agilent 1260 Series HPLC-UV system equipped with a Waters, XBridge BEH C18, 2.1 mm \times 100 mm column (pore size 135 Å, particle size 3.5 μm) was used for the chromatographic fractionation of crude extracts. The same HPLC gradient was used as for the high-resolution electrospray ionization mass spectrometry (HRESIMS) instrument (described below). The flow through was collected in 30 s intervals into a 96-well microtiter plate. Afterward, the plates were dried by a constant nitrogen-flush for 40 min, inoculated with 150 μl indicator bacteria per well and incubated as described above. After 24 h the plates were evaluated and documented employing a custom-made mirror stand and a CANON EOS 10D digital camera.

Mass Spectra

Electrospray ionization mass spectrometry (ESIMS) spectra in positive and negative mode were obtained with an Agilent 1260 Infinity Series HPLC-UV system (column 2.1 mm \times 50 mm, 1.7 μm , C18 Acquity UPLC BEH (Waters), solvent A: H_2O + 0.1% formic acid; solvent B: ACN + 0.1% formic acid, gradient: 5% B for 0.5 min increasing to 100% B in 19.5 min, maintaining 100% B for 5 min, FR 0.6 ml/min, UV detection 200–600 nm) equipped with a diode array detector and an ESIontrap MS detector (Amazon, Bruker).

High-resolution electrospray ionization mass spectrometry spectra were obtained with an Agilent 1200 series HPLC-UV system [solvent A: $\text{H}_2\text{O}/\text{ACN}$ (95/5) + 5 mM/l of NH_4Ac + 40 $\mu\text{l}/\text{l}$ of acetic acid; solvent B: $\text{H}_2\text{O}/\text{ACN}$ (5/95) + 5 mM/l of NH_4Ac + 40 $\mu\text{l}/\text{l}$ of acetic acid, gradient: 10% B increasing to 100% B in 30 min, maintained 100% B for 10 min; FR = 0.3 ml/min; UV detection 200–600 nm] combined with an ESI-TOF-MS (Maxis, Bruker; scan range 100–2500 m/z, rate 2 Hz, capillary voltage 4500 V, dry temperature 200°C).

RESULTS

Chemically Defined Growth Conditions for Marine and Limnic Planctomycetes

We selected the marine species *R. baltica* SH1 DSM 10527 and the limnic organism *P. limnophila* DSM 3776 as model Planctomycetes together with the phylogenetically distant and recently isolated strain Pan216 (**Supplementary Figure S1**) for subsequent experiments. For both established model species, optimized growth conditions in complex media, containing rather high amounts of yeast extract and peptone, have been previously described (Jogler et al., 2011; Jeske et al., 2013). The optimal growth conditions in rich media for strain Pan216 were determined in this study (see Materials and Methods).

To enable ecomimetic experiments that mimic certain natural conditions in the laboratory, and to optimize HPLC detection and fractionation, we developed a chemically defined and carbon source free maintain medium for limnic- (MM1) and marine conditions (MM2). *P. limnophila*, *R. baltica*, and Pan216 cells survived under such conditions, but were not able to divide and grow without supplementation of any maintain medium with a carbon source (**Figure 1**, red curves). After a starvation period (5–9 days) in the respective Maintain Media, all three strains were able to fully recover when specific carbon and nitrogen sources were added. Remarkably, *P. limnophila* grew even more efficiently in MM1 + glucose (same growth rate but higher biomass attained; **Figure 1A**, blue curve) or MM1 + NAG (lower growth rate but higher biomass attained; **Figure 1A**, pink curve), than in the originally described isolation medium (**Figure 1A**, green curve). *R. baltica* grew less efficiently with MM2 + glucose (**Figure 1B**, blue curve) or MM2 + NAG (**Figure 1B**, pink curve) and did not reach the same OD₆₀₀ compared to the medium culture broth M2 (**Figure 1B**, green curve). Pan216 grew best if fed with M1H NAG ASW medium developed in this study (**Figure 1C**, green curve). The chemically defined MM media were also supplemented with other carbon sources such as the complex polysaccharide dextran (**Figure 1**, orange curves) that provided growth for *P. limnophila* and Pan216 but not for *R. baltica*. In the case of *R. baltica*, the supplementation of NAG (**Figure 1B**, pink curve) led to initial biofilm formation resulting in an early decrease of the cultures optical density. This effect was even stronger after adding dextran (**Figure 1B**, orange curve) and explains why the optical density was lower than in the control culture (**Figure 1B**, red curve) without any carbon source added. Thus certain carbon sources might trigger a lifestyle switch from planktonic growth to biofilm formation.

The adsorber resin XAD binds unspecifically to both secreted secondary metabolites and components of the complex growth media M1 and M2, resulting in visible media component signals in HPLC measurements even when no-bacteria medium control samples were measured (**Supplementary Figures S2A,C**). However, extraction of our newly developed MM1 and MM2 media with XAD showed no media component signals in HPLC analysis (**Supplementary Figures S2B,C**), making them the preferred choice to investigate the influence of trigger substances on secondary metabolite production in Planctomycetes.

Ecomimetic Cultivation of Planctomycetes

The chemically defined Maintain Media (MM) were developed to enable ecomimetic experiments which attempt to recreate environmental situations under defined conditions in the laboratory. The rational was that certain environmental cues, such as a particular carbon source, would stimulate secondary metabolite production in Planctomycetes, and consequently alter the peak profile in subsequent HPLC analysis. For a proof of principle, we simulated the planctomycetal interaction with cyanobacteria by adding a key component of bacterial cell walls –NAG – to our MM. Since cyanobacteria occur in both, marine- and limnic habitats, we performed the evaluation of our MMs with *R. baltica* (marine) and *P. limnophila* (limnic) in MM2 and MM1 respectively. After cultivation with XAD for 3 days at 28°C, XAD extracts were analyzed via HPLC. For *P. limnophila*, three minor peaks were exclusively detected when cells were cultivated with glucose as sole carbon source (**Figure 2A**, black asterisk), while one peak was unique to cultivation with NAG as sole carbon source (**Figure 2A**, red asterisk). When cultivated with glucose, *R. baltica* produced secondary metabolites that led to five major and five minor peaks in the HPLC chromatogram (**Figure 2B**, green curve). In contrast, when fed with NAG, the subsequent HPLC chromatogram contains two additional minor peaks (**Figure 2B**, black arrows) while one minor peak vanished (**Figure 2B**, black asterisk). Three of the major peaks were significantly higher (**Figure 2B**, red asterisk), while one showed less signal intensity (**Figure 2B**, red arrow). The overall signal intensity of *P. limnophila* extracts showed less variation between the cultivation conditions than *R. baltica* did. However, comparison of extracts from *P. limnophila* (**Figures 2C,D**, blue) and *R. baltica* (**Figures 2C,D**, red) showed that both organisms display entirely different HPLC peak patterns.

Thus our Maintain Media allow ecomimetic experiments that lead to the production of different metabolites in response to different carbon sources.

Screening of Planctomycetal Extracts for Antimicrobial Activity

One aim of this study was to develop cultivation techniques that could stimulate the production of bioactive molecules with antimicrobial activity as demonstrated in the previous section. However, extracts obtained in such ecomimetic experiments require a screening procedure to determine potential antimicrobial activity. Thus, for the first time we demonstrate different screening methods for planctomycetal extracts and strains and evaluated their usefulness.

The semi-quantitative agar plate diffusion assay was used to determine the inhibitory effect of *R. baltica* cell- and XAD resin extracts obtained from *R. baltica* cultures against *B. subtilis*. While the negative control and the cell extract disks showed no influence on bacterial growth, the planctomycetal XAD extract displayed a zone of *B. subtilis* growth inhibition, pointing toward an antibiotic molecule produced by *R. baltica* (**Figure 4A**).

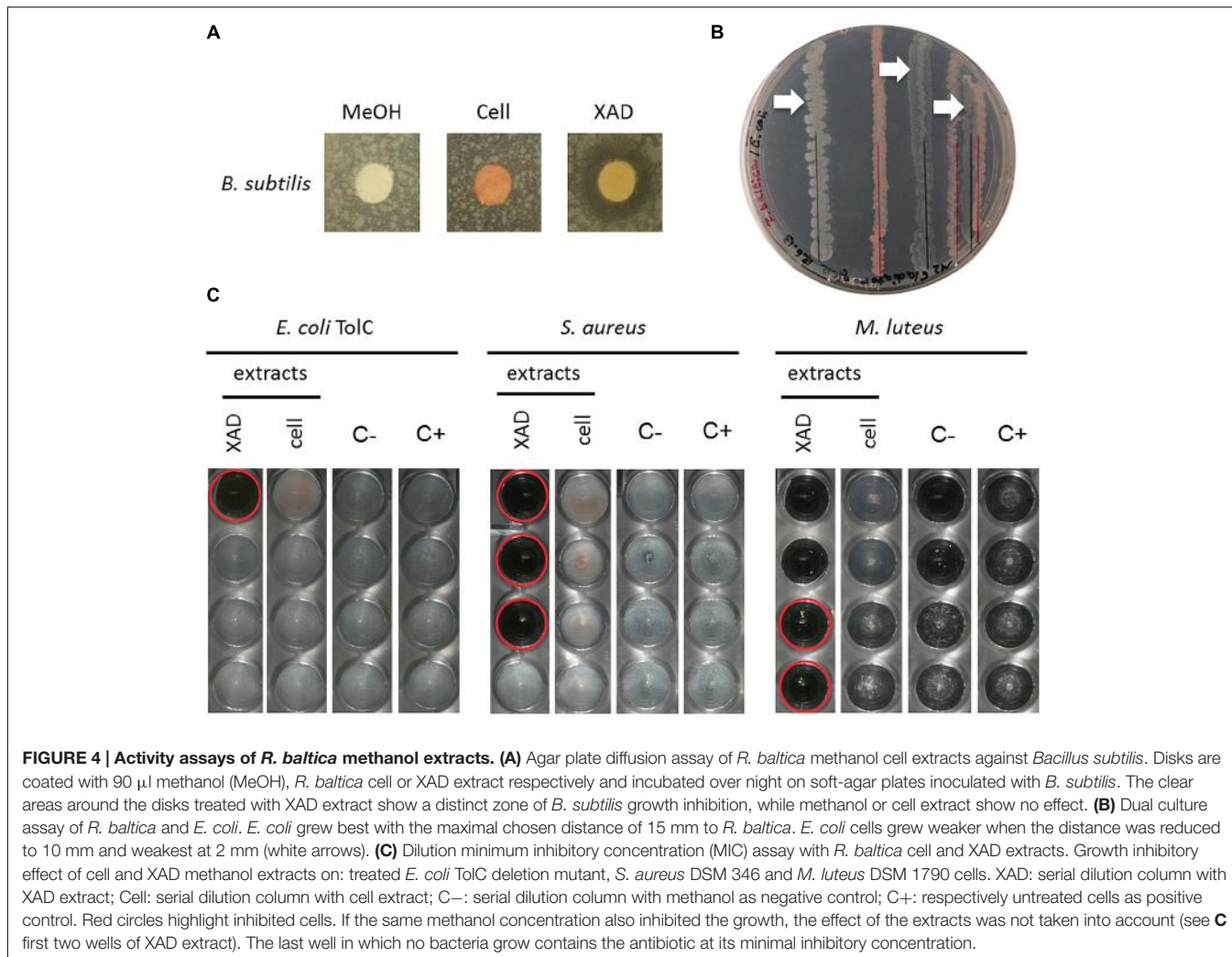


FIGURE 4 | Activity assays of *R. baltica* methanol extracts. (A) Agar plate diffusion assay of *R. baltica* methanol cell extracts against *Bacillus subtilis*. Disks are coated with 90 µl methanol (MeOH), *R. baltica* cell or XAD extract respectively and incubated over night on soft-agar plates inoculated with *B. subtilis*. The clear areas around the disks treated with XAD extract show a distinct zone of *B. subtilis* growth inhibition, while methanol or cell extract show no effect. **(B)** Dual culture assay of *R. baltica* and *E. coli*. *E. coli* grew best with the maximal chosen distance of 15 mm to *R. baltica*. *E. coli* cells grew weaker when the distance was reduced to 10 mm and weakest at 2 mm (white arrows). **(C)** Dilution minimum inhibitory concentration (MIC) assay with *R. baltica* cell and XAD extracts. Growth inhibitory effect of cell and XAD methanol extracts on: treated *E. coli* TolC deletion mutant, *S. aureus* DSM 346 and *M. luteus* DSM 1790 cells. XAD: serial dilution column with XAD extract; Cell: serial dilution column with cell extract; C-: serial dilution column with methanol as negative control; C+: respectively untreated cells as positive control. Red circles highlight inhibited cells. If the same methanol concentration also inhibited the growth, the effect of the extracts was not taken into account (see **C** first two wells of XAD extract). The last well in which no bacteria grow contains the antibiotic at its minimal inhibitory concentration.

The dual culture assay revealed that reducing the distance between *R. baltica* and *E. coli* K12 increased the growth inhibition effect (**Figure 4B**). *E. coli* grew to highest density with the maximum chosen distance of 15 mm. When the distance to *R. baltica* was reduced to 10 mm, the *E. coli* grew less well. Ultimately, only minor growth of *E. coli* was observed when the distance was reduced to 2 mm distance.

The MIC assay was performed for *R. baltica* extracts (**Figure 4C**). Several dilution series were prepared against *E. coli* TolC, *S. aureus* and *M. luteus*. Only the highest concentration of *R. baltica* XAD extract in the first well showed an effect against the *E. coli* TolC strain (**Figure 4C**: XAD). However, a strong inhibitory effect against *S. aureus* was observed with the *R. baltica* XAD extract (**Figure 4C**: XAD). The first three wells of the dilution series showed a distinct inhibition of growth. The lowest concentration in which the bacterial growth was inhibited therefore contained the antibiotic at MIC. In contrast, *S. aureus* treated with the cell extract grew normally and showed no signs of growth inhibition (**Figure 4C**: cell).

Likewise, only the XAD extract had a strong inhibitory effect against *M. luteus* in the first four wells (**Figure 4C**: XAD), whereas

the cell extract had no effect on *M. luteus* (**Figure 4C**: cell). However, since no bacterial growth could be detected in the first two wells of the dilution series for the negative control, the effect of the first two wells in the XAD column might be caused by methanol rather than by a potential antibiotic within the crude extract. However, bacteria were not inhibited in the third well of the negative control, so extracts with activity at this dilution could still contain an active compound.

Thus, all three evaluated screening methods, agar plate diffusion, dual culture, and MIC assay were useful to analyze planctomycetal antimicrobial activity. For the first time we demonstrated antibacterial activity of *R. baltica* against both, Gram-negative and Gram-positive bacteria.

Correlation of Antimicrobial Activity with Distinct HPLC Peaks

After development of ecomimetic cultivation, biological screening methods, and protocols to facilitate the analysis of planctomycetal antibiotic production, next the HPLC signals need to be correlated with biological activity to facilitate structure elucidation of the antibiotic molecules. Thus, we deve-

loped a procedure that allows correlation of HPLC peaks with antimicrobial activity of planctomycetal extracts. Again, a limnic (*P. limnophila*) and a marine species (strain Pan216) were chosen for the proof of principle study. After cultivation and extraction of cultures with adsorbent resin, the MIC assay screening against indicator strains (Supplementary Table S1) was performed. Once the analyzed extract showed an activity against one of the indicator strains (Figures 4C and 5), a semi preparative HPLC run was performed (Figure 5). Our integrated approach consists of utilizing HPLC instruments coupled with both HRESIMS as well as a fractionation collector for 96-well microtiter plates, which are used in a subsequent bioassay against the prior determined strains. Both HPLC systems were equipped equally, so that chromatograms and retention times can directly be compared. Thereby it is possible to assign the activity observed for the crude extract to individual peaks, and simultaneously to determine their molecular formula (Figure 5; Table 1). Furthermore, tandem mass spectrometry (MS/MS) and UV/Vis spectra can sometime provide early information about the chemical structure of the desired substance. Although, the HPLC gradient and solvents can be varied, the use of a water/acetonitrile (ACN) system provided best chromatographic separation and we suggest this as standard procedure for the analysis of planctomycetal extracts. Since the use of formic acid did not lead to the reproducible detection of bioactive wells, we concluded that some of the bioactive compounds might be degraded under acidic conditions and consequently we used an acetate buffered solvent system instead.

Two replicate cultivation and extraction experiments were performed for both *P. limnophila* and strain Pan216.

Fractionation of *P. limnophila* replicate R1 resulted in inhibition of various wells. The obtained results were not reproducible and no activity could be assigned to peaks in the UV chromatogram.

In contrast, repeated fractionation of 15 μ l extract each for *P. limnophila* replicate R2 led to reproducible inhibition of *B. subtilis* growth in well 'B6', which had been collected from 23 to 23.5 min (Table 1). The chromatogram showed a major peak at this retention time (Figure 5A). The same peak was observed at a retention time of 22.4 min in the HRESIMS system. Its molecular formula $C_{26}H_{51}NO_6$ was deduced from its $[M+H]^+$ peak at m/z 474.3880 as well as its $[M+Na]^+$, $[2M+H]^+$, and $[2M+Na]^+$ peaks at m/z 496.3608, 947.7514, and 969.7325, respectively (Table 1). The assignment of the molecular ion cluster was further confirmed by the observation of the $[M+CO_2H]^-$ peak at m/z 518.3 in the ESIMS spectrum measured in negative mode. A search with the molecular formula $C_{26}H_{51}NO_6$ in the Dictionary of Natural Products (DNPs) on DVD resulted in no known metabolites (Table 1).

In the case of strain Pan216, both replicates resulted in different inhibition patterns as well. For replicate R1 inhibition of wells B7, C7, and G7 was observed that correspond to three major peaks of the slightly lipophilic region of the chromatogram (Figure 5B). These three peaks were detected in HRESIMS spectrum at 25.1, 25.8, and 27.6 min and molecular formulae of $C_{18}H_{30}O_2$, $C_{22}H_{32}O_2$, and $C_{22}H_{34}O_2$ were assigned from their $[M+H]^+$ and $[M+Na]^+$ peak pairs (Table 1). These assignments were further confirmed by $[M+H]^+ [M-H]^-$ pairs in positive/negative mode ESIMS spectra. The search for these molecular formulae in the DNP resulted in 122, 38, and 61 hits (Table 1).

Neither of those peaks were observed in the chromatogram of Pan216 replicate R2 nor was activity observed in wells B7-G7. Instead, well C6 (23.5–24 min) was constantly inhibited. The corresponding peak shows characteristic UV absorption maxima at 244 and 294 nm, which might suggest an aromatic residue. The $[M+H]^+$ peak in the HRESIMS spectrum at m/z 294.0532 could indicate the molecular formula as $C_{12}H_{11}N_3O_4S$, which would explain the observed +2 satellite

TABLE 1 | Antibacterial metabolites found in *P. limnophila* and Pan216.

| Organism | Rt [min] | m/z^a | Molecular formula | Hits in DNP | DBE | MS/MS | Possible fragments |
|-------------------------|----------|-----------------|----------------------------|-------------|-----|----------|---------------------|
| <i>P. limnophila</i> R2 | 22.4 | 474.3880 | $C_{26}H_{51}NO_6$ | 0 | 2 | 456.3685 | $C_{26}H_{50}NO_5$ |
| | | 947.7514 | $C_{52}H_{103}N_2O_{12}$ | | | 317.2845 | $C_{22}H_{37}O$ |
| | | 969.7333 | $C_{52}H_{102}N_2O_{12}Na$ | | | 236.1495 | $C_{10}H_{22}NO_5$ |
| Pan216 R1 | 27.6 | 331.2642 | $C_{22}H_{35}O_2$ | 132 | 6 | 313.2532 | $C_{20}H_{34}ONa$ |
| | | 353.2461 | $C_{22}H_{34}O_2Na$ | | | 295.2429 | $C_{20}H_{32}Na$ |
| Pan216 R2 | 25.8 | 329.2481 | $C_{22}H_{33}O_2$ | 38 | 7 | 271.2429 | $C_{18}H_{30}ONa$ |
| | | 301.2143 | $C_{18}H_{30}O_2Na$ | | | 247.1703 | $C_{14}H_{24}O_2Na$ |
| | 25.1 | 301.2143 | $C_{18}H_{30}O_2Na$ | 61 | 4 | 233.1551 | $C_{13}H_{22}O_2Na$ |
| | | 294.0532 | $C_{12}H_{11}N_3O_4S$ | | | 217.1954 | $C_{14}H_{26}Na$ |
| | 21.8 | 329.2481 | $C_{22}H_{33}O_2$ | 0 | 8 | 203.1792 | $C_{13}H_{24}Na$ |
| | | 301.2143 | $C_{18}H_{30}O_2Na$ | | | 187.1119 | $C_{11}H_{16}ONa$ |
| | 21.8 | 294.0532 | $C_{12}H_{11}N_3O_4S$ | | | 177.1638 | $C_{11}H_{22}Na$ |
| | | 294.0532 | | | | / | / |

^aBold mass was further processed by MS/MS.

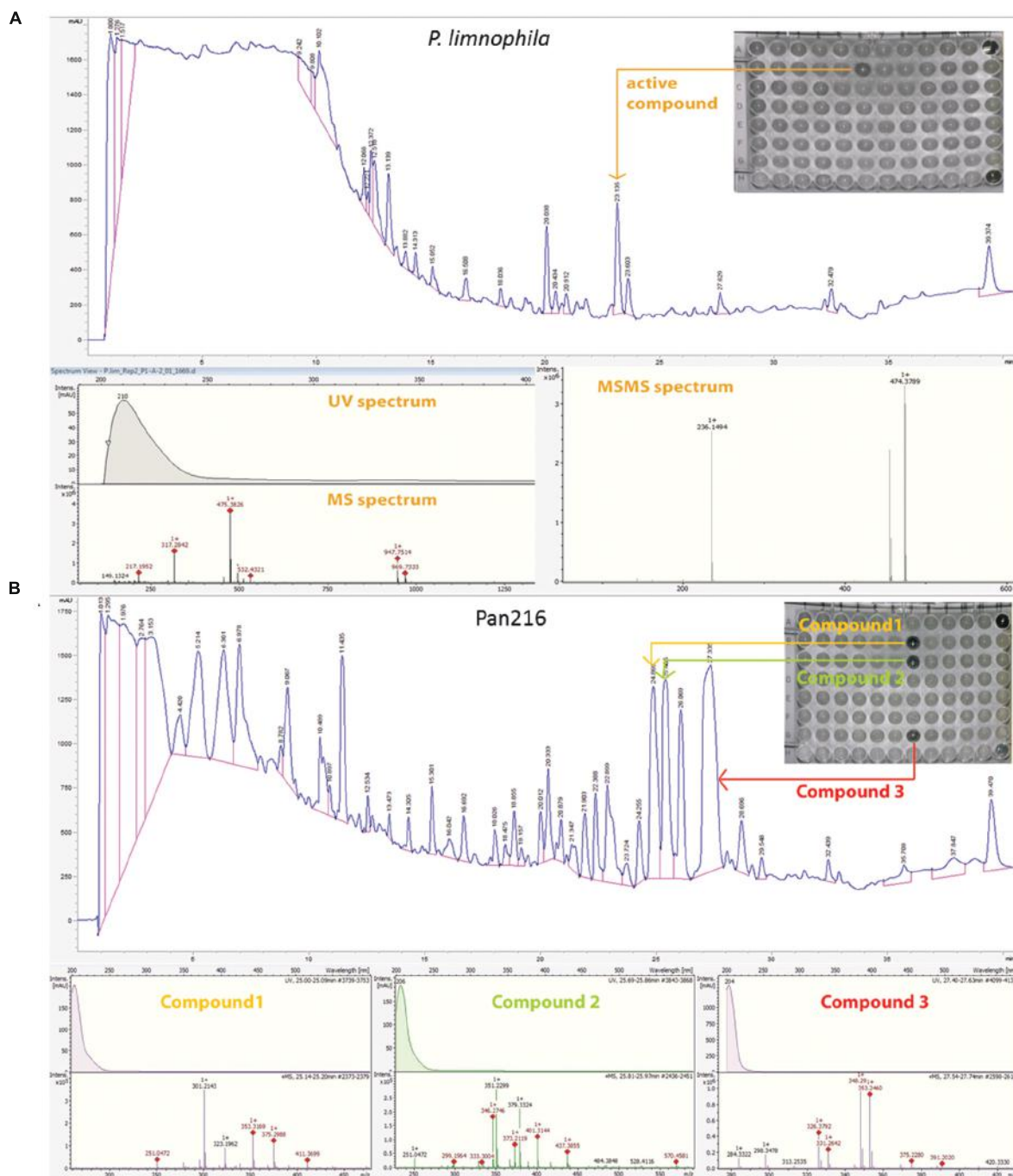


FIGURE 5 | Fractionation analysis of planctomycetal crude extracts. (A) Combined chromatogram of HPLC fractionations, UV/Vis, mass- and tandem mass (MS/MS) spectrometry to identify the active compound, which causes the growth inhibition of *P. limnophila* crude extract #2 against *B. subtilis* on a 96 well plate. Fractionation of 15 μ L extract for *P. limnophila* replicate #2 led to reproducible inhibition of *B. subtilis* growth in well 'B6', which had been collected from 23 to 23.5 min. The chromatogram shows a major peak at this retention time. The same peak was observed at a retention time of 22.4 min in the HRESIMS system. Its molecular formula $C_{26}H_{41}NO_6$ was deduced from its $[M+H]^+$ peak at m/z 474.3880 as well as its $[M+Na]^+$, $[2M+H]^+$, and $[2M+Na]^+$ peaks at m/z 496.3608, 947.7514, and 969.7325, respectively (Table 1). The assignment of the molecular ion cluster was further confirmed by the observation of the $[M+CO_2H]^-$ peak at m/z 518.3 in the ESIMS spectrum measured in negative mode. **(B)** Combined chromatogram of HPLC fractionations, UV/Vis, mass spectrometry to identify three active compounds, which causes growth inhibition of *B. subtilis* of Pan216 crude extract #1 in a 96 well plate. In case of strain Pan216 both replicates resulted in different inhibition patterns as well. Inhibition of wells B7, C7, and G7 was observed that correspond to three major peaks of the slightly lipophilic region of the chromatogram. These three peaks were observed in HRESIMS spectrum at 25.1, 25.8, and 27.6 min; molecular formulae of $C_{18}H_{30}O_2$, $C_{22}H_{32}O_2$, and $C_{22}H_{34}O_2$ were assigned from their $[M+H]^+$ and $[M+Na]^+$ peak pairs (Table 1). These assignments were further confirmed by $[M+H]^+/ [M-H]^-$ pairs in positive/negative mode ESIMS spectra. Wells A12 and H12 are negative controls treated with tetracycline and crude extract respectively.

in the molecular ion cluster as the ^{34}S isotope. However, the other possibilities for the molecular formula $\text{C}_{13}\text{H}_{12}\text{NO}_5\text{P}$ and $\text{C}_{20}\text{H}_7\text{NO}_2$ cannot be excluded. In the ESIMS spectra in negative mode $[\text{M} - \text{H}]^-$ respectively $[2\text{M} - \text{H}]^-$ peaks at 291.1 and 585.0 confirm the assignment. There is no known natural product included in the DNP for any of the three molecular formulae.

Thus we demonstrated a procedure to correlate HPLC peaks of planctomycetal extracts with antimicrobial activity that allows subsequent purification of the compound of interest. Initial data pointed towards novel bioactive molecules with antimicrobial activity produced by Planctomycetes.

Cultivation of Planctomycetes in Process Controlled Bioreactors

Thus far we have presented tools and procedures for the discovery of planctomycetal bioactive molecules, yet one important feature is missing if they are to be useful: large scale cultivation. Anammox Planctomycetes are routinely cultivated in different types of bioreactors in small, large and industry scale, mainly for waste water treatment (for review see, van Niftrik and Jetten, 2012). However, little to no experience exists with the planctomycetal orders Phycisphaerales and Planctomycetales. The known species belonging to the order Phycisphaerales have small genomes with few secondary metabolite related clusters while species of the order Planctomycetales were found to comprise large genomes with many secondary metabolite related genes (Jeske et al., 2013). Among Planctomycetales, only the cultivation of *R. baltica* in a small-scale custom-made chemostat was described thus far (Frank et al., 2011). However, such experiments were not performed with the intention to obtain secondary metabolites.

In this study, we developed the required media and procedures to cultivate both limnic (*P. limnophila*) and marine (*R. baltica*) Planctomycetes in a 10 l bench-top bioreactor (BIOSTAT®B, Sartorius). Our protocols (see Materials and Methods) fit to batch (Figure 3) and fed-batch (Supplementary Figure S3) cultivation in different sized stirring tank reactors as our reactor system allows seamless scale-up, at least for up to 100 l.

First, we determined optimal growth conditions in maintain medium supplemented with glucose (Figures 3A,B) and obtained optimal biomass production, whereby the pH was kept constant at 7.5 for *R. baltica* and at 7.2 for *P. limnophila*. Since HEPES is used routinely to buffer planctomycetal culture media, the future scale-up might be limited by high costs of this chemical. Thus, we explored different buffer systems and found that at least the growth of *P. limnophila* is not affected by phosphate buffering (see Materials and Methods). Growth was measured by OD₆₀₀ and dry weight, while glucose consumption was determined in addition (Figures 3A,B). While both curves, dry weight and OD₆₀₀, comprise a similar shape for *R. baltica*, the slope of the OD₆₀₀ curve for *P. limnophila* is steeper than the curve representing dry weight measurements.

Paralleling the extraction procedure employed for flask cultures, we added XAD to the bioreactor that was finally harvested with an analyze sieve prior to extraction. Thus, even for planctomycetal large-scale cultures our procedure allows small

volume downstream processes, significantly reducing the amount of organic solvents and effort for the extraction process.

When two independent *P. limnophila* 5 l cultivation batches were employed for XAD extraction and subsequent HPLC analysis, the resulting metabolite profiles differed slightly (Supplementary Figure S4). Eight minor peaks (red asterisks) and one major peak (black asterisks) occurred only in one of the two replicates, while only the three major peaks (black arrows) were found in both extracts.

Thus, we developed a large scale cultivation approach for aerobic Planctomycetes that reduces cost and effort but still lacks 100% reproducibility.

DISCUSSION

The aim of this pilot study was to develop the tools and procedures required to produce, isolate, and analyze secondary metabolites from Planctomycetes. We employed different marine and limnic Planctomycetes as a proof of principal for each step of our pipeline.

The first step was the development of cultivation conditions that support the production of secondary metabolites. To determine a suitable cultivation strategy, we took the ecology of Planctomycetes into account. It has been demonstrated by both us and others that Planctomycetes interact with phototrophs, such as cyanobacteria, in marine and limnic habitats and that the Planctomycetes can even dominate biofilms in these carbon-rich ecological niches (Bengtsson and Øvreås, 2010; Bengtsson et al., 2010, 2012; Pizzetti et al., 2011a,b; Jeske et al., 2013). Due to the slow growth of Planctomycetes, we hypothesized that their dominance in biofilms could be due to production of antibiotics, which could provide an advantage over faster-growing bacteria. To elucidate whether environmental cues can trigger the production of secondary metabolites, we first developed both a limnic (MM1) and a marine (MM2) Maintain Medium (Figure 1). This development is vital, because it dramatically reduces the culture-media components in acetone extracts to zero (Supplementary Figure S2). Thus, the MM allows for easy detection and characterization of produced metabolites. In addition, changes in production of bioactive molecules caused by altered growth conditions could be easily monitored. Such alterations could, for example, be achieved by supplementing the MM with different carbon sources. Furthermore, ecomimetic experiments can replicate the environmental interactions of Planctomycetes and phototrophs in a chemically defined manner, allowing for determination of environmental cues which are currently unknown. In a proof of principle study we found that NAG, a main component of the cyanobacterial cell wall, altered the secreted secondary metabolome of both *P. limnophila* and *R. baltica* (Figure 2). This finding is not surprising, since it is well-known that changes in the composition of cultivation media can affect the biosynthesis of secondary metabolites (Berdy, 2005). In the past, selection of growth media composition to stimulate the expression of 'silent' secondary metabolite genes or clusters was rather random. Here, we utilize the chemical characteristics of the planctomycetal ecological niche to guide alterations of

the medium composition which led to the production of novel secondary metabolites. Algae and bacteria produce a multitude of different compounds and it has been shown by both our group and others that many of these molecules can be utilized by Planctomycetes (Wegner et al., 2012; Jeske et al., 2013). Thus, our Maintain Medium provides a base medium that allows for addition of many kinds of substrate combinations. Subsequent analysis of changes in the secondary metabolome can be correlated with environmental cues (substrates) present in the media. Furthermore, the addition of XAD adsorber resin allowed for easy and low solvent-volume extraction and analysis of such molecules.

After developing chemically defined growth conditions and ecomimetic, the second step in our pipeline is the screening for biological activity. We successfully evaluated agar plate diffusion, dual culture, and MIC assays and found all three methods very useful to screen Planctomycetes. An initial screen with the cheap and easy dual culture approach allows for determination of potential antibiotic producers, whilst the agar plate diffusion and the MIC assay allow for further purification of extracts and isolation of active components. Most importantly, we found evidence for antimicrobial activity of Planctomycetes against both Gram-negative and Gram-positive bacteria. This finding might support our hypothesis of the planctomycetal interaction with phototrophs.

The third step is the correlation of bioactivity in a crude extract with a particular HPLC peak. This step is crucial for isolation and purification of bioactive compounds, facilitating subsequent structure elucidation. We developed a comprehensive approach by combining analytical and preparative HPLC with direct fractionation of extracts into 96-well plates that can be subsequently employed for activity screening (Figure 4). While the elucidation of distinct structures is beyond the scope of this study we gained some insights into the chemical composition of planctomycetal antibiotic molecules. For example, in *P. limnophila* replicate #2, an active metabolite had a molecular formula of $C_{26}H_{51}NO_6$, which is not present in the DNP, suggesting it could be a novel compound. Although *de novo* structure elucidation is impossible with MS/MS data alone, early indications can be obtained by fragmentation ions. For example, fragments of the aforementioned compound indicate that the structure consists of a long aliphatic chain and a heteroatom-containing core structure. Pan216 replicate #2 contained an active metabolite with molecular formula of $C_{12}H_{11}N_3O_4S$, this was also not in the DNP and suggests a new natural product. UV absorption maxima at 244 and 294 nm might indicate an aromatic or heteroaromatic residue. However, Pan216 replicate #1 showed no evidence of this active metabolite. Three distinct metabolites inhibiting the growth of *B. subtilis* were also produced in Pan216 replicate #2. The active metabolites had molecular formulae of $C_{22}H_{34}O_2$, $C_{22}H_{32}O_2$, and $C_{18}H_{30}O_2$, which corresponds to 6, 7, and 4° of unsaturation, respectively. Dozens of compounds are known for these molecular formulae and so we cannot identify these metabolites nor state that these metabolites are new.

Both the metabolome and the bioactivity varied strongly between the replicates of *P. limnophila* and strain Pan216,

implying that the production of secondary metabolites is highly variable, responsible factors could include the inoculum, oxygenation, growth stage, formation of aggregates, as well as degradation of compounds during cultivation. Thus, this study revealed that single planctomycetal strains might be able to produce a multitude of antimicrobial secondary metabolites. Therefore, Planctomycetes do not only contain the gene clusters for secondary metabolite production, but actually produce compounds with antibacterial activity. However, structure elucidation of such bioactive molecules requires large scale cultivation of planctomycetal producer strains.

To facilitate future structure elucidation attempts, the last step of our pipeline is the cultivation of marine and limnic Planctomycetes in large scale stirring tank bioreactors. We choose a 5 l volume in 10 l computer controlled bioreactors as this allows for easy scale-up. While establishing the protocols we noticed a disparity between the approximate doubling times determined by OD₆₀₀ (57 h) and dry weight (47 h) for *P. limnophila*, and OD₆₀₀ (62 h) and dry weight (41 h) for *R. baltica*. Therefore, future experiments using dry weight instead of optical density might provide better correlation between growth phase and secondary metabolite production. Whilst HPLC analysis of crude extracts of two replicates of 5 l *P. limnophila* batch cultures showed differences, the most prominent peaks were reproducible and would be the obvious candidates for structure elucidation. Once these prominent compounds have been determined, batch culture of *P. limnophila* may have to be further studied to enable isolation of the compounds which appear more variable in their production. It is possible that the life cycle switch of *P. limnophila* could cause fluctuations in the secondary metabolome (Jogler et al., 2011). *P. limnophila* daughter cells are flagellated and live as planktonic swimmers before developing into stalked sessile cells which are capable of dividing and forming biofilms (Jogler et al., 2011). If both cell types react to environmental cues in the same way remains unknown. The cultures used in our pilot study were not synchronized and thus the ratio between stalked sessile cells and flagellated swimmer cells might have varied among individual experiments. In addition, increased formation of cell aggregates might explain both the differences in production of secondary metabolites and the differences between OD₆₀₀ and dry weight measurements. This is because aggregates give different OD₆₀₀ values than single free-living cells. Despite such limitations, our approach will allow for the large scale production of planctomycetal compounds. For future studies, alternative reactor models and synchronization of cultures could increase reproducibility in the production of planctomycetal secondary metabolites.

In summary, we presented a pipeline for the utilization of Planctomycetes as sources of novel antibiotics. Screening of marine and limnic planctomycetal species demonstrated discovery of antimicrobial compounds. This finding further supports our hypothesis of allelopathic interactions between phototrophs and Planctomycetes, and emphasizes the usefulness of ecomimetic experiments to stimulate the production of bioactive molecules. This work will provide the starting point for the exploration of Planctomycetes as a currently untapped source of novel bioactive molecules.

AUTHOR CONTRIBUTIONS

OJ and CJ designed the project. OJ and MK cultivated all required bacteria with the help from MJ and extracted crude extracts from planctomycetal cultures. MK, OJ, and FS performed HPLC analysis. MK performed bioreactor experiments and measurements of biomass and glucose consumption. OJ performed with the help of MK activity assays. FS and BF performed HPLC fractionation and mass spectra analysis. PR did phylogenetic analysis. OJ and CJ wrote the manuscript with the help from FS and JW and input from all other authors.

ACKNOWLEDGMENTS

We thank Birte Trunkwalter, Diana Telkemeyer, and Anja Heuer for skillful technical assistance, Prof. Dr. Marc Stadler for support, and Robert Barnett for proofreading the manuscript. This work was supported by the Leibniz Institute DSMZ and by the Deutsche Forschungsgemeinschaft (DFG joint grant SU 936/1-1 and JO 893/4-1).

SUPPLEMENTARY MATERIAL

The Supplementary Material for this article can be found online at: <http://journal.frontiersin.org/article/10.3389/fmcb.2016.01242>

FIGURE S1 | Phylogenetic position of strain Pan216 within the phylum Planctomycetes. The 16S rRNA gene-based tree was reconstructed under the maximum likelihood criterion with 1000 bootstrap resamplings and rooted to a cluster of sequences from anammox Planctomycetes (not shown). Strains of interest (isolate Pan216, *Planctopirus limnophila* and *Rhodopirellula baltica*) are

highlighted in black and bold-faced. Validly published planctomycetal type strains are indicated by gray font and serve as matrix to pronounce the distinct phylogenetic position of strain Pan216. To estimate reliability of the tree branches, maximum parsimony and neighbor joining phylogenetic trees (not shown) were calculated (1000 bootstrap resamplings) and branch support was compared to the maximum likelihood phylogenetic tree. Black dots express bootstrap support values >70%, gray dots express support values >50% but <70%.

FIGURE S2 | High performance liquid chromatography analysis of the marine and limnic cultivation media for Planctomycetes. **(A)** Full medium M1 for limnic Planctomycetes shows high signal peaks after a retention time from 3 to 10 min (intensity up to 8×10^5 Au). **(B)** The chemically defined MM1 shows no detectable signal peaks compared to its full medium M1. **(C)** Full medium M2 for marine Planctomycetes shows high signal peaks after retention time from 20 to 50 min (intensity up to 4×10^5 Au). **(D)** The chemically defined MM2 shows no detectable signal peaks compared to M2.

FIGURE S3 | Dry weight determination of *P. limnophila* cells over 17 days of cultivation in 5 l fermentation with NAG. The dry weight of *P. limnophila* cells increased from 0.6 g/l volume to 2.9 g/l volume after 17 days cultivation. The culture was fed after 7 days with 25 ml NAG and 10 ml vitamin solution (red arrow). This demonstrates that a similar dry-weight could be achieved with NAG as sole carbon source if a fed- batch procedure is employed.

FIGURE S4 | Reproducibility of the HPLC spectra of two distinct *P. limnophila* methanol extracts of 5 l fermentation. In both HPLC spectra of the two distinct extracts similar signal peaks could be detected with slight shifts in retention time and intensity but also differences could be observed. Eight minor peaks (red asterisks) and one major peak (black asterisk) occurred only in one of the two replicates, while only the three major peaks (black arrows) were found in both extracts. The HPLC spectrum of the first extract (green curve) showed the first signal peak after 7 min and a second after 15 min but no peak at 10 min while the HPLC spectrum of the second run (purple curve) showed the first peak at 10 but not after 7 or 15 min. The HPLC spectrum of the second extract revealed six signal peaks after a retention time of 25–32 min and an intensity of 1.56×10^5 Au up to 10^6 Au. In the first extract an additional signal peak at 24 min was detected, the intensity of the signal peak at 25 min decreased from 10^6 Au to 9×10^5 Au, while the peaks at 26 and 27 min were absent. A further additional signal peak in the HPLC spectrum of the first extract was detected at 52 min that was absent in the analysis of the second extract.

REFERENCES

- Bengtsson, M. M., and Øvreås, L. (2010). Planctomycetes dominate biofilms on surfaces of the kelp *Laminaria hyperborea*. *BMC Microbiol.* 10:261. doi: 10.1186/1471-2180-10-261
- Bengtsson, M. M., Sjøtun, K., Lanzen, A., and Øvreås, L. (2012). Bacterial diversity in relation to secondary production and succession on surfaces of the kelp *Laminaria hyperborea*. *ISME J.* 6, 2188–2198. doi: 10.1038/ismej.2012.67
- Bengtsson, M. M., Sjøtun, K., and Øvreås, L. (2010). Seasonal dynamics of bacterial biofilms on the kelp *Laminaria hyperborea*. *Aquat. Microb. Ecol.* 60, 71–83. doi: 10.3354/ame01409
- Berdy, J. (2005). Bioactive microbial metabolites. *J. Antibiot.* 58, 1–26. doi: 10.1038/ja.2005.1
- Christie-Oleza, J. A., Piña-Villalonga, J. M., Bosch, R., Nogales, B., and Armengaud, J. (2012). Comparative proteogenomics of twelve *Roseobacter* exoproteomes reveals different adaptive strategies among these marine bacteria. *Mol. Cell. Proteomics* 11, M111-013110. doi: 10.1074/mcp.m111.013110
- Cooper, M. A., and Shlaes, D. (2011). Fix the antibiotics pipeline. *Nature* 472:32. doi: 10.1038/472032a
- Donadio, S., Monciardini, P., and Sosio, M. (2007). Polyketide synthases and nonribosomal peptide synthetases: the emerging view from bacterial genomics. *Nat. Prod. Rep.* 24, 1073–1109. doi: 10.1039/b514050c
- Fowler, T., Walker, D., and Davies, S. C. (2014). The risk/benefit of predicting a post-antibiotic era: is the alarm working? *Ann. N. Y. Acad. Sci.* 1323, 1–10. doi: 10.1111/nyas.12399
- Frank, C. S., Langhammer, P., Fuchs, B. M., and Harder, J. (2011). Ammonium and attachment of *Rhodopirellula baltica*. *Arch. Microbiol.* 193, 365–372. doi: 10.1007/s00203-011-0681-1
- Fuerst, J. A., and Sagulenko, E. (2011). Beyond the bacterium: planctomycetes challenge our concepts of microbial structure and function. *Nat. Rev. Microbiol.* 9, 403–413. doi: 10.1038/nrmicro2578
- Gade, D., Stührmann, T., Reinhardt, R., and Rabus, R. (2005). Growth phase dependent regulation of protein composition in *Rhodopirellula baltica*. *Environ. Microbiol.* 7, 1074–1084. doi: 10.1111/j.1462-2920.2005.00784.x
- Glöckner, F. O., Kube, M., Bauer, M., Teeling, H., Lombardot, T., Ludwig, W., et al. (2003). Complete genome sequence of the marine planctomycete *Pirellula* sp. strain 1. *Proc. Natl. Acad. Sci. U.S.A.* 100, 8298–8303. doi: 10.1073/pnas.1431443100
- Jeske, O., Jogler, M., Petersen, J., Sikorski, J., and Jogler, C. (2013). From genome mining to phenotypic microarrays: planctomycetes as source for novel bioactive molecules. *Antonie Van Leeuwenhoek* 104, 551–567. doi: 10.1007/s10482-013-0007-1
- Jeske, O., Schüler, M., Schumann, P., Schneider, A., Boedeker, C., Jogler, M., et al. (2015). Planctomycetes do possess a peptidoglycan cell wall. *Nat. Commun.* 6:7116. doi: 10.1038/ncomms8116
- Jogler, C., Glöckner, F. O., and Kolter, R. (2011). Characterization of *Planctomyces limnophilus* and development of genetic tools for its manipulation establish it as a model species for the phylum Planctomycetes. *Appl. Environ. Microbiol.* 77, 5826–5829. doi: 10.1128/AEM.05132-11
- Jogler, C., Waldmann, J., Huang, X., Jogler, M., Glöckner, F. O., Mascher, T., et al. (2012). Identification of proteins likely to be involved in morphogenesis, cell

- division, and signal transduction in Planctomycetes by comparative genomics. *J. Bacteriol.* 194, 6419–6430. doi: 10.1128/JB.01325-12
- Jogler, M., and Jogler, C. (2013). “Towards the development of genetic tools for Planctomycetes,” in *New Models for Cell Structure, Origins and Biology: Planctomycetes*, ed. J. A. Fuerst (Heidelberg: Springer).
- Lage, O. M., and Bondoso, J. (2014). Planctomycetes and macroalgae, a striking association. *Front. Microbiol.* 5:267. doi: 10.3389/fmicb.2014.00267
- Lane, D. J. (ed.) (1991). *16S/23S rRNA Sequencing*. Chichester: Wiley.
- Lee, K. C., Webb, R. I., and Fuerst, J. A. (2009). The cell cycle of the planctomycete *Gemmata obscuriglobus* with respect to cell compartmentalization. *BMC Cell Biol.* 10:4. doi: 10.1186/1471-2121-10-4
- Ludwig, W., Strunk, O., Westram, R., Richter, L., Meier, H., Yadhukumar, et al. (2004). ARB: a software environment for sequence data. *Nucleic Acids Res.* 32, 1363–1371. doi: 10.1093/nar/gkh293
- Morris, R. M., Longnecker, K., and Giovannoni, S. J. (2006). Pirellula and OM43 are among the dominant lineages identified in an Oregon coast diatom bloom. *Environ. Microbiol.* 8, 1361–1370. doi: 10.1111/j.1462-2920.2006.01029.x
- Müller, R., and Wink, J. (2014). Future potential for anti-infectives from bacteria – how to exploit biodiversity and genomic potential. *Int. J. Med. Microbiol.* 304, 3–13. doi: 10.1016/j.ijmm.2013.09.004
- Pilhofer, M., Rappl, K., Eckl, C., Bauer, A. P., Ludwig, W., Schleifer, K. H., et al. (2008). Characterization and evolution of cell division and cell wall synthesis genes in the bacterial phyla Verrucomicrobia, Lentisphaerae, Chlamydiae, and Planctomycetes and phylogenetic comparison with rRNA genes. *J. Bacteriol.* 190, 3192–3202. doi: 10.1128/JB.01797-07
- Pizzetti, I., Fuchs, B. M., Gerdts, G., Wichels, A., Wiltshire, K. H., and Amann, R. (2011a). Temporal variability of coastal Planctomycetes clades at kabeltonne station, North Sea. *Appl. Environ. Microbiol.* 77, 5009–5017. doi: 10.1128/AEM.02931-10
- Pizzetti, I., Gobet, A., Fuchs, B. M., Amann, R., and Fazi, S. (2011b). Abundance and diversity of Planctomycetes in a Tyrrhenian coastal system of central Italy. *Aquat. Microb. Ecol.* 65, 129–141. doi: 10.3354/ame01535
- Pruesse, E., Peplies, J., and Glöckner, F. O. (2012). SINA: accurate high-throughput multiple sequence alignment of ribosomal RNA genes. *Bioinformatics* 28, 1823–1829. doi: 10.1093/bioinformatics/bts252
- Strous, M., Heijnen, J. J., Kuenen, J. G., and Jetten, M. S. M. (1998). The sequencing batch reactor as a powerful tool for the study of slowly growing anaerobic ammonium-oxidizing microorganisms. *Appl. Microbiol. Biotechnol.* 50, 589–596. doi: 10.1007/s002530051340
- Tekniepe, B. L., Schmidt, J. M., and Starr, M. P. (1981). Life cycle of a budding and appendaged bacterium belonging to morphotype IV of the *Blastocaulis*-*Planctomycetes* group. *Curr. Microbiol.* 5, 1–6. doi: 10.1007/BF01566588
- van Niftrik, L., and Jetten, M. S. (2012). Anaerobic ammonium-oxidizing bacteria: unique microorganisms with exceptional properties. *Microbiol. Mol. Biol. Rev.* 76, 585–596. doi: 10.1128/MMBR.05025-11
- van Teeseling, M. C., Mesman, R. J., Kuru, E., Espaillet, A., Cava, F., Brun, Y. V., et al. (2015). Anammox Planctomycetes have a peptidoglycan cell wall. *Nat. Commun.* 6:6878. doi: 10.1038/ncomms7878
- Wegner, C. E., Richter-Heitmann, T., Klindworth, A., Klockow, C., Richter, M., Achstetter, T., et al. (2012). Expression of sulfatases in *Rhodopirellula baltica* and the diversity of sulfatases in the genus *Rhodopirellula*. *Mar. Genomics* 9, 51–61. doi: 10.1016/j.margen.2012.12.001
- Wilson, M. C., Mori, T., Ruckert, C., Uria, A. R., Helf, M. J., Takada, K., et al. (2014). An environmental bacterial taxon with a large and distinct metabolic repertoire. *Nature* 506, 58–62. doi: 10.1038/nature12959
- Zhao, J., Yang, N., and Zeng, R. (2008). Phylogenetic analysis of type I polyketide synthase and nonribosomal peptide synthetase genes in Antarctic sediment. *Extremophiles* 12, 97–105. doi: 10.1007/s00792-007-0107-9

Conflict of Interest Statement: The authors declare that the research was conducted in the absence of any commercial or financial relationships that could be construed as a potential conflict of interest.

Copyright © 2016 Jeske, Surup, Ketteniß, Rast, Förster, Jogler, Wink and Jogler. This is an open-access article distributed under the terms of the Creative Commons Attribution License (CC BY). The use, distribution or reproduction in other forums is permitted, provided the original author(s) or licensor are credited and that the original publication in this journal is cited, in accordance with accepted academic practice. No use, distribution or reproduction is permitted which does not comply with these terms.



Planctomycetes as Novel Source of Bioactive Molecules

Ana P. Graça^{1,2}, Rita Calisto^{1,2} and Olga M. Lage^{1,2*}

¹ Departamento de Biologia, Faculdade de Ciências, Universidade do Porto, Porto, Portugal, ² CIMA—Centro Interdisciplinar de Investigação Marinha e Ambiental—Universidade do Porto, Porto, Portugal

OPEN ACCESS

Edited by:

Damien Paul Devos,
Universidad Pablo de Olavide,
de Sevilla, Spain

Reviewed by:

Suleyman Yildirim,
Istanbul Medipol University
International School of Medicine,
Turkey
Christian Jogler,
DSMZ, Germany

*Correspondence:

Olga M. Lage
olga.lage@fc.up.pt

Specialty section:

This article was submitted to
Evolutionary and Genomic
Microbiology,
a section of the journal
Frontiers in Microbiology

Received: 03 May 2016

Accepted: 26 July 2016

Published: 12 August 2016

Citation:

Graça AP, Calisto R and Lage OM
(2016) Planctomycetes as Novel
Source of Bioactive Molecules.
Front. Microbiol. 7:1241.
doi: 10.3389/fmicb.2016.01241

Marine environments are a fruitful source of bioactive compounds some of which are the newest leading drugs in medicinal therapeutics. Of particular importance are organisms like sponges and macroalgae and their associated microbiome. *Planctomycetes*, abundant in macroalgae biofilms, are promising producers of bioactive compounds since they share characteristics, like large genomes and complex life cycles, with the most bioactive bacteria, the *Actinobacteria*. Furthermore, genome mining revealed the presence of secondary metabolite pathway genes or clusters in 13 analyzed *Planctomycetes* genomes. In order to assess the antimicrobial production of a large and diverse collection of *Planctomycetes* isolated from macroalgae from the Portuguese coast, molecular, and bioactivity assays were performed in 40 bacteria from several taxa. Two genes commonly associated with the production of bioactive compounds, nonribosomal peptide synthetases (NRPS), and polyketide synthases (PKS) genes were screened. Molecular analysis revealed that 95% of the planctomycetes potentially have one or both secondary bioactive genes; 85% amplified with PKS-I primers and 55% with NRPS primers. Some of the amplified genes were confirmed to be involved in secondary metabolite pathways. Using bioinformatic tools their biosynthetic pathways were predicted. The secondary metabolite genomic potential of strains LF1, UC8, and FC18 was assessed using *in silico* analysis of their genomes. Aqueous and organic extracts of the *Planctomycetes* were evaluated for their antimicrobial activity against an environmental *Escherichia coli*, *E. coli* ATCC 25922, *Pseudomonas aeruginosa* ATCC 27853, *Staphylococcus aureus* ATCC 25923, *Bacillus subtilis* ATCC 6633, and a clinical isolate of *Candida albicans*. The screening assays showed a high number of planctomycetes with bioactive extracts revealing antifungal (43%) and antibacterial (54%) activity against *C. albicans* and *B. subtilis*, respectively. Bioactivity was observed in strains from *Rhodopirellula lusitana*, *R. rubra*, *R. baltica*, *Roseimarinima ulvae*, and *Planctomyces brasiliensis*. This study confirms the bioactive capacity of *Planctomycetes* to produce antimicrobial compounds and encourages further studies envisaging molecule isolation and characterization for the possible discovery of new drugs.

Keywords: **planctomycetes, antibiotic activity, antifungal activity, PKS and NRPS genes, screening, secondary metabolite, genome mining**

INTRODUCTION

Diseases like cancer and antibiotic resistance impose us a pressing need for the discovery of new effective leads in their treatment. Since the discovery of penicillin, the miracle drug of the twentieth century by Fleming in 1928, we assisted to a boom of molecules release with antibiotic capacity. Due to excessive and incorrect use of antibiotics and the capacity of bacteria to escape their action, we witnessed, in the last decade, to a dramatic increase of bacterial pathogens presenting multidrug resistance to antibacterial agents (Roca et al., 2015). The search for novel bioactive molecules has been essentially based on terrestrial organisms. However, in the last decades, attention has been paid to marine samples. The unique characteristics of the marine environment allied to its unexplored and unknown biologic diversity makes the marine habitats a potential great source of new bioactive molecules. Moreover, microorganisms, in their adaptation to a multitude of different and sometimes extreme marine conditions, are holders of a myriad of metabolic pathways including secondary metabolite activity that are not found in terrestrial ecosystems (Karabi et al., 2016). Furthermore, they are easily and sustainably cultivated in large scale at a reasonable cost which are good characteristics for technological exploitation (Waites et al., 2001; Debbab et al., 2010).

Bioactive compounds, often produced as secondary metabolites, can be, for example alkaloids, sugars, steroids, terpenoids, peptides, and polyketides (Simmons et al., 2005). These substances are mainly produced as a defense strategy and can be used by man as antibacterial, antifungal, antiviral, antitumor, and immunosuppressive among other potential medicines (Laport et al., 2009). The production of secondary metabolites involves complex molecular structures and biochemical pathways (Hutchinson, 2003). Nonribosomal peptides and polyketides are biocompounds synthesized by two classes of enzymes: the nonribosomal peptides synthetases (NRPS) and polyketide synthases (PKS), respectively (Grozdanov and Hentschel, 2007). These enzymes are responsible for many secondary metabolites that exhibit an important biological activity and may be valuable drugs (Hutchinson, 2003; Ansari et al., 2004; Kennedy et al., 2007). These pathway systems have been studied and described mainly in *Actinobacteria* but are also present in other bacterial taxa and even in filamentous fungi and plants (Ayuso-Sacido and Genilloud, 2005). PKS and NRPS genes are codified by gene clusters presents in the genome of various groups of bacteria (Donadio et al., 2007; Graça et al., 2013, 2015).

Planctomycetes are a bacterial phylum with very particular features that make them good candidates for the production of novel bioactive molecules. They possess complex life cycles and quite large genomes for prokaryotes, characteristics that are typical of bacteria known for their bioactive potential like *Streptomyces* and *Myxobacteria* (Jeske et al., 2013). In their adaptation to a wide range of habitats, including extreme environments (Lage and Bondoso, 2014), planctomycetes developed diversified metabolisms still unexploited. Other characteristics make them unique. These include a complex cell plan (Lage et al., 2013; Santarella-Mellwig et al., 2013),

polar budding of many members (Ward et al., 2006), and the absence of the bacterial division protein FtsZ (Pilhofer et al., 2008), the presence of membrane coat-like proteins (Santarella-Mellwig et al., 2010), and endocytosis (Lonhienne et al., 2010). Although much is still unknown about planctomycetes secondary metabolism, some recent studies have recently pointed out their bioactive potential. Donadio et al. (2007) analyzed the genome of *Rhodopirellula baltica* SH1255 and verified the presence of two small NRPSs, two monomodular PKSs, and a bimodular NRPS-PKS which may be involved in the synthesis of five different, unknown products. In Antarctic sediments, Zhao et al. (2008) identified planctomycetal type I polyketide synthase domains. Using a comprehensive genome mining approach for the analyses of 13 genomes, Jeske et al. (2013) found 102 candidate genes or clusters.

In our study, we explored the bioactive potential of a unique collection of planctomycetes isolated from the biofilm of macroalgae by genome mining, as well as PKS-I and NRPS gene molecular analyses and antimicrobial bioactivity screenings. As biofilms are complex highly dynamic structured ecosystems where strong chemical competition occurs and planctomycetes are relatively slow growing bacteria, these bacteria should possess well-equipped chemical machinery to be able to fight for their survival and impose themselves in such a competing environment.

MATERIALS AND METHODS

Biological Material

The 40 planctomycetes under study, belonging to 10 taxa, were isolated from macroalgae surfaces biofilms within the scope of several diversity and phylogenetic studies carried out in rocky beaches in north of Portugal (Lage and Bondoso, 2011). The bacteria were maintained in pure culture at 25°C in M600/M14 agar medium (Lage and Bondoso, 2011). The phylogenetic relationship of the strains are shown in a phylogenetic tree constructed using the sequences available in GenBank database. The sequences of UC49.2 and FC9.2 were assigned with the following accession numbers—KX495344–KX495345. The sequences were aligned using clustalW, and a final maximum likelihood (ML) phylogenetic tree was generated using the aligned 1316 bp applying the general time reversible model with gamma distributed with invariant sites (G+I) rates in MEGA6.06.

The panel of target microorganisms used in the screening assays were an environmental strain of *E. coli* (Cabral and Marques, 2006), *E. coli* ATCC 25922, *Pseudomonas aeruginosa* ATCC 27853, *Staphylococcus aureus* ATCC 25923, *Bacillus subtilis* ATCC 6633, and a clinical isolate of *C. albicans*.

Amplification and Sequencing of PKS-I and NRPS Genes

Total genomic DNA was extracted from pure cultures using the E.Z.N.A. Bacterial DNA Isolation Kit (Omega), following the recommended instructions. In order to perform the screening of the genomic bioactive potential the degenerate

primers MDPQQRF (5'-RTRGAYCCNCAGCAICG-3') and HGTGTr (5'-VGTNCCNGTGCCRTG-3') and MTRF2 [5'-GCNGG(C/T)GG(C/T)GCNTA(C/T)GTNCC-3'] and DKF (5'-GTGCCGGTNCCRTGNGYYTC-3') were used for the amplification of PKS-I (Kim et al., 2005) and NRPS (Neilan et al., 1999), respectively. These primers amplify for the alpha keto synthetase of PKS-I and core motif-V of NRPS genes. The amplification mixture was composed of 12.5 μ L of NZYtaq 2 \times Green Master Mix, 2 μ L of each primer, 1 μ L genomic DNA as template, and completed with sterilized ultrapure water to a final volume of 25 μ L. The amplification parameters for both primers were identical and the PCR amplifications were performed in a MyCyclerTM Thermo Cycler (Bio-Rad) as described in Graça et al. (2013). The PCR products were visualized after electrophoresis in a 1.2% agarose gel with 1 \times TAE buffer in a VWR GenoPlex. The expected PCR products size of PKS-I and NRPS genes were 750 and 1000 bp, respectively.

Bands with several sizes were excised and purified using Illustra GFX PCR DNA and Gel Band Purification Kit (GE Healthcare) and directly sequenced using appropriate primers. The sequences were manually corrected and consensus constructed by means of Vector NTI Advance 11.5.3. Data used for UC8 PKS-I was the portion of the annotated genome that matched with the amplicon sequenced, with additional 200 bp above and after alignment, in order to retrieve more information for the analysis.

In silico Analysis of PKS-I and NRPS Genes

The resulting consensus sequences of the strains were searched through Basic Local Alignment Search Tool (BLAST), classified in the Nucleotide collection of the National Center of Biotechnology Information (NCBI) based on somewhat similarity. Information regarding similarity and coverage values was assessed for the validation of the amplification of the targeted genes.

Natural Product Domain Seeker—NaPDoS, a bioinformatic tool to search for PKS and NRPS modules and to predict bioactive pathway products, was used based on the FASTA file with the nucleotide sequences choosing Predicted coding sequences or PCR products. The sequences were screened to detect and extract C- (NRPS) and KS- (PKS) domains and candidate secondary metabolites domains (Ziemert et al., 2012).

Blast2go is a fast bioinformatics tool that uses several public databases to assign a biological function to a sequence by identifying similar characterized sequences. This tool was used to compare and confirm results obtained by manual search and NaPDoS. Gene synteny of the results obtained in the prediction of the metabolite pathways were analyzed in SynTax (Oberto, 2013). Nucleotide sequences of the genes were translated into amino acidic sequences using ExPASy tool and the longer sequences translated were used to construct a phylogenetic tree. Phylogenetic and molecular evolutionary analyses were conducted using MEGA version 6 (Tamura et al., 2013). Sequences were aligned using clustalW, and a final ML phylogenetic tree was generated applying Equal input model after searching for the fittest model also in MEGA6.06. Sequences with small size were removed from the analysis.

The sequences used in this study were submitted to GenBank database and the accession number assigned for PKS and NRPS gene sequences were KX306801–KX306815. Since some sequences did not reach enough size to be submitted in this database they are provided as Supplementary Material (Annex I).

Secondary Metabolite Related In silico Analysis of Planctomycete Genomes

The genomes of strains *Rubriphilella obstinata* LF1^T (GenBank: LWSK00000000), *Roseimarinima ulvae* UC8^T (GenBank: LWSJ00000000) and *Planctomycetes* strain FC18 (GenBank: LWSI00000000) used in this study were previously curated and annotated (unpublished results). The contigs were searched for their genomic bioactive potential using antibiotics and Secondary Metabolites Analysis Shell—antiSMASH 3.0 (Weber et al., 2015) and NaPDoS annotation pipelines. The antiSMASH analysis retrieved information of the biosynthetic clusters and of biosynthetic, transport, and regulatory genes present in the submitted genomes by gathering data of several *in silico* secondary metabolite analyses tools. The NaPDoS tool was used as referred above but using the Genome or metagenome contigs (DNA) option. These two tools were used as a complement and for data confirmation.

Antimicrobial Screenings

The screening of antimicrobial activity was performed in 35 planctomycetes (Table 1). Actively growing strains were initially pre-cultured in M600 medium, at 25°C, 220 r.p.m. for 2 days. Each planctomycete was then incubated in M600 and M607 media (Lage and Bondoso, 2011) for 7 days, at 25°C and 220 r.p.m. Each culture was then used to prepare four types of bacterial extracts: 1 aqueous and 3 organic. The organic extracts, for which a mixture of acetone plus 10% DMSO was used, were obtained from culture broth (A/C), cell pellet (A/P), and supernatant (A/S). Two milliliters of culture were used for the A/C; another 2 mL of culture were centrifuged at 13,300 r.p.m. for 5 min and the supernatant (A/S) and pellet (A/P) collected. To these three samples, 2 mL of the solvent mixture were added. These mixtures were incubated for 1 h under continuous shaking and 2 mL of the upper phase (organic) were removed to a new tube and dried to half volume (twice concentrated). To the A/P extracts, sterilized distilled water was added up to 1 mL. To obtain the aqueous supernatant extract (F), 2 mL of culture were centrifuged at 13,300 r.p.m. for 5 min and the supernatant filter sterilized through a 0.22 μ m (Graça et al., 2015).

The target microorganisms used were grown overnight in 10 mL of Luria Broth (LB) medium, at 37°C and 220 r.p.m. Cultures absorbance was measured at 600 nm and the cell concentration adjusted to 2.5×10^5 CFU/mL.

The extracts were assayed in 96 well-plates in triplicates three times. Ninety microliter of each target culture were incubated with 10 μ L of each extract. The cultures were also incubated with 10 μ L of the respective positive control: amphotericin B (0.19, 0.39, 0.78, and 1.56 μ g.mL⁻¹) against *C. albicans*, rifampicin (62.5, 125, 250, and 500 mg.mL⁻¹) against *E. coli* and *P. aeruginosa* and chloramphenicol (3.75, 7.5, 15, and 30 μ g.mL⁻¹) against *B. subtilis* and *S. aureus*. LB medium (100 μ L) was used

TABLE 1 | Results of the molecular analysis and screening of the bioactive potential of the studied Planctomycetes.

| Strain | Genera | Bioactivity against | Bioactivity against | PKS-I size amplicon | NRPS size amplicon | PKS-I genes closest similar result using blastn in NCBI | Similarity; Coverage result using blastn in NCBI | PKS-I genes closest similar result using blastn in NCBI | Similarity; Coverage prediction pathway product | NRPS genes closest similar result using blastn in NCBI | NRPS genes closest similar result using blastn in NCBI | NRPS genes closest similar result using blastn in NCBI | Similarity; Coverage prediction pathway product | Coverage prediction pathway product |
|--------|---|---------------------|---------------------|---------------------|--------------------|---|--|---|---|---|--|--|---|-------------------------------------|
| Rb SH1 | <i>Rhodopirellula</i> <i>baltica</i> | Bioactive | Bioactive | 750 bp | 1000 bp | <i>Rhodopirellula baltica</i> SH 1 complete genome; segment 22/24 | 99%; 99% | <i>Rhodopirellula baltica</i> SH 1 complete genome; segment 22/24 | 100%; 97% epothilone | NSR | — | — | — | — |
| UC21 | <i>Rhodopirellula</i> <i>baltica</i> | Bioactive | Bioactive | 750 bp | — | — | — | — | — | — | — | — | — | — |
| UC49.1 | <i>Rhodopirellula</i> <i>baltica</i> | Bioactive | Bioactive | 750 bp | 1000 bp | <i>Rhodopirellula baltica</i> SH 1 complete genome; segment 22/24 | 97%; 100% | <i>Rhodopirellula baltica</i> SH 1 complete genome; segment 22/24 | 100%; 97% epothilone | — | — | — | — | — |
| FC92 | <i>Rhodopirellula</i> sp. | Bioactive | Bioactive | — | 750 bp | Alpha proteobacterium F16 beta ketosynthase gene, partial cds | 85%; 98% | beta ketosynthase, partial [alpha] proteobacterium F16 | 88%; 100% microcystin | Matched with — PKSI | — | — | — | — |
| FF4 | <i>Rhodopirellula</i> sp. | Not Bioactive | Bioactive | 1000 bp | 750 bp | — | — | NSR | — | NSR | — | — | — | — |
| FC3 | <i>Rhodopirellula</i> <i>rubra</i> | Bioactive | Not Bioactive | 750 bp | 1000 bp | — | — | NSR | — | NSR | — | — | — | — |
| FC17 | <i>Rhodopirellula</i> <i>rubra</i> | Not assayed | Not assayed | — | 1000 bp | — | — | — | — | NSR | — | — | — | — |
| FC15 | <i>Rhodopirellula</i> <i>rubra</i> | Not assayed | Not assayed | 750 bp | 1000 bp | — | — | NSR | — | NSR | — | — | — | — |
| MsF5.1 | <i>Rhodopirellula</i> <i>rubra</i> | Not Bioactive | Not Bioactive | 750 bp | — | — | — | NSR | — | — | — | — | — | — |
| OJF1 | <i>Rhodopirellula</i> <i>rubra</i> | Not assayed | Not assayed | 750 bp | 1000 bp | <i>Rhodopirellula baltica</i> SH 1 complete genome; segment 3/24, dipeptidyl peptidase IV | 90%; 100% | — | — | <i>Myxococcus stipitatus</i> DSM 14675, complete genome, non-ribosomal peptide synthetase | 83%; 34% | surfactin synthetase [<i>Rhodopirellula</i> sp. SWK7] | 94%; 98% HC-Toxin | — |
| LF2 | <i>Rhodopirellula</i> <i>rubra</i> | Not Bioactive | Not Bioactive | 750 bp | — | <i>Rhodopirellula baltica</i> SH 1 complete genome; segment 11/24 | 73%; 68% | putative membrane protein [<i>Rhodopirellula</i> sp. SWK7] | 97%; 100% | — | — | — | — | — |

(Continued)

TABLE 1 | Continued

| Strain | Genera | Bioactivity against <i>Candida albicans</i> | Bioactivity against <i>Bacillus subtilis</i> | PKS-I size amplicon | NRPS size amplicon | PKS-I genes closest similar result using blast in NCBI | Similarity; Coverage result using blast in NCBI | PKS-I genes closest similar result using blast in NCBI | Similarity; Coverage result using blast in NCBI | NRPS genes closest similar result using blastp in NCBI | Similarity; Coverage result using blastp in NCBI | NRPS genes closest similar result using blastp in NCBI | Similarity; Coverage result using blastp in NCBI |
|--------|--------------------------------|---|--|---------------------|--------------------|---|---|--|---|--|--|--|--|
| UC9 | <i>Rhodopirellula rubra</i> | Not Bioactive | Bioactive | 750 bp | 750 bp | — | — | NSR | — | <i>Pancromyces brasiliensis</i> DSM 5305, complete genome, prolyl oligopeptidase | 68%; 40% NSR | Prolyl endopeptidase [Rhodopirellula salentini] NSR | 98%; 100% Bactracin |
| Cc06 | <i>Rhodopirellula lusitana</i> | Not Bioactive | Bioactive | 600 bp | 1000 bp | — | — | NSR | — | <i>Pancromyces brasiliensis</i> DSM 5305, complete genome, prolyl oligopeptidase | — | — | — |
| Cc08 | <i>Rhodopirellula lusitana</i> | Not Bioactive | Bioactive | 600 bp | 1000 bp | Alpha proteobacterium F16 beta ketosynthase gene, partial cds | 85%; 100% partial [alpha] proteobacterium F16 | beta ketosynthase, partial [alpha] proteobacterium F16 | 88%; 89% | pikromycin | Matched with PKS1 | — | — |
| FC24 | <i>Rhodopirellula lusitana</i> | Bioactive | Not Bioactive | 750 bp | 1000 bp | <i>Pirellula staleyi</i> DSM 6068, complete genome | 66%; 94% DSM 6068, complete genome | DUF1501 | 91%; 100% | — | NSR | — | — |
| FC25 | <i>Rhodopirellula lusitana</i> | Not Bioactive | Bioactive | 750 bp | — | <i>Pirellula staleyi</i> DSM 6068, complete genome | 66%; 93% DSM 6068, complete genome | DUF1501 | 91%; 100% | — | — | — | — |
| FC26 | <i>Rhodopirellula lusitana</i> | Not Bioactive | Not Bioactive | 750 bp | — | — | — | NSR | — | <i>Rhodopirellula salentini</i> NSR | — | — | — |
| FC27 | <i>Rhodopirellula lusitana</i> | Not Bioactive | Bioactive | 750 bp | — | — | — | NSR | — | — | — | — | — |
| SM4 | <i>Rhodopirellula lusitana</i> | Bioactive | Bioactive | 750 bp | 1000 bp | — | — | NSR | — | — | NSR | — | — |
| UC13 | <i>Rhodopirellula lusitana</i> | Bioactive | Bioactive | 750 bp | 1000 bp | — | — | NSR | — | <i>Noardia cyriadigeorgica</i> GUH-2 chromosome | 72%; 60% hypothetical protein SMAC_05551 | [<i>Sordaria macrospora</i>] k-hell | 87%; 82% |

(Continued)

TABLE 1 | Continued

| Strain | Genera | Bioactivity against <i>Candida albicans</i> | Bioactivity against <i>Bacillus subtilis</i> | PKS-I size amplicon | NRPS size amplicon | PKS-I genes closest similar result using blastn in NCBI | Similarity; Coverage result using blastn in NCBI | PKS-I genes closest similar result using blastn in NCBI | Similarity; Coverage result using blastn in NCBI | NRPS genes closest similar result using blastn in NCBI | Similarity; Coverage result using blastn in NCBI | NRPS genes closest similar result using blastn in NCBI | Similarity; Coverage result using blastn in NCBI |
|--------|---------------------------------|---|--|---------------------|--------------------|--|--|---|--|--|--|--|--|
| UC16 | <i>Rhodopirellula lusitana</i> | Not Bioactive | Bioactive | 750 bp | 1000 bp | — | — | NSR | — | — | — | — | — |
| UC17 | <i>Rhodopirellula lusitana</i> | Bioactive | Bioactive | — | — | — | — | — | — | — | — | — | — |
| UC20 | <i>Rhodopirellula lusitana</i> | Not Bioactive | Bioactive | — | — | — | — | — | — | — | — | — | — |
| UC22 | <i>Rhodopirellula lusitana</i> | Not Bioactive | Not Bioactive | 750 bp | 1000 bp | — | NSR | — | — | NSR | — | — | — |
| UC31 | <i>Rhodopirellula lusitana</i> | Bioactive | Bioactive | 750 bp | 1000 bp | — | NSR | — | — | NSR | — | — | — |
| UC33 | <i>Rhodopirellula lusitana</i> | Not assayed | Not assayed | 750 bp | 1000 bp | — | NSR | — | — | NSR | — | — | — |
| UC36 | <i>Rhodopirellula lusitana</i> | Bioactive | Bioactive | 600 bp | 1000 bp | — | NSR | — | — | NSR | — | — | — |
| UC38 | <i>Rhodopirellula lusitana</i> | Not Bioactive | Not Bioactive | 600 bp | 1000 bp | Alpha proteobacterium F16 beta ketosynthase gene, partial cds | 86%; 100% beta ketosynthase, partial [alpha] proteobacterium F16 | 92%; 100% stigmatellin | Matched with PKS1 | — | — | — | — |
| UC49.2 | <i>Rhodopirellula lusitana</i> | Not Bioactive | Not Bioactive | 600 bp | — | — | NSR | — | — | NSR | — | — | — |
| UF6 | <i>Rhodopirellula lusitana</i> | Not Bioactive | Bioactive | 1000 bp | 1000 bp | — | NSR | — | — | NSR | — | — | — |
| LF1 | <i>Rubripirellula obscurata</i> | Not assayed | Not assayed | 750 bp | — | — | NSR | — | — | — | — | — | — |
| UC8 | <i>Roseimarinina ulvae</i> | Not Bioactive | Not Bioactive | 750 bp | 1000 bp | Chondromyces croaticus strain Cm c5, complete genome, polyketides synthase | 70%; 91% | — | myxothiazol | — | — | — | — |
| UF2 | <i>Roseimarinina ulvae</i> | Bioactive | Not Bioactive | 1000 bp | — | Brassica rapa subsp. pekinensis clone KBrB081M20, complete sequence | 81%; 16% | — | — | — | — | — | — |

(Continued)

TABLE 1 | Continued

| Strain | Genera | Bioactivity against <i>Candida albicans</i> | Bioactivity against <i>Bacillus subtilis</i> | PKS-I size amplicon | NRPS size amplicon | PKS-I genes closest similar result using blastn in NCBI | Similarity; Coverage | PKS-I genes closest similar result using blastn in NCBI | Similarity; Coverage | NAPDOS prediction pathway product | NRPS genes closest similar result using blastn in NCBI | NRPS genes closest similar result using blastn in NCBI | NRPS genes closest similar result using blastn in NCBI | Similarity; NAPDOS coverage prediction pathway product |
|-----------|----------------------------------|---|--|---------------------|--------------------|--|----------------------|---|----------------------|-----------------------------------|--|--|--|--|
| UF3 | <i>Roseimarinitima ulvae</i> | Bioactive | Not Bioactive | 750 bp | — | <i>Myxococcus hanskus</i> strain mixupis, complete genome. Malonyl CoA-acyl carrier protein transacylase | 66%; 94% | polyketide synthase domain [Nostoc sp. ATCC 53789] | 65%; 99% | stigmatellin | — | — | — | — |
| UF4.2 | <i>Roseimarinitima ulvae</i> | Bioactive | Not Bioactive | 750 bp | — | <i>Nonomuraea spiralis</i> strain IMC A-0156 | 71%; 59% | — | — | stigmatellin | — | — | — | — |
| FC18 | New genus | Not Bioactive | Not Bioactive | — | 1000 bp | — | — | — | — | — | — | — | — | — |
| FF15 | New genus | Not Bioactive | Not Bioactive | 750 bp | 850 bp | <i>Lyngbya majuscula</i> CCAP 1446/4 clone 7 polyketide synthase gene, partial cds | 83%; 100% | <i>Lyngbya majuscula</i> CCAP 1446/4 | 96%; 98% | stigmatellin | NSR | — | — | — |
| Pdt sp. | <i>Planctomyces</i> | Not Bioactive | Not Bioactive | 600 bp | — | — | — | NSR | — | — | — | — | — | — |
| UIF1 Ent1 | <i>Planctomyces</i> | Not Bioactive | Not Bioactive | 600 bp | 850 bp | — | — | NSR | — | — | NSR | — | — | — |
| Gr7 | <i>Planctomyces brasiliensis</i> | Bioactive | Bioactive | 750 bp | — | <i>Procentrum micans</i> polyketide synthase | 82%; 99% | polyketide synthase domain protein [Procentrum micans] | 98%; 96% | myxalamid | — | — | — | — |

NSR, No Sequence Resulted; Blast was searched in NCBI using somewhat similar sequences and the selected hit was the one with the highest coverage. Blastp was searched in NCBI using somewhat similar sequences and the selected hit was the one with the highest similarity. NaPDOS is a webserver tool that allows the prediction of biosynthetic pathways.

as negative control and 100 µL of the target cultures were used to control the normal growth of the strains, both done in triplicate. To ensure that neither the solvent mixture (acetone+DMSO) nor the media induced inhibition of the cultures, 10 µL of each condition was assayed with 90 µL of culture of each target strain as controls. The inoculated plates were incubated at 37°C and 220 r.p.m for 24 h. Initial and final absorbance measurements were performed at 600 nm in a Multiskan GO plate reader (Thermo Scientific) and analyses of the assays were carried out as described in Graça et al. (2015). Extracts were only considered bioactive when inhibitory values above 20% were obtained in two or more assays showing, thus, consistency in the results.

RESULTS

The genomic potential of *Planctomycetes* to produce bioactive compounds was assessed by amplification and sequencing of PKS-I and NRPS genes and analysis *in silico* of tree genomes (UC8, LF1, and FC18). Furthermore, screening assays were performed in order to assess the production of antimicrobial molecules.

PKS-I and NRPS Genes, Molecular, and *In silico* Analysis

The search for the conserved motifs of the ketosynthase of the PKS-I genes and core motif V of NRPS genes was performed in 40 planctomycetes of 10 different taxa (Table 1; Figure S1). Amplicons with several sizes were obtained from 38 strains and bands extracted, DNA purified and sequenced. Only 24 strains were amplified for the expected product size (750 bp) and 10 for other product sizes with the PKS-I primers. With the NRPS primers, 17 planctomycetes amplified for the expected product size (1000 bp) and five for other product sizes (Table 1). Since these genes are understudied in *Planctomycetes*, amplicons of unexpected sizes were also sequenced. It was only possible to retrieve sequences from 18 amplicons. Seven out of the 11 amplicons with 750 bp and 2 amplicons with 600 bp amplified with PKS-I primers confirmed the presence of the ketosynthase gene in the planctomycetes. Two ketosynthase genes were confirmed with the sequencing of NRPS amplicons of 600 bp. Two amplicons of PKS-I genes with 750 bp were found with potential to codify for a DUF1501 domain-containing protein (FC24 and FC25), one for a putative membrane protein (LF2) and another for a *Rhodopirellula* dipeptidyl peptidase IV (OJF1). Concerning the NRPS amplification, only three amplicons provided sequences confirming the presence of NRPS modules (UC13, OJF1, and UC9). The Blast2go tool analysis of the sequenced amplicons confirmed the results obtained in the previous step using Blast in NCBI database (Table S1).

The phylogenetic tree using the amino acids corresponding to the amplified PKS-I and the NRPS sequences revealed that the PKS-I clustered together but were separated from the NRPS with the exception of *R. ulvae* UF4.2 PKS-I which may be a hybrid PKS-NRPS (Figure 1). The PKS-I from two strains of *R. baltica* clustered together as well as those of *Rhodopirellula lusitana*. When considering the site sampling, phylogeny

(Figure S1), or macroalgal host-origin of the planctomycetes analyzed (Lage and Bondoso, 2011), no correlation could be obtained.

NaPDoS analysis showed that 10 of the amplified genes encoded for modular KS and have somewhat similarity with known secondary metabolite pathways involved in the production of antitumor (UC49.1, UC8, and Rb), antibiotic (Gr7 and CcC8), antifungal (Gr7), quinol inhibitor (FF15, UF4.2, UF3, and UC38), and toxins (FC9.2) (Table 1). Regarding NRPS genes, NaPDoS *in silico* analysis showed a codification of C domain with potential production of a toxin for OJF1 and a DCL domain with potential production of bacitracin for UC9. Since the percentage of similarity of the sequences obtained using the NaPDoS is less than 80%, the prediction had to be confirmed by blastnr. Furthermore, *R. ulvae* strains most probably have uncharacterized biosynthetic gene clusters since similarities lower than 85% were obtained with blastnr. In fact, comparing the different analyses *in silico* performed, all the strains belonging to the taxa *R. ulvae* (UC8, UF3, and UF4.2) showed the presence of a PKS-I gene cluster not yet characterized being the highest percentage of similarity of 71% in strain UF4.2.

Secondary Metabolite Related *In silico* Analysis of UC8, FC18, and LF1 Genomes

Nowadays, several are the tools available to search for biosynthetic clusters, which are able to predict and provide information on the genomic potential for the production of bioactive compounds. In this work, antiSMASH, and NaPDoS tools were used. The antiSMASH analysis showed that LF1 was the one with higher number of biosynthetic clusters (9), followed by UC8 (8), and FC18 (5; Figure 2). UC8 is the only strain that possesses PKS-I clusters and LF1 the only one that possesses a resorcinol cluster.

However, a closer analysis of the clusters related to secondary metabolites revealed that UC8 is the strain with higher number of biosynthetic genes (43), followed by LF1 (35), and FC18 (16; Figure 3). The genes codifying for glycosyl transferase group I, AMP-dependent synthethase, and ligase, terpene-cyclase, polyprenyl synthase, and phytene synthase are shared by all the strains. Additionally to these genes, UC8, and LF1 are the strains that share more genes (7), while UC8 and FC18 share 3 genes, and LF1 and FC18 only one. Regarding unique biosynthetic genes, UC8 is again the one that possesses the higher number with 18 genes, LF1 has 15 genes, and FC18 only 6 (Figure 3).

Although LF1 is the strain with the higher number of biosynthetic clusters it does not have any kind of NRPS gene (Figure 2) and contains the lowest number of regulatory genes (Figure S2). LF1's genome also contains in one cluster a codification for an unknown biosynthetic pathway with a regulatory gene similar to a LuxR response regulator and another cluster coding for a terpene which has an AraC family transcriptional regulator and two sigma-54 dependent transcriptional regulators. One cluster of UC8 is a hybrid NRPS-PKS-I which encodes for an epothilone biosynthetic gene and holds a tetR family transcriptional regulator. A PKS-I cluster of

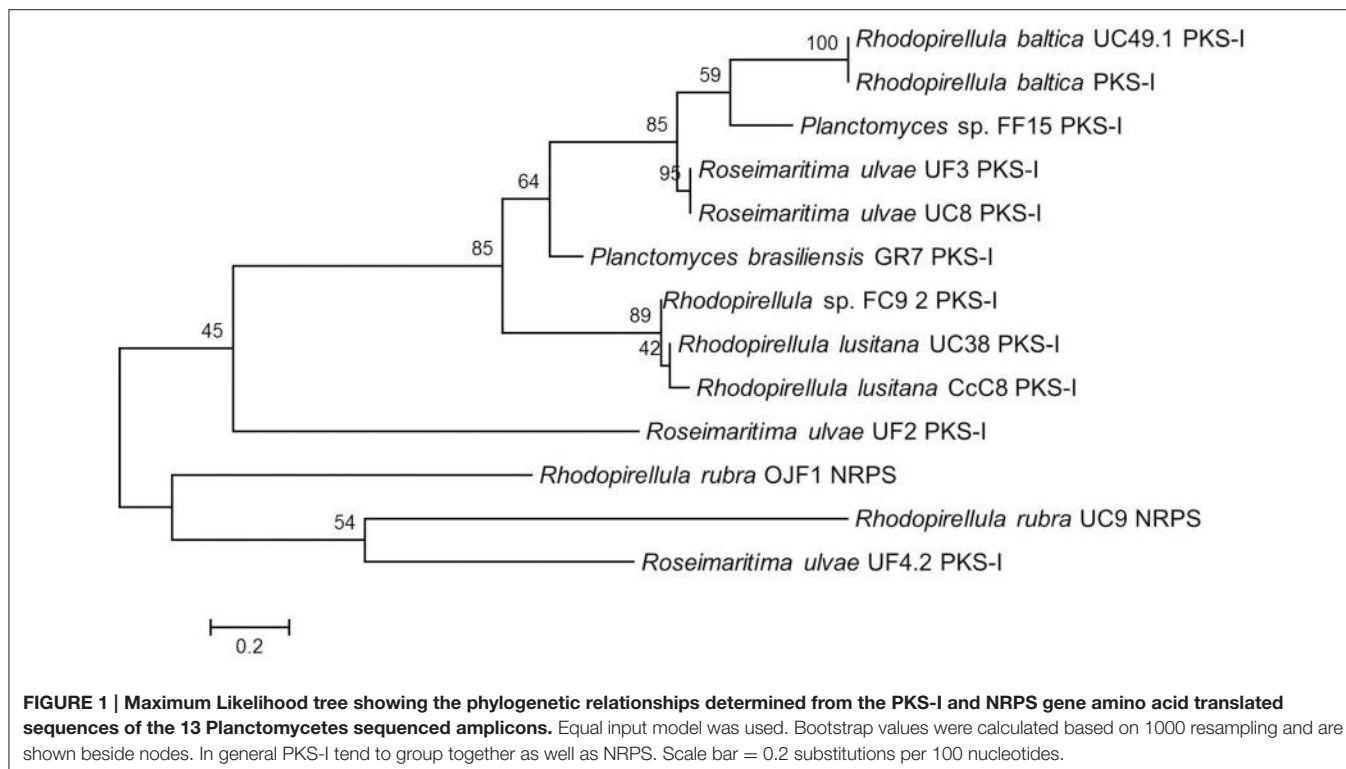


FIGURE 1 | Maximum Likelihood tree showing the phylogenetic relationships determined from the PKS-I and NRPS gene amino acid translated sequences of the 13 Planctomycetes sequenced amplicons. Equal input model was used. Bootstrap values were calculated based on 1000 resampling and are shown beside nodes. In general PKS-I tend to group together as well as NRPS. Scale bar = 0.2 substitutions per 100 nucleotides.

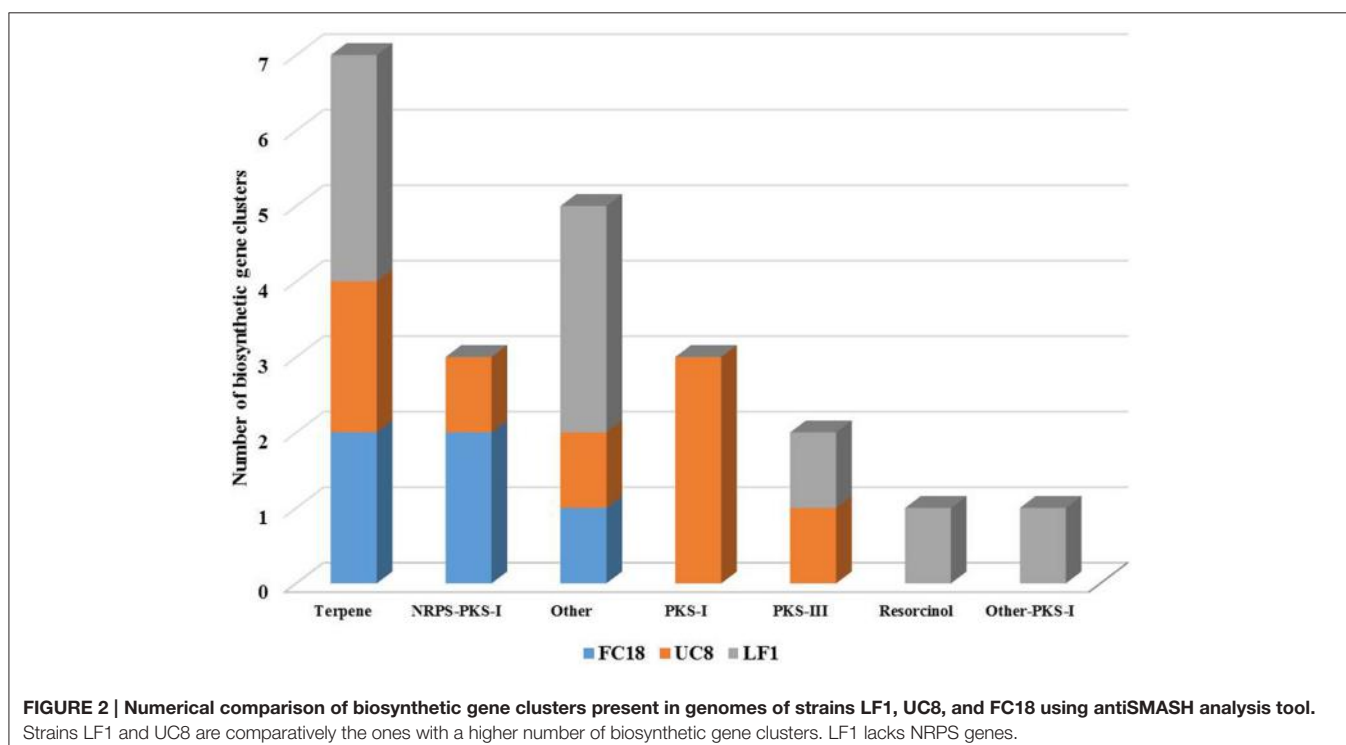


FIGURE 2 | Numerical comparison of biosynthetic gene clusters present in genomes of strains LF1, UC8, and FC18 using antiSMASH analysis tool. Strains LF1 and UC8 are comparatively the ones with a higher number of biosynthetic gene clusters. LF1 lacks NRPS genes.

UC8 holds a *GntR* family transcriptional regulator. There are still five clusters with unknown attributed function and in all the clusters there are still some uncharacterized biosynthetic, transport and regulatory genes (Figure 2; Figure S2).

NaPDoS analysis of genomes secondary pathways confirmed (1) gene similarities lower than 80%; (2) lack of any kind of NRPS genes in LF1; (3) the presence of NRPS-PKS hybrids in FC18 and UC8; and (4) that UC8 was the strain with the highest

number of secondary metabolite genes (**Figure 4**). Hepatotoxic (FC18), anticancer (FC18 and UC8), antifungal (LF1, UC8, and FC18), and antibiotic (LF1) activities were predicted by NaPDos.

Bioactivity Assays with Planctomycetes

The production of bioactive compounds by the planctomycetes was only assessed in 35 strains due to growth limitation (**Table 1**). Two culture media (M600 and M607) and four types of extracts were assayed. Forty-three percent (15 strains) of the strains were active against *C. albicans* and 54% (19 strains) against *Bacillus subtilis*. Low activity was detected against the two strains of *E. coli* and no activity was obtained against *P. aeruginosa* and *S. aureus*.

Figure 5 shows planctomycetes inhibition obtained against *C. albicans*. The two more relevant extracts due to consistency and level of inhibition were the aqueous supernatants of the culture broths (F) in M600 from SM4 (average activity of 60%) and from UC13 (average activity of 52%). The majority of the bioactive extracts against *C. albicans* are from bacteria incubated in medium M600 (83%). UC13 was the only strain that induced inhibition with all extracts from M600. Three extracts were bioactive for SM4: pellet (A/P), organic supernatant (A/S), and aqueous supernatant (F). Only the supernatant extracts (A/S and F) from the strains UC31, FC27 when incubated in M600 were active. For *R. baltica* SH1^T only extracts A/C and F in M600 were active. Strains FC3, FC9.2, UC36, and Gr7 only induced bioactivity when the extracts were obtained from the pellet. Strains UF2 and UF4.2 induced bioactivity with the aqueous supernatant (F) when incubated in M600. However, when these strains were incubated in M607 the bioactive extract was obtained from the organic crude extract.

Regarding *Bacillus subtilis* (**Figure 6**), the strains with consistent higher values of inhibitions were the organic supernatants (A/S) in M600 of CcC8, UC31, and UF6 (average activity of 52, 50, and 48%, respectively). However, the crude extract of UF6 in M600 was the most inhibitory one with 66% of average inhibition. The nine extracts with higher activity against *B. subtilis* had approximately the same inhibitory activity as 7.5 µg/ml chloramphenicol (the third concentration of the MIC). The extracts obtained from strains incubated in M600 (77 strains) were more active than the ones incubated in M607. Sixty-eight percent of the bioactive extracts were obtained from the supernatant of the cultures broths [organic (A/S) or aqueous (F)]. No pellet extract was active. While F extract in M600 obtained from FC9.2 was the least inhibitory (22% inhibition), the value of inhibition raised to 35% when the supernatant was extracted with acetone. The bioactive extracts of CcC6 in M607, CcC8 in M607, FC27 in M607, SM4 in M600, and UF6 in M600 were A/C and A/S which may indicate that the bioactive molecules are possibly polar and secreted to the media. Also FF4, UC13, and UC20 may produce bioactive molecules to the media since all the bioactive extracts were obtained from A/S and F extracts.

Ten strains were able to produce both antibiotic and antifungal compounds: *R. baltica* SH1^T; UC49.1; UC21; SM4; UC13; UC17; UC31; UC36, Gr7; and FC9.2. In this work, 24 planctomycetes (69%) revealed bioactivity potential.

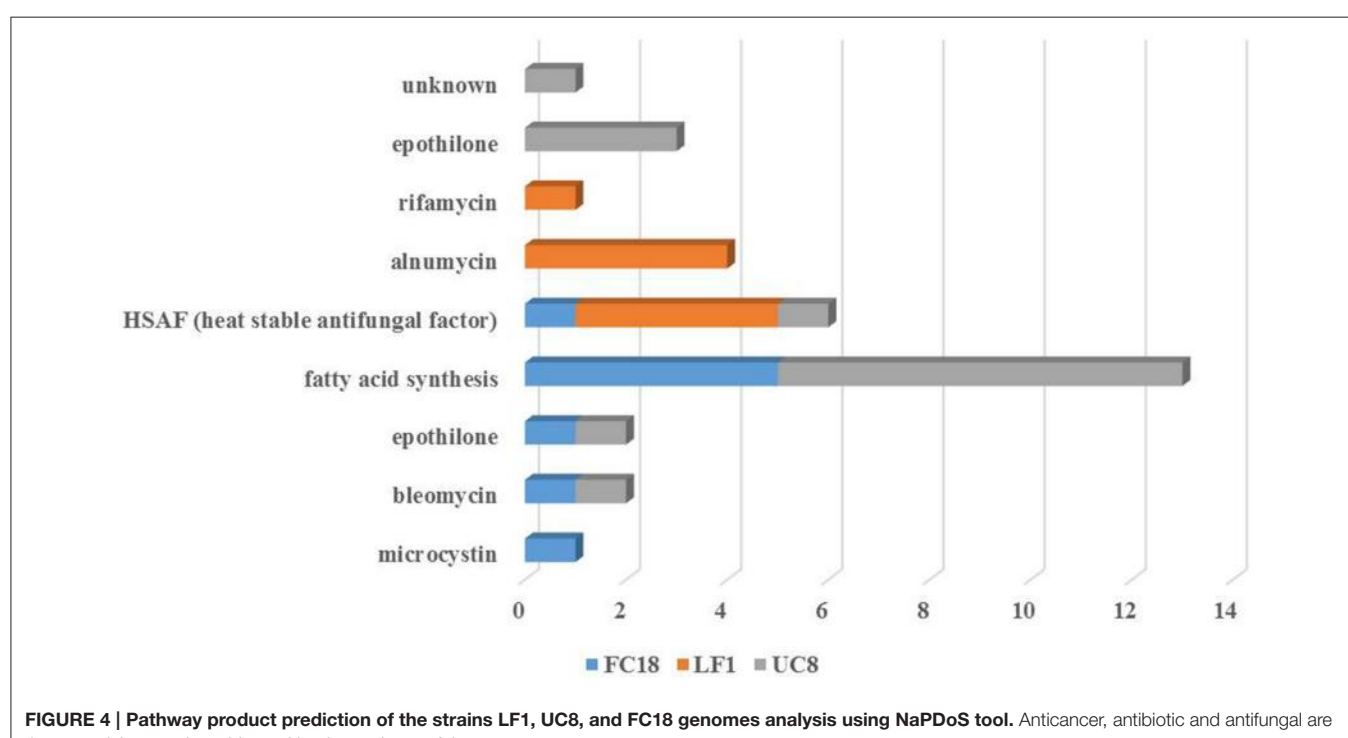
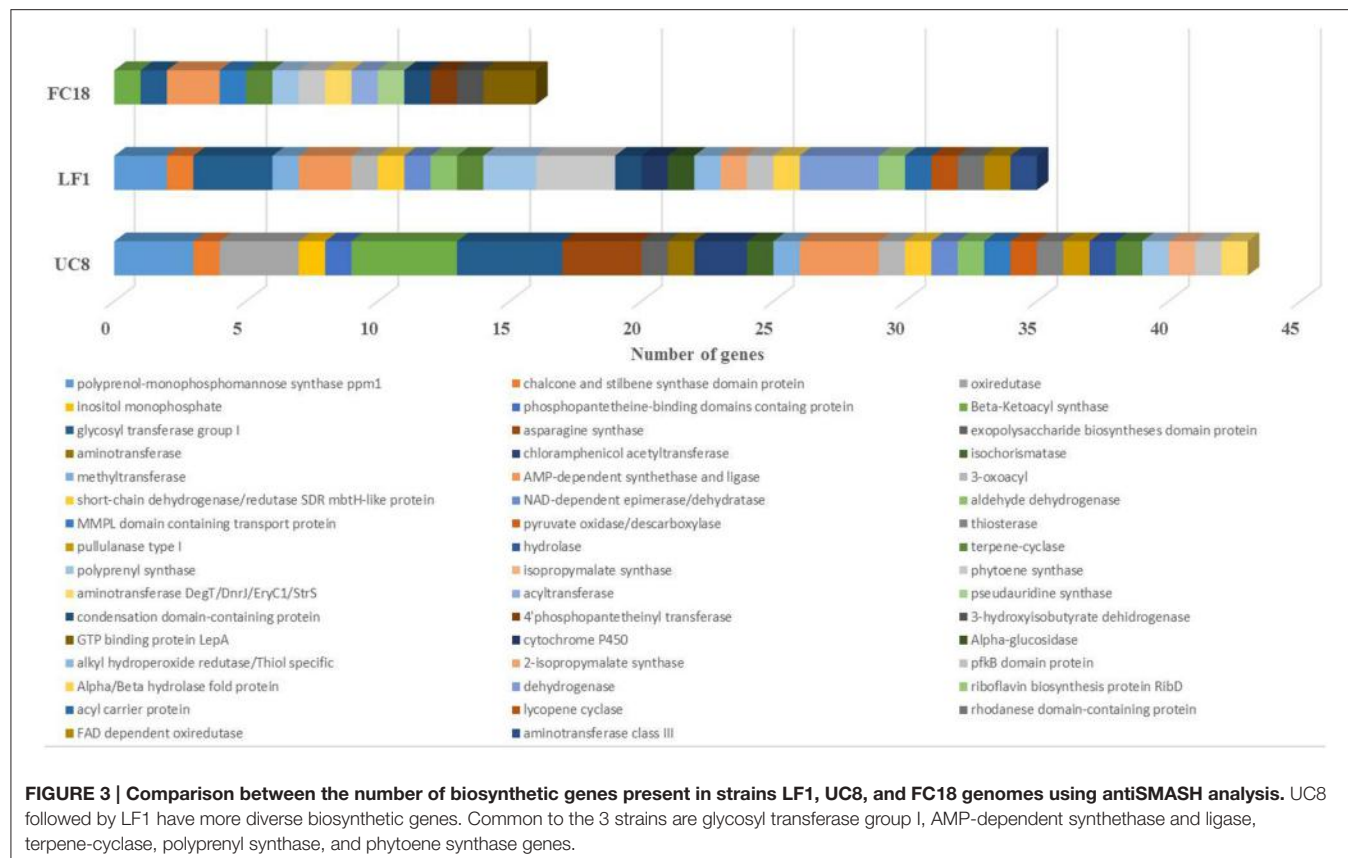
DISCUSSION

Nonribosomal peptides and polyketides are important groups of secondary metabolites accounting for a significant portion of known natural products (Walsh, 2004; Wang et al., 2014). In an extensive genome mining of NRPS and PKS genes across the three domains, Wang et al. (2014) observed that NRPS and type I PKS clusters were more frequent in the phyla *Proteobacteria*, *Firmicutes*, *Actinobacteria*, and *Cyanobacteria*. Regarding *Planctomycetes* only a significant lower number (seven) was analyzed of which five possessed PKS and hybrid NRPS/PKS clusters. These results are in accordance with ours since we only detected PKS and hybrids genes.

In our screening, although a high number of amplicons was obtained for both type I PKS (66%) and NRPS (47%) genes, only a reduced number could be confirmed to be PKS or NRPS genes after sequencing. This may be due to the presence of more than one KS and NRPS domain which may interfere with the direct sequencing of the amplicons. Furthermore, four non-specific amplifications (LF2, FC24, FC25, and UF2) were also obtained with these primers which indicate the necessity to confirm the amplifications obtained by sequencing. The phylogenetic analyses of the retrieved PKS-I and NRPS sequences also suggested that some planctomycetes that clustered together (**Figure 1**; FC9.2, UC38, CcC8) may possess hybrid NRPS/PKS-I modules because the amplified PKS-I sequences (**Table 1**) were obtained with NRPS primers. The detection of PKS genes with NRPS primers may also be a result of the low specificity of the degenerate primers used in our work. Tambadou et al. (2014) also obtained sequences without similarity to the A domain of NRPSs in their study with marine mudflat bacteria.

The molecular analysis performed (**Table 1**) confirmed the previous genome mining result obtained for *R. baltica* SH1^T which showed the presence of a type I PKS gene in this bacterium (Jeske et al., 2013). Furthermore, the NaPDos tool predicted that this gene, present in both *R. baltica* strains SH1 and UC49.1, may encode for an epothilone. Gene structural similarity between the two *R. baltica* is also evidenced by their phylogenetic relationship (**Figure 1**). Although no absolute confirmation can be taken regarding putative products, the analysis of the closest similar products indicates an epothilone pathway for the two strains of *R. baltica*. Epothilones are a new class of tubulin target agents effective against human malignant disease (Cheng et al., 2008). Originally epothilone was discovered from *Sorangium cellulosum*, a myxobacterium isolated from the banks of Zambesi River in Africa, and showed to be highly cytotoxic *in vitro* to the human T-24 bladder carcinoma cell line (Gerth et al., 1996).

The presence of a polyketide synthase gene in *Planctomyces* strain Gr7 is shared with *Planctomyces brasiliensis* (Jeske et al., 2013) and these two planctomycetes have a 16 S rRNA gene similarity of 100% (Lage and Bondoso, 2011) which demonstrates their closeness. A predicted myxalamid pathway was foreseen for the type I PKS gene sequenced from *Planctomyces* strain Gr7. Myxalamids are antibiotics produced by the myxobacterium *Myxococcus xanthus* and are known to block the respiration chain at the site of complex I, i.e., NADH:ubiquinone oxidoreductase (Gerth et al., 1983).



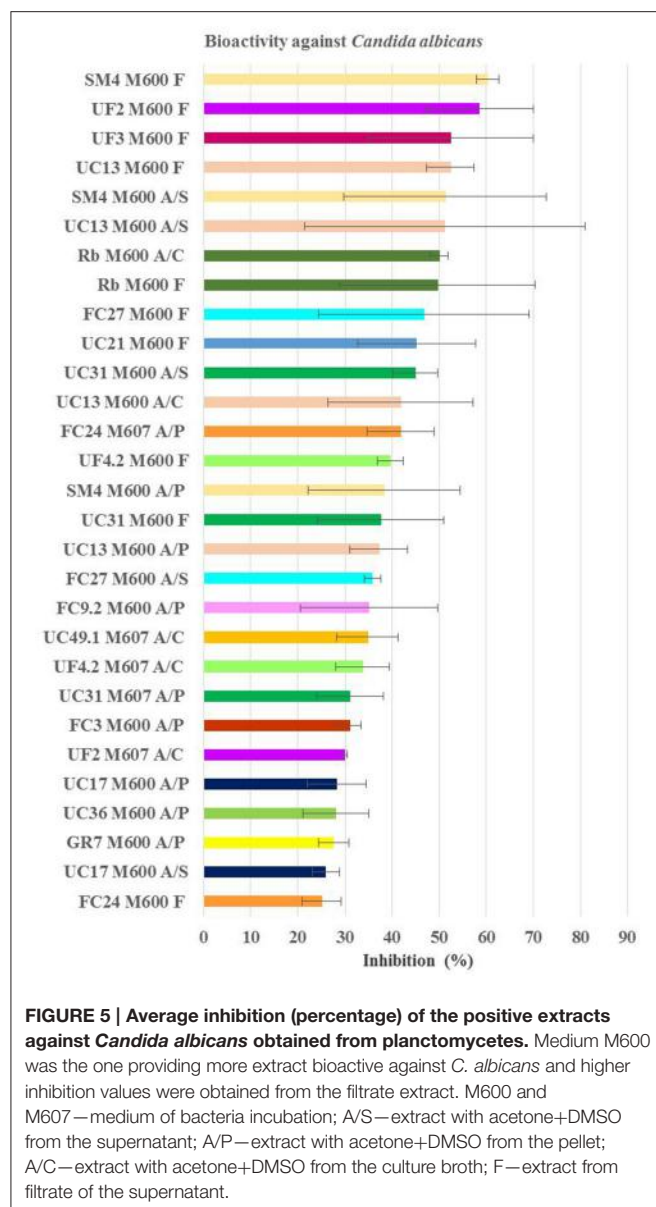


FIGURE 5 | Average inhibition (percentage) of the positive extracts against *Candida albicans* obtained from planctomycetes. Medium M600 was the one providing more extract bioactive against *C. albicans* and higher inhibition values were obtained from the filtrate extract. M600 and M607—medium of bacteria incubation; A/S—extract with acetone+DMSO from the supernatant; A/P—extract with acetone+DMSO from the pellet; A/C—extract with acetone+DMSO from the culture broth; F—extract from filtrate of the supernatant.

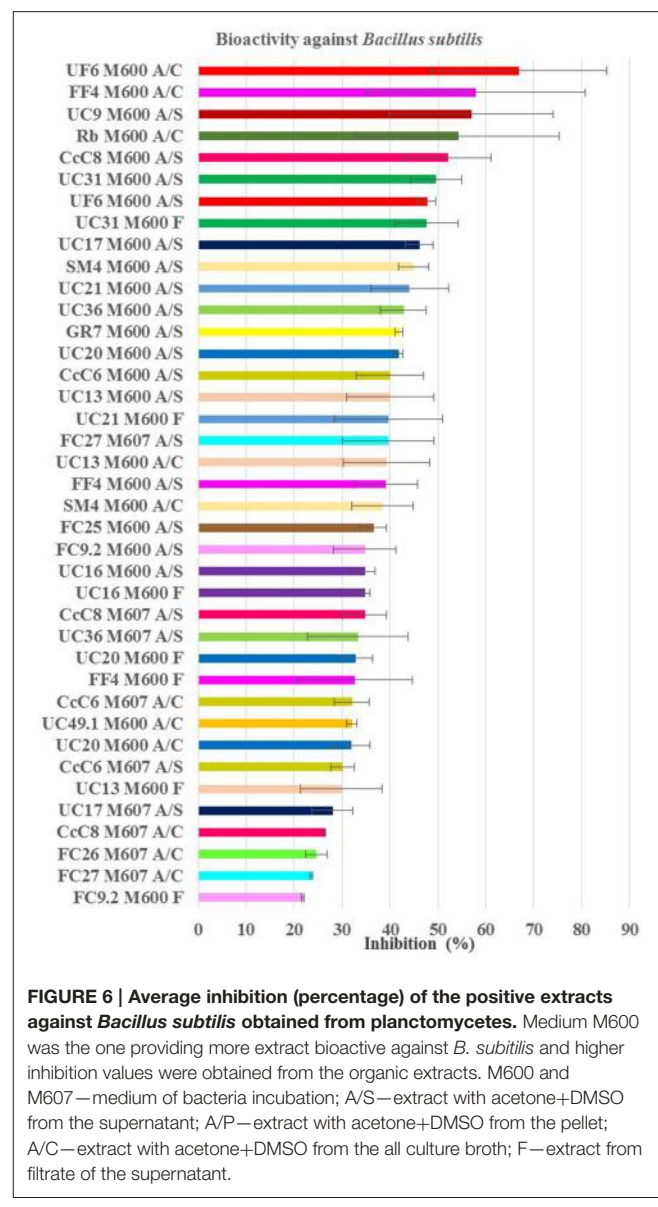


FIGURE 6 | Average inhibition (percentage) of the positive extracts against *Bacillus subtilis* obtained from planctomycetes. Medium M600 was the one providing more extract bioactive against *B. subtilis* and higher inhibition values were obtained from the organic extracts. M600 and M607—medium of bacteria incubation; A/S—extract with acetone+DMSO from the supernatant; A/P—extract with acetone+DMSO from the pellet; A/C—extract with acetone+DMSO from the culture broth; F—extract from filtrate of the supernatant.

R. lusitana strain UC38, *R. ulvae* UF3, and UF4.2 and an uncharacterized new genus, strain FF15, revealed to amplify a type I PKS gene with a predicted production of stigmatellin which is an antibiotic produced by the myxobacterium *Stigmatella aurantiaca* (Oettmeier et al., 1985). This antibiotic is a potent electron transfer inhibitor of photosynthetic and respiratory electron transports, inhibiting the quinol oxidation (Qo) site of the cytochrome b6f complex of thylakoid membranes, of the cytochrome bc1 complex (ubiquinol-cytochrome c reductase or complex III) in mitochondria and of the bacterial photosynthetic reaction center (Thierbach et al., 1984; Giangiacomo et al., 1987).

R. ulvae UC8 amplified also for a type I PKS gene that potentially encodes for a myxothiazol which is an antifungal antibiotic from the myxobacterium *Myxococcus fulvus* (Gerth et al., 1980). Although its binding site is different of that of stigmatellin, myxothiazol also is a competitive inhibitor

of ubiquinol. It binds at the quinol oxidation (Qo) site of the mitochondrial cytochrome bc1 complex (Ouchane et al., 2002). On the original screening of myxothiazol, Gerth et al. (1980) observed growth inhibition of *B. subtilis* in plate culture although no MIC concentration was determined. However, good effectiveness of this antibiotic was detected against filamentous fungi (Gerth et al., 1980). In our study no bioactivity was detected by *R. ulvae* UC8 against neither *C. albicans* nor *B. subtilis* so optimization of growth conditions is needed in order to attempt the induction of such synthetic pathway.

Our results suggest that *Planctomycetes* potentially may have several similar secondary metabolite pathways (epothilone, stigmatellin, myxothiazol, myxamid) to *Myxobacteria*. This bacterial group is known for their complex cell cycle, bioactive potential, and large genomes (Schneiker et al., 2007; Huntley et al., 2012). Also the gene synteny analysis revealed higher

similarity with *Myxobacteria* PKS-I genes than with other *Planctomycetes* (**Figure S3**).

Besides secondary pathways related to *Myxobacteria*, other pathways are also present. Microcystin pathway is possibly encoded by *R. lusitana* CcC8 and *Rhodopirellula* sp. FC9.2. The synteny analysis of the PKS-I amplicon from FC9.2 revealed its similarity to mcyE gene from *Microcystis aeruginosa* NIES 843 (**Figure S3**). Microcystins are a class of cyclic heptapeptide toxins produced by several freshwater cyanobacteria namely members of *Microcystis*, *Planktothrix*, *Anabaena*, *Oscillatoria*, and *Nostoc* but recent evidence also suggest that they are also being produced in the oceans by a number of cosmopolitan marine species (Vareli et al., 2013). Microcystin biosynthesis gene cluster has a highly conserved organization which includes NRPS, PKS, and hybrid NRPS-PKS genes as has been characterized in the genus *Microcystis* (Noguchi et al., 2009).

Regarding NRPS, UC9 demonstrated putative capacity for the production of bacitracin, a mixture of cyclic peptides with antibiotic properties through the inhibition of the cell wall synthesis, produced by strains of *Bacillus licheniformis* (Stone and Strominger, 1971). However, when gene synteny of the NRPS was analyzed, closer similarity was obtained with genes from Planctomycetes and with a different strain of *Bacillus* (**Figure S3**) Furthermore, *R. rubra* OJF1 NRPS matches a HC-toxin that is the host-selective toxin of the maize pathogen (Walton, 2006).

Noteworthy is the low similarity of the predicted pathways obtained in the analysis with NaPDoS tool databases which can reveal the undiscovered pathways possessed by these strains. The blastnr PKS-I and NRPS values obtained are indicative of new secondary pathways, especially the PKS-I amplified from *R. ulvae* strains which have the lowest similarity to their closest relatives. Although the other planctomycetes strains used in this study possess higher similarity values, their closest relatives do not have their pathways characterized.

In the genome analysis of the three planctomycetes (LF1, FC18, and UC8), besides PKS and NRPS clusters, a resorcinol cluster was found in LF1. Resorcinol can be used as an antiseptic and disinfectant in the treatment of chronic skin diseases such as psoriasis, hidradenitis suppurativa, and eczema, as an oxidative hair coloring product and as a food additive [SCCS (Scientific Committee on Consumer Safety), 2010]. Furthermore, terpene clusters are present in the three genomes. Terpenes comprehend the largest class of plant natural products (Boutanaev et al., 2015) but their bacterial origin has been known for many years and terpene synthases are widely distributed in bacteria (Yamada et al., 2015). Terpenes seem to be present in all planctomycetes genomes (Jeske et al., 2013; Aghnatiotis et al., 2015) and terpenoid synthases may be likely involved in carotenoid synthesis (Jeske et al., 2013).

Strain LF1 has a transcriptional regulator of the AraC family associated with the cluster coding for a terpene. These regulators are widespread among bacteria and may be involved in the stress responses to virulence (Frota et al., 2004). LF1 also has extracytoplasmic function sigma factor (ECFs), two sigma-54 dependent transcription regulators. This particular ECF has been regulated to various cellular processes like mobility, virulence, biofilm formation, and nitrogen assimilation (Francke et al.,

2011). Although different ECFs were found, their presence in planctomycetes has been previously described (Jogler et al., 2012). Through the study of transcriptional regulators and transporter genes found associated to the biosynthetic clusters, the production of the secondary metabolites may be optimized as well as their signaling induction.

The genomes analyzed sustain the relation between large genomes and high number of biosynthetic clusters (Jeske et al., 2013). However, FC18 is the strain with lower number of biosynthetic clusters and genes which could be related to the fact that it was the one that also provided the lowest information for the annotation analysis. Also the absence of NRPS genes in LF1 is in line with Jeske et al. (2013) where, summing up all the results, only 38% of the planctomycetes possess any type of NRPS genes. The secondary metabolite potential of our strains falls short of that of *Gemmata assimilans* and *Schlesneria paludicola* which are still the strains with the highest number of secondary metabolites pathways (Aghnatiotis et al., 2015)

The products obtained by pathway prediction of the three genomes using NaPDoS showed that these strains are potentially able to produce a heat-stable antifungal factor (**Figure 4**). This novel model of antifungal activity is encoded by a hybrid NRPS-PKS that induces inhibition against a wide range of fungal species (Yu et al., 2007). Furthermore, UC8 and FC18 showed genomic potential to produce anticancer agents due to the potential presence of epothilone and bleomycin pathways. Bleomycin is a polyamine antibiotic produced by *Streptomyces verticillus* known for its use in cancer treatment and also its toxicity to bacteria and some tissues (Cohen and Josephine, 1976). Strain LF1 possesses genomic potential for the production of antibiotics with predicted pathways for rifamycin and alnumycin that can show different bioactive properties. Ryfamycin is an important antibiotic produced by several bacterial strains like *Nocardia* RSP-3, *Amycolatopsis mediterranei*, marine *Actinobacteria* and the marine sponge bacteria *Salinispora* and it is used to treat tuberculosis leprosy and AIDS-related mycobacterial infections (El-Tayeb et al., 2004; Kim et al., 2006; Hewavitharana et al., 2007; Mahalaxmi et al., 2008). Alnumycin, initially discovered from an endophytic *Streptomyces* sp., is an antibiotic with several biological activities like inhibition of Gram positive bacteria and human leukemia cells (Bieber et al., 1998).

Merging the information from the molecular and screening assays we were able to confirm the genomic potential of nine strains (SH1, UC49.1, FC9.2, UC9, CcC8, UC13, UF3, UF4.2, Gr7). However, for 3 strains (UC38, UC8 and FF15), their bioactivity is still undisclosed. This may be due to the specificity of the produced compounds that may target different strains or possess activities not screened for, such as antitumor or antimalarial, or even to the need of different induction conditions for the production of the compounds.

Stepping to the antimicrobial production, *R. baltica* showed antibiotic and antifungal capacity. *R. lusitana* was the species with the highest values of bioactivity against both *C. albicans* and *B. subtilis*. Although *R. rubra* amplified for PKS-I and NRPS genes no secondary metabolite pathway could be predicted with NaPDoS and only bioactivity was detected against *B. subtilis* by one strain (UC9). *R. ulvae* putatively possesses genes encoding for the production of the antibiotics myxothiazol and stigmatellin

and demonstrated high level of activity against *C. albicans* with the filtrate extracts of UF2, UF3, and UF4.2, lower activity with organic crude (A/C) extracts and no activity against *B. subtilis*. The novel genus of strain FF15 showed putative synthetic capacity for the production of stigmatellin but no bioactivity could be detected. *P. brasiliensis* Gr7 demonstrated a great antimicrobial capacity and the genomic potential production of myxalamid.

Regarding the bioactivity screening, while some pellet extracts were bioactive against *C. albicans*, none was active against *B. subtilis* showing that the antifungal compounds were released to the external medium. This is reinforced by the fact that most of the bioactive extracts were obtained from the supernatants (F). The fact that the number of bioactive supernatant extracts obtained with acetone is lower than the aqueous ones can be explained by low affinity of the molecules with the organic solvent used. Occasionally, the pellet and supernatant extracts obtained from a strain were both active while the crude was not, suggesting, thus, an effect among the molecules extracted. This effect may be due to interference with binding sites or counter active actions of the molecules (Jia et al., 2009).

Bioactivity against *C. albicans* and *B. subtilis* was mainly obtained when the planctomycetes were grown in M600 (respectively, 83 and 77% of the extracts), which is, comparatively to M607, a medium with four fold yeast extract, peptone and glucose. M600 appears to be the best medium for bioactivity screenings of planctomycetes. It seems to favor their antimicrobial production due to the favorable higher organic medium conditions and/or the higher biomass yield (absorbance measurements obtained when the bacteria were grown with M600 were in general twice higher than the ones obtained when incubated with M607—data not shown). These favor the growth of fast growing heterotrophs which compete against slower growing microorganisms like planctomycetes (doubling times of several hours to days). The complexity of species and interactions in biofilms impose the development of survival strategies for their members. Moreover, all strains were isolated from the surface of macroalgae, where they are subjected to high levels of released polysaccharides and various forms of environmental stresses like abrupt and broad changes in salinity and temperature, high light intensities, and pollution. As antimicrobials production was higher under higher organic medium conditions, we postulate that high levels of organic carbon may favorably trigger the production of antimicrobials by planctomycetes, a plus for bacteria fighting for their presence in biofilms. Several compounds, mainly polysaccharides, released by macroalgae were identified as potential triggers for secondary metabolite production (Jeske et al., 2013). *In vitro* antibiotics production is commonly favored by starvation conditions which are opposite to the hypothesis here formulated. However, we do not know antibiotics role in the natural environment and how they favor the producing organisms, but it is believed that they control other microbes competing with their neighbors for space and resources (Clardy et al., 2009; Hibbing et al., 2010).

Our results provide diverse and consistent evidence of secondary metabolite production by several planctomycetes with the production of putative novel metabolites of biotechnological

interest. Furthermore, the study of planctomycetes compounds that are already known is of the utmost importance as they may have different properties, namely regarding side effects. The presence of genes related to bioactive pathways or bioactivity production in all strains here studied seem to be indicative of their potential ability to fight against their competitor in the biofilm of macroalgae. The analysis of the three genomes (FC18, LF1, and UC8) also revealed that these strains possess a great potential to cope with environmental stress (unpublished results). We should emphasize that this is the first study reporting a high percentage of Planctomycetes extracts with a great antibiotic and antifungal activity against *Bacillus subtilis* and *C. albicans*. Further, studies into the secondary molecules production by these scarcely studied bacteria open the door to new promising and challenging biotechnological studies.

AUTHOR CONTRIBUTIONS

Conceived and designed the experiments: AG, OL. Performed the experiments: AG, RC. Analyzed the results: AG, RC, OL. Wrote the manuscript: AG, RC, OL. All authors have read and approved the manuscript.

FUNDING

This research was partially supported by the Strategic Funding UID/Multi/04423/2013 through national funds provided by FCT—Foundation for Science and Technology and European Regional Development Fund (ERDF), in the framework of the programme PT2020 and by the Structured Program of R&D&I INNOVMAR – Innovation and Sustainability in the Management and Exploitation of Marine Resources (reference NORTE-01-0145-FEDER-000035, Research Line NOVELMAR), funded by the Northern Regional Operational Programme (NORTE2020) through the European Regional Development Fund (ERDF).

SUPPLEMENTARY MATERIAL

The Supplementary Material for this article can be found online at: <http://journal.frontiersin.org/article/10.3389/fmich.2016.01241>

Annex 1 | PKS-I sequences not used in the phylogenetic tree because of their small bp size and not submitted to GenBank database.

Table S1 | Results of the *in silico* analysis performed with the Blast2go tool. These results confirm the ones obtained manually by search with Blastnr in GenBank database.

Figure S1 | Phylogenetic 16 S rDNA tree generated by maximum-likelihood analysis based in General Time Reversible model and Gamma distributed with Invariant sites (G+I) indicating the relationship of the Planctomycetes used in this work. Bar—0.05 substitutions per 1000 nucleotides.

Figure S2 | Number and description of transport and regulatory genes present in strains LF1, UC8, and FC18 genomes reported by antiSMASH analysis. UC8 is the strain with higher number of regulatory genes.

Figure S3 | Result of the synteny analysis of Planctomycetes PKS and NRPS amplicons sequences with the closest strains as matched in

REFERENCES

- Aghnatiros, R., Cayrou, C., Garibal, M., Robert, C., Azza, S., Raoult, D., et al. (2015). Draft genome of *Gemmata massiliiana* sp. nov, a water-borne Planctomycetes species exhibiting two variants. *Stand. Genomic Sci.* 10, 120. doi: 10.1186/s40793-015-0103-0
- Ansari, M. Z., Yadav, G., Gokhale, R. S., and Mohanty, D. (2004). NRPS-PKS: a knowledge-based resource for analysis of NRPS/PKS megasynthases. *Nucleic Acids Res.* 32, W405–W413. doi: 10.1093/nar/gkh359
- Ayuso-Sacido, A., and Genilloud, O. (2005). New PCR primers for the screening of NRPS and PKS-I systems in actinomycetes: detection and distribution of these biosynthetic gene sequences in major taxonomic groups. *Microb. Ecol.* 49, 10–24. doi: 10.1007/s00248-004-0249-6
- Bieber, B., Nuske, J., Ritzau, M., and Grafe, U. (1998). Alnumycin a new naphthoquinone antibiotic produced by an endophytic *Streptomyces* sp. *J. Antibiot.* 51, 381–382. doi: 10.7164/antibiotics.51.381
- Boutanaev, A. M., Moses, T., Zi, J., Nelson, D. R., Mugford, S. T., Peters, R. J., et al. (2015). Investigation of terpene diversification across multiple sequenced plant genomes. *Proc. Natl. Acad. Sci. U.S.A.* 112, E81–E88. doi: 10.1073/pnas.1419547112
- Cabral, J. P., and Marques, C. (2006). Faecal coliform bacteria in Febros river (northwest Portugal): temporal variation, correlation with water parameters, and species identification. *Environ. Monit. Assess.* 118, 21–36. doi: 10.1007/s10661-006-0771-8
- Cheng, K. L., Bradley, T., and Budman, D. R. (2008). Novel microtubule-targeting agents – the epithilones. *Biologics* 2, 789–811. doi: 10.2147/BTT.S3487
- Clardy, J., Fischbach, M., and Currie, C. (2009). The natural history of antibiotics. *Curr. Biol.* 19, R437–R441. doi: 10.1016/j.cub.2009.04.001
- Cohen, S. S., and Josephine, I. (1976). Synthesis and the lethality of bleomycin in bacteria. *Cancer Res.* 36, 2768–2774.
- Debbab, A., Aly, A. H., Lin, W. H., and Proksch, P. (2010). Bioactive compounds from marine bacteria and fungi. *Microb. Biotechnol.* 3, 544–563. doi: 10.1111/j.1751-7915.2010.00179.x
- Donadio, S., Monciardini, P., and Sosio, M. (2007). Polyketide synthases and nonribosomal peptide synthetases: the emerging view from bacterial genomics. *Nat. Prod. Rep.* 24, 1073–1109. doi: 10.1039/b514050c
- El-Tayeb, O. M., Salama, A. A., Hussein, M. M. M., and El-Sedawy, H. F. (2004). Optimization of industrial production of rifamycin B by *Amycolatopsis mediterranei*. I. The role of colony morphology and nitrogen sources in productivity. *Afr. J. Biotechnol.* 3, 266–272. doi: 10.5897/AJB2004.000-2049
- Francke, C., Kormelink, T. G., Hagemeijer, Y., Overmars, L., Sluijter, V., Moeselaar, R., et al. (2011). Comparative analyses imply that the enigmatic Sigma factor 54 is a central controller of the bacterial exterior. *BMC Genomics* 12:385. doi: 10.1186/1471-2164-12-385
- Frota, C. C., Papavinasasundaram, K. G., Davis, E. O., and Colston, M. J. (2004). The AraC family transcriptional regulator Rv1931c plays a role in the virulence of mycobacterium tuberculosis. *Infect. Immun.* 72, 5483–5486. doi: 10.1128/IAI.72.9.5483-5486.2004
- Gerth, K., Bedorf, N., Höfle, G., Irschik, H., and Reichenbach, H. (1996). Epothilons A and B: antifungal and cytotoxic compounds from *Sorangium cellulosum* (Myxobacteria). Production, physico-chemical and biological properties. *J. Antibiot.* 49, 560–563. doi: 10.7164/antibiotics.49.560
- Gerth, K., Irschik, H., Reichenbach, H., and Trowitzsch, W. (1980). Myxothiazol, an antibiotic from *Myxococcus fulvus* (myxobacterales). I. Cultivation, isolation, physico-chemical and biological properties. *J. Antibiot.* 33, 1474–1479. doi: 10.7164/antibiotics.33.1474
- Gerth, K., Jansen, R., Reifenstahl, G., Höfle, G., Irschik, H., Kunze, B., et al. (1983). The myxalamids, new antibiotics from *Myxococcus xanthus* (Myxobacterales). I. Production, physico-chemical and biological properties, and mechanism of action. *J. Antibiot.* 36, 1150–1156. doi: 10.7164/antibiotics.36.1150
- Giangiacomo, K. M., Robertson, D. E., and Dutton, P. L. (1987). “Stigmatellin and other electron transfer inhibitors as probes for the QB binding site in the reaction center of photosynthetic bacteria,” in *Progress in Photosynthesis Research*, ed J. Biggins (Dordrecht: Martinus Nijhoff), 409–412.
- Graça, A. P., Bondoso, J., Gaspar, H., Xavier, J. R., Monteiro, M. C., de la Cruz, M., et al. (2013). Antimicrobial activity of heterotrophic bacterial communities from the marine sponge *Erylus discophorus* (Astrophorida, Geodiidae). *PLoS ONE* 8:e78992. doi: 10.1371/journal.pone.0078992
- Graça, A. P., Viana, F., Bondoso, J., Correia, M. I., Gomes, L., Humanes, M., et al. (2015). The antimicrobial activity of heterotrophic bacteria isolated from the marine sponge *Erylus deficiens* (Astrophorida, Geodiidae). *Front. Microbiol.* 6:389. doi: 10.3389/fmicb.2015.00389
- Grozdanov, L., and Hentschel, U. (2007). An environmental genomics perspective on the diversity and function of marine sponge-associated microbiota. *Curr. Opin. Microbiol.* 10, 215–220. doi: 10.1016/j.mib.2007.05.012
- Hewavitharana, A. K., Shaw, P. N., Kim, T. K., and Fuerst, J. A. (2007). Screening of rifamycin producing marine sponge bacteria by LC-MS-MS. *J. Chromatogr. B Analyt. Technol. Biomed. Life Sci.* 852, 362–366. doi: 10.1016/j.jchromb.2007.01.042
- Hibbing, M. E., Fuqua, C., Parsek, M. R., and Peterson, S. B. (2010). Bacterial competition: surviving and thriving in the microbial jungle. *Nat. Rev. Microbiol.* 8, 15–25. doi: 10.1038/nrmicro2259
- Huntley, S., Zhang, Y., Treuner-Lange, A., Kneip, S., Sensen, C. W., and Søgaard-Andersen, L. (2012). Complete genome sequence of the fruiting myxobacterium *Coralloccoccus coralloides* DSM 2259. *J. Bacteriol.* 194, 3012–3013. doi: 10.1128/JB.00397-12
- Hutchinson, C. R. (2003). Polyketide and non-ribosomal peptide synthases: falling together by coming apart. *Proc. Natl. Acad. Sci. U.S.A.* 100, 3010–3012. doi: 10.1073/pnas.0730689100
- Jeske, O., Jogler, M., Petersen, J., Sikorski, J., and Jogler, C. (2013). From genome mining to phenotypic microarrays: planctomycetes as source for novel bioactive molecules. *Antonie Van Leeuwenhoek* 104, 551–567. doi: 10.1007/s10482-013-0007-1
- Jia, J., Zhu, F., Ma, X., Cao, Z. W., Li, Y., and Chen, Y. Z. (2009). Mechanisms of drug combinations: interaction and network perspectives. *Nat. Rev. Drug Discov.* 8, 111–128. doi: 10.1038/nrd2683
- Jogler, C., Waldmann, J., Huang, X., Jogler, M., Glöckner, F. O., Mascher, T., et al. (2012). Identification of proteins likely to be involved in morphogenesis, cell division, and signal transduction in planctomycetes by comparative genomics. *J. Bacteriol.* 194, 6419–6430. doi: 10.1128/JB.01325-12
- Karabi, B., Dipak, P., and Sankar, N. S. (2016). Marine bacteria: a potential tool for antibacterial activity. *J. Appl. Environ. Microbiol.* 4, 25–29. doi: 10.12691/jaem-4-1-3
- Kennedy, J., Marchesi, J. R., and Dobson, A. D. W. (2007). Metagenomic approaches to exploit the biotechnological potential of the microbial consortia of marine sponges. *Appl. Microbiol. Biotechnol.* 75, 11–20. doi: 10.1007/s00253-007-0875-2
- Kim, T. K., Hewavitharana, A. K., Shaw, P. N., and Fuerst, J. A. (2006). Discovery of a new source of rifamycin antibiotics in marine sponge *Actinobacteria* by phylogenetic prediction. *Appl. Environ. Microbiol.* 72, 2118–2125. doi: 10.1128/AEM.72.3.2118-2125.2006
- Kim, T. K., Mary, J., Garson, M. J., and Fuerst, J. A. (2005). Marine actinomycetes related to the salinospora group from the great barrier reef sponge *pseudoceratinia clavata*. *Environ. Microbiol.* 7, 509–518. doi: 10.1111/j.1462-2920.2005.00716.x
- Lage, O. M., and Bondoso, J. (2011). Planctomycetes diversity associated with macroalgae. *FEMS Microbiol. Ecol.* 78, 366–375. doi: 10.1111/j.1574-6941.2011.01168.x
- Lage, O. M., and Bondoso, J. (2014). Planctomycetes and macroalgae, a striking association. *Front. Microbiol.* 5:267. doi: 10.3389/fmicb.2014.00267
- Lage, O. M., Bondoso, J., and Lobo-da-Cunha, A. (2013). Insights into the ultrastructural morphology of novel Planctomycetes. *Antonie Van Leeuwenhoek* 104, 467–476. doi: 10.1007/s10482-013-9969-2
- NaPDoS.** All the strains were also searched against *Planctomycetales* group for synteny. Only the results with higher similarity are shown.

- Laport, M. S., Santos, O. C. S., and Muricy, G. (2009). Marine sponges: potential sources of new antimicrobial drugs. *Curr. Pharm. Biotechnol.* 10, 86–105. doi: 10.2174/138920109787048625
- Lonhienne, T. G., Sagulenko, E., Webb, R. I., Lee, K. C., Franke, J., and Devos, D. P., et al. (2010). Endocytosis-like protein uptake in the bacterium *Gemmata obscuriglobus*. *Proc. Natl. Acad. Sci. U.S.A.* 107, 12883–12888. doi: 10.1073/pnas.1001085107
- Mahalaxmi, Y., Rao, C. S., Suvarnalaxmi, G., Sathish, T., Sudhakar, P., and Prakasham, R. S. (2008). Rifamycin B production pattern in Nocardia RSP-3 strain and influence of barbital on antibiotic production. *Curr. Trends Biotechnol. Pharmacy* 2, 208–216.
- Neilan, B. A., Dittmann, E., Rouhiainen, L., Amanda, R., Schaub, V., et al. (1999). Nonribosomal peptide synthesis and toxicogenicity of cyanobacteria nonribosomal peptide synthesis and toxicogenicity of cyanobacteria. *J. Bacteriol.* 181, 4089–4097
- Noguchi, T., Shinohara, A., Nishizawa, A., Asayama, M., Nakano, T., Hasegawa, M., et al. (2009). Genetic analysis of the microcystin biosynthesis gene cluster in *Microcystis* strains from four bodies of eutrophic water in Japan. *J. Gen. Appl. Microbiol.* 55, 111–123. doi: 10.2323/jgam.55.111
- Oberto, J. (2013). SyntTax: a web server linking synteny to prokaryotic taxonomy. *BMC Bioinformatics.* 14:4. doi: 10.1186/1471-2105-14-4
- Oettmeier, W., Godde, D., and Höfle, G. (1985). Stigmatellin. A dual type inhibitor of photosynthetic electron transport. *Biochim. Biophys. Acta* 807, 216–219. doi: 10.1016/0005-2728(85)90125-2
- Ouchane, S., Agalidis, I., and Astier, C. (2002). Natural resistance to inhibitors of the ubiquinol cytochrome c oxidoreductase of rubrivivax gelatinosus: sequence and functional analysis of the cytochrome bc1 complex. *J. Bacteriol.* 184, 3815–3822 doi: 10.1128/jb.184.14.3815-3822.2002
- Pilhofer, M., Rappl, K., Eckl, C., Bauer, A. P., Ludwig, W., Schleifer, K. H., et al. (2008). Characterization and evolution of cell division and cell wall synthesis genes in the bacterial phyla Verrucomicrobia, Lentisphaerae, Chlamydiae, and Planctomycetes and phylogenetic comparison with rRNA genes. *J. Bacteriol.* 190, 3192–3202. doi: 10.1128/JB.01797-07
- Roca, I., Akova, M., Baquero, F., Carlet, J., Cavalieri, M., Coenen, S., et al. (2015). The global threat of antimicrobial resistance: science for intervention. *New Microbes New Infect.* 6, 22–29. doi: 10.1016/j.nmni.2015.02.007
- Santarella-Mellwig, R., Franke, J., Jaedicke, A., Gorjanacz, M., Bauer, U., Budd, A., et al. (2010). The compartmentalized Bacteria of the Planctomycetes-Verrucomicrobia-Chlamydiae superphylum have membrane coat-like proteins. *PLoS Biol.* 8:e1000281. doi: 10.1371/journal.pbio.1000281
- Santarella-Mellwig, R., Pruggnaller, S., Roos, N., Mattaj, I. W., and Devos, D. P. (2013). Three-dimensional reconstruction of bacteria with a complex endomembrane system. *PLoS Biol.* 11:e1001565. doi: 10.1371/journal.pbio.1001565
- SCCS (Scientific Committee on Consumer Safety) (2010). *Opinion on Resorcinol. COLIPA n° A11*. Brussels: European Union.
- Schneiker, S., Perlava, O., Kaiser, O., Gerth, K., Alici, A., Altmeier, M. O., et al. (2007). Complete genome sequence of the myxobacterium *Sorangium cellulosum*. *Nat. Biotechnol.* 25, 1281–1289. doi: 10.1038/nbt1354
- Simmons, T. L., Andrianasolo, E., McPhail, K., Flatt, P., and Gerwick, W. H. (2005). Marine natural products as anticancer drugs. *Mol. Cancer Ther.* 4, 333–342.
- Stone, K. J., and Strominger, J. L. (1971). Mechanism of action of bacitracin: complexation with metal ion and C 55 -isoprenyl pyrophosphate. *Proc. Natl. Acad. Sci. U.S.A.* 68, 3223–3227. doi: 10.1073/pnas.68.12.3223
- Tambadou, F., Lanneluc, I., Sablé, S., Klein, G. L., Doghri, I., Sopéna, V., et al. (2014). Novel nonribosomal peptide synthetase (NRPS) genes sequenced from intertidal mudflat bacteria. *FEMS Microbiol. Lett.* 357, 123–130. doi: 10.1111/1574-6968.12532
- Tamura, K., Stecher, G., Peterson, D., Filipski, A., and Kumar, S. (2013). MEGA6: Molecular Evolutionary Genetics Analysis version 6.0. *Mol. Biol. Evol.* 30, 2725–2729. doi: 10.1093/molbev/mst197
- Thierbach, G., Kunze, B., and Höfle, G. (1984). The mode of action of stigmatellin, a new inhibitor of the cytochrome bc1 segment of the respiratory chain. *Biochim. Biophys. Acta* 765, 227–235. doi: 10.1016/0005-2728(84)90017-3
- Vareli, K., Jaeger, W., Touka, A., Frillingos, S., Briasoulis, E., and Sainis, I. (2013). Hepatotoxic seafood poisoning (HSP) due to microcystins: a threat from the ocean? *Mar. Drugs* 11, 2751–2768. doi: 10.3390/md11082751
- Waites, M. J., Morgan, N. L., Higton, G., and Rockey, J. S. (2001). *Industrial Microbiology: An Introduction*. Oxford: Blackwell Science.
- Walsh, C. T. (2004). Polyketide and nonribosomal peptide antibiotics: modularity and versatility. *Science* 303, 1805–1810. doi: 10.1126/science.1094318
- Walton, J. D. (2006). HC-toxin. *Phytochemistry* 67, 1406–1413. doi: 10.1016/j.phytochem.2006.05.033
- Wang, H., Fewer, D. P., Holm, L., Rouhiainen, L., and Sivonen, K. (2014). Atlas of nonribosomal peptide and polyketide biosynthetic pathways reveals common occurrence of nonmodular enzymes. *Proc. Natl. Acad. Sci. U.S.A.* 24, 9259–9264. doi: 10.1073/pnas.1401734111
- Ward, N., Staley, J. T., Fuerst, J. A., Giovannoni, S., Schlesner, H., and Stackebrandt, E. (2006). “The order Planctomycetales, including the genera planctomyces, pirellula, gemmata and isosphaera and the candidatus genera brocadia, kuenenia and scalindua,” in *The Prokaryotes: A Handbook on the Biology of Bacteria*, Vol. 7, eds M. Dworkin, S. Falkow, E. Rosenberg, K. H. Schleifer and E. Stackebrandt (New York, NY: Springer), 757–793.
- Weber, T., Blin, K., Duddela, S., Krug, D., Kim, H. U., Brucolieri, R., et al. (2015). antiSMASH 3.0—a comprehensive resource for the genome mining of biosynthetic gene clusters *Nucleic Acids Res.* 1, W237–W243. doi: 10.1093/nar/gkv437
- Yamada, Y., Kuzuyama, T., Komatsu, M., Shin-ya, K., Omura, S., Cane, D. E., et al. (2015). Terpene synthases are widely distributed in bacteria. *Proc. Natl. Acad. Sci. U.S.A.* 112, 857–862. doi: 10.1073/pnas.1422108112
- Yu, F. G., Zaleta-Rivera, K., Zhu, X. C., Huffman, J., Millet, J. C., Harris, S. D., et al. (2007). Structure and biosynthesis of heat-stable antifungal factor (HSAF), a broad-spectrum antimycotic with a novel mode of action. *Antimicrob. Agents Chemother.* 51, 64–72. doi: 10.1128/AAC.00931-06
- Zhao, J., Yang, N., and Zeng, R. (2008). Phylogenetic analysis of type I polyketide synthase and nonribosomal peptide synthetase genes in Antarctic sediment. *Extremophiles* 12, 97–105. doi: 10.1007/s00792-007-0107-9
- Ziemert, N., Podell, S., Penn, K., Badger, J. H., Allen, E., and Jensen, P. R. (2012). The natural product domain seeker napdos: a phylogeny based bioinformatic tool to classify secondary metabolite gene diversity. *PLoS ONE* 7:e34064. doi: 10.1371/journal.pone.0034064

Conflict of Interest Statement: The authors declare that the research was conducted in the absence of any commercial or financial relationships that could be construed as a potential conflict of interest.

Copyright © 2016 Graça, Calisto and Lage. This is an open-access article distributed under the terms of the Creative Commons Attribution License (CC BY). The use, distribution or reproduction in other forums is permitted, provided the original author(s) or licensor are credited and that the original publication in this journal is cited, in accordance with accepted academic practice. No use, distribution or reproduction is permitted which does not comply with these terms.



Identification and Partial Characterization of a Novel UDP-N-Acetylenolpyruvoylglucosamine Reductase/UDP-N-Acetylmuramate:L-Alanine Ligase Fusion Enzyme from *Verrucomicrobium spinosum* DSM 4136^T

OPEN ACCESS

Edited by:

Laura Van Niftrik,
Radboud University, Netherlands

Reviewed by:
Felipe Cava,

The Laboratory of Molecular Infection
Medicine Sweden, Sweden
Alexander John Frederick Egan,
Newcastle University, UK

***Correspondence:**
André O. Hudson
aohsbi@rit.edu

[†]These authors have contributed
equally to this work.

Specialty section:

This article was submitted to
Evolutionary and Genomic
Microbiology,
a section of the journal
Frontiers in Microbiology

Received: 11 January 2016

Accepted: 07 March 2016

Published: 23 March 2016

Citation:

Naqvi KF, Patin D, Wheatley MS,
Savka MA, Dobson RCJ, Gan HM,
Barreteau H, Blanot D,
Mengin-Lecreux D and Hudson AO
(2016) Identification and Partial
Characterization of a Novel UDP-N-
Acetylenolpyruvoylglucosamine
Reductase/UDP-N-
Acetylmuramate:L-Alanine Ligase
Fusion Enzyme from
Verrucomicrobium spinosum DSM
4136^T. *Front. Microbiol.* 7:362.
doi: 10.3389/fmicb.2016.00362

Kubra F. Naqvi^{1†}, Delphine Patin^{2†}, Matthew S. Wheatley¹, Michael A. Savka¹, Renwick C. J. Dobson^{3,4}, Han Ming Gan^{5,6}, Hélène Barreteau², Didier Blanot², Dominique Mengin-Lecreux² and André O. Hudson^{1*}

¹ Thomas H. Gosnell School of Life Sciences, Rochester Institute of Technology, Rochester, NY, USA, ² Institute for Integrative Biology of the Cell, CEA, CNRS, Univ Paris-Sud, Université Paris-Saclay, Orsay, France, ³ Biomolecular Interaction Centre, School of Biological Sciences, University of Canterbury, Christchurch, New Zealand, ⁴ Department of Biochemistry and Molecular Biology, Bio21 Molecular and Biotechnology Institute, The University of Melbourne, Parkville, VIC, Australia,

⁵ Monash University Malaysia Genomics Facility, Monash University Malaysia, Selangor, Malaysia, ⁶ School of Science, Monash University Malaysia, Selangor, Malaysia

The enzymes involved in synthesizing the bacterial cell wall are attractive targets for the design of antibacterial compounds, since this pathway is essential for bacteria and is absent in animals, particularly humans. A survey of the genome of a bacterium that belongs to the phylum Verrucomicrobia, the closest free-living relative to bacteria from the Chlamydiales phylum, shows genetic evidence that *Verrucomicrobium spinosum* possesses a novel fusion open reading frame (ORF) annotated by the locus tag (VspiD_010100018130). The ORF, which is predicted to encode the enzymes UDP-N-acetylenolpyruvoylglucosamine reductase (MurB) and UDP-N-acetylmuramate:L-alanine ligase (MurC) that are involved in the cytoplasmic steps of peptidoglycan biosynthesis, was cloned. *In vivo* analyses using functional complementation showed that the fusion gene was able to complement *Escherichia coli* murB and murC temperature sensitive mutants. The purified recombinant fusion enzyme (MurB/C_VS) was shown to be endowed with UDP-N-acetylmuramate:L-alanine ligase activity. *In vitro* analyses demonstrated that the latter enzyme had a pH optimum of 9.0, a magnesium optimum of 10 mM and a temperature optimum of 44–46°C. Its apparent *K_m* values for ATP, UDP-MurNac, and L-alanine were 470, 90, and 25 μM, respectively. However, all attempts to demonstrate an *in vitro* UDP-N-acetylenolpyruvoylglucosamine reductase (MurB) activity were unsuccessful. Lastly, Hidden Markov Model-based similarity search

and phylogenetic analysis revealed that this fusion enzyme could only be identified in specific lineages within the *Verrucomicrobia* phylum.

Keywords: MurB, MurC, UDP-N-acetylenolpyruvoylglucosamine reductase, UDP-N-acetyl muramate:L-alanine ligase, fusion enzyme, bacterial cell wall, peptidoglycan, *Verrucomicrobium spinosum*

INTRODUCTION

Bacteria belonging to the *Verrucomicrobia* phylum are Gram-negative heterotrophic organisms that are generally found in soil and fresh water environments. The phylum is considered to have two sister phyla, Chlamydiae and Lentisphaerae (Cho et al., 2004). Members of the *Verrucomicrobia* are of interest due to their close evolutionary relationship to bacteria from the genus Chlamydia in addition to their unusual morphology of possessing wart-like and tube-like appendages that protrude from the cell membrane, commonly referred to as prosthæcae (Wagner and Horn, 2006; McGroty et al., 2013). Most of the research that has been done with bacteria from this phylum has been done using *Verrucomicrobium spinosum* as the model organism. The bacterium was found to employ the type III secretion system and is pathogenic toward *Drosophila melanogaster* and *Caenorhabditis elegans* (Sait et al., 2011). In addition, research from our group recently demonstrated that the bacterium employs the L,L-diaminopimelate aminotransferase (DapL) pathway for the synthesis of *meso*-diaminopimelate involved both in the cross-linking of peptidoglycan (PG) and in lysine anabolism (Nachar et al., 2012; McGroty et al., 2013). Due to the morphological complexity and unusual cellular plan of *V. spinosum*, the synthesis of PG is of interest to our group given its close relationship to the pathogenic organisms from the genus Chlamydia. In addition, the recent discovery of PG in Chlamydia has made this project more intriguing, given the fact that even though β -lactam antibiotics are effective against Chlamydia, definitive evidence of PG in Chlamydial species has been lacking until this recent discovery (Pilhofer et al., 2013; Packiam et al., 2015).

Cell wall PG (also named murein) is ubiquitous in the bacterial domain. The PG of bacteria is composed of tandem repeats of the sugars N-acetylglucosamine (GlcNAc) and N-acetylmuramic acid (MurNAc) cross-linked by a short peptide stem containing usually L-lysine or *meso*-diaminopimelate at the third position (Park, 1987; Vollmer et al., 2008). Due to its rigid structure and tensile strength, the PG has several overarching roles such as protecting the osmotic integrity of the cell in addition to maintaining the shape of the bacteria.

The synthesis of PG in bacteria occurs *via* a pathway that has three distinct steps: the cytoplasmic, membrane, and periplasmic steps. In the cytoplasmic steps, the nucleotide sugar-linked precursor UDP-MurNAc-pentapeptide is synthesized in a series of reactions catalyzed by the enzymes MurA, MurB, MurC, MurD, MurE, MurF, and Ddl (Figure 1) (Barreteau et al., 2008). The next steps in PG formation are the synthesis of the lipid precursor intermediates, undecaprenyl-diphospho-MurNAc-pentapeptide (lipid I) and

undecaprenyl-diphospho-MurNAc-(pentapeptide)-GlcNAc (lipid II), by the enzymes MraY and MurG, respectively; these reactions occur at the level of the cytoplasmic membrane (Bouhss et al., 2008). The ultimate steps in the pathway are the transglycosylation and transpeptidation reactions, characterized by the polymerization of the sugar-peptide units and their incorporation into the growing PG; these reactions take place in the extra-cytoplasmic space and are catalyzed by the penicillin-binding proteins (PBPs) (Figure 1) (Scheffers and Pinho, 2005).

The first three cytoplasmic steps of the PG synthesis pathway, which are the topic of this paper, are as follows. First, UDP-N-acetylglucosamine-1-carboxyvinyltransferase (MurA, EC 2.5.1.7) catalyzes the transfer of the enolpyruvyl moiety from phosphoenolpyruvate to the 3'-hydroxyl end of UDP-GlcNAc to produce UDP-N-acetylenolpyruvoylglucosamine (UDP-GlcNAc-EP) (Figure 1) (Marquardt et al., 1992; Wanke et al., 1992). Then, UDP-N-acetylenolpyruvoylglucosamine reductase (MurB, EC 1.3.1.98) catalyzes the reduction of the enolpyruvyl moiety of UDP-GlcNAc-EP to lactyl ether to produce UDP-N-acetyl muramic acid (UDP-MurNAc) (Figure 2A) (Benson et al., 1993; Tayeh et al., 1995). Finally, UDP-N-acetyl muramate:L-alanine ligase (MurC, EC 6.3.2.8) catalyzes the third reaction, which consists in the addition of L-Ala to the carboxyl group of UDP-MurNAc to produce UDP-MurNAc-L-Ala (Figure 2B) (Liger et al., 1995; Falk et al., 1996; Gubler et al., 1996).

Here we report the identification and biochemical partial characterization of a novel MurB/C fusion enzyme from *V. spinosum*. While *in vitro* assays demonstrate that the enzyme is able to catalyze the ligase (MurC) reaction, attempts to demonstrate the reductase (MurB) activity *in vitro* were unsuccessful. Nevertheless, *in vivo* analyses demonstrated that the fusion gene is able to functionally complement two *Escherichia coli* strains that harbor mutations in the *murB* and *murC* genes. Given the facts that (i) the MurB and MurC enzymes are not normally fused and are encoded by separate ORFs as is the case of the two *E. coli* proteins (Pucci et al., 1992; Liger et al., 1995), and (ii) the PG biosynthesis pathway is essential and is only present in the bacterial domain, the identification and characterization of this unusual fusion enzyme involved in PG biosynthesis in *V. spinosum*, a close relative of the pathogenic organism Chlamydia, is intriguing. This study has the potential to contribute to the further understanding of the kinetic, physical and structural properties of enzymes involved in the synthesis of PG in order to facilitate the development and/or discovery of antibacterial compounds that are able to combat current and emerging bacterial infections and diseases, especially those that are deemed to be resistant to antibiotics that are currently used in a clinical setting.

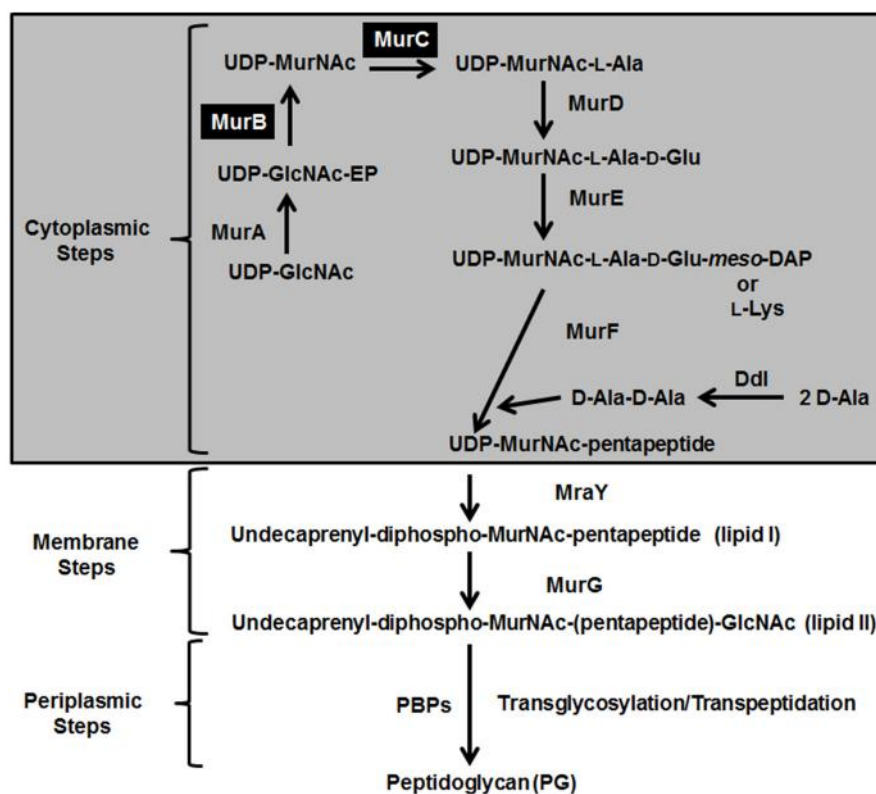


FIGURE 1 | Schematic representation depicting the three stages of PG biosynthesis in bacteria. The cytoplasmic, membrane, and periplasmic steps are shown. The abbreviations of the enzymes are as follows: MurA, UDP-N-acetylglucosamine 1-carboxyvinyltransferase; MurB, UDP-N-acetylenolpyruvoylglycosamine reductase; MurC, UDP-N-acetylmuramate:L-alanine ligase; MurD, UDP-N-acetylmuramoyl-L-alanine:D-glutamate ligase; MurE, UDP-N-acetylmuramoyl-D-alanyl-D-glutamate:2,6-diaminopimelate ligase or UDP-N-acetylmuramoyl-L-alanyl-D-glutamate:L-lysine ligase; MurF, UDP-N-acetylmuramoyl-tripeptide:D-alanyl-D-alanine ligase; Ddl, D-alanine:D-alanine ligase; MraY, phospho-N-acetylmuramoyl-pentapeptide transferase; MurG, undecaprenyl-diphospho-N-acetylmuramoyl-pentapeptide β -N-acetylglucosaminyl transferase; and PBPs, penicillin-binding proteins. The enzymatic activities theoretically carried by the MurB/C fusion enzyme from *V. spinosum* are shaded in black. UDP-GlcNAc-EP stands for UDP-N-acetylenolpyruvoylglycosamine.

MATERIALS AND METHODS

Materials

L-[¹⁴C]Ala (5.99 GBq.mmol⁻¹) and L-[¹⁴C]Ser (6.07 GBq.mmol⁻¹) were purchased from Perkin Elmer, [¹⁴C]Gly (3.88 GBq.mmol⁻¹) from CEA, and UDP-[¹⁴C]GlcNAc (2 GBq.mmol⁻¹) from ARC Isobio. UDP-[¹⁴C]MurNAc was prepared according to published procedure (Bouhss et al., 2002). UDP-GlcNAc-EP was purchased from the BaCWAN facility.

V. spinosum Growth Conditions/Plasmids and Strains used in this Study

V. spinosum DSM 4136^T was cultured in R2A medium supplemented with 5% (w/v) artificial sea water at 26°C (Schlesner, 1987). The plasmids and strains used in this study are listed in Table 1.

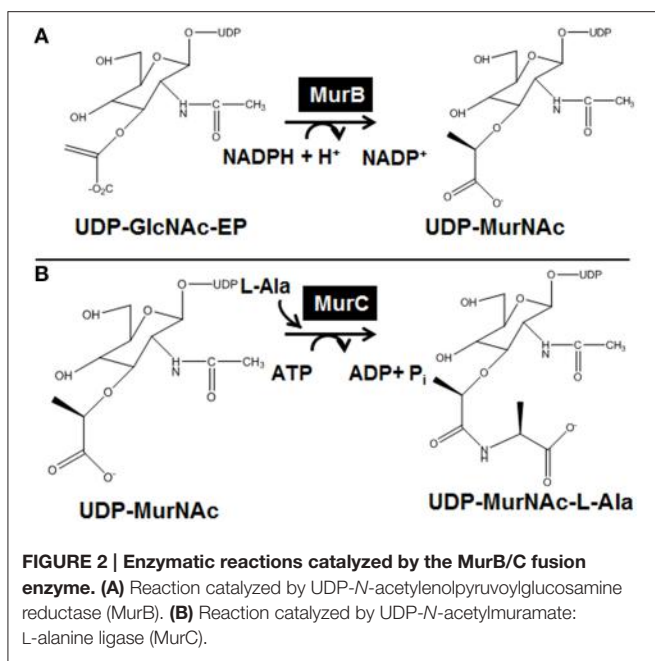
Domain Mapping of MurB/C_{Vs} Identification

The protein family (Pfam) domains of MurB/C_{Vs} were identified using the Pfam server (<http://pfam.sanger.ac.uk/>)

and (<http://pfam.janelia.org/>) (Finn et al., 2014). The conserved domain database (CDD) (<http://www.ncbi.nlm.nih.gov/Structure/cdd/cdd.shtml>) was used to identify the domains of MurB/C_{Vs} (Marchler-Bauer et al., 2015).

Identification of Lineages Containing Fused MurB/C Protein and Phylogenetic Analysis of MurB and MurC Proteins

Publicly available draft and complete genome sequences belonging to members of the phylum Planctomycetes, Verrucomicrobia, Chlamydiae, and Lentisphaerae (PVC) were downloaded from NCBI. The proteomes were re-predicted with Prodigal version 2.6 (Hyatt et al., 2010) and then used for phylogenomic tree construction with PhyloPhlAN (Segata et al., 2013). The manually curated database of protein families known as TIGFAMs was used to identify MurB (TIGR00179) and MurC (TIGR00182) proteins (Haft et al., 2003). The predicted whole proteomes were subjected to similarity search based on the hidden Markov model (HMM) profiles TIGR00179 and TIGR00182 using HMMsearch (-cut_tc option) (Eddy, 2011), and species containing unusual composition of MurB and MurC, i.e., fused MurB/C, missing MurB, and/or missing MurC, were



annotated in the constructed species tree. Additionally, the gene organization of contigs containing the fused *murB/C* open reading frame (ORF) was further analyzed with EasyFig version 2.1 (Sullivan et al., 2011). Additional MurB and MurC proteins were also mined from the UniProt (<http://www.uniprot.org/>) (The UniProt Consortium) to be included for phylogenetic analysis. Briefly, the proteins were aligned and trimmed using mafft-linsi and trimal (-gappyout setting) (Capella-Gutiérrez et al., 2009; Katoh and Standley, 2013), and phylogenetic inference was performed using IQ-TREE version 1.3.10 (Nguyen et al., 2014) and visualized using FigTree version 1.4.2 (<http://tree.bio.ed.ac.uk/software/figtree/>).

PCR Amplification and Cloning of the *V. spinosum murB/C* Open Reading Frame (ORF)

The ORF annotated by the locus tag (VspID_010100018130) UDP-N-acetylenolpyruvoylglucosamine reductase /UDP-N-acetyl muramate:L-alanine ligase was amplified by PCR using the primers *murB/C_{Vs}*-forward (5'-CACCATGAATCACGCC GTCGTCAGTTGTTGAAG-3') and *murB/C_{Vs}*-reverse (5'-GTCGACCTATAGCGGAAGCGGTTCCCTTCTCGCCAAT-3'). The underlined sequence represents the restriction enzyme site used to facilitate sub-cloning of the ORF while the bold sequences represent initiation and termination codons. The PCR reaction contained 12 pmol of forward and reverse primers, 1 mM MgSO₄, 0.5 mM of each of the four deoxynucleotide triphosphates, 0.5 ng of genomic DNA and 1 unit of Platinum Pfx DNA polymerase (Invitrogen Corporation, Carlsbad, CA, USA). PCR conditions were: 1 cycle at 94°C for 2 min, followed by 30 cycles of 94°C for 15 s, 60°C for 30 s, and 72°C for 3 min. The *murB/C* PCR fragment was ligated into the plasmid pET100D/topo (Invitrogen Corporation, Carlsbad, CA, USA)

TABLE 1 | Plasmids and strains used in this study.

| Plasmids and strains | Sources/References |
|---|---|
| PLASMIDS | |
| pET100D/topo | Invitrogen, USA |
| pBAD33 | Guzman et al., 1995 |
| pET100D:: <i>murB/C_{Vs}</i> | This study |
| pBAD33:: <i>murB/C_{Vs}</i> | This study |
| pTrcHis60 | Pompeo et al., 1998 |
| pTrcHis60:: <i>murB_{Vs}</i> -1 | This study |
| pTrcHis60:: <i>murB_{Vs}</i> -2 | This study |
| pTrcHis60:: <i>murC_{Vs}</i> -1 | This study |
| pTrcHis60:: <i>murC_{Vs}</i> -2 | This study |
| pTrcHis60:: <i>murC_{Ec}</i> | Liger et al., 1995 |
| STRAINS | |
| <i>Verrucomicrobium spinosum</i> DSM 4136 ^T | Schlesner, 1987 |
| 5-alpha competent cells | New England Biolabs, USA |
| Rosetta codon plus RIPL | Agilent, Technologies, USA |
| Rosetta (DE3) pLysS | Novagen, USA |
| <i>E. coli</i> <i>murB</i> (ST5) CGSC Strain # 6442 | Matsuzawa et al., 1969; Miyakawa et al., 1972 |
| <i>E. coli</i> <i>murC</i> (ST222) CGSC Strain # 5988 | Miyakawa et al., 1972 |
| <i>E. coli</i> <i>murC</i> (H1119) | Wijsman, 1972 |
| <i>E. coli</i> <i>murB</i> (pBAD33) | This study |
| <i>E. coli</i> <i>murC</i> (pBAD33) | This study |
| <i>E. coli</i> <i>murB</i> (pBAD33:: <i>murB/C_{Vs}</i>) | This study |
| <i>E. coli</i> <i>murC</i> (pBAD33:: <i>murB/C_{Vs}</i>) | This study |

to produce the plasmid pET100D::*murB/C_{Vs}*. The recombinant protein encoded by this plasmid carries an N-terminal MRGSHHHHHGMASMTGGQQMGRDLYDDDDKDHPFT additional sequence containing a hexa-histidine tag (bold) derived from the pET100D plasmid. To confirm the fidelity of the PCR reaction, the ORF was sequenced from pET100D using the T7 promoter primer, 5'-TAATACGACTCACTATAGGG-3' and the T7 reverse primer, 5'-TAGTTATTGCTCAGCGGTGG-3'. The cloned *murB/C* ORF was 100% identical to the sequence deposited in the Integrated Microbial Genomes public database (<http://img.jgi.doe.gov/cgi-bin/w/main.cgi>).

Cloning of *murC* and *murB* Domains

The *murC* and *murB* domains of the MurB/C_{Vs} fusion protein were also cloned separately in expression vectors, as follows. The *murC* domain sequence (two different end points were chosen) was amplified by PCR by using *murC_{Vs}*-forward (5'-GCGCTCATGAATCACGCCGTCGTCAGTTGTTGA-3') as the forward primer and either *murC_{Vs}*-reverse-1 (5'-GCGCAGATTGCCTCGCGATTGAGCACCCTAGT GAG-3') or *murC_{Vs}*-reverse-2 (5'-GCGCAGATTGACCGT GCCACCGCCTTCGCGATTGAG-3') as the reverse primer, designed to end the MurC domain at the Gly477 and Val481 residues, respectively. The underlined sequences correspond to introduced *Bsp*H I and *Bgl*II restriction sites and the *murC* gene initiation codon is indicated in bold. The two PCR

products were digested by *Bsp*HI and *Bgl*II and inserted between the compatible *Nco*I and *Bgl*II sites of the expression vector p_{Trc}His60 that allows expression of proteins with a C-terminal hexa-histidine tag under the control of the IPTG-inducible *trc* promoter (Pompeo et al., 1998). The two plasmids thus generated, p_{Trc}His60::*murC_{Vs}*-1 and p_{Trc}His60::*murC_{Vs}*-2, directed expression of Met1-Gly477 and Met1-Val481 fragments from the MurB/C_{Vs} fusion protein (770 residues in total), respectively, fused to a C-terminal tag extension consisting in Arg-Ser-His₆.

Similarly, the *murB* domain sequence (two different starting points were chosen) was amplified by using either *murB_{Vs}*-forward-1 (5'-GAAGCCATGGGCACGGTCAAGCTCTATGA GCGATG-3') or *murB_{Vs}*-forward-2 (5'-GCGCTCATGAAGC TCTATGAGCCGATGGCCAACCAC-3') as the forward primer and *murB*_{Vs}-reverse (5'-GCGCAGATCTTAGCGGAAGCGG TTCCTCTTCGCCAATG-3') as the reverse primer. *Nco*I, *Bsp*HI and *Bgl*II restriction sites introduced in these sequences are underlined and the *murB* gene initiation codons are indicated in bold. The two PCR products were digested by *Nco*I or *Bsp*HI and *Bgl*II and inserted between the compatible *Nco*I and *Bgl*II sites of the vector p_{Trc}His60. The two plasmids thus generated, p_{Trc}His60::*murB_{Vs}*-1 and p_{Trc}His60::*murB_{Vs}*-2, directed expression of the Gly479-Leu770 and Lys482-Leu770 fragments (preceded by a Met residue) from the MurB/C_{Vs} fusion protein, respectively, here too with a C-terminal tag consisting in Arg-Ser-His₆.

Expression and Purification of Recombinant MurB/C_{Vs}

The *E. coli* Rosetta (DE3) pLysS strain (Novagen) was transformed with the plasmid pET100D::*murB/C_{Vs}* and grown at 37°C in 2YT medium containing 50 µg.mL⁻¹ ampicillin and 25 µg.mL⁻¹ chloramphenicol. An overnight pre-culture of the resulting strain was used to inoculate 2YT medium (2-liter cultures). The culture was incubated with shaking at 37°C. When the optical density reached 0.9, the temperature of the culture was decreased to 20°C and IPTG was added at a 1 mM final concentration. Growth was continued for 18 h at 20°C. Cells were harvested at 4°C and the pellet was washed with cold 20 mM phosphate buffer, pH 7.2, containing 1 mM dithiothreitol (buffer A). Bacteria were resuspended in buffer A (12 mL) and disrupted by sonication in the cold using a Bioblock Vibracell 72412 sonicator. The resulting suspension was centrifuged at 4°C for 30 min at 200,000 × g with a Beckman TL100 apparatus, and the pellet was discarded. The supernatant was kept at -20°C.

The His₆-tagged protein was purified on Ni²⁺-nitrotriaceate (Ni²⁺-NTA)-agarose following the manufacturer's recommendations (Qiagen). All procedures were performed at 4°C. The supernatant was mixed for 1 h with the polymer previously washed with buffer A containing 0.3 M KCl and 10 mM imidazole. Washing and elution steps were performed with a discontinuous gradient of imidazole (20–300 mM) in buffer A containing 0.3 M KCl. Protein contents were analyzed by sodium dodecyl sulfate-polyacrylamide gel electrophoresis (SDS-PAGE) and relevant fractions were

pooled and dialyzed against 100 volumes of buffer A. At this step, precipitation of a significant part of the protein was observed. The non-precipitated protein was concentrated on an Amicon Ultra 50,000 molecular mass cutoff filter. Glycerol (10% final concentration) was added for storage at -20°C. Protein concentrations were determined by quantitative amino acid analysis with a Hitachi L8800 analyzer (ScienceTec) after hydrolysis of samples at 105°C for 24 h in 6 M HCl containing 0.05% 2-mercaptoethanol. No attempts were made to remove the additional sequence containing the hexa-histidine tag after protein purification.

Construction of the Plasmid to Facilitate Functional Complementation

The plasmid used for functional complementation of the *E. coli* *murB* and *murC* mutants was produced by sub-cloning the *Xba*I and *Sal*I fragment from the pET100D::*murB/C_{Vs}* plasmid into pBAD33 to produce the plasmid pBAD33::*murB/C_{Vs}*, which is under control of the arabinose inducible promoter (Guzman et al., 1995). The protein produced from the pBAD33 construct is identical to the protein produced from the pET100D construct. Note that there is an *Xba*I site 20 base pairs upstream of the ribosome binding site of the pET100D vector that was used to facilitate sub-cloning from pET100D into pBAD33.

Functional Complementation of the *E. coli* *murB* and *murC* Thermosensitive Mutants

The *E. coli* *murB* mutant (ST5-strain #6442) [thr-1, araC14, leuB6 (Am), secA216, fhuA61, lacY1, galT23, λ⁻ trp-84, his-215, thyA710, rpsL263 (strR), xylA5, mtl-1, murB1-(ts), thi-1] and *murC* mutant (ST222-strain #5988) [thr-1, araC14, leuB6 (Am), murC3(ts), secA216, fhuA61, lacY1, galT23, λ⁻ trp-84, his-215, thyA710, rpsL263 (strR), xylA5, mtl-1, thi-1] were both obtained from the Coli Genetic Stock Center (<http://cgsc.biology.yale.edu/>). These mutants were transformed with the pBAD33 vector or the pBAD33::*murB/C_{Vs}* plasmid and transformants were selected on LB agar medium supplemented with 50 µg.mL⁻¹ thymine, 34 µg.mL⁻¹ chloramphenicol, and 0.2% (w/v) arabinose at 30°C. Colonies were then replica-plated onto LB agar medium plus 0.2% (w/v) arabinose and 10 µg.mL⁻¹ thymine. Liquid cultures were also performed in LB medium supplemented with arabinose and thymine. In both cases, the growth phenotype was assessed at 30 and 42°C for up to 24 h.

As described above, the individual *murC* and *murB* domains from the *murB/C_{Vs}* fusion gene were also cloned separately in the p_{Trc}His60 vector that allows high-level gene expression under control of the strong IPTG-dependent *trc* promoter. The resulting plasmids p_{Trc}His60::*murB_{Vs}* and p_{Trc}His60::*murC_{Vs}* were then tested for functional complementation, using the *E. coli* *murB* mutant ST5 and the *murC* mutant strain H1119 (Wijsman, 1972), respectively. Transformants were selected on LB agar medium supplemented with 100 µg.mL⁻¹ ampicillin and 50 µg.mL⁻¹ thymine at 30°C and were subsequently replicated on similar plates incubated at 30°C or 42°C, in the presence or absence of 0.5 mM IPTG. Growth was observed after 24 h of incubation.

Determination of the Kinetic Constants of the MurC Activity

The standard MurC activity assay (Liger et al., 1995) measured the formation of UDP-MurNAc-L-Ala in a mixture (final volume, 40 μ L) containing 100 mM Tris-HCl, pH 9.0, 10 mM MgCl₂, 3 mM ATP, 10 mM ammonium sulfate, 0.5 mg.mL⁻¹ bovine serum albumin (BSA), 0.9 mM UDP-MurNAc, 0.3 mM L-[¹⁴C]Ala (400 Bq), and enzyme (20 μ L of an appropriate dilution in buffer A). For the determination of the K_m values for UDP-MurNAc, UDP-[¹⁴C]MurNAc was used as the radiolabelled substrate.

In all cases, the mixtures were incubated for 30 min at 37°C and the reactions were stopped by the addition of glacial acetic acid (10 μ L) followed by lyophilization. Radioactive substrate and product were then separated by HPLC on a Nucleosil 100C₁₈ 5 μ m column (150 \times 4.6 mm; Alltech France) using 50 mM ammonium formate, pH 3.2, at a flow rate of 0.6 mL.min⁻¹. Radioactivity was detected with a flow detector (model LB506-C1, Berthold) using the Quicksafe Flow 2 scintillator (Zinsser Analytic) at 0.6 mL.min⁻¹. Quantification was performed with the Radiostar software (Berthold).

For the determination of the kinetic constants, the same assay was used with various concentrations of one substrate and fixed concentrations of the others. In all cases, the enzyme concentration was chosen so that substrate consumption was <20%, the linearity being ensured within this interval even at the lowest substrate concentration. Data were fitted to the equation $v = V_{max}S/(K_m + S)$ by the Levenberg-Marquardt method (Press et al., 1986), where v is the initial velocity and S is the substrate concentration, and values \pm standard deviation at 95% of confidence were calculated. The MDFitt software developed by M. Desmadril (I2BC, Orsay, France) was used for this purpose.

In vitro Spectrophotometric Assay of the MurB Activity

The MurB spectrophotometric assay was performed as described previously (Benson et al., 1993). The reaction mixture contained, in a final volume of 100 μ L, 50 mM Tris-HCl, pH 8.0, 20 mM KCl, 0.5 mM dithiothreitol, 0.1 mM UDP-GlcNAc-EP, and 0.15 mM NADPH. The mixture was placed in a 1-cm path length cell and the reaction was started by the addition of the enzyme. The decrease in NADPH absorbance at 340 nm was monitored with a Jasco V-630 spectrophotometer.

In vitro Coupled Assay of the MurA/MurB Activities

The reaction mixture contained, in a final volume of 40 μ L, 50 mM Tris-HCl, pH 7.6, 25 mM KCl, 0.1 mM NADPH, 55 μ M UDP-[¹⁴C]GlcNAc (500 Bq), 75 μ M phosphoenolpyruvate, *E. coli* MurA (1 μ g), and enzyme. In some experiments, 5 mM ATP, 10 mM MgCl₂, and 0.15 mM L-Ala were included. After 30 min at 37°C, the reaction was stopped by the addition of glacial acetic acid (8 μ L) followed by lyophilization. The radioactive substrate and product were separated on a Nucleosil 100C₁₈ 5 μ m column (150 \times 4.6 mm; Alltech France) using 50 mM ammonium formate, pH 3.2, at a flow rate of 0.6 mL.min⁻¹. Detection and quantification of the radioactivity were performed

as described above. The retention times for UDP-GlcNAc, UDP-GlcNAc-EP, UDP-MurNAc, and UDP-MurNAc-L-Ala were 6, 10, 12, and 20 min, respectively.

MurB/C_{VS} Cleavage Assay

For the cleavage assay, *V. spinosum* was grown in liquid medium R2A medium supplemented with 5% (w/v) artificial sea water at 26°C for 5 days. Following centrifugation, the cells were lysed by sonication in the following buffer systems 50 mM Tris-HCl, pH 7.6, 50 mM Tris-HCl, pH 8.5, and 50 mM HEPES-KOH, pH 7.6. The purified recombinant enzyme (7.5 μ g) was incubated with 15 μ g of *V. spinosum* extract at 30°C. The proteins were resolved on a 10% (w/v) acrylamide gel and stained with Coomassie blue for visualization. Protein concentration was measured using the Bradford assay with BSA as the standard (Bradford, 1976).

RESULTS

Identification of the MurB/C Fusion Enzyme from *V. spinosum*

The complete set of genes in *V. spinosum* required for the *de novo* synthesis of PG was initially identified from a comparative analysis of the *V. spinosum* proteome using the known PG biosynthesis proteins as queries (Nachar et al., 2012). The search revealed an anomaly when it was realized that both the MurB and MurC proteins were encoded by a single locus tag VspID_010100018130 (Table 2).

Domain Mapping of the MurB/C Fusion Enzyme from *V. spinosum*

The length of the MurB and MurC *E. coli* proteins are 342 and 491 residues, respectively, and the lengths of the MurB/C fusion enzyme protein is 770 residues. As such, we were interested to assess if the fusion enzyme had the domains that are indicative of typical MurB and MurC enzymes. Domains were identified using the NCBI's CDD and the protein families database (Pfam) (Finn et al., 2014; Marchler-Bauer et al., 2015). The CDD and Pfam analyses resulted in the identification of the following domains: (1) the Mur ligase catalytic domain (Pfam01225), (2) the Mur ligase middle domain (Pfam08245), (3) the Mur ligase family amino acid-binding domain (Pfam02875), (4) the FAD-binding domain (Pfam01565), and (5) the UDP-N-acetylenolpyruvylglucosamine reductase C-terminal domain (Pfam02873). This analysis also demonstrated that the residues responsible for the MurC activity were located toward the N-terminal end of the fusion enzyme, while those for the MurB activity are located toward the C-terminal end. MurC and MurB are separated by a linker region of ~100 residues as depicted in the schematic. For comparison, the figure also depicts the domain structures of the *E. coli* MurB and MurC enzymes (Figure 3).

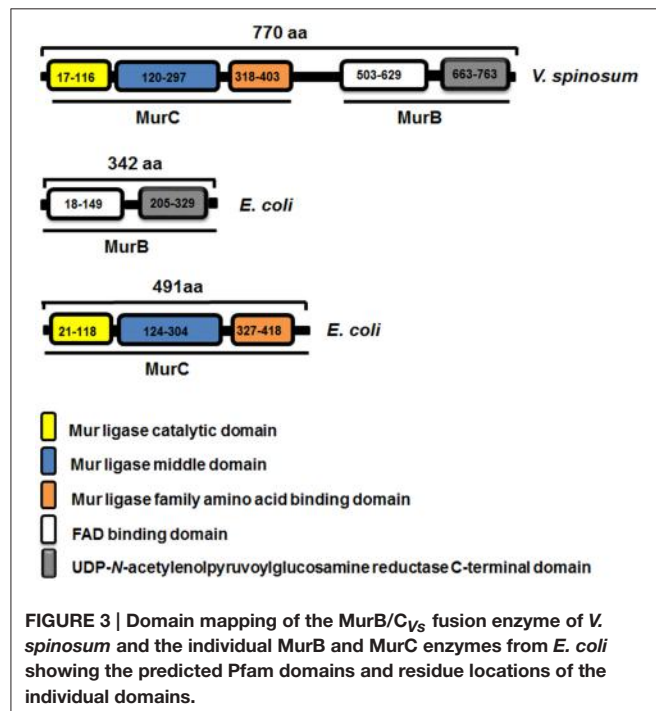
The murB/C_{VS} Gene is able to Functionally Complement the *E. coli* murB and murC Mutants

The *E. coli* strains ST5 and ST222 obtained from the Coli Genetic Stock Center harbor mutations in the *murB* and *murC*

TABLE 2 | List of PG biosynthesis genes from *V. spinosum*.

| Protein symbol | Gene product name | EC # | Locus Tag |
|----------------|---|-----------------|---------------------------|
| MurA | UDP-N-acetylglucosamine 1-carboxyvinyltransferase | 2.5.1.7 | VspiD_010100011745 |
| MurB | UDP-N-acetylenolpyruoylglicosamine reductase | 1.3.1.98 | VspiD_010100018130 |
| MurC | UDP-N-acetyl muramate:L-alanine ligase | 6.3.2.8 | VspiD_010100018130 |
| MurI | Glutamate racemase | 5.1.1.3 | VspiD_01010008415 |
| MurD | UDP-N-acetyl muramoyl-L-alanine:D-glutamate ligase | 6.3.2.9 | VspiD_010100019115 |
| MurE | UDP-N-acetyl muramoyl-L-alanyl-D-glutamate:2,6-diaminopimelate ligase | 6.3.2.13 | VspiD_010100019130 |
| MurF | UDP-N-acetyl muramoyl-tripeptide:D-alanyl-D-alanine ligase | 6.3.2.10 | VspiD_010100019125 |
| AlaR | Alanine racemase | 5.1.1.1 | VspiD_01010000100 |
| Ddl | D-alanine:D-alanine ligase | 6.3.2.4 | VspiD_010100018175 |
| MraY | Phospho-N-acetyl muramoyl-pentapeptide transferase | 2.7.8.13 | VspiD_010100019120 |
| MurG | Undecaprenyl-diphospho-N-acetyl muramoyl-pentapeptide β -N-acetylglucosaminyl transferase | 2.4.1.227 | VspiD_010100019100 |
| UppP | Undecaprenyl-diphosphate phosphatase | 3.6.1.27 | VspiD_010100026230 |
| PBP | D-alanyl-D-alanine carboxypeptidase-class C | 3.4.16.4 | VspiD_010100024635 |
| PBP | Multimodular transpeptidase-transglycosylase-class A | 2.4.1.129 | VspiD_010100022270 |
| PBP | Penicillin-binding protein 1C-class A | 2.4.1.129 | VspiD_01010006740 |
| PBP | Penicillin-binding protein 2-class A | 2.4.1.129 | VspiD_010100020475 |
| PBP | Peptidoglycan transpeptidase-class B | 2.4.1.129 | VspiD_010100007940 |
| PBP | Peptidoglycan transpeptidase-class B | 2.4.1.129 | VspiD_010100017450 |
| PBP | Peptidoglycan synthetase FtsL-class B | 2.4.1.129 | VspiD_010100019135 |
| PBP | Cell elongation specific D,D-transpeptidase-class B | 2.4.1.129 | VspiD_010100018680 |

The information for MurB and MurC is in bold. EC # denotes enzyme classification number.



genes, respectively. These mutations result in a temperature-sensitive growth phenotype where the mutants are able to grow at the permissive temperature of 30°C, but not at the non-permissive temperature of 42°C (Matsuzawa et al., 1969;

Miyakawa et al., 1972). To answer the question of whether the fusion gene is able to complement the *murB* and *murC* *E. coli* mutants, the mutant strains were transformed with an empty vector (pBAD33) or with a vector containing the *murB/C* gene (pBAD33::*murB/C_{VS}*). Using replica-plating, the results from this analysis demonstrate that at the permissive temperature of 30°C, the mutant strains harboring the vector control (pBAD33) and the vector containing the recombinant gene (pBAD33::*murB/C_{VS}*) were both able to grow. However, when exposed to the non-permissive temperature of 42°C, only the strains expressing the *murB/C* recombinant gene were able to grow (Figure 4A). This result was corroborated by assessing bacterial growth in liquid medium over a period of 24 h. At 30°C the mutants harboring the vector-only and the *murB/C*-expressing vector grew as expected. The growth phenotype at the non-permissive temperature of 42°C demonstrated that only the mutant strains expressing the *murB/C* gene were able to grow when compared to the vector-only controls (Figure 4B). The lack of growth based on the optical density of the vector-only controls at 42°C can be attributed to rapid lysis of the cells due to the lack of proper peptidoglycan synthesis (Figure 4B). The assessment of crude soluble protein extracts from the complementation experiment using SDS-PAGE analysis confirmed the production of the recombinant MurB/C fusion enzyme (~87.3 kDa) in the mutant backgrounds grown at 42°C that was not present in the extracts from the mutant harboring the vector-only control when both were under inducing conditions using arabinose (Figure 4C). Together, these analyses demonstrated that the recombinant MurB/C fusion enzyme from *V. spinosum* was endowed with the reductase (MurB) and ligase (MurC) activities,

and that the amount produced was sufficient to sustain the growth of the *E. coli* mutants.

Attempts to clone and assay the *in vivo* activity of the individual MurB and MurC domains of the MurB/C_{Vs} fusion protein were then made. Protein dissection was performed on the basis of the mapping experiments described above, i.e., alignment of the *V. spinosum* protein sequence with that of MurB and MurC ortholog proteins from *E. coli*. These two domains were cloned in the pTrcHis60 vector, in each case in two versions: with the MurC domain starting at the Met1 residue and terminating either at the Gly477 or the Val481 residue, and the MurB domain starting either at the Gly479 or the Lys482 residue (preceded by a Met residue) and terminating at the last residue (Leu770) of the fusion protein. The two pTrcHis60::murC_{Vs} constructs thus generated complemented the thermosensitive murC mutant strain H1119, indicating that the shortest version ending at Gly477 clearly exhibited MurC activity. IPTG was not required for complementation, indicating that basal expression of the murC_{Vs} domain from the pTrcHis60 vector was sufficient to sustain cell growth and viability of the murC mutant at the non-permissive temperature of 42°C (**Supplemental Figure 1**). However, the two other pTrcHis60::murB_{Vs} constructs failed to

complement the growth defect of the murB mutant strain ST5 and induction of gene expression with 0.5 mM IPTG yielded the same result. The latter finding could be interpreted in several ways: inappropriate design of the murB domain initiation codon, physical instability of these truncated forms of the fusion protein, or inability of the MurB domain to function independently (absolute requirement for the presence of the MurC domain). Our data show that this is not the case for the MurC domain whose activity did not depend on the presence of the MurB domain.

Properties and Kinetic Parameters of MurC Activity from MurB/C_{Vs}

The *in vitro* L-alanine-ligase activity of the MurB/C_{Vs} fusion enzyme was revealed using a radioactive assay, which was also used to determine the properties and kinetic parameters (**Table 3**). The optimal pH and temperature for MurC_{Vs} were found to be 9.0 and 44–46°C, respectively. As it is the case for the other Mur ligases (Barreteau et al., 2008), magnesium ions were essential for the activity: the optimal concentration was 10 mM. It was shown that the addition of 10 mM ammonium sulfate and 0.5 mg·mL⁻¹ BSA increased the activity by 35 and

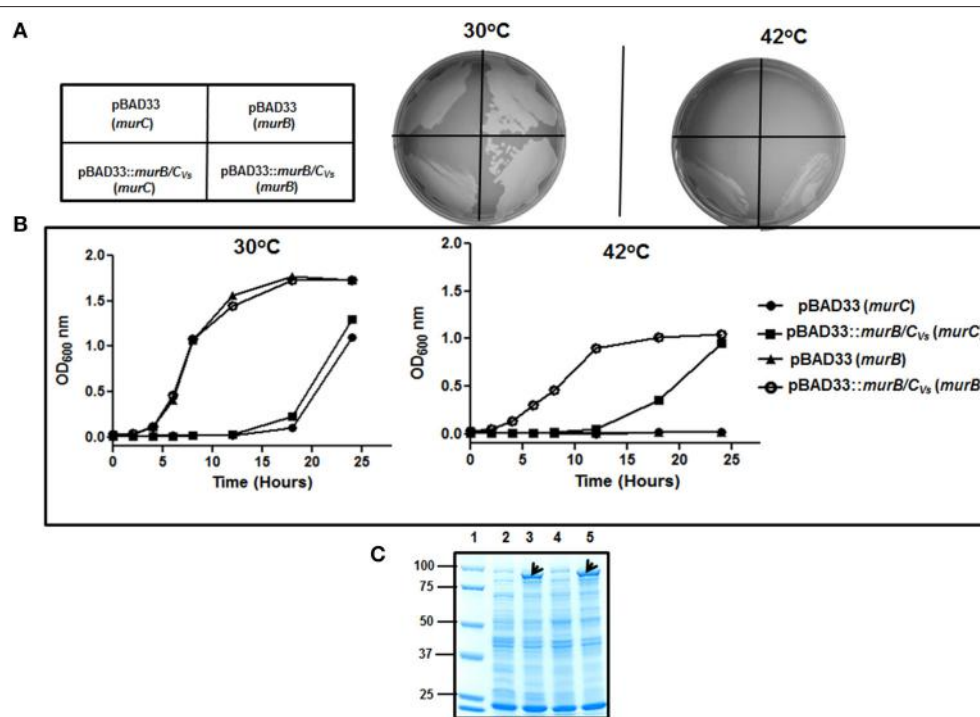


FIGURE 4 | Functional complementation analysis of the *E. coli* murB and murC mutants. (A) Replica-plating experiment of the murC and murB mutants transformed with pBAD33 and pBAD33::murB/C_{Vs} grown at 30 and 42°C. **(B)** Analysis of the complementation experiment at 30 and 42°C in liquid culture assessing the growth phenotype by measurement of the optical density (OD) at 600 nm for a 24 h period. The growth experiments were done four times giving the similar growth profiles. The graphs in **(B)** represent one of those growth curves. **(C)** SDS-PAGE analysis of proteins from the complementation experiment to assess the expression of MurB/C in the mutant backgrounds. Lane (1), protein ladder (kDa). Lane (2), 10 µg of protein extract from the *E. coli* murC mutant harboring pBAD33 grown at 30°C. Lane (3), 10 µg of protein extract from the *E. coli* murC mutant harboring pBAD33::murB/C_{Vs} grown at 42°C. Lane (4), 10 µg of protein extract from the *E. coli* murB mutant harboring pBAD33 grown at 30°C. Lane (5), 10 µg of protein extract from the *E. coli* murB mutant harboring pBAD33::murB/C_{Vs} grown at 42°C. Crude extracts were obtained via sonication after 24 h from the samples grown at 30°C and 42°C. The black arrows show expression of the MurB/C recombinant enzyme. The proteins were resolved on a 10% (w/v) acrylamide gel and stained with Coomassie blue for visualization.

TABLE 3 | Properties and apparent kinetic parameters of *V. spinosum* MurC in comparison with its orthologs from *E. coli* and *C. trachomatis*.

| Kinetic parameter | MurC _{VS} ^a | MurC _{Ec} ^b | MurC _{Ct} ^c |
|--|---------------------------------|---------------------------------|---------------------------------|
| Optimal pH | 9.0 | 8.6 | 8.0–8.5 |
| Optimal Mg ²⁺ concentration (mM) | 10 | 10–20 | 20 |
| Optimal temperature (°C) | 44–46 | 45 | nd ^d |
| K _m ^{ATP} (μM) | 470 ± 160 | 450 | 162 |
| K _m ^{UDP-MurNAc} (μM) | 90 ± 25 | 100 | 196 |
| K _m ^{L-Ala} (μM) | 25 ± 10 | 20 | 124 |
| V _{max} (nmol.min ⁻¹ .mg ⁻¹) | 5500 ± 50 | 17300 | 73.8 |

^aThe apparent kinetic parameters were determined as described in Section Materials and Methods. The concentrations of the fixed substrates were 5 mM for ATP, 1 mM for UDP-MurNAc, and 0.2 mM for L-Ala. The concentration ranges for the varied substrates were 0.2–5 mM for ATP, 25–500 μM for UDP-MurNAc, and 10–400 μM for L-Ala.

^bFrom (Liger et al., 1995).

^cFrom (Hesse et al., 2003).

^dnd, not determined.

TABLE 4 | Specificity of MurC_{VS} for the amino acid substrate.

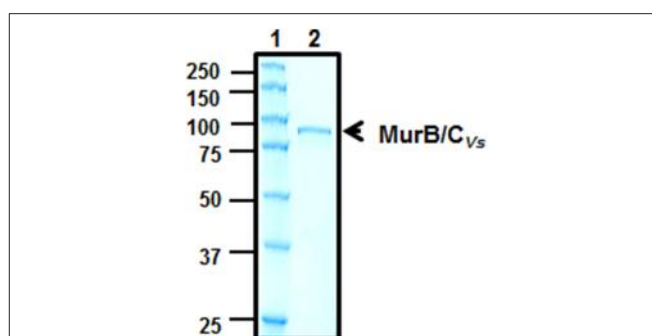
| Substrate | Enzymatic activity (nmol·min ⁻¹ ·mg ⁻¹) ^a |
|-----------|---|
| L-Ala | 4900 ± 250 |
| L-Ser | 3200 ± 130 |
| Gly | 3570 ± 220 |

^aDetermined as described in Section Materials and Methods with fixed concentrations of ATP (5 mM), UDP-MurNAc (1.5 mM), and amino acid (1.5 mM).

55%, respectively. With L-alanine as the amino acid substrate, the apparent *k_{cat}* of the enzyme was 480 min⁻¹ (*V_{max}*, ca. 5500 nmol·min⁻¹·mg⁻¹). Amino acids Gly and L-Ser, which are found at position 1 of the peptide stem in some bacteria (Schleifer and Kandler, 1972; Vollmer et al., 2008), were also tested as substrates (Table 4). L-Ala was the best substrate, which is in agreement with the amino acid composition of *V. spinosum* peptidoglycan (McGroty et al., 2013). However, the difference with the two others was not as important as for the *E. coli* MurC ortholog (Liger et al., 1995).

Attempts to Demonstrate the *In vitro* MurB Activity from MurB/C_{VS}

Several attempts were made to measure the *in vitro* reductase activity of MurB/C_{VS} with two assays: a spectrophotometric assay using commercial UDP-GlcNAc-EP and NADPH, and a coupled MurA/MurB assay using UDP-[¹⁴C]GlcNAc and *E. coli* MurA. However, neither decrease of absorbance at 340 nm nor appearance of labeled UDP-MurNAc occurred, even at high protein concentrations. It was checked that the expected reaction took place in both assays when MurB/C_{VS} was replaced by *E. coli* MurB (data not shown). In order to ascertain that the absence of reaction in the coupled assay was not due to strong inhibition by the MurB product, L-alanine, ATP, and Mg²⁺ were added so that the MurC_{VS} activity might displace the reaction toward the right. A new radioactive compound appeared, but its retention time (25 min) was not consistent with that of UDP-MurNAc-L-Ala (20 min) (data not shown). It was presumably the result of the

**FIGURE 5 | Purification of MurB/C by affinity chromatography.** Lane (1), protein ladder (kDa). Lane (2), 0.5 μg of purified MurB/C. The proteins were resolved on a 10% (w/v) acrylamide gel and stained with Coomassie blue for visualization.

direct addition of L-alanine to UDP-GlcNAc-EP, a reaction that has been shown to occur with *E. coli* MurC (Liger et al., 1995).

Is MurB/C_{VS} Active as a Fusion Enzyme *in vivo*?

The SDS-PAGE showing the expression of the MurB/C_{VS} in the *murB* and *murC* mutant backgrounds demonstrated that the recombinant enzyme was not cleaved in *E. coli* (Figure 4C). However, given the fact that there is a 100-residue linker region between the MurC and MurB domains (Figure 3), we were interested in answering the question of whether the fusion enzyme is cleaved in *V. spinosum*. This would indicate that after translation, the enzyme is processed by a protease to create two separate and distinct polypeptides of MurB and MurC. To answer this question, the purified recombinant enzyme (Figure 5) was used in a cleavage assay using crude soluble protein extract from *V. spinosum*. The assay showed that the recombinant enzyme was not cleaved when incubated with an extract from *V. spinosum* over a period of 120 min (Figure 6). It should be noted that the result was consistent when the assay was done using several concentrations of *V. spinosum* protein extract of up to 15 μg and several buffer systems with varying pH values (data not shown). Based on the complementation, and supported by the cleavage assay, it is probable that the enzyme is active as a fusion enzyme in *V. spinosum*. Fusion enzymes involved in PG biosynthesis are not a new phenomenon; a MurC/Ddl fusion enzyme from *Chlamydia trachomatis* has been characterized and it was shown that the D-Ala:D-Ala ligase activity of the Ddl domain is dependent on the fusion structure of the MurC/Ddl protein (McCoy and Maurelli, 2005). Our present data show that at least the MurC domain of the *V. spinosum* MurB/C fusion protein is functionally independent as its expression allowed complementation of a temperature-conditional *murC* defect in *E. coli*.

Unusual MurB and MurC Composition is Prevalent in the Currently Sequenced Members of Verrucomicrobia

PhyloPhlAn-generated species tree of the PVC clade supports the monophyletic placement of the major lineage (SH-likelihood

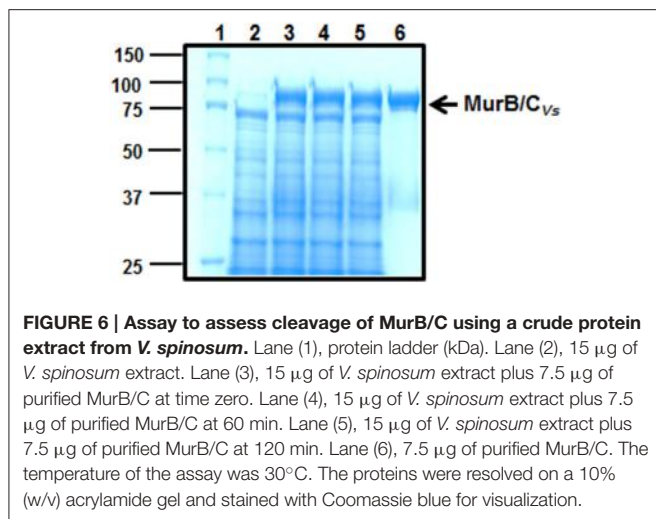


FIGURE 6 | Assay to assess cleavage of MurB/C using a crude protein extract from *V. spinosum*. Lane (1), protein ladder (kDa). Lane (2), 15 μ g of *V. spinosum* extract. Lane (3), 15 μ g of *V. spinosum* extract plus 7.5 μ g of purified MurB/C at time zero. Lane (4), 15 μ g of *V. spinosum* extract plus 7.5 μ g of purified MurB/C at 60 min. Lane (5), 15 μ g of *V. spinosum* extract plus 7.5 μ g of purified MurB/C at 120 min. Lane (6), 7.5 μ g of purified MurB/C. The temperature of the assay was 30°C. The proteins were resolved on a 10% (w/v) acrylamide gel and stained with Coomassie blue for visualization.

branch support of >0.90). A slightly lower than average SH-likeness support value of 0.94 was observed in the branch splitting the Chlamydiae and Lentisphaerae clades which presumably is due to low taxon sampling ($N = 1$) of the Lentisphaerae clade (Figure 7A). Fused MurB/C is present in all the currently sequenced members of Verrucomicrobiales (9/9) and Methylacidiphilales (3/3). These members usually exhibit a conserved *ftsW-murG-murB/C-ddLB-ftsQ* gene organization (Figure 7B) with the exception of *V. spinosum* DSM 4138, the type species and type strain for the genus *Verrucomicrobium* and species *V. spinosum*, respectively. In *V. spinosum* DSM 4138, the *murB/C* gene is flanked by genes that are not directly related to cell-wall synthesis. However, the monophyletic grouping of MurB/C protein (including that of *V. spinosum* DSM 4138) suggests that fused MurB/C is an authentic molecular signature in specific lineages of the phylum Verrucomicrobia and is not a result of inter-phylum horizontal gene transfer (Supplemental Figures 2A,B). TIGRFAM search failed to detect MurC domain in the predicted proteome from members of the class Opitutae (Figure 7A, green-colored branch). Despite lowering the detection threshold limit for MurC to the least stringent limit, e.g. noise cutoff, the MurC domain still could not be detected, thus supporting the absence of authentic MurC domain in this lineage. However, it is worth noting that the MurB proteins detected in nearly all members from Opitutae are longer than usual and contain the Mur ligase domain located at the N-terminal (Supplemental Figure 3 and data not shown), suggesting that although the N-terminal region has diverged substantially from the typical MurC, it may still share partially overlapping function with MurC.

DISCUSSION

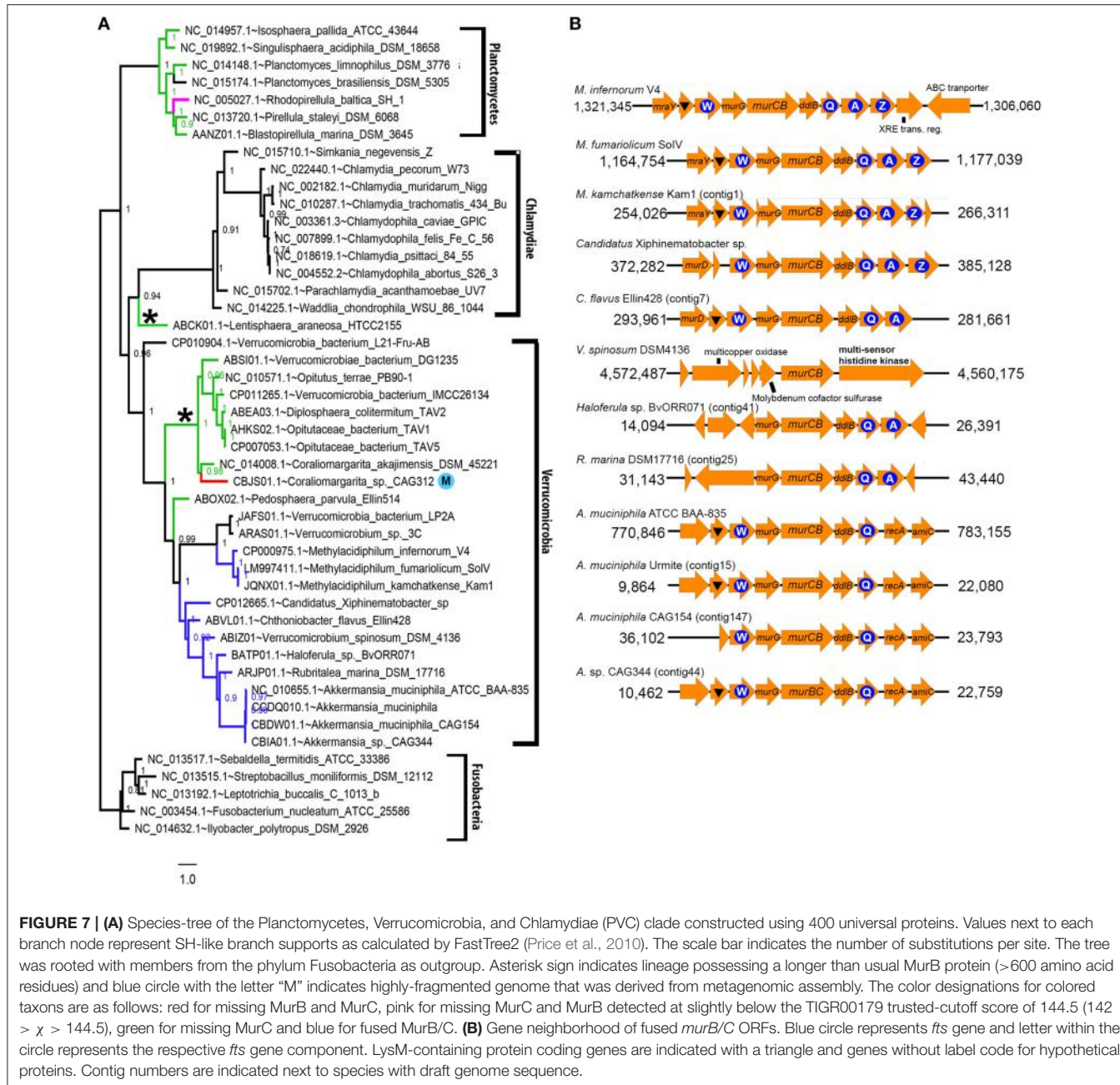
In the present paper, the *in vivo* MurB and MurC activities of the MurB/C_{Vs} fusion enzyme were revealed by functional complementation experiments. Furthermore, the protein was shown to be endowed with MurC ligase activity *in vitro* through

a specific radioactive assay. In Table 3, the properties and kinetic parameters of the MurC_{Vs} activity are compared with those of a reference ortholog (*E. coli*) and a phylogenetically related ortholog (*C. trachomatis*). The enzymes from *V. spinosum* and *E. coli* are comparable regarding their kinetic parameters. The maximum velocity of MurC_{Vs} is three-fold lower (but the k_{cat} value is only two-fold lower due to the high molecular mass of the fusion enzyme) when compared to the *E. coli* MurC. In addition, the optimal pH value (9.0) of the MurC_{Vs} falls within the range found for most Mur ligases (8.0–9.2) (Patin et al., 2009) and the observed pH optimum is comparable to that of MurE from *V. spinosum* (9.6). It is possible that such values of pH ≥ 9 reflect environmental factors such as the natural habitat of *V. spinosum* (McGroty et al., 2013). On the other hand, MurC enzymes from *V. spinosum* and *C. trachomatis* have quite different kinetic parameters. The main difference is the maximum velocity, which is 75-fold lower for *C. trachomatis* MurC when compared to the MurC from *V. spinosum*. Although many reasons can be put forward to explain such a low maximum velocity, a physiological explanation might be related to the slower growth rate of *C. trachomatis* given the fact that it is an intracellular parasite (Hesse et al., 2003).

Although L-alanine is the best substrate *in vitro*, L-serine and glycine are also reasonable substrates (Table 4). From the *in vitro* data, the discrimination between the three amino acids *in vivo* is much less obvious than for MurC from *E. coli* (Liger et al., 1995). Nevertheless, the determination of the amino acid composition of PG from *V. spinosum* proves undoubtedly that L-Ala is the amino acid found at position 1 of the peptide stem (McGroty et al., 2013). With *C. trachomatis* MurC, the discrimination was even less obvious, since the three amino acids were added to UDP-MurNAc with similar V_{max}/K_m values, thereby preventing us from deducing which amino acid was present in the putative chlamydial PG (Hesse et al., 2003; Patin et al., 2012). The recent mass spectrometric detection, from *C. trachomatis*-infected cell lysates, of muropeptides with alanine or glycine at position 1 strongly suggests that these amino acid are both used as MurC substrates by *C. trachomatis* *in vivo* (Packiam et al., 2015).

While the MurC_{Vs} activity could be totally characterized, the MurB_{Vs} activity could not be detected *in vitro*, even with the use of two different assays. Attempts to modify the assay conditions (different pH value, NADH instead of NADPH) were unsuccessful. A plausible explanation for the lack of MurB_{Vs} activity could be the denaturation of the MurB domain during or after the purification steps. Even though a cryoprotectant was included in the storage buffer, such a phenomenon cannot be ruled out. Another explanation would be that an unidentified cofactor(s) is necessary for activity which we are not aware of at this time. Nevertheless, the functional complementation of the *E. coli* murB thermosensitive strain by the murB/C_{Vs} gene proves that the MurB_{Vs} domain is active *in vivo* conditions.

Based on phylogenetic and protein domain scanning, most members of the Verrucomicrobia possess different compositions of MurB and MurC proteins. In some lineages, both proteins are fused as is the case for *V. spinosum*. In others, the MurC seems to be absent. Given the phenotype of Verrucomicrobia regarding the unusual body plan with respect to wart-like and



projections radiating from the central body, one would expect that PG biosynthesis would have an integral role pertaining to the shape of the bacterium (McGroarty et al., 2013). Theoretically, the possession of a fusion protein that catalyzes sequential steps in a particular pathway may constitute an advantage when compared to a system where these orthologous proteins are separate. These advantages may include control of the expression of two genes as a single unit, substrate channeling due to proximity of the catalysts, higher catalytic activities, etc. Whether such an advantage, if it exists, influences growth and development of *V. spinosum* is currently not known. Further studies to determine the structure of the MurB/C fusion enzyme would help shed some

light regarding the catalytic properties of the enzyme, especially since we were not able to demonstrate the MurB activity.

In summary, we present the first description of a MurB/C fusion enzyme from *V. spinosum*. *In vitro* biochemical analyses demonstrated that the enzyme is capable of catalyzing the ligase (MurC) reaction at position 1 on the peptide stem. *In vitro* analyses to demonstrate the MurB reductase were not successful even though *in vivo* analyses demonstrated that the fusion gene is able to functionally complement *E. coli* strains that harbor mutations in the *murB* and *murC* genes. Furthermore, dissection experiments showed that the MurB domain of the fusion protein was not essential for the UDP-N-acetylmuramate:L-alanine

ligase activity of the MurC domain. As this is the first description of a MurB/C fusion enzyme, there are no structural studies in the literature. Therefore, studies to solve the structure of fusion enzymes such as MurB/C_{Vs} and MurC/Ddl from *C. trachomatis* would help elucidate properties of the enzyme and have the potential to provide information regarding the rational design and/or identification of compounds that are deemed inhibitory and that could be developed as antibiotics. As such, this study lays the foundation regarding the further understanding of the kinetic, physical, and structural properties of a novel enzyme involved in the synthesis of PG.

AUTHOR CONTRIBUTIONS

All authors listed, have made substantial, direct and intellectual contribution to the work, and approved it for publication.

ACKNOWLEDGMENTS

AH, KN, MW, and MS thank the Thomas H. Gosnell School of Life Sciences (GSOLS) and the College of Science (COS) at the Rochester Institute of Technology (RIT) for ongoing support. This work was supported by a Dean's Research Initiation (D-RIG) awarded to AH by the COS at RIT. HG acknowledges the support from the Monash University Malaysia Tropical Medicine and Biology Multidisciplinary Platform. RD acknowledges the

following for funding support in part: (1) the Ministry of Business, Innovation, and Employment (contract UOCX1208), (2) the New Zealand Royal Society Marsden Fund (contract UOC1013), and (3) the US Army Research Laboratory and US Army Research Office under contract/grant number W911NF-11-1-0481. This work was also supported by grants from the Centre National de la Recherche Scientifique (UMR 9198).

SUPPLEMENTARY MATERIAL

The Supplementary Material for this article can be found online at: <http://journal.frontiersin.org/article/10.3389/fmicb.2016.00362>

Supplemental Figure 1 | Growth of *E. coli* murC thermosensitive strain H1119 transformed by vector pTrcHis60 (A), pTrcHis60::murC_{Ec} (B), pTrcHis60::murC_{Vs}-1 (C), and pTrcHis60::murC_{Vs}-2 (D).

Supplemental Figure 2 | Maximum likelihood tree of (A) MurB and (B) MurC proteins. Both trees are constructed using IQ-TREE version 1.3.10 with the optimized LG+G4 model. Value next to branch corresponds to IQ-TREE ultrafast bootstrap support value. Taxons containing fused MurB/MurC are colored red. The scale bar indicates the number of substitutions per site.

Supplemental Figure 3 | Complete InterProScan analysis of longer-than-usual MurB protein identified from the draft genome of Verrucomicrobiae bacterium DG1235 (accession number: ABSI01). The MurC domain corresponding to InterProScan ID IPR005758 (HAMAP: MF_00046; TIGRFAMs: TIGR01082) was absent from this MurB protein. However, domains corresponding to a general Mur ligase (N-terminal catalytic, central, and C-terminal domains) are present in the N-terminal region.

REFERENCES

- Barreteau, H., Kovač, A., Boniface, A., Sova, M., Gobec, A., and Blanot, D. (2008). Cytoplasmic steps of peptidoglycan biosynthesis. *FEMS Microbiol. Rev.* 32, 168–207. doi: 10.1111/j.1574-6976.2008.00104.x
- Benson, T. E., Marquardt, J. L., Marquardt, A. C., Etzkorn, F. A., and Walsh, C. T. (1993). Overexpression, purification, and mechanistic study of UDP-N-acetylenolpyruvylglucosamine reductase. *Biochemistry* 32, 2024–2030. doi: 10.1021/bi00059a019
- Bouhss, A., Dementin, S., van Heijenoort, J., Parquet, C., and Blanot, D. (2002). MurC and MurD synthetases of peptidoglycan synthesis: borohydride trapping of acyl-phosphate intermediates. *Methods Enzymol.* 354, 189–196.
- Bouhss, A., Trunkfield, A. E., Bugg, T. D., and Mengin-Lecreux, D. (2008). The biosynthesis of peptidoglycan lipid-linked intermediates. *FEMS Microbiol. Rev.* 32, 208–233. doi: 10.1111/j.1574-6976.2007.00089.x
- Bradford, M. M. (1976). A rapid and sensitive method for the quantification of microgram quantities of protein utilizing the principle of protein dye binding. *Anal. Biochem.* 72, 248–254. doi: 10.1016/0003-2697(76)90527-3
- Capella-Gutiérrez, S., Silla-Martínez, J. M., and Gabaldón, T. (2009). trimAl: a tool for automated alignment trimming in large-scale phylogenetic analyses. *Bioinformatics* 25, 1972–1973. doi: 10.1093/bioinformatics/btp348
- Cho, J. C., Vergin, K. L., Morris, R. M., and Giovannoni, S. J. (2004). Lentisphaera araneosa gen. nov., sp. nov., a transparent exopolymer producing marine bacterium, and the description of a novel bacterial phylum, Lentisphaerae. *Environ. Microbiol.* 6, 611–621. doi: 10.1111/j.1462-2920.2004.00614.x
- Eddy, S. R. (2011). Accelerated profile HMM searches. *PLoS Comput. Biol.* 7:e1002195. doi: 10.1371/journal.pcbi.1002195
- Falk, P. J., Ervin, K. M., Volk, K. S., and Ho, H. T. (1996). Biochemical evidence for the formation of a covalent acyl-phosphate linkage between UDP-N-acetylmuramate and ATP in the *Escherichia coli* UDP-N-acetylmuramate:L-alanine ligase-catalyzed reaction. *Biochemistry* 35, 1417–1422. doi: 10.1021/bi952078b
- Finn, D., Bateman, A., Clements, J., Coggill, P., Eberhardt, R. Y., Eddy, S. R., et al. (2014). Pfam: the protein families database. *Nucleic Acids Res.* 42, D222–D230. doi: 10.1093/nar/gkt1223
- Gubler, M., Appoldt, Y., and Keck, W. (1996). Overexpression, purification, and characterization of UDP-N-acetylglucosamine:N-acetylmuramyl-L-alanine ligase from *Escherichia coli*. *J. Bacteriol.* 178, 906–910.
- Guzman, L. M., Belin, D., Carson, M. J., and Beckwith, J. (1995). Tight regulation, modulation, and high level expression by vectors containing the arabinose pBAD promoter. *J. Bacteriol.* 177, 4121–4130.
- Haft, D. H., Selengut, J. D., and White, O. (2003). The TIGRFAMs database of protein families. *Nucleic Acids Res.* 31, 371–373. doi: 10.1093/nar/gkg128
- Hesse, L., Bostock, J., Dementin, S., Blanot, D., Mengin-Lecreux, D., and Chopra, I. (2003). Functional and biochemical analysis of *Chlamydia trachomatis* MurC, an enzyme displaying UDP-N-acetylglucosamine:N-acetylmuramyl-L-alanine ligase activity. *J. Bacteriol.* 185, 6507–6512. doi: 10.1128/JB.185.22.6507-6512.2003
- Hyatt, D., Chen, G. L., LoCascio, P. F., Land, M. L., Larimer, F. W., and Hauser, L. J. (2010). Prodigal: prokaryotic gene recognition and translation initiation site identification. *BMC Bioinformatics* 11:119. doi: 10.1186/1471-2105-11-119
- Katoh, K., and Standley, D. M. (2013). MAFFT multiple sequence alignment software version 7: improvements in performance and usability. *Mol. Biol. Evol.* 30, 772–780. doi: 10.1093/molbev/mst010
- Liger, D., Masson, A., Blanot, D., van Heijenoort, J., and Parquet, C. (1995). Over-production, purification and properties of the uridine-diphosphate-N-acetylmuramate:L-alanine ligase from *Escherichia coli*. *Eur. J. Biochem.* 230, 80–87. doi: 10.1111/j.1432-1033.1995.0080i.x
- Marchler-Bauer, A., Derbyshire, M. K., Gonzales, N. R., Lu, S., Chitsaz, F., Geer, L. Y., et al. (2015). CDD: NCBI's conserved domain database. *Nucleic Acids Res.* 43, D222–D226. doi: 10.1093/nar/gku1221
- Marquardt, J. L., Siegele, D. A., Kolter, R., and Walsh, C. T. (1992). Cloning and sequencing of *Escherichia coli* murZ and purification of its product, a UDP-N-acetylglucosamine enolpyruvyl transferase. *J. Bacteriol.* 174, 5748–5752.

- Matsuzawa, H., Matsuhashi, M., Oka, A., and Sugino, Y. (1969). Genetic and biochemical studies on cell wall peptidoglycan synthesis in *Escherichia coli* K-12. *Biochem. Biophys. Res. Commun.* 36, 682–689. doi: 10.1016/0006-291X(69)90360-X
- McCoy, A. J., and Maurelli, A. T. (2005). Characterization of *Chlamydia* MurC-Ddl, a fusion protein exhibiting D-alanyl-D-alanine ligase activity involved in peptidoglycan synthesis and D-cycloserine sensitivity. *Mol. Microbiol.* 57, 41–52. doi: 10.1111/j.1365-2958.2005.04661.x
- McGroty, S. E., Pattaniyil, D. T., Patin, D., Blanot, D., Ravichandran, A. C., Suzuki, H., et al. (2013). Biochemical characterization of UDP-N-acetyl muramoyl-L-alanyl-D-glutamate: meso-2,6-diaminopimelate ligase (MurE) from *Verrucomicrobium spinosum* DSM 4136(T). *PLoS ONE* 8:e66458. doi: 10.1371/journal.pone.0066458
- Miyakawa, T., Matsuzawa, H., Matsuhahi, M., and Sugino, Y. (1972). Cell wall peptidoglycan mutants of *Escherichia coli* K-12: existence of two clusters of genes, *mra* and *mrb*, for cell wall peptidoglycan synthesis. *J. Bacteriol.* 112, 950–958.
- Nachar, V. R., Savka, F. C., McGroty, S. E., Donovan, K. A., North, R. A., Dobson, R. C. J., et al. (2012). Genomic and biochemical analysis of the diaminopimelate and lysine biosynthesis pathway in *Verrucomicrobium spinosum*: identification and partial characterization of L,L-diaminopimelate aminotransferase and UDP-N-acetyl muramoylalanyl-D-glutamyl-2,6-meso-diaminopimelate ligase. *Front. Microbiol.* 3:183. doi: 10.3389/fmicb.2012.00183
- Nguyen, L. T., Schmidt, H. A., von Haeseler, A., and Minh, B. Q. (2014). IQ-TREE: A fast and effective stochastic algorithm for estimating maximum likelihood phylogenies. *Mol. Biol. Evol.* 32, 268–274. doi: 10.1093/molbev/msu300
- Packiam, M., Weinrick, B., Jacobs, W. R. Jr., and Maurelli, A. T. (2015). Structural characterization of muropeptides from *Chlamydia trachomatis* peptidoglycan by mass spectrometry resolves “chlamydial anomaly”. *Proc. Natl. Acad. Sci. U.S.A.* 112, 11660–11665. doi: 10.1073/pnas.1514026112
- Park, J. T. (1987). “Murein synthesis,” in *Escherichia coli* and *Salmonella typhimurium: Cellular and Molecular Biology*, Vol. 1, eds F. C. Neidhardt, J. L. Ingraham, K. B. Low, B. Magasanik, M. Schaechter, and H. E. Umbarger (Washington, DC: American Society for Microbiology), 663–671.
- Patin, D., Bostock, J., Blanot, D., Mengin-Lecreux, D., and Chopra, I. (2009). Functional and biochemical analysis of the *Chlamydia trachomatis* ligase MurE. *J. Bacteriol.* 191, 7430–7435. doi: 10.1128/JB.01029-09
- Patin, D., Bostock, J., Chopra, I., Mengin-Lecreux, D., and Blanot, D. (2012). Biochemical characterization of the chlamydial MurF ligase, and possible sequence of the chlamydial peptidoglycan pentapeptide stem. *Arch. Microbiol.* 194, 505–512. doi: 10.1007/s00203-011-0784-8
- Pilhofer, M., Aistleitner, K., Biboy, J., Gray, J., Kuru, E., Hall, E., et al. (2013). Discovery of chlamydial peptidoglycan reveals bacteria with murein sacci but without FtsZ. *Nat. Commun.* 4:2856. doi: 10.1038/ncomms3856
- Pompeo, F., van Heijenoort, J., and Mengin-Lecreux, D. (1998). Probing the role of cysteine residues in glucosamine-1-phosphate acetyltransferase activity of the bifunctional GlmU protein from *Escherichia coli*: Site-directed mutagenesis and characterization of the mutant enzymes. *J. Bacteriol.* 180, 4799–4803.
- Press, W. H., Flannery, B. P., Teukolsky, S. A., and Vetterling, W. T. (1986). *Numerical Recipes: The Art of Scientific Computing*. Cambridge: Cambridge University Press.
- Price, M. N., Dehal, P. S., and Arkin, A. P. (2010). FastTree 2 – approximately maximum-likelihood trees for large alignments. *PLoS ONE* 5:e9490. doi: 10.1371/journal.pone.0009490
- Pucci, M. J., Discotto, L. F., and Dougherty, T. J. (1992). Cloning and identification of the *Escherichia coli* murB DNA sequence, which encodes UDP-N-acetylenolpyruvoylglucosamine reductase. *J. Bacteriol.* 174, 1690–1693.
- Sait, M., Kamneva, O. K., Fay, D. S., Kirienko, N. V., Polek, J., Shirasu-Hiza, M. M., et al. (2011). Genomic and experimental evidence suggests that *Verrucomicrobium spinosum* interacts with eukaryotes. *Front. Microbiol.* 2:211. doi: 10.3389/fmicb.2011.00211
- Scheffers, D. J., and Pinho, M. G. (2005). Bacterial cell wall synthesis: new insights from localization studies. *Microbiol. Mol. Biol. Rev.* 69, 585–607. doi: 10.1128/MMBR.69.4.585-607.2005
- Schleifer, K. H., and Kandler, O. (1972). Peptidoglycan types of bacterial walls and their taxonomic implications. *Bacteriol. Rev.* 36, 407–477.
- Schlesner, H. (1987). *Verrucomicrobium spinosum* gen. nov., sp. nov.: a fimbriated prostheteate bacterium. *Syst. Appl. Microbiol.* 10, 54–56. doi: 10.1016/S0723-2020(87)80010-3
- Segata, N., Börnigen, D., Morgan, X. C., and Huttenhower, C. (2013). PhyloPhAn is a new method for improved phylogenetic and taxonomic placement of microbes. *Nat. Commun.* 4, 2304. doi: 10.1038/ncomms3304
- Sullivan, M. J., Petty, N. K., and Beatson, S. A. (2011). Easyfig: a genome comparison visualizer. *Bioinformatics* 27, 1009–1010. doi: 10.1093/bioinformatics/btr039
- Tayeh, M. A., Dotson, G. D., Clemens, J. C., and Woodard, R. W. (1995). Overproduction and one-step purification of *Escherichia coli* UDP-N-acetylglucosamine enolpyruvyl reductase. *Protein Expr. Purif.* 6, 757–762. doi: 10.1006/prep.1995.0006
- Vollmer, W., Blanot, D., and de Pedro, M. A. (2008). Peptidoglycan structure and architecture. *FEMS Microbiol. Rev.* 32, 149–167. doi: 10.1111/j.1574-6976.2007.00094.x
- Wagner, M., and Horn, M. (2006). The *Planctomycetes*, *Verrucomicrobia*, *Chlamydiae* and sister phyla comprise a superphylum with biotechnological and medical relevance. *Curr. Opin. Biotechnol.* 17, 241–249. doi: 10.1016/j.copbio.2006.05.005
- Wanke, C., Falchetto, R., and Amrhein, N. (1992). The UDP-N-acetylglucosamine 1-carboxyvinyl-transferase of *Enterobacter cloacae*. Molecular cloning, sequencing of the gene and overexpression of the enzyme. *FEBS Lett.* 301, 271–276. doi: 10.1016/0014-5793(92)80255-F
- Wijsman, H. J. (1972). A genetic map of several mutations affecting the mucopeptide layer of *Escherichia coli*. *Genet. Res.* 20, 65–74. doi: 10.1017/S0016672300013598

Conflict of Interest Statement: The authors declare that the research was conducted in the absence of any commercial or financial relationships that could be construed as a potential conflict of interest.

Copyright © 2016 Naqvi, Patin, Wheatley, Savka, Dobson, Gan, Barreteau, Blanot, Mengin-Lecreux and Hudson. This is an open-access article distributed under the terms of the Creative Commons Attribution License (CC BY). The use, distribution or reproduction in other forums is permitted, provided the original author(s) or licensor are credited and that the original publication in this journal is cited, in accordance with accepted academic practice. No use, distribution or reproduction is permitted which does not comply with these terms.



Three Novel Species with Peptidoglycan Cell Walls form the New Genus *Lacunisphaera* gen. nov. in the Family Opitutaceae of the Verrucomicrobial Subdivision 4

Patrick Rast¹, Ines Glöckner², Christian Boedeker¹, Olga Jeske¹, Sandra Wiegand¹, Richard Reinhardt³, Peter Schumann⁴, Manfred Rohde⁵, Stefan Spring⁶, Frank O. Glöckner⁷, Christian Jogler^{1,8*} and Mareike Jogler^{1*}

OPEN ACCESS

Edited by:

Damien Paul Devos,
Pablo de Olavide University, Spain

Reviewed by:

Seong Woon Roh,
Korea Basic Science Institute,
South Korea

George Liechti,

Uniformed Services University of the
Health Sciences, USA

*Correspondence:

Christian Jogler
christian@jogler.de

Mareike Jogler
mareike@jogler.de

Specialty section:

This article was submitted to
Evolutionary and Genomic
Microbiology,
a section of the journal
Frontiers in Microbiology

Received: 28 September 2016

Accepted: 27 January 2017

Published: 13 February 2017

Citation:

Rast P, Glöckner I, Boedeker C, Jeske O, Wiegand S, Reinhardt R, Schumann P, Rohde M, Spring S, Glöckner FO, Jogler C and Jogler M (2017) Three Novel Species with Peptidoglycan Cell Walls form the New Genus *Lacunisphaera* gen. nov. in the Family Opitutaceae of the Verrucomicrobial Subdivision 4. *Front. Microbiol.* 8:202.

doi: 10.3389/fmicb.2017.00202

¹ Microbial Cell Biology and Genetics, Leibniz-Institut DSMZ-Deutsche Sammlung von Mikroorganismen und Zellkulturen GmbH, Braunschweig, Germany, ² Institute for Pharmacology, Toxicology and Clinical Pharmacy, University of Technology, Braunschweig, Germany, ³ Max Planck Genome Center, Max Planck Institute for Plant Breeding Research, Köln, Germany,

⁴ Department of Central Services, Leibniz-Institut DSMZ-Deutsche Sammlung von Mikroorganismen und Zellkulturen GmbH, Braunschweig, Germany, ⁵ Central Facility for Microscopy, Helmholtz Centre for Infection Research, Braunschweig, Germany, ⁶ Department Microorganisms, Leibniz-Institut DSMZ-Deutsche Sammlung von Mikroorganismen und Zellkulturen GmbH, Braunschweig, Germany, ⁷ Department of Molecular Ecology, Max Planck Institute for Marine Microbiology, Bremen, Germany, ⁸ Department of Microbiology, Institute for Water and Wetland Research, Faculty of Science, Radboud University, Nijmegen, Netherlands

The cell wall of free-living bacteria consists of peptidoglycan (PG) and is critical for maintenance of shape as dissolved solutes cause osmotic pressure and challenge cell integrity. Surprisingly, the subdivision 4 of the phylum Verrucomicrobia appears to be exceptional in this respect. Organisms of this subdivision are described to be devoid of muramic or diaminopimelic acid (DAP), usually found as components of PG in bacterial cell walls. Here we describe three novel bacterial strains from a freshwater lake, IG15^T, IG16b^T, and IG31^T, belonging to a new genus in the subdivision 4 of Verrucomicrobia which we found to possess PG as part of their cell walls. Biochemical analysis revealed the presence of DAP not only in these novel strains, but also in *Opitutus terrae* PB90-1^T, the closest described relative of strains IG15^T, IG16b^T, and IG31^T. Furthermore, we found that nearly all genes necessary for peptidoglycan synthesis are present in genomes of subdivision 4 members, as well as in the complete genome sequence of strain IG16b^T. In addition, we isolated and visualized PG-sacculi for strain IG16b^T. Thus, our results challenge the concept of peptidoglycan-less free-living bacteria. Our polyphasic taxonomy approach places the novel strains in a new genus within the family Opitutaceae, for which the name *Lacunisphaera* gen. nov. is proposed. Strain designations for IG15^T, IG16b^T and IG31^T are *Lacunisphaera parvula* sp. nov. (=DSM 26814 = LMG 29468), *L. limnophila* sp. nov. (=DSM 26815 = LMG 29469) and *L. anatis* sp. nov. (=DSM 103142 = LMG 29578) respectively, with *L. limnophila* IG16b^T being the type species of the genus.

Keywords: peptidoglycan, subdivision 4, Verrucomicrobia, *Lacunisphaera*, ornithine

INTRODUCTION

In aquatic environments, abiotic factors such as salinity and temperature, but also intrinsic metabolism-related mechanisms challenge the cellular integrity of microorganisms and their ability to proliferate. Protective elements may be of a structural nature, such as S-layers, or the avoidance of osmotic stress by living in dependency of host organisms which provide stable conditions for survival (Miles, 1992; Engelhardt, 2007). Members of the class Mollicutes for example lack a peptidoglycan cell wall (Razin, 2006), are osmotically fragile and exhibit pleomorphism (Miles, 1992). Thus, they depend on an eukaryotic host to provide an osmotically stable environment for living.

On the other hand, free-living bacteria usually possess cell wall structures including three dimensionally cross-linked polymeric glycan strands, interconnected by short peptide elements, a structure commonly known as peptidoglycan (PG) to protect cellular integrity. Among bacteria only few exceptions are described while all controversy discussed species belong to the Planctomycetes-Verrucomicrobia-Chlamydiae (PVC) superphylum (Wagner and Horn, 2006). In many respects, this PVC-superphylum seems to challenge our concept of the prokaryotic cell (Lee et al., 2009; Fuerst and Sagulenko, 2011; Jacquier et al., 2015; Rivas-Marín et al., 2016). In particular, the suggested absence of PG in Planctomycetes (König et al., 1984), Chlamydia (Fox et al., 1990) and subdivision 4 Verrucomicrobia (Yoon, 2011) is remarkable. While the assumed lack of PG seems to be associated with the lack of the otherwise universal bacterial cell division protein FtsZ in Planctomycetes (Pilhofer et al., 2008; Jogler et al., 2012) and Chlamydia (Stephens et al., 1998), subdivision 4 Verrucomicrobia encode the tubulin homolog FtsZ (Pilhofer et al., 2008). However, Planctomycetes were recently found to possess a PG cell wall (Jeske et al., 2015; van Teeseling et al., 2015). For Chlamydia, the existence of PG was demonstrated but a canonical PG sacculus was not isolated (Liechti et al., 2014; Packiam et al., 2015). However, for some other members of the phylum Chlamydiae a PG sacculus was identified (Pilhofer et al., 2013). Chlamydia are obligate intracellular pathogens (Jacquier et al., 2015) and thus dwell in an environment isotonic to their cytoplasm, they do not necessarily require a peptidoglycan sacculus to maintain cell shape. Accordingly, recent evidence suggests that PG forms an MreB regulated ring at mid-cell to allow cell division in pathogenic Chlamydia (Liechti et al., 2016). In contrast a typical bacterial sacculus was reported for the free-living Planctomycetes that have to withstand various osmotic challenges in their natural habitats (Jeske et al., 2015; van Teeseling et al., 2015), while free-living bacteria of the verrucomicrobial subdivision 4 are still considered to lack a PG sacculus. This bacterial group belongs to the phylum Verrucomicrobia which is divided into six so-called subdivisions. Thus far, cultured representatives are available for subdivisions 1–4. Recently for subdivision 5 the new Phylum Kiritimatiellaeota was proposed, with one characterized isolate (Spring et al., 2016). Playing a crucial role in environmental nutrient cycles, members of the Verrucomicrobia have not only been found to degrade a variety of complex polymeric compounds in, e.g., soil communities (Wang et al., 2014, 2015),

some were also identified as methanotrophs (Sharp et al., 2013; van Teeseling et al., 2014). Increasing efforts to extend the knowledge about this environmentally important phylum have led to the successful isolation and description of several new species in recent years (Lee et al., 2014; Kim et al., 2015). However, the majority of new strains brought into pure culture is affiliated with subdivision 1. Therefore, the scarce data existing to date leaves inconclusive results about the suspected peptidoglycan anomaly of subdivision 4 Verrucomicrobia. Furthermore, thus far only two genomes from validly described species (*Opitutus terrae* and *Coraliomargarita akajimensis*) are available. Both genomes were not yet analyzed for PG related genes with state-of-the-art bioinformatic methods (Jeske et al., 2015). Some members of this subdivision have been found to be resistant to various β -lactam antibiotics, indicating either absence of PG or an resistance mechanism such as β -lactamases. For other strains the presence of typical cellular PG building blocks was not investigated at the time of their description (Shieh and Jean, 1998; Choo et al., 2007), leaving open the question whether peptidoglycan exists in verrucomicrobial subdivision 4. Members of this subdivision have been isolated from soil communities and leafs, while most strains originate from aquatic habitats, including freshwater lakes, marine waters and extreme habitats such as hot springs (Shieh and Jean, 1998; Chin et al., 2001; Choo et al., 2007; Yoon et al., 2007c, 2010). Here we describe the targeted isolation of subdivision 4 Verrucomicrobia, using antibiotic agents as selective markers for β -lactam resistant bacteria. Our strategy led to the successful cultivation of three novel strains from surface fresh water samples. By biochemical, microscopic and computational analysis we found that the novel and previously reported members of the verrucomicrobial subdivision 4 possess PG as part of their cell walls.

Our findings challenge the proposed absence of peptidoglycan among subdivision 4 Verrucomicrobia, while at the same time extending the scarce pool of cultivated species in this environmentally important phylum.

MATERIALS AND METHODS

Sample Collection and Preparation

Surface freshwater samples were collected in triplicates from a local pond ($52^{\circ} 9' 38''$ N, $10^{\circ} 32' 40''$ E, Wolfenbüttel, Germany) on August 30th, 2012 after the observation of a massive cyanobacterial blooming event. Water was collected in sterile polypropylene bottles, immediately transferred to the laboratory, homogenized and processed within 2 h.

Culture Media and Bacterial Isolation

Cultivation medium M1H was prepared with double distilled water containing 0.25 g/l peptone (BactoTM), 0.25 g/l yeast extract (BactoTM), 2.38 g/l HEPES (Serva), 20 ml/l mineral salt solution and a pH adjusted to 8.0 with 5 M KOH. After sterilization, the medium was complemented with 10 ml/l of a 2.5% glucose solution, 5 ml/l double concentrated vitamin solution, 1 ml/l of 100 mg/ml carbenicillin and 20 mg/ml cycloheximide stock solutions, respectively. Solid medium was

prepared with three times washed 12 g/l agar (BactoTM) and cooled to 55°C prior to the addition of heat sensitive solutions. Both, mineral salt solution and double concentrated vitamin solution were prepared according to DSMZ medium 621, while metal salts solution consisted of 250 mg/l Na-EDTA, 1095 mg/l ZnSO₄·7H₂O, 500 mg/l FeSO₄·7H₂O, 154 mg/l MnSO₄·H₂O, 39.5 mg/l CuSO₄·7H₂O, 20.3 mg/l CoCl₂·6H₂O, and 17.7 mg/l Na₂B₄O₇·10H₂O of which 50 ml were added per liter of mineral salt solution.

For initial bacterial isolation, solid M1H medium was supplemented with 100 µl of carbenicillin stock solution (100 mg/ml), dried for 30 min and inoculated with 100 µl homogenized sample material per plate in a 10–10⁻² dilution series and incubated at 20°C in the dark until colony formation became visible. Single colonies were inoculated on fresh solid medium with respective antibiotics. Pure cultures were cryopreserved in M1H medium supplemented with 50% glycerol or 5% DMSO and stored at -80°C. Strains isolated and later identified as members of the verrucomicrobial subdivision 4 were designated IG15^T, IG16b^T and IG31^T. Unless otherwise indicated, verrucomicrobial strains were cultivated at 28°C to ensure reproducibility of cultivation dependent experiments.

Cultivation medium of thin layer chromatography (TLC) reference strains, *Bacillus subtilis* DSM 10 and *Escherichia coli* DSM 498, was standard LB medium contained 10 g/l tryptone, 10 g/l sodium chloride and 5 g/l yeast extract at pH 7.0 (Bertani, 1951).

For *O. terrae* PB90-1^T cultivation was performed following the recommendations of the Leibniz Institute DSMZ (DSMZ medium no. 295).

Molecular Identification and Phylogenetic Analysis

Novel isolates were identified by direct sequencing of the 16S rRNA gene after amplification with the optimized universal primers 8f (5'-AGA GTT TGA TCM TGG CTC AG-3') and 1492r (5'-GGY TAC CTT GTT ACG ACT T-3') modified from (Lane, 1991). PCR reactions were performed directly on single colonies for identification or liquid cultures to check for purity, using the *Taq* DNA Polymerase Kit (Qiagen) with one reaction of 25 µl containing 11 µl PCR-grade H₂O, 2.5 µl 10x CoralLoad buffer, 2.5 µl Q-Solution, 0.5 µl dNTPs (10 mM each), 1 µl sterile bovine serum albumin solution (20 mg/ml), 0.5 µl MgCl₂ solution (25 mM), 0.125 µl *Taq*-Polymerase (1 U/µl) and 1 µl of each primer (10 pmol). The employed protocol consisted of two steps, the first step with an initial denaturation at 94°C, 5 min, 10 cycles of denaturation at 94°C, 30 s, annealing at 59°C, 30 s, elongation at 72°C, 1 min, followed by the second step with 20 cycles denaturation at 94°C, 30 s, annealing at 54°C, 30 s, elongation at 72°C, 1 min and a final elongation step at 72°C, 7 min. All PCRs were carried out in an Applied Biosystems[®] Veriti[®] thermal cycler (Thermo Fisher Scientific) and PCR products were stored at 4°C until Sanger sequencing.

To generate near full length 16S sequences, additional primers (compare Supplementary Table S1) were used for sequencing and assembly of the resulting sequences was performed with

the ContigExpress application of the Vector NTI[®] Advance 10 software (Thermo Fisher Scientific).

Alignment of near full length 16S rRNA sequences was performed using the SINA web aligner (Pruesse et al., 2012), corrected manually and used for phylogenetic tree reconstruction. Tree reconstruction was performed with the ARB software package (Ludwig et al., 2004) using the Maximum Likelihood RAxML module and rate distribution model GTR GAMMA running the rapid bootstrap analysis algorithm, the Neighbor Joining tool with Felsenstein correction for DNA and Maximum Parsimony method employing the Phylip DNAPARS module. Bootstrap values for all three methods were computed with 1,000 resamplings including the *E. coli* 16S rRNA gene positions 101–1,371. The analysis involved 68 nucleotide sequences of described type strains and uncultured clones, related to the novel strains (compare Supplementary Table S2). 16S rRNA gene identity values of novel isolates and related type strains were calculated using neighbor joining clustering of the ARB package.

Characterization of Novel Isolates Morphological, Physiological, and Biochemical Analysis

Bacterial cells were immobilized on a 1% agarose-pad in MatTek 35 mm glass-bottom dishes and imaged under phase-contrast illumination using a Nikon Eclipse Ti invers microscope at 100× magnification and the Nikon DS-Ri2 camera. To determine the cell size of the novel strains, 100 individual cells of each strain were measured using the NIS-Elements software V4.3 (Nikon Instruments).

For field emission scanning electron microscopy (FESEM) bacteria were fixed in 1% formaldehyde in HEPES buffer (3 mM HEPES, 0.3 mM CaCl₂, 0.3 mM MgCl₂, 2.7 mM sucrose, pH 6.9) for 1 h on ice and washed one time with HEPES buffer. Cover slips with a diameter of 12 mm were coated with a poly-L-lysine solution (Sigma-Aldrich) for 10 min, washed in distilled water and air-dried. 50 µl of the fixed bacteria solution was placed on a cover slip and allowed to settle for 10 min. Cover slips were then fixed in 1% glutaraldehyde in TE buffer (20 mM TRIS, 1 mM EDTA, pH 6.9) for 5 min at room temperature and subsequently washed twice with TE-buffer before dehydrating in a graded series of acetone (10, 30, 50, 70, 90, and 100%) on ice for 10 min at each concentration. Samples from the 100% acetone step were brought to room temperature before placing them in fresh 100% acetone. Samples were then subjected to critical-point drying with liquid CO₂ (CPD 300, Leica). Dried samples were covered with a gold/palladium (80/20) film by sputter coating (SCD 500, Bal-Tec) before examination in a field emission scanning electron microscope (Zeiss Merlin) using the Everhart Thornley HESE2-detector and the inlens SE-detector in a 25:75 ratio at an acceleration voltage of 5 kV.

Temperature optima of the novel isolates were determined by optical density measurements of growing cultures at 600 nm (OD_{600nm}). Strains were inoculated 1:10 from early stationary phase cultures in glass tubes with M1H medium and incubated under constant agitation in temperature controlled shakers (for exact temperatures tested, compare Supplementary Figure S1).

Measurements were performed in triplicates and each tube served as its own blank prior to inoculation. Resulting growth curves were analyzed by plotting change of OD_{600nm} during exponential growth phases (slope values), of each individual temperature against temperature values in °C.

To determine the pH optimum, M1H medium was buffered to pH values of 5.0, 6.0, 6.5, 7.0, 7.5, 8.0, 8.5, 9.0, and 10.0 using 10 mM MES, HEPES, HEPPS and CHES buffers, corresponding to their individual buffer range. OD_{600nm} was determined in glass tubes, incubated at 28°C, with three replicates as measure of growth. Catalase activity was determined by bubble formation with fresh 3% H₂O₂ solution. Cytochrom oxidase activity was determined using Bactident® Oxidase test stripes (Merck Millipore) following the manufacturer's instructions. Gram properties were determined by reaction of fresh biomass with fresh 3% KOH solution (Suslow et al., 1982).

Substrate utilization of the isolated strains was investigated using the Biolog GN2 MicroLog™ test panel for Gram-negative bacteria. Sterile glass tubes were prepared in duplicates with a basic medium mixture containing 15.7 ml IF-0a inoculation fluid (Biolog), 160 µl of 1 M HEPES buffer (pH 8.0) and 80 µl double concentrated vitamin solution. Tubes were inoculated with bacterial colony material from exponentially growing cultures to a turbidity of 56–68%. Two individual plates per strain were evaluated. To enable the comparison of the derived data, the data of each single experiment were normalized to 100. Only values corresponding to >25% utilization were considered as positive. The heat map graphic was obtained in the R environment (R Core Team, 2015) by using the heatmap.2() function of the gplots package.

Analysis of Cellular Fatty Acids

Biomass of the isolated strains was obtained from liquid cultures grown in M1H medium at 28°C until stationary phase. The obtained biomasses were stored at –20°C. For fatty acid analysis, 30 mg of lyophilized biomass was processed according to the standards of the Identification Service of the German Collection of Microorganisms and Cell Cultures (DSMZ) (Miller, 1982; Kuykendall et al., 1988).

Determination of Molar G + C Content

Strains were grown in liquid culture to stationary phase and biomass was obtained by centrifugation. For strains IG15^T and IG31^T, the molar G + C content was determined by the service facilities of the DSMZ. In brief, genomic DNA is isolated (Cashion et al., 1977), hydrolyzed, dephosphorylated (Mesbah et al., 1989) and analyzed by HPLC (Tamaoka and Komagata, 1984) in comparison to DNA standards from organisms with published genome sequences and a G + C content range from 43 to 72 mol%. G + C content of strain IG16b^T was determined during genome sequencing with the Pacific Bioscience sequencer.

Antibiotic Susceptibility

Tolerance of IG15^T and IG16b^T toward β-lactam antibiotic agents was investigated in a treatment assay using carbenicillin. Strains were inoculated as triplicates 1:10 in glass tubes with M1H medium and final concentrations of 0, 500, 1000, or 2000 mg/l

carbenicillin were added. Tubes were incubated at 28°C and growth was measured as change in optical density at 600 nm. After 120 h of incubation, cell viability was investigated by FESEM and cell numbers per ml were calculated by counting with a Neubauer chamber.

Genome Sequencing of Strain IG16b^T

DNA Extraction and Purity Control

To obtain high molecular weight DNA of strain IG16b^T, nucleic acid was extracted from whole-cells using a tweaked Genomic DNA kit protocol with Genomic tips 100/G (Qiagen). The protocol was performed as recommended by the manufacturer with one exception: incubation time with digestive enzymes was prolonged to an overnight step to ensure complete lysis of bacterial cells. An aliquot of the extracted DNA was used to prepare 16S rRNA clone libraries (Zero Blunt® PCR Cloning kit; Invitrogen) and resulting clones were sequenced to ensure purity of the extracted DNA.

Sequencing and Gene Content Analysis

De novo genome sequencing of strain IG16b^T was performed using a PacBio RS sequencer. Single molecule real-time (SMRT) bell™ libraries (Pacific Bioscience) were prepared using ~10 µg genomic DNA. Sequencing data was processed and assembled using the SMRT analysis software. The closed and complete chromosome of strain IG16b^T was annotated using the Prokka annotation tool (Seemann, 2014) and subjected to analysis for putative genomic islands and phage regions using IslandViewer3 (Dhillon et al., 2015) and PHAST (Zhou et al., 2011), respectively. The verrucomicrobial genomes for the gene content analysis were derived from NCBI and IMG (Markowitz et al., 2012) in April 2016 and had to match the following criteria upon CheckM analysis (Parks et al., 2015): completeness > 90, contamination < 5 and strain heterogeneity < 20. Orthologs were detected by Proteinortho (Lechner et al., 2011), a tool that identifies the reciprocal best hits from the given protein sequences. The genome plot was then generated with BRIG (Alikhan et al., 2011).

Peptidoglycan Analysis

Identification of Peptidoglycan Synthesis Genes and β-lactamase Protein Homologs

The presence of peptidoglycan synthesis genes was analyzed using blastp (Altschul et al., 1997), while protein sequences of *Phycisphaera mikurensis* FYK2301M01^T or *Gimesia maris* 534-30^T served as query and were compared with protein sequences encoded in the genomes of *O. terrae* PB90-1^T, *C. akajimensis* 04OKA010-24^T and strain IG16b^T. β-lactamase encoding genes were detected in IG16, *O. terrae* and *C. akajimensis* as previously described (Bush, 2013; Jeske et al., 2015). For both analysis, homologous proteins required an identity >30%, an e-value lower than 1e⁻⁶ and a conserved domain architecture.

Lysozyme Assay

Susceptibility to lysozyme was investigated by incubation of the novel strains in M1H medium. Since strain IG31^T showed no lysis after 24 h in M1H medium, osmotic stress was

increased by incubation of cells in ddH₂O (negative controls as well as lysozyme treated cells). Lysozyme was added to a final concentration of 10 mg/ml and cells were incubated for up to 24 h at 37°C under constant agitation at 300 rpm. Bacterial cells were immobilized on a 1% agarose-pad in MatTek 35 mm glass-bottom dishes and imaged under phase-contrast illumination using a Nikon Eclipse Ti invers microscope at 100× magnification and the Nikon DS-Ri2 camera (Nikon Instruments). Cell viability was checked by microscopy after 1, 3, 6, and 24 h of incubation in M1H medium or ddH₂O until cell lysis was observed.

Biochemical Analysis of Peptidoglycan Building Blocks

The presence of diaminopimelic acid (DAP) was investigated employing thin-layer chromatography and gas chromatography/mass spectrometry (GC/MS). Thin-layer chromatography of whole-cell hydrolysates of strains IG15^T, IG16b^T, IG31^T as well as reference strains *B. subtilis* DSM 10 and *E. coli* DSM 498 was performed as previously described (Staneck and Roberts, 1974). Novel isolates were grown in M1H medium at 28°C to stationary phase and cells were harvested by centrifugation. *B. subtilis* and *E. coli* served as organismic controls, grown in 50 ml LB medium at 37°C overnight and harvested by centrifugation, while a mixture of purified DAP isomers (Sigma) was used as detection standard.

Whole-cell hydrolysates of strains IG15^T, IG16b^T, IG31^T as well as of *O. terrae* PB90-1^T (DSM 11246) were analyzed using a gas chromatography/mass spectrometry (GS/MS)-based method (Schumann, 2011), previously employed to quantify the peptidoglycan marker DAP and in addition ornithine in a new proposed Verrucomicrobia related phylum (Spring et al., 2016). In brief, cell pellets were obtained from liquid cultures (grown as described above) and biomass was lyophilized. Samples were standardized for the quantification of diagnostic diamino acids by supplementing lyophilized biomass with 2 µmol of norleucine as internal standard. The hydrolysates (200 µl 4N HCl, 100°C, 16 h) of the samples were dried in a vacuum desiccator. Amino acids derivatized to N-heptafluorobutyryl isobutylesters and were resolved in ethyl acetate and analyzed by GC/MS (Singlequad 320, Varian; electron impact ionization, scan range 60 to 800 m/z). The DAP derivative was detected in extracted ion chromatograms using the characteristic fragment ion set 380, 324, 306, and 278 m/z at a retention time of 22.17 min. A fragment ion of 266 m/z with a retention time of 15.13 min was indicative of the presence of ornithine.

Preparation of IG16b^T Sacculi

Cells of IG16b^T were harvested from 2 l of stationary phase cultures grown in M1H medium at 28°C, by centrifugation at room temperature following a protocol established by van Teeseling et al. (2015). In brief, cells were boiled at 100°C for 1 h with 4% SDS, while being gently mixed by inverting the reaction tube several times in 15 min intervals. Lysates were transferred to Float-a-Lyzer® dialysis tubes (SpectrumLabs, DG Breda, Netherlands) and dialyzed against deionized water in a five-liter beaker over the course of 3 days (water was exchanged

two times). Dialyzed samples were stored at RT until analysis by transmission electron microscopy (TEM).

Negative Staining of IG16b^T Sacculi

Thin carbon support films were prepared by sublimation of a carbon thread onto a freshly cleaved mica surface. Lysate containing the sacculi was adsorbed onto a carbon film for 1 min and negatively stained with 1% (w/v) aqueous uranyl acetate, pH 5.0 (Valentine et al., 1968). After air-drying, samples were examined in a TEM 910 transmission electron microscope (Carl Zeiss, Oberkochen, Germany) at an acceleration voltage of 80 kV and calibrated magnifications using a line replica. Images were recorded digitally with a Slow-Scan CCD-Camera (ProScan, 1024x1024, Scheuring, Germany) with ITEM-Software (Olympus Soft Imaging Solutions, Münster, Germany).

Nucleotide Sequence Accession Numbers

Near full-length sequences of the 16S ribosomal RNA genes as well as the complete genome sequence of strain IG16b^T were deposited with the National Center for Biotechnology Information (NCBI) and are available under KX058881 (IG15^T), KX058882 (IG16b^T), KX058883 (IG31^T) and CP016094 (IG16b^T whole genome).

RESULTS

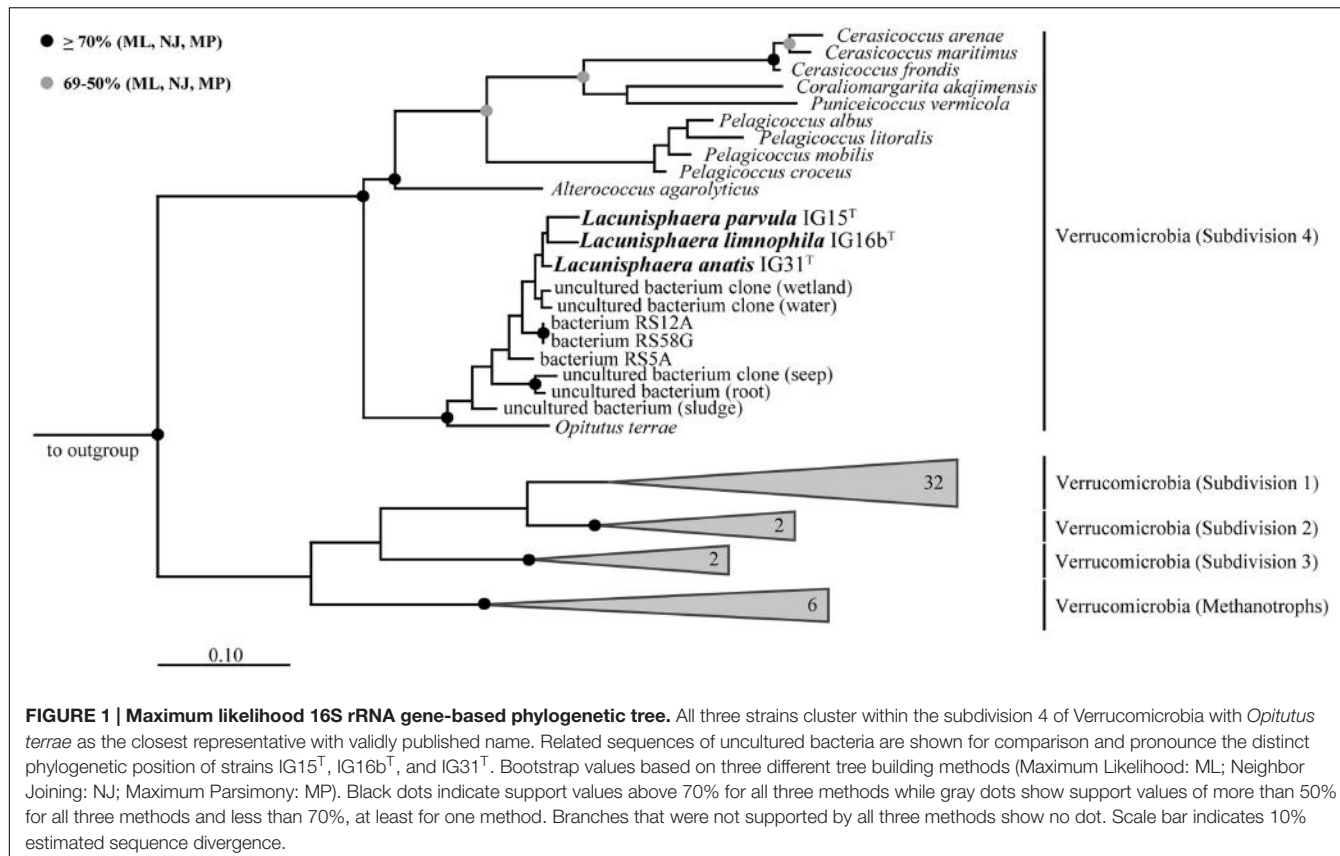
Novel Species of the Verrucomicrobial Subdivision 4

Isolation and Identification

Surface water samples from a local duck pond were used for the targeted isolation of novel subdivision 4 Verrucomicrobia. Given that members of subdivision 4 were thought to lack peptidoglycan, β-lactam antibiotics were used as selection pressure to enrich target bacteria. Obtained colonies of β-lactam resistant bacteria were screened by 16S rRNA gene sequencing analysis and three isolates were identified as members of the verrucomicrobial subdivision 4. Phylogenetic tree reconstruction based on near full-length 16S rRNA gene sequences (Figure 1) revealed that strains IG15^T, IG16b^T, and IG31^T belong to the family of *Opitutaceae*, sharing 92.21, 92.39, and 92.90% sequence identity with the closest related species *O. terrae* PB90-1^T, respectively (Table 1). Based on recent threshold values for 16S rRNA gene sequence comparison (Rosselló-Móra and Amann, 2015), the novel strains represent three distinct species that form a novel genus within the family *Opitutaceae*, with IG15^T, IG16b^T, and IG31^T being the type strains.

Morphological, Physiological, and Biochemical Characterization of Novel Strains

Cells of strains IG15^T, IG16b^T, and IG31^T were investigated using light microscopic and electron microscopic techniques, revealing a coccoid cell shape with cells present as mono- or diplococci (Figures 2 and 3). No chain or rosette formation was observed. IG15^T cells were the smallest of the three strains in average, measuring 0.6 ± 0.1 µm (diameter of single cocci



with standard deviation; $n = 100$ cells) while cells of $IG16b^T$ and $IG31^T$ measured 0.9 ± 0.2 and $0.6 \pm 0.1 \mu\text{m}$ in diameter, respectively (Figure 2D). In wide-field microscopy experiments, cell size variability of all three strains (compare Figure 2) became more evident than in scanning electron microscopy, where cells appeared smaller in size (compare Figure 3) due to osmotic stress during fixation. During exponential growth, cells of strain $IG15^T$ and $IG31^T$ were highly motile, while $IG16b^T$ showed only very few motile cells. While culture agitation was not necessary for growth, cells of strain $IG15^T$ produced an extracellular matrix when grown under constant agitation (90 rpm) (Figures 3A,B) with cells embedded in loose aggregates. No extracellular matrix formation was observed for strain $IG16b^T$ and $IG31^T$ (Figures 3C–F). All strains grow aerobically. Temperature and pH optima measurements revealed a mesophilic growth profile with growth temperatures from 13–38, 13–36, and 20–36°C for strains $IG15^T$, $IG16b^T$, and $IG31^T$, respectively. Optical density changes during exponential growth pointed to optimum growth temperatures of 33, 32, and 30°C, respectively (Supplementary Figure S1). $IG15^T$ and $IG16b^T$ were able to grow in pH ranges from 6.0 to 9.0, with an optimum between 7.5 and 8.0. The pH optimum for strain $IG31^T$ was not determined, since its pH growth properties are likely to be similar to strains $IG15^T$ and $IG16b^T$. Additionally, results of the oxidase assays were positive and determination of catalase activity showed negative results for all three strains. Strains were found to be Gram-negative by reaction with 3% KOH solution (Suslow et al., 1982). Substrate

TABLE 1 | 16S rRNA gene sequence identity matrix indicating similarity between the three verrucomicrobial isolates and the next relative *Opitutus terrae* PB90-1.

| 16S rRNA gene sequence similarity [%] | <i>Opitutus terrae</i> PB90-1 T | $IG15^T$ | $IG16b^T$ | $IG31^T$ |
|---------------------------------------|-----------------------------------|----------|-----------|----------|
| <i>Opitutus terrae</i> | 100 | 92.21 | 92.39 | 92.90 |
| PB90-1 T | | | | |
| $IG15^T$ | 92.21 | 100 | 97.07 | 97.55 |
| $IG16b^T$ | 92.39 | 97.07 | 100 | 97.71 |
| $IG31^T$ | 92.90 | 97.55 | 97.71 | 100 |

Similarity values were calculated using neighbor joining clustering.

utilization profiles of strain $IG15^T$ and $IG16b^T$ showed similar patterns in terms of sugar and sugar acid utilization, while strain $IG31^T$ was clearly distinct, utilizing substrates such as glycyl-L-glutamic acid, L-rhamnose and succinic acid mono-methyl ester (Figure 4). Cellular fatty acid analysis identified iso-C_{15:0} as major component of $IG15^T$ and $IG16b^T$ cell walls with 33.3 and 48.6%, respectively, while $IG31^T$ only contained 9.1% of this particular fatty acid (Supplementary Table S3). Furthermore, $IG31^T$ possessed iso-C_{14:0} as major component (15.4%).

Antibiotic Susceptibility of Strains $IG15^T$ and $IG16b^T$

Antibiotic susceptibility of strains $IG15^T$ and $IG16b^T$ toward β -lactams was investigated by treatment with carbenicillin. Optical density (OD_{600nm}) measurements indicated growth at

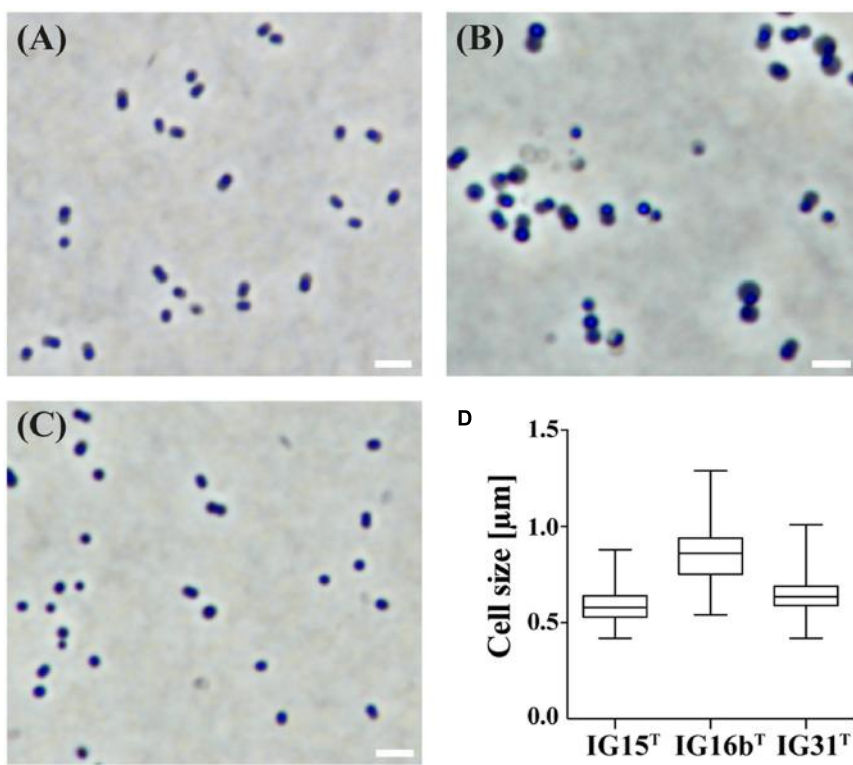


FIGURE 2 | Investigation of cell morphology and size by light microscopy. The morphology and average cell size of IG15^T (A), IG16b^T (B), and IG31^T (C) was investigated by light microscopy under phase-contrast illumination. Cells of strain IG15^T (A), IG16b^T (B), and IG31^T (C) are of coccoid morphology and grow as mono- or diplococci. Cell size was determined by measuring 100 individual cells per strain (D) and average cell size with standard deviation differed from $0.6 \pm 0.1 \mu\text{m}$ (IG15^T), $0.9 \pm 0.2 \mu\text{m}$ (IG16b^T) to $0.6 \pm 0.1 \mu\text{m}$ (IG31^T). Scale bar indicates $2 \mu\text{m}$.

all tested antibiotic concentrations for both strains, as values increased over time (Supplementary Figures S2A,B). However, size measurements based on SEM micrographs revealed that treated cells of both strains were significantly increased in size when compared to untreated samples (Figure 5; $p = 0.0001$). Furthermore, the number of cells per ml was significantly lower (about 10-fold) in treated samples (Supplementary Figure S2C; $p = 0.001$). Thus, the increase of OD_{600nm} was rather caused by swelling of the cells, than by multiplication after cell division.

Genome Sequencing and Gene Content Analysis of IG16b^T

The genome of strain IG16b^T was obtained solely with single molecule real-time sequencing (PacBio). Sequencing read length was 3823 bp in average and yielded 616 mega bp of sequencing data from 6 SMRT cells with a coverage of $\sim 80\times$ per base. Chromosome size was determined at 4,199,284 bp in length and bear a GC content of 66.5 mol%. Annotation with Prokka revealed the presence of 3575 coding sequences, 3 rRNA and 50 tRNA entries (Table 2). In Figure 6 the results of gene content analysis based on reciprocal blast are shown in a circular plot. Known genomes of subdivision 4 Verrucomicrobia are compared to the IG16b^T chromosome, thereby revealing its unique genomic regions (Figure 6, gray boxes). Some of these regions were also predicted to be genomic islands (Figure 6, gray zones, outer

rim), originating from horizontal gene transfer, and mainly hold hypothetical proteins or proteins with domains of unknown function. All predicted prophage regions (Figure 6, yellow zones, outer rim) were incomplete (Supplementary Table S4), thus no intact prophage exists in the chromosome of strain IG16b^T.

Peptidoglycan in the Verrucomicrobial Subdivision 4

Bioinformatic Analysis of Peptidoglycan Synthesis Genes and β -lactamase Homologs

Using comparative genomics, we analyzed the genomes of strain IG16b^T, *O. terrae* PB90-1^T and *C. akajimensis* 04OKA010-24^T (compare Table 2) with respect to genes required for the synthesis of peptidoglycan (PG). Results of our blast-based approach led to the conclusion that all investigated organisms harbor almost all genes essential for the synthesis of PG (Supplementary Table S5). Interestingly, for the penicillin binding proteins only ftsI was identified above threshold. Gene products of *murB* and *murC* were encoded polycistronic in IG16b^T, *O. terrae* and *C. akajimensis* (compare Supplementary Table S5, orange boxes) leading to the identification of the same protein when investigated with the query protein sequences for MurB and MurC.

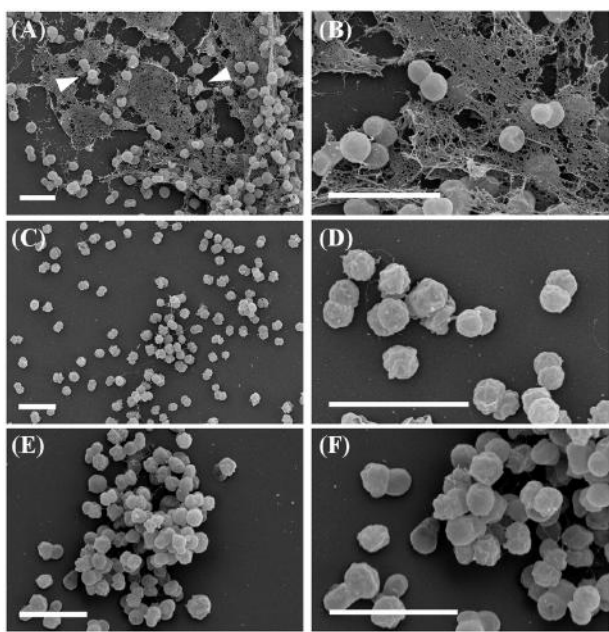


FIGURE 3 | Field emission scanning electron microscopy. Strains show coccoid morphology with organization as mono- or diplococci. Micrographs of IG15^{T} cells (**A**, overview; **B**, close up) illustrate the formation of multicellular aggregates embedded in an extracellular matrix substance (white arrowheads). In contrast, cells of IG16b^{T} (**C**, overview; **D**, close up) or IG31^{T} (**E**, overview; **F**, close up) did not produce an extracellular matrix. Scale bar indicates 2 μm .

Tolerance of β -lactam-derived antibiotic agents in bacteria is often related to one of several modes of resistance, including efflux or exclusion mechanisms, alterations in target proteins or the most common cause being the presence of β -lactamases to degrade the antibiotic compound (Poole, 2004). Growth of strains IG15^{T} , IG16b^{T} , and IG31^{T} on solid media supplemented with the β -lactam carbenicillin gave rise to the assumptions that these strains possess a mode of tolerance against β -lactams. Employing comparative genomics, we analyzed the presence of β -lactamase genes in the genomes of strain IG16b^{T} , *O. terrae* and *C. akajimensis* (see Supplementary Tables S6 and S7). For IG16b^{T} and *O. terrae*, three β -lactamases were identified, while for *C. akajimensis* no β -lactamase was found with the tested criteria. Our findings suggest that a tolerance mechanism against carbenicillin exists in strain IG16b^{T} and is at least partially due to the presence of β -lactamases, leading to the survival of the organism until the antibiotic agent is decayed from the cultivation medium.

Lysozyme Susceptibility Assay

Treatment with lysozyme leads to the disruption of the cell envelope by hydrolytic cleavage of β -1,4-linkages in the peptidoglycan complex (Johnson et al., 1968). Untreated cells of strains IG15^{T} , IG16b^{T} , and IG31^{T} maintained typical coccoid cell morphology, while all three strains displayed a loss of mobility during incubation at 37°C (Figures 7A–C, respectively). Cells that were treated with lysozyme for up to 24 h at 37°C in either

culture medium (IG15^{T} and IG16b^{T}) or ddH₂O (IG31^{T}) showed different susceptibility levels toward the lysozyme treatment. Cells of strain IG15^{T} showed no lysis in M1H medium after 1, 3, or 6 h, but were lysed after 24 h of incubation (Figure 7D; white arrowheads). Cells of strain IG16b^{T} were destroyed after 3 h incubation in M1H medium (Figure 7E; white arrowheads). Since strain IG31^{T} showed no lysis after 24 h in M1H medium, osmotic stress was increased by incubation of cells in ddH₂O and cells were disrupted in ddH₂O after 24 h (Figures 7D,F; white arrowheads).

Biochemical Evidence for the Presence of Peptidoglycan Building Blocks

First, the presence of DAP was investigated for strains IG15^{T} , IG16b^{T} , and IG31^{T} by TLC and no DL-DAP was detected. In contrast, Gram-negative and Gram-positive reference strains, *E. coli* DSM498 and *B. subtilis* DSM10, respectively, showed signals for DAP (Supplementary Figure S3), with *E. coli* giving only a weak signal. However, we analyzed whole-cell hydrolysates of IG15^{T} , IG16b^{T} , and IG31^{T} using a more sensitive GC/MS method that previously revealed DAP in Planctomycetes. Despite negative results in TLC, we found the specific ion peaks, characteristic for DAP (compare Figure 8B), indicating the presence of peptidoglycan in IG15^{T} , IG16b^{T} , and IG31^{T} and *O. terrae* PB90-1 $^{\text{T}}$. The same ion peaks were previously detected for *E. coli* DSM 498 (Spring et al., 2016), the identical *E. coli* strain we here used in our TLC experiment. In addition, ornithine was detected in the whole cell hydrolysates of all three novel strains and the closest related type strain, *O. terrae* (Figure 8A). A quantitative estimation, based on the internal standard used, revealed that DAP and ornithine occurred in nearly equivalent, albeit low amounts in strains IG15^{T} and IG16b^{T} while ornithine was the dominant substance detected for *O. terrae* and strain IG31^{T} (Table 3). However, quantities of DAP for strains IG15^{T} (7 nmol), IG16b^{T} (6 nmol), IG31^{T} (3 nmol) and *O. terrae* (4 nmol) were nearly 10-fold lower than those detected for the control *E. coli* strain (63 nmol), investigated in the study of Spring et al. (2016), which explains why no signal of DAP was visible in TLC experiments for strains IG15^{T} , IG16b^{T} , and IG31^{T} , but a weak signal for *E. coli* (compare Supplementary Figure S3). Furthermore, proteins essential for DAP biosynthesis via the aminotransferase pathway are present in the genome of strain IG16b^{T} (LysC :WP_069962807.1, WP_069963418.1; Asd: WP_069963129.1; DapA: WP_069962952.1; DapB: WP_069962953.1; DapL: WP_069960938.1; DapF: WP_069963382.1) as well as a alanine racemase (WP_069962553.1).

Thus, we conclude despite negative results in TLC, that all analyzed strains contain DAP as diagnostic diamino acid of peptidoglycan. Additionally, ornithine was detected which is a part of the peptidoglycan backbone of certain gram-negative bacteria (Yanagihara et al., 1984; Spring et al., 2016).

Cell Sacculi of IG16b^{T}

To give the ultimate proof that PG exists in the novel strains isolated in this study cell sacculi were extracted from strain



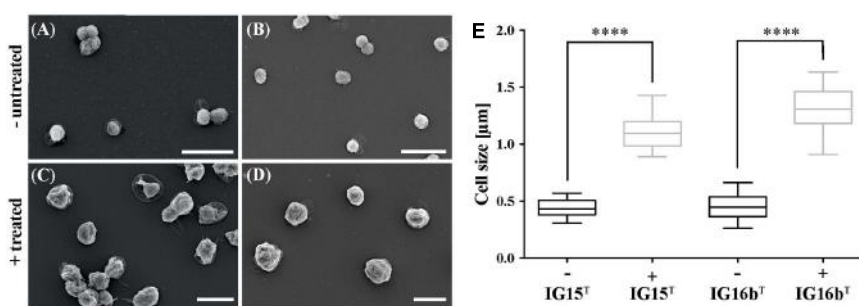


FIGURE 5 | Effect of carbenicillin treatment on IG15^T and IG16b^T cells. Cells of IG15^T and IG16b^T were treated with carbenicillin for 120 h at 28°C. Untreated cells IG15^T and IG16b^T (**A,B**) showed no change in morphology, while size of treated cells (**C,D**; 2 mg/ml carbenicillin) was significantly increased (**E**). Cell size was calculated by counting 20–32 cells per treatment condition. **** = $p < 0.0001$. Scale bar indicates 2 μm .

TABLE 2 | Basic genome information of the newly sequenced strain IG16b^T and other described subdivision 4 Verrucomicrobia.

| Feature | IG16b ^T | <i>Opitutus terrae</i> PB90-1 ^T | <i>Coraliomargarita</i> <i>akajimensis</i> 04OKA010-24 ^T |
|-------------------|--------------------|---|---|
| Size [bases] | 4,199,284 | 5,957,605 | 3,750,771 |
| Genes | 3575 | 4612 | 3120 |
| GC content [mol%] | 66.5 | 65.3 | 53.6 |
| rRNA entries | 3 | 4 | 6 |
| tRNA entries | 50 | 65 | 46 |

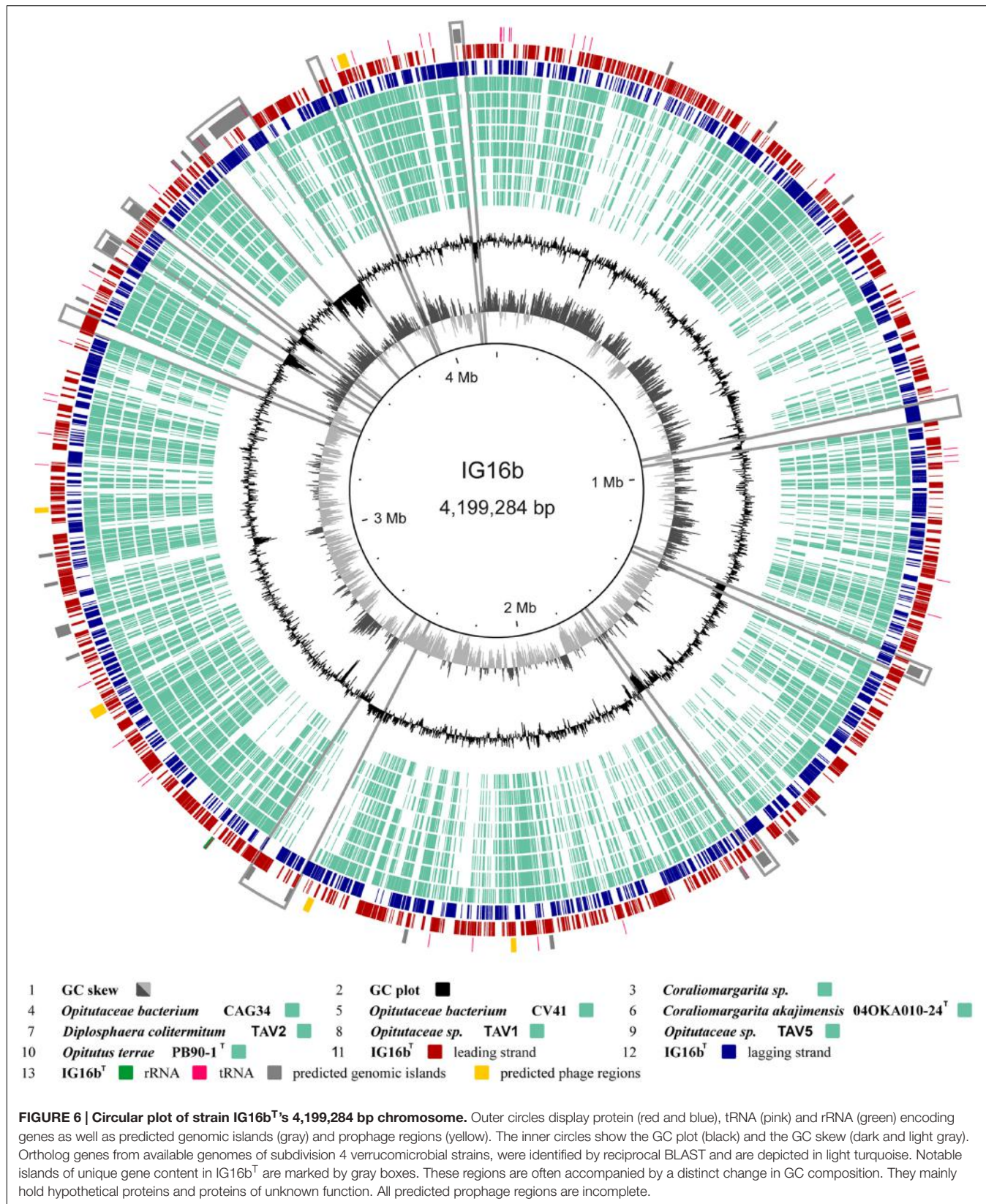
IG16b^T and investigated by TEM. TEM imaging revealed the presence of cell sacculi (Figure 9; Supplementary Figure S4) with remaining protein accumulations (white arrowheads) being present in the sample investigated.

The isolation of PG sacculi together with the presence of DAP and PG synthesis genes, suggests that the claim of verrucomicrobial subdivision 4 lacking peptidoglycan, is not entirely justifiable (compare Table 4).

DISCUSSION

All free-living bacteria possess a peptidoglycan cell wall (PG) to withstand environmental osmotic challenges and to maintain cell shape (Vollmer et al., 2008), with subdivision 4 Verrucomicrobia being described as one of the few exceptions (Yoon, 2011). Since it was recently demonstrated that Planctomycetes possess a PG cell wall (Jeske et al., 2015) despite oppositional previous reports (König et al., 1984), we revisited the question if subdivision 4 Verrucomicrobia are indeed an exception to this otherwise universal cell biological bacterial trait. Given that only a few representatives of the verrucomicrobial subdivision 4 are available in axenic culture, we applied a selective β -lactam-based cultivation approach considering the putative lack of PG to specifically enrich subdivision 4 Verrucomicrobia from a limnic water sample. As β -lactam antibiotics prevent PG formation and remodeling during cell division by irreversible interaction with penicillin-binding proteins involved in the final step of PG synthesis (Waxman and Strominger, 1983), subdivision

4 Verrucomicrobia should comprise intrinsic resistance if no PG *per se* exists. Accordingly, all three strains described in this study were obtained from plates initially containing carbenicillin. However, all novel verrucomicrobial strains grew only after 4 months of incubation, indicating rather antibiotic degradation through hydrolysis than an intrinsic resistance against β -lactam antibiotics. Thus, we analyzed the genome of the novel strain IG16b^T in more detail to reveal the nature of its cell wall architecture and possible resistance mechanism to β -lactam antibiotics. First, we employed bioinformatics and found strain IG16b^T to encode β -lactamase proteins that can confer resistance against β -lactam antibiotics such as carbenicillin. Second, we incubated cultures of strains IG16b^T and IG15^T with carbenicillin concentrations of 500–2000 mg/l, which were far above the 100 mg/l working concentration usually used as selection pressure for β -lactamase mediated resistance in molecular laboratory approaches (Green and Sambrook, 2012). Accordingly, SEM analysis revealed that carbenicillin treated cells were inhibited in cell division and increased in size. However, they withstood the antibiotic reagent and resumed growth, once carbenicillin was depleted from the cultivation medium, as happened through hydrolysis over time once they were initially isolated from the environment. Similar behavior has been observed for *Chlamydia psittaci*, where presence of penicillin led to swelling of reticulate bodies and incomplete cell division, while cells transferred to penicillin-free medium resumed division (Matsumoto and Manire, 1970). Our observations thus rather suggest a mode of tolerance, possibly enabled by β -lactamases, than a mode of intrinsic resistance due to the absence of PG in the novel isolates. In case of intrinsic resistance, increase of carbenicillin concentration would have had no effect on cell division. However, the degradation capability of β -lactamases can be titrated to a point, where the enzyme cannot confer resistance anymore and the cell becomes affected as observed in changes of morphology in this study. Thus, this finding provided us with the ample motivation to further analyze PG in our strains. To do this comprehensively, we analyzed the genome of strain IG16b^T (obtained in this study) along with the published genomes of *O. terrae* (van Passel et al., 2011) and *C. akajimensis* (Mavromatis et al., 2010) employing



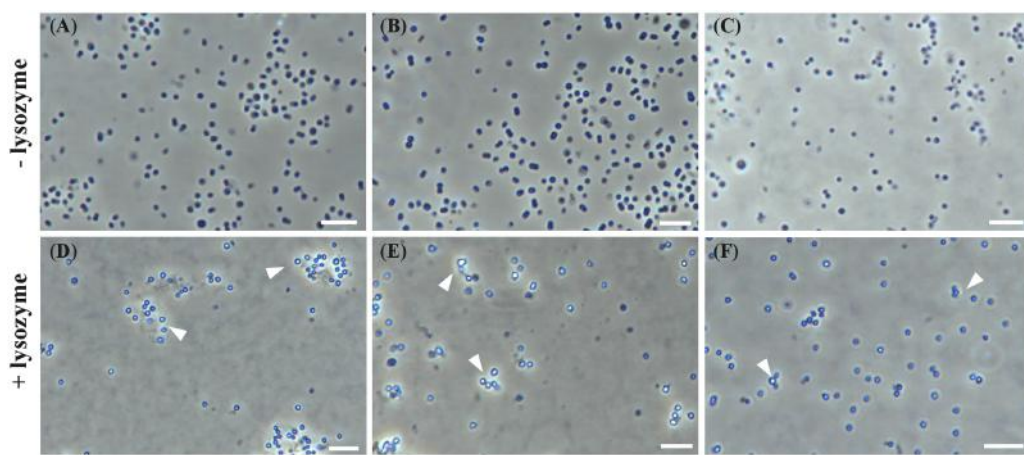


FIGURE 7 | Effect of lysozyme treatment on strains $IG15^T$, $IG16b^T$, and $IG31^T$. Cells of all three strains were incubated with lysozyme. Untreated cells served as negative controls. Cell morphology was investigated by light microscopy. All strains were susceptible to lysozyme treatment, leading to disruption of the cells shape (D–F; white arrowheads), while cells in negative controls remained healthy during the whole incubation time (A–C). The isolates showed different resistance to the lysozyme treatment. Cells of isolate $IG15^T$ (D) and $IG31^T$ (F) were disrupted after 24 h of incubation in M1H medium or ddH₂O, respectively. In contrast, cells of strain $IG16b^T$ (E) lysed after 3 h of incubation in M1H medium. Scale bar indicates 5 μ m.

complementary blast methods that were previously used to identify PG synthesis related genes in Planctomycetes (Jeske et al., 2015). We found that *O. terrae*, *C. akajimensis* and strain $IG16b^T$ harbor nearly all genes essential for the synthesis of PG. Thus, from a genomic perspective based on all available type strain genomes, it is likely that subdivision 4 Verrucomicrobia can synthesize PG.

Employing a previously described procedure (Jeske et al., 2015), we next demonstrated that all three novel strains, $IG15^T$, $IG16b^T$, and $IG31^T$, are susceptible to the treatment with lysozyme, an enzyme that destroys beta-1,4 glycosidic bonds in the peptidoglycan structure, leading to disruption of the bacterial cell envelope (Johnson et al., 1968). Our results indicate different tolerance levels of strains $IG15^T$, $IG16b^T$, and $IG31^T$ against lysozyme, under laboratory culture conditions (in M1H medium) or under osmotic stress ($IG31^T$ in ddH₂O).

Even though all evidence so far points toward the existence of an peptidoglycan cell wall in strains $IG15^T$, $IG16b^T$, and $IG31^T$, we obtained no signals for the diagnostic peptidoglycan-specific structural element DAP when performing TLC experiments. This result is consistent with previous reports that led to the conclusion that subdivision 4 Verrucomicrobia lack PG (Yoon et al., 2007a). However, we analyzed whole-cell hydrolysates of our strains and *O. terrae* PB90-1^T using a modified version – capable of quantification- of a highly sensitive method based on gas chromatography and mass spectrometry (GC/MS) detection that previously revealed DAP in Planctomycetes (Jeske et al., 2015). We found the specific ion set characteristic for DAP, while quantification of DAP in whole-cell hydrolysates of our strains and *O. terrae* revealed that this marker was only present in low quantities, possibly explaining why less sensitive methods such as TLC failed to detect DAP. Furthermore, all proteins essential for DAP synthesis were detected within the

genome of strain $IG16b^T$. In addition, we surprisingly detected the non-proteinogenic diamino acid ornithine that was, until recently, thought to be an exception in PG among Gram-negative bacteria limited to *Spirochaetaceae* (Schleifer and Joseph, 1973; Yanagihara et al., 1984). At this point, it cannot be excluded that ornithine could have been extracted from certain amino lipids or other cell components instead of peptidoglycan, because only whole-cell hydrolysates were analyzed. However, ornithine was recently identified in whole-cell hydrolysates of both, the proposed phylum Kiritimatiellaeota -formally known as verrucomicrobial subdivision 5- and representatives of the phylum Lentisphaerae (Spring et al., 2016), indicating that more Gram-negative bacteria display such alterations in their PG cell walls. Spring et al. additionally analyzed whole-cell hydrolysates of *E. coli* DSM 498, the same strain we used for TLC analysis, and found much higher quantities of DAP (63 nmol) than we did for our strains (compare Table 3), consequently supporting the observation of TLC being a method unfit to detect DAP in cases where only low quantities are present in the cell walls of the investigated organism.

To ultimately proof the existence of peptidoglycan sacculi, we isolated them from strain $IG16b^T$ and visualized them employing TEM (Figure 9).

Based on our findings, we conclude that subdivision 4 Verrucomicrobia do possess PG sacculi. Contrary previous reports used methods such as TLC (Yoon et al., 2007c) that did not detect DAP in subdivision 4 Verrucomicrobia in our hands as well (Supplementary Figure S3). Thus, future analyses must meet a new standard in PG detection, set by others and us, to justify the claim that a certain free-living bacterial strain lacks PG (Pilhofer et al., 2013; Jeske et al., 2015; Packiam et al., 2015; van Teeseling et al., 2015).

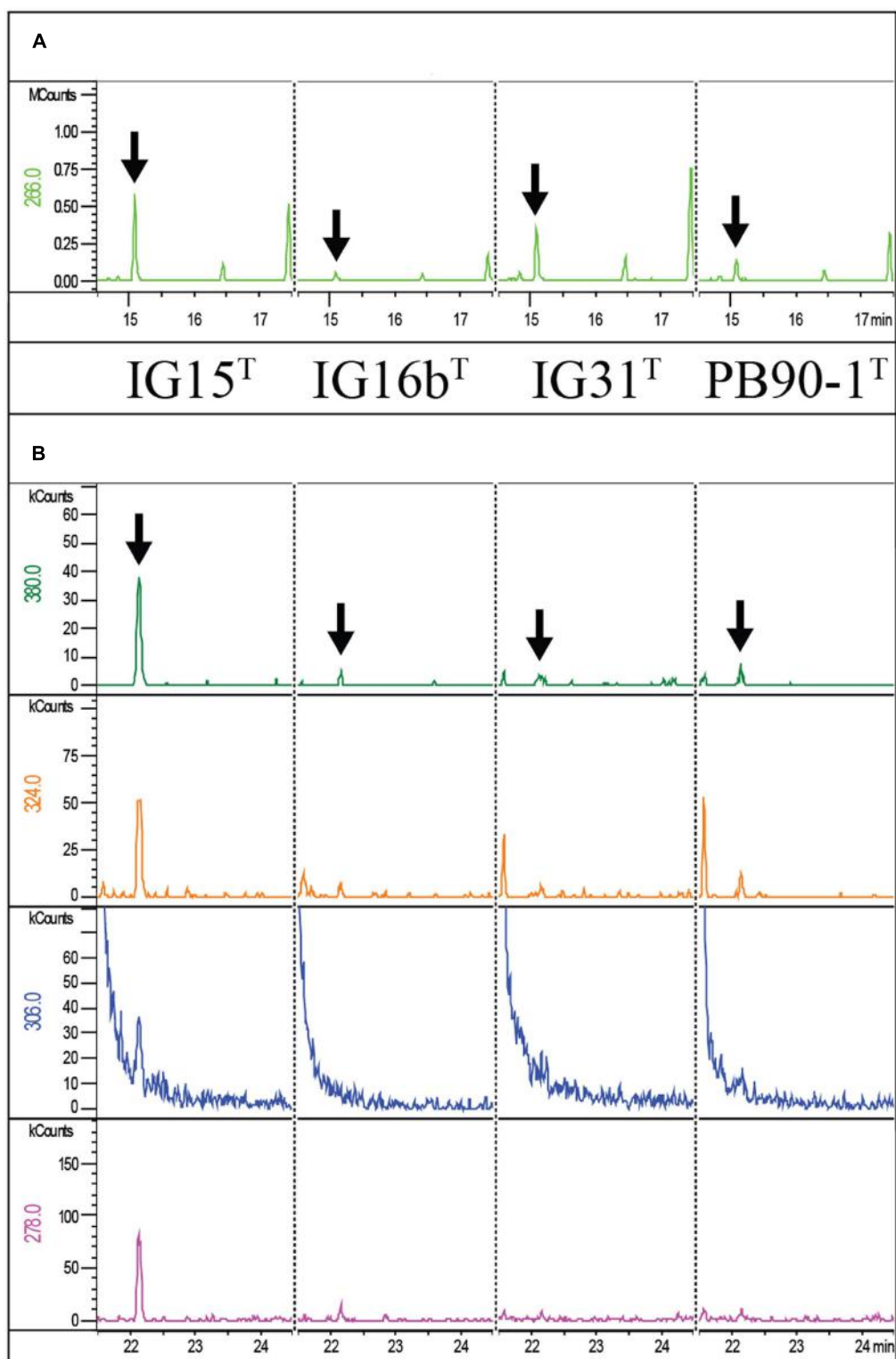


FIGURE 8 | Mass spectrometric detection of diaminopimelic acid and ornithine in IG15^T, IG16b^T, IG31^T and *O. terrae* PB90-1^T. Extracted Ion chromatograms of ornithine (**A**) and the DAP derivative (N-heptafluorobutyryl DAP isobutylester) (**B**) from whole-cell hydrolysates of strains IG15^T, IG16b^T, IG31^T and *O. terrae* PB90-1^T are shown. Masses of the ornithine fragment (266 m/z) were detected for IG15^T, IG16b^T, IG31^T, *O. terrae* PB90-1^T at 15.13 min retention time. Masses of DAP fragments (380, 324, 306, and 278 m/z) were detected for IG15^T, IG16b^T, IG31^T and *O. terrae* PB90-1^T at 22.17 min retention time. Peaks confirming the presence of amino acids are highlighted for ornithine (**A**; black arrows) and DAP (**B**; black arrows) for all strains analyzed.

TABLE 3 | Content of diagnostic diamino acids of peptidoglycan in whole-cell hydrolysates of *Opitutus terrae* PB90-1^T and strains IG15^T, IG16b^T, and IG31^T.

| Organism | DAP | Orn |
|--|-----|-----|
| <i>Opitutus terrae</i> PB90-1 ^T | 4 | 11 |
| IG15 ^T | 7 | 9 |
| IG16b ^T | 6 | 6 |
| IG31 ^T | 3 | 18 |

Values are nmol of diamino acid per 1.0 mg lyophilized biomass. DAP, diaminopimelic acid; Orn, ornithine.

Based on recent results (Pilhofer et al., 2013; Jeske et al., 2015; Packiam et al., 2015; van Teeseling et al., 2015) and the outcome of this study we further postulate -applying the *lex parsimoniae*- that all free-living bacteria require a PG cell wall to maintain cell shape integrity in habitats with osmotic conditions different from their cytosol.

Description of *Lacunisphaera* gen. nov.

Lacunisphaera (La.cu.ni.sphae.ra N.L. fem. n. *lacuna*, a little lake, referring to the origin of the organism; N.L. fem. n. *sphaera*, a ball, globe, sphere; N.L. fem. n. *Lacunisphaera*, a spherical microorganism from a lake).

Cells are Gram-negative, aerobic cocci. Mono- or diplococci are formed, but no chains or rosettes. Cells are motile during exponential growth phase, but not in late stationary phase. No spore formation was observed. Members test positive for cytochrome oxidase activity, but show no catalase activity in reaction with H₂O₂. Extracellular matrix formation in liquid culture is observed for some members when cultured under constant agitation. This is not true for the type species. The molar G + C content is between 65 and 67 mol%. Members contain peptidoglycan with DAP and ornithine as diamino acids. The predominant cellular fatty acid of the type species is iso-C_{15:0}. Members belong to the phylum Verrucomicrobia, class *Opitutae*, order *Opitutales*, family *Opitutaceae*. The type species of the genus is *Lacunisphaera limnophila*.

Description of *Lacunisphaera parvula* sp. nov.

Lacunisphaera parvula (*par.vu.la*, L. adj. *parvula* small, referring to the size of individual cells).

Main attributes are as given for the genus. Colonies grown on M1H agar were round, smooth and cream colored, while aging colonies became translucent. An extracellular matrix compound is produced in liquid cultures when kept under constant agitation, but formation was not observed on solid media. Cells are present as mono- or diplococci, but form aggregates when embedded in the extracellular matrix compound. Single cells measured 0.6 ± 0.1 μm in diameter. Substrates utilized were D-cellobiose, maltose, gentiobiose, α-D-lactose, sucrose, turanose, lactulose, succinic acid, thymidine, inosine, uridine, succinic acid mono-methyl

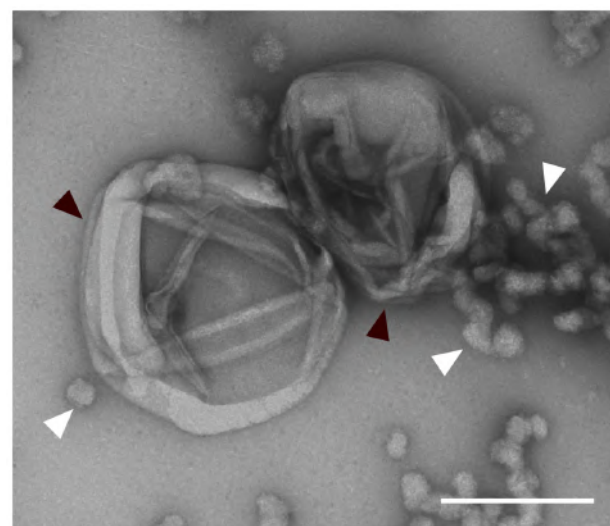


FIGURE 9 | Extracted peptidoglycan sacculus of strain IG16b^T. Cells were boiled in 4% SDS for 1 h and unbound SDS was dialyzed against ddH₂O over the course of 3 days. Sacculi were negatively stained with 1% aqueous uranyl acetate and imaged by transmission electron microscopy (black arrowheads). Protein-bound SDS is seen in the sample (white arrowheads). Scale bar indicates 0.2 μm.

ester, L-rhamnose, D-alanine, malonic acid, L-aspartic acid, D-melibiose, β-methyl-D-glucoside, D-fructose, α-D-glucose, D-D-trehalose, bromosuccinic acid, α-cyclodextrin, dextrin, tween 80, α-ketoglutaric acid, D-gluconic acid, D-sorbitol, glycogen, D-galactose, D-raffinose, α-D-glucose-1-phosphate, D-mannose, D-glucosaminic acid, D-saccharic acid, L-alanine, D,L-lactic acid, D-galacturonic acid, D-glucuronic acid and succinamic acid. Cells grew in M1H medium at temperatures between 12 and 38°C, while 33°C was the optimum. Cells did not grow below 10°C and above 38°C. pH values between 6.0 and 9.0 were tolerated for growth, while the optimum was between 7.5 and 8.0. Major cellular fatty acids were iso-C_{15:0} (33.3%), C_{16:0} (10.2%), iso-C_{13:0} 3-OH (8.7%), C_{16:1} ω5c (8.4%) and iso-C_{11:0} (4.9%). The G + C content of the DNA of the type strain is 65.9 mol%. The type strain is IG15^T (=DSM 26814 = LMG 29468) and was isolated from the surface water column of a freshwater lake during a cyanobacterial blooming event.

Description of *Lacunisphaera limnophila* sp. nov.

Lacunisphaera limnophila (*lim.no' phi.la* Gr. n. *limnos* lake; Gr. adj. *philus* loving; N.L. adj. *limnophila* lake loving).

Overall characteristics are as described for the genus. Colonies grown on M1H agar were round, smooth and cream colored, while aging colonies became translucent. Liquid cultures appeared pale yellowish. Cells are present as mono- or diplococci and form no chains or rosettes. Single cells measured 0.9 ± 0.2 μm in diameter. Substrates utilized were D-cellobiose, maltose, gentiobiose, α-D-lactose, sucrose,

TABLE 4 | Taxonomic affiliation and detected presence of peptidoglycan (DAP) in strains *IG15^T*, *IG16b^T*, *IG31^T* and validly published type strains within subdivision 4 Verrucomicrobia.

| Taxonomic rank | | | | | Peptidoglycan (DAP) | | Peptidoglycan synthesis genes |
|----------------|-----------------|------------------|------------------|--|---------------------|------------|-------------------------------|
| Class | Order | Family | Genus | Species | Literature | This study | This study |
| Opitutae | Opitutales | Opitutaceae | Opitutus | <i>Opitutus terrae</i> ¹ | n.d. | + | + |
| | | | Alterococcus | <i>Alterococcus agarolyticus</i> ² | n.d. | n.d. | n.d. |
| | | | Lacunisphaera | <i>Lacunisphaera parvula</i> <i>IG15^{T,3}</i> | n.d. | + | n.d. |
| | | | | <i>Lacunisphaera limnophila</i> <i>IG16b^{T,4}</i> | n.d. | + | + |
| | | | | <i>Lacunisphaera anatis</i> <i>IG31^{T,5}</i> | n.d. | + | n.d. |
| Opitutae | Puniceicoccales | Puniceicoccaceae | Puniceicoccus | <i>Puniceicoccus vermicola</i> ⁶ | n.d. | n.d. | n.d. |
| | | | Cerasicoccus | <i>Cerasicoccus arenae</i> ⁷ | — | n.d. | n.d. |
| | | | | <i>Cerasicoccus frondis</i> ⁸ | — | n.d. | n.d. |
| | | | Pelagicoccus | <i>Pelagicoccus croceus</i> ¹⁰ | — | n.d. | n.d. |
| | | | | <i>Pelagicoccus litoralis</i> ¹¹ | — | n.d. | n.d. |
| | | | | <i>Pelagicoccus albus</i> ¹² | — | n.d. | n.d. |
| | | | | <i>Pelagicoccus mobilis</i> ¹³ | — | n.d. | n.d. |
| | | | Coraliomargarita | <i>Coraliomargarita akajimensis</i> ¹⁴ | — | n.d. | + |

¹PB90-1^T (Chin et al., 2001; this study); ²ADT3^T (Shieh and Jean, 1998); ³IG15^T (this study); ⁴IG16b^T (this study); ⁵IG31^T (this study); ⁶IMCC1545^T (Choo et al., 2007); ⁷YM26-026^T (Yoon et al., 2007a); ⁸YM31-066^T (Yoon et al., 2010); ⁹YM31-114^T (Yoon et al., 2010); ¹⁰N5FB36-5^T (Yoon et al., 2007b); ¹¹H-MN57^T (Yoon et al., 2007d); ¹²YM14-201^T (Yoon et al., 2007d); ¹³O2PA-Ca-133^T (Yoon et al., 2007d); ¹⁴04OKA010-24^T (Yoon et al., 2007c). —, negative; n.d., not determined; +, positive.

turanose, lactulose, thymidine, inosine, glycy-L-aspartic acid, glucuronamide, pyruvic acid methyl ester, L-leucin, hydroxyl-L-proline, D-melibiose, β-methyl-D-glucoside, D-fructose, α-D-glucose, D-trehalose, glycogen, D-galactose, D-raffinose, α-D-glucose-1-phosphate and D-mannose. Cells grew in M1H medium at temperatures between 13 and 36°C, while 32°C was the optimum. Cells did not grow below 10°C and above 36°C. pH values between 6.0 and 9.0 were tolerated for growth, while the optimum was between 7.5 and 8.0. Major cellular fatty acids were iso-C_{15:0} (48.6%), Anteiso-C_{15:0} (12.1%), iso-C_{15:1} ω9c (10.3%), iso-C_{13:0} 3-OH (6.6%) and iso-C_{13:0} (5.0%). The genome based G + C content of coding sequences is 66.5 mol%. The type strain is *IG16b^T* (=DSM 26815 = LMG 29469) and was isolated from the particle-containing fraction of surface water from a freshwater lake. The 4,199,284 bp genome of *L. limnophila* *IG16b^T* was similar, yet distinct from other sequenced verrucomicrobial species in terms of gene content (Figure 6). In most cases, such differences were associated with genomic islands which indicate frequent horizontal gene transfer.

Description of *Lacunisphaera anatis* sp. nov.

Lacunisphaera anatis (*a.na.tis* L. fem. n. *anatis* with the ducks, referring to the term ‘duck pond’ describing a lake or pond inhabited by ducks).

Overall characteristics are as described for the genus. Colonies grown on M1H agar were round, smooth and cream colored, while aging colonies became translucent. Cells are present as mono- or diplococci and form no chains or aggregates.

Single cells measured 0.6 ± 0.1 μm in diameter. Substrates utilized were glycy-L-glutamic acid, succinic acid, thymidine, inosine, uridine, succinic acid mono-methyl ester, L-rhamnose, and D-fructose. Cells grew in M1H medium at temperatures between 15 and 36°C, while 30°C was the optimum. Cells did not grow below 12°C and above 36°C. pH values between 6.0 and 9.0 were tolerated for growth, while the optimum was between 7.5 and 8.0. Major cellular fatty acids were iso-C_{14:0} (15.4%), iso-C_{14:0} (15.4%), C_{16:0} (12.1%), Anteiso-C_{15:0} (10.6%) and iso-C_{16:0} (10.1%). The G + C content of the DNA of the type strain is 67.2 mol%. The type strain is *IG31^T* (=DSM 103142 = LMG 29578) and was isolated from surface freshwater containing biomass of a cyanobacterial bloom.

AUTHOR CONTRIBUTIONS

PR did most of the experimental laboratory work and wrote the main part of the manuscript body and functions as first author. IG helped with the isolation of the novel strains and with cultivation measurements. CB performed all light microscopic work and cell size measurements. OJ conducted blast analysis for the detection of peptidoglycan synthesis genes and β-lactamases. SW analyzed the gene content and generated substrate utilization heatmaps. RR coordinated sequencing of the *IG16b* genome sequence with Pacific Bioscience. PS did the gas chromatographic analysis of PG in the new strains. MR performed scanning electron microscopy experiments. SS cultivated reference strains for GC MS and fatty acid analysis and contributed in literature research

toward ornithin in PG layers. FG analyzed sequencing data and was involved in genome assembly of IG16b's genome sequence. CJ is PI and together with MJ functions as corresponding author. MJ and CJ, along with PR designed the study and helped with experimental setups and design.

FUNDING

This work was kindly funded by the Deutsche Forschungsgemeinschaft (JO 893/3-1). We thank Pacific Bioscience for genome sequencing.

REFERENCES

- Alikhan, N. F., Petty, N. K., Ben Zakour, N. L., and Beatson, S. A. (2011). BLAST Ring Image Generator (BRIG): simple prokaryote genome comparisons. *BMC Genomics* 12:402. doi: 10.1186/1471-2164-12-402
- Altschul, S. F., Madden, T. L., Schaffer, A. A., Zhang, J., Zhang, Z., Miller, W., et al. (1997). Gapped BLAST and PSI-BLAST: a new generation of protein database search programs. *Nucleic Acids Res.* 25, 3389–3402. doi: 10.1093/nar/25.17.3389
- Bertani, G. (1951). Studies on lysogenesis. I. The mode of phage liberation by lysogenic *Escherichia coli*. *J. Bacteriol.* 62, 293–300.
- Bush, K. (2013). The ABCD's of beta-lactamase nomenclature. *J. Infect. Chemother.* 19, 549–559. doi: 10.1007/s10156-013-0640-7
- Cashion, P., Hodler-Franklin, M. A., McCully, J., and Franklin, M. (1977). A rapid method for base ratio determination of bacterial DNA. *Anal. Biochem.* 81, 461–466. doi: 10.1016/0003-2697(77)90720-5
- Chin, K. J., Liesack, W., and Janssen, P. H. (2001). *Opitutus terrae* gen. nov., sp. nov., to accommodate novel strains of the division 'Verrucomicrobia' isolated from rice paddy soil. *Int. J. Syst. Evol. Microbiol.* 51(Pt 6), 1965–1968. doi: 10.1099/00207713-51-6-1965
- Choo, Y. J., Lee, K., Song, J., and Cho, J. C. (2007). *Puniceicoccus vermicola* gen. nov., sp. nov., a novel marine bacterium, and description of *Puniceicoccaceae* fam. nov., *Puniceicoccales* ord. nov., *Opitutaceae* fam. nov., *Opitutales* ord. nov. and *Opitutia* classis nov. in the phylum 'Verrucomicrobia'. *Int. J. Syst. Evol. Microbiol.* 57(Pt 3), 532–537. doi: 10.1099/ijss.0.04616-0
- Dhillon, B. K., Laird, M. R., Shay, J. A., Winsor, G. L., Lo, R., Nizam, F., et al. (2015). IslandViewer 3: more flexible, interactive genomic island discovery, visualization and analysis. *Nucleic Acids Res.* 43, W104–W108. doi: 10.1093/nar/gkv401
- Engelhardt, H. (2007). Are S-layers exoskeletons? The basic function of protein surface layers revisited. *J. Struct. Biol.* 160, 115–124. doi: 10.1016/j.jsb.2007.08.003
- Fox, A., Rogers, J. C., Gilbart, J., Morgan, S., Davis, C. H., Knight, S., et al. (1990). Muramic acid is not detectable in *Chlamydia psittaci* or *Chlamydia trachomatis* by gas chromatography-mass spectrometry. *Infect. Immun.* 58, 835–837.
- Fuerst, J. A., and Sagulenko, E. (2011). Beyond the bacterium: planctomycetes challenge our concepts of microbial structure and function. *Nat. Rev. Microbiol.* 9, 403–413. doi: 10.1038/nrmicro2578
- Green, M. R., and Sambrook, J. (2012). *Molecular Cloning: A Laboratory Manual*. New York, NY: Cold Spring Harbor Laboratory Press.
- Jacquier, N., Viollier, P. H., and Greub, G. (2015). The role of peptidoglycan in chlamydial cell division: towards resolving the chlamydial anomaly. *FEMS Microbiol. Rev.* 39, 262–275. doi: 10.1093/femsre/fuv001
- Jeske, O., Schüler, M., Schumann, P., Schneider, A., Boedeker, C., Jogler, M., et al. (2015). Planctomycetes do possess a peptidoglycan cell wall. *Nat. Commun.* 6:7116. doi: 10.1038/ncomms8116
- Jogler, C., Waldmann, J., Huang, X., Jogler, M., Glöckner, F. O., Mascher, T., et al. (2012). Identification of proteins likely to be involved in morphogenesis, cell division, and signal transduction in Planctomycetes by comparative genomics. *J. Bacteriol.* 194, 6419–6430. doi: 10.1128/JB.01325-12
- Johnson, L. N., Phillips, D. C., and Rupley, J. A. (1968). The activity of lysozyme: an interim review of crystallographic and chemical evidence. *Brookhaven Symp. Biol.* 21, 120–138.
- Kim, M., Pak, S., Rim, S., Ren, L., Jiang, F., Chang, X., et al. (2015). *Luteolibacter arcticus* sp. nov., isolated from high Arctic tundra soil, and emended description of the genus *Luteolibacter*. *Int. J. Syst. Evol. Microbiol.* 65(Pt 6), 1922–1928. doi: 10.1099/ijss.0.000202
- König, E., Schlesner, H., and Hirsch, P. (1984). Cell wall studies on budding bacteria of the Planctomyces/Pasteuria group and on a *Prosthecomicrobium* sp. *Arch. Microbiol.* 138, 200–205. doi: 10.1007/BF00402120
- Kuykendall, L. D., Roy, M. A., Neill, J. J., and Devine, T. E. (1988). Fatty acids, antibiotic resistance, and deoxyribonucleic acid homology groups of *Bradyrhizobium japonicum*. *Int. J. Syst. Evol. Microbiol.* 38, 358–361. doi: 10.1099/00207713-38-4-358
- Lane, D. J. (ed.) (1991). *16S/23S rRNA Sequencing*. Hoboken NJ: Wiley.
- Lechner, M., Findeiss, S., Steiner, L., Marz, M., Stadler, P. F., and Prohaska, S. J. (2011). Proteinortho: detection of (co-)orthologs in large-scale analysis. *BMC Bioinformatics* 12:124. doi: 10.1186/1471-2105-12-124
- Lee, J., Park, B., Woo, S. G., Lee, J., and Park, J. (2014). *Prosthecobacter algae* sp. nov., isolated from activated sludge using algal metabolites. *Int. J. Syst. Evol. Microbiol.* 64(Pt 2), 663–667. doi: 10.1099/ijss.0.052787-0
- Lee, K. C., Webb, R. I., Janssen, P. H., Sangwan, P., Romeo, T., Staley, J. T., et al. (2009). Phylum Verrucomicrobia representatives share a compartmentalized cell plan with members of bacterial phylum Planctomycetes. *BMC Microbiol.* 9:5. doi: 10.1186/1471-2180-9-5
- Liechti, G., Kuru, E., Packiam, M., Hsu, Y. P., Tekkam, S., Hall, E., et al. (2016). Pathogenic chlamydia lack a classical sacculus but synthesize a narrow, mid-cell peptidoglycan ring, regulated by MreB, for cell division. *PLoS Pathog.* 12:e1005590. doi: 10.1371/journal.ppat.1005590
- Liechti, G. W., Kuru, E., Hall, E., Kalinda, A., Brun, Y. V., van Nieuwenhze, M., et al. (2014). A new metabolic cell-wall labelling method reveals peptidoglycan in *Chlamydia trachomatis*. *Nature* 506, 507–510. doi: 10.1038/nature12892
- Ludwig, W., Strunk, O., Westram, R., Richter, L., Meier, H., Yadhukumar, et al. (2004). ARB: a software environment for sequence data. *Nucleic Acids Res.* 32, 1363–1371. doi: 10.1093/nar/gkh293
- Markowitz, V. M., Chen, I. M., Palaniappan, K., Chu, K., Szeto, E., Grechkin, Y., et al. (2012). IMG: the integrated microbial genomes database and comparative analysis system. *Nucleic Acids Res.* 40, D115–D122. doi: 10.1093/nar/gkr1044
- Matsumoto, A., and Manire, G. P. (1970). Electron microscopic observations on the effects of penicillin on the morphology of *Chlamydia psittaci*. *J. Bacteriol.* 101, 278–285.
- Mavromatis, K., Abt, B., Brambilla, E., Lapidus, A., Copeland, A., Deshpande, S., et al. (2010). Complete genome sequence of *Coraliomargarita akajimensis* type strain (04OKA010-24). *Stand. Genomic. Sci.* 2, 290–299. doi: 10.4056/sigs.952166
- Mesbah, M., Premachandran, U., and Whitman, W. B. (1989). Precise measurement of the G+C content of deoxyribonucleic acid by high-performance liquid chromatography. *Int. J. Syst. Bacteriol.* 39, 159–167. doi: 10.1099/00207713-39-2-159
- Miles, R. J. (1992). Catabolism in mollicutes. *J. Gen. Microbiol.* 138, 1773–1783. doi: 10.1099/00221287-138-9-1773

ACKNOWLEDGMENTS

We thank Anja Heuer for versatile and skillful technical assistance. Gabriele Pötter we thank for technical assistance in fatty acid analysis and thin layer chromatography of the novel strains.

SUPPLEMENTARY MATERIAL

The Supplementary Material for this article can be found online at: <http://journal.frontiersin.org/article/10.3389/fmib.2017.00202/full#supplementary-material>

- Miller, L. T. (1982). Single derivatization method for routine analysis of bacterial whole-cell fatty acid methyl esters, including hydroxy acids. *J. Clin. Microbiol.* 16, 584–586.
- Packiam, M., Weinrick, B., Jacobs, W. R. Jr., and Maurelli, A. T. (2015). Structural characterization of muropeptides from *Chlamydia trachomatis* peptidoglycan by mass spectrometry resolves “chlamydial anomaly”. *Proc. Natl. Acad. Sci. U.S.A.* 112, 11660–11665. doi: 10.1073/pnas.1514026112
- Parks, D. H., Imelfort, M., Skennerton, C. T., Hugenholtz, P., and Tyson, G. W. (2015). CheckM: assessing the quality of microbial genomes recovered from isolates, single cells, and metagenomes. *Genome Res.* 25, 1043–1055. doi: 10.1101/gr.186072.114
- Pilhofer, M., Aistleitner, K., Biboy, J., Gray, J., Kuru, E., Hall, E., et al. (2013). Discovery of chlamydial peptidoglycan reveals bacteria with murein sacci but without FtsZ. *Nat. Commun.* 4:2856. doi: 10.1038/ncomms3856
- Pilhofer, M., Rappl, K., Eckl, C., Bauer, A. P., Ludwig, W., Schleifer, K. H., et al. (2008). Characterization and evolution of cell division and cell wall synthesis genes in the bacterial phyla Verrucomicrobia, Lentisphaerae, Chlamydiae, and Planctomycetes and phylogenetic comparison with rRNA genes. *J. Bacteriol.* 190, 3192–3202. doi: 10.1128/JB.01797-07
- Poole, K. (2004). Resistance to beta-lactam antibiotics. *Cell Mol. Life Sci.* 61, 2200–2223. doi: 10.1007/s00018-004-4060-9
- Pruesse, E., Peplies, J., and Glöckner, F. O. (2012). SINA: accurate high-throughput multiple sequence alignment of ribosomal RNA genes. *Bioinformatics* 28, 1823–1829. doi: 10.1093/bioinformatics/bts252
- Razin, S. (2006). “The genus mycoplasma and related genera (Class Mollicutes),” in *The Prokaryotes*, eds M. Dworkin, S. Falkow, E. Rosenberg, K.-H. Schleifer, and E. Stackebrandt (Berlin: Springer), 836–904.
- R Core Team. (2015). *R: A Language Environment for Statistical Computing*. Available at: <https://www.r-project.org/>
- Rivas-Marin, E., Canosa, I., and Devos, D. P. (2016). Evolutionary cell biology of division mode in the bacterial planctomycetes-verrucomicrobia-chlamydiae superphylum. *Front. Microbiol.* 7:1964. doi: 10.3389/fmicb.2016.01964
- Rosselló-Móra, R., and Amann, R. (2015). Past and future species definitions for Bacteria and Archaea. *Syst. Appl. Microbiol.* 38, 209–216. doi: 10.1016/j.syapm.2015.02.001
- Schleifer, K. H., and Joseph, R. (1973). A directly cross-linked L-ornithine-containing peptidoglycan in cell walls of *Spirochaeta stenostrepta*. *FEBS Lett.* 36, 83–86. doi: 10.1016/0014-5793(73)80342-4
- Schumann, P. (2011). “5 - Peptidoglycan Structure,” in *Methods in Microbiology*, eds R. Fred and O. Aharon (Cambridge, MA: Academic Press), 101–129.
- Seemann, T. (2014). Prokka: rapid prokaryotic genome annotation. *Bioinformatics* 30, 2068–2069. doi: 10.1093/bioinformatics/btu153
- Sharp, C. E., Op den Camp, H. J., Tamas, I., and Dunfield, P. F. (2013). “Unusual members of the PVC superphylum: the methanotrophic Verrucomicrobia genus “*Methylacidiphilum*”,” in *Planctomycetes: Cell Structure, Origins and Biology*, ed. J. A. Fuerst (New York, NY: Humana Press), 211–227.
- Shieh, W. Y., and Jean, W. D. (1998). *Alterococcus agarolyticus*, gen.nov., sp.nov., a halophilic thermophilic bacterium capable of agar degradation. *Can. J. Microbiol.* 44, 637–645. doi: 10.1139/cjm-98-44-7-637
- Spring, S., Bunk, B., Sproer, C., Schumann, P., Rohde, M., Tindall, B. J., et al. (2016). Characterization of the first cultured representative of Verrucomicrobia subdivision 5 indicates the proposal of a novel phylum. *ISME J.* 10, 2801–2816. doi: 10.1038/ismej.2016.84
- Staneck, J. L., and Roberts, G. D. (1974). Simplified approach to identification of aerobic actinomycetes by thin-layer chromatography. *Appl. Microbiol.* 28, 226–231.
- Stephens, R. S., Kalman, S., Lammel, C., Fan, J., Marathe, R., Aravind, L., et al. (1998). Genome sequence of an obligate intracellular pathogen of humans: *Chlamydia trachomatis*. *Science* 282, 754–759. doi: 10.1126/science.282.5389.754
- Suslow, T. V., Schroth, M. N., and Isaka, M. (1982). Application of a rapid method for gram differentiation of plant pathogenic saprophytic bacteria without staining. *Am. Phytopathol. Soc.* 72, 917–918. doi: 10.1094/Phyto-72-917
- Tamaoka, J., and Komagata, K. (1984). Determination of DNA base composition by reversed-phase high-performance liquid chromatography. *FEMS Microbiol. Lett.* 25, 125–128. doi: 10.1111/j.1574-6968.1984.tb01388.x
- Valentine, R. C., Shapiro, B. M., and Stadtman, E. R. (1968). Regulation of glutamine synthetase. XII. Electron microscopy of the enzyme from *Escherichia coli*. *Biochemistry* 7, 2143–2152. doi: 10.1021/bi00846a017
- van Passel, M. W., Kant, R., Palva, A., Copeland, A., Lucas, S., Lapidus, A., et al. (2011). Genome sequence of the verrucomicrobe *Opitutus terrae* PB90-1, an abundant inhabitant of rice paddy soil ecosystems. *J. Bacteriol.* 193, 2367–2368. doi: 10.1128/JB.00228-11
- van Teeseling, M. C., Mesman, R. J., Kuru, E., Espaillat, A., Cava, F., Brun, Y. V., et al. (2015). Anammox Planctomycetes have a peptidoglycan cell wall. *Nat. Commun.* 6:6878. doi: 10.1038/ncomms7878
- van Teeseling, M. C., Pol, A., Harhangi, H. R., van der Zwart, S., Jetten, M. S. M., Op den Camp, H. J., et al. (2014). Expanding the verrucomicrobial methanotrophic world: description of three novel species of *Methylacidiphilum* gen. nov. *Appl. Environ. Microbiol.* 80:6782. doi: 10.1128/AEM.01838-14
- Vollmer, W., Blanot, D., and de Pedro, M. A. (2008). Peptidoglycan structure and architecture. *FEMS Microbiol. Rev.* 32, 149–167. doi: 10.1111/j.1574-6976.2007.00094.x
- Wagner, M., and Horn, M. (2006). The *Planctomycetes*, *Verrucomicrobia*, *Chlamydiae* and sister phyla comprise a superphylum with biotechnological and medical relevance. *Curr. Opin. Biotechnol.* 17, 241–249. doi: 10.1016/j.copbio.2006.05.005
- Wang, G., Huang, X., Ng, T. B., Lin, J., and Ye, X. Y. (2014). High phylogenetic diversity of glycosyl hydrolase family 10 and 11 xylanases in the sediment of Lake Dabusu in China. *PLoS ONE* 9:e112798. doi: 10.1371/journal.pone.0112798
- Wang, X., Sharp, C. E., Jones, G. M., Grasby, S. E., Brady, A. L., and Dunfield, P. F. (2015). Stable-isotope probing identifies uncultured planctomycetes as primary degraders of a complex heteropolysaccharide in soil. *Appl. Environ. Microbiol.* 81, 4607–4615. doi: 10.1128/AEM.00055-15
- Waxman, D. J., and Strominger, J. L. (1983). Penicillin-binding proteins and the mechanism of action of beta-lactam antibiotics. *Annu. Rev. Biochem.* 52, 825–869. doi: 10.1146/annurev.bi.52.070183.004141
- Yanagihara, Y., Kamisango, K., Yasuda, S., Kobayashi, S., Mifuchi, I., Azuma, I., et al. (1984). Chemical compositions of cell walls and polysaccharide fractions of spirochetes. *Microbiol. Immunol.* 28, 535–544. doi: 10.1111/j.1348-0421.1984.tb00706.x
- Yoon, J. (2011). Phylogenetic studies on the bacterial phylum ‘Verrucomicrobia’. *Microbiol. Cult. Coll.* 27, 61–65.
- Yoon, J., Matsuo, Y., Matsuda, S., Adachi, K., Kasai, H., and Yokota, A. (2007a). *Cerasicoccus arenae* gen. nov., sp. nov., a carotenoid-producing marine representative of the family *Puniceicoccaceae* within the phylum ‘Verrucomicrobia’ isolated from marine sand. *Int. J. Syst. Evol. Microbiol.* 57(Pt 9), 2067–2072. doi: 10.1099/ijss.0.651020
- Yoon, J., Oku, N., Matsuda, S., Kasai, H., and Yokota, A. (2007b). *Pelagicoccus croceus* sp. nov., a novel marine member of the family *Puniceicoccaceae* within the phylum ‘Verrucomicrobia’ isolated from seagrass. *Int. J. Syst. Evol. Microbiol.* 57(Pt 12), 2874–2880. doi: 10.1099/ijss.0.65286-0
- Yoon, J., Yasumoto-Hirose, M., Katsuta, A., Sekiguchi, H., Matsuda, S., Kasai, H., et al. (2007c). *Coraliomargarita akajimensis* gen. nov., sp. nov., a novel member of the phylum ‘Verrucomicrobia’ isolated from seawater in Japan. *Int. J. Syst. Evol. Microbiol.* 57(Pt 5), 959–963. doi: 10.1099/ijss.0.64755-0
- Yoon, J., Yasumoto-Hirose, M., Matsuo, Y., Nozawa, M., Matsuda, S., Kasai, H., et al. (2007d). *Pelagicoccus mobilis* gen. nov., sp. nov., *Pelagicoccus albus* sp. nov. and *Pelagicoccus litoralis* sp. nov., three novel members of subdivision 4 within the phylum ‘Verrucomicrobia’ isolated from seawater by in situ cultivation. *Int. J. Syst. Evol. Microbiol.* 57(Pt 7), 1377–1385. doi: 10.1099/ijss.0.64970-0
- Yoon, J., Matsuo, Y., Matsuda, S., Kasai, H., and Yokota, A. (2010). *Cerasicoccus maritimus* sp. nov. and *Cerasicoccus frondis* sp. nov., two peptidoglycan-less marine verrucomicrobial species, and description of Verrucomicrobia phyl. nov., nom. rev. *J. Gen. Appl. Microbiol.* 56, 213–222. doi: 10.2323/jgam.56.213

Zhou, Y., Liang, Y., Lynch, K. H., Dennis, J. J., and Wishart, D. S. (2011). PHAST: a fast phage search tool. *Nucleic Acids Res.* 39, W347–W352. doi: 10.1093/nar/gkr485

Conflict of Interest Statement: The authors declare that the research was conducted in the absence of any commercial or financial relationships that could be construed as a potential conflict of interest.

Copyright © 2017 Rast, Glöckner, Boedecker, Jeske, Wiegand, Reinhardt, Schumann, Rohde, Spring, Glöckner, Jogler and Jogler. This is an open-access article distributed under the terms of the Creative Commons Attribution License (CC BY). The use, distribution or reproduction in other forums is permitted, provided the original author(s) or licensor are credited and that the original publication in this journal is cited, in accordance with accepted academic practice. No use, distribution or reproduction is permitted which does not comply with these terms.



Characterization of Outer Membrane Proteome of *Akkermansia muciniphila* Reveals Sets of Novel Proteins Exposed to the Human Intestine

Noora Ottman^{1,2}, Laura Huuskonen³, Justus Reunananen^{3,4}, Sjef Boeren⁵, Judith Klievink⁶, Hauke Smidt¹, Clara Belzer¹ and Willem M. de Vos^{1,3,6*}

¹ Laboratory of Microbiology, Wageningen University, Wageningen, Netherlands, ² Metapopulation Research Centre, University of Helsinki, Helsinki, Finland, ³ Department of Veterinary Biosciences, University of Helsinki, Helsinki, Finland,

⁴ Microbiology and Biotechnology, Department of Food and Environmental Sciences, University of Helsinki, Helsinki, Finland,

⁵ Laboratory of Biochemistry, Wageningen University, Wageningen, Netherlands, ⁶ Immunobiology, Department of Bacteriology and Immunology, and Research Programs Unit, University of Helsinki, Helsinki, Finland

OPEN ACCESS

Edited by:

Laura Van Niftrik,
Radboud University Nijmegen,
Netherlands

Reviewed by:

Suleyman Yildirim,
Istanbul Medipol University
International School of Medicine,
Turkey

Naomi L. Ward,
University of Wyoming, USA

*Correspondence:

Willem M. de Vos
willems.devos@wur.nl

Specialty section:

This article was submitted to
Evolutionary and Genomic
Microbiology,
a section of the journal
Frontiers in Microbiology

Received: 01 April 2016

Accepted: 12 July 2016

Published: 26 July 2016

Citation:

Ottman N, Huuskonen L, Reunananen J, Boeren S, Klievink J, Smidt H, Belzer C and de Vos WM (2016) Characterization of Outer Membrane Proteome of *Akkermansia muciniphila* Reveals Sets of Novel Proteins Exposed to the Human Intestine. *Front. Microbiol.* 7:1157.
doi: 10.3389/fmicb.2016.01157

Akkermansia muciniphila is a common member of the human gut microbiota and belongs to the Planctomycetes-Verrucomicrobia-Chlamydiae superphylum. Decreased levels of *A. muciniphila* have been associated with many diseases, and thus it is considered to be a beneficial resident of the intestinal mucus layer. Surface-exposed molecules produced by this organism likely play important roles in colonization and communication with other microbes and the host, but the protein composition of the outer membrane (OM) has not been characterized thus far. Herein we set out to identify and characterize *A. muciniphila* proteins using an integrated approach of proteomics and computational analysis. Sarkosyl extraction and sucrose density-gradient centrifugation methods were used to enrich and fractionate the OM proteome of *A. muciniphila*. Proteins from these fractions were identified by LC-MS/MS and candidates for OM proteins derived from the experimental approach were subjected to computational screening to verify their location in the cell. In total we identified 79 putative OM and membrane-associated extracellular proteins, and 23 of those were found to differ in abundance between cells of *A. muciniphila* grown on the natural substrate, mucin, and those grown on the non-mucus sugar, glucose. The identified OM proteins included highly abundant proteins involved in secretion and transport, as well as proteins predicted to take part in formation of the pili-like structures observed in *A. muciniphila*. The most abundant OM protein was a 95-kD protein, termed PilQ, annotated as a type IV pili secretin and predicted to be involved in the production of pili in *A. muciniphila*. To verify its location we purified the His-Tag labeled N-terminal domain of PilQ and generated rabbit polyclonal antibodies. Immunolectron microscopy of thin sections immunolabeled with these antibodies demonstrated the OM localization of PilQ, testifying for its predicted function as a type IV pili secretin in *A. muciniphila*. As pili structures are known to be involved in the modulation of host immune responses,

this provides support for the involvement of OM proteins in the host interaction of *A. muciniphila*. In conclusion, the characterization of *A. muciniphila* OM proteome provides valuable information that can be used for further functional and immunological studies.

Keywords: *Akkermansia muciniphila*, outer membrane, gut microbiota, proteomics, pili, PVC superphylum

INTRODUCTION

Akkermansia muciniphila is a Gram-negative, anaerobic bacterium, which colonizes the mucus layer of the human gastrointestinal (GI) tract (Derrien et al., 2004). *A. muciniphila* is considered to be an important member of the GI microbiota, because of the inverse correlation between its abundance and several intestinal disorders, including inflammatory bowel diseases and obesity (Png et al., 2010; Karlsson et al., 2012; Rajilic-Stojanovic et al., 2013). Moreover, experiments with germ-free mice mono-associated with *A. muciniphila*, or conventional mice on a high fat diet that are fed *A. muciniphila*, have shown that *A. muciniphila* plays a role in host immune response, restoration of mucus layer thickness and mucus production (Derrien et al., 2011; Everard et al., 2013; Shin et al., 2014). In addition, extracellular vesicles from *A. muciniphila* were shown to have protective effects on the development of dextran sulfate sodium (DSS) induced colitis in mice (Kang et al., 2013). Finally, *A. muciniphila* has also been shown to adhere to intestinal epithelium and improve enterocyte monolayer integrity of Caco-2 cells (Reunanan et al., 2015). These findings suggest important host-bacteria interactions, the mechanisms of which are yet to be discovered (see Derrien et al., 2016 for a recent review).

Bacterial outer membrane (OM) proteins play important roles in communication with other microbes and the host, as well as in colonization and substrate transport (Tseng et al., 2009; Galdiero et al., 2012). Subcellular fractionation techniques combined with mass spectrometry-based proteomic analysis are powerful tools for identifying proteins in different bacterial compartments. These techniques have been successfully used for studying the protein composition of intestinal bacteria, such as the OM of *Bacteroides fragilis* and *Bacteroides thetaiotaomicron* (Elhenawy et al., 2014; Wilson et al., 2015), surface proteins of *Propionibacterium freudenreichii* (Le Marechal et al., 2015) and OM vesicles of *Escherichia coli* Nissle 1917 (Aguilera et al., 2014).

Akkermansia muciniphila is a member of the Planctomycetes-Verrucomicrobia-Chlamydiae (PVC) superphylum, which contains bacteria from several groups and various environments with different lifestyles (Wagner and Horn, 2006; Gupta et al., 2012; Kamneva et al., 2012). Bacteria from this superphylum were previously suggested to have a compartmentalized cell plan with a cytoplasmic membrane as the outermost membrane, and an intracytoplasmic membrane containing a condensed nucleoid and ribosomes (Lee et al., 2009). However, these observations have been challenged by more recent data suggesting that the PVC cell plan is actually a variation, not an exception, of the Gram-negative cell plan, and that the bacteria have an outer and

an inner membrane (IM) with possible invaginations of the IM inside the cytoplasm (Devos, 2014).

There is limited information available on the membrane structure and composition of *A. muciniphila*, and most reports have focused on *in silico* analysis of Verrucomicrobia membranes, instead of experimental approaches (Santarella-Mellwig et al., 2010; Kamneva et al., 2012; Speth et al., 2012). Recently, the proteome of a termite hindgut representative of the Verrucomicrobia, *Diplosphaera colotermitum* TAV2, was experimentally studied, but this report did not focus on membrane proteins (Isanapong et al., 2013). The presence of OM biomarkers, including genes involved in lipopolysaccharide (LPS) insertion, in the genome of *A. muciniphila* was confirmed computationally (Speth et al., 2012). We have experimentally verified the presence of LPS in *A. muciniphila* (Ottman, 2015). No genes coding for membrane coat-like proteins were found in *A. muciniphila*, unlike in some other Verrucomicrobia (Santarella-Mellwig et al., 2010).

In the present study, we set out to identify and characterize *A. muciniphila* proteins using an integrated approach of proteomics and computational analysis. Successful extraction of OM proteins was established, and the proteins were identified with liquid chromatography-tandem mass spectrometry (LC-MS/MS). The abundance of *A. muciniphila* proteins in the OM fraction was compared to the whole proteome of *A. muciniphila* and a fraction enriched for intracellular proteins. Candidates for OM proteins derived from the proteomics analysis were subjected to computational screening to verify their location in the cell. The OM location of the most abundant membrane protein, termed PilQ, in *A. muciniphila* was confirmed by immunoelectron microscopy. PilQ is predicted to be a secretin involved in the production of type IV pilins, long surface exposed filaments involved in a variety of functions, including motility and adherence to host cells, and found in virtually all prokaryotes, including the PVC superphylum (Berry and Pelicic, 2015). We also explored the presence of these proteins as a function of the growth on mucus, resulting in the identification of several OM proteins related to mucosal colonization. The results indicate that *A. muciniphila* produces OM proteins involved in secretion and transport in high abundance, and these, including PilQ, may be involved in its capacity to interact with the host.

MATERIALS AND METHODS

Bacterial Growth Conditions

Akkermansia muciniphila Muc^T (ATCC BAA-835) was grown in a basal medium as described previously, except without the

addition of rumen fluid (Derrien et al., 2004). The medium was supplemented with either hog gastric mucin (0.5 %, Type III; Sigma-Aldrich, St. Louis, MO, USA) purified by ethanol precipitation as described previously (Miller and Hoskins, 1981), or D-glucose (10 mM, Sigma-Aldrich). The medium with glucose was also supplemented with BactoTM casitone (BD, Sparks, MD, USA), BBLTM yeast extract (BD), tryptone (Oxoid Ltd, Basingstoke, Hampshire, England), peptone (Oxoid Ltd) (2 g/l each) and L-threonine (Sigma-Aldrich) (2 mM). Incubations were performed in serum bottles sealed with butyl-rubber stoppers at 37°C under anaerobic conditions provided by a gas phase of 182 kPa (1.5 atm) N₂/CO₂. Growth was measured by following optical density at 600 nm (OD₆₀₀) using a spectrophotometer.

Bacterial Fractionation Methods

Membrane proteins of *A. muciniphila* were isolated from liquid cultures with two different methods, using either *N*-lauroyl-sarcosine (sarkosyl) or sucrose density-gradient centrifugation, as described previously, with minor modifications (Hobb et al., 2009).

Briefly, for sarkosyl treatments, 250 ml cultures of *A. muciniphila* were grown on mucin for 16 h (OD₆₀₀ = 1.56) or on glucose for 40 h (OD₆₀₀ = 0.34). Cells were harvested, washed twice with phosphate buffered saline (PBS) and resuspended in 9 ml 10 mM HEPES, pH 7.4, and lysed by passing the culture three times through a French press (Aminco, American Instrument Co., Inc., Silver Spring, Maryland, USA) at 1000 psi (40 K cell). The lysed cell preparation was centrifuged at 10 000 g for 10 min at 4°C to remove cell debris and unlysed cells. The membranes were collected by ultracentrifugation of the supernatant at 100 000 g for 1 h at 4°C. The supernatant was collected and stored at -20°C. This sample was later analyzed by LC-MS/MS as the intracellular fraction. The pellet was resuspended in 2 ml 10 mM HEPES, pH 7.4, washed in a total volume of 10 ml 10 mM HEPES, pH 7.4, and spun again in the ultracentrifuge (using the conditions described above). The pellet was resuspended in 5 ml 1 % (w/v) *N*-lauroylsarcosine (sarkosyl) (Sigma-Aldrich) in 10 mM HEPES, pH 7.4, and incubated at 37°C for 30 min with shaking to solubilize cytoplasmic membranes. The sarkosyl-treated membranes were spun at 100 000 g for 1 h at 4°C and the pellet was washed with 7 ml 10 mM HEPES, pH 7.4. Following the final ultracentrifugation, the pellet containing the OM fraction was resuspended in 1 ml 10 mM HEPES, pH 7.4 and stored at -20°C.

For the sucrose-density gradient centrifugation treatments, 250 ml cultures of *A. muciniphila* were grown on mucin for 16 h (OD₆₀₀ = 1.51) or on glucose for 40 h (OD₆₀₀ = 0.35). Cells were harvested, washed twice with phosphate buffered saline (PBS) and resuspended in 7 ml 10 mM HEPES, pH 7.4, and lysed by passing the culture three times through a French press at 1000 psi (40K cell). The lysed cells preparation was centrifuged at 10 000 g for 10 min at 4°C. The supernatant was ultracentrifuged at 100 000 g for 60 min at 4°C to pellet the total membranes. The membrane pellet was washed in 10 ml 10 mM HEPES, 0.05 M EDTA pH 7.5 (HE buffer) and ultracentrifuged again. The final membranes were homogenized in 2 ml HE buffer.

Continuous sucrose gradients were prepared by layering sucrose solutions (prepared in HE buffer) into 14 × 95 mm polyallomer ultracentrifuge tubes (Seton Scientific, Petaluma, CA, USA) in the following order: 0.4 ml 60% (w/v), 0.9 ml 55%, 2.2 ml 50%, 2.2 ml 45%, 2.2 ml 40%, 1.3 ml 35% and 0.4 ml 30%. Total membranes were layered on top of each gradient, with no more than 2.5 ml per gradient. Sucrose gradients were centrifuged in a TST 41.14-41000 RPM swinging-bucket rotor (Kontrol) at 250 000 g for 16 h at 4°C. The sucrose gradient tubes were then removed from the rotor buckets and 500 µl fractions (24 fractions for each gradient) were collected from the bottom of each gradient by puncturing the tube with a needle and allowing the sample to drip out by gravity. The samples were stored in 2 ml low binding tubes (Eppendorf, Hamburg, Germany) at -20°C.

For comparison, the whole proteome fraction was obtained from *A. muciniphila* cultures grown with mucin or glucose as the carbon source. Bacterial cells from an overnight 2 ml culture were spun down, washed with PBS and suspended into 500 µl of PBS. Cells were lysed by sonication, using a Branson sonifier equipped with a 3 mm tip (four pulses of 20 s with 30 s rest on ice in-between each pulse, strength of the pulse was 4). The samples were stored in 2 ml low binding tubes (Eppendorf, Hamburg, Germany) at -20°C.

Protein Identification by Mass Spectrometry

To determine the protein content of cell extracts, the Qubit[®] Protein Assay Kit (Life technologies, Eugene, OR, USA) was used according to the manufacturer's instructions. Samples were loaded on a 10% acrylamide separation gel (25201, PreciseTM Protein Gels, Thermo Scientific, Rockford, IL, USA) using the mini-PROTEAN 3 cell (Bio-Rad Laboratories, Hercules, CA, USA). The electrophoresis procedure was according to the manufacturer's instructions. Gels were stained using Coomassie Brilliant Blue (CBB) R-250 as indicated in the protocol of the mini-PROTEAN 3 system.

In-gel digestion of proteins and purification of peptides were done following a modified version of a previously described protocol (Rupakula et al., 2013). Disulphide bridges in proteins were reduced by covering whole gels with reducing solution (10 mM dithiothreitol, pH 7.6, in 50 mM NH₄HCO₃), and the gels were incubated at 60°C for 1 h. Alkylation was performed for 1 h by adding 25 ml of iodoacetamide solution (10 mM iodoacetamide in 100 mM Tris-HCl, pH 8.0). Gels were thoroughly rinsed with demineralized water in between steps. Each of the used gel lanes was cut into either five slices (sarkosyl-extracted OM, intracellular proteins and whole proteome) or one slice (sucrose density-gradient centrifugation samples), and the slices were cut into approximately 1 mm × 1 mm × 1 mm cubes and transferred to separate 0.5 ml protein LoBind tubes (Eppendorf, Hamburg, Germany). Enzymatic digestion was done by adding 50 µl of trypsin solution (5 ng/µl trypsin in 50 mM NH₄HCO₃) to each tube, and by incubating at room temperature overnight with gentle shaking. Extraction of peptides was performed with manual sonication in an ultrasonic water bath for 1 s before the supernatant was transferred to

a clean protein LoBind tube. Trifluoroacetic acid (10%) was added to the supernatant to reach a pH between 2 and 4. The supernatant was used for LC-MS/MS analysis. Samples were measured by nLC-MS/MS with a Proxeon EASY nLC and a LTQ-Orbitrap XL mass spectrometer as previously described (Lu et al., 2011).

LC-MS data analysis was performed as described previously (Rupakula et al., 2013) with false discovery rates (FDRs) set to 0.01 on peptide and protein level, and additional result filtering (minimally 2 peptides necessary for protein identification of which at least one is unique and at least one is unmodified). To analyze the abundance of proteins in the fractions, their label-free quantification (LFQ) intensities was compared (Cox et al., 2014). Non-existing LFQ intensity values due to not enough quantified peptides were substituted with a value lower than the LFQ intensity value for the least abundant, quantified protein. The mass spectrometry proteomics data have been deposited to the ProteomeXchange Consortium via the PRIDE (Vizcaino et al., 2016) partner repository with the dataset identifier PXD004400.

Enzyme Activity Assay

Enzyme activity was tested in the OM and intracellular fractions by incubating them at 37°C with colorimetric or fluorimetric substrates, as described previously (Rosendale et al., 2012). The following substrate/enzyme combinations were used: 4-nitrophenyl *N*-acetyl- β -D-glucosaminide/*N*-acetyl- β -glucosaminidase, *p*-nitrophenyl-alpha-L-fucoside/fucosidase, PNP *N*-acetyl-glucosamine-sulfate/GlcNAc-sulfatase, and 2'-*(4-methylumbelliferyl)- α -D-N-acetylneurameric acid/sialidase. Substrates were purchased from Carbosynth (Compton, Berkshire, UK). Reaction volume was 20 μ l and substrate concentration was 1 mM in each reaction. All reactions were performed in duplicate.*

Bioinformatics Analysis

Proteins were categorized based on results of SignalP v.4.0 (set for Gram-negative bacteria) (Petersen et al., 2011), LipoP v.1.0 (Juncker et al., 2003), SecretomeP v.2.0 (set for Gram-negative bacteria) (Bendtsen et al., 2005), TMHMM v.2.0 (Krogh et al., 2001) and BOMP (Berven et al., 2004). Subcellular localization was determined using CELLO v.2.5 (set for Gram-negative bacteria) (Yu et al., 2004) and PSORTb v3.0 (set for Gram-negative bacteria) (Yu et al., 2010). BLAST searches were run against the non-redundant (nr) database at <http://blast.ncbi.nlm.nih.gov/> using default settings. TIGRFAM and Pfam were used for screening proteins with PEP-CTERM domains (Selengut et al., 2007; Finn et al., 2014).

Overproduction and Purification of Amuc_1098A Protein

The DNA coding for the N-terminal half of PilQ, the product of the gene with locus tag Amuc_1098, was amplified by PCR from the chromosomal DNA of *A. muciniphila* using a primer pair containing NdeI site (5'ATACATATGGATGGC GGCGCCGTCGGAACCTC; restriction site in italics) and XhoI

site (5'ATACTCGAGGGCTTAAGGCCGGAGGAGCTTT; restriction site in italics) (Sigma-Aldrich). The obtained PCR product was digested with NdeI and XhoI and cloned into similarly digested pET26b vector (Novagen) and transformed into *E. coli* TOP10 (Invitrogen). Agarose gel electrophoresis and sequencing were used to verify the right insert and the obtained plasmid (termed pAmuc_1098A) was subsequently transformed into the expression strain *E. coli* BL21 (DE3) (Invitrogen) containing plasmid pSJS1240 (Kim et al., 1998) and transformants were selected for resistance to kanamycin and spectinomycin (both at 50 μ g/ml). Protein production was induced in an exponentially growing aerobic culture at optical density at 600 nm of approximately 0.5 by adding isopropyl β -D-1-thiogalactopyranoside (IPTG) to a final concentration of 1 mM. After a further overnight incubation at 37°C, cells were collected and lysed by sonication and the protein, referred to as P-Amuc_1098A, was purified under native conditions using Ni-NTA His Bind Resin (Novagen) according to manufacturer's instructions. The purity was tested with sodium dodecyl sulfate-polyacrylamide gel electrophoresis (SDS-PAGE).

Generation of Polyclonal Antibody against P-Amuc_1098A Protein

Polyclonal rabbit antibodies were produced against P-Amuc_1098A protein with an immunization protocol as described previously (Johnston et al., 1991), at the Laboratory Animal Centre of the University of Helsinki. In short, a rabbit was immunized four times with 3 weeks interval for each injection. Pre-immunization sera were collected before initiating the immunization. In the first immunization, purified P-Amuc_1098A protein (192 μ g) was mixed with an equal amount of Freund's complete adjuvant. For the subsequent immunizations (booster injections), P-Amuc_1098A protein (96 μ g) was diluted 1:1 volume in Freund's incomplete adjuvant and injected into rabbit. Blood was collected from the rabbit 10 days after the last booster injection. The blood was allowed to clot for 1–2 h at 37°C after which the blood clot was separated from the serum by centrifugation at 3 000 g for 10 min. Then the serum was divided into aliquots and stored at –80°C prior to use.

Immunogold Labeling and Electron Microscopy of Thin Sections

Immunogold labeling of *A. muciniphila* thin sections was performed as described previously with minor changes (Reunanen et al., 2012). In short, *A. muciniphila* cells were grown in mucin medium for two overnights and washed once with phosphate buffer (0.1 M Na-phosphate, pH 7.4) before fixation. The fixed cells were embedded in Lowicryl HM20 resin, 50 nm thin sections were cut from polymerized Lowicryl and mounted on nickel grids. Grids containing the *A. muciniphila* thin sections were treated with anti-P-Amuc_1098A rabbit immune serum (1:5 dilution), and subsequently with protein A conjugated to 10 nm diameter gold particles. Finally, the grids were post-stained with uranyl acetate and lead citrate using an UltroStain apparatus (Leica). The grids were examined and

images obtained with a JEOL JEM-1400 transmission electron microscope (Jeol Ltd., Tokyo, Japan).

Statistical Analysis

Statistical analysis of the results from the enzyme activity assay was performed by one-way analysis of variance (ANOVA) using IBM SPSS software (IBM SPSS Statistics 22); *p* values <0.05 were considered significant.

RESULTS

Akkermansia muciniphila OM proteins were isolated using two different methods, based on either selective sarkosyl extraction or sedimentation gradient centrifugation of membrane proteins, derived from cells grown with mucin or glucose as major carbon and energy sources (Figure 1). Label-free mass spectrometry of the trypsin-treated fractions was performed to identify the extracted proteins in comparison with those recovered from total cells (whole proteome). In addition, the location of the identified proteins was predicted by using the CELLO software. To determine the abundance of proteins within the fractions from different cellular locations, we compared their LFQ intensities as these are commonly used as a proxy for absolute protein abundance in mass spectrometry data analysis (Cox et al., 2014).

An over 20-fold enrichment of predicted OM proteins was achieved in the sarkosyl-treated membranes in comparison with the whole proteome and intracellular fraction of both mucin and glucose-grown cells of *A. muciniphila* (Figures 1A,B). Moreover, the predicted periplasmic and extracellular proteins were slightly enriched in the OM fraction at the expense of cytoplasmic proteins that were enriched in the intracellular fraction.

Complementary to the sarkosyl treatment procedure, we applied sucrose density gradient centrifugation of *A. muciniphila* membrane fractions obtained from cells grown on mucin or glucose. Analysis of the recovered proteins from each fraction revealed different protein abundance in the mucin versus glucose-grown cell membranes, likely reflecting the adaptation to the different environmental conditions (Supplementary Figure S1). The abundance of OM proteins was the lowest in the fraction with the lowest sucrose density, and increased along the gradient for proteins derived from both growth conditions (Figures 1C,D). However, the enrichment of predicted OM proteins was not more than a factor of 2–5 by the sucrose gradient centrifugation and hence it was evident that the sarkosyl treatment procedure was superior (Figures 1C,D).

The sarkosyl-treated OM fraction was compared with the intracellular fraction derived from the same *A. muciniphila* cells (Figures 1A,B) for the activity of four relevant mucin-degrading

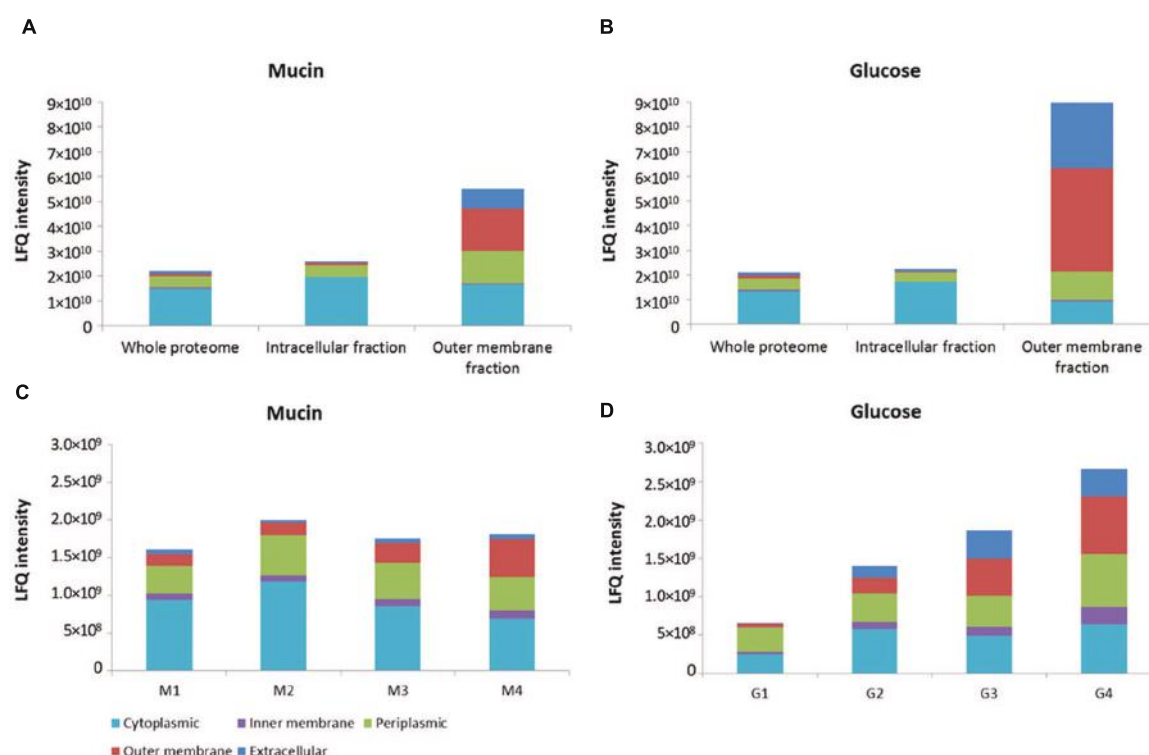


FIGURE 1 | Distribution of proteins from different bacterial compartments in isolated fractions. OM fraction isolated from sarkosyl-extracted membranes in comparison to whole proteome and intracellular fraction of both mucin and glucose-grown cells of *A. muciniphila* (A,B). Fractions of sucrose density-gradient centrifugation (see Supplementary Figure S1) of membranes of *A. muciniphila* grown on mucin or glucose (C,D). Label-free quantification (LFQ) intensity was used as a proxy for absolute protein abundance. CELLO software was used to predict protein localization.

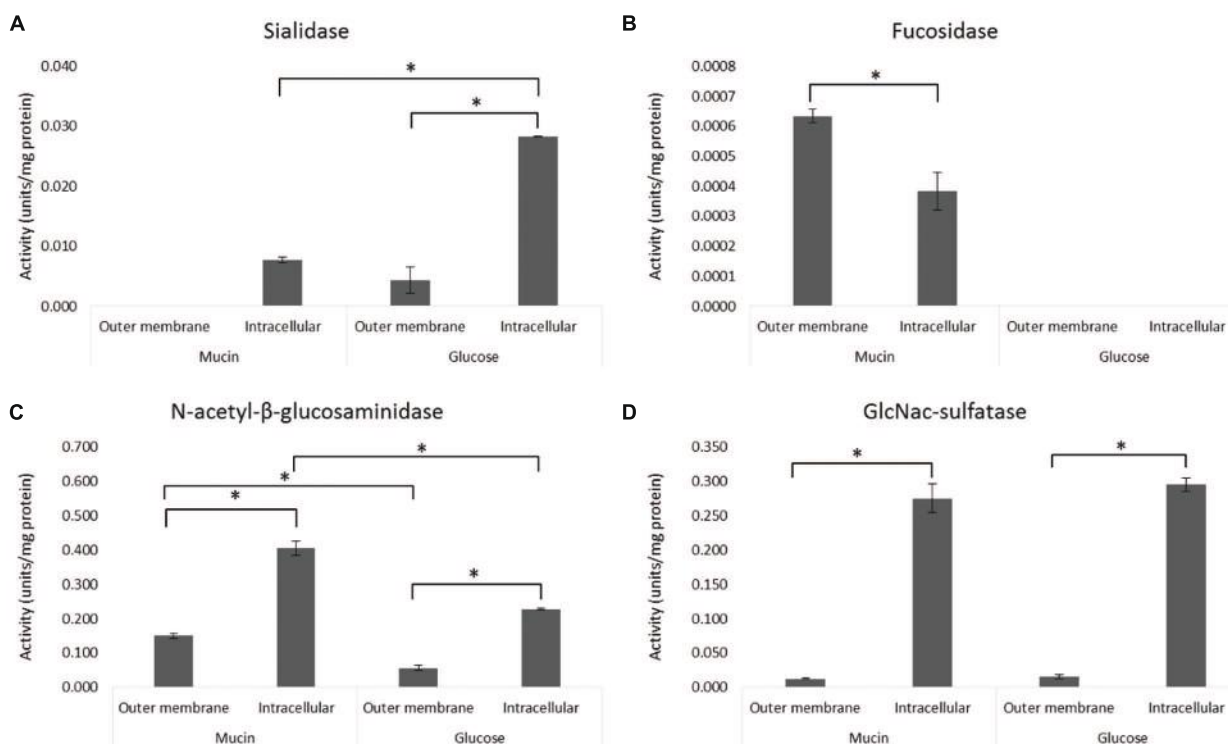


FIGURE 2 | Activity of mucin-degrading enzymes in the OM and intracellular fractions. The enzyme activity of sialidase (A), fucosidase (B), *N*-acetyl- β -glucosaminidase (C), and GlcNAc-sulfatase (D) was determined from OM and intracellular (including periplasmic space) fractions of *A. muciniphila* grown on mucin or glucose as described in Figure 1. Average of duplicate measurements is shown. Significant differences ($p < 0.05$) in the enzyme activities between samples are indicated with an asterisks.

enzymes (sialidase, fucosidase, *N*-acetyl- β -glucosaminidase, GlcNAc-sulfatase) (Figure 2). Except for the fucosidase activity, it appeared that the sialidase, *N*-acetyl- β -glucosaminidase and GlcNAc-sulfatase activity was significantly higher in the intracellular than the OM fractions, for both glucose and mucin-grown cells (Figures 2A,C,D). As none of the candidate enzymes for these activities was predicted to be located in the OM, this supported the purification of OM proteins by the sarkosyl treatment. In contrast, most candidate proteins were predicted to carry a signal sequence and hence their presence in the intracellular fraction indicated that they are at least partly among the periplasmic space proteins that are also found in this fraction (Figures 1A,B). Different results were obtained for the fucosidase activity (Figure 2B). This enzymatic activity was enriched in the OM fraction, which is compatible with the experimentally verified OM location of one of the fucosidases (encoded by the gene with locus tag Amuc_0146; see below). Remarkably, this fucosidase activity was strongly induced in the extracts of *A. muciniphila* grown on mucin, which is in line with the production of 1,2-propanediol from fucose during growth on mucin but not on glucose (Ottman, 2015).

Analysis of the *A. muciniphila* Proteome

While over 1000 different proteins could be identified in the total *A. muciniphila* proteome, the number of sarkosyl-treated

OM proteins amounted to slightly lower amounts (812 and 719 proteins from the mucin and glucose grown cells, respectively) but exceeded those found in the sucrose gradient fractions (up to \sim 500 proteins), indicative of the efficiency of the detergent treatment (Supplementary Table S1). Of further interest was the comparison of the protein abundances of these sarkosyl-treated OM proteins and the intracellular proteins obtained from the same *A. muciniphila* cells, grown on either mucin or glucose (Figure 3). The resulting comparative proteome plots showed that many of the predicted OM proteins were highly abundant in the OM fraction with a relative LFQ intensity above 8.5. Remarkably, several predicted extracellular, periplasmic and cytoplasmic proteins (12, 12, and 14, respectively) were also similarly abundant and enriched in the OM fraction in *A. muciniphila* cells grown on either mucin or glucose. Hence, all the proteins with an LFQ intensity above 8.5 and proteins predicted as OM proteins by CELLO or PSORTb (a total of 145) were further analyzed as described below.

Identification, Annotation and Classification of *A. muciniphila* OM Proteins

Next, we confirmed the predicted localization of the 145 proteins that were experimentally found to be enriched in the OM fraction by applying several criteria, supported by advanced

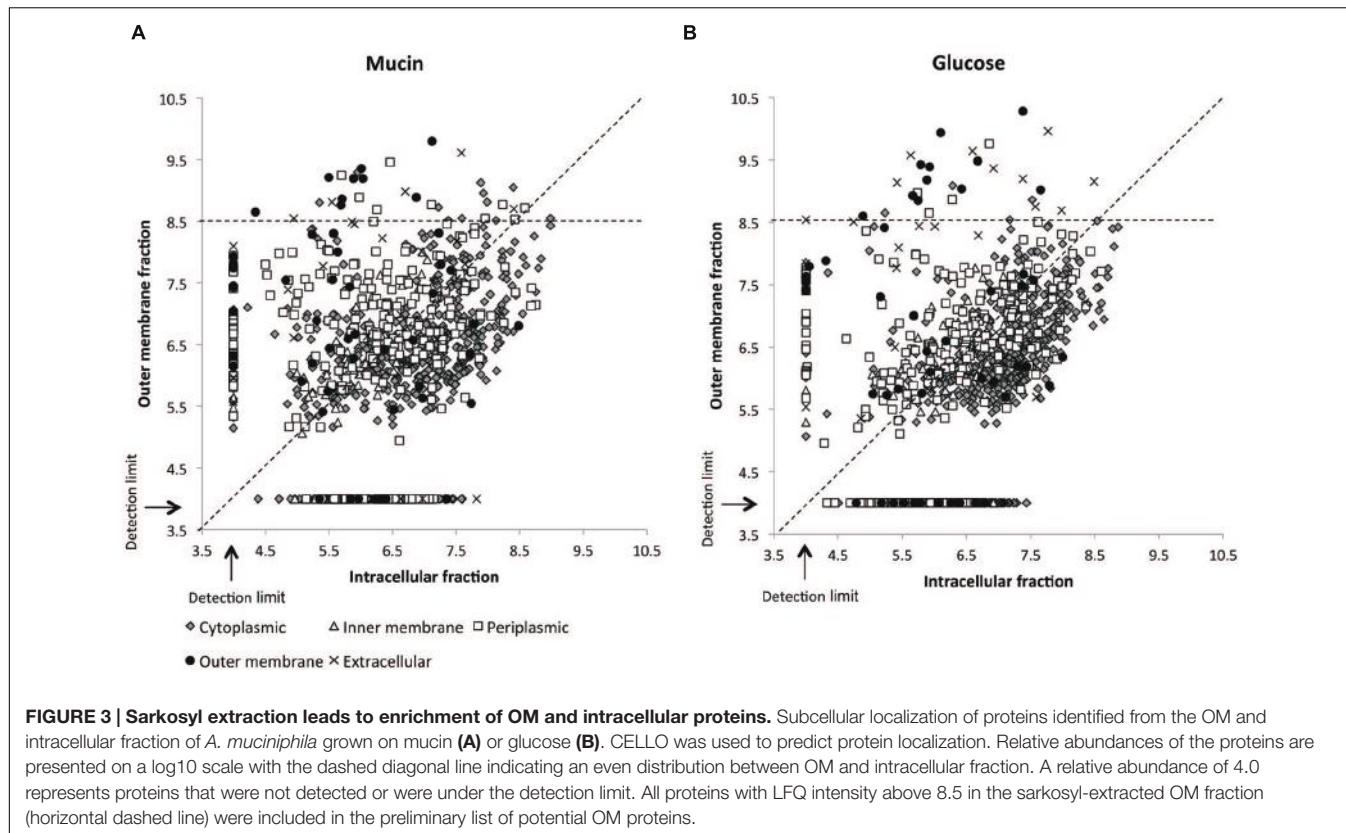


FIGURE 3 | Sarkosyl extraction leads to enrichment of OM and intracellular proteins. Subcellular localization of proteins identified from the OM and intracellular fraction of *A. muciniphila* grown on mucin (A) or glucose (B). CELLO was used to predict protein localization. Relative abundances of the proteins are presented on a log10 scale with the dashed diagonal line indicating an even distribution between OM and intracellular fraction. A relative abundance of 4.0 represents proteins that were not detected or were under the detection limit. All proteins with LFQ intensity above 8.5 in the sarkosyl-extracted OM fraction (horizontal dashed line) were included in the preliminary list of potential OM proteins.

bioinformatic predictions: a protein was considered as a potential OM protein if (1) both CELLO and PSORTb programs predicted the protein to be localized in the OM, (2) the Lipop software predicted the protein to be a lipoprotein, (3) BOMP software predicted the presence of beta-barrel(s), or (4) the protein had no signal protein, but SecretomeP predicted unclassical secretion (Supplementary Figure S2). Proteins that had a signal peptide but did not fulfill any of the above criteria were assumed to be periplasmic. After applying these criteria, 73 proteins from mucin-grown cells and 76 proteins from glucose-grown cells in the isolated OM fractions were predicted to be true OM proteins. Moreover, 5 out of the 14 cytoplasmic and 9 out of the 12 periplasmic proteins included in the preliminary list were identified as true OM proteins. In total, 79 truly predicted OM and membrane-associated extracellular proteins were identified (Supplementary Table S2). It is of interest to note that the majority of these were also present in the sucrose density-gradient samples: 62 proteins for the mucin-grown and 58 proteins for the glucose-grown condition (data not shown).

Additionally, we searched for potential OM proteins, which were not present in either of the sarkosyl-extracted protein fractions. The *A. muciniphila* genome was found to encode additional 17 proteins, which were predicted as OM proteins according to the applied criteria (see above), and 12 (71%) of these were uncharacterized proteins (Supplementary Table S3). Two of the proteins (products of genes tagged as Amuc_0356 and Amuc_0480) were found to be present in the sucrose density-gradient fractions. Three of the proteins (products of

genes tagged as Amuc_0983, Amuc_1011 and Amuc_1945) were present in low amounts when the whole proteome of *A. muciniphila* was analyzed. However, all these proteins are likely to be produced, since RNA-seq analysis of *A. muciniphila* grown on mucin or glucose confirmed the production of transcripts for the corresponding 17 genes (Ottman, 2015).

The proteins identified as true OM proteins had multiple and different functions (Supplementary Figure S3). Nine proteins obtained from cells grown at both conditions were OM proteins containing an autotransporter barrel domain. OM proteins enriched during growth on mucin (total of four) or on glucose (total of three) were found to be involved in RND (Resistance-Nodulation-Division) efflux systems. Mucin-grown cells contained three and glucose-grown cells two YD repeat proteins. The function of many of the predicted OM proteins was unknown (26 proteins for mucin-grown and 29 for glucose-grown cells). BLAST searches were performed for all uncharacterized proteins with LFQ intensity above 8.5, but this did not reveal any closely related proteins.

Influence of Environmental Growth Conditions on OM Protein Abundances

From the identified OM proteins, 23 out of the 79 showed more than a 10-fold change in abundance between *A. muciniphila* grown on either mucin or glucose (Supplementary Table S2). Six out of the nine proteins containing an autotransporter barrel domain were present at a higher level in glucose-grown as

compared to mucin-grown cells. In addition, a two-component regulator propeller domain protein and a peptidase were more abundant in mucin-grown cells, whilst a glycoside hydrolase family 16 protein and peptidyl-prolyl *cis-trans* isomerase were present in higher abundance in glucose-grown cells (products of genes with locus tags Amuc_0371 and Amuc_0576 as well as Amuc_2108 and Amuc_1026, respectively). Many uncharacterized proteins were among the ones with highest fold-change differences between the two conditions. There were four uncharacterized proteins (products of genes with locus tags Amuc_0789, Amuc_0837, Amuc_1333, Amuc_2165) exclusively found in the OM fraction extracted from glucose-grown cells and one uncharacterized protein (encoded by the gene with locus tag Amuc_0006), exclusively found in mucin-grown cells.

BLAST searches and subsequent TIGRFAM and PFAM analyses revealed that three of the glucose-exclusive proteins in the OM fraction contained a PEP-CTERM domain (Supplementary Table S4). This domain is thought to be involved in protein sorting and cell surface localization (Haft et al., 2006). The domain includes the motif Pro-Glu-Pro (PEP), which is considered a potential recognition or processing site, followed by a predicted transmembrane helix and a cluster rich in basic amino acids. These target proteins are generally destined to transit cellular membranes during their biosynthesis and undergo further posttranslational modifications, such as glycosylation. PEP-CTERM domains have been first identified in the predicted proteome of *Verrucomicrobium spinosum* and have only been found in the genomes of several Gram-negative bacteria that encode EpsH (exopolysaccharide locus protein H), including members of the PVC cluster (Haft et al., 2012). An EpsH-like gene is also found in the genome of *A. muciniphila* and upon further screening for the presence of PEP-CTERM proteins encoded by the genome of *A. muciniphila*, we found 23 predicted proteins containing this domain (Supplementary Table S4). The synthesis of 9 of these was confirmed by mass spectrometry, as they were present in at least one of the analyzed bacterial fractions. However, these appeared to be differentially regulated as some were only found in *A. muciniphila* grown on either glucose or mucin.

Abundant OM Proteins and OM Location of the PilQ Protein in *A. muciniphila*

Three OM proteins (encoded by the genes with locus tags Amuc_0336, Amuc_1310 and Amuc_1098) were the most highly abundant in *A. muciniphila* grown on mucin or glucose, altogether making up to 20–40% of the total OM protein (Supplementary Table S2). BLAST analysis predicted the 17-kD protein encoded by the gene with locus tag Amuc_1310 to belong to a protein superfamily that includes several *Rickettsia* genus-specific 17 kD-surface antigen proteins, suggesting its potential interaction with the environment. The 82-kD protein encoded by the gene with locus tag Amuc_0336 could be annotated as a TonB-dependent receptor and showed low but significant similarity (sequence identity ~25%) to TonB-dependent receptors from *Pseudomonas* spp, which are OM proteins involved in heme and iron transport (Takase et al., 2000).

By far the most prominent protein, which was found to be over twofold more abundant than any other OM protein, is the product of gene with locus tag Amuc_1098, further termed PilQ. The 907-residue protein PilQ was initially annotated as a types II and III secretion system protein (see Supplementary Table S2) and contains a highly conserved pilus secretin domain at position 650–876, while its N-terminal part has a conserved domain at position 71–239 of a beta-barrel assembly machinery (BAM) containing three tetratricopeptide repeats. Highly similar homologues (25–40% identity) of the *A. muciniphila* PilQ are predicted to be produced by other Verrucomicrobia, such as *V. spinosum*, *Halofeferula* sp. and *Lentisphaera araneosa*, the homologue of the latter being annotated as the type IV fimbrial biogenesis protein PilQ. These results strongly suggests that Verrucomicrobia, and specifically *A. muciniphila*, may produce type IV pili that are secreted in a process that involves the OM located secretin PilQ (Berry and Pelicic, 2015).

Previous electron microscope (EM) images from *A. muciniphila* have revealed pili-like structures (Derrien et al., 2004). Therefore, we used immunogold labeling of *A. muciniphila* thin sections to determine the location of PilQ. The N-terminal domain of PilQ (termed P-Amuc_1098A) labeled with a C-terminal His-Tag was overproduced and purified from *E. coli* since the gene for the entire PilQ could not be stably maintained in the *E. coli* host Top10 (data not shown). Polyclonal rabbit antibodies against the purified termed P-Amuc_1098A were generated, labeled with protein A-conjugated gold particles, and used to treat thin sections of *A. muciniphila* cells that were subsequently examined by transmission electron microscopy (Figure 4). The results show that a major part of the protein A-gold particles were located in the OM, confirming the location of PilQ in the OM of *A. muciniphila*. Moreover, each thin section has various PilQ molecules, as is to be expected by the high level of abundance of the OM protein PilQ in *A. muciniphila*.

DISCUSSION

Using a combination of experimental mass-spectrometry based identification and advanced bioinformatics, we identified 79 putative OM proteins in *A. muciniphila*, which comprises 3.6% of the 2176 predicted protein-coding sequences in this mucus-degrading intestinal bacterium. This fraction is slightly higher than that found in other Gram-negative bacteria where it was estimated that 2–3% of the genome codes for OM proteins (Molloy et al., 2000; Wimley, 2003). As we included membrane-associated extracellular proteins in the analysis, the actual number of OM proteins in *A. muciniphila* is presumably somewhat lower. Extracellular proteins were included as they may be involved in communication with the host and are therefore of great interest. Seven complementary bioinformatic algorithms were applied to characterize *A. muciniphila* OM and extracellular proteins based on the predicted secretion signals, occurrence of transmembrane strands, presence of beta-barrel structures and attachment to the cell wall by lipid motifs. Moreover, the enrichment of the OM fractions was characterized by analysis of the activity of mucin-degrading

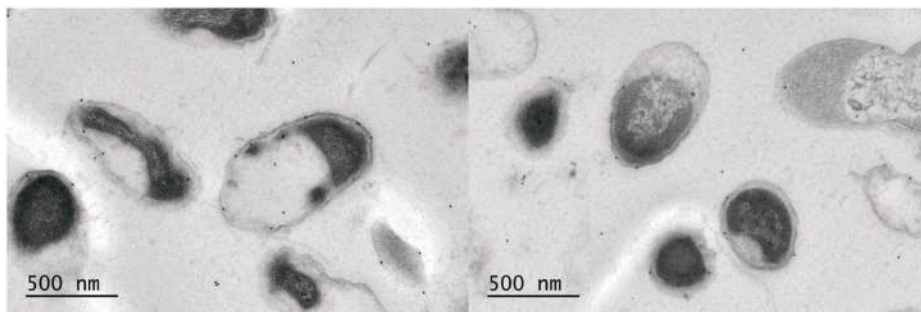


FIGURE 4 | Immunoelectron microscopy labeling of *A. muciniphila* thin sections visualizes PilQ to be localized on the OM. The cells were labeled with anti-P-Amuc_1098A antibodies and detection was done by using 10-nm protein A-conjugated gold particles. Two representative electronmicrographs are shown.

enzymes in *A. muciniphila*. This included the sialidase activity, encoded by two secreted enzymes that recently were purified and characterized (Tailford et al., 2015).

Since it was discovered that sarkosyl can selectively solubilize cytoplasmic and inner membranes while conserving the integrity of the OM, this ionic detergent has been widely used in the purification of OM proteins in Gram-negative bacteria (Rhomberg et al., 2004; Brown et al., 2010; Moumene et al., 2015). In comparison to other methods, sarkosyl extraction leads to higher purity and better reproducibility of the OM extracts, while the basis for OM resistance to this detergent is not known (Filip et al., 1973; Frankel et al., 1991). In our study, sarkosyl-treatment was superior to the sucrose gradient centrifugation of *A. muciniphila* membranes and led to enrichment of OM proteins (Figure 1). Several proteins from other cellular locations were also present and the high sensitivity of LC-MS/MS might be one of the reasons why so many proteins were identified from the fractions. Hence, by optimizing the protocol, the abundance of non-OM proteins could be further reduced.

More insight into the OM proteome biosynthesis of *A. muciniphila* was generated through isolation and identification of proteins covering the most important pathways of OM biogenesis. The YaeT protein (the product of the gene with locus tag Amuc_1053), which is an essential protein for OM protein biogenesis due to its role in insertion of beta-barrel proteins into the OM (Werner and Misra, 2005; Tokuda, 2009), was among the 10 most highly abundant proteins in the extracted OM fractions. Furthermore, the organic solvent tolerance protein (encoded by the gene with the locus tag Amuc_1439), known also as increased membrane permeability (Imp) protein, needed for LPS transport to the bacterial cell surface (Bos et al., 2004), was found in high abundance. These results support the typical Gram-negative membrane architecture of *A. muciniphila*. However, we obtained no support for the presence of an intracytoplasmic membrane as is found in some PVC species (Lee et al., 2009). A recent study on the abundance of *A. muciniphila* in antibiotic-treated subjects has reported partial compartmentalization of some *A. muciniphila* cells (Doubourg et al., 2013). However, *A. muciniphila* does not contain the highly conserved genetic module, termed DUF1501, preferentially present in compartmentalized PVC species, nor

the Planctomycetes and Verrumicrobia metabolosome genes (Kamneva et al., 2012).

The *A. muciniphila* protein PilQ was found to be the most highly produced OM protein in *A. muciniphila*, regardless of the growth conditions. The primary structure of the *A. muciniphila* PilQ includes a N-terminal BAM domain with three tetratricopeptide repeats, resembling the pilin proteins that are essential for the folding and insertion of proteins in the OM of Gram-negative bacteria and involved in the biogenesis of type IV pili (Koo et al., 2013). Moreover, the *A. muciniphila* PilQ includes a C-terminal secretin domain, which is highly conserved in all secretins that allow passage through the OM of type IV pilins, long surface exposed filaments involved in a variety of functions, including motility and adherence to host cells (Berry and Pelicic, 2015). No atomic structures of secretins have been solved yet but advanced EM analysis has recently provided insight in the *Thermus thermophilus* and *Myxococcus xanthus* pilin machineries, showing that the PilQ of these bacteria form the OM channels as well as part of the periplasmic ring where type IV pili are being extruded (Burkhardt et al., 2011; Chang et al., 2016). The structure of the *A. muciniphila* PilQ is unique but conserved in proteins predicted to be produced by other Verrucomicrobia, including *V. spinosum*, *Haloferrula* sp. and *L. araneosa*. We found the *A. muciniphila* PilQ to be enriched in the sarkosyl-resistant OM fraction, which is in line with the observation that the well-characterized *T. thermophilus* PilQ is resistant to sarkosyl treatment (Burkhardt et al., 2011). The immunogold labeling results presented here confirm the localization of PilQ in the OM of *A. muciniphila*. Based on this observation, the demonstrated OM location and the predicted structural homology of PilQ, we propose that the *A. muciniphila* PilQ is involved in the formation of type IV pili. The earlier observed protruding filaments in *A. muciniphila* could represent such type IV pili but further studies are needed to confirm this (Derrien et al., 2004). Hence, PilQ is an interesting candidate for immune signaling in *A. muciniphila*, as the type IV pili are known to be involved in a variety of interactions with the host (Ehara et al., 1993; Craig and Li, 2008; von Ossowski et al., 2013).

Other groups of OM proteins found to be produced by *A. muciniphila* were autotransporters, RND multidrug efflux pumps and YD proteins. Autotransporters are an extensive family

of proteins, which can be either secreted or cell-surface-exposed, and function for example as enzymes, adhesins, cytotoxins or mediate bacterial motility (Grijpstra et al., 2013). They have mainly been studied for their virulence-related properties in pathogens but are also commonly found in non-pathogenic bacteria. RND multidrug efflux pumps exist in a tripartite form traversing both the OM and IM, and thus they are able to efficiently pump out drug molecules directly into extracellular space (Nikaido, 2011). The function of YD proteins is not very well studied but they have been suggested to be involved in carbohydrate binding and bacterial interactions with eukaryotic host cells (Jackson et al., 2009; Koskinen et al., 2013).

In addition to the OM proteins produced by *A. muciniphila*, we identified another 12 OM proteins from the genome using *in silico* analysis. These were not present in any of the studied fractions. Based on RNA-seq data all the genes encoding these proteins are transcriptionally active (Ottman, 2015), suggesting that their absence from the proteomics dataset could be due to a methodological reason, such as their low level production, high hydrophobicity, or post-translational modification. While we can presently not distinguish between these possibilities, we have been able to detect proteins that are post-translationally modified. These include the PEP-CTERM proteins that are involved in a specific sortase system and may be heavily post-translationally modified, including removal of N-terminal and C-terminal transmembrane domains and extensive glycosylation (Haft et al., 2012). *A. muciniphila* was predicted to encode 23 PEP-CTERM proteins and we detected nine of these by mass spectrometry. The proteins were present in relatively low abundance in the whole proteome samples, which may explain the difficulty in detecting them. Higher levels of PEP-CTERM proteins were detected in the intracellular fractions compared to OM fractions but we cannot exclude the possibility that this is related to different levels of glycosylation. While originally detected in *V. spinosum* but widely spread in the Gram-negatives, including the PVC cluster, peptides of the PEP-CTERM proteins have so far been experimentally identified in several Archaea (Haft et al., 2012). Hence, these findings suggest that *A. muciniphila* may be a well-suited model organism for studying the bacterial PEP-CTERM/exosortase system that so far has been little characterized.

Among the highly abundant proteins in the OM fractions were several proteins annotated as cytoplasmic, including six ribosomal proteins. It is possible that these proteins were so abundant in the cultures that they ended up in high concentrations also in the OM fraction, but it may also be that they have secondary roles in the bacteria. Proteins that are able to perform two or more functions are called moonlighting proteins (Copley, 2012). Several glycolytic, housekeeping and ribosomal proteins are often found on the surface of bacteria where they develop other functions (Henderson and Martin, 2011; Sherry et al., 2011).

The presence of specific OM proteins in Gram-negative bacteria is modulated by the available carbon and energy sources

(Papasotiriou et al., 2008; Haussmann et al., 2009; Yang et al., 2011). The abundance of one third of the putative *A. muciniphila* OM proteins was altered during growth on glucose in comparison to mucin. However, for most of these proteins, the presence of other proteins with the same function was found in both conditions. This suggests that the specific function is not missing, but is taken over by a different protein. Unfortunately, many of the proteins that were most affected by the difference in carbon sources remain uncharacterized, despite efforts to search for related proteins. This is a common issue when handling proteomics data, especially as *A. muciniphila* belongs to the PVC superphylum, which has not been studied extensively yet. Further research into the function of these proteins could reveal important characteristics of *A. muciniphila*.

This study provides the first proteomic characterization of *A. muciniphila* OM proteins. We have identified highly abundant proteins involved in secretion and transport, as well as many uncharacterized proteins. In particular, we confirmed by immunoelectron microscopy the localization of the most abundant OM protein PilQ that is predicted to be involved in type IV pili formation by *A. muciniphila*.

AUTHOR CONTRIBUTIONS

NO, HS, CB, WdV conceived and designed the experiments. NO, LH, JR, SB, JK performed the experiments. NO, CB, WdV analyzed the data. NO and WdV drafted the manuscript and all authors contributed to the final article.

FUNDING

This work was supported by Advanced Research Grant 250172 (MicrobesInside) of the European Research Council and the Netherlands Organization for Scientific Research (Spinoza Award and SIAM Gravity Grant 024.002.002) to WdV, the European Community's Seventh Framework Programme (FP7/2007-2013) under grant agreement n°215553-2 to NO, and the Finland Academy of Sciences (252803 to JR, and 141130 to WdV).

ACKNOWLEDGMENT

This manuscript includes content that first appeared in Ottman, 2015 as partial fulfillment of obtaining the Ph.D. degree by NO.

SUPPLEMENTARY MATERIAL

The Supplementary Material for this article can be found online at: <http://journal.frontiersin.org/article/10.3389/fmicb.2016.01157>

REFERENCES

- Aguilera, L., Tolozza, L., Gimenez, R., Odona, A., Oliveira, E., Aguilar, J., et al. (2014). Proteomic analysis of outer membrane vesicles from the probiotic strain *Escherichia coli* Nissle 1917. *Proteomics* 14, 222–229. doi: 10.1002/pmic.201300328
- Bendtsen, J. D., Kierner, L., Fausbøll, A., and Brunak, S. (2005). Non-classical protein secretion in bacteria. *BMC Microbiol.* 5:58. doi: 10.1186/1471-2180-5-58
- Berry, J. L., and Pelicic, V. (2015). Exceptionally widespread nanomachines composed of type IV pilins: the prokaryotic Swiss Army knives. *FEMS Microbiol. Rev.* 39, 134–154. doi: 10.1093/femsre/fuu001
- Berven, F. S., Flikka, K., Jensen, H. B., and Eidhammer, I. (2004). BOMP: a program to predict integral beta-barrel outer membrane proteins encoded within genomes of Gram-negative bacteria. *Nucleic Acids Res.* 32, W394–W399. doi: 10.1093/nar/gkh351
- Bos, M. P., Tefsen, B., Geurtzen, J., and Tommassen, J. (2004). Identification of an outer membrane protein required for the transport of lipopolysaccharide to the bacterial cell surface. *Proc. Natl. Acad. Sci. U.S.A.* 101, 9417–9422. doi: 10.1073/pnas.0402340101
- Brown, R. N., Romine, M. F., Schepmoes, A. A., Smith, R. D., and Lipton, M. S. (2010). Mapping the subcellular proteome of *Shewanella oneidensis* MR-1 using sarkosyl-based fractionation and LC-MS/MS protein identification. *J. Proteome Res.* 9, 4454–4463. doi: 10.1021/pr100215h
- Burkhardt, J., Vonck, J., and Averhoff, B. (2011). Structure and function of PilQ, a secretin of the DNA transporter from the thermophilic bacterium *Thermus thermophilus* HB27. *J. Biol. Chem.* 286, 9977–9984. doi: 10.1074/jbc.M110.212688
- Chang, Y. W., Rettberg, L. A., Treuner-Lange, A., Iwasa, J., Sogaard-Andersen, L., and Jensen, G. J. (2016). Architecture of the type IVa pilus machine. *Science* 351:aad2001. doi: 10.1126/science.aad2001
- Copley, S. D. (2012). Moonlighting is mainstream: paradigm adjustment required. *Bioessays* 34, 578–588. doi: 10.1002/bies.201100191
- Cox, J., Hein, M. Y., Luber, C. A., Paron, I., Nagaraj, N., and Mann, M. (2014). Accurate proteome-wide label-free quantification by delayed normalization and maximal peptide ratio extraction, termed MaxLFQ. *Mol. Cell. Proteomics* 13, 2513–2526. doi: 10.1074/mcp.M113.031591
- Craig, L., and Li, J. (2008). Type IV pili: paradoxes in form and function. *Curr. Opin. Struct. Biol.* 18, 267–277. doi: 10.1016/j.sbi.2007.12.009
- Derrien, M., Belzer, C., and de Vos, W. M. (2016). *Akkermansia muciniphila* and its role in regulating host functions. *Microb. Pathog.* doi: 10.1016/j.micpath.2016.02.005 [Epub ahead of print].
- Derrien, M., Van Baarlen, P., Hooiveld, G., Norin, E., Muller, M., and de Vos, W. M. (2011). Modulation of mucosal immune response, tolerance, and proliferation in mice colonized by the mucin-degrader *Akkermansia muciniphila*. *Front. Microbiol.* 2:166. doi: 10.3389/fmicb.2011.00166
- Derrien, M., Vaughan, E. E., Plugge, C. M., and de Vos, W. M. (2004). *Akkermansia muciniphila* gen. nov., sp. nov., a human intestinal mucin-degrading bacterium. *Int. J. Syst. Evol. Microbiol.* 54, 1469–1476. doi: 10.1099/ijss.0.02873-0
- Devos, D. P. (2014). PVC bacteria: variation of, but not exception to, the Gram-negative cell plan. *Trends Microbiol.* 22, 14–20. doi: 10.1016/j.tim.2013.10.008
- Dubourg, G., Lagier, J. C., Armougom, F., Robert, C., Audoly, G., Papazian, L., et al. (2013). High-level colonization of the human gut by Verrucomicrobia following broad-spectrum antibiotic treatment. *Int. J. Antimicrob. Agents* 41, 149–155. doi: 10.1016/j.ijantimicag.2012.10.012
- EHara, M., Ichinose, Y., Iwami, M., Utsunomiya, A., Shimodori, S., Kangethe, S. K., et al. (1993). Immunogenicity of *Vibrio cholerae* O1 fimbriae in animal and human cholera. *Microbiol. Immunol.* 37, 679–688. doi: 10.1111/j.1348-0421.1993.tb01692.x
- Elhenawy, W., Debely, M. O., and Feldman, M. F. (2014). Preferential packing of acidic glycosidases and proteases into *Bacteroides* outer membrane vesicles. *MBio* 5:e00909-14. doi: 10.1128/mBio.00909-14
- Everard, A., Belzer, C., Geurts, L., Ouwerkerk, J. P., Druart, C., Bindels, L. B., et al. (2013). Cross-talk between *Akkermansia muciniphila* and intestinal epithelium controls diet-induced obesity. *Proc. Natl. Acad. Sci. U.S.A.* 110, 9066–9071. doi: 10.1073/pnas.1219451110
- Filip, C., Fletcher, G., Wulff, J. L., and Earhart, C. F. (1973). Solubilization of the cytoplasmic membrane of *Escherichia coli* by the ionic detergent sodium-lauryl sarcosinate. *J. Bacteriol.* 115, 717–722.
- Finn, R. D., Bateman, A., Clements, J., Coggill, P., Eberhardt, R. Y., Eddy, S. R., et al. (2014). Pfam: the protein families database. *Nucleic Acids Res.* 42, D222–D230. doi: 10.1093/nar/gkt1223
- Frankel, S., Sohn, R., and Leinwand, L. (1991). The use of sarkosyl in generating soluble protein after bacterial expression. *Proc. Natl. Acad. Sci. U.S.A.* 88, 1192–1196. doi: 10.1073/pnas.88.4.1192
- Galdiero, S., Falanga, A., Cantani, M., Tarallo, R., Della Pepa, M. E., D'Oriano, V., et al. (2012). Microbe-host interactions: structure and role of Gram-negative bacterial porins. *Curr. Protein Pept. Sci.* 13, 843–854. doi: 10.2174/138920312804871120
- Grijpstra, J., Arenas, J., Rutten, L., and Tommassen, J. (2013). Autotransporter secretion: varying on a theme. *Res. Microbiol.* 164, 562–582. doi: 10.1016/j.resmic.2013.03.010
- Gupta, R. S., Bhandari, V., and Naushad, H. S. (2012). Molecular signatures for the PVC clade (Planctomycetes, Verrucomicrobia, Chlamydiae, and Lentisphaerae) of bacteria provide insights into their evolutionary relationships. *Front. Microbiol.* 3:327. doi: 10.3389/fmicb.2012.00327
- Haft, D. H., Paulsen, I. T., Ward, N., and Selengut, J. D. (2006). Exopolysaccharide-associated protein sorting in environmental organisms: the PEP-CTERM/EpsH system. Application of a novel phylogenetic profiling heuristic. *BMC Biol.* 4:29. doi: 10.1186/1741-7007-4-29
- Haft, D. H., Payne, S. H., and Selengut, J. D. (2012). Archaeosortases and exosortases are widely distributed systems linking membrane transit with posttranslational modification. *J. Bacteriol.* 194, 36–48. doi: 10.1128/JB.06026-11
- Haussmann, U., Qi, S. W., Wolters, D., Rogner, M., Liu, S. J., and Poetsch, A. (2009). Physiological adaptation of *Corynebacterium glutamicum* to benzoate as alternative carbon source – a membrane proteome-centric view. *Proteomics* 9, 3635–3651. doi: 10.1002/pmic.200900025
- Henderson, B., and Martin, A. (2011). Bacterial virulence in the moonlight: multitasking bacterial moonlighting proteins are virulence determinants in infectious disease. *Infect. Immun.* 79, 3476–3491. doi: 10.1128/IAI.00179-11
- Hobb, R. I., Fields, J. A., Burns, C. M., and Thompson, S. A. (2009). Evaluation of procedures for outer membrane isolation from *Campylobacter jejuni*. *Microbiology* 155, 979–988. doi: 10.1099/mic.0.024539-0
- Isanapong, J., Sealy Hambright, W., Willis, A. G., Boonmee, A., Callister, S. J., Burnum, K. E., et al. (2013). Development of an ecophysiological model for *Diplosphaera colofermitum* TAV2, a termite hindgut Verrucomicrobium. *ISME J.* 7, 1803–1813. doi: 10.1038/ismej.2013.74
- Jackson, A. P., Thomas, G. H., Parkhill, J., and Thomson, N. R. (2009). Evolutionary diversification of an ancient gene family (rhs) through C-terminal displacement. *BMC Genomics* 10:584. doi: 10.1186/1471-2164-10-584
- Johnston, B. A., Eisen, H., and Fry, D. (1991). An evaluation of several adjuvant emulsion regimens for the production of polyclonal antisera in rabbits. *Lab. Anim. Sci.* 41, 15–21.
- Juncker, A. S., Willenbrock, H., Von Heijne, G., Brunak, S., Nielsen, H., and Krogh, A. (2003). Prediction of lipoprotein signal peptides in Gram-negative bacteria. *Protein Sci.* 12, 1652–1662. doi: 10.1110/ps.0303703
- Kamneva, O. K., Knight, S. J., Liberles, D. A., and Ward, N. L. (2012). Analysis of genome content evolution in pvc bacterial super-phylum: assessment of candidate genes associated with cellular organization and lifestyle. *Genome Biol. Evol.* 4, 1375–1390. doi: 10.1093/gbe/evs113
- Kang, C. S., Ban, M., Choi, E. J., Moon, H. G., Jeon, J. S., Kim, D. K., et al. (2013). Extracellular vesicles derived from gut microbiota, especially *Akkermansia muciniphila*, protect the progression of dextran sulfate sodium-induced colitis. *PLoS ONE* 8:e76520. doi: 10.1371/journal.pone.0076520
- Karlsson, C. L., Onnerfalt, J., Xu, J., Molin, G., Ahrne, S., and Thorngren-Jerneck, K. (2012). The microbiota of the gut in preschool children with normal and excessive body weight. *Obesity (Silver Spring)* 20, 2257–2261. doi: 10.1038/oby.2012.110
- Kim, R., Sandler, S. J., Goldman, S., Yokota, H., Clark, A. J., and Kim, S. H. (1998). Overexpression of archaeal proteins in *Escherichia coli*. *Biotechnol. Lett.* 20, 207–210. doi: 10.1023/A:1005305330517

- Koo, J., Tang, T., Harvey, H., Tammam, S., Sampaleanu, L., Burrows, L. L., et al. (2013). Functional mapping of PilF and PilQ in the *Pseudomonas aeruginosa* type IV pilus system. *Biochemistry* 52, 2914–2923. doi: 10.1021/bi3015345
- Koskinen, S., Lamoureux, J. G., Nikolakakis, K. C., t'Kint de Roodenbeke, C., Kaplan, M. D., Low, D. A., et al. (2013). Rhs proteins from diverse bacteria mediate intercellular competition. *Proc. Natl. Acad. Sci. U.S.A.* 110, 7032–7037. doi: 10.1073/pnas.1300627110
- Krogh, A., Larsson, B., von Heijne, G., and Sonnhammer, E. L. (2001). Predicting transmembrane protein topology with a hidden Markov model: application to complete genomes. *J. Mol. Biol.* 305, 567–580. doi: 10.1006/jmbi.2000.4315
- Le Marechal, C., Peton, V., Ple, C., Vroland, C., Jardin, J., Briard-Bion, V., et al. (2015). Surface proteins of *Propionibacterium freudenreichii* are involved in its anti-inflammatory properties. *J. Proteomics* 113, 447–461. doi: 10.1016/j.jprot.2014.07.018
- Lee, K. C., Webb, R. I., Janssen, P. H., Sangwan, P., Romeo, T., Staley, J. T., et al. (2009). Phylum Verrucomicrobia representatives share a compartmentalized cell plan with members of bacterial phylum Planctomycetes. *BMC Microbiol.* 9:5. doi: 10.1186/1471-2180-9-5
- Lu, J., Boeren, S., de Vries, S. C., van Valenberg, H. J., Vervoort, J., and Hettinga, K. (2011). Filter-aided sample preparation with dimethyl labeling to identify and quantify milk fat globule membrane proteins. *J. Proteomics* 75, 34–43. doi: 10.1016/j.jprot.2011.07.031
- Miller, R. S., and Hoskins, L. C. (1981). Mucin degradation in human colon ecosystems. Fecal population densities of mucin-degrading bacteria estimated by a “most probable number” method. *Gastroenterology* 81, 759–765.
- Molloy, M. P., Herbert, B. R., Slade, M. B., Rabilloud, T., Nouwens, A. S., Williams, K. L., et al. (2000). Proteomic analysis of the *Escherichia coli* outer membrane. *Eur. J. Biochem.* 267, 2871–2881. doi: 10.1046/j.1432-1327.2000.01296.x
- Moumene, A., Marcelino, I., Ventosa, M., Gros, O., Lefrancois, T., Vachiery, N., et al. (2015). Proteomic profiling of the outer membrane fraction of the obligate intracellular bacterial pathogen *Ehrlichia ruminantium*. *PLoS ONE* 10:e0116758. doi: 10.1371/journal.pone.0116758
- Nikaido, H. (2011). Structure and mechanism of RND-type multidrug efflux pumps. *Adv. Enzymol. Relat. Areas Mol. Biol.* 77, 1–60.
- Ottman, N. (2015). *Host Immunostimulation and Substrate Utilization of the Gut Symbiont Akkermansia muciniphila*. Ph.D. dissertation, Wageningen University, Wageningen.
- Papasotiriou, D. G., Markoutsas, S., Meyer, B., Papadioti, A., Karas, M., and Tsiotis, G. (2008). Comparison of the membrane subproteomes during growth of a new *Pseudomonas* strain on lysogenic broth medium, glucose, and phenol. *J. Proteome Res.* 7, 4278–4288. doi: 10.1021/pr800192n
- Petersen, T. N., Brunak, S., von Heijne, G., and Nielsen, H. (2011). SignalP 4.0: discriminating signal peptides from transmembrane regions. *Nat Methods* 8, 785–786. doi: 10.1038/nmeth.1701
- Png, C. W., Linden, S. K., Gilshenan, K. S., Zoetendal, E. G., McSweeney, C. S., Sly, L. I., et al. (2010). Mucolytic bacteria with increased prevalence in IBD mucosa augment in vitro utilization of mucin by other bacteria. *Am. J. Gastroenterol.* 105, 2420–2428. doi: 10.1038/ajg.2010.281
- Rajilic-Stojanovic, M., Shanahan, F., Guarner, F., and de Vos, W. M. (2013). Phylogenetic analysis of dysbiosis in ulcerative colitis during remission. *Inflamm. Bowel Dis.* 19, 481–488. doi: 10.1097/MIB.0b013e31827fec6d
- Reunanan, J., Kainulainen, V., Huuskonen, L., Ottman, N., Belzer, C., Huhtinen, H., et al. (2015). *Akkermansia muciniphila* adheres to enterocytes and strengthens the integrity of epithelial cell layer. *Appl. Environ. Microbiol.* 81, 3655–3662. doi: 10.1128/AEM.04050-14
- Reunanan, J., von Ossowski, I., Hendrickx, A. P. A., Palva, A., and de Vos, W. M. (2012). Characterization of the SpaCBA pilus fibers in the probiotic *Lactobacillus rhamnosus* GG. *Appl. Environ. Microbiol.* 78, 2337–2344. doi: 10.1128/Aem.07047-11
- Rhomberg, T. A., Karlberg, O., Mini, T., Zimny-Arndt, U., Wickenberg, U., Rottgen, M., et al. (2004). Proteomic analysis of the sarcosine-insoluble outer membrane fraction of the bacterial pathogen *Bartonella henselae*. *Proteomics* 4, 3021–3033. doi: 10.1002/pmic.200400933
- Rosendale, D. I., Blatchford, P. A., Sims, I. M., Parkar, S. G., Carnachan, S. M., Hedderley, D., et al. (2012). Characterizing kiwifruit carbohydrate utilization in vitro and its consequences for human faecal microbiota. *J. Proteome Res.* 11, 5863–5875. doi: 10.1021/pr300646m
- Rupakula, A., Kruse, T., Boeren, S., Holliger, C., Smidt, H., and Maillard, J. (2013). The restricted metabolism of the obligate organohalide respiring bacterium *Dehalobacter restrictus*: lessons from tiered functional genomics. *Philos. Trans. R. Soc. Lond. B Biol. Sci.* 368:20120325. doi: 10.1098/rstb.2012.0325
- Santarella-Mellwig, R., Franke, J., Jaedicke, A., Gorjanacz, M., Bauer, U., Budd, A., et al. (2010). The compartmentalized bacteria of the planctomycetes-verrucomicrobia-chlamydia superphylum have membrane coat-like proteins. *PLoS Biol.* 8:e1000281. doi: 10.1371/journal.pbio.1000281
- Selengut, J. D., Haft, D. H., Davidsen, T., Ganapathy, A., Gwinn-Giglio, M., Nelson, W. C., et al. (2007). TIGRFAMs and Genome Properties: tools for the assignment of molecular function and biological process in prokaryotic genomes. *Nucleic Acids Res.* 35, D260–D264. doi: 10.1093/nar/gkl1043
- Sherry, A. E., Inglis, N. F., Stevenson, A., Fraser-Pitt, D., Everest, P., Smith, D. G., et al. (2011). Characterisation of proteins extracted from the surface of *Salmonella Typhimurium* grown under SPI-2-inducing conditions by LC-ESI/MS/MS sequencing. *Proteomics* 11, 361–370. doi: 10.1002/pmic.200900802
- Shin, N. R., Lee, J. C., Lee, H. Y., Kim, M. S., Whon, T. W., Lee, M. S., et al. (2014). An increase in the *Akkermansia* spp. population induced by metformin treatment improves glucose homeostasis in diet-induced obese mice. *Gut* 63, 727–735. doi: 10.1136/gutjnl-2012-303839
- Speth, D. R., van Teeseling, M. C., and Jetten, M. S. (2012). Genomic analysis indicates the presence of an asymmetric bilayer outer membrane in planctomycetes and verrucomicrobia. *Front. Microbiol.* 3:304. doi: 10.3389/fmicb.2012.00304
- Tailford, L. E., Owen, C. D., Walshaw, J., Crost, E. H., Hardy-Goddard, J., Le Gall, G., et al. (2015). Discovery of intramolecular trans-sialidases in human gut microbiota suggests novel mechanisms of mucosal adaptation. *Nat. Commun.* 6:7624. doi: 10.1038/ncomms8624
- Takase, H., Nitanai, H., Hoshino, K., and Otani, T. (2000). Requirement of the *Pseudomonas aeruginosa* tonB gene for high-affinity iron acquisition and infection. *Infect. Immun.* 68, 4498–4504. doi: 10.1128/Iai.68.8.4498-4504.2000
- Tokuda, H. (2009). Biogenesis of outer membranes in Gram-negative bacteria. *Biosci. Biotechnol. Biochem.* 73, 465–473. doi: 10.1271/bbb.80778
- Tseng, T. T., Tyler, B. M., and Setubal, J. C. (2009). Protein secretion systems in bacterial-host associations, and their description in the Gene Ontology. *BMC Microbiol.* 9(Suppl. 1):S2. doi: 10.1186/1471-2180-9-S1-S2
- Vizcaino, J. A., Csordas, A., del-Toro, N., Dianes, J. A., Griss, J., Lavidas, I., et al. (2016). 2016 update of the PRIDE database and its related tools. *Nucleic Acids Res.* 44, D447–D456. doi: 10.1093/nar/gkv1145
- von Ossowski, I., Pietila, T. E., Rintahaka, J., Nummenmaa, E., Makinen, V. M., Reunanan, J., et al. (2013). Using recombinant Lactococci as an approach to dissect the immunomodulating capacity of surface piliation in probiotic *Lactobacillus rhamnosus* GG. *PLoS ONE* 8:e64416. doi: 10.1371/journal.pone.0064416
- Wagner, M., and Horn, M. (2006). The Planctomycetes, Verrucomicrobia, Chlamydiae and sister phyla comprise a superphylum with biotechnological and medical relevance. *Curr. Opin. Biotechnol.* 17, 241–249. doi: 10.1016/j.copbio.2006.05.005
- Werner, J., and Misra, R. (2005). YaeT (Omp85) affects the assembly of lipid-dependent and lipid-independent outer membrane proteins of *Escherichia coli*. *Mol. Microbiol.* 57, 1450–1459. doi: 10.1111/j.1365-2958.2005.04775.x
- Wilson, M. M., Anderson, D. E., and Bernstein, H. D. (2015). Analysis of the outer membrane proteome and secretome of *Bacteroides fragilis* reveals a multiplicity of secretion mechanisms. *PLoS ONE* 10:e0117732. doi: 10.1371/journal.pone.0117732
- Wimley, W. C. (2003). The versatile beta-barrel membrane protein. *Curr. Opin. Struct. Biol.* 13, 404–411. doi: 10.1016/S0959-440X(03)00099-X
- Yang, J. N., Wang, C., Guo, C., Peng, X. X., and Li, H. (2011). Outer membrane proteome and its regulation networks in response to glucose

- concentration changes in *Escherichia coli*. *Mol. Biosyst.* 7, 3087–3093. doi: 10.1039/c1mb05193h
- Yu, C. S., Lin, C. J., and Hwang, J. K. (2004). Predicting subcellular localization of proteins for Gram-negative bacteria by support vector machines based on n-peptide compositions. *Protein Sci.* 13, 1402–1406. doi: 10.1110/ps.03479604
- Yu, N. Y., Wagner, J. R., Laird, M. R., Melli, G., Rey, S., Lo, R., et al. (2010). PSORTb 3.0: improved protein subcellular localization prediction with refined localization subcategories and predictive capabilities for all prokaryotes. *Bioinformatics* 26, 1608–1615. doi: 10.1093/bioinformatics/btq249

Conflict of Interest Statement: The authors declare that the research was conducted in the absence of any commercial or financial relationships that could be construed as a potential conflict of interest.

Copyright © 2016 Ottman, Huuskonen, Reunanen, Boeren, Klievink, Smidt, Belzer and de Vos. This is an open-access article distributed under the terms of the Creative Commons Attribution License (CC BY). The use, distribution or reproduction in other forums is permitted, provided the original author(s) or licensor are credited and that the original publication in this journal is cited, in accordance with accepted academic practice. No use, distribution or reproduction is permitted which does not comply with these terms.



The S-Layer Protein of the Anammox Bacterium *Kuenenia stuttgartiensis* Is Heavily O-Glycosylated

Muriel C. F. van Teeseling^{1*†}, Daniel Maresch², Cornelia B. Rath³, Rudolf Figl², Friedrich Altmann², Mike S. M. Jetten¹, Paul Messner³, Christina Schäffer³ and Laura van Niftrik^{1*}

OPEN ACCESS

Edited by:

Martin G. Klotz,
Queens College of The City University
of New York, USA

Reviewed by:

Sonja-Verena Albers,
University of Freiburg, Germany
Reinhard Rachel,
University of Regensburg, Germany

*Correspondence:

Muriel C. F. van Teeseling
murielvanteeseling@gmail.com
Laura van Niftrik
l.vanniftrik@science.ru.nl

†Present address:

Muriel C. F. van Teeseling,
Department of Molecular Biology
and Laboratory for Molecular Infection
Medicine Sweden, Umeå Centre
for Microbial Research, Umeå,
Sweden

Specialty section:

This article was submitted to
Evolutionary and Genomic
Microbiology,
a section of the journal
Frontiers in Microbiology

Received: 11 June 2016

Accepted: 13 October 2016

Published: 01 November 2016

Citation:

van Teeseling MCF, Maresch D,
Rath CB, Figl R, Altmann F,
Jetten MSM, Messner P, Schäffer C
and van Niftrik L (2016) The S-Layer
Protein of the Anammox Bacterium
Kuenenia stuttgartiensis Is Heavily
O-Glycosylated.
Front. Microbiol. 7:1721.
doi: 10.3389/fmicb.2016.01721

¹ Department of Microbiology, Institute for Water and Wetland Research, Faculty of Science, Radboud University, Nijmegen, Netherlands, ² Division of Biochemistry, Department of Chemistry, University of Natural Resources and Life Sciences, Vienna, Austria, ³ NanoGlycobiology Unit, Department of NanoBiotechnology, University of Natural Resources and Life Sciences, Vienna, Austria

Anaerobic ammonium oxidation (anammox) bacteria are a distinct group of Planctomycetes that are characterized by their unique ability to perform anammox with nitrite to dinitrogen gas in a specialized organelle. The cell of anammox bacteria comprises three membrane-bound compartments and is surrounded by a two-dimensional crystalline S-layer representing the direct interaction zone of anammox bacteria with the environment. Previous results from studies with the model anammox organism *Kuenenia stuttgartiensis* suggested that the protein monomers building the S-layer lattice are glycosylated. In the present study, we focussed on the characterization of the S-layer protein glycosylation in order to increase our knowledge on the cell surface characteristics of anammox bacteria. Mass spectrometry (MS) analysis showed an O-glycan attached to 13 sites distributed over the entire 1591-amino acid S-layer protein. This glycan is composed of six monosaccharide residues, of which five are *N*-acetylhexosamine (HexNAc) residues. Four of these HexNAc residues have been identified as GalNAc. The sixth monosaccharide in the glycan is a putative dimethylated deoxyhexose. Two of the HexNAc residues were also found to contain a methyl group, thereby leading to an extensive degree of methylation of the glycan. This study presents the first characterization of a glycoprotein in a planctomycete and shows that the S-layer protein Kustd1514 of *K. stuttgartiensis* is heavily glycosylated with an O-linked oligosaccharide which is additionally modified by methylation. S-layer glycosylation clearly contributes to the diversification of the *K. stuttgartiensis* cell surface and can be expected to influence the interaction of the bacterium with other cells or abiotic surfaces.

Keywords: anammox bacteria, *Kuenenia stuttgartiensis*, S-layer, glycoprotein, O-glycan, methylation

INTRODUCTION

From early on in the study of Planctomycetes, their cell biology has been a topic that has sparked much interest (Fuerst and Webb, 1991; Fuerst, 1995; Lindsay et al., 1997, 2001). First thought to share a special evolutionary link with eukaryotes (Fuerst, 1995; Devos and Reynaud, 2010; Forterre and Gribaldo, 2010; Fuerst and Sagulenko, 2012), Planctomycetes are now emerging

as a special case of Gram-negative bacteria (Speth et al., 2012; Devos, 2014a,b; Jeske et al., 2015; van Teeseling et al., 2015) harboring at least two membrane-enclosed compartments of which the innermost is often characterized by a curved membrane. The width of the periplasmic space in many species varies over the cell volume due to the complex membrane invaginations of the cytoplasmic membrane.

A special case within the Planctomycetes are the anammox bacteria which perform anaerobic oxidation of ammonium with nitrite to dinitrogen gas (Kartal et al., 2011b). Anammox bacteria are present in marine environments, freshwater and soil (Schmid et al., 2007; Dale et al., 2009; Humbert et al., 2010; Zhu et al., 2013; Sonnighand et al., 2014) where they contribute significantly to the loss of fixed nitrogen. They are also applied in sustainable nitrogen removal systems worldwide (Kartal et al., 2010). Both in nature and in laboratory settings they often occur in clusters in which the cells are attached to other anammox cells and cells of other species (Woebken et al., 2007; Russ et al., 2014). Anammox bacteria can also attach to abiotic surfaces as is exemplified by the common occurrence of biofilms in anammox enrichment bioreactors (Botchkova et al., 2015). Since so far anammox bacteria cannot be grown in pure culture, all anammox species officially have a “*Candidatus*” status. The anammox cell plan comprises a third membrane-enclosed compartment called anammoxosome (Lindsay et al., 2001). This prokaryotic organelle is the location of the anammox reaction that supports the energy for growth of these bacteria (Neumann et al., 2014). In contrast to other planctomycetes, it is the membrane of the anammoxosome instead of the cytoplasmic membrane that is curved. In this case the membrane curvature is hypothesized to provide an enlarged surface area for the many membrane-associated proteins involved in the anammox reaction (van Niftrik et al., 2004; van Teeseling et al., 2013).

The cell envelope of Planctomycetes has been an object of many studies. Early studies (in non-anammox Planctomycetes) reported the almost ubiquitous macromolecule peptidoglycan to be absent and proteinaceous cell walls to be present instead (König et al., 1984; Liesack et al., 1986; Cayrou et al., 2010). Recently, it was discovered that both non-anammox (Jeske et al., 2015) and anammox (van Teeseling et al., 2015) Planctomycetes do have a peptidoglycan cell wall. In addition, the model species “*Candidatus Kuenenia stuttgartiensis*” (referred to as *K. stuttgartiensis* throughout the manuscript) was found to have a proteinaceous two-dimensional crystalline surface (S-) layer (van Teeseling et al., 2014). S-layers have been found in almost all phylogenetic branches of Gram-positive and Gram-negative Bacteria as well as in Archaea (Fagan and Fairweather, 2014), but this was the first report in a cultured planctomycete. It is generally assumed that S-layers provide a selection advantage to the cells, by one or several of the reported functions: osmoprotection (Engelhardt, 2007b), maintenance of the cell shape and integrity (Engelhardt, 2007a; Klingl et al., 2011), protection against predation (Tara et al., 2009; Chanyi et al., 2013) and attachment of exoenzymes (Egelseer et al., 1995). S-layers are formed by the intrinsic self-assembly capability of the constituting S-layer (glyco)protein monomers. Covalently linked glycans are often found in S-layers and these glycans are

highly diverse in terms of composition and structure (Messner et al., 2013). The *K. stuttgartiensis* S-layer is composed of many copies of the modified protein Kustd1514 that has an apparent molecular mass of 250 kDa and also occurs in unmodified form (160 kDa), albeit to a lesser extent.

Since the S-layer is the outermost cell envelope layer and therefore, the structure that is in contact with the outside environment it is expected to have an important function for the cells. This hypothesis is strengthened by the observation that *K. stuttgartiensis* cells have not lost their S-layer during prolonged culturing under laboratory conditions – even though this is a frequent observation for other S-layer bearing bacteria (Sleytr and Messner, 1983). Because of the lack of a genetic system in anammox bacteria, it was not possible to test the importance of the S-layer via a knock-out mutant. In this study, we set out to characterize this S-layer in more detail, focusing on the modification of the S-layer protein. Previously, the detection of the 160-kDa S-layer protein with the carbohydrate-specific periodic acid Schiff (PAS), stain migrating at an apparent molecular weight of ~250 kDa, indicated this protein to be glycosylated (van Teeseling et al., 2014). In this study, we performed a detailed mass spectrometry (MS) analysis to find out how the glycans are attached to the S-layer protein, which sugars constitute the glycan and if and how these sugars are further modified.

MATERIALS AND METHODS

K. stuttgartiensis Enrichment Culture

Free-living planktonic *K. stuttgartiensis* cells were grown in an enrichment culture (~95% *K. stuttgartiensis*) in a membrane bioreactor as described previously (Kartal et al., 2011a).

Preparation of *K. stuttgartiensis* S-Layer Glycoproteins

The S-layer was enriched from *K. stuttgartiensis* cells concentrated in their original growth medium (van de Graaf et al., 1995) which were frozen at -20°C. Thawed cells were resuspended in 20 mM potassium phosphate buffer pH 7 with 750 mM 6-amino caproic acid, and broken in a French Press (three passages at 138 MPa). The membrane fraction, which contains the S-layer as one of the most abundant proteins, was collected after ultracentrifugation (184000 g, 60 min). This enriched S-layer protein sample was washed three times in the above-mentioned buffer and stored until further use.

PNGaseF Treatment of S-Layer Protein

To release putative N-glycans, S-layers, enriched as described before (van Teeseling et al., 2014), were incubated with peptide-N-glycosidase F (PNGaseF; ~0,25 units of PNGaseF per µg of enriched S-layer protein) at 37°C for 10 h in 20 mM potassium phosphate buffer pH 7. As a negative control, enriched S-layer protein was incubated without PNGaseF. After incubation, the samples were analyzed via SDS-PAGE on 8% slab gels using Laemmli running buffer (Laemmli, 1970) followed by staining with Coomassie Brilliant Blue G250.

MS/MS Analysis of S-Layer Glycopeptides

MS/MS was performed on trypically digested S-layer glycoprotein bands excised from an SDS-PAGE gel to which enriched S-layers (described above) were applied following the protocol as described before (Kolarich et al., 2012). In brief, bands were destained, S-alkylated and digested with sequencing grade trypsin (Promega, Vienna, Austria). The peptide mixture was analyzed using a Dionex Ultimate 3000 system directly linked to a QTOF instrument (maXis 4G, Bruker) equipped with the standard ESI source in the positive ion, data-dependent mode. MS-scans were recorded (range: 150–2200 m/z, spectra rate: 1 Hz) and the six highest peaks were selected for fragmentation. Instrument calibration was performed using an ESI calibration mixture (Agilent). For separation of the peptides, a Thermo BioBasic C18 column (5 µm particle size, 150 mm × 0.36 mm) was used. A gradient from 97% solvent A (65 mM ammonium formate) and 3% solvent B (100% acetonitrile) to 32% solvent B in 45 min was applied at a flow rate of 6 µl/min. Analysis data was converted to XML files and evaluated against the target sequence using X! Tandem¹ with the following settings: reversed sequences no; check parent ions for charges 1, 2, and 3 yes; models found with peptide log e lower -1 and proteins log e lower -1; residue modifications; oxidation on M, W and deamidation of N, Q; isotope error was considered; fragment type was set to monoisotopic; refinement was used with standard parameters; fragment mass error of 0.1 Da and ± 7 ppm parent mass error; fragment types b and y ions; maximum parent ion charge of 4; missed cleavage sites allowed was set to 2; semi-cleavage yes. The MS² trace was manually screened for ions of tryptic peptides derived by complete loss of sugars from the parent glycopeptide.

RP-HPLC Detection of Monosaccharide Components of the S-Layer Glycan

To determine the monosaccharide composition of the glycan attached to the S-layer glycoprotein, S-layer glycoprotein bands were excised from SDS-PAGE gels, destained and incubated with pepsin (Sigma-Aldrich, P6887) in 5% formic acid. Extracted material was dried, resuspended in 4 M trifluoroacetic acid and hydrolyzed at 100°C for 4 h. The resulting monosaccharides were labeled with 2-aminobenzoic acid (Anumula, 1994) and analyzed by RP-HPLC using a volatile buffer system (Windwarder et al., 2016).

RESULTS

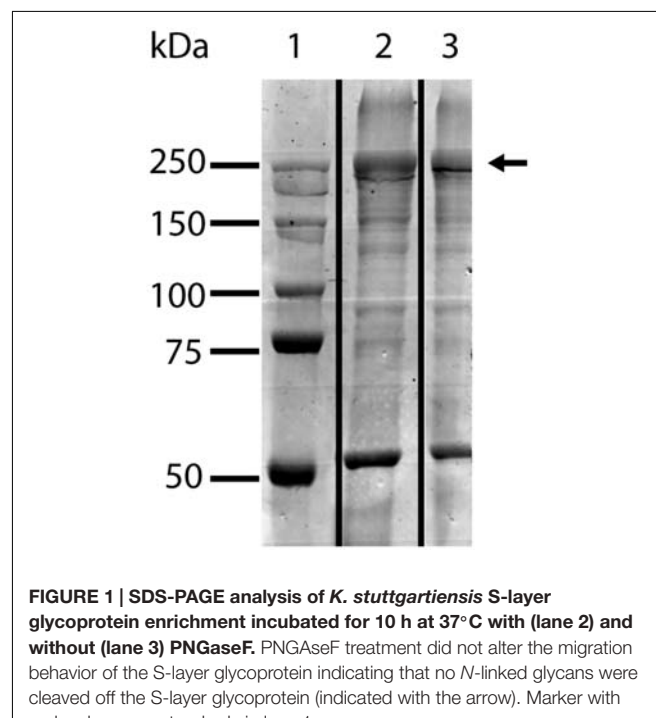
PNGaseF Treatment of *K. stuttgartiensis* S-Layer Glycoprotein

Previous results suggested that the S-layer protein Kustd1514 is a glycoprotein, since the carbohydrate-specific PAS stain colored the Kustd1514 band at approximately 250 kDa strongly (van Teeseling et al., 2014). To verify these results and to

test if the S-layer glycans were linked to the protein via an N-glycosidic bond, the enriched S-layer glycoprotein was treated with PNGaseF. This enzyme specifically releases N-linked glycans from the protein by cleaving the amide linkage between asparagine and oligosaccharides with a chitobiose core. SDS-PAGE demonstrated that incubation with PNGaseF did not cleave the glycoprotein, since the pattern on an SDS gel was identical to that of the untreated sample (Figure 1). This result indicated that, provided the S-layer protein is indeed a glycoprotein, the glycan is most probably O-glycosidically linked to the protein.

MS/MS Analysis of Tryptic (glyco)peptides from the S-Layer Glycoprotein Kustd1514

The ~250-kDa band that was shown before to represent modified Kustd1514 (van Teeseling et al., 2014) was excised from an SDS-gel, digested with trypsin and subjected to mass spectrometric analysis. ESI-MS/MS spectra of mammalian N- and O-glycoproteins are often characterized by the occurrence of a peak for the peptide ion plus one HexNAc residue ("Y₁ ion") (Irungu et al., 2008). Likewise, oxonium ions of HexNAc and oligomers are usually found. However, these strategies were not so suitable for this sample because no prior knowledge was present on the glycan composition. Indeed these strategies did not identify signals belonging to glycopeptides. However, a signal was noticed where a double peak with a 14-Da mass difference was seen. This could indicate O-methylation of a glycan. The base peak of the fragment spectrum had the mass of the doubly charged peptide LGTQATSALPLIALTK and in



¹www.thegpm.org/tandem/

fact the spectrum contained a series of y and b fragments confirming the identity of this peptide (**Figure 2**). Notably, this Kustd1514 peptide does not contain any Asn residue and hence the modification can be designated as an O-glycan, confirming the PNGaseF results. The glycan found on this peptide gave rise to a mass increment of 1203.507 Da, which could not be readily explained in terms of plain sugar units. However, the fragment at m/z 908.029 was followed by two more fragments spaced by m/z 101.54 (=203.07/2) as is typical of HexNAc residues. The gap to the naked peptide mass at m/z 799.48 amounted to a mass indicative of an O-methylated HexNAc. The picture was completed by ions from the non-reducing end of the sugar moiety (B-series) starting with m/z = 407.17, which comprises two HexNAc units. This B₂ ion is then elongated either by m/z 203.07 (=HexNAc) or by a residue with m/z 174.09, which could be a di-methylated deoxyhexose or –even more exceptional- a trimethylated pentose that sits on the terminal or penultimate HexNAc of the non-reducing end. The parent ion of this glycopeptide was accompanied by a peak that was larger by m/z 4.67 (=14.02/3 Da), which indicates an additional methyl group. The MS/MS spectrum, which because of the selected window size comprises fragments of both these precursors, indicated that this additional methyl group is attached to the terminal HexNAc disaccharide. Together with the monosaccharide analysis (described below), which identified the HexNAc component as a GalNAc, the model shown in **Figure 3** was devised. A survey of the elution region of this O-glycopeptide indicated it as being the dominant, if not only, glycoform of Kustd1514.

RP-HPLC Detection of Monosaccharide Components of S-Layer Glycoprotein

Since there is no mass difference between sugar epimers, MS cannot distinguish between different HexNAc or dHex sugars. Therefore, we analyzed the glycopeptides used for MS analysis as 2-aminobenzoic acid derivatives with a volatile buffer system for RP-HPLC that allowed verifying the nature of peaks by MS (Windwarder et al., 2016). Three major peaks were observed. The largest peak was identified as glucose, which most likely was a contamination introduced with the pepsin. Another peak with the mass of a HexNH₂ exactly eluted like GalNH₂. The third peak did not co-elute with any of the available standards and had the mass of a mono-methylated HexNAc. No peak with the mass accounting for the 174 Da component in the MS/MS spectra could be found in the time window considered.

MS/MS Analysis Showed Glycosylation Sites at the S-Layer Protein

Further inspection of the MS/MS data revealed a total of ten peptides carrying the described O-glycan (**Figure 3**). One of these peptides carried two copies of the glycan, while another peptide was found to contain three copies of the glycan. Thus, a total of 13 different sites at the S-layer protein was identified that carry this O-glycan. The majority of the O-glycans was attached to the N-terminal half of the 1576-amino acid protein and only

two glycans were found to be attached to the C-terminal half (**Figure 4**).

DISCUSSION

The cell envelope has been a crucial structure in interpreting the controversial planctomycetal cell plan. Only recently peptidoglycan was revealed in several planctomycetes (Jeske et al., 2015; van Teeseling et al., 2015) and a proteinaceous S-layer was described in the anammox bacterium *K. stuttgartiensis* (van Teeseling et al., 2014). As at the time of the discovery of the S-layer, the peptidoglycan layer in these bacteria had not yet been found, it was hypothesized that the S-layer provided integrity and strength to the anammox cells (van Teeseling et al., 2014). Now it is known that the S-layer is not the only cell wall component and even though it cannot be excluded that the S-layer is still necessary in providing additional strength and integrity as an exoskeleton (as suggested by Engelhardt, 2007a), it is also well possible that the S-layer has a different function for *K. stuttgartiensis*. By describing an O-glycan that is present in the cell envelope of the anammox bacterium *K. stuttgartiensis*, the present study adds to a more in-depth knowledge of planctomycetal cell envelopes and shows that glycoproteins can make up an important part of these structures.

The O-glycan described in this study was found attached to the *K. stuttgartiensis* S-layer protein Kustd1514 at thirteen different sites on ten different peptides. With the methods used it was not possible to identify at which amino acids within these peptides the glycans were attached. Knowing that the glycan is an O-glycan, we searched for serine and threonine residues in these peptide sequences, since the glycans are expected to be bound to these residues. The identified peptides all harbor a serine and all but one contain threonine residues. Therefore, we can conclude that the glycan at least in multiple of the cases attaches to the serine residue. However, not all glycans can bind to a serine, since the peptide that carries the triple glycosylation has only one serine and therefore two of the three glycans can be assumed to be bound to a threonine. It seems most likely that the glycan is always attached to the protein via an O-linkage, even though some asparagine residues were observed in the glycopeptides. This also fits with previous findings of bacterial S-layer proteins that are exclusively glycosylated via O-linkages, even though some other glycoproteins in Bacteria and S-layer glycoproteins in Archaea can show N-glycosylation (Ristl et al., 2011; Jarrell et al., 2014).

Glycosylation sites are often characterized by a specific sequence that is recognized by the enzyme that couples the glycan to the protein, either as an entire glycan coupled via an O-oligosaccharyltransferase (O-OTase) or monosaccharide by monosaccharide in an O-OTase independent pathway (Iwashiki et al., 2013). Since the glycopeptides that were identified with MS analysis were rather long and only one glycoprotein was analyzed it is difficult to point to a recognition sequence for O-glycosylation in *K. stuttgartiensis*. However, analysis of the glycopeptides showed seventeen potential glycosylation sites where the serine or threonine is preceded by a glycine (**Figure 4**).

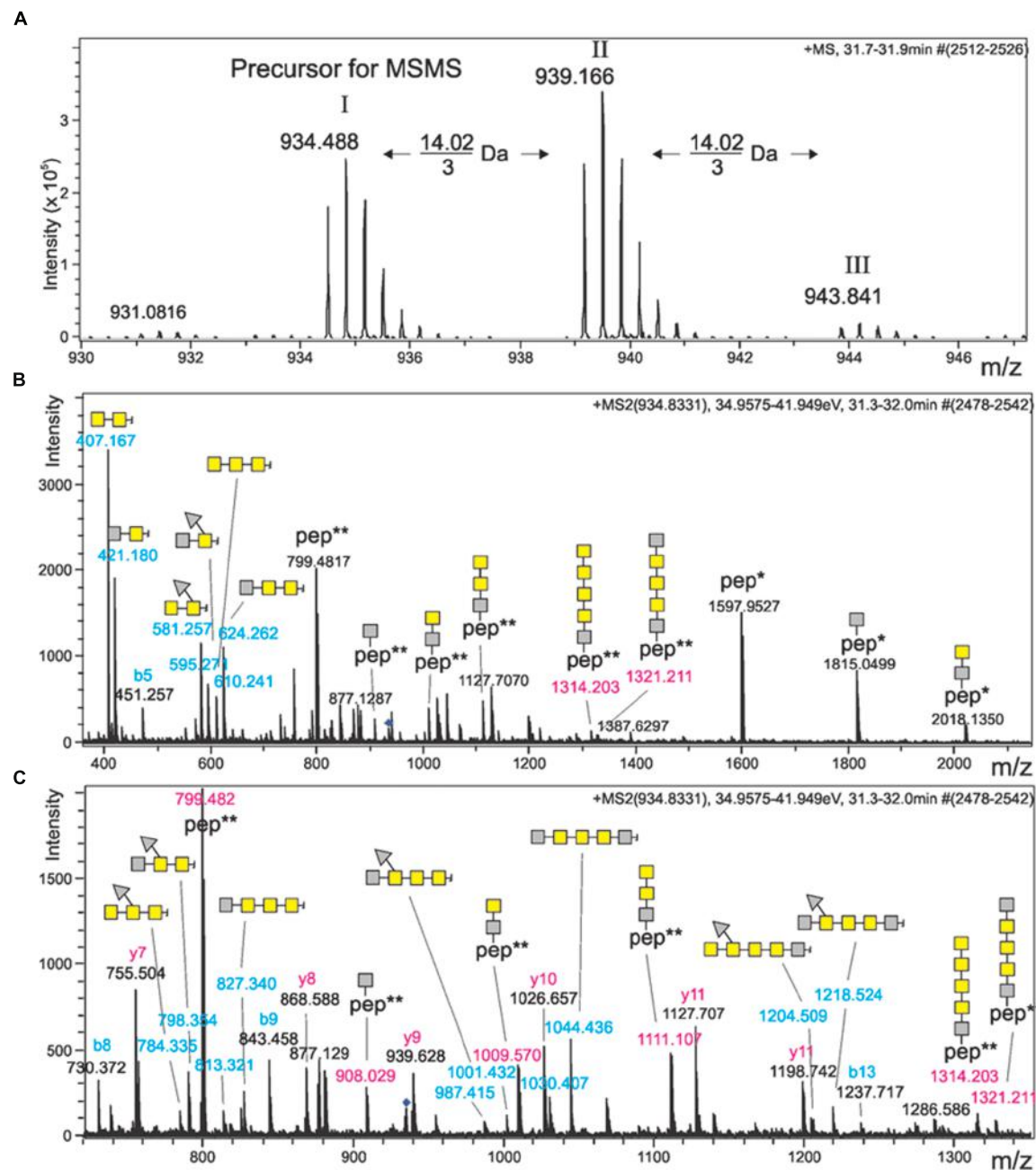


FIGURE 2 | Mass spectrometric analysis of the *K. stuttgartiensis* glycopeptide prepared in this study. **(A)** Shows the sum spectrum of the triply charged ion of glycopeptide LGTQATSALPLIALTK, which comes in three versions spaced by 14.02/3 Da. **(B,C)** Depict the same MS/MS spectrum of compound I with different x-axis. Note that the precursor mass selection window was chosen large enough to co-select peak II. Mass values printed in blue depict B-ions of the non-reducing end of the glycan. Glycopeptide masses (Y-ions) are written in red, whereas the peptide-only fragment masses are given in black. Yellow squares denote N-acetylgalactosamine residues, while gray squares stand for a methylated HexNAc. Gray triangles represent di-methylated deoxyhexose. * and ** indicate the charge state of peptide ions.

Since in each glycopeptide the sequence GT/SX (in which X is variable) is present at least once (and at least twice in the peptide carrying two glycans and at least three times in the peptide carrying three glycans), it seems probable that GT/SX is the recognition sequence. Since this sequence is also present

on multiple sites in the S-layer protein outside of the identified glycopeptides, additional clues are probably present that steer the glycosylation toward the sequences inside the glycopeptides. In some bacteria, the same (O-)glycan can be coupled to several (often cell envelope-associated or excreted) proteins (Nothaft and

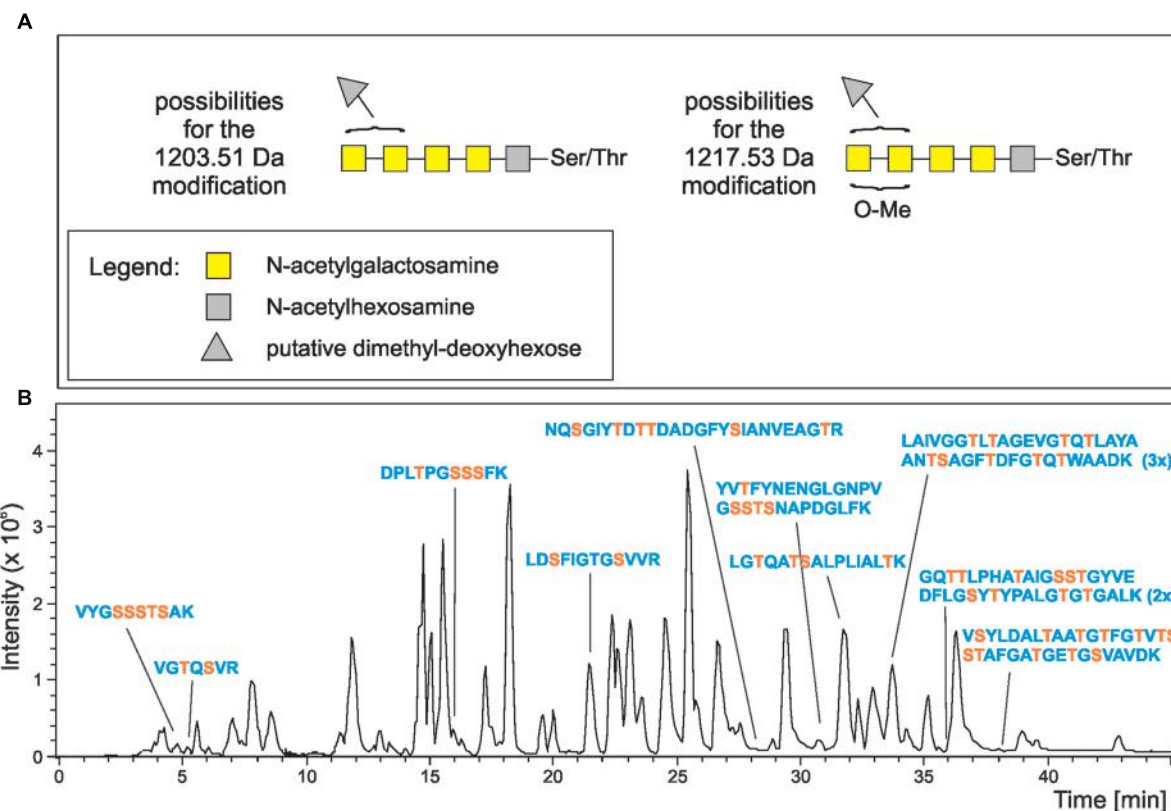


FIGURE 3 | Structure model of the *K. stuttgartiensis* S-layer glycoprotein O-glycan and its occurrence. (A) Summarizes our current view of the O-glycan on the Kustd1514 S-layer glycoprotein. As the exact location of the 174-Da unit and the methyl group are not known, several isomeric structures are possible. The brackets indicate the possible locations of the methyl group (O-Me) and the 174-Da component (gray triangle). Again, yellow squares denote N-acetylgalactosamine residues, while gray squares stand for a methylated HexNAc. **(B)** Shows the base peak ion chromatogram of the tryptic digest of *K. stuttgartiensis* S-layer glycoprotein. The SDS-PAGE band of the protein Kustd1514 was S-alkylated, digested with trypsin and subjected to reversed-phase HPLC with mass spectrometric detection. Peaks of peptides found to carry one or more of the O-glycan units found on LGTQATSALPIALI^{TK} are designated. Serine and threonine residues are depicted in orange.

Szymanski, 2010; Posch et al., 2011; Iwashkiw et al., 2013) and it remains to be investigated if the described glycan is also present at other proteins of *K. stuttgartiensis*.

Since almost no unglycosylated variants of the glycopeptides were found, it seems that most of the thirteen identified glycosylation sites are occupied by glycans in one and the same mature glycoprotein. Therefore, it can be concluded that the amount of glycosylation is rather exceptional for Bacteria. Another indication for a high degree of glycosylation of the S-layer protein is the large difference between the apparent molecular mass of the glycosylated (250 kDa) and native protein (160 kDa). The nominal mass of all glycans described in this study (~1.2 kDa in case of full glycosylation of the thirteen identified sites) cannot explain this difference. However, glycosylation often leads to pronounced, unexpected shifts in apparent molecular mass (Magnelli et al., 2011), as it affects the binding of SDS. Furthermore, O-glycosylation sites tend to be located in more rigid regions of a protein, which leads to inappropriate calibration with globular proteins (Léonard et al., 2005, 2010). In Bacteria, the number of glycosylation sites per protein is often below 10 (Iwashkiw et al., 2013) and most of the known S-layer proteins

have been described to have two to four glycosylation sites per S-layer protein (Ristl et al., 2011). In archaeal S-layers, a higher amount of glycosylation sites has been described. In the case of the N-glycan of the archaeon *Sulfolobus acidocaldarius* S-layer protein, an exceptionally high number of 45 potential glycosylation sites has been described, of which nine have been experimentally verified to carry a glycan (Peyfoon et al., 2010).

The O-glycan described in this study consists of six monosaccharides and is shorter than most bacterial S-layer glycans, which can contain up to 150 monosaccharides (Messner et al., 2008). Almost all O-glycans coupled to bacterial S-layers contain a repeating unit that is linked to the protein via a core oligosaccharide (Messner et al., 2008; Ristl et al., 2011; Fagan and Fairweather, 2014), with the so far only exception provided by the O-linked oligosaccharide decorating the S-layer proteins of *Tannerella forsythia* (Posch et al., 2011). The *K. stuttgartiensis* S-layer O-glycan has no repeating units and, thus, shares its S-layer glycan building plan with *T. forsythia*. The presence of methyl groups in the *K. stuttgartiensis* S-layer is in itself not exceptional, since methylation has been described before for

| | |
|------|--|
| ↓ | |
| 1 | MKRPGLNLKGNWLSMAGVLFLMLALVMVASNAKAATGSFDRDHYLPQLG |
| 51 | TSDYDRAWIMVEDSTATGTTISVTQALTSGESATYTLVGGSSTAFTTHK |
| 101 | GQTTLPHATAIGSSTGYVEDFLGSYTYPALGTGTGALK**LITGGLGSSAPG |
| 151 | NAANGTDGVLKVNNSDTLALVYSGATLDTASVSIIGANDSTIEITTASPW |
| 201 | GTSVDTGVNVEDATANVKITVVDPNVNLNPNLKEVIGLQDGFTTGLASAG |
| 251 | SSRVRVQVIDQDSATGDLTGATASNIILVETGKNTGSFVATGKVY GSSS |
| 301 | TSAKSNLRLGTTSAFANGYDGSAITLGGPTGPSVTQILEVTADKLAI |
| 351 | VGGTLTAGEVGTQTLAYAANTSAGFTDFGTQTAADK***VVVGIRGTNDEVS |
| 401 | LFGNPTSNTSAYLPSSTRIFKLIDGANYCLVKITGSVGSTTATLSNGTYG |
| 451 | VETGGSSAGSITVTLDAFVLAGARSGDSVK VSYLDALTAATGTFGTVTSS |
| 501 | TAFGATGETGSVAVDKTSVDINDFFAITVVDGNLNTSSTARGSVASGDWN |
| 551 | GTTTNSRGDRLKVAGYSNSSFVIDLQHQDGSRV GQTQSVRISSTDGSLI W |
| 601 | VPNSLSDSTYGFDRDPLTP GSSSFK LGTQATSALPLIALTKGNSTSAQSTL |
| 651 | SSANANSFVATTDAVAGTVEISPDTGTHWVAVPITETGINSSTFVGTLIGFD |
| 701 | FTAARVTTDTTLTRTTAFSDSTDYTTITFANSEFNSTNR LDSFIGTGSV |
| 751 | RVRDDFSQEFAQEVVSVAGSTMVTKLASSTSFTPYKTIQVIGNDMTTAR |
| 801 | EDTLSNGAKVFRIGGFFGATYRIRYNDAKDADGNYKAGDTLAATASDVGF |
| 851 | QTYDGELESTNVSGTIGPNQYVVVTLVDEDLNTSTSSKQTTEPDRTESGT |
| 901 | RYVTFYNEGLGNPVGSSTSNA PDGLFKNGFTAKVLYASKLSNVLSSVD |
| 951 | QSSNTIDFKLEETAVNSGTFKGSFQLSSSSSTLNSSDRLQVSSGDSIYVH |
| 1001 | YNDSAPSATAEDNSTNYRVVGPLSIELSIGSLLLSKAKAYLSGDTVVVSVV |
| 1051 | DDDQNTTSGQDTLTDKLKIEGSNYSTGGALTLDLVESGNTSGTFLATFTT |
| 1101 | GTETVETSANLGKVKQAEGGVTVTYTDSSPSNTTVTETLSFGSYDATIE |
| 1151 | FNADSYGLGTYAIVTLADAERNTSHTGTETLLDDVFIQTSSVNSTMRLV |
| 1201 | ETGNDTGTGVGSILVTSSGATTEFNQIQGAEGE |
| 1251 | LT |
| 1301 | TVTDTAAITAATVTPSPTPTPGVTPPGITPTPGLPTPSLIPGLGSVEGF |
| 1351 | VTDAATG DGIEGATVR NQSGIYTD TTADGFYSIANVEA GTR FTAVALG |
| 1401 | YVPSAPTAIVVTAGGTTNLDFA |
| 1451 | LVASVQGTPITPTPGLPTPSLIPGLGSVEGF |
| 1501 | Y |
| 1551 | DN |
| | ECPAQGVVKRKLTSAKKIKVTPASQKTDRTGQATFTVKAKK |
| | NKGKANVKFGVKGVKTPKVNVSLSK |

FIGURE 4 | Amino acid sequence of the S-layer glycoprotein Kustd1514 with glycopeptides detected via MS in bold and putative glycosylation recognition sites in these peptides in red. The peptide followed by ** was found with two glycans attached, the peptide followed by *** was carrying three glycans. The putative amino acid cleavage site of the signal peptidase is indicated with an arrow. The blank space in line 601 is inserted to indicate that these two glycopeptides on both side of the blank space have both been identified.

S-layer glycans in both Bacteria (Schäffer et al., 1999, 2002; Messner et al., 2008; Posch et al., 2011) and Archaea (Paul and Wieland, 1987; Kärcher et al., 1993; Magidovich et al., 2010), as well as in Eukaryotes (Staudacher, 2012). With up to five methyl groups in six monosaccharides, the degree of methylation of the *K. stuttgartiensis* S-layer glycan is however, higher than has been

described for bacterial S-layer glycans. In most other bacterial S-layer glycans methylation has thus far only been described for the terminal sugar residue at the non-reducing end (Messner et al., 2008). In the glycan described here at least one of the methyl groups is present at another site, being the reducing-end sugar residue (Figure 3).

The specific identity of the methylated HexNAc could not be clarified via monosaccharide analysis since no methylated HexNAc standards were included in the analysis. Since, however, one of the two methylated HexNac residues was found in an unmethylated state as well (**Figures 2B,C**) and no other unmethylated HexNAcs were found other than GalNAc, it seems most probable that this HexNAc is a GalNAc which is methylated in some cases. Also the 174-Da component could not be identified with the RP-HPLC approach, since no peak was observed that could stem from this component. Maybe the peak stemming from this component eluted outside of the observed region or the amount was too low to be detected. At this point it remains to be elucidated if the 174-Da component is indeed a dimethylated deoxyhexose, a trimethylated pentose or even something else. Dimethylated deoxyhexose, however has been found in multiple bacteria before (Takaichi et al., 2001; Schorey and Sweet, 2008).

An intriguing question concerning the glycosylation of Kustd1514 is which effect on, and which function for, the cells these glycans have. Such an extensive glycosylation is expected to have an impact on the physicochemical properties of the S-layer, and thereby the interface of the cell that is seen by the extracellular environment. Indeed, glycosylation was shown to increase the hydration of the S-layer protein in the bacterium *Geobacillus stearothermophilus* (Schuster and Sleytr, 2015). Possibly the glycosylation of Kustd1514 protects the protein from protease degradation, since this was shown in the case of N-glycosylation of S-layer proteins in Archaea (Yurist-Doutsch et al., 2008, 2010; Kaminski et al., 2010) and several bacterial non-S-layer O-glycans (Herrmann et al., 1996). Another described role of protein glycosylation in Bacteria is attachment, for instance to eukaryotic cells (Swanson and Kuo, 1994; Lindenthal and Elsinghorst, 1999) and cellulose (Miron and Forsberg, 1999). Since attachment to other cells and abiotic surfaces is a common characteristic of anammox bacteria it could well be that the glycosylation of the S-layer plays a role in attachment. Since in anammox bacteria no genetic system is present and attempts to grow anammox cells in pure culture have not succeeded up to now, it will be very difficult to test the role of the S-layer glycans.

In summary, this study describes an O-glycan that is linked to the S-layer protein of the anammox bacterium *K. stuttgartiensis*. The O-glycan is composed of six monosaccharide residues, and built up of five HexNAc residues – of which four have been

confirmed to be GalNAc. One of these HexNAcs is always methylated and a second one is methylated in some cases. In addition a putative dimethylated deoxyhexose completes the glycan. Compared to most other structurally elucidated bacterial S-layer glycans, this glycan is shorter, shows an extensive degree of methylation and is linked to many different sites of the protein. This study deepens the understanding of the cell envelope of the anammox Planctomycetes and provides the first description of a planctomycetal glycoprotein.

AUTHOR CONTRIBUTIONS

All listed authors have made substantial, direct and intellectual contribution to the work, and approved it for publication.

FUNDING

MvT and MJ are supported by the European Research Council (ERC232937) and MvT received additional support from EMBO (ALTF1396-2015) and the European Commission via the Marie Curie Actions (Marie Curie Actions LTFCOFUND2013, GA-2013-609409). LvN received support from the Netherlands Organisation for Scientific Research (VENI grant 863.09.009). PM and CS are supported by the Austrian Science Fund FWF (project P24305-B20 to PM and projects P21954-B20 and P24317-B22 to CS). DM and CR are supported by the FWF Doctoral programme BioToP W1224.

ACKNOWLEDGMENTS

Paul Kosma is acknowledged for helpful discussions and Paul Kosma and Andreas Hofinger-Horvath are acknowledged for preliminary NMR measurements. Hans Wessels is acknowledged for LC-MS/MS analysis of glycoprotein bands in an earlier stage of the research. We thank Sonja Zayni for help with a prior monosaccharide analysis, Andrea Scheberl for help with chromatographic purification of S-layer glycopeptides and Eva Bönisch for advice and help with preparing S-layer glycopeptides. Monique van Scherpenzeel is acknowledged for the kind gift of PNGaseF. We thank Joachim Reimann and Christina Ferousi for the *Kuenenia stuttgartiensis* cells.

REFERENCES

- Anumula, K. R. (1994). Quantitative determination of monosaccharides in glycoproteins by high-performance liquid chromatography with highly sensitive fluorescence detection. *Anal. Biochem.* 220, 275–283. doi: 10.1006/abio.1994.1338
- Botchkova, E. A., Plakunov, V. K., and Nozhevnikova, A. N. (2015). Dynamics of biofilm formation on microscopic slides submerged in an anammox bioreactor. *Microbiology* 84, 456–460. doi: 10.1134/S0026261715030029
- Cayrou, C., Raoult, D., and Drancourt, M. (2010). Broad-spectrum racemase antibiotic resistance of Planctomycetes organisms determined by Etest. *J. Antimicrob. Chemother.* 65, 2119–2122. doi: 10.1093/jac/dkq290
- Chanyi, R. M., Ward, C., Pechey, A., and Koval, S. F. (2013). To invade or not to invade: two approaches to a prokaryotic predatory life cycle. *Can. J. Microbiol.* 59, 273–279. doi: 10.1139/cjm-2013-0041
- Dale, O. R., Tobias, C. R., and Song, B. (2009). Biogeographical distribution of diverse anaerobic ammonium oxidizing (anammox) bacteria in Cape Fear River Estuary. *Environ. Microbiol.* 11, 1194–1207. doi: 10.1111/j.1462-2920.2008.01850.x
- Devos, D. P. (2014a). Re-interpretation of the evidence for the PVC cell plan supports a Gram-negative origin. *Antonie Van Leeuwenhoek* 105, 271–274. doi: 10.1007/s10482-013-0087-y
- Devos, D. P. (2014b). PVC bacteria: variation of, but not exception to, the Gram-negative cell plan. *Trends Microbiol.* 22, 14–20. doi: 10.1016/j.tim.2013.10.008

- Devos, D. P., and Reynaud, E. G. (2010). Intermediate steps. *Science* 330, 1187–1188. doi: 10.1126/science.1196720
- Egelseer, E., Schocher, I., Sára, M., and Sleytr, U. B. (1995). The S-layer from *Bacillus stearothermophilus* DSM 2358 functions as an adhesion site for a high-molecular-weight amylase. *J. Bacteriol.* 177, 1444–1451.
- Engelhardt, H. (2007a). Are S-layers exoskeletons? The basic function of protein surface layer revisited. *J. Struct. Biol.* 160, 115–124. doi: 10.1016/j.jsb.2007.08.003
- Engelhardt, H. (2007b). Mechanism of osmoprotection by archaeal S-layers: a theoretical study. *J. Struct. Biol.* 160, 190–199. doi: 10.1016/j.jsb.2007.08.004
- Fagan, R. P., and Fairweather, N. F. (2014). Biogenesis and functions of bacterial S-layers. *Nat. Rev. Microbiol.* 12, 211–222. doi: 10.1038/nrmicro3213
- Forterre, P., and Gribaldo, S. (2010). Bacteria with a eukaryotic touch: a glimpse of ancient evolution? *Proc. Natl. Acad. Sci. U.S.A.* 107, 12739–12740. doi: 10.1073/pnas.1007720107
- Fuerst, J. A. (1995). The planctomycetes: emerging models for microbial ecology, evolution and cell biology. *Microbiology* 141, 1493–1506. doi: 10.1099/13500872-141-7-1493
- Fuerst, J. A., and Sagulenko, E. (2012). Keys to eukaryality: planctomycetes and ancestral evolution of cellular complexity. *Front. Microbiol.* 3:167. doi: 10.3389/fmicb.2012.00167
- Fuerst, J. A., and Webb, R. I. (1991). Membrane-bounded nucleoid in the eubacterium *Gemmata obscuriglobus*. *Proc. Natl. Acad. Sci. U.S.A.* 88, 8184–8188. doi: 10.1073/pnas.88.18.8184
- Herrmann, J. L., O'Gaora, P., Gallagher, A., Thole, J. E., and Young, D. B. (1996). Bacterial glycoproteins: a link between glycosylation and proteolytic cleavage of a 19 kDa antigen from *Mycobacterium tuberculosis*. *EMBO J.* 15, 3547–3554.
- Humbert, S., Tarnawski, S., Fromin, N., Mallet, M.-P., Aragno, M., and Zopfi, J. (2010). Molecular detection of anammox bacteria in terrestrial ecosystems: distribution and diversity. *ISME J.* 4, 450–454. doi: 10.1038/ismej.2009.125
- Irungu, J., Go, E. P., Zhang, Y., Dalpathado, D. S., Liao, H.-X., Haynes, B. F., et al. (2008). Comparison of HPLC/ESI-FTICR MS versus MALDI-TOF/TOF MS for glycopeptide analysis of a highly glycosylated HIV envelope glycoprotein. *J. Am. Soc. Mass Spectrom.* 19, 1209–1220. doi: 10.1016/j.jasms.2008.05.010
- Iwashiki, J. A., Vozza, N. F., Kinsella, R. L., and Feldman, M. F. (2013). Pour some sugar on it: the expanding world of bacterial protein O-linked glycosylation. *Mol. Microbiol.* 89, 14–28. doi: 10.1111/mmi.12265
- Jarrell, K. F., Ding, Y., Meyer, B. H., Albers, S.-V., Kaminski, L., and Eichler, J. (2014). N-linked glycosylation in Archaea: a structural, functional, and genetic analysis. *Microbiol. Mol. Biol. Rev.* 78, 304–341. doi: 10.1128/MMBR.00052-13
- Jeske, O., Schüler, M., Schumann, P., Schneider, A., Boedeker, C., Jogler, M., et al. (2015). Planctomycetes do possess a peptidoglycan cell wall. *Nat. Commun.* 6:7116. doi: 10.1038/ncomms8116
- Kaminski, L., Abu-Qarn, M., Guan, Z., Naparstek, S., Ventura, V. V., Raetz, C. R. H., et al. (2010). AglJ adds the first sugar of the N-linked pentasaccharide decorating the *Haloflexax volcanii* S-layer glycoprotein. *J. Bacteriol.* 192, 5572–5579. doi: 10.1128/JB.00705-10
- Kärcher, U., Schröder, H., Haslinger, E., Allmaier, G., Schreiner, R., Wieland, F., et al. (1993). Primary structure of the heterosaccharide of the surface glycoprotein of *Methanothermus fervidus*. *J. Biol. Chem.* 268, 26821–26826.
- Kartal, B., Geerts, W., and Jetten, M. S. M. (2011a). “Cultivation, detection, and ecophysiology of anaerobic-ammonium-oxidizing bacteria,” in *Methods in Enzymology*, Vol. 486, ed. M. G. Klotz (San Diego, CA: Academic Press), 89–109.
- Kartal, B., Maalcke, W. J., de Almeida, N. M., Cirpus, I., Gloerich, J., Geerts, W., et al. (2011b). Molecular mechanisms of anaerobic ammonium oxidation. *Nature* 479, 127–130. doi: 10.1038/nature10453
- Kartal, B., Kuenen, J. G., and van Loosdrecht, M. C. M. (2010). Sewage treatment with anammox. *Science* 328, 702–703. doi: 10.1126/science.1185941
- Klingl, A., Moissl-Eichinger, C., Wanner, G., Zweck, J., Huber, H., Thomm, M., et al. (2011). Analysis of the surface proteins of *Acidithiobacillus ferrooxidans* strain SP5/1 and the new, pyrite-oxidizing *Acidithiobacillus* isolate HV2/2, and their possible involvement in pyrite oxidation. *Arch. Microbiol.* 193, 867–882. doi: 10.1007/s00203-011-0720-y
- Kolarich, D., Jensen, P. H., Altmann, F., and Packer, N. H. (2012). Determination of site-specific glycan heterogeneity on glycoproteins. *Nat. Protoc.* 7, 1285–1298. doi: 10.1038/nprot.2012.062
- König, E., Schlesner, H., and Hirsch, P. (1984). Cell wall studies on budding bacteria of the Planctomyces-Pasteuria group and on a *Prosthecomicrobium* sp. *Arch. Microbiol.* 138, 200–205. doi: 10.1007/BF00402120
- Laemmli, U. K. (1970). Cleavage of structural proteins during the assembly of the head of bacteriophage T4. *Nature* 15, 680–685. doi: 10.1038/227680a0
- Léonard, R., Petersen, B. O., Himly, M., Kaar, W., Wopfner, N., Kolarich, D., et al. (2005). Two novel types of O-glycans on the mugwort pollen allergen art v 1 and their role in antibody binding. *J. Biol. Chem.* 280, 7932–7940. doi: 10.1074/jbc.M410407200
- Léonard, R., Wopfner, N., Pabst, M., Stadlmann, J., Petersen, B. O., Duus, J. Ø., et al. (2010). A new allergen from Ragweed (*Ambrosia artemisiifolia*) with homology to art v 1 from Mugwort. *J. Biol. Chem.* 285, 27192–27200. doi: 10.1074/jbc.M110.127118
- Liesack, W., König, H., Schlesner, H., and Hirsch, P. (1986). Chemical composition of the peptidoglycan-free cell envelopes of budding bacteria of the *Pirellula/Planctomyces* group. *Arch. Microbiol.* 145, 361–366. doi: 10.1007/BF00470872
- Lindenthal, C., and Elsinghorst, E. A. (1999). Identification of a glycoprotein produced by enterotoxigenic *Escherichia coli*. *Infect. Immun.* 67, 4084–4091.
- Lindsay, M. R., Webb, R. I., and Fuerst, J. A. (1997). Pirellulosomes: a new type of membrane-bounded cell compartment in planctomycete bacteria of the genus *Pirellula*. *Microbiology* 143, 739–748. doi: 10.1099/00221287-143-3-739
- Lindsay, M. R., Webb, R. I., Strous, M., Jetten, M. S. M., Butler, M. K., Forde, R. J., et al. (2001). Cell compartmentalization in planctomycetes: novel types of structural organization for the bacterial cell. *Arch. Microbiol.* 175, 413–429. doi: 10.1007/s002030100280
- Magidovich, H., Yurist-Doutsch, S., Konrad, Z., Ventura, V. V., Dell, A., Hitchen, P. G., et al. (2010). AglP is an S-adenosyl-L-methionine-dependent methyltransferase that participates in the N-glycosylation pathway in *Haloflexax volcanii*. *Mol. Microbiol.* 76, 190–199. doi: 10.1111/j.1365-2958.2010.07090.x
- Magnelli, P. E., Bielik, A. M., and Guthrie, E. P. (2011). Identification and characterization of protein glycosylation using specific endo- and exoglycosidases. *J. Vis. Exp.* 58, 3749. doi: 10.3791/3749
- Messner, P., Schäffer, C., and Kosma, P. (2013). Bacterial cell-envelope glycoconjugates. *Adv. Carbohydr. Chem. Biochem.* 69, 209–272. doi: 10.1016/B978-0-12-408093-5.00006-X
- Messner, P., Steiner, K., Zarschler, K., and Schäffer, C. (2008). S-layer nanoglycobiology of bacteria. *Carbohydr. Res.* 343, 1934–1951. doi: 10.1016/j.carres.2007.12.025
- Miron, J., and Forsberg, C. W. (1999). Characterisation of cellulose-binding proteins that are involved in the adhesion mechanism of *Fibrobacter intestinalis* DR7. *Appl. Microbiol. Biotechnol.* 51, 491–497. doi: 10.1007/s002530051422
- Neumann, S., Wessels, H. J. C. T., Rijpstra, W. I. C., Sinninghe Damsté, J. S., Kartal, B., Jetten, M. S. M., et al. (2014). Isolation and characterization of a prokaryotic cell organelle from the anammox bacterium *Kuenenia stuttgartiensis*. *Mol. Microbiol.* 94, 794–802. doi: 10.1111/mmi.12816
- Nothaft, H., and Szymbanski, C. M. (2010). Protein glycosylation in bacteria: sweeter than ever. *Nat. Rev. Microbiol.* 8, 765–778. doi: 10.1038/nrmicro2383
- Paul, G., and Wieland, F. (1987). Sequence of the halobacterial glycosaminoglycan. *J. Biol. Chem.* 262, 9587–9593.
- Peyfoon, E., Meyer, B., Hitchen, P. G., Panico, M., Morris, H. R., Haslam, S. M., et al. (2010). The S-layer glycoprotein of the crenarchaeote *Sulfolobus acidocaldarius* is glycosylated at multiple sites with chitobiose-linked N-glycans. *Archaea* 2010: 754101. doi: 10.1155/2010/754101
- Posch, G., Pabst, M., Brecker, L., Altmann, F., Messner, P., and Schäffer, C. (2011). Characterization and scope of S-layer protein O-glycosylation in *Tannerella forsythia*. *J. Biol. Chem.* 266, 38714–38724. doi: 10.1074/jbc.M111.284893
- Ristl, R., Steiner, K., Zarschler, K., Zayni, S., Messner, P., and Schäffer, C. (2011). The S-layer glycome- adding to the sugar coat of bacteria. *Int. J. Microbiol.* 2011: 127870. doi: 10.1155/2011/127870
- Russ, L., Speth, D. R., Jetten, M. S. M., den Camp, H. J. M., and Kartal, B. (2014). Interactions between anaerobic ammonium and sulfur-oxidizing bacteria in a laboratory scale model system. *Environ. Microbiol.* 16, 3487–3498. doi: 10.1111/1462-2920.12487
- Schäffer, C., Müller, N., Christian, R., Graninger, M., Wugeditsch, T., Scheberl, A., et al. (1999). Complete glycan structure of the S-layer glycoprotein of *Aneurinibacillus thermaoerophilus* GS4-97. *Glycobiology* 9, 407–414. doi: 10.1093/glycob/9.4.407

- Schäffer, C., Wugeditsch, T., Kählig, H., Scheberl, A., Zayni, S., and Messner, P. (2002). The surface layer (S-layer) glycoprotein of *Geobacillus stearothermophilus* NRS 2004/3a. Analysis of its glycosylation. *J. Biol. Chem.* 277, 6230–6239.
- Schmid, M. C., Risgaard-Petersen, N., van de Vossenberg, J., Kuypers, M. M. M., Lavik, G., Petersen, J., et al. (2007). Anaerobic ammonium-oxidizing bacteria in marine environments: widespread occurrence but low diversity. *Environ. Microbiol.* 9, 1476–1484. doi: 10.1111/j.1462-2920.2007.01266.x
- Schorey, J. S., and Sweet, L. (2008). The mycobacterial glycopeptidolipids: structure, function, and their role in pathogenesis. *Glycobiology* 18, 832–841. doi: 10.1093/glycob/cwn076
- Schuster, B., and Sleytr, U. B. (2015). Relevance of glycosylation of S-layer proteins for cell surface properties. *Acta Biomater.* 19, 149–157. doi: 10.1016/j.actbio.2015.03.020
- Sleytr, U. B., and Messner, P. (1983). Crystalline surface layers on bacteria. *Annu. Rev. Microbiol.* 37, 311–339. doi: 10.1146/annurev.mi.37.100183.001523
- Sonthiphand, P., Hall, M. W., and Neufeld, J. D. (2014). Biogeography of anaerobic ammonia-oxidizing (anammox) bacteria. *Front. Microbiol.* 5:399. doi: 10.3389/fmicb.2014.00399
- Speth, D. R., van Teeseling, M. C. F., and Jetten, M. S. M. (2012). Genomic analysis indicates the presence of an asymmetric bilayer outer membrane in Planctomycetes and Verrucomicrobia. *Front. Microbiol.* 3:304. doi: 10.3389/fmicb.2012.00304
- Staudacher, E. (2012). Methylation- an uncommon modification of glycans. *Biol. Chem.* 393, 675–685. doi: 10.1515/hzs-2012-0132
- Swanson, A. F., and Kuo, C.-C. (1994). Binding of the glycan of the major outer membrane protein of *Chlamydia trachomatis* to HeLa cells. *Infect. Immun.* 62, 24–28.
- Takaichi, S., Maoka, T., and Masamoto, K. (2001). Myxoxanthophyll in *Synechocystis* sp. PCC 6803 is myxol 2'-dimethyl-fucoside, (3R,2'S)-myxol 2'-(2,4-di-O-methyl- α -L-fucoside), not rhamnoside. *Plant. Cell Physiol.* 42, 756–762. doi: 10.1093/pcp/pce098
- Tarao, M., Jezbera, J., and Hahn, M. W. (2009). Involvement of cell surface structures in size-independent grazing resistance of freshwater Actinobacteria. *Appl. Environ. Microbiol.* 75, 4720–4726. doi: 10.1128/AEM.00251-09
- van de Graaf, A. A., Mulder, A., de Bruijn, P., Jetten, M. S. M., Robertson, L. A., and Kuennen, J. G. (1995). Anaerobic oxidation of ammonium is a biologically mediated process. *Appl. Environ. Microbiol.* 61, 1246–1251.
- van Niftrik, L., Fuerst, J. A., Sinnighe Damsté, J. S., Kuenen, J. G., Jetten, M. S. M., and Strous, M. (2004). The anammoxosome: an intracytoplasmic compartment in anammox bacteria. *FEMS Microbiol. Lett.* 233, 7–13. doi: 10.1016/j.femsle.2004.01.044
- van Teeseling, M. C. F., de Almeida, N. M., Klingl, A., Speth, D. R., den Camp, H. J. M., Rachel, R., et al. (2014). A new addition to the cell plan of anammox bacteria: “*Candidatus Kuenenia stuttgartiensis*” has a protein surface layer at the outermost layer of the cell. *J. Bacteriol.* 196, 80–89. doi: 10.1128/JB.00988-13
- van Teeseling, M. C. F., Mesman, R. J., Kuru, E., Espaillat, A., Cava, F., Brun, Y. V., et al. (2015). Anammox planctomycetes have a peptidoglycan cell wall. *Nat. Commun.* 6:6878. doi: 10.1038/ncomms7878
- van Teeseling, M. C. F., Neumann, S., and van Niftrik, L. (2013). The anammoxosome organelle is crucial for the energy metabolism of anaerobic ammonium oxidizing bacteria. *J. Mol. Microbiol. Biotechnol.* 23, 104–117. doi: 10.1159/000346547
- Windwarder, M., Figl, R., Svehla, E., Mócsai, R. T., Faracet, J.-B., Staudacher, E., et al. (2016). “Hypermethylation” of anthranilic acid-labeled sugars confers the selectivity required for liquid chromatography-mass spectrometry. *Anal. Biochem.* 514, 24–31. doi: 10.1016/j.ab.2016.09.008
- Woebken, D., Fuchs, B. M., Kuypers, M. M. M., and Amann, R. (2007). Potential interactions of particle-associated anammox bacteria with bacterial and archaeal partners in the Namibian upwelling system. *Appl. Environ. Microbiol.* 73, 4648–4657. doi: 10.1128/AEM.02774-06
- Yurist-Doutsch, S., Abu-Qarn, M., Battaglia, F., Morris, H. R., Hitchen, P. G., Dell, A., et al. (2008). aglF, aglG, and aglL, novel members of a gene island involved in the N-glycosylation of the *Haloflexax volcanii* S-layer glycoprotein. *Mol. Microbiol.* 69, 1234–1245. doi: 10.1111/j.1365-2958.2008.06352.x
- Yurist-Doutsch, S., Magidovich, H., Ventura, V. V., Hitchen, P. G., Dell, A., and Eichler, J. (2010). N-glycosylation in Archaea: on the coordinated actions of *Haloflexax volcanii* AglF and AglM. *Mol. Microbiol.* 75, 1047–1058. doi: 10.1111/j.1365-2958.2009.07045.x
- Zhu, G., Wang, S., Wang, W., Wang, Y., Zhou, L., Jiang, B., et al. (2013). Hotspots of anaerobic ammonium oxidation at land-freshwater interfaces. *Nat. Geosci.* 6, 103–107. doi: 10.1038/ngeo1683

Conflict of Interest Statement: The authors declare that the research was conducted in the absence of any commercial or financial relationships that could be construed as a potential conflict of interest.

Copyright © 2016 van Teeseling, Maresch, Rath, Figl, Altmann, Jetten, Messner, Schäffer and van Niftrik. This is an open-access article distributed under the terms of the Creative Commons Attribution License (CC BY). The use, distribution or reproduction in other forums is permitted, provided the original author(s) or licensor are credited and that the original publication in this journal is cited, in accordance with accepted academic practice. No use, distribution or reproduction is permitted which does not comply with these terms.



Evolutionary Cell Biology of Division Mode in the Bacterial *Planctomycetes-Verrucomicrobia-Chlamydiae* Superphylum

Elena Rivas-Marín, Inés Canosa and Damien P. Devos *

Centro Andaluz de Biología del Desarrollo, Consejo Superior de Investigaciones Científicas, Junta de Andalucía, Universidad Pablo de Olavide, Seville, Spain

OPEN ACCESS

Edited by:

Boran Kartal,
Max-Planck-Gesellschaft, Germany

Reviewed by:

Christian Jogler,
Deutsche Sammlung von
Mikroorganismen und Zellkulturen,
Germany
Daan R. Speth,
California Institute of Technology, USA

*Correspondence:

Damien P. Devos
damienpddevos@gmail.com

Specialty section:

This article was submitted to
Evolutionary and Genomic
Microbiology,
a section of the journal
Frontiers in Microbiology

Received: 05 September 2016

Accepted: 23 November 2016

Published: 06 December 2016

Citation:

Rivas-Marín E, Canosa I and Devos DP (2016) Evolutionary Cell Biology of Division Mode in the Bacterial *Planctomycetes-Verrucomicrobia-Chlamydiae* Superphylum. *Front. Microbiol.* 7:1964.
doi: 10.3389/fmicb.2016.01964

Bacteria from the *Planctomycetes*, *Verrucomicrobia*, and *Chlamydiae* (PVC) superphylum are exceptions to the otherwise dominant mode of division by binary fission, which is based on the interaction between the FtsZ protein and the peptidoglycan (PG) biosynthesis machinery. Some PVC bacteria are deprived of the FtsZ protein and were also thought to lack PG. How these bacteria divide is still one of the major mysteries of microbiology. The presence of PG has recently been revealed in *Planctomycetes* and *Chlamydiae*, and proteins related to PG synthesis have been shown to be implicated in the division process in *Chlamydiae*, providing important insights into PVC mechanisms of division. Here, we review the historical lack of observation of PG in PVC bacteria, its recent detection in two phyla and its involvement in chlamydial cell division. Based on the detection of PG-related proteins in PVC proteomes, we consider the possible evolution of the diverse division mechanisms in these bacteria. We conclude by summarizing what is known and what remains to be understood about the evolutionary cell biology of PVC division modes.

Keywords: PVC superphylum, peptidoglycan, cell division, budding, ftsZ, dcw cluster

INTRODUCTION

Most bacteria divide by binary fission using a mechanism centered on the interaction between the FtsZ protein and the peptidoglycan (PG) biosynthesis machinery. With limited exceptions, both FtsZ and PG are ubiquitous in bacteria. Amongst those exceptions are the members of the *Planctomycetes*, *Verrucomicrobia*, and *Chlamydiae* (PVC) superphylum, which encompasses these three phyla as well as the *Lentisphaerae* and some uncultured candidate phyla, such as the *Candidatus Omnitrophica* (previously known as OP3; Wagner and Horn, 2006; Fuerst, 2013a; Devos and Ward, 2014) (Figure 1).

The *Chlamydiae* phylum was initially restricted to members of the family *Chlamydiaceae* due to their human pathogenicity, but now includes the families *Parachlamydiaceae*, *Waddliaeae*, *Criblamydiaceae*, and *Simkaniaeae* of the order *Chlamydiales* (Bertelli and Greub, 2013). These newly described families of chlamydia-related bacteria diverged from the *Chlamydiaceae* more than 700 million years ago (Horn et al., 2004). The phyla *Lentisphaerae* and *Verrucomicrobia* form a separate group within the PVC superphylum, with the latter containing the orders *Opitutales*, *Puniceicoccales*, and *Verrucomicrobiales*, amongst others. Within the *Planctomycetes*, three orders

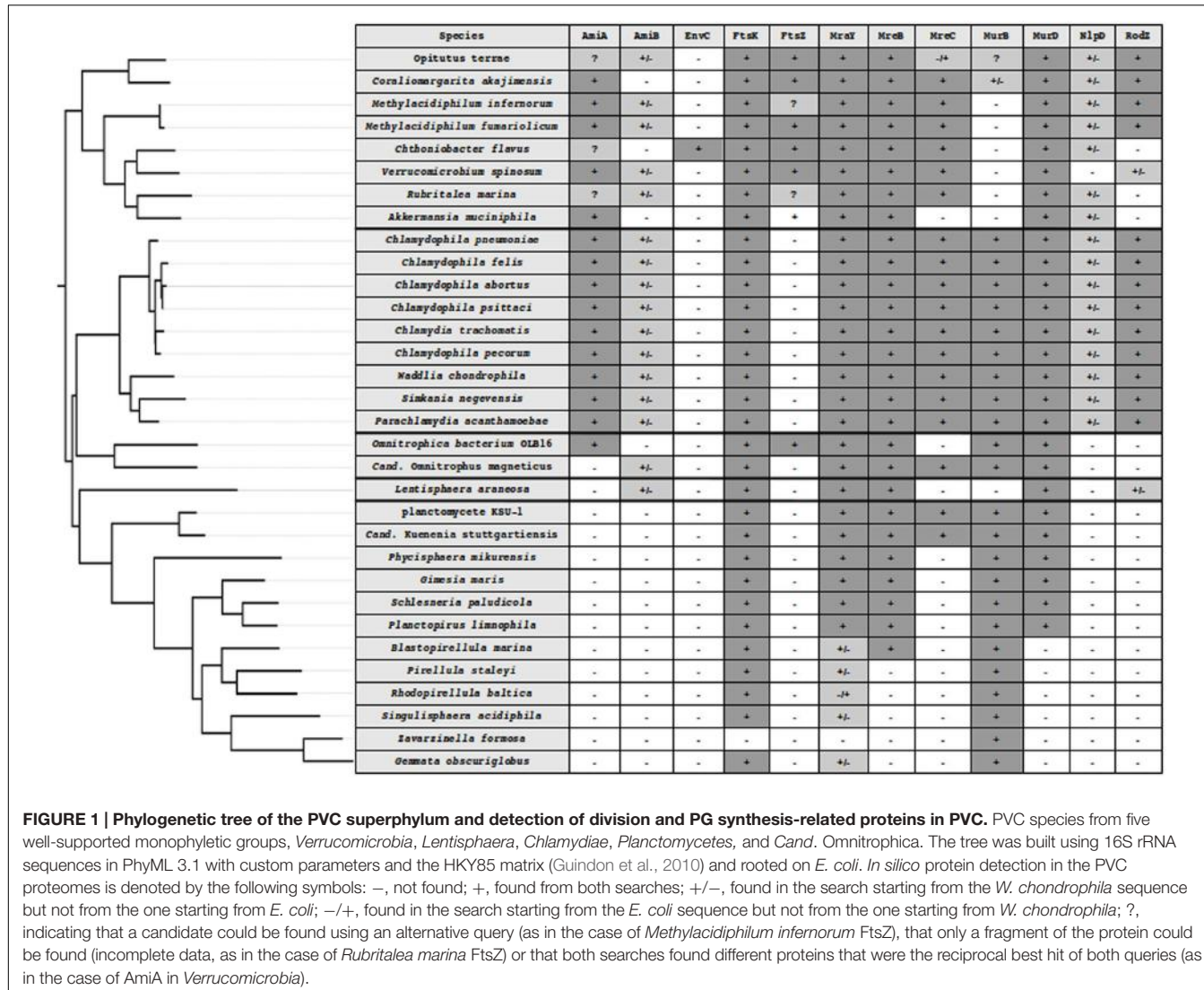


FIGURE 1 | Phylogenetic tree of the PVC superphylum and detection of division and PG synthesis-related proteins in PVC. PVC species from five well-supported monophyletic groups, *Verrucomicrobia*, *Lentisphaera*, *Chlamydiae*, *Planctomycetes*, and *Cand. Omnitrophica*. The tree was built using 16S rRNA sequences in PhyML 3.1 with custom parameters and the HKY85 matrix (Guindon et al., 2010) and rooted on *E. coli*. *In silico* protein detection in the PVC proteomes is denoted by the following symbols: -, not found; +, found from both searches; +/-, found in the search starting from the *W. chondrophila* sequence but not from the one starting from *E. coli*; -/+ found in the search starting from the *E. coli* sequence but not from the one starting from *W. chondrophila*; ?, indicating that a candidate could be found using an alternative query (as in the case of *Methylacidiphilum infernorum* FtsZ), that only a fragment of the protein could be found (incomplete data, as in the case of *Rubritalea marina* FtsZ) or that both searches found different proteins that were the reciprocal best hit of both queries (as in the case of AmiA in *Verrucomicrobia*).

are recognized: *Cand. Brocadiales*, *Phycisphaerales*, and *Planctomycetales*. The *Cand. Brocadiales* is a deep-branching order responsible for anaerobic ammonium oxidation (anammox; van Niftrik, 2013). The *Phycisphaerales* only contain a few species that are still uncultured and for which limited description is available (Fukunaga et al., 2009). The order *Planctomycetales* is formed by the *Gemmata*, *Blastopirellula*, and *Pirellula* genera, amongst others. The *Cand. Omnitrophica* phylum was recently added to the PVC group with scarce information available, including genomic one.

Bacteria belonging to the PVC superphylum are fascinating for their peculiar biology. Their lifestyles range from the free-living soil and aquatic *Planctomycetes*, *Verrucomicrobia*, and *Lentisphaerae*, through the commensal and mutualistic *Verrucomicrobia* and *Lentisphaerae*, to the obligate pathogens of the *Chlamydiae*. *Cand. Omnitrophica* are mostly found in fresh water. Cell division is one of the particularities of this superphylum: some PVC species, such as the members of the order *Planctomycetales*, divide by budding, whereas most

others divide by binary fission (Figure 2). Although *Chlamydiae* were previously described as dividing by binary fission, new data have revealed an asymmetric division in *Chlamydinia trachomatis* (Abdelrahman et al., 2016). With the exception of the *Verrucomicrobia* and *Cand. Omnitrophica*, PVC bacteria also lack the FtsZ protein, the central player of bacterial division. How bacteria deprived of FtsZ divide without this landmark protein is unknown. Some members of the PVC superphylum have also been described as lacking PG. The lack of both PG and FtsZ, and the different mode of division observed in *Planctomycetes* and *Chlamydiae*, once represented one of the biggest mysteries of microbiology – as well as an excellent breeding ground for hypotheses on the evolution of new modes of cell division.

Evolutionary cell biology is a recent field that aims to meld an understanding of evolutionary processes with variation in intracellular structure, based on the comparison of mechanisms between species (Lynch et al., 2014). The development of a new division mode is one of the most important evolutionary transitions. How a binary fission mechanism based on FtsZ

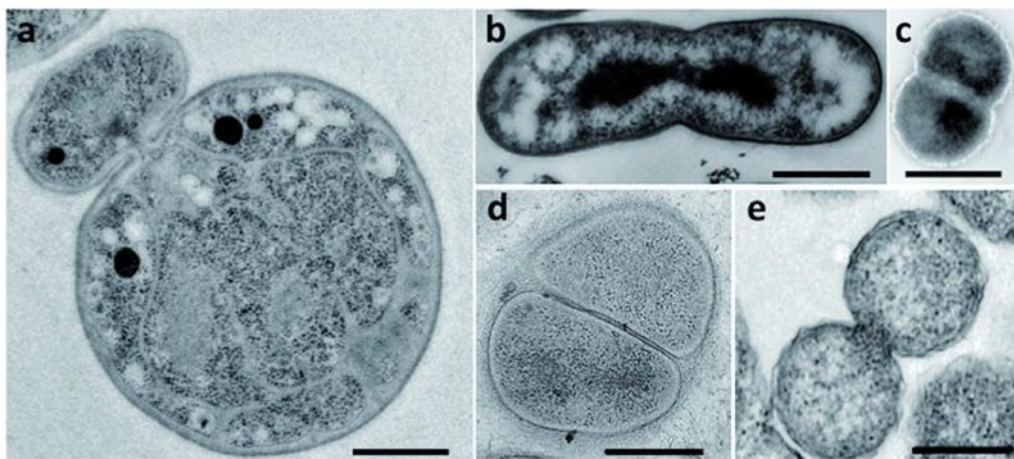


FIGURE 2 | Division modes in the PVC superphylum. Transmission electron micrographs of thin sections of dividing cells from (a) *G. obscuriglobus* (Santarella-Mellwig, personal communication), (b) *Chthoniobacter flavus* [adapted with permission from Sangwan et al. (2004), License number 3662961133966], (c) *L. araneosa* [adapted with permission from Cho et al. (2004), License number 3662980203389], (d) *P. mikurensis* [reprinted with permission from Fukunaga et al. (2009)], and (e) *C. trachomatis* [adapted with permission from Lewis et al. (2014)]. Scale bars, 0.5 μm .

evolved into an FtsZ-independent mechanism of division by budding is a major question in this field.

Various publications have recently revealed the presence of PG in some planctomycetal and chlamydial species, suggesting that it is also present in other species in these phyla and in other PVC phyla (Pilhofer et al., 2013; Liechti et al., 2014, 2016; Jeske et al., 2015; van Teeseling et al., 2015). Furthermore, a link between PG synthesis at the septum and division in *Chlamydiae* is emerging, offering clues about the mechanism of bacterial division without FtsZ (Liechti et al., 2016).

Here, we review the most striking features of the PVC bacteria that are linked to cell division without FtsZ and the involvement of PG in this process. We first summarize the historical analyses that led to the conclusion that PG was absent from some of these bacteria. We then recapitulate the recent detection of PG in some chlamydias and planctomycetes, as well as the role of PG, PG-related and division proteins in chlamydial division. Based on the detection of PG-related proteins in PVC proteomes, we evaluate

the possible evolution of division mechanisms in these bacteria. Finally, we discuss the implications of these findings for division in *Chlamydiae* and their extrapolation to the other PVC phyla.

Binary Fission and PG Synthesis

In the majority of bacteria, cell division is performed by binary fission. There are a few exceptions: a small proportion of bacteria use mechanisms such as intracellular offspring production or multiple fission (Angert, 2005). Budding is an alternative mode that has been reported in many bacterial lineages, including some members of *Cyanobacteria*, *Firmicutes*, *Planctomycetes*, and the prosthecate proteobacteria. Recent research also reveals that *C. trachomatis* divides asymmetrically, which is reminiscent of budding (Abdelrahman et al., 2016; Liechti et al., 2016). In model organisms, such as *Escherichia coli*, division by binary fission is realized using a molecular machinery assembled around the FtsZ protein, a homolog of the eukaryotic tubulin (Figure 3) (den Blaauwen et al., 2008; Erickson et al., 2010). FtsZ is one

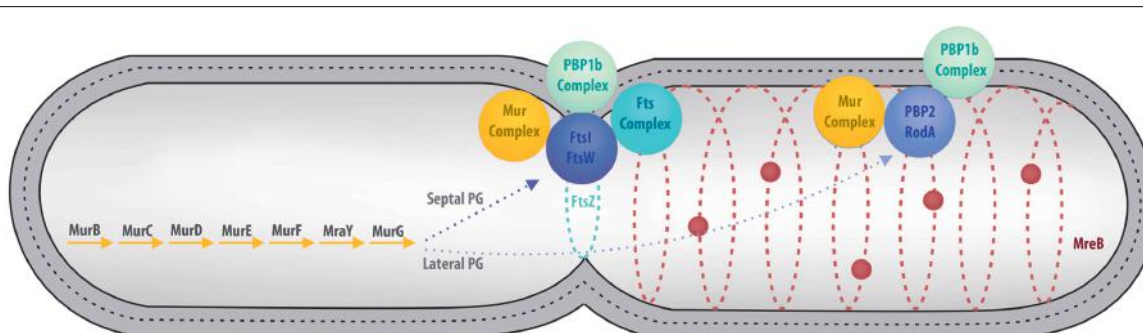


FIGURE 3 | Overview of cell division in model organisms. Major cell division and PG synthesis complexes are represented. Cytoplasmic steps of PG synthesis enzymes (**Left**), major cell division and septal PG synthesis complexes (**Center**), and elongation of lateral PG complexes (**Right**) are represented by colored spheres. PG is represented by a dotted line between the inner and outer membranes.

of the first proteins to localize at the division site in the middle of the cell. It forms a ring while recruiting the components of the division machinery, the divisome, including FtsA, FtsI, FtsK, FtsL, and FtsW, as well as PBP1b, EnvC, NlpD, and the Tol-Pal system (Lutkenhaus et al., 2012). During division, the FtsZ ring and the associated divisome contract, pulling the membranes toward the inside of the cell. As a consequence of its central role in division, FtsZ is present in almost all bacteria. Only a few groups, including *Chlamydiae*, *Planctomycetes*, and some of the *Mollicutes*, are unusual in that they lack a recognizable homolog of FtsZ (Figure 1; Supplementary Table S1).

Peptidoglycan also plays an important role in division by binary fission. PG is a net-like heteropolymer comprising linear glycan strands that are assembled from two sugar precursors, *N*-acetyl-glucosamine acid (GlcNAc) and *N*-acetyl-muramic acid (MurNAc), through β -(1,4)-glycosidic bonds and stabilized through peptide bridges containing D-amino acids. PG has a structural role: it surrounds the bacterial cell, forming an exoskeleton, the sacculus, that amongst other functions, protects cells from osmotic stress. The sacculus is so stable that it can be purified as a single entity (den Blaauwen et al., 2008). The presence of PG is one of the characteristics that differentiates bacteria from the other two domains of life, archaea and eukaryotes. There are, however, a few exceptions to the PG universality in bacteria, which are now restricted to the *Mollicutes* but until recently also included the *Chlamydiae* and *Planctomycetes*.

The PVC Melting Pot

Peptidoglycan has historically been thought to be absent from the periplasm of most PVC bacteria. Early attempts failed to detect PG in *Chlamydiae* (Garrett et al., 1974; Fox et al., 1990), efforts to purify chlamydial sacculi were unsuccessful (Caldwell et al., 1981; Barbour et al., 1982), and periplasmic density layers between the inner and outer membranes were not detected by electron microscopy (Tamura et al., 1971; Huang et al., 2010). Surprisingly, bacteria from the *Chlamydiae* are sensitive to β -lactam antibiotics, which inhibit PG synthesis (Matsumoto and Manire, 1970). In addition, most available chlamydial genomes encode functional enzymes for PG synthesis, and the functionality of a nearly complete biosynthesis pathway in several species is well supported (Hesse et al., 2003; McCoy et al., 2003; McCoy and Maurelli, 2005, 2006; Patin et al., 2009, 2012). These contradictory observations have been referred to as the “chlamydial anomaly” (Moulder, 1993). By contrast, *Planctomycetes* are resistant to all PG-targeting antibiotics (Cayrou et al., 2010), and early biochemical analyses were unable to detect PG components in isolated cell envelopes of various strains (König et al., 1984; Stackebrandt et al., 1986). Thus, PG was thought to be absent from *Planctomycetes*. Nevertheless, the growth of the anammox planctomycetes *Cand. Kuenenia stuttgartiensis* has been shown to be inhibited by lysozyme and penicillin, which both act on PG (Hu et al., 2013). PG had also been detected in some, but not all, verrucomicrobial species investigated (Yoon et al., 2007a,b, 2008a,b, 2010). In agreement, most PG synthesis genes were detected in *Verrucomicrobium spinosum* and the functionality of at least one of them has been

confirmed (McGroty et al., 2013). Recently, PG has been detected in subdivision 5 of *Verrucomicrobia* (Spring et al., 2016).

In addition, and of chief interest here, is the observation that PVC bacteria encode a diversity of division proteins. *Verrucomicrobia*, *Lentisphaera araneosa*, and *Omnitrophica bacterium* OLB16 encode the FtsZ protein and synthesize PG, whereas the *Planctomycetes* and *Chlamydiae* lack FtsZ as well as other division proteins (Figure 1; Supplementary Table S1). Whereas the *Verrucomicrobia* and *Lentisphaerae*, as well as the lowest branching *Planctomycetes* orders, *Cand. Brocadiales* and *Phycisphaerales*, divide by binary fission, members of the order *Planctomycetales* divide by budding. *Chlamydiae* were previously described as dividing by binary fission, however, asymmetric polarized cell division that might resemble budding has recently been reported in *C. trachomatis* (Abdelrahman et al., 2016; Liechti et al., 2016). This intracellular pathogen has differential localization of major cell components, such as the major outer-membrane protein and lipopolysaccharide present on opposite poles of the cell (Abdelrahman et al., 2016).

Thus, the *Verrucomicrobia* were classified as Gram-negative bacteria dividing by binary fission with FtsZ and PG (Krieg, 2011); the *Chlamydiae* as PG-deprived Gram-negative bacteria dividing by binary fission without FtsZ; and the *Planctomycetes* as dividing by budding without FtsZ and PG, but also as defining a “third cell plan” (Fuerst, 2013b).

PG Detection in PVC Members

The first analysis to address the conservation of the division and cell wall (*dcw*) cluster in PVC genomes failed to detect some key PG synthesis genes and concluded that the last common ancestor of the PVC superphylum possessed a ‘classical’ *dcw* cluster (Pilhofer et al., 2008). Major modifications, mostly losses, were found in the *Planctomycetes*. The presence of genes was recently re-addressed using a profile-based method more appropriate for detecting remote relationships between proteins (Jeske et al., 2015; van Teeseling et al., 2015). Contrary to previous analyses, these studies revealed that all planctomycetal and chlamydial species investigated harbored the genes essential for PG synthesis.

Given the detection of PG synthesis enzymes in the chlamydial and planctomycetal genomes, the presence of PG in their cell walls was re-evaluated (Pilhofer et al., 2013; Liechti et al., 2014; Jeske et al., 2015; van Teeseling et al., 2015). Using a combination of methods, PG was observed in four planctomycetes strains: *Gemmata obscuriglobus*, *Planctopirus limnophila*, *Rhodopirellula baltica*, and strain L21-Rpul-D3 (Jeske et al., 2015). Those methods included a radioactive kinase assay to detect the transfer of a radioactive γ -phosphoryl group from [γ -³²P]-ATP to GlcNAc and MurNAc monomers, gas chromatography and mass spectrometry to reveal the presence of the PG component 2,6-diaminopimelic acid, visualization of cell wall sacculi disruption after lysozyme treatment, and direct visualization of a thin PG layer by electron microscopy in vitrified cells. The presence of PG was simultaneously reported for the anammox planctomycete *Cand. Kuenenia stuttgartiensis* (van Teeseling et al., 2015). A similar set of methods was used, including direct observation of sacculi digestion by lysozyme, incorporation of PG specific probes, chemical analyses

using ultra-performance liquid chromatography and mass spectrometry, and direct visualization of the cell wall layer by cryo-electron microscopy of vitreous sections. Similarly, the use of mass spectrometry and fluorescent labeling dyes combined with electron cryotomography and a PG synthesis inhibitor revealed the presence of a PG sacculus in *Protochlamydia amoebophila*, a symbiotic member of the *Chlamydiae* (Pilhofer et al., 2013). However, the same technique failed to reveal PG in *Simkania negevensis*, a pathogenic chlamydial-like bacterium. This lack of detection is in agreement with the resistance of this bacterium to penicillin and phosphomycin (Pilhofer et al., 2013), but is at odds with the presence of genes coding for most PG synthesis enzymes in its genome (**Supplementary Table S1**). In addition, two of the *S. negevensis* genes, *amiA* and *nlpD*, have been shown to encode functional proteins that are active in *E. coli* (Frandi et al., 2014). A new metabolic cell-wall labeling method based on D-amino acid dipeptide and click chemistry revealed the presence of PG in *C. trachomatis* (Liechti et al., 2014). Remarkably, whereas a typical, cell-surrounding sacculus is formed in *P. amoebophila*, only a ring-like band is observed at mid-cell in *C. trachomatis* (Liechti et al., 2014).

Individually, these reports provide compelling evidence for the presence of PG in the cell wall of the investigated strains. Taken together, the direct and indirect evidence accumulated from orthogonal sources constitutes irrefutable proof of PG synthesis in phylogenetically dispersed strains of the PVC superphylum. In addition, PG has been detected in strains belonging to the genus Prosthecobacter and in strain L21-Fru-ABT from the *Verrucomicrobia* (Hedlund et al., 1996; Spring et al., 2016). Combined with the genomic data, these detections strongly suggest that PG synthesis takes place in most, if not all, members of the PVC superphylum. To the best of our knowledge, the synthesis of PG has not yet been tested in *Lentisphaeraea*, although the only genomic sequence information available so far suggests that *L. araneosa* is capable of PG synthesis (**Figure 1; Supplementary Table S1**). These data strongly supports that PVC bacteria are a variation of, not an exception to, the Gram-negative cell plan, putting a clear end to the controversy about the planctomycetal cell plan (Fuerst, 2013b; Devos, 2014a,b; Sagulenko et al., 2014).

Clarifying the ‘Chlamydial Anomaly’

Considerable modifications of the chlamydial PG structure and timing of its synthesis have recently been revealed in four pathogenic strains: *C. trachomatis*, *C. muridarum*, *Chlamydophila psittaci*, and *C. caviae* (Liechti et al., 2016). The use of chemical probes with super-resolution microscopy demonstrated that PG in these species is limited to a narrow ring at the division plane only during the replicative stage (Liechti et al., 2014, 2016). Because the host immune system recognizes and responds to PG, the authors suggest that members of the family *Chlamydiaceae*, all of which are pathogens, may limit the synthesis of PG to the place and time that are absolutely necessary, i.e., the division septum of replicating cells (Liechti et al., 2016). Thus, PG synthesis is crucial to chlamydial division, even in pathogenic strains, which have reduced it to a minimum. This spatiotemporally limited synthesis of PG explains why it was not detected before and also

why *Chlamydiae* are susceptible to antibiotics, thus resolving the ‘chlamydial anomaly.’

Historical Considerations

The detection of PG in *Planctomycetes* and *Chlamydiae* poses the question of why it remained undetected for so long. In the case of *Chlamydiae*, it was due mostly to technical limitations, combined with the restricted presence of PG in time and space in pathogenic strains (Pilhofer et al., 2013; Liechti et al., 2014, 2016). The case of *Planctomycetes* appears to be different. Since early analyses (König et al., 1984; Liesack et al., 1986; Stackebrandt et al., 1986), the absence of PG in *Planctomycetes* cell walls was not reconsidered, despite several investigations into these bacteria and their structure (Fuerst, 2005, 2013b; Fuerst and Sagulenko, 2013; Sagulenko et al., 2014). Planctomycetal sacculi was purified in the presence of SDS and high temperature, but instead of PG, a proteinaceous cell wall was found (Stackebrandt et al., 1986). However, protein recovery was only 51%, with no indication of what comprised the remaining 49% of the envelope. It is unlikely that the sacculi consisted exclusively of proteins, as proteins of mesophilic organisms cannot resist hours of boiling in SDS and would be denatured under those conditions. Attempts to determine the presence of PG in *Planctomycetes* never involved lysozyme treatment, until recently (Giovannoni et al., 1987; Hu et al., 2013; Jeske et al., 2015; van Teeseling et al., 2015).

Given that PG is present in *Planctomycetes*, their resistance to β-lactam antibiotics might appear confusing (Cayrou et al., 2010). This resistance is possibly due to the presence of putative β-lactamases encoded in their genomes (Kahane et al., 1993). At least one putative β-lactamase gene is present in each *Planctomycetes* genome, often in multiple copies. For instance, there are 13 putative β-lactamases encoded in the *P. limnophila* genome (Labutti et al., 2010). By contrast, *Chlamydiae* are sensitive to β-lactam antibiotics despite the presence of β-lactamases in their genomes (Bertelli et al., 2010).

Chlamydial Division

The detection of PG in PVC species and its interaction with division proteins are important, as they provide potential clues about PVC division mechanisms. The few PVC species for which division mechanisms have been investigated so far belong to the *Chlamydiae* (Jacquier et al., 2015). Chlamydial division was previously believed to resemble FtsZ-dependent binary fission (Brown and Rockey, 2000; Abdelrahman and Belland, 2005). However, an asymmetric polarized division mode has recently been revealed in *Chlamydiaceae* (Abdelrahman et al., 2016) and progress on understanding the link between chlamydial PG and division has been reported (Jacquier et al., 2015). This new knowledge allows us to draw a preliminary model of chlamydial division that reveals important modifications to the mechanisms of division in model organisms. In particular, the central role of MreB (a bacterial homolog of actin) and its interaction with PG synthesis enzymes at the septum is emerging.

Division is tightly regulated in *Chlamydiales*, as only one specific cell type, the reticulate body, is metabolically active and able to divide. Expression analyses of several division and PG biosynthesis genes in *C. trachomatis* and *C. pneumoniae*

show that these genes are over-expressed in the dividing forms compared with the non-dividing forms (Albrecht et al., 2010, 2011). Typical peptide components of PG accumulate at the chlamydial division site, as in most other bacteria (Jacquier et al., 2014). These PG precursors are required for proper localization of PG- and MreB-binding proteins at the division septum (Jacquier et al., 2014). The activity of MurA, MurF, and MurG, which are involved in the early and mid-phase stages of PG synthesis, are required to organize the chlamydial septum, further supporting the understanding that PG synthesis is required for division (Liechti et al., 2014).

The cytoskeletal proteins MreB and RodZ, which are responsible for cell-shape determination in model organisms, seem to play an important role in this process in *Chlamydiae*, as they may bring together the PG biosynthesis and remodeling enzymes to the divisome (Jacquier et al., 2015). Indeed, it appears that FtsZ-less *Chlamydiae* uses MreB to define the division plane by interaction with FtsK, which in turn may recruit PBP2, FtsI (also called PBP3) and likely other unidentified proteins (Ouellette et al., 2012). Co-localization results suggest that MreB polymerization is required to guide new PG incorporation along the PG ring in *Chlamydiales* (Gaballah et al., 2011; Liechti et al., 2016), supporting the proposal that MreB acts as the division plane organizer in pathogenic chlamydias. However, MreB does not seem to be an early cell division protein like FtsZ, because it is recruited late at the septum (Gaballah et al., 2011). Like FtsZ, MreB appears to be a central coordinator of the large multi-protein PG synthesizing complex that cooperates to direct cell elongation. This complex includes PBP2, RodA and many additional partners, such as MreC, MreD, and RodZ, that are involved in the stabilization and/or regulation of this machinery. *C. pneumoniae* MreB has been shown to interact with MurF, MraY, and MurG, three key components of lipid II biosynthesis (Gaballah et al., 2011). In *W. chondrophila*, RodZ is recruited early to the septal site in a process that is dependent on the presence and dispersal of cell wall precursors (Jacquier et al., 2014). The endopeptidase NlpD localizes at the division plane in *Chlamydiae* and its septal sequestration depends on prior cell wall synthesis (Frandi et al., 2014). Thus, the division mechanisms of *Chlamydiae* share similarities but also have important differences with model organisms.

Evolutionary Cell Biology of Division Modes in PVC Bacteria

The diversity of characteristics of related bacteria makes the PVC superphylum particularly attractive for the field of evolutionary cell biology. To paraphrase Theodosius Dobzhansky, it could be said that “nothing in PVC cell division makes sense except in the light of evolutionary cell biology.” Some clues about PVC division can be derived from the limited knowledge available about division in the *Chlamydiae* and from gene conservation in other species. We thus revisited the presence of the main genes involved in PG synthesis and division in the PVC proteomes for a representative set of genomes across the superphylum (Figure 1; Supplementary Table S1). It is unclear if the inability to detect some proteins is due to their absence or represents a false negative

result. The latter nevertheless indicates a profound modification of the protein sequences and thus most likely of the molecular mechanisms associated with it.

The diversity of division modes and proteins observed in PVC species is due to divergent evolution from a common ancestor (Figure 4). The most parsimonious explanation for the gene distribution of the *dcw* cluster is that the last PVC common ancestor was a Gram-negative bacterium that divided by binary fission using PG and FtsZ, and that had a mostly classical *dcw* cluster, as suggested by others (Pilhofer et al., 2008; Jogler et al., 2012). Within the PVC superphylum, species have diverged from this common ancestor, accumulating differences including gene losses but also modifications of the function of existing genes (Figure 1; Supplementary Table S1). How gene losses are related to modifications of this division mechanism is one of the main questions remaining in this field. Even in the PVCs containing FtsZ, modifications of the division modes are to be expected, as demonstrated by the losses of molecular components. Due to the diversity of phenotypes and genotypes encountered in the PVC superphylum, generalization of their features is a difficult exercise.

First and foremost, FtsZ, the landmark protein of binary fission that is conserved in almost all bacteria, is not found in *Chlamydiae* or in *Planctomycetes*. It is detected only in *Omnitrophica bacterium* OLB16, and it is not clear if its absence in the other two members of the *Cand. Omnitrophica* is real or merely a result of incomplete data. On the other side of the spectrum of conservation, a putative FtsK protein, the DNA translocase, is likely to be present in all genomes (its absence in *Zavarzinella formosa* is likely due to incomplete data). The same applies to MraY, an integral membrane enzyme that catalyzes the transfer of the PG precursor to the lipid carrier undecaprenyl phosphate, forming the lipid I.

In between those two extremes, interesting intermediary cases are found. MreB is found in almost all PVC proteomes, with the exception of some of the budding planctomycetes. This conservation supports the central role of MreB in the absence of FtsZ. In model organisms, MreB requires the membrane proteins MreC and MreD for the organization of the PG (White et al., 2010). Interestingly, MreD is not found in any PVC proteomes, while MreC shows a patchy distribution: it is found in verrucomicrobias and chlamydias, and in two out of three binary fission planctomycetes, but not in *L. araneosa* or in the budding planctomycetes (with the possible exception of *Planctomyces brasiliensis*, which is probably a false positive). The protein RodZ might form the link between MreB and the PG-modifying penicillin-binding proteins (PBPs), and it locates early at the septum in *Chlamydiae* (Jacquier et al., 2014). Interestingly, RodZ is only found in *Chlamydiae* and *Verrucomicrobia* but not in *Planctomycetes* or in *L. araneosa*. Thus, important modifications of division mode due to the lack of RodZ are expected. This is in agreement with the fact that the chlamydial RodZ is truncated, lacking its C-terminal periplasmic domain, and cannot complement an *E. coli* RodZ mutant (Ouellette et al., 2014).

The peptidase NlpD is another protein that localizes at the septum in chlamydial pathogens (Frandi et al., 2014). NlpD, like RodZ, is found only in *Chlamydiae* and *Verrucomicrobia*, and not

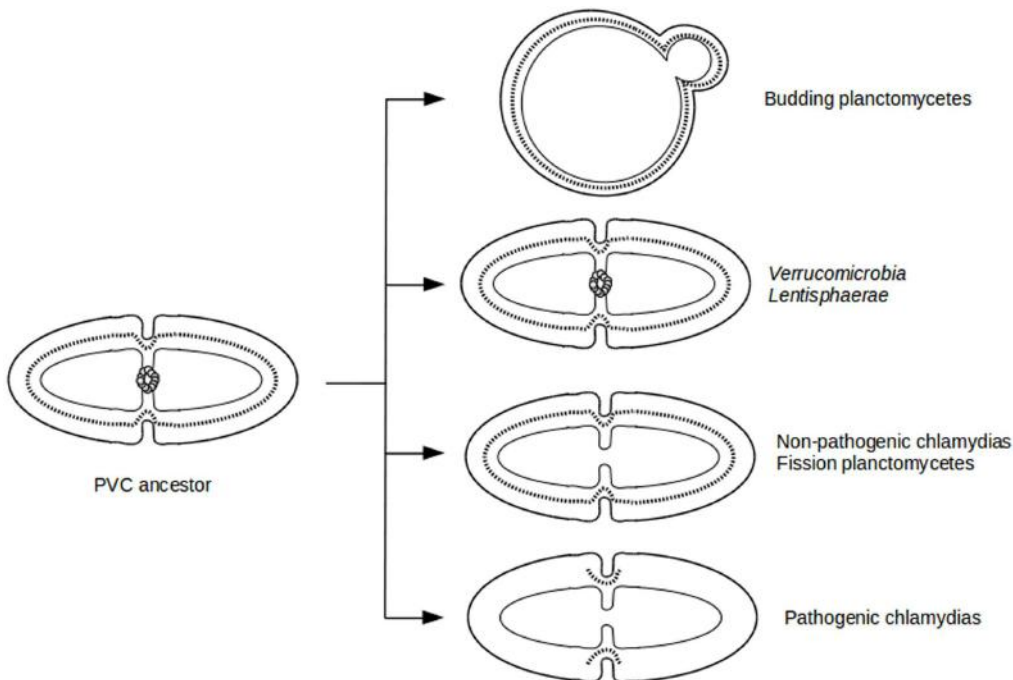


FIGURE 4 | Evolutionary cell biology of division modes in PVCs. Schematic representation of cell division modes in the last PVC common ancestor (**Left**) and in current PVC species (**Right**). Outer and inner membranes are in thick and thin lines, respectively. PG layer is in dotted line. FtsZ proteins are represented as a ring of gray spheres.

in *Planctomycetes* or *Lentisphaera*. The amidase activator EnvC is not found in any PVC proteomes (with a single exception, which is probably a false positive). In model organisms, EnvC is a regulator of the cell wall amidases AmiA and AmiB. Like NlpD, AmiA is found in *Chlamydiae* and *Verrucomicrobia*, but not in *Planctomycetes*, *Omnitrophica*, or *Lentisphaera*. AmiB is detected in *Chlamydiae*, *L. araneosa*, and only one *Omnitrophica*, but only in five members of the *Verrucomicrobia* (out of nine) and not at all in *Planctomycetes*. Most PG synthesis enzymes are found in PVC members, with the exception of some budding planctomycetes.

Hence, this pattern of undetected proteins illustrates important modifications of the cell division modes in the various branches of the PVC superphylum. The diverse division modes in PVC bacteria offer a fascinating field of study for the years to come.

REMARKS AND OPEN QUESTIONS

Great progress has been made in uncovering the division modes in members of the PVC superphylum. Many relevant discoveries reveal new questions that require further research to answer. The data presented here calls for a few remarks and questions.

First, PG is almost universal in bacteria, with a few exceptions limited to obligate intracellular bacteria, and is one of the true features defining bacteria (including bacteria-derived organelles such as plastids). The recent detection of PG in PVC members,

combined with genomic information, suggests that it is present in most PVC species. The only bacterial group that is possibly devoid of a PG cell wall is the *Mollicutes*. In addition, to the best of our knowledge, the mollicutes *Phytoplasma* sp., *Ureaplasma* sp., and *Mycoplasma mobile* are the only species deprived of both FtsZ and PG (Bernander and Ettema, 2010).

Second, PVC bacteria are variations of, but not exceptions to, the Gram-negative cell plan (Devos, 2014a). The presence of PG in PVC species definitively resolves this controversy.

Third, most PVC bacteria have a well developed endomembrane system. This system can take the form of invaginations of the cytoplasmic membrane toward the inside of the cell (as observed in most planctomycetes), of evaginations of the outer membrane (in some verrucomicrobias), or of a tubulo-vesicular network in the periplasm of the cell (in the planctomycete *G. obscuriglobus*; Santarella-Mellwig et al., 2013; Acehan et al., 2014; Devos, 2014a). The anammox planctomycetes even appear to display the first prokaryotic organelle with a compartment apparently separated from the inner membrane (Neumann et al., 2014). How the PG organizes within or around this endomembrane system, including the periplasmic tubulo-vesicular network, is another intriguing feature that requires deeper investigation. How PG is synthesized and organized in the bud is yet another interesting area of research.

Fourth, during evolutionary divergence from their common ancestor with a classical FtsZ-based binary fission mode of division, PVC members have evolved different modifications,

including the loss of FtsZ and the development of alternative division mechanisms and modes, raising various questions for evolutionary cell biology. What forces and constraints acted on which proteins and processes? What has been the evolutionary pressure behind those innovations? Given the degradation of the *dcw* cluster, the total conservation of some genes, such as *mreB* or *ftsK*, is intriguing.

Fifth, recent progress has been made in deciphering the chlamydial division mechanism, which requires the active synthesis of PG, suggesting a role at the septum related to that of PG in classical Gram-negative species. This opens up more important questions. How much of the ancestral division mechanism is conserved in current species? And what are the differences? What is the role of PG in division without FtsZ? Has MreB replaced FtsZ, as has been suggested (Jacquier et al., 2015)? A key question is how to transfer the chlamydial knowledge to other PVCs.

Sixth, recent advances in the field of PVC genetic manipulation are providing us with better tools to answer some of these questions. Genetic tools have been described recently in the three initial PVC phyla *Planctomycetes*, *Verrucomicrobia*, and *Chlamydiae* (Domman et al., 2011; Jogler et al., 2011; Kari et al., 2011; Wang et al., 2011; Gérard et al., 2013; Erbilgin et al., 2014; Kokes et al., 2015; Rivas-Marín et al., 2016). The analyses reported here and elsewhere constitute a very good place not only to continue deciphering the modes of division of *Chlamydiae*, but also to start exploring those of the other PVC members. The isolation and characterization of new PVC members is important, as it will provide more information about the diversity of division modes in PVC bacteria. Is there an intermediary organism with a mode of division between binary fission and budding? Genome information for additional PVC species is needed to evaluate the conservation of division proteins (and mechanisms) in this superphylum.

CONCLUSION

The PVC bacterial superphylum presents an unparalleled opportunity for the study of evolutionary cell biology of division modes. We are looking forward to progress in this fascinating field.

REFERENCES

- Abdelrahman, Y., Ouellette, S. P., Belland, R. J., and Cox, J. V. (2016). Polarized cell division of Chlamydia trachomatis. *PLOS Pathog.* 12:e1005822. doi: 10.1371/journal.ppat.1005822
- Abdelrahman, Y. M., and Belland, R. J. (2005). The chlamydial developmental cycle. *FEMS Microbiol. Rev.* 29, 949–959. doi: 10.1016/j.femsre.2005.03.002
- Acehan, D., Santarella-Mellwig, R., and Devos, D. P. (2014). A bacterial tubulovesicular network. *J. Cell Sci.* 127, 277–280. doi: 10.1242/jcs.137596
- Albrecht, M., Sharma, C. M., Dittrich, M. T., Müller, T., Reinhardt, R., Vogel, J., et al. (2011). The transcriptional landscape of Chlamydia pneumoniae. *Genome Biol.* 12:R98. doi: 10.1186/gb-2011-12-10-r98
- Albrecht, M., Sharma, C. M., Reinhardt, R., Vogel, J., and Rudel, T. (2010). Deep sequencing-based discovery of the Chlamydia trachomatis transcriptome. *Nucleic Acids Res.* 38, 868–877. doi: 10.1093/nar/gkp1032
- Angert, E. R. (2005). Alternatives to binary fission in bacteria. *Nat. Rev. Microbiol.* 3, 214–224. doi: 10.1038/nrmicro1096
- Barbour, A. G., Amano, K., Hackstadt, T., Perry, L., and Caldwell, H. D. (1982). Chlamydia trachomatis has penicillin-binding proteins but not detectable muramic acid. *J. Bacteriol.* 151, 420–428.
- Bernander, R., and Ettema, T. J. (2010). FtsZ-less cell division in archaea and bacteria. *Curr. Opin. Microbiol.* 13, 747–752. doi: 10.1016/j.mib.2010.10.005
- Bertelli, C., Collynn, F., Croxatto, A., Rückert, C., Polkinghorne, A., Kebbi-Beghdadi, C., et al. (2010). The *Waddlia* genome: a window into chlamydial biology. *PLoS ONE* 5:e10890. doi: 10.1371/journal.pone.0010890

AUTHOR CONTRIBUTIONS

All authors listed, have made substantial, direct and intellectual contribution to the work, and approved it for publication.

FUNDING

ER-M and DD are supported by the Spanish Ministry of Economy and Competitiveness (Grant BFU2013-40866-P) and the Junta de Andalucía (CEIC Grant C2A program to DD). IC is supported by the Spanish Ministry of Economy and Competitiveness (Grant BIO2014-57545-R).

ACKNOWLEDGMENTS

We thank Rachel Santarella-Mellwig (EMBL, Heidelberg, Germany) for helpful comments on the manuscript, Eduardo Santero (CABD, Seville, Spain) for support, and Nicola Bordin (CABD) for building the phylogenetic tree.

SUPPLEMENTARY MATERIAL

The Supplementary Material for this article can be found online at: <http://journal.frontiersin.org/article/10.3389/fmicb.2016.01964/full#supplementary-material>

TABLE S1 | Division and cell wall cluster and PG synthesis protein detection in PVC. Due to the divergence of the PVC species from model organisms and for the sake of completeness, two complementary searches were combined (Sheet 1). We first performed two iterations of Psi-Blast using the *W. chondrophila* (Sheet 2) and *E. coli* (Sheet 3) proteins as a query on the non-redundant GenBank (nr) database, using default parameters and accepting hits with an e-value below 10^{-3} . One additional iteration was run on the PVC proteomes with the obtained profile as query. A reciprocal search was then used to verify that the starting proteins were found when using the hit as a query. The PVC hit was only accepted if the reciprocal search found the starting sequence. Each cell contains two identifiers, if the reciprocal best hits are different, the first one corresponding to the hit from the *W. chondrophila* search (left), followed by the hit from the *E. coli* search (right). In most cases, the two approaches hit the same proteins, reinforcing their results. Only one identifier is indicated if the reciprocal best hits are the same. Sheets 2 and 3 show the e-values of detection corresponding to the searches from the *W. chondrophila* and *E. coli* proteins, respectively. NA, not applicable; PF, binary fission planctomycetes; PB, budding planctomycetes.

Albrecht, M., Sharma, C. M., Reinhardt, R., Vogel, J., and Rudel, T. (2010). Deep sequencing-based discovery of the Chlamydia trachomatis transcriptome. *Nucleic Acids Res.* 38, 868–877. doi: 10.1093/nar/gkp1032

Angert, E. R. (2005). Alternatives to binary fission in bacteria. *Nat. Rev. Microbiol.* 3, 214–224. doi: 10.1038/nrmicro1096

Barbour, A. G., Amano, K., Hackstadt, T., Perry, L., and Caldwell, H. D. (1982). Chlamydia trachomatis has penicillin-binding proteins but not detectable muramic acid. *J. Bacteriol.* 151, 420–428.

Bernander, R., and Ettema, T. J. (2010). FtsZ-less cell division in archaea and bacteria. *Curr. Opin. Microbiol.* 13, 747–752. doi: 10.1016/j.mib.2010.10.005

Bertelli, C., Collynn, F., Croxatto, A., Rückert, C., Polkinghorne, A., Kebbi-Beghdadi, C., et al. (2010). The *Waddlia* genome: a window into chlamydial biology. *PLoS ONE* 5:e10890. doi: 10.1371/journal.pone.0010890

- Bertelli, C., and Greub, G. (2013). "Phyla related to planctomycetes: members of the phylum Chlamydiae and their implications for planctomycetes cell biology," in *Planctomycetes: Cell Structure, Origins and Biology*, ed. J. A. Fuerst (New York, NY: Humana Press), 229–241. doi: 10.1007/978-1-62703-502-6_10
- Brown, W. J., and Rockey, D. D. (2000). Identification of an antigen localized to an apparent septum within dividing chlamydiae. *Infect. Immun.* 68, 708–715. doi: 10.1128/IAI.68.2.708-715.2000
- Caldwell, H. D., Kromhout, J., and Schachter, J. (1981). Purification and partial characterization of the major outer membrane protein of *Chlamydia trachomatis*. *Infect. Immun.* 31, 1161–1176.
- Cayrou, C., Raoult, D., and Drancourt, M. (2010). Broad-spectrum antibiotic resistance of Planctomycetes organisms determined by Etest. *J. Antimicrob. Chemother.* 65, 2119–2122. doi: 10.1093/jac/dkq290
- Cho, J.-C., Vergin, K. L., Morris, R. M., and Giovannoni, S. J. (2004). *Lentisphaera araneosa* gen. nov., sp. nov., a transparent exopolymer producing marine bacterium, and the description of a novel bacterial phylum, *Lentisphaerae*. *Environ. Microbiol.* 6, 611–621. doi: 10.1111/j.1462-2920.2004.00614.x
- den Blaauwen, T., de Pedro, M. A., Nguyen-Distèche, M., and Ayala, J. A. (2008). Morphogenesis of rod-shaped sacculi. *FEMS Microbiol. Rev.* 32, 321–344. doi: 10.1111/j.1574-6976.2007.00090.x
- Devos, D. P. (2014a). PVC bacteria: variation of, but not exception to, the gram-negative cell plan. *Trends Microbiol.* 22, 14–20. doi: 10.1016/j.tim.2013.10.008
- Devos, D. P. (2014b). Re-interpretation of the evidence for the PVC cell plan supports a gram-negative origin. *Antonie Van Leeuwenhoek* 105, 271–274. doi: 10.1007/s10482-013-0087-y
- Devos, D. P., and Ward, N. L. (2014). Mind the PVCs. *Environ. Microbiol.* 16, 1217–1221. doi: 10.1111/1462-2920.12349
- Domman, D. B., Steven, B. T., and Ward, N. L. (2011). Random transposon mutagenesis of *Verrucomicrobium spinosum* DSM 4136(T). *Arch. Microbiol.* 193, 307–312. doi: 10.1007/s00203-010-0666-5
- Erbilgin, O., McDonald, K. L., and Kerfeld, C. A. (2014). Characterization of a planctomycetal organelle: a novel bacterial microcompartment for the aerobic degradation of plant saccharides. *Appl. Environ. Microbiol.* 80, 2193–2205. doi: 10.1128/AEM.03887-13
- Erickson, H. P., Anderson, D. E., and Osawa, M. (2010). FtsZ in bacterial cytokinesis: cytoskeleton and force generator all in one. *Microbiol. Mol. Biol. Rev.* 74, 504–528. doi: 10.1128/MMBR.00021-10
- Fox, A., Rogers, J. C., Gilbart, J., Morgan, S., Davis, C. H., Knight, S., et al. (1990). Muramic acid is not detectable in *Chlamydia psittaci* or *Chlamydia trachomatis* by gas chromatography-mass spectrometry. *Infect. Immun.* 58, 835–837.
- Frandi, A., Jacquier, N., Théraulaz, L., Greub, G., and Viollier, P. H. (2014). FtsZ-independent septal recruitment and function of cell wall remodelling enzymes in chlamydial pathogens. *Nat. Commun.* 5:4200. doi: 10.1038/ncomms5200
- Fuerst, J. A. (2005). Intracellular compartmentation in planctomycetes. *Annu. Rev. Microbiol.* 59, 299–328. doi: 10.1146/annurev.micro.59.030804.121258
- Fuerst, J. A. (ed.) (2013a). *Planctomycetes: Cell Structure, Origins and Biology*. Totowa, NJ: Humana Press.
- Fuerst, J. A. (2013b). The PVC superphylum: exceptions to the bacterial definition? *Antonie Van Leeuwenhoek* 104, 451–466. doi: 10.1007/s10482-013-9986-1
- Fuerst, J. A., and Sagulenko, E. (2013). Nested bacterial boxes: nuclear and other intracellular compartments in Planctomycetes. *J. Mol. Microbiol. Biotechnol.* 23, 95–103. doi: 10.1159/000346544
- Fukunaga, Y., Kurahashi, M., Sakiyama, Y., Ohuchi, M., Yokota, A., and Harayama, S. (2009). *Phycisphaera mikurensis* gen. nov., sp. nov., isolated from a marine alga, and proposal of *Phycisphaeraceae* fam. nov., *Phycisphaerales* ord. nov. and *Phycisphaerae* classis nov. in the phylum Planctomycetes. *J. Gen. Appl. Microbiol.* 55, 267–275. doi: 10.2323/jgam.55.267
- Gaballah, A., Kloekner, A., Otten, C., Sahl, H.-G., and Henrichfreise, B. (2011). Functional analysis of the cytoskeleton protein MreB from *Chlamydophila pneumoniae*. *PLoS ONE* 6:e25129. doi: 10.1371/journal.pone.0025129
- Garrett, A. J., Harrison, M. J., and Manire, G. P. (1974). A search for the bacterial mucopeptide component, muramic acid, in *Chlamydia*. *J. Gen. Microbiol.* 80, 315–318. doi: 10.1099/00221287-80-1-315
- Gérard, H. C., Mishra, M. K., Mao, G., Wang, S., Hali, M., Whittum-Hudson, J. A., et al. (2013). Dendrimer-enabled DNA delivery and transformation of *Chlamydia pneumoniae*. *Nanomed. Nanotechnol. Biol. Med.* 9, 996–1008. doi: 10.1016/j.nano.2013.04.004
- Giovannoni, S. J., Godchaux, W., Schabtach, E., and Castenholz, R. W. (1987). Cell wall and lipid composition of *Isosphaera pallida*, a budding eubacterium from hot springs. *J. Bacteriol.* 169, 2702–2707. doi: 10.1128/JB.169.6.2702-2707.1987
- Guindon, S., Dufayard, J.-F., Lefort, V., Anisimova, M., Hordijk, W., and Gascuel, O. (2010). New algorithms and methods to estimate maximum-likelihood phylogenies: assessing the performance of PhyML 3.0. *Syst. Biol.* 59, 307–321. doi: 10.1093/sysbio/syq010
- Hedlund, B. P., Gosink, J. J., and Staley, J. T. (1996). Phylogeny of *Prosthecobacter*, the fusiform caulobacters: members of a recently discovered division of the bacteria. *Int. J. Syst. Bacteriol.* 46, 960–966. doi: 10.1099/00207713-46-960
- Hesse, L., Bostock, J., Dementin, S., Blanot, D., Mengin-Lecreux, D., and Chopra, I. (2003). Functional and biochemical analysis of *Chlamydia trachomatis* MurC, an enzyme displaying UDP-N-acetylglucosamine:amino acid ligase activity. *J. Bacteriol.* 185, 6507–6512. doi: 10.1128/JB.185.22.6507-6512.2003
- Horn, M., Collingro, A., Schmitz-Esser, S., Beier, C. L., Purkhold, U., Fartmann, B., et al. (2004). Illuminating the evolutionary history of chlamydiae. *Science* 304, 728–730. doi: 10.1126/science.1096330
- Hu, Z., van Aken, T., Jetten, M. S. M., and Kartal, B. (2013). Lysozyme and penicillin inhibit the growth of anaerobic ammonium-oxidizing planctomycetes. *Appl. Environ. Microbiol.* 79, 7763–7769. doi: 10.1128/AEM.02467-13
- Huang, Z., Chen, M., Li, K., Dong, X., Han, J., and Zhang, Q. (2010). Cryo-electron tomography of *Chlamydia trachomatis* gives a clue to the mechanism of outer membrane changes. *J. Electron Microscop. (Tokyo)* 59, 237–241. doi: 10.1093/jmicro/dfp057
- Jacquier, N., Frandi, A., Pillonel, T., Viollier, P. H., Viollier, P., and Greub, G. (2014). Cell wall precursors are required to organize the chlamydial division septum. *Nat. Commun.* 5:3578. doi: 10.1038/ncomms4578
- Jacquier, N., Viollier, P. H., and Greub, G. (2015). The role of peptidoglycan in chlamydial cell division: towards resolving the chlamydial anomaly. *FEMS Microbiol. Rev.* 39, 262–275. doi: 10.1093/femsre/fuv001
- Jeske, O., Schüler, M., Schumann, P., Schneider, A., Boedeker, C., Jogler, M., et al. (2015). Planctomycetes do possess a peptidoglycan cell wall. *Nat. Commun.* 6:7116. doi: 10.1038/ncomms8116
- Jogler, C., Glöckner, F. O., and Kolter, R. (2011). Characterization of planctomycetes limnophilus and development of genetic tools for its manipulation establish it as a model species for the phylum planctomycetes. *Appl. Environ. Microbiol.* 77, 5826–5829. doi: 10.1128/AEM.05132-11
- Jogler, C., Waldmann, J., Huang, X., Jogler, M., Glöckner, F. O., Mascher, T., et al. (2012). Identification of proteins likely to be involved in morphogenesis, cell division, and signal transduction in planctomycetes by comparative genomics. *J. Bacteriol.* 194, 6419–6430. doi: 10.1128/JB.01325-12
- Kahane, S., Gonen, R., Sayada, C., Elion, J., and Friedman, M. G. (1993). Description and partial characterization of a new chlamydial-like microorganism. *FEMS Microbiol. Lett.* 109, 329–333. doi: 10.1111/j.1574-6968.1993.tb06189.x
- Kari, L., Goheen, M. M., Randall, L. B., Taylor, L. D., Carlson, J. H., Whitmire, W. M., et al. (2011). Generation of targeted *Chlamydia trachomatis* null mutants. *Proc. Natl. Acad. Sci. U.S.A.* 108, 7189–7193. doi: 10.1073/pnas.1102229108
- Kokes, M., Dunn, J. D., Granek, J. A., Nguyen, B. D., Barker, J. R., Valdivia, R. H., et al. (2015). Integrating chemical mutagenesis and whole-genome sequencing as a platform for forward and reverse genetic analysis of chlamydias. *Cell Host Microbe* 17, 716–725. doi: 10.1016/j.chom.2015.03.014
- König, E., Schlesner, H., and Hirsch, P. (1984). Cell wall studies on budding bacteria of the *Planctomycetes/Pasteuria* group and on a *Prosthecomicrobium* sp. *Arch. Microbiol.* 138, 200–205. doi: 10.1007/BF00402120
- Krieg, N. R. (2011). *Bergey's Manual of Systematic Bacteriology: The Bacteroidetes, Spirochaetes, Tenericutes (Mollicutes), Acidobacteria, Fibrobacteres, Fusobacteria, Dictyoglomata, Gemmatimonadetes, Lentisphaerae, Verrucomicrobia, Chlamydiae, and Planctomycetes*, Vol. 4. Berlin: Springer.

- Labutti, K., Sikorski, J., Schneider, S., Nolan, M., Lucas, S., Glavina Del Rio, T., et al. (2010). Complete genome sequence of *Planctomyces limnophilus* type strain (Mu 290). *Stand. Genomic Sci.* 3, 47–56. doi: 10.4056/sigs.1052813
- Lewis, M. E., Belland, R. J., AbdelRahman, Y. M., Beatty, W. L., Aiyar, A. A., Zea, A. H., et al. (2014). Morphologic and molecular evaluation of Chlamydia trachomatis growth in human endocervix reveals distinct growth patterns. *Front. Cell. Infect. Microbiol.* 4:71. doi: 10.3389/fcimb.2014.00071
- Liechti, G., Kuru, E., Packiam, M., Hsu, Y.-P., Tekkam, S., Hall, E., et al. (2016). Pathogenic chlamydia lack a classical sacculus but synthesize a narrow, mid-cell peptidoglycan ring, regulated by MreB, for cell division. *PLOS Pathog.* 12:e1005590. doi: 10.1371/journal.ppat.1005590
- Liechti, G. W., Kuru, E., Hall, E., Kalinda, A., Brun, Y. V., VanNieuwenhze, M., et al. (2014). A new metabolic cell-wall labelling method reveals peptidoglycan in Chlamydia trachomatis. *Nature* 506, 507–510. doi: 10.1038/nature12892
- Liesack, W., König, H., Schlesner, H., and Hirsch, P. (1986). Chemical composition of the peptidoglycan-free cell envelopes of budding bacteria of the *Pirella/Planctomyces* group. *Arch. Microbiol.* 145, 361–366. doi: 10.1007/BF00470872
- Lutkenhaus, J., Pichoff, S., and Du, S. (2012). Bacterial cytokinesis: from Z ring to divisome. *Cytoskeleton* 69, 778–790. doi: 10.1002/cm.21054
- Lynch, M., Field, M. C., Goodson, H. V., Malik, H. S., Pereira-Leal, J. B., Roos, D. S., et al. (2014). Evolutionary cell biology: two origins, one objective. *Proc. Natl. Acad. Sci. U.S.A.* 111, 16990–16994. doi: 10.1073/pnas.1415861111
- Matsumoto, A., and Manire, G. P. (1970). Electron microscopic observations on the effects of penicillin on the morphology of Chlamydia psittaci. *J. Bacteriol.* 101, 278–285.
- McCoy, A. J., and Maurelli, A. T. (2005). Characterization of Chlamydia MurC-Ddl, a fusion protein exhibiting D-alanyl-D-alanine ligase activity involved in peptidoglycan synthesis and D-cycloserine sensitivity. *Mol. Microbiol.* 57, 41–52. doi: 10.1111/j.1365-2958.2005.04661.x
- McCoy, A. J., and Maurelli, A. T. (2006). Building the invisible wall: updating the chlamydial peptidoglycan anomaly. *Trends Microbiol.* 14, 70–77. doi: 10.1016/j.tim.2005.12.004
- McCoy, A. J., Sandlin, R. C., and Maurelli, A. T. (2003). In vitro and in vivo functional activity of Chlamydia MurA, a UDP-N-acetylglucosamine enolpyruvyl transferase involved in peptidoglycan synthesis and fosfomycin resistance. *J. Bacteriol.* 185, 1218–1228. doi: 10.1128/JB.185.4.1218-1228.2003
- McGroty, S. E., Pattaniyil, D. T., Patin, D., Blanot, D., Ravichandran, A. C., Suzuki, H., et al. (2013). Biochemical characterization of UDP-N-acetyl muramoyl-L-alanyl-D-glutamate: meso-2,6-diaminopimelate ligase (MurE) from *Verrucomicrobium spinosum* DSM 4136(T). *PLoS One* 8:e66458. doi: 10.1371/journal.pone.0066458
- Moulder, J. W. (1993). Why is Chlamydia sensitive to penicillin in the absence of peptidoglycan? *Infect. Agents Dis.* 2, 87–99.
- Neumann, S., Wessels, H. J. C. T., Rijpstra, W. I. C., Sinninghe Damsté, J. S., Kartal, B., Jetten, M. S. M., et al. (2014). Isolation and characterization of a prokaryotic cell organelle from the anammox bacterium *Kuenenia stuttgartiensis*. *Mol. Microbiol.* 94, 794–802. doi: 10.1111/mmi.12816
- Ouellette, S. P., Karimova, G., Subtil, A., and Ladant, D. (2012). Chlamydia co-opts the rod shape-determining proteins MreB and Pbp2 for cell division. *Mol. Microbiol.* 85, 164–178. doi: 10.1111/j.1365-2958.2012.08100.x
- Ouellette, S. P., Rueden, K. J., Gauliard, E., Persons, L., de Boer, P. A., and Ladant, D. (2014). Analysis of MreB interactors in Chlamydia reveals a RodZ homolog but fails to detect an interaction with MraY. *Front. Microbiol.* 5:279. doi: 10.3389/fmicb.2014.00279
- Patin, D., Bostock, J., Blanot, D., Mengin-Lecreulx, D., and Chopra, I. (2009). Functional and biochemical analysis of the Chlamydia trachomatis ligase MurE. *J. Bacteriol.* 191, 7430–7435. doi: 10.1128/JB.01029-09
- Patin, D., Bostock, J., Chopra, I., Mengin-Lecreulx, D., and Blanot, D. (2012). Biochemical characterisation of the chlamydial MurF ligase, and possible sequence of the chlamydial peptidoglycan pentapeptide stem. *Arch. Microbiol.* 194, 505–512. doi: 10.1007/s00203-011-0784-8
- Pilhofer, M., Aistleitner, K., Biboy, J., Gray, J., Kuru, E., Hall, E., et al. (2013). Discovery of chlamydial peptidoglycan reveals bacteria with murein sacculi but without FtsZ. *Nat. Commun.* 4:2856. doi: 10.1038/ncomms3856
- Pilhofer, M., Rappaport, K., Eckl, C., Bauer, A. P., Ludwig, W., Schleifer, K.-H., et al. (2008). Characterization and evolution of cell division and cell wall synthesis genes in the bacterial phyla Verrucomicrobia, Lentisphaerae, Chlamydiae, and Planctomycetes and phylogenetic comparison with rRNA genes. *J. Bacteriol.* 190, 3192–3202. doi: 10.1128/JB.01797-07
- Rivas-Marín, E., Canosa, I., Santero, E., and Devos, D. P. (2016). Development of genetic tools for the manipulation of the planctomycetes. *Front. Microbiol.* 7:914. doi: 10.3389/fmicb.2016.00914
- Sagulenko, E., Morgan, G. P., Webb, R. I., Yee, B., Lee, K.-C., and Fuerst, J. A. (2014). Structural studies of planctomycete gemmata obscuriglobus support cell compartmentalisation in a bacterium. *PLoS ONE* 9:e91344. doi: 10.1371/journal.pone.0091344
- Sangwan, P., Chen, X., Hugenholtz, P., and Janssen, P. H. (2004). Chthoniobacter flavus gen. nov., sp. nov., the first pure-culture representative of subdivision two, Spartobacteria classis nov., of the phylum Verrucomicrobia. *Appl. Environ. Microbiol.* 70, 5875–5881. doi: 10.1128/AEM.70.10.5875-5881.2004
- Santarella-Mellwig, R., Pruggnaller, S., Roos, N., Mattaj, I. W., and Devos, D. P. (2013). Three-dimensional reconstruction of bacteria with a complex endomembrane system. *PLoS Biol.* 11:e1001565. doi: 10.1371/journal.pbio.1001565
- Spring, S., Bunk, B., Spröer, C., Schumann, P., Rohde, M., Tindall, B. J., et al. (2016). Characterization of the first cultured representative of Verrucomicrobia subdivision 5 indicates the proposal of a novel phylum. *ISME J.* doi: 10.1038/ismej.2016.84 [Epub ahead of print].
- Stackebrandt, E., Wehmeyer, U., and Liesack, W. (1986). 16S ribosomal RNA and cell wall analysis of gemmata obscuriglobus, a new member of the order Planctomycetales. *FEMS Microbiol. Lett.* 37, 289–292. doi: 10.1111/j.1574-6968.1986.tb01810.x
- Tamura, A., Matsumoto, A., Manire, G. P., and Higashi, N. (1971). Electron microscopic observations on the structure of the envelopes of mature elementary bodies and developmental reticulate forms of Chlamydia psittaci. *J. Bacteriol.* 105, 355–360.
- van Niftrik, L. (2013). Cell biology of unique anammox bacteria that contain an energy conserving prokaryotic organelle. *Antonie Van Leeuwenhoek* 104, 489–497. doi: 10.1007/s10482-013-9990-5
- van Teeseling, M. C. F., Mesman, R. J., Kuru, E., Espaillat, A., Cava, F., Brun, Y. V., et al. (2015). Anammox Planctomycetes have a peptidoglycan cell wall. *Nat. Commun.* 6:6878. doi: 10.1038/ncomms7878
- Wagner, M., and Horn, M. (2006). The Planctomycetes, Verrucomicrobia, Chlamydiae and sister phyla comprise a superphylum with biotechnological and medical relevance. *Curr. Opin. Biotechnol.* 17, 241–249. doi: 10.1016/j.copbio.2006.05.005
- Wang, Y., Kahane, S., Cutcliffe, L. T., Skilton, R. J., Lambden, P. R., and Clarke, I. N. (2011). Development of a transformation system for Chlamydia trachomatis: restoration of glycogen biosynthesis by acquisition of a plasmid shuttle vector. *PLoS Pathog.* 7:e1002258. doi: 10.1371/journal.ppat.1002258
- White, C. L., Kitich, A., and Gober, J. W. (2010). Positioning cell wall synthetic complexes by the bacterial morphogenetic proteins MreB and MreD. *Mol. Microbiol.* 76, 616–633. doi: 10.1111/j.1365-2958.2010.07108.x
- Yoon, J., Matsuo, Y., Adachi, K., Nozawa, M., Matsuda, S., Kasai, H., et al. (2008a). Description of *Persicirhabdus sediminis* gen. nov., sp. nov., *Roseibacillus ishigakijimensis* gen. nov., sp. nov., *Roseibacillus ponti* sp. nov., *Roseibacillus persicus* sp. nov., *Luteolibacter pohnpeiensis* gen. nov., sp. nov. and *Luteolibacter algae* sp. nov., six marine members of the phylum “Verrucomicrobia”, and emended descriptions of the class Verrucomicrobiae, the order Verrucomicrobiales and the family Verrucomicrobiaceae. *Int. J. Syst. Evol. Microbiol.* 58, 998–1007. doi: 10.1099/ijsm.0.65520-0
- Yoon, J., Matsuo, Y., Katsuta, A., Jang, J.-H., Matsuda, S., Adachi, K., et al. (2008b). *Haloferula rosea* gen. nov., sp. nov., *Haloferula hareniae* sp. nov., *Haloferula phyci* sp. nov., *Haloferula helveola* sp. nov. and *Haloferula sargassicola* sp. nov., five marine representatives of the family Verrucomicrobiaceae within the phylum “Verrucomicrobia”. *Int. J. Syst. Evol. Microbiol.* 58, 2491–2500. doi: 10.1099/ijsm.0.2008/000711-0
- Yoon, J., Matsuo, Y., Matsuda, S., Adachi, K., Kasai, H., and Yokota, A. (2007a). *Cerasicoccus arenae* gen. nov., sp. nov., a carotenoid-producing marine representative of the family Punicicoccaceae within the phylum

- "Verrucomicrobia", isolated from marine sand. *Int. J. Syst. Evol. Microbiol.* 57, 2067–2072. doi: 10.1099/ijss.0.65102-0
- Yoon, J., Matsuo, Y., Matsuda, S., Adachi, K., Kasai, H., and Yokota, A. (2007b). *Rubritalea spongiae* sp. nov. and *Rubritalea tangerina* sp. nov., two carotenoid- and squalene-producing marine bacteria of the family Verrucomicrobiaceae within the phylum "Verrucomicrobia", isolated from marine animals. *Int. J. Syst. Evol. Microbiol.* 57, 2337–2343. doi: 10.1099/ijss.0.65243-0
- Yoon, J., Matsuo, Y., Matsuda, S., Kasai, H., and Yokota, A. (2010). *Cerasicoccus maritimus* sp. nov. and *Cerasicoccus frondis* sp. nov., two peptidoglycan-less marine verrucomicrobial species, and description of Verrucomicrobia phyl. nov., nom. rev. *J. Gen. Appl. Microbiol.* 56, 213–222. doi: 10.2323/jgam.56.213

Conflict of Interest Statement: The authors declare that the research was conducted in the absence of any commercial or financial relationships that could be construed as a potential conflict of interest.

Copyright © 2016 Rivas-Marín, Canosa and Devos. This is an open-access article distributed under the terms of the Creative Commons Attribution License (CC BY). The use, distribution or reproduction in other forums is permitted, provided the original author(s) or licensor are credited and that the original publication in this journal is cited, in accordance with accepted academic practice. No use, distribution or reproduction is permitted which does not comply with these terms.



OPEN ACCESS

Edited by:

Damien Paul Devos,
Universidad Pablo de Olavide, Spain

Reviewed by:

Marc Strous,
University of Calgary, Canada
Jonathan Badger,
National Cancer Institute, USA

***Correspondence:**

Lloyd Vaughan
vaughanl@vetpath.uzh.ch

†Present Address:

Alexander G. J. Fehr,
Institute of Microbiology and Infection,
School of Biosciences, University of
Birmingham, Birmingham, UK;

Maja Ruetten,
Pathovet AG, Tagelswangen,
Switzerland;

Helena M. B. Seth-Smith,
Clinical Microbiology, University
Hospital Basel, Basel, Switzerland and
Department of Biomedicine, University
of Basel, Basel, Switzerland;

Andrea Voegtlín,
Institute of Virology and Immunology,
Mittelhaeusern, Switzerland

Specialty section:

This article was submitted to
Evolutionary and Genomic
Microbiology,
a section of the journal
Frontiers in Microbiology

Received: 10 September 2016

Accepted: 01 November 2016

Published: 18 November 2016

Citation:

Fehr AGJ, Ruetten M, Seth-Smith HMB, Nufer L, Voegtlín A, Lehner A, Greub G, Crosier PS, Neuhauss SCF and Vaughan L (2016) A Zebrafish Model for Chlamydia Infection with the Obligate Intracellular Pathogen *Waddlia chondrophila*. *Front. Microbiol.* 7:1829. doi: 10.3389/fmicb.2016.01829

A Zebrafish Model for *Chlamydia* Infection with the Obligate Intracellular Pathogen *Waddlia chondrophila*

Alexander G. J. Fehr^{1†}, Maja Ruetten^{1†}, Helena M. B. Seth-Smith^{1,2†}, Lisbeth Nufer¹, Andrea Voegtlín^{3†}, Angelika Lehner⁴, Gilbert Greub⁵, Philip S. Crosier⁶, Stephan C. F. Neuhauss⁷ and Lloyd Vaughan^{1*}

¹ Vetsuisse Faculty, Institute for Veterinary Pathology, University of Zurich, Zurich, Switzerland, ² Functional Genomics Center Zurich, Molecular and Life Sciences, University of Zurich, Zurich, Switzerland, ³ Vetsuisse Faculty, Institute of Veterinary Bacteriology, University of Zurich, Zurich, Switzerland, ⁴ Vetsuisse Faculty, Institute for Food Safety and Hygiene, University of Zurich, Zurich, Switzerland, ⁵ Institute of Microbiology, University Hospital Center and University of Lausanne, Lausanne, Switzerland, ⁶ Department of Molecular Medicine and Pathology, School of Medical Sciences, University of Auckland, Auckland, New Zealand, ⁷ Institute of Molecular Life Sciences, University of Zurich, Zurich, Switzerland

Obligate intracellular chlamydial bacteria of the Planctomycetes-Verrucomicrobia-Chlamydiae (PVC) superphylum are important pathogens of terrestrial and marine vertebrates, yet many features of their pathogenesis and host specificity are still unknown. This is particularly true for families such as the *Waddliaceae* which, in addition to epithelia, cellular targets for nearly all *Chlamydia*, can infect and replicate in macrophages, an important arm of the innate immune system or in their free-living amoebal counterparts. An ideal pathogen model system should include both host and pathogen, which led us to develop the first larval zebrafish model for chlamydial infections with *Waddlia chondrophila*. By varying the means and sites of application, epithelial cells of the swim bladder, endothelial cells of the vasculature and phagocytosing cells of the innate immune system became preferred targets for infection in zebrafish larvae. Through the use of transgenic zebrafish, we could observe recruitment of neutrophils to the infection site and demonstrate for the first time that *W. chondrophila* is taken up and replicates in these phagocytic cells and not only in macrophages. Furthermore, we present evidence that myeloid differentiation factor 88 (MyD88) mediated signaling plays a role in the innate immune reaction to *W. chondrophila*, eventually by Toll-like receptor (TLRs) recognition. Infected larvae with depleted levels of MyD88 showed a higher infection load and a lower survival rate compared to control fish. This work presents a new and potentially powerful non-mammalian experimental model to study the pathology of chlamydial virulence *in vivo* and opens up new possibilities for investigation of other members of the PVC superphylum.

Keywords: zebrafish, PVC superphylum, *Chlamydia*, *Waddlia*, swim bladder infection, endothelial cells, neutrophils, MyD88

INTRODUCTION

The bacterial species *Waddlia chondrophila* is a purported abortifacient pathogen of cattle (Dilbeck-Robertson et al., 2003), first isolated from a cow abortion in the United States (Dilbeck et al., 1990) and subsequently from a similar case in Germany (Henning et al., 2002). The *Waddliaceae* is one of eight families described to date, within the phylum *Chlamydiae* (Collingro et al., 2011; Taylor-Brown et al., 2015), all of which are obligate intracellular pathogens able to infect a variety of hosts covering much of the animal kingdom. The best known family of this phylum is the *Chlamydiaceae*, classical pathogens of humans and animals, some of which are known for their high zoonotic potential and ability to cross species borders, such as *Chlamydia psittaci*, the agent of psittacosis in birds and humans and *Chlamydia abortus*, an agent of fetal death and abortion in ruminants and humans (Longbottom and Coulter, 2003). *Waddlia chondrophila* may similarly pose a zoonotic risk, based on evidence from serological tests and quantitative real-time PCR in cases of human miscarriage and respiratory disease (Baud et al., 2007, 2011, 2014; Haider et al., 2008; Goy et al., 2009). A marked difference to the *Chlamydiaceae*, however, is the additional ability of *W. chondrophila* to infect and replicate in phagocytic cells, including macrophages and free-living amoebae, at least *in vitro* (Goy et al., 2008; Lamothe and Greub, 2010). This considerably complicates experiments to uncover the infection mechanisms and routes *W. chondrophila* uses *in vivo*, adding to the intrinsic difficulty of tracing infectious processes in whole animals. This knowledge is, however, key to the design and application of effective treatment strategies for the *Waddliaceae* in particular and for the *Chlamydiae* as a whole.

In vitro data indicates that *Waddlia* may be able to infect quite different hosts, widening the choice available when considering model organisms. The first cultivation of *W. chondrophila* was achieved in bovine turbinate cells and mouse macrophages (Dilbeck et al., 1990; Kocan et al., 1990). Subsequent *in vitro* studies showed that *W. chondrophila* is potentially a highly versatile pathogen, able to infect and replicate in McCoy cells, buffalo green monkey cells, human fibroblasts (Henning et al., 2002), Vero cells, human pneumocytes and endometrial cells (Kebbi-Beghdadi et al., 2011b), as well as in human macrophages (Goy et al., 2008). During the infection of macrophages, *W. chondrophila* avoids degradation by successfully preventing the fusion of the endosome with a lysosome and relocating in a vacuole expressing endoplasmic reticulum (ER) markers (Croxatto and Greub, 2010). Freshwater amoebae of the genus *Acanthamoeba* are also susceptible to infection with *W. chondrophila* (Lamothe and Greub, 2010). Furthermore, *W. chondrophila* was recently found to be able to invade and proliferate in two fish cell lines derived from fathead minnow (*Pimephales promelas*; EPC-175) and rainbow trout (*Oncorhynchus mykiss*; RTG-2) (Kebbi-Beghdadi et al., 2011a). In addition to mammalian hosts, *W. chondrophila* has been isolated from aquatic environments as diverse as sediments from the eastern Mediterranean Sea (Polymenakou et al., 2005) and freshwater samples from well water sources in Spain (Codony et al., 2012). According to these findings, it has been speculated

that freshwater protists and fish could potentially serve as an aquatic reservoir for *W. chondrophila*, that one possible transmission route is water-borne and by inference, that fish may not only be a valuable alternative model but also a natural host.

Indeed, chlamydial disease affects both marine as well as freshwater fishes causing the disease epitheliocystis (Hoffman et al., 1969; Draghi et al., 2004; Meijer et al., 2006; Stride et al., 2014) in which bacteria-filled intracellular inclusions are found infecting gill and skin epithelia. Several chlamydial agents of epitheliocystis have been described so far, some of which are closely related to the *Waddliaceae* such as *Ca. Clavichlamydia salmonicola* (Karlsen et al., 2008), *Ca. Syngnamydia venezia* (Fehr et al., 2013) and *Ca. Syngnamydia salmonis* (Nylund et al., 2015), whereas others are more distantly related such as members of the deep rooted Piscichlamydia clade, *Ca. Piscichlamydia salmonis* (Draghi et al., 2004; Schmidt-Posthaus et al., 2012), *Ca. Parilichlamydiaceae* (Stride et al., 2013a), *Ca. Similichlamydiaceae* (Stride et al., 2013b,c; Steigen et al., 2015; Seth-Smith et al., this issue), and *Ca. Actinochlamydiaceae* (Steigen et al., 2013). In a ground breaking study, Lagkouvardos and colleagues discovered up to 181 new putative families of the *Chlamydiae* from primarily marine and fresh water sources, of which the *Waddliaceae* formed a prominent clade (Lagkouvardos et al., 2014).

Expanding genomic information has greatly improved our understanding of potential mechanisms underlying host diversity and disease pathology and is an essential step for establishing a model pathogen-host system. The availability of the *W. chondrophila* genome provided precious information on putative virulence factors of these bacteria (Bertelli et al., 2010), however, there is a great need to develop animal models to test the ideas coming from these efforts (Bachmann et al., 2014). Ideally, such an animal model would lend itself to high throughput screening and share an immune system with close similarities to that of humans and other animal hosts. As a model organism in infection biology, the zebrafish (*Danio rerio*) has become increasingly popular. Many infection systems using larval and adult zebrafish have been successfully developed over the past decade (Kanther and Rawls, 2010; Meijer and Spaink, 2011; Fehr et al., 2015). Its small size, ease of breeding, high fertility and genetic tractability combined with transparent larval stages combine to make it an attractive model organism for science. The zebrafish immune system displays many similarities to that of mammals, with counterparts for most of the human immune cell types (Meeker and Trede, 2008) and have conserved mechanisms for the recognition of microbes like Toll-like receptors (TLRs) (Hall et al., 2009). The zebrafish innate immune system starts to develop as early as 24 h post fertilization (hpf) with a population of primitive macrophages which derive from cells located in a region of the yolk sac near the heart (Herbomel et al., 1999). At 2 days post fertilization (dpf), subpopulations of macrophages can already be observed throughout the organism along with neutrophils whose development initiates between 32 and 48 hpf. The development of the adaptive immune system lags behind, with the first lymphocytes observed from 4 dpf, although fully developed adaptive immunity takes another 4 weeks to mature (Meijer and Spaink, 2011). For this reason, it is possible to

exclusively observe the reaction of the innate immune system within an infection during the first week of larval development. Previous studies have proposed that recognition by TLRs could mediate an efficient immune reaction against chlamydial infection leading to bacterial clearance (Naiki et al., 2005), while in other cases TLR dependent recruitment of innate immune cells had an adverse effect by enhancing the bacterial load during an infection (Rodriguez et al., 2005). The activation of TLRs initiates an inflammatory response through signaling cascades that lead to cytokine production which promote recruitment of leukocytes to the infection site and phagocytosis of invading pathogens (Newton and Dixit, 2012). A key factor for TLR signal transduction is the downstream adaptor molecule MyD88, which interacts with all known TLRs and members of the interleukin-1 receptor (IL-1R) family, resulting in the induction of nuclear factor-kappaB (NF- κ B) and mitogen-activated protein kinase (MAPK) signaling (Medzhitov et al., 1998; Warner and Nunez, 2013).

Zebrafish larvae have been used to study infections of many different bacterial pathogens like *Mycobacterium marinum*, *Salmonella typhimurium*, *Vibrio anguillarum*, *Listeria monocytogenes*, *Pseudomonas aeruginosa*, *Burkholderia cenocepacia*, *Staphylococcus aureus*, *Streptococcus iniae*, *Shigella flexneri*, and *Cronobacter turicensis* (Herbomel et al., 1999; Davis et al., 2002; van der Sar et al., 2003; O'Toole et al., 2004; Brannon et al., 2009; Clatworthy et al., 2009; Levraud et al., 2009; Vergunst et al., 2010; Adams et al., 2011; Prajsnar et al., 2012; Harvie et al., 2013; Mostowy et al., 2013; Fehr et al., 2015). However, none of these pathogens are obligate intracellular bacteria. By developing an infection model with *W. chondrophila*, we demonstrate the first zebrafish infection model for an obligate intracellular pathogen and member of the Chlamydiae. We established alternate routes of infection and analyzed preferred target cells for *Waddlia* infection *in vivo* and have taken initial steps to elucidate molecular mechanisms regulating infection, including the impact of MyD88 signaling in knockdown larvae.

MATERIALS AND METHODS

Zebrafish Strains and Husbandry

Zebrafish (*D. rerio*) strains used in this study were predominantly *albino* mutants (*slc45a2^{b4/+}*) and transgenic fish of the *Tg(lyz:DsRED2)nz50* line that produce red fluorescent protein in cells of the myelomonocytic lineage able to migrate to inflammatory sites and phagocytose bacteria (Hall et al., 2007), primarily neutrophils from 50 h post fertilization (hpf) (Clatworthy et al., 2009). In addition, the *Tg(fli1a:eGFP)* line which produces green fluorescent protein in endothelial cells, was used to visualize the vascular system (Lawson and Weinstein, 2002). Adult fish were kept at a 14/10 h light/dark cycle at a pH of 7.5 and 27°C. Eggs were obtained from natural spawning between adult fish which were set up pairwise in separate breeding tanks. Embryos were raised in petri dishes with E3 medium (5 mM NaCl, 0.17 mM KCl, 0.33 mM CaCl₂, 0.33 mM MgSO₄) containing 0.3 µg/ml of methylene blue at 28°C. From 24 hpf, 0.003% 1-phenyl-2-thiourea (PTU) was added to prevent melanin synthesis. The *albino* mutants lack

melanised melanophores, and for these PTU treatment was not necessary. Staging of embryos was performed according to Kimmel et al. (1995).

Research was conducted with ethics approval (no. 216/2012) from the animal research ethics committee of the Veterinary Office, Public Health Department, Canton of Zurich (Switzerland). Larvae were maintained up until 7 days post fertilization (dpf), at which time all were euthanized by applying an overdose of 4 g/l buffered tricaine (MS-222, Ethyl 3-aminobenzoate methanesulfonate, Sigma-Aldrich) in accordance with ethical procedures.

Bacterial Cultures

Waddlia chondrophila strain WSU 86-1044 (ATCC VR-1470) were grown within *Acanthamoeba castellanii* strain ATCC 30010 in 25 cm² cell culture flasks containing 10 ml of peptone yeast extract glucose (PYG) broth (Greub and Raoult, 2002). Cultures were harvested after 5 days and filtered through a 5 µm membrane to remove remaining amoebae. The flow-through was centrifuged at 7000 g for 15 min. The resulting pellet of bacterial elementary bodies (EBs) was then suspended in E3 medium for bath immersion or phosphate buffered saline (PBS) for microinjection experiments. The infectivity of *W. chondrophila* was tested in Epithelioma Papulosum Cyprini (EPC) cells, to investigate the infection process and morphology of the bacteria in these fish epithelial cells (Supplementary Material Figure S1). Subsequently, Inclusion Forming Units (IFU) of the cultures were determined by infecting monolayers of EPC cells in 24-well plates with a 10-fold dilution series of 1 µl of the bacterial suspension at 28°C. After 24 h cells were fixed with 4% paraformaldehyde and subsequently stained with a primary rabbit anti-*Waddlia* antibody and detected with a secondary goat anti-rabbit-IgG conjugated to a fluorescent AlexaFluor dye. After imaging with a fluorescent microscope, inclusions were counted in Imaris (Bitplane) to calculate a mean IFU value.

Bath Immersion Experiments

Zebrafish embryos between 24 hpf and 4 dpf were incubated in groups of 15 for each time point and each condition in 24-well plates with E3 medium containing 2 × 10⁹ IFU/ml of *W. chondrophila* at 28°C. Embryos younger than 48 hpf were manually dechorionated prior to immersion. After 4 h of incubation embryos were washed twice in fresh E3 medium and transferred to 6-well plates containing 4 ml of E3 medium per well and further incubated at 28°C. Embryos were then observed under a binocular microscope for signs of disease and survival twice a day. At several time points embryos from each group were euthanized in E3 medium containing 4 mg/ml buffered tricaine (MS-222).

Microinjection Experiments

For microinjections of *W. chondrophila* into zebrafish larvae bacteria were first harvested from a 5 days old amoebal co-culture as described above. The concentration of the *W. chondrophila* EBs was adjusted to 1000–2000 IFU/nl in PBS and 0.085% phenol red was added to visualize the injection procedure. Injections were done using pulled borosilicate glass microcapillary injection

needles (Science Products, 1210332, 1 mm O.D. × 0.78 mm I.D.) and a PV830 Pneumatic PicoPump (World Precision Instruments). Prior to intravenous injections embryos of 2 dpf were manually dechorionated and anaesthetised with 200 mg/l buffered tricaine (MS-222). Afterwards embryos were aligned on an agar plate and injected with 1 nl of the *W. chondrophila* suspension into the Duct of Cuvier, also known as common cardinal vein. Prior determination of the injected volume was performed by injection of a droplet into mineral oil and measurement of its approx. diameter over a scale bar. For swim bladder injections 4 dpf larvae were treated similarly but dechorionisation was not necessary because larvae were already hatched. 4 dpf larvae were then injected with a volume of 2 nl into the lumen of the swim bladder. After injections, infected larvae were allowed to recover in a petri dish with fresh E3 medium for 15 min. Subsequently, larvae were transferred in 6-well plates in groups of about 15 larvae in 4 ml E3 medium per well, incubated at 28°C and observed under a stereomicroscope twice a day. Samples for Immunofluorescence (IF), Transmission Electron Microscopy (TEM) and quantitative Polymerase Chain Reaction (qPCR) were taken at 0, 12, 24, 36, 48, 60 and 72 h post infection (hpi). Sampled larvae were euthanized with an overdose of 4 g/l buffered tricaine and transferred into different buffers and fixatives for subsequent analyses respectively.

Whole Mount Immunofluorescence (IF) and Histological Stainings

For IF stainings, whole zebrafish larvae were fixed in 4 % paraformaldehyde at 4°C overnight followed by 100 % methanol overnight at -20°C. Samples were rehydrated in 50% methanol for 5 min and subsequently in H₂O for 1 h before blocking in PBST (PBS containing 1% BSA, 1% DMSO, 0.5% Triton X-100, 2.5% goat serum) for 6–8 h at room temperature. Larvae were then incubated with primary antibody overnight at 4°C. Primary antibody was detected by incubation with a secondary goat anti-IgG antibody conjugated to a fluorescent AlexaFluor

dye (Life Technologies) at 4°C overnight. Additionally 4'-6-diamin-2-phenylindole (DAPI) was added to visualize bacterial and host DNA. Stained larvae were prepared for microscopy on objective slides mounted in 1.5% agarose, 50% glycerol and screened under a fluorescence microscope. Positive samples were subsequently screened in more detail for *W. chondrophila* inclusions by Confocal Laser Scanning Microscopy (CLSM).

For histological examination, whole zebrafish larvae were fixed in 4% paraformaldehyde at 4°C and embedded in cubes of cooked egg white in order to position them correctly for histological sections. These cubes containing the larvae were dehydrated in an ascending alcohol series ending in xylene and afterwards embedded in paraffin. Paraffin blocks were cut in 2–3 μm thin sections, mounted on glass slides and stained using a routine protocol for haematoxylin and eosin (HE) staining.

Light-Microscopy and Image Analysis

Overview images were taken with an upright light microscope (Olympus BX61) with both bright field and fluorescence modules. The fluorescence filter cube used was optimized for DAPI/FITC/TRIC. For higher resolution images, 3D-image stacks of whole mount samples were prepared using CLSM (Leica TCS SP5, Leica Microsystems). Various combinations of the fluorophors AlexaFluor dyes 594, 546, 488, GFP, dsRED, and DAPI were sequentially excited in descending series with the 594, 561, 488, and 405 nm laser lines, with emission signals collected within the respective range of wave lengths. Three-dimensional image stacks were collected sequentially (to prevent blue-green-red channel cross-talk) and according to Nyquist criteria and deconvolved using HuygensPro via the Huygens Remote Manager v2.1.2 (SVI, Netherlands). Images were further analyzed with Imaris 7.6.1 (Bitplane, Zurich, Switzerland) and aligned with Adobe Photoshop Elements 12. Fluorescent cells were quantified with the Imaris fluorescent spot counting tool.

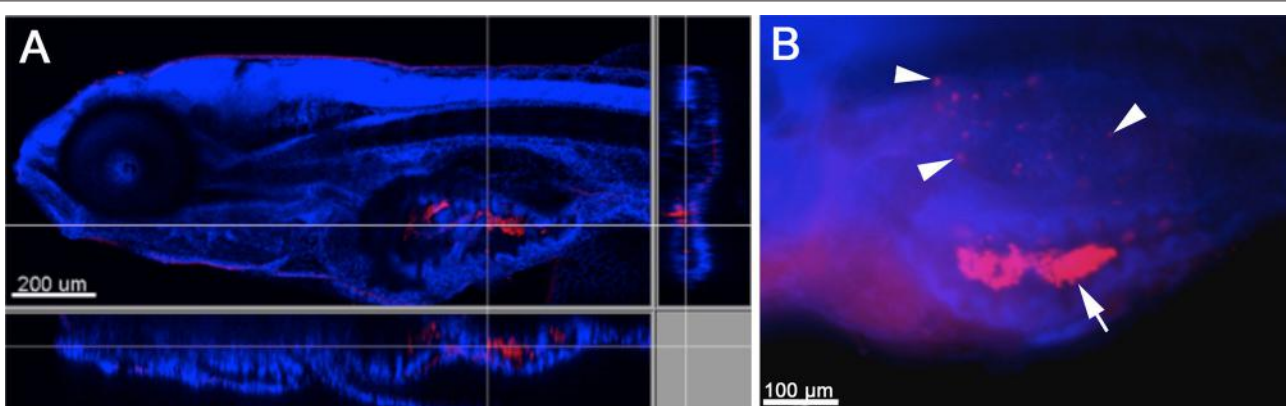


FIGURE 1 | Infection of zebrafish larvae with *W. chondrophila* via bath-immersion at 4 dpf followed by IF staining with an anti-*Waddlia* antibody (red) and DAPI (blue). Section view of a CLSM acquired 3D stack of a larva at 4 hpi. The section view exhibits a large amount of swallowed *W. chondrophila* inside the lumen of the intestine (**A**). Fluorescence light-microscope appearance of the trunk region of a larva at 48 hpi shows in addition to the accumulation of *W. chondrophila* in the gut lumen (arrow), an infection of the swim bladder with bacterial inclusions (arrow heads) visible inside the epithelium (**B**).

Transmission Electron Microscopy

For electron microscopy, larvae were fixed in a mixed solution of 1% paraformaldehyde and 2.5% glutaraldehyde in 0.1 M sodium phosphate buffer, pH 7.5 at 4°C overnight. Samples were prepared by embedding into epoxy resin and for TEM

microscopy according to standard procedures. Epoxy resin blocks were screened for larval location using semithin sections (1 µm) which were stained with toluidine blue (Sigma-Aldrich) to visualize tissue. Ultrathin sections (80 nm) were mounted on copper grids (Merck Eurolab AG, Dietlikon, Switzerland),

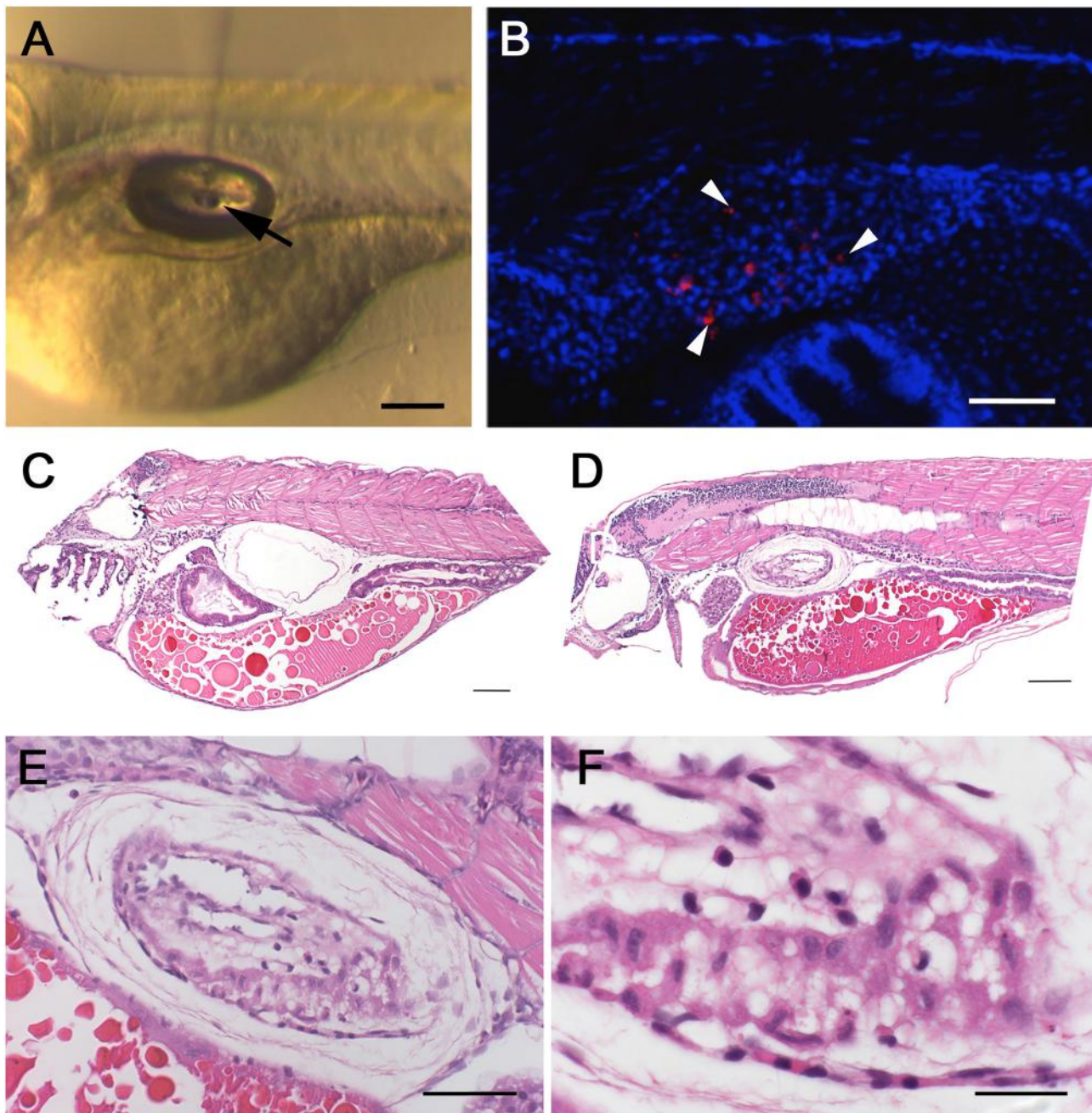


FIGURE 2 | **Swim bladder infection in 4–5 dpf old larvae.** Microinjection of *W. chondrophila* EBs directly into the lumen of the swim bladder of 4 dpf larvae. A drop of approx. 1 nl of the bacterial suspension can be seen hanging on the tip of the injection needle (arrow) inside the air filled lumen of the swim bladder (**A**). CLSM acquired 3D stack of the trunk region of a larva at 36 hpi, after IF staining with an anti-*Waddlia* antibody (red) and DAPI (blue). The swim bladder in the center of the image exhibits several bacterial inclusions (arrow heads) inside the epithelium (**B**). Histology on HE-stained sections of the swim bladder of a PBS injected control larva (**C**) with normal appearance and of an infected larva (**D**) showing clear pathological changes, including thickening of the epithelium (**E**) and infiltration of innate immune cells like macrophages and neutrophils (**F**). Scale bars (**A–D**) 100 µm, (**E**) 50 µm, and (**F**) 20 µm.

contrasted with uranyl acetate dihydrate (Sigma-Aldrich) and lead citrate (Merck Eurolab AG) and investigated using a Philips CM10 transmission electron microscope. Images were processed with Imaris (Bitplane) and assembled for publication using Adobe Photoshop.

Quantitative PCR

A qPCR system was designed against the 16S rRNA gene from *W. chondrophila* (forward: 5'-AGTCGGCTACACCAAGTATGC-3', reverse: 5'-TGGCGAAGGCCGTTTC-3', probe: 5'-FAM-TTCGCTCCCCTAGCTTCGGGCAT-TAMRA-3'), allowing quantification of the bacterial load of individual infected larvae. The TaqMan qPCR system was designed and validated against quantified serial dilutions of the target sequence cloned into the pCR2.1 plasmid and against total DNA extracts of non-infected larvae. Serial dilutions of pCR2.1 containing the target sequence were used as standards in each run. Total DNA of individual larvae was extracted with a MagNA Pure LC (Roche) robot and eluted in 100 µl elution buffer. Reactions were carried out on a StepOne Plus real-time PCR system (Applied Biosystems). TaqMan Fast Advanced reagents (Applied Biosystems) were used according to the manufacturer's instructions with 5 µl input DNA in a total reaction volume of 20 µl.

Morpholino Knockdown

Knockdown of MyD88 expression was done by standard microinjection of 1 nl of a 5 mM solution of anti-Myd88 morpholino (5'-GTTAACACTGACCCTGTGGATCAT-3', Gene Tools; Bates et al., 2007; Cambier et al., 2014) into the early zygote immediately after fertilization using borosilicate glass microcapillary injection needles (Harvard Apparatus, 30-0019, 1 mm O.D. × 0.58 mm I.D.) and an Eppendorf FemtoJet. A group of control larvae was injected with 1 nl of a control morpholino (5'-CCTCTTACCTCAGTTACAATTATA-3', Gene Tools) with no known target in zebrafish at the same concentration in parallel. Levels of MyD88 protein in morphant and control larvae were analyzed by Western Blot at 3, 4, and 5 dpf with a mouse

anti-myd88 antibody, detected with a goat anti-mouse-IgG antibody conjugated to horseradish peroxidase (HRP).

RESULTS

W. chondrophila is capable of infecting Zebrafish Larvae via Bath-Immersion

In order to first establish whether *W. chondrophila* can infect zebrafish through an oral or dermal route, embryos and larvae of different stages were incubated in a suspension of *W. chondrophila* infectious particles or EBs, in a bath-immersion experiment. While younger embryos and larvae of up to 72 hpf (hours post fertilization) stages could not be infected with this method, 4 dpf (days post fertilization) larvae appeared to swallow (Figure 1A) the bacteria and interestingly, succumbed to an infection of their swim bladder which we detected by IF staining (Figure 1B).

Swim Bladder Infection Can Be Provoked via Microinjection

The swim bladder provides the only possibility to examine infections of air-exposed epithelium in fish and, as such, is a putative model for equivalent epithelia in humans, in particular the lungs. In this context, the spontaneous bath-immersion induced infection of the swim bladder and especially the attachment to the cilia of the epithelium was an exciting finding, although infection via bath immersion carried inherent experimental variability due to varying local concentrations of *W. chondrophila* and different gulping rates of individual larvae. Therefore, we tried direct microinjection of 10³ *W. chondrophila* EBs into the swim bladder lumen of 4 dpf larvae (Figure 2A). The resulting infection was comparable to that seen using bath-immersion but under more controlled conditions, confirming that directed injection can be used as a more reproducible method of establishing infection. In addition to live *W. chondrophila*, two groups of control embryos were injected with either heat-inactivated *W. chondrophila* or PBS in parallel.

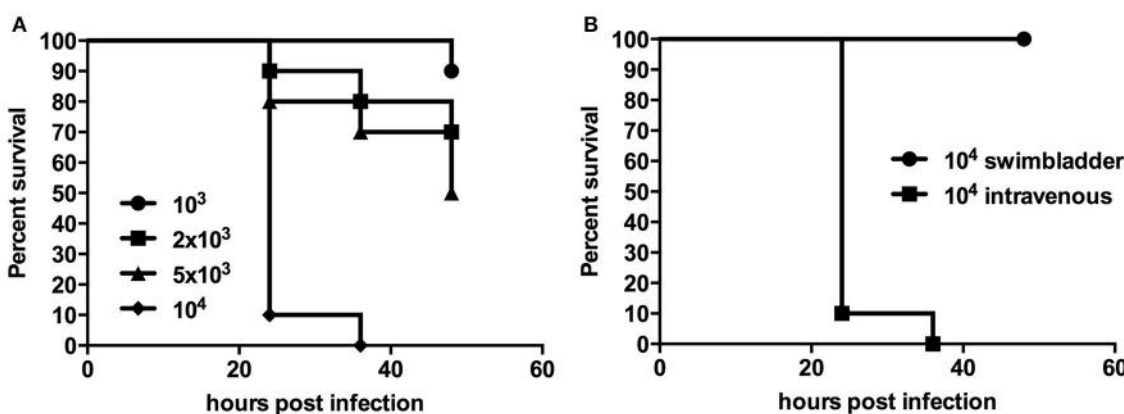


FIGURE 3 | Survival rates of larvae with a systemic infection after injection of different dosages of *W. chondrophila* show diminished survival with increasing dosage (A), while injection into the swim bladder has no impact on larval survival (B).

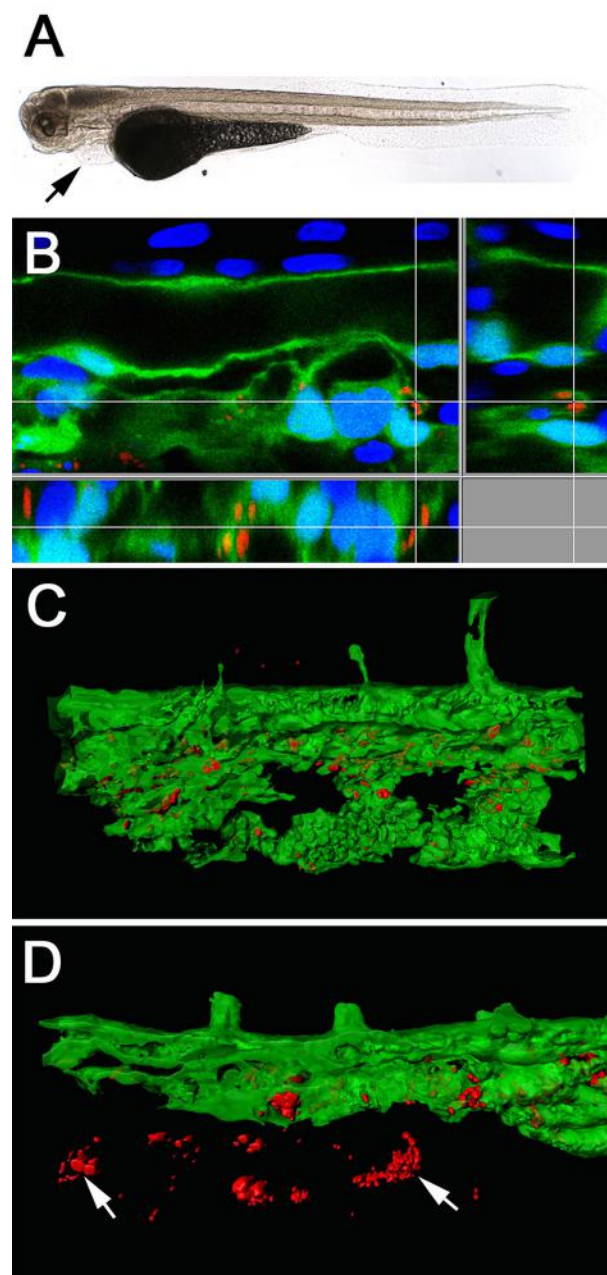


FIGURE 4 | Light-microscope appearance of a transgenic *Tg(fli1a:eGFP)* larva at 48 hpi after intravenous injection of live bacteria (**A**), showing an impaired blood flow ending in an almost completely stopped circulation, accompanied by pericardial oedema formation (arrow). Section view of a CLSM acquired 3D stack (**B**) after IF staining with an anti-*Waddlia* antibody, showing the infection of GFP expressing endothelial cells (green) with *W. chondrophila* (red). Host cell nuclei were stained with DAPI (blue). Surface rendering of the tail artery and caudal vein shows the distribution of the inclusions inside the vasculature at 24 hpi (**C**) and 36 hpi (**D**), showing bacterial spread across endothelial bounds (arrows).

Samples were taken at 4, 24, 48, 72, and 96 hpi and screened for the presence of *W. chondrophila* inclusions by confocal laser scanning microscopy CLSM (Laser Scanning Microscopy)

and TEM (Transmission Electron Microscopy). *W. chondrophila* inclusions were detected in the epithelium of the swim bladder as well as in adjacent tissues at 24–48 hpi (**Figure 2B**). In haematoxylin and eosin (HE) stained samples, the swim bladder walls of infected larvae were markedly thickened when compared with control animals (**Figures 2C,D**). The epithelial cells lining the cavity were piled up and were no longer a single cell row, with the cells themselves exhibiting a cuboidal instead of a flattened morphology (**Figure 2E**). The epithelium was surrounded by a moderate proliferation of fibroblasts resulting in a fibrosis, as has been described in mice for chlamydial lung infections (Jupelli et al., 2013). Neutrophils were also found to have migrated into the epithelial cell layers (**Figure 2F**). No increase in mortality was observed up until the end of the observation period of 3 days post infection (dpi) and infected larvae showed no altered behavior compared to control larvae.

Intravenous Microinjection of *W. chondrophila* Causes a Systemic Infection

Chlamydial infection of vascular tissue has been an area of intense interest in the past, and not without controversy in respect to atherosclerosis (recently reviewed by Campbell and Rosenfeld (2014)). It is also an aspect which is difficult to follow *in vivo* in other animal models but which is readily accessible in younger zebrafish larval stages by intravenous injection. We injected 48 hpf embryos intravenously via the Duct of Cuvier, also known as common cardinal vein with 10^3 – 10^4 *W. chondrophila* EBs. In comparison to the non-lethal swim bladder infection, a systemic infection caused a dosage dependent mortality rate of injected larvae (**Figures 3A,B**). The injection resulted in a rapid systemic infection with mortalities up to 100% within the first 24 h for the highest tested dosage (10^4) and a LD₅₀ within 48 hpi of approximately 5×10^3 . A dosage of 2×10^3 *W. chondrophila* EBs was chosen for the following experiments to produce moderate mortalities of between 20 and 30% at 72 hpi. With that dosage larvae showed an increasingly impaired blood circulation between 24 and 48 hpi, resulting in the formation of a pericardial oedema (**Figure 4A**). Histologically, no tissue alterations could be seen.

To follow the distribution of *W. chondrophila* in the vascular system we used the transgenic *Tg(fli1a:eGFP)* line, which expresses green fluorescent protein in all endothelial cells. Tracking the infection with IF using an anti-*Waddlia* antibody, the maximal number of *W. chondrophila* inclusions were found at 36–48 hpi, distributed throughout the whole embryo, and with inclusions located both within the vasculature and beyond the bounds of the endothelium (**Figures 4B–D**). Cell types that were identified to be susceptible to *W. chondrophila* invasion during a systemic infection were predominantly endothelial cells and phagocytosing innate immune cells. Especially in regions where the blood is flowing more slowly, such as the fine capillary network of the tail muscles and veins, infection of the endothelium was more common.

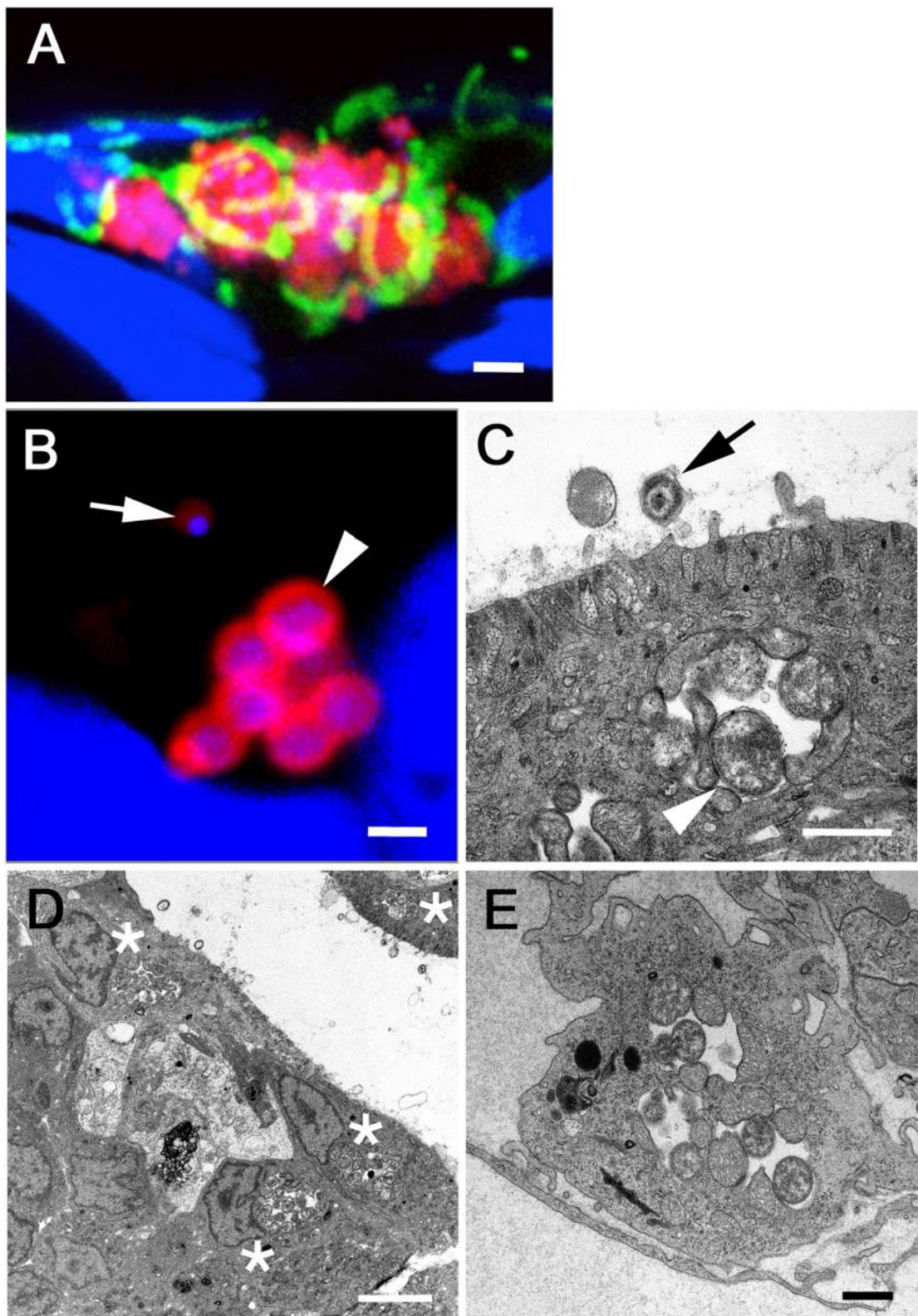


FIGURE 5 | CLSM acquired 3D image of *W. chondrophila* inclusions inside the swim bladder epithelium (A) after IF staining of *Waddlia* (red), mitochondria (green) and DAPI staining of host cell and bacterial DNA (blue). The image shows the formation of several bacteria containing vacuoles inside epithelial cells,

(Continued)

FIGURE 5 | Continued

accompanied by the recruitment and close association with host cell mitochondria. Close-ups of single inclusions with CLSM (**B**) and TEM (**C**) reveal typical features of the chlamydial life cycle, such as transformation from the smaller infectious EB with condensed DNA (arrow) to the larger and metabolically active RB form with finely distributed chromatin (arrow head), dividing inside the vacuole. TEM images show also the morphology of infected epithelial cells of the swim bladder (**D**) and endothelial cells of blood vessels (**E**), usually containing a single perinuclear inclusion (asterisks), strongly associated with host cell mitochondria. Scale bars (**A**) 2 μm , (**B,C,E**) 1 μm and (**D**) 5 μm .

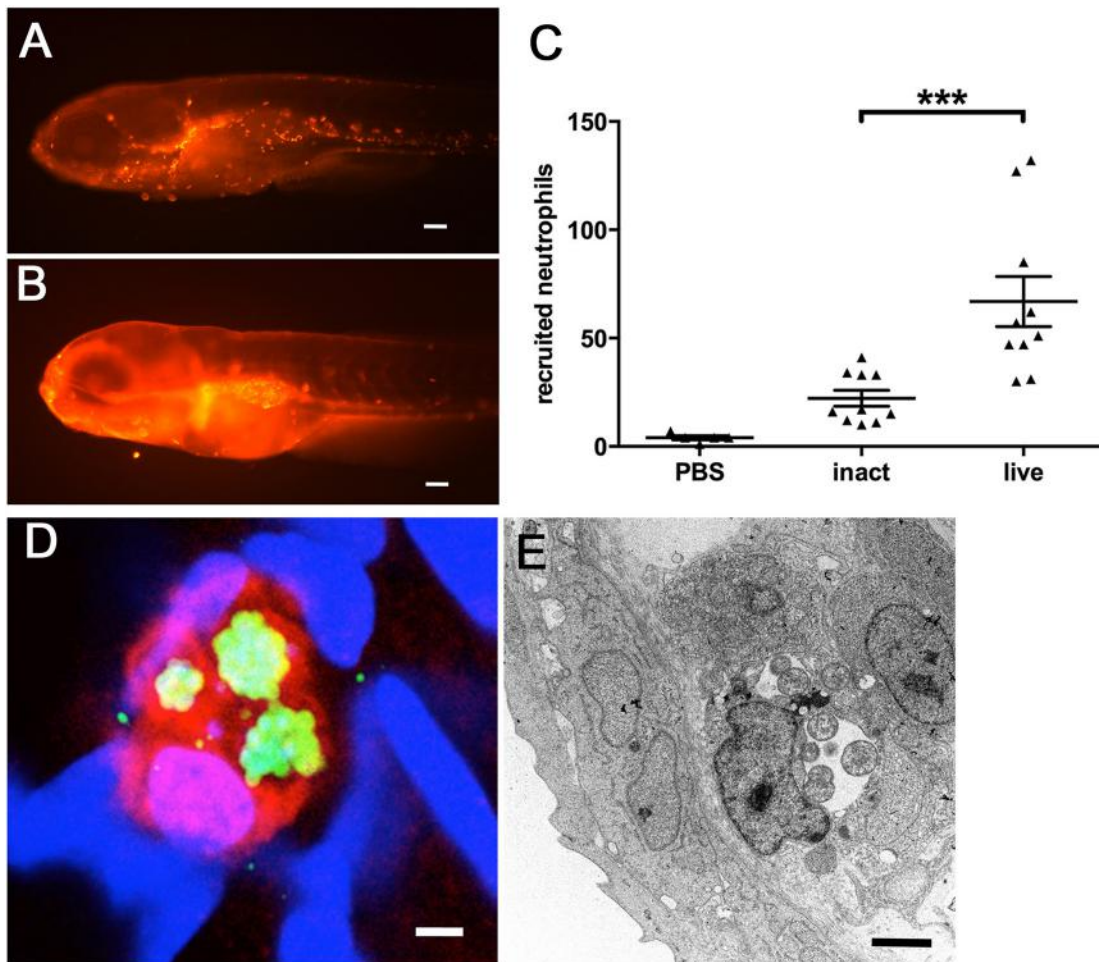


FIGURE 6 | Neutrophil recruitment and uptake of *W. chondrophila* monitored in transgenic Tg(lyzC:dsRed^{nz50}) larvae at 8 hpi. Whilst the swim bladder of a healthy larva is usually nearly devoid of innate immune cells (**A**), the injection of *W. chondrophila* into the swim bladder activates strong neutrophil recruitment (**B**). Quantification of recruited neutrophils (**C**) shows a significantly increased reaction to live *W. chondrophila* (live) compared to heat-inactivated (inact) bacteria or with sterile PBS injected control larvae, ***p < 0.001. After the uptake by a neutrophil *W. chondrophila* can successfully avoid its degradation and instead start replicating inside the phagosome to form an inclusion shown by 3D-CLSM (**D**) and TEM (**E**). (**D**) shows a 3D acquired z-stack image of a dsRed expressing neutrophil (red) of the transgenic Tg(lyzC:dsRed^{nz50}) line, harboring three *W. chondrophila* inclusions, visualized by antibody staining (green). DNA was stained with DAPI (blue). The TEM image in (**E**) shows a zebrafish phagocyte containing two inclusions of replicating *W. chondrophila* RBs. Scale bars (**A,B**) 100 μm , (**D**) 1 μm and (**E**) 2 μm .

Morphology of *W. chondrophila* Inside Zebrafish Host Cells

To investigate the morphological features of *W. chondrophila* infection in zebrafish larvae, we performed detailed TEM and CLSM analyses of infected larvae after IF staining with an anti-*Waddlia* antibody and an anti-OxPhosIV antibody to stain mitochondria. *W. chondrophila* could be found to infect different cells of the zebrafish, predominantly epithelial cells of the

swim bladder, phagocytes of the innate immune system and endothelial cells (Figure 5). The chlamydial inclusions inside these cells exhibited features typical for a *Waddlia* infection, including the transformation from the round shaped smaller (up to 0.5 μm in diameter) metabolically almost inactive but infectious EBs with highly condensed DNA, to the larger (about 0.9 μm in diameter) replicating reticulate bodies (RBs) with finely distributed chromatin inside a bacteria containing

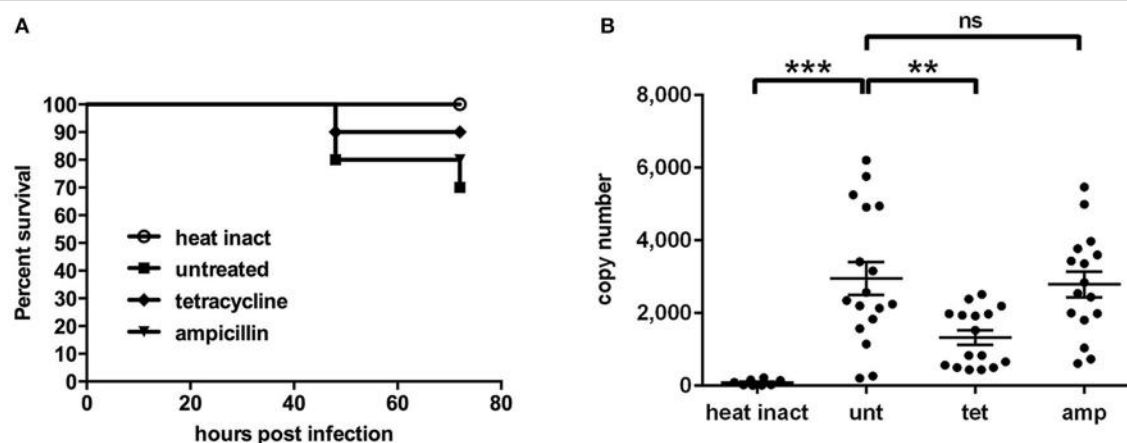


FIGURE 7 | Survival rates (A) and bacterial load (B) are shown for larvae after intravenous injection of live *W. chondrophila* and subsequent treatment with 30 µg/ml tetracycline (tet) or 30 µg/ml ampicillin (amp) or left untreated (unt). Another group was injected with heat inactivated *W. chondrophila* (heat inact) for comparison. For survival rates (A) 10 larvae of each condition were observed in three independent experiments, respectively. The bacterial load (B) was determined at 36 hpi by qPCR of total DNA extracts from homogenates of individual larvae, targeting the *W. chondrophila* 16S rRNA sequence. Statistical analysis was done by one-way ANOVA with Bonferroni's posttest. * $p < 0.001$, ** $p < 0.01$, ns = not significant. Mean values ± SEM are shown by horizontal bars.**

vacuole. Further, host cell mitochondria were readily recruited and closely associated with the inclusion, a characteristic for *Waddlia* infection *in vitro* (Croxatto and Greub, 2010) and now shown *in vivo*. While epithelial and endothelial cells usually contained a single perinuclear inclusion, individual phagocytes could harbor several inclusions of dividing bacteria. In TEM images of larvae that were injected into the swim bladder, some bacteria were in close relation to microvilli on the epithelial cell surface while others were found within the cytoplasm of these cells. The morphological structure of these bacteria on the surface resembled as well the typical morphology known for infectious particles of *W. chondrophila* (Rusconi et al., 2013). The perinuclear bacteria containing vacuoles inside epithelial cells were closely associated with host cell mitochondria and ER and are typical for actively replicating *W. chondrophila* observed *in vitro* (Rusconi et al., 2013).

Innate Immune Reaction to *W. chondrophila* Includes a Strong Recruitment of Neutrophils

The zebrafish innate immune system reacts to *W. chondrophila* with a strong recruitment of inflammatory cells to the infection site, as we already observed in our histology analysis (Figure 2).

This recruitment of inflammatory cells could be confirmed by using larvae of the transgenic Tg(*lyzC:dsRed*^{nz50}) line, whose neutrophils express red fluorescent protein, easily assessable by fluorescence microscopy. Since the zebrafish swim bladder is an enclosed compartment, usually devoid of immune cells, we used our swim bladder infection assay in order to quantify the induced recruitment of neutrophils following microinjection. In these larvae, large numbers of neutrophils could be detected clustered inside the swim bladder (Figure 6B), compared to PBS injected control larvae (Figure 6A). We quantified the recruitment by counting the fluorescent neutrophils using the

image analysis package of Imaris (Video S1). The results show further a significantly increased response of neutrophil invasion to live *W. chondrophila* compared to heat-inactivated bacteria (Figure 6C). Phagocytosed *W. chondrophila* show the ability to survive and replicate inside neutrophils (Figures 6D,E).

Systemically Infected Larvae Can Be Rescued by Antibiotic Treatment with Tetracycline

In vitro studies have previously shown that *W. chondrophila* is susceptible to antibiotics of the tetracycline group, but is resistant to β-lactam antibiotics (Goy and Greub, 2009). Therefore we compared the effect of tetracycline and ampicillin on *W. chondrophila* infections *in vivo* by using our systemic infection assay, for which we compared the survival rates of differently treated larvae. In order to additionally quantify and compare the bacterial burden of individual larvae during the infection, we furthermore developed a specific quantitative PCR targeting the two-copy *W. chondrophila* 16S rRNA gene.

While treatment with tetracycline significantly ($p < 0.01$) reduced *W. chondrophila* replication *in vivo* and increased the survival rate (Figure 7), treatment with ampicillin had a small but non-significant impact on the bacterial load compared to untreated larvae. Formation and distribution of *W. chondrophila* inclusions in untreated and ampicillin treated larvae were similar. In tetracycline treated larvae inclusion formation was strongly attenuated. Furthermore heat-inactivated bacteria were quickly cleared from the system.

Effect of MyD88 on Infection with *W. chondrophila*

The signaling molecule MyD88 has been shown to play a central role for pathogen recognition, immune reaction and survival of infected individuals during *Chlamydia* infection in several *in*

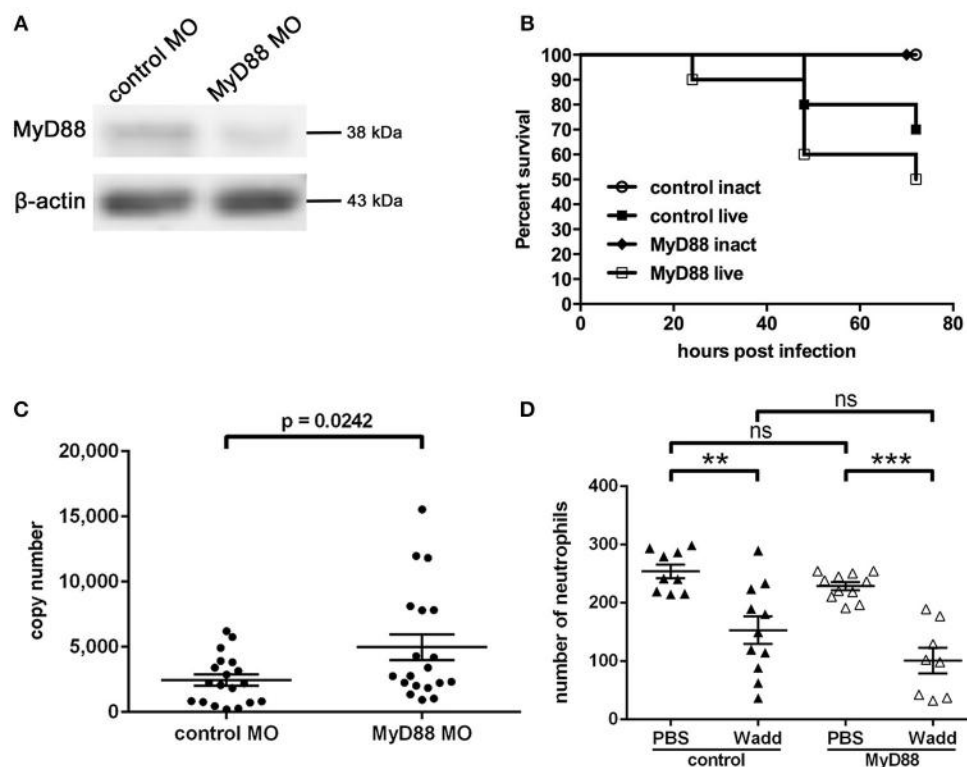


FIGURE 8 | Morpholino knockdown of MyD88, verified by Western Blot analysis (A) of zebrafish MyD88 at 4 dpf, showing a depleted level of the protein in morphant fish. β -actin served as loading control. Survival rates of control and MyD88 depleted larvae at 36 hpi (B) show differences after intravenous injection of *W. chondrophila*. Morphant larvae show a slightly reduced survival rate compared to control larvae. Survival rates of 10 larvae for each condition were observed in three independent experiments, respectively. The bacterial load, determined by qPCR, (C) of MyD88 depleted larvae at 36 hpi is significantly ($p = 0.0242$) higher compared to control larvae. Statistical analysis was done by Student's unpaired *t*-test. Mean values \pm SEM are shown by horizontal bars. Total numbers of neutrophils of whole individual control and MyD88 depleted larvae (D) were determined in the transgenic Tg(*lyzC:dsRed*)^{nz50} line at 36 hpi after intravenous injection of PBS or live *W. chondrophila* by counting dsRed expressing neutrophils after IF staining with an anti-dsRED antibody and subsequent CLSM analysis. The acquired 3D stacks of whole larvae were analyzed with the fluorescent spot counting tool in Imaris (Bitplane). The results show a significant depletion of neutrophils after injection of *W. chondrophila* compared to PBS injection in both normal and MyD88 depleted larvae with no significant differences between the two groups. Statistical analysis was done by one-way ANOVA with Bonferroni's posttest. *** $p < 0.001$, ** $p < 0.01$, ns = not significant. Mean values \pm SEM are shown by horizontal bars.

vivo studies. Now we wished to address how MyD88 mediated signaling affects the infection with *W. chondrophila* in our zebrafish model. To investigate whether MyD88 signaling has a function during *W. chondrophila* infection in zebrafish, we knocked down MyD88 expression by injection of a specific morpholino at the 1-cell stage. The resulting knockdown lasted for up to 4 dpf as determined by Western Blot (Figure 8A). Survival rates and bacterial loads were compared between control and MyD88 knockdown larvae during systemic infection. Our results show, that MyD88 morphant larvae exhibited a 20% lower survival rate compared to control larvae with a similar initial injection dose of 2×10^3 *W. chondrophila* EBs (Figure 8B). Furthermore, the bacterial load of MyD88 morphant larvae at 36 hpi was higher compared to control larvae (Figure 8C).

Additionally, to compare the total numbers of neutrophils during a systemic infection between morphant and control fish we injected transgenic Tg(*lyzC:dsRed*)^{nz50} larvae either with sterile PBS, heat-inactivated *W. chondrophila* or live *W. chondrophila* (10^3 EBs) at 2 dpf. Subsequently, total numbers

of neutrophils within individual larvae were counted with the cell counting tool in Imaris. At 36 hpi, these numbers were found to be significantly depleted upon the systemic infection with *W. chondrophila* compared to PBS injected larvae, although no differences between MyD88 morphant and control fish were evident (Figure 8D).

DISCUSSION

We present the first zebrafish infection model for an obligate intracellular pathogen and member of the PVC superphylum, *W. chondrophila*, which produces a non-lethal swim bladder infection and a lethal systemic infection in zebrafish larvae. Primary target cells are epithelial cells of the swim bladder, endothelial cells of the vascular system and innate immune phagocytes. Moreover, in this study, we show for the first time that *W. chondrophila* can successfully survive and grow within zebrafish neutrophils. By using zebrafish larvae between 2 and 5 dpf our model provides the opportunity to study specifically

the reaction of the innate immune system to a *W. chondrophila* infection.

The zebrafish swim bladder is an air-exposed epithelium, regarded as a homologous organ to the mammalian lung, having similar developmental and molecular ontogeny (Winata et al., 2009; Flores et al., 2010). Oral uptake of *W. chondrophila* by 4 dpf larvae results in a swim bladder infection, which can be reproducibly replicated by direct microinjection of *W. chondrophila* into the swim bladder. Since *W. chondrophila* has been linked to cases of pneumonia in humans (Haider et al., 2008), as have related organisms such as *Chlamydia pneumoniae* and *C. psittaci*, our model could provide a new approach to investigate aspects of human respiratory disease caused by these pathogens *in vivo*. Even more we could demonstrate that *W. chondrophila* enters the swim bladder epithelial cells and goes into the life cycle typical for these organisms forming metabolic active RB as described in mice with *C. pneumoniae* infections. A fibrosis surrounding the swim bladder was found to develop within few days after inoculation (Jupelli et al., 2013). Similarly to experimental infections of rodent lungs with other members of the order chlamydiales (Roger et al., 2010), the injection of live *W. chondrophila* into the swim bladder causes a strong recruitment of neutrophils to the infection site, compared to lack of neutrophil recruitment when using heat-inactivated bacteria. While zebrafish macrophages are known to react to invading bacteria at all locations, neutrophils are able to phagocytise surface associated bacteria in a vacuum-cleaner-like manner (Colucci-Guyon et al., 2011). Thus from our findings, it is possible that live *W. chondrophila* EBs adhere efficiently to the epithelium of the swim bladder, while heat-inactivated bacteria are unable to do so. The adhesion of live bacteria could lead to an increased neutrophil recruitment to the infection site.

Intravenous injection of *W. chondrophila* into zebrafish larvae leads to a strongly impaired blood circulation and subsequent oedema formation, as is typical for severe systemic inflammatory states such as sepsis, with the ensuing increased mortality correlating with increased dosage. This reaction was only provoked by injection of live infectious EBs and not by the use of heat-inactivated *W. chondrophila*. The infection triggers a strong innate immune response, evidenced by the initial recruitment and subsequent depletion of phagocytes. In addition to macrophages, we show for the first time that epithelial cells and neutrophils are among the preferred target cells for infection by *W. chondrophila* *in vivo*. The involvement of neutrophils in the host response to *W. chondrophila* was unexpected and is a new finding of this study which will stimulate a re-evaluation of the relative importance of macrophages and neutrophils in the initial clearance of chlamydial infections. Infection of endothelial cells has already been shown *in vitro* for *Chlamydia pneumoniae* (Godzik et al., 1995; Gaydos et al., 1996), suggesting at the time that these chlamydial pathogens may play a possible role in the development of vascular disease. Our findings with intravenously injected *W. chondrophila* now provide *in vivo* evidence to support this idea with another chlamydial pathogen and by using the zebrafish, a readily tractable model for future investigations.

W. chondrophila was first proposed as an abortifacient agent in ruminants (Dilbeck et al., 1990; Henning et al., 2002; Dilbeck-Robertson et al., 2003) and more recently in humans (Baud et al., 2007, 2011, 2014; Haider et al., 2008; Goy et al., 2009; Goy and Greub, 2009). The pathological mechanisms for this are unknown, although other chlamydial abortifacient agents are thought to act via a permanent infection of the intestine and from there via sepsis infecting the placenta and fetus. Aborted placentas of ewes after infections with *C. abortus* show, in addition to large areas of necrotic trophoblasts, a severe necrotizing vasculitis (Buxton et al., 2002). That *W. chondrophila* is able to establish an infection within vessel endothelium is a new finding and offers a potential mechanism to promote invasion of the placental tissues from the blood circulation.

Treatment of the infected larvae with tetracycline significantly reduces the bacterial load and increases the larval survival rate, while treatment with ampicillin is ineffective. Nevertheless, even without antibiotic treatment, the bacterial load starts to decrease after 72 hpi in surviving larvae. The infection is greatly reduced by 4 dpi although isolated inclusions or infection loci can remain. This experimental zebrafish model may thus be used to test new antibiotics *in vivo* during the initial infection window and may be used to investigate the effect of anti-virulence compounds such as Type III secretion system (T3SS) inhibitors, recently shown to be effective *in vitro* (Bertelli et al., 2010).

Our results show that although phagocytes are susceptible to infection with *W. chondrophila*, the innate immune system on its own is able to mount an effective initial counter strike against *W. chondrophila* infection in surviving larvae. Furthermore, we found that MyD88 mediated signaling contributes to an increased survival and a reduced bacterial load in control larvae compared to MyD88 morphants. These findings indicate a possible role of MyD88 dependent activation and recruitment of innate immune cells, including neutrophils, for an efficient reaction to *W. chondrophila* infection. On the other hand, we could not observe differences in phagocyte depletion between control and morphant larvae, which indicates that recruitment and phagocytosis of *W. chondrophila* could basically also be mediated by a MyD88 independent manner. MyD88 mediated signaling has also been found to contribute to the generation of an effective early immune response and increased host survival in a mouse model for *Chlamydia pneumoniae* infection (Naiki et al., 2005). Furthermore, it has been shown that *Parachlamydia acanthamoebiae* is recognized and internalized by macrophages in a MyD88 independent manner (Roger et al., 2010), while on the other hand in another mouse model it was shown that neutrophil recruitment to *Chlamydia pneumoniae* infection is strongly depending on MyD88 signaling, although in this case, recruitment of neutrophils initially increased the bacterial load (Rodriguez et al., 2005).

The potential role of MyD88 signaling at later time points of an infection needs to be further investigated. Possible subsequent recognition of the *W. chondrophila* bacteria containing vacuole inside infected phagocytes by endosomal TLRs or cytoplasmic nucleotide binding oligomerization domain (NOD)-like receptors acting in association with MyD88 mediated signaling could lead to a more efficient response of the innate immune

system to *W. chondrophila* infection. An essential role for the recognition and defensive reaction induced by NOD-like receptors has already been shown for *Chlamydia pneumoniae* and *Chlamydia trachomatis* (Buchholz and Stephens, 2008; Shimada et al., 2009). Whether *W. chondrophila* is also recognized by intracellular pattern recognition receptors is another key aspect for future studies.

Taken together, our results complement those from mouse models, but offers new insights into pathogenesis and immune response during *Chlamydia* infections. In particular, the use of different injection sites permits a staged analysis of separate events in an infection and the opportunity to understand the molecular mechanisms guiding these processes. The genetic tractability of the model is a particularly opportune addition to the tools available to the *Chlamydia* field, being potentially high throughput for screening of novel anti-chlamydial agents and especially useful given the recent progress in development of transgenic *Chlamydia* (Gérard et al., 2013; Song et al., 2013). The zebrafish model presented here offers chlamydial researchers in particular, and the PVC field in general, a powerful new experimental tool.

AUTHOR CONTRIBUTIONS

AF, AL, AV, HS, LV, MR, PC, and SN conceived and designed the experiments. AF, AL, HS, LN, LV, MR, and SN performed the experiments. AF, AL, AV, GG, HS, LN, LV, MR, PC, and

SN analyzed the data. AF, GG, HS, LV, MR, and PC wrote the manuscript.

FUNDING

This study was supported by the EU through Marie Curie IEF grant number 332058, the SBF through COST Action 867: Fish Welfare in European Aquaculture and by the Swiss National Science Foundation (SNF), grant number 310030_138533/1. The funders had no role in study design, data collection and interpretation, or the decision to submit the work for publication.

ACKNOWLEDGMENTS

We would like to thank Kara Dannenhauer for fish maintenance and the Center of Microscopy and Image Analysis of the University of Zurich for providing microscopic equipment and support. The laboratory work was partly performed using the logistics of the Center for Clinical Studies at the Vetsuisse Faculty of the University of Zurich.

SUPPLEMENTARY MATERIAL

The Supplementary Material for this article can be found online at: <http://journal.frontiersin.org/article/10.3389/fmicb.2016.01829/full#supplementary-material>

REFERENCES

- Adams, K. N., Takaki, K., Connolly, L. E., Wiedenhoft, H., Winglee, K., Humbert, O., et al. (2011). Drug tolerance in replicating mycobacteria mediated by a macrophage-induced efflux mechanism. *Cell* 145, 39–53. doi: 10.1016/j.cell.2011.02.022
- Bachmann, N. L., Polkinghorne, A., and Timms, P. (2014). Chlamydia genomics: providing novel insights into chlamydial biology. *Trends Microbiol.* 22, 464–472. doi: 10.1016/j.tim.2014.04.013
- Bates, J. M., Akerlund, J., Mittge, E., and Guillemain, K. (2007). Intestinal alkaline phosphatase detoxifies lipopolysaccharide and prevents inflammation in zebrafish in response to the gut microbiota. *Cell Host Microbe* 2, 371–382. doi: 10.1016/j.chom.2007.10.010
- Baud, D., Goy, G., Osterheld, M. C., Borel, N., Vial, Y., Pospischil, A., et al. (2011). *Waddlia chondrophila*: from bovine abortion to human miscarriage. *Clin. Infect. Dis.* 52, 1469–1471. doi: 10.1093/cid/cir205
- Baud, D., Goy, G., Osterheld, M. C., Croxatto, A., Borel, N., Vial, Y., et al. (2014). Role of *Waddlia chondrophila* placental infection in miscarriage. *Emerging Infect. Dis.* 20, 460–464. doi: 10.3201/eid2003.131019
- Baud, D., Thomas, V., Arafa, A., Regan, L., and Greub, G. (2007). *Waddlia chondrophila*, a potential agent of human fetal death. *Emerging Infect. Dis.* 13, 1239–1243. doi: 10.3201/eid1308.070315
- Bertelli, C., Collynn, F., Croxatto, A., Rückert, C., Polkinghorne, A., Kebbi-Beghdadi, C., et al. (2010). The *Waddlia* genome: a window into chlamydial biology. *PLoS ONE* 5:e10890. doi: 10.1371/journal.pone.0010890
- Brannon, M. K., Davis, J. M., Mathias, J. R., Hall, C. J., Emerson, J. C., Crosier, P. S., et al. (2009). *Pseudomonas aeruginosa* Type III secretion system interacts with phagocytes to modulate systemic infection of zebrafish embryos. *Cell. Microbiol.* 11, 755–768. doi: 10.1111/j.1462-5822.2009.01288.x
- Buchholz, K. R., and Stephens, R. S. (2008). The cytosolic pattern recognition receptor NOD1 induces inflammatory interleukin-8 during *Chlamydia trachomatis* infection. *Infect. Immun.* 76, 3150–3155. doi: 10.1128/IAI.00104-08
- Buxton, D., Anderson, I. E., Longbottom, D., Livingstone, M., Wattegedera, S., and Entrican, G. (2002). Ovine Chlamydial abortion: characterization of the inflammatory immune response in placental tissues. *J. Comp. Pathol.* 127, 133–141. doi: 10.1053/jcpa.2002.0573
- Cambier, C. J., Takaki, K. K., Larson, R. P., Hernandez, R. E., Tobin, D. M., Urdahl, K. B., et al. (2014). Mycobacteria manipulate macrophage recruitment through coordinated use of membrane lipids. *Nature* 505, 218–222. doi: 10.1038/nature12799
- Campbell, L. A., and Rosenfeld, M. E. (2014). Persistent *C. pneumoniae* infection in atherosclerotic lesions: rethinking the clinical trials. *Front. Cell Infect. Microbiol.* 4:34. doi: 10.3389/fcimb.2014.00034
- Clatworthy, A. E., Lee, J. S., Leibman, M., Kostun, Z., Davidson, A. J., and Hung, D. T. (2009). *Pseudomonas aeruginosa* infection of zebrafish involves both host and pathogen determinants. *Infect. Immun.* 77, 1293–1303. doi: 10.1128/IAI.01181-08
- Codony, F., Pittipaldi, M., López, E., Morató, J., Agustí, G., (2012). Well water as a possible source of *Waddlia chondrophila* infections. *Microb. Environ.* 27, 529–532. doi: 10.1264/jsme2.ME12048
- Collingro, A., Tischler, P., Weinmaier, T., Penz, T., Heinz, E., Brunham, R. C., et al. (2011). Unity in variety—the pan-genome of the Chlamydiae. *Mol. Biol. Evol.* 28, 3253–3270. doi: 10.1093/molbev/msr161
- Colucci-Guyon, E., Tinevez, J. Y., Renshaw, S. A., and Herbomel, P. (2011). Strategies of professional phagocytes *in vivo*: unlike macrophages, neutrophils engulf only surface-associated microbes. *J. Cell Sci.* 124(Pt 18), 3053–3059. doi: 10.1242/jcs.082792
- Croxatto, A., and Greub, G. (2010). Early intracellular trafficking of *Waddlia chondrophila* in human macrophages. *Microbiology* 156(Pt 2), 340–355. doi: 10.1099/mic.0.034546-0
- Davis, J. M., Clay, H., Lewis, J. L., Ghori, N., Herbomel, P., and Ramakrishnan, L. (2002). Real-time visualization of Mycobacterium-macrophage interactions leading to initiation of granuloma formation in zebrafish embryos. *Immunity* 17, 693–702. doi: 10.1016/S1074-7613(02)00475-2

- Dilbeck, P. M., Evermann, J. F., Crawford, T. B., Ward, A. C. S., Leathers, C. W., Holland, C. J., et al. (1990). Isolation of a previously undescribed Rickettsia from an aborted bovine fetus. *J. Clin. Microbiol.* 28, 814–816.
- Dilbeck-Robertson, P., McAllister, M. M., Bradway, D., and Evermann, J. F. (2003). Results of a new serologic test suggest an association of *Waddlia Chondrophila* with Bovine Abortion. *J. Veterin. Diagnost. Investig.* 15, 568–569. doi: 10.1177/104063870301500609
- Draghi, A. II., Popov, V. L., Kahl, M. M., Stanton, J. B., Brown, C. C., Tsongalis, G. J., et al. (2004). Characterization of “*Candidatus piscichlamydia salmonis*” (order Chlamydiales), a chlamydia-like bacterium associated with epitheliocystis in farmed Atlantic salmon (*Salmo salar*). *J. Clin. Microbiol.* 42, 5286–5297. doi: 10.1128/JCM.42.11.5286-5297.2004
- Fehr, A., Eshwar, A. K., Neuhauss, S. C. F., Ruetten, M., Lehner, A., and Vaughan, L. (2015). Evaluation of zebrafish as a model to study the pathogenesis of the opportunistic pathogen *Cronobacter turicensis*. *Emerg. Microb Infect* 4:e30. doi: 10.1038/emi.2015.30
- Fehr, A., Walther, E., Schmidt-Posthaus, H., Nufer, L., Wilson, A., Svercel, M., et al. (2013). *Candidatus Syngnathymia venezia*, a novel member of the phylum Chlamydiae from the broad nosed pipefish, *Syngnathus typhle*. *PLoS ONE* 8:e70853. doi: 10.1371/journal.pone.0070853
- Flores, M. V., Crawford, K. C., Pullin, L. M., Hall, C. J., Crosier, K. E., and Crosier, P. S. (2010). Dual oxidase in the intestinal epithelium of zebrafish larvae has anti-bacterial properties. *Biochem. Biophys. Res. Commun.* 400, 164–168. doi: 10.1016/j.bbrc.2010.08.037
- Gaydos, C. A., Summersgill, J. T., Sahney, N. N., Ramirez, J. A., and Quinn, T. C. (1996). Replication of *Chlamydia pneumoniae* *in vitro* in human macrophages, endothelial cells, and aortic artery smooth muscle cells. *Infect. Immun.* 64, 1614–1620.
- Gérard, H. C., Mishra, M. K., Mao, G., Wang, S., Hali, M., Whittum-Hudson, J. A., et al. (2013). Dendrimer-enabled DNA delivery and transformation of *Chlamydia pneumoniae*. *Nanomedicine* 9, 996–1008. doi: 10.1016/j.nano.2013.04.004
- Godzik, K. L., O’Brien, E. R., Wang, S., and Kuo, C. (1995). *In vitro* susceptibility of human vascular wall cells to infection with *Chlamydia pneumoniae*. *J. Clin. Microbiol.* 33, 2411–2414.
- Goy, G., Croxatto, A., and Greub, G. (2008). *Waddlia chondrophila* enters and multiplies within human macrophages. *Microbes Infect.* 10, 556–562. doi: 10.1016/j.micinf.2008.02.003
- Goy, G., Croxatto, A., Posfay-Barbe, K. M., Gervaix, A., and Greub, G. (2009). Development of a real-time PCR for the specific detection of *Waddlia chondrophila* in clinical samples. *Eur. J. Clin. Microbiol. Infect. Dis.* 28, 1483–1486. doi: 10.1007/s10096-009-0804-7
- Goy, G., and Greub, G. (2009). Antibiotic susceptibility of *Waddlia chondrophila* in *Acanthamoeba castellanii* amoebae. *Antimicrob. Agents Chemother.* 53, 2663–2666. doi: 10.1128/AAC.00046-09
- Greub, G., and Raoult, D. (2002). Crescent bodies of *Parachlamydia acanthamoeba* and its life cycle within *Acanthamoeba polyphaga*: an electron micrograph study. *Appl. Environ. Microbiol.* 68, 3076–3084. doi: 10.1128/aem.68.6.3076-3084.2002
- Haider, S., Collingro, A., Walochnik, J., Wagner, M., and Horn, M. (2008). Chlamydia-like bacteria in respiratory samples of community-acquired pneumonia patients. *FEMS Microbiol. Lett.* 281, 198–202. doi: 10.1111/j.1574-6968.2008.01099.x
- Hall, C., Flores, M. V., Chien, A., Davidson, A., Crosier, K., and Crosier, P. (2009). Transgenic zebrafish reporter lines reveal conserved Toll-like receptor signaling potential in embryonic myeloid leukocytes and adult immune cell lineages. *J. Leukoc. Biol.* 85, 751–765. doi: 10.1189/jlb.0708405
- Hall, C., Flores, M. V., Storm, T., Crosier, K., and Crosier, P. (2007). The zebrafish lysozyme C promoter drives myeloid-specific expression in transgenic fish. *BMC Dev. Biol.* 7:42. doi: 10.1186/1471-213X-7-42
- Harvie, E. A., Green, J. M., Neely, M. N., and Huttenlocher, A. (2013). Innate immune response to *Streptococcus iniae* infection in zebrafish larvae. *Infect. Immun.* 81, 110–121. doi: 10.1128/IAI.00642-12
- Henning, K., Schares, G., Granzow, H., Polster, U., Hartmann, M., Hotzel, H., et al. (2002). *Neospora caninum* and *Waddlia chondrophila* strain 2032/99 in a septic stillborn calf. *Vet. Microbiol.* 85, 285–292. doi: 10.1016/S0378-1135(01)00510-7
- Herbomel, P., Thisse, B., and Thisse, C. (1999). Ontogeny and behaviour of early macrophages in the zebrafish embryo. *Development* 126, 3735–3745.
- Hoffman, G. L., Dunbar, C. E., Wolf, K., and Zwillingberg, L. O. (1969). Epitheliocystis, a new infectious disease of the bluegill (*Lepomis macrochirus*). *Antonie Van Leeuwenhoek* 35, 146–158.
- Jupelli, M., Shimada, K., Chiba, N., Slepchenko, A., Alsabeh, R., Jones, H. D., et al. (2013). *Chlamydia pneumoniae* infection in mice induces chronic lung inflammation, iBALT formation, and fibrosis. *PLoS ONE* 8:e77447. doi: 10.1371/journal.pone.0077447
- Kanther, M., and Rawls, J. F. (2010). Host-microbe interactions in the developing zebrafish. *Curr. Opin. Immunol.* 22, 10–19. doi: 10.1016/j.co.2010.01.006
- Karlsen, M., Nylund, A., Watanabe, K., Helvik, J. V., Nylund, S., and Plarre, H. (2008). Characterization of ‘*Candidatus Clavochlamydia salmonicola*’: an intracellular bacterium infecting salmonid fish. *Environ. Microbiol.* 10, 208–218. doi: 10.1111/j.1462-2920.2007.01445.x
- Kebbi-Beghdadi, C., Batista, C., and Greub, G. (2011a). Permissivity of fish cell lines to three Chlamydia-related bacteria: *Waddlia chondrophila*, *Estrella lausannensis* and *Parachlamydia acanthamoebae*. *FEMS Immunol. Med. Microbiol.* 63, 339–345. doi: 10.1111/j.1574-695X.2011.00856.x
- Kebbi-Beghdadi, C., Cisse, O., and Greub, G. (2011b). Permissivity of Vero cells, human pneumocytes and human endometrial cells to *Waddlia chondrophila*. *Microbes Infect.* 13, 566–574. doi: 10.1016/j.micinf.2011.01.020
- Kimmel, C. B., Ballard, W. W., Kimmel, S. R., Ullmann, B., and Schilling, T. F. (1995). Stages of embryonic development of the zebrafish. *Develop. Dyn.* 203, 253–310.
- Kocan, K. M., Crawford, T. B., Dilbeck, P. M., Evermann, J. F., and McGuire, T. C. (1990). Development of a Rickettsia isolated from an aborted bovine fetus. *J. Bacteriol.* 172, 5949–5955.
- Lagkouvardos, I., Weinmaier, T., Lauro, F. M., Cavicchioli, R., Rattei, T., and Horn, M. (2014). Integrating metagenomic and amplicon databases to resolve the phylogenetic and ecological diversity of the Chlamydiae. *ISME J.* 8, 115–125. doi: 10.1038/ismej.2013.142
- Lamoth, F., and Greub, G. (2010). Amoebal pathogens as emerging causal agents of pneumonia. *FEMS Microbiol. Rev.* 34, 260–280. doi: 10.1111/j.1574-6976.2009.00207.x
- Lawson, N. D., and Weinstein, B. M. (2002). *In vivo* imaging of embryonic vascular development using transgenic zebrafish. *Dev. Biol.* 248, 307–318. doi: 10.1006/dbio.2002.0711
- Levraud, J. P., Disson, O., Kissa, K., Bonne, I., Cossart, P., Herbomel, P., et al. (2009). Real-time observation of listeria monocytogenes-phagocyte interactions in living zebrafish larvae. *Infect. Immun.* 77, 3651–3660. doi: 10.1128/IAI.00408-09
- Longbottom, D., and Coulter, L. J. (2003). Animal Chlamydioses and Zoonotic implications. *J. Comp. Pathol.* 128, 217–244. doi: 10.1053/jcpa.2002.0629
- Medzhitov, R., Preston-Hurlburt, P., Kopp, E., Stadlen, A., Chen, C., Ghosh, S., et al. (1998). MyD88 is an adaptor protein in the hToll/IL-1 receptor family signaling pathways. *Mol. Cell* 2, 253–258.
- Meeker, N. D., and Trede, N. S. (2008). Immunology and zebrafish: spawning new models of human disease. *Dev. Comp. Immunol.* 32, 745–757. doi: 10.1016/j.dci.2007.11.011
- Meijer, A. H., and Spaink, H. P. (2011). Host-pathogen interactions made transparent with the zebrafish model. *Curr. Drug Targets* 12, 1000–1017. doi: 10.2174/138945011795677809
- Meijer, A., Roholl, P. J., Ossewaarde, J. M., Jones, B., and Nowak, B. F. (2006). Molecular evidence for association of chlamydiales bacteria with epitheliocystis in leafy seadragon (*Phycodurus eques*), silver perch (*Bidyanus bidyanus*), and barramundi (*Lates calcarifer*). *Appl. Environ. Microbiol.* 72, 284–290. doi: 10.1128/AEM.72.1.284-290.2006
- Mostowy, S., Boucrot, L., Mazon Moya, M. J., Sirianni, A., Boudinot, P., Hollinshead, M., et al. (2013). The zebrafish as a new model for the *in vivo* study of *Shigella flexneri* interaction with phagocytes and bacterial autophagy. *PLoS Pathog.* 9:e1003588. doi: 10.1371/journal.ppat.1003588
- Naiki, Y., Michelsen, K. S., Schröder, N. W., Alsabeh, R., Slepchenko, A., Zhang, W., et al. (2005). MyD88 is pivotal for the early inflammatory response and subsequent bacterial clearance and survival in a mouse model of *Chlamydia pneumoniae* pneumonia. *J. Biol. Chem.* 280, 29242–29249. doi: 10.1074/jbc.M503225200
- Newton, K., and Dixit, V. M. (2012). Signaling in innate immunity and inflammation. *Cold Spring Harb. Perspect. Biol.* 4:a006049. doi: 10.1101/cshperspect.a006049

- Nylund, S., Steigen, A., Karlsbakk, E., Plarre, H., Andersen, L., Karlsen, M., et al. (2015). Characterization of '*Candidatus Syngnathia salmonis*' (Chlamydiales, Simkaniaeae), a bacterium associated with epitheliocystis in Atlantic salmon (*Salmo salar* L.). *Arch. Microbiol.* 197, 17–25. doi: 10.1007/s00203-014-1038-3
- O'Toole, R., Von Hofsten, J., Rosqvist, R., Olsson, P. E., and Wolf-Watz, H. (2004). Visualisation of zebrafish infection by GFP-labelled *Vibrio anguillarum*. *Microb. Pathog.* 37, 41–46. doi: 10.1016/j.micpath.2004.03.001
- Polymenakou, P. N., Bertilsson, S., Tselepidis, A., and Stephanou, E. G. (2005). Bacterial community composition in different sediments from the Eastern Mediterranean Sea: a comparison of four 16S ribosomal DNA clone libraries. *Microb. Ecol.* 50, 447–462. doi: 10.1007/s00248-005-0005-6
- Prajnar, T. K., Hamilton, R., Garcia-Lara, J., McVicker, G., Williams, A., Boots, M., et al. (2012). A privileged intraphagocyte niche is responsible for disseminated infection of *Staphylococcus aureus* in a zebrafish model. *Cell. Microbiol.* 14, 1600–1619. doi: 10.1111/j.1462-5822.2012.01826.x
- Rodriguez, N., Fend, F., Jennen, L., Schiemann, M., Wantia, N., da Costa, C. U. P., et al. (2005). Polymorphonuclear neutrophils improve replication of *Chlamydia pneumoniae* *In vivo* upon MyD88-Dependent Attraction. *J. Immunol.* 174, 4836–4844. doi: 10.4049/jimmunol.174.8.4836
- Roger, T., Casson, N., Croxatto, A., Entenza, J. M., Pusztaszeri, M., Akira, S., et al. (2010). Role of MyD88 and Toll-like receptors 2 and 4 in the sensing of *Parachlamydia acanthamoebae*. *Infect. Immun.* 78, 5195–5201. doi: 10.1128/IAI.00786-10
- Rusconi, B., Lienard, J., Aeby, S., Croxatto, A., Bertelli, C., and Greub, G. (2013). Crescent and star shapes of members of the Chlamydiales order: impact of fixative methods. *Antonie Van Leeuwenhoek* 104, 521–532. doi: 10.1007/s10482-013-9999-9
- Schmidt-Posthaus, H., Polkinghorne, A., Nufer, L., Schifferli, A., Zimmermann, D. R., Segner, H., et al. (2012). A natural freshwater origin for two chlamydial species, *Candidatus Piscichlamydia salmonis* and *Candidatus Clavochlamydia salmonicola*, causing mixed infections in wild brown trout (*Salmo trutta*). *Environ. Microbiol.* 14, 2048–2057. doi: 10.1111/j.1462-2920.2011.02670.x
- Shimada, K., Chen, S., Dempsey, P. W., Sorrentino, R., Alsabeh, R., Slepchenko, A. V., et al. (2009). The NOD/RIP2 pathway is essential for host defenses against *Chlamydophila pneumoniae* lung infection. *PLoS Pathog.* 5:e1000379. doi: 10.1371/journal.ppat.1000379
- Song, L., Carlson, J. H., Whitmire, W. M., Kari, L., Virtaneva, K., Sturdevant, D. E., et al. (2013). *Chlamydia trachomatis* plasmid-encoded Pgp4 is a transcriptional regulator of virulence-associated genes. *Infect. Immun.* 81, 636–644. doi: 10.1128/IAI.01305-12
- Steigen, A., Karlsbakk, E., Plarre, H., Watanabe, K., Övergård, A. C., Brevik, Ø., et al. (2015). A new intracellular bacterium, *Candidatus Similichlamydia labri* sp. nov. (Chlamydiaceae) producing epitheliocysts in ballan wrasse, *Labrus bergylta* (Pisces, Labridae). *Arch. Microbiol.* 197, 311–318. doi: 10.1007/s00203-014-1061-4
- Steigen, A., Nylund, A., Karlsbakk, E., Akoll, P., Fiksdal, I. U., Nyland, S., et al. (2013). 'Cand. Actinochlamydia clariae' gen. nov., sp. nov., a Unique Intracellular Bacterium Causing Epitheliocystis in Catfish (*Clarias gariepinus*) in Uganda. *PLoS ONE* 8:e66840. doi: 10.1371/journal.pone.0066840
- Stride, M. C., Polkinghorne, A., Miller, T. L., Groff, J. M., LaPatra, S. E., and Nowak, B. F. (2013a). Molecular characterization of "Candidatus Parilichlamydia carangidicola", a Novel Chlamydia-Like Epitheliocystis Agent in Yellowtail Kingfish, *Seriola lalandi* (Valenciennes), and the Proposal of a New Family, "Candidatus Parilichlamydiaceae" fam. nov. (Order Chlamydiales). *App. Environ. Microbiol.* 79, 1590–1597. doi: 10.1128/AEM.02899-12
- Stride, M. C., Polkinghorne, A., Miller, T. L., and Nowak, B. F. (2013b). Molecular characterization of "Candidatus Similichlamydia latridicola" gen. nov., sp. nov. (Chlamydiales: "Candidatus Parilichlamydiaceae"), a novel Chlamydia-like epitheliocystis agent in the striped trumpeter, *Latris lineata* (Forster). *App. Environ. Microbiol.* 79, 4914–4920.
- Stride, M. C., Polkinghorne, A., Powell, M. D., and Nowak, B. F. (2013c). "Candidatus similichlamydia laticola," a novel Chlamydia-like agent of epitheliocysts in seven consecutive cohorts of farmed Australian barramundi, *Lates calcarifer* (Bloch). *PLoS ONE* 8:e82889. doi: 10.1371/journal.pone.0082889
- Stride, M. C., Polkinghorne, A., and Nowak, B. F. (2014). Chlamydial infections of fish: diverse pathogens and emerging causes of disease in aquaculture species. *Vet. Microbiol.* 170, 19–27. doi: 10.1016/j.vetmic.2014.01.022
- Taylor-Brown, A., Vaughan, L., Greub, G., Timms, P., and Polkinghorne, A. (2015). Twenty years of research into Chlamydia-like organisms: a revolution in our understanding of the biology and pathogenicity of members of the phylum Chlamydiae. *Pathog. Dis.* 73, 1–15. doi: 10.1093/femspd/ftu009
- van der Sar, A. M., Musters, R. J. P., van Eeden, F. J. M., Appelmelk, B. J., Vandebroucke-Grauls, C. M. J. E., and Bitter, W. (2003). Zebrafish embryos as a model host for the real time analysis of *Salmonella typhimurium* infections. *Cell. Microbiol.* 5, 601–611. doi: 10.1046/j.1462-5822.2003.00303.x
- Vergunst, A. C., Meijer, A. H., Renshaw, S. A., and O'Callaghan, D. (2010). *Burkholderia cenocepacia* creates an intramacrophage replication niche in zebrafish embryos, followed by bacterial dissemination and establishment of systemic infection. *Infect. Immun.* 78, 1495–1508. doi: 10.1128/IAI.00743-09
- Warner, N., and Nunez, G. (2013). MyD88: a critical adaptor protein in innate immunity signal transduction. *J. Immunol.* 190, 3–4. doi: 10.4049/jimmunol.1203103
- Winata, C. L., Korzh, S., Kondrychyn, I., Zheng, W., Korzh, V., and Gong, Z. (2009). Development of zebrafish swimbladder: the requirement of Hedgehog signaling in specification and organization of the three tissue layers. *Dev. Biol.* 331, 222–236. doi: 10.1016/j.ydbio.2009.04.035

Conflict of Interest Statement: The authors declare that the research was conducted in the absence of any commercial or financial relationships that could be construed as a potential conflict of interest.

Copyright © 2016 Fehr, Ruetten, Seth-Smith, Nufer, Voegtl, Lehner, Greub, Crosier, Neuhauss and Vaughan. This is an open-access article distributed under the terms of the Creative Commons Attribution License (CC BY). The use, distribution or reproduction in other forums is permitted, provided the original author(s) or licensor are credited and that the original publication in this journal is cited, in accordance with accepted academic practice. No use, distribution or reproduction is permitted which does not comply with these terms.



Ca. Similichlamydia in *Epitheliocystis* Co-infection of Gilthead Seabream Gills: Unique Morphological Features of a Deep Branching Chlamydial Family

OPEN ACCESS

Edited by:

Laura van Niftrik,
Radboud University Nijmegen,
Netherlands

Reviewed by:

Matthias Horn,
University of Vienna, Austria
Reinhard Rachel,
University of Regensburg, Germany

*Correspondence:

Lloyd Vaughan
vaughan@vetpath.uzh.ch

†Present Address:

Helena M. B. Seth-Smith,
Clinical Microbiology, University
Hospital Basel, Basel, Switzerland;
Department of Biomedicine, University
of Basel, Basel, Switzerland

Specialty section:

This article was submitted to
Evolutionary and Genomic
Microbiology,
a section of the journal
Frontiers in Microbiology

Received: 07 September 2016

Accepted: 13 March 2017

Published: 30 March 2017

Citation:

Seth-Smith HMB, Katharios P,
Dourala N, Mateos JM, Fehr AGJ,
Nufer L, Ruetten M, Guevara Soto M
and Vaughan L (2017) Ca.
Similichlamydia in *Epitheliocystis*
Co-infection of Gilthead Seabream
Gills: Unique Morphological Features
of a Deep Branching Chlamydial
Family. *Front. Microbiol.* 8:508.
doi: 10.3389/fmicb.2017.00508

Helena M. B. Seth-Smith^{1,2†}, Pantelis Katharios³, Nancy Dourala⁴, José M. Mateos⁵,
Alexander G. J. Fehr¹, Lisbeth Nufer¹, Maja Ruetten^{1,6}, Maricruz Guevara Soto^{1,7} and
Lloyd Vaughan^{1,6*}

¹ Vetsuisse Faculty, Institute for Veterinary Pathology, University of Zürich, Zürich, Switzerland, ² Functional Genomics Center Zürich, University of Zürich, Zürich, Switzerland, ³ Hellenic Center for Marine Research, Institute of Marine Biology, Biotechnology and Aquaculture, Heraklion, Greece, ⁴ Selonda Aquaculture, Athens, Greece, ⁵ Center for Microscopy and Image Analysis, University of Zürich, Zürich, Switzerland, ⁶ Pathovet AG, Tagelswangen, Switzerland, ⁷ Department of Infectious Diseases and Pathobiology, Centre of Fish and Wildlife Health, University of Bern, Bern, Switzerland

The Planctomycetes-Verrucomicrobia-Chlamydiae (PVC) bacterial superphylum constitutes a broad range of organisms with an intriguing array of ultrastructural morphologies, including intracellular membranes and compartments and their corresponding complex genomes encoding these forms. The phylum Chlamydiae are all obligate intracellular bacteria and, although much is already known of their genomes from various families and how these regulate the various morphological forms, we know remarkably little about what is likely the deepest rooting clade of this phylum, which has only been found to contain pathogens of marine and fresh water vertebrates. The disease they are associated with is called epitheliocystis; however, analyses of the causative agents is hindered by an inability to cultivate them for refined *in vitro* experimentation. For this reason, we have developed tools to analyse both the genomes and the ultrastructures of bacteria causing this disease, directly from infected tissues. Here we present structural data for a member of the family Ca. Similichlamydiaceae from this deep-rooted clade, which we have identified using molecular tools, in epitheliocystis lesions of gilthead seabream (*Sparus aurata*) in Greece. We present evidence that the chlamydial inclusions appear to develop in a perinuclear location, similar to other members of the phylum and that a chlamydial developmental cycle is present, with chlamydial forms similar to reticular bodies (RBs) and elementary bodies (EBs) detected. Division of the RBs appeared to follow a budding process, and larger RBs with multiple condensed nucleoids were detected using both transmission electron microscopy (TEM) and by focused-ion beam, scanning electron microscopy (FIB-SEM). As model hosts, fish offer many advantages for investigation, and we hope by these efforts to encourage others to explore the biology of fish pathogens from the PVC.

Keywords: epitheliocystis, Planctomycetes-Verrucomicrobia-Chlamydiae-superphylum, Piscichlamydia, Similichlamydia

INTRODUCTION

Epitheliocystis is a common disease of wild and cultured fish, characterized by cyst-like inclusions in gill and skin epithelium. It was first described in bluegill (*Lepomis macrochirus*) (Hoffman et al., 1969) and since then has been observed in more than 80 different fish species (Stride et al., 2014) in both marine and freshwater environments (Nowak and LaPatra, 2006). The first studies combined molecular and morphological techniques to provide firm supportive data for *Chlamydia*-like organisms, reflected in the naming of *Candidatus Piscichlamydia salmonis* (Draghi et al., 2004) and *Candidatus Clavichlamydia salmonicola* (Karlsen et al., 2008). At the same time, these two new species also defined new families which could not better illustrate the diversity amongst a rapidly expanding phylum *Chlamydiae*.

The *Ca. Clavichlamydiaceae* remain the closest water-based relatives and immediate ancestors to the *Chlamydiaceae*, chlamydial pathogens of land vertebrates and major human disease agents (Taylor-Brown et al., 2015). This is also reflected in their morphologies, with predicted chlamydial developmental cycles, including peripheral, dividing reticular bodies (RBs), intermediate bodies (IBs), and the infectious particles or elementary bodies (EBs), the latter showing the head and tail form only observed in *Ca. Clavichlamydia salmonicola* until now (Karlsen et al., 2008; Schmidt-Posthaus et al., 2012; Guevara Soto et al., 2016).

The *Ca. Piscichlamydiaceae*, in contrast, were the first representatives of a new deeply branching clade, found exclusively in marine and fresh water vertebrates. A chlamydial developmental cycle was evident, although this differed in key aspects to the *Ca. Clavichlamydiaceae*, including cytoplasmic bridges linking dividing or budding RBs found throughout the inclusion and a differing host response (Schmidt-Posthaus et al., 2012), indicating that this group of bacteria utilizes a different pathological armory. An exciting development was the recent addition of new candidate families to this deep-branching clade, variously found in Southern hemisphere waters and including the *Ca. Parilichlamydiaceae* infecting yellow tail kingfish (*Seriola lalandi*) (Stride et al., 2013a), members of the *Ca. Similichlamydiaceae* infecting striped trumpeter (*Latris lineata*) and barramundi (*Lates calcarifer*) (Stride et al., 2013b,c), *Ca. Actinochlamydiaceae* causing epitheliocystis in catfish (*Clarias gariepinus*) in a Ugandan lake system (Steigen et al., 2013), and new species of the *Ca. Similichlamydiaceae* infecting ballan wrasse (*Labrus bergylta*) used as cleaner fish in salmon farms off the Norwegian coast (Steigen et al., 2015). These all share the property of stimulating a moderate host response, although the nature of the chlamydial inclusions and their developmental cycles differ from other *Chlamydiae*.

Early studies describing the diverse cyst types and bacterial forms detected in sparid (Paperna, 1977; Crespo et al., 1999) and salmonid (Nylund et al., 1998) epitheliocystis assumed

the causative organisms primarily to belong to the phylum *Chlamydiae*, but also raised the possibility of mixed infections with rickettsia-like bacteria containing cysts. The careful study of mixed epitheliocystis infections in Norwegian salmon (Steinum et al., 2010), pointing to an as yet unknown agent, led to the first identification of a beta-proteobacterium causing epitheliocystis (Toenshoff et al., 2012). Other species of beta-proteobacteria have since been identified in mixed epitheliocystis infections of gilthead seabream (*Sparus aurata*) (Qi et al., 2016; Seth-Smith et al., 2016), as have gamma-proteobacteria been identified in cysts from lake trout (*Salvelinus namaycush*) (Contador et al., 2016), Cobia larvae (Mendoza et al., 2013), and sharpsnout seabream (*Diplodus puntazzo*) larvae (Katharios et al., 2015). In none of these bacterial infections were chlamydial developmental cycles evident.

Epitheliocystis in gilthead seabream, which is one of the major cultured species in the Mediterranean, was first reported several decades ago (Paperna, 1977; Crespo et al., 1999). During a recent survey of the disease in cultured gilthead seabream in Greece during 2012–2013 we identified a more complex disease scenario with several bacterial species co-infecting the fish cohort gills. Using 16S rRNA gene sequencing combined with fluorescent *in situ* hybridization (FISH), we identified two species of a novel beta-proteobacterial genus, *Candidatus Ichthyocystis*, as the main pathogens (Qi et al., 2016; Seth-Smith et al., 2016). Complicating the analysis even further, new species of the *Ca. Piscichlamydiaceae* and *Ca. Similichlamydiaceae* were also identified molecularly, of which the latter was the dominant chlamydial agent and these results we now present here. FISH with a probe recognizing both families localized these agents to morphologically separable inclusions from the dominant *Ca. Ichthyocystis* agents (Seth-Smith et al., 2016, Supplementary Figure 3). We now present detailed molecular, transmission electron microscopy (TEM) and focused ion beam-scanning electron microscopy (FIB-SEM) analyses to reaffirm the unique aspects of the *Ca. Similichlamydia* developmental cycles which, although clearly chlamydial in nature, share features found in representatives of the *Planctomycetes*, raising questions concerning the mechanisms of cell division in the *Chlamydiae*. Although epitheliocystis has been reported in Greece and in gilthead seabream, this is the first report with molecular evidence connecting the disease with members of the *Chlamydiae*.

METHODS

Fish Sampling

Sampling of juvenile gilthead seabream (*S. aurata*) was carried out in Selonda SA farms in Saronikos (sampled November 2012 randomly; 2012Sar) and Argolida (sampled June 2013 during an epitheliocystis outbreak; 2013Arg), as previously described (Seth-Smith et al., 2016). Sampling formed part of the routine monitoring of fish health on the farms by one of the authors (ND). Gill arches from individual fish were taken in parallel into 10% buffered formalin, RNALater and pure ethanol, with the 2013Arg samples also taken into M4RT *Chlamydia* transport medium (Remel Microtest M4RT, Thermo Fisher, Switzerland)

Abbreviations: FIB-SEM, focused ion beam-scanning electron microscopy; TEM, transmission electron microscopy; CLSM, confocal laser scanning microscopy; EB, elementary body; RB, reticular body; IB, intermediate body; FISH, fluorescent *in situ* hybridisation.

and sterile sea water and sent chilled by overnight courier to Switzerland. All samples were kept chilled and further processed immediately upon arrival.

TEM and Histology

Screening of gill samples with standard histology was performed on samples fixed in 10% neutral buffered formalin, followed by dehydration in an ascending alcohol series ending in xylol and afterwards embedded in paraffin. Paraffin blocks were cut in 2–3 μm thin sections, mounted on glass slides and stained using a routine protocol for haematoxylin and eosin (HE) staining.

For electron microscopy, formalin-fixed gill tissues were post-fixed in a mixed solution of 1% paraformaldehyde and 2.5% glutaraldehyde in 0.1 M sodium phosphate buffer, pH 7.5 at 4°C overnight. Samples were prepared for TEM by embedding into epoxy resin according to standard procedures (Seth-Smith et al., 2016). Epoxy resin blocks were screened for epitheliocystis lesions using semithin sections (1 μm) which were stained with toluidine blue (Sigma-Aldrich). Ultrathin sections (80 nm) were mounted on copper grids (Merck Eurolab AG, Dietlikon, Switzerland), contrasted with uranyl acetate dihydrate (Sigma-Aldrich), and lead citrate (Merck Eurolab AG) and investigated using a Philips CM10 transmission electron microscope. Images were processed with Imaris 7.6.1 (Bitplane, Oxford Instruments) and assembled into panels for publication and annotated using Photoshop (Adobe).

Focused Ion Beam-Scanning Electron Microscopy (FIB-SEM)

Sample blocks were fixed in 2.5% glutaraldehyde in 0.2 M sodium cacodylate buffer, pH 7.4 at room temperature overnight, followed by 1% osmium tetroxide, and contrasted with 2% aqueous uranyl acetate. Sample dehydration was in an ethanol series, then propylene oxide and embedded in Epon 812 resin. Semithin and ultrathin sections were obtained to identify the regions containing cysts. The selected blocks were attached to 12 mm stubs by conductive carbon cement followed by carbon coating. 3D datasets were acquired with a FIB-SEM Auriga 40 Crossbeam (Zeiss, Oberkochen, Germany) using the FIBICS Nanopatterning engine (Fibics Inc, Ottawa, Canada). The gallium-ion beam for milling was used at 30 kV, 600 pA current and the images were acquired at an acceleration voltage of 1.5 kV using an in-lens energy selective backscattered electron detector (ESB) with a grid voltage of 1.3 kV. The resolution was set to 5 nm in the XY axes and 5–10 nm in the Z axis. The image stacks were aligned with TrackEM2 (Cardona et al., 2012). The aligned dataset was visualized with Imaris 7.6.1. To better visualize the shape of the bacteria as well as for showing a dividing bacterium the FIB-SEM dataset was segmented with the software Ilastik, 1.1 (Sommer et al., 2011).

Bacterial Identification

Identification of chlamydial bacteria was carried out using *Chlamydiae*-specific 16S rRNA gene primers (Everett et al., 1999; Draghi et al., 2004). Positive bands were analyzed further only when template free negative controls showed no signal. 16S rRNA gene amplicons were cloned into Topo vector pCR2.1 prior to capillary sequencing from both ends (Microsynth, Balgach). The resulting reads were assembled (CLC Main Workbench 7.0.2, CLC bio, Qiagen), compared using blastn against the Genbank database and used to create alignments with reference sequences using Muscle and PhyML v3 within Seaview v4 (Gouy et al., 2010). Only unique sequences from each sample were included in the analysis. Representative 16S rRNA gene sequences have been deposited with EMBL with the following accession numbers: LN612731-4 representing 2012Sar3_5c, 2013Arg23_1c, 2013Arg33_2c, and 2013Arg14_4c respectively.

Fluorescent In situ Hybridization (FISH)

FISH was performed on the Ventana Discovery XT automated platform using the probe shown in Table 1. Automated deparaffinization was followed by pretreatment with 0.2 M HCl in PBS then pepsin ($500 \mu\text{g ml}^{-1}$ in this buffer) for 4 min. Following addition of 50 ng probe per slide in a hybridization buffer comprising $6 \times \text{SSC}$, $5 \times \text{Denhardt's solution}$, and 12% dextran sulfate, samples were denatured at 90°C for 4 min and hybridized at 48°C overnight. A wash with $2 \times \text{SSC}$ at 48°C was followed by manual post staining with 4'-6-diamin-2-phenylindole (DAPI) at $10 \mu\text{g ml}^{-1}$ to visualize bacterial and host DNA for 10–30 min.

FISH and HE sections were scanned on a Hamamatsu Nanozoomer 2.0 HT scanner for an overview of the section, and high resolution imaging was performed on the Leica SP5 resonant confocal laser scanning microscope. Deconvolution was performed using Huygens (Ponti et al., 2007) and images were prepared with Imaris 7.6.1 (Bitplane, Oxford Instruments) and assembled into panels for publication and annotated using Photoshop CS4 extended, version 11.0.2 or CS6 extended, version 13.0x32 (Adobe).

RESULTS

Identification of Chlamydial Agents Present in Infected Gills

In total, five gilthead seabream gill samples from Saronikos bay (2012) and 16 samples from Argolida (2013) were screened for the presence of chlamydial sequences. All samples had visible epitheliocystis lesions under histopathological examination, although infection intensities were higher in Argolida fish. The majority of the cysts were attributed

TABLE 1 | Probe used in FISH.

| Probe | Specificity (sp) | Sequence/fluorophore | Position (<i>E.coli</i> numbering) | Reference |
|------------|------------------------------------|--------------------------------|-------------------------------------|-------------------------|
| Pisci-0312 | Ca. Piscichlamydia/Similichlamydia | 5'-AGTCCCAGTGTTGGCGATCG-3' Cy3 | 304–323 | Seth-Smith et al., 2016 |

to *Candidatus Ichthyocystis* spp. (Seth-Smith et al., 2016), yet amplification with *Chlamydiae*-specific 16S rRNA gene primers also gave clear products which were cloned and sequenced.

Phylogenetic analysis of the 67 sequences from *Chlamydiae*-specific primers (**Figure 1**) showed 63 sequences, derived from all 21 fish studied from both Saronikos and Argolida, clustering very closely with each other and *Ca. Similichlamydia*. These

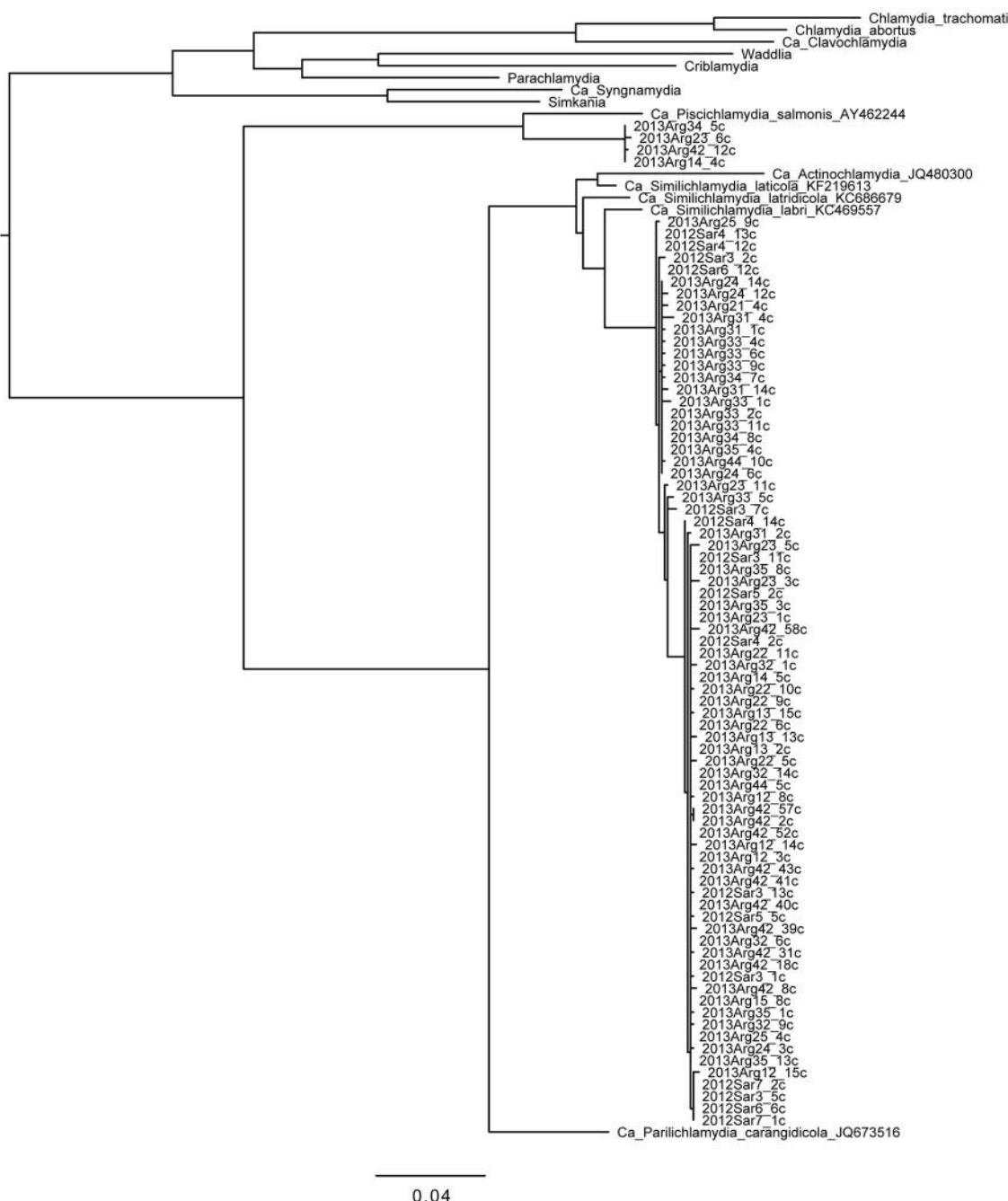


FIGURE 1 | Phylogenetic tree of chlamydial 16S rRNA gene sequences obtained from gilthead seabream gills. Reference sequences from the phylum as a whole and from the deep-rooted “fish-Chlamydia” clade (provisional families *Ca. Piscichlamydiae*, *Parilichlamydiae*, *Actinochlamydiae*, and *Similichlamydiae*) are shown to put the sequences we obtained in this study in context. Clones from fish samples are named from the gill sample with the postscript “c” denoting amplification with *Chlamydiae*-specific primers. Four of the novel sequences from four fish from Argolida are more closely related to *Ca. P. salmonis*; 63 of the novel sequences from Saronikos and Argolida are more closely related to *Ca. S. labri* and *Ca. S. latridicola*. Sequences (~1,100 bp) were aligned and phylogenies generated within Seaview with 100 bootstraps. Branches separating the novel sequences from the reference sequences have bootstraps of 97% (*Piscichlamydiae* clade) and 100% (*Similichlamydiae* clade). Scale bar indicates number of substitutions per site.

share 97.2% nucleotide identity with a *Ca. Similichlamydia labri* sequence (accession number KC469554) over 1,075 bp from Norwegian ballan wrasse (Steigen et al., 2015) and 97% identity with *Ca. Similichlamydia latridicola* from striped trumpeter (Stride et al., 2013b). Thus, these may belong to a novel genus, but further full-length 16S rRNA gene sequencing would be required to confirm this (Yarza et al., 2014). There are two main clusters of sequences within this group: one of 19 sequences varying by 0–4 bp represented by 2013Arg33_2c, and the other of 41 sequences varying by 0–3 bp represented by 2013Arg23_1c.

Additionally, four sequences from four Argolida fish were analyzed and found to cluster with the *Ca. Piscichlamydia* and differ from each other by 0–2 bp. These share 94.1% identity over 1,091 bp with *Ca. Piscichlamydia salmonis* 16S rRNA gene sequence (accession number AY462244), indicating that they are likely to be distantly related members of this genus (Yarza et al., 2014). Thus, many novel strains of environmental *Chlamydia*, related to both *Ca. Similichlamydia* and *Ca. Piscichlamydia*, were found in the gills of this gilthead seabream cohort.

Chlamydial Load and Morphological Features of Chlamydial Cysts

Previous, quantitative analysis by qPCR comparing copy numbers of *Chlamydiae* and *Ca. Ichthyocystis* spp. showed that mixed infections were commonly observed, and the ratios of the infectious agents differed widely in individual fish, ranging from 1:5 to 1:3,000 (Seth-Smith et al., 2016, Supplementary Material).

These results were reflected in semithin sections stained with toluidine blue (Figure 2), allowing a clear differentiation between the dominant darkly staining and densely packed cysts of *Ca. Ichthyocystis* sp. and the fewer, lightly staining, thick walled chlamydial cysts. In smallest chlamydial cysts, presumably reflecting earlier stages of development, the perinuclear location of the intracellular cyst is readily evident, pressed to the side of the cell, reminiscent of *Ca. Piscichlamydia* (Schmidt-Posthaus et al., 2012) or a typical chlamydial type inclusion (Taylor-Brown et al., 2015). This can be seen in serial sections of a small cyst shown in Figure 2, where the cell wall thickness becomes quite marked through the increasingly oblique sectioning angles, relative to the cyst. Even in larger, presumably later stage cysts, only a single nucleus deformed by the cyst inclusion is evident. The clustering of chlamydial cysts along one of the three gill arches in this section is helpful for illustrating the different cyst morphologies, although the proportion of chlamydial to *Ca. Ichthyocystis* sp. cysts is normally lower, consistent with the relative loads previously determined molecularly (Seth-Smith et al., 2016, Supplementary Material).

FISH with a probe recognizing both *Ca. Similichlamydia* and *Ca. Piscichlamydia* of this deep branching chlamydial clade, gave a positive signal only with the chlamydial cysts (Figure 3A) and did not react with the generally larger *Ca. Ichthyocystis* sp. cysts. Conversely, *Ca. Ichthyocystis* sp. specific probes only reacted with these larger cysts (Seth-Smith et al.,

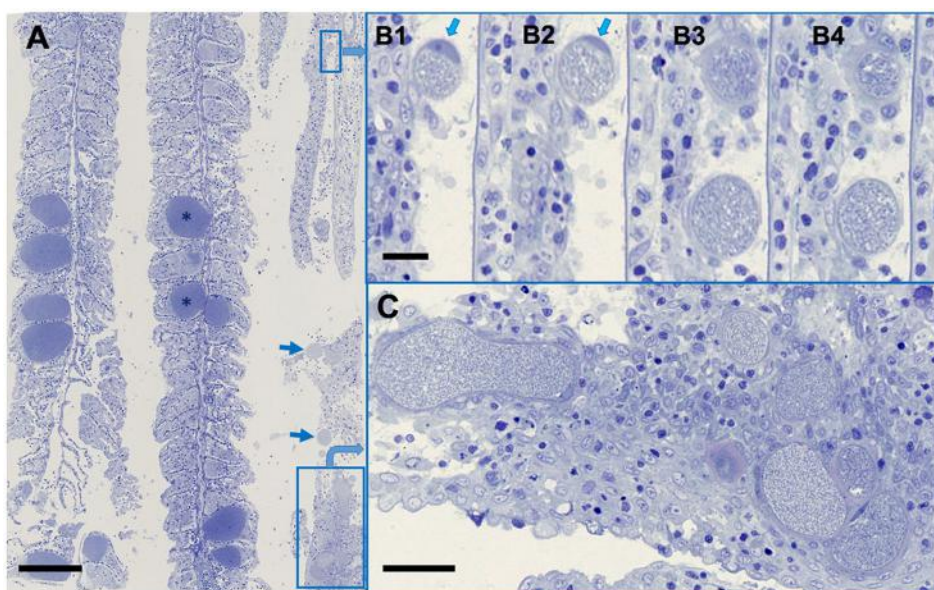


FIGURE 2 | *Ca. Ichthyocystis* sp. and *Ca. Similichlamydia* sp. cysts in adjacent gilthead seabream gill filaments. **(A)** An overview, with the darkly stained *Ca. Ichthyocystis* sp. cysts (*) typically attached to the base of the primary lamella, and filling the space between two secondary lamellae, which become surrounded by proliferating epithelial cells, completely embedding the cyst. The *Ca. Similichlamydia* sp. cysts (boxed or with arrows) are lightly stained, often in clusters, and typically localized within the base of the primary lamella. **(B1–B4)** Serial 1 μm sections (although not sequential) of two small cysts with host cell nucleus (arrows) pressed between the inclusion and the cellular membrane. Regions shown were enlarged from region of small rectangular box, upper right of overview **(A)**. **(C)** Higher magnification of boxed region, lower right **(A)**, for better visualization of similichlamydial cysts, all with broad inclusion membranes. Semi-thin 1 μm sections were stained with toluidine blue and imaged using a Hamamatsu Nanoozometer slide scanner, equipped with a 25 \times NA 0.75 objective lens, producing images with pixel sizes of 0.25 μm . Scale bars are 100 μm in **(A)**, 10 μm in **(B1–B4)**, and 25 μm in **(C)**.

2016, Supplementary Figure 3), and did not detect the chlamydial cysts.

Using the semithin sections for orientation, ultrathin sections were prepared and similichlamydial cysts were selected for TEM, whereby an attempt was made to cover as many stages of the putative developmental cycle as possible (Figure 3). The broad cell walls of smaller early stage cysts, detected in histology, revealed itself to be an intricate tubular or vesicular network,

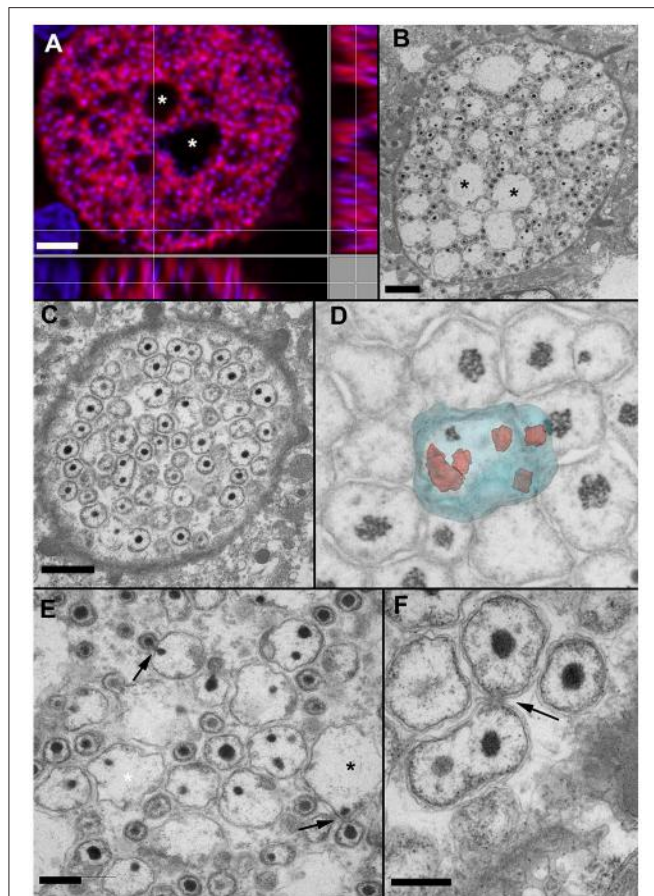


FIGURE 3 | *In situ* hybridization (**A**) and EM of early (**C,D**) and mid-stage (**A,B,E,F**) cysts. (**A**) Orthogonal projection of *Ca. Similichlamydia* labeled cyst from sample 2013Arg23, stained with Pisci0312-Cy3 in red and DAPI in blue and visualized with CLSM. (**B**) An equivalent cyst prepared for TEM, with similar vacuolar spaces (*) evident in both cysts and the condensed bacterial nucleoids of the IBs and EBs staining with DAPI in (**A**) and electron-dense in (**B**). (**C**) At a putatively earlier stage, the cysts are filled with amorphous bacterial forms, which can contain multiple condensed nucleoids, shown here with TEM. (**D**) The forms in **C** can best be visualized using 3D imaging with FIB-SEM. Here is a snapshot from a 3D FIB-SEM stack (see **Video S1**) showing a segmented reconstruction of a large amorphous RB containing multiple condensed nucleoids. (**E**) A higher magnification image of (**B**) reveals what appears to be an asymmetrical budding of IBs, with individual bacteria first being enclosed by an outer membrane, prior to release from the RB. The large electron-lucent spaces may well represent remnant RBs, left over after the budding process is complete. (**F**) Asymmetrical budding of smaller RBs is also evident, as is a reticular network, often observed within the host cell and enclosing the inclusion, as can be seen in the bottom right hand corner of this image. Scale bars (**A,B**) (2 μ m), (**C**) (1 μ m), (**E,F**) (0.5 μ m).

often enmeshing mitochondria as well as darkly staining deposits, possibly lipid containing, and intimately connecting with the chlamydial inclusion membrane (see also **Video S1**). In contrast to clavichlamydial cysts (Steinum et al., 2010; Schmidt-Posthaus et al., 2012), we detected no projections penetrating the inclusion membrane and associated with or attached to dividing (RB-like) bacteria. Dividing bacteria were detected throughout the putative early stage inclusions (Figures 3C,D,F, **Video S2**), indicative that nutrients from the host and within the inclusions are either freely solubilized in the inclusion liquor or their transport utilizes vesicular-based mechanisms. Rather than a replication initiated by simple division of RBs, once they reach a critical mass, the RBs appear quite amorphous in size and form, with up to eight nucleoids detected within a single RB (Figure 3D and **Video S2**). Here the use of FIB-SEM was invaluable in unequivocally visualizing the multinucleoid nature of these amorphous RBs. New bacteria appear to arise by budding (Figures 3B,C,E,F), which always occurs at one position from a given parent cell, indicative of a polar process. This is especially marked in the budding bodies shown in Figure 3E, where condensed nucleoids can be seen on both sides of the neck connecting the budding cells. The loose, wavy bacterial membranes and the many filamentous particles within the bacterial bodies are likely to be artifacts of the fixation and embedding process.

Putative late stage inclusions (Figure 4) contain uniform populations of EB-like forms, with features similar to those described for the closely related *Ca. Actinochlamydia* (Steigen et al., 2013). A condensed nucleoid is typically localized in a polar fashion adjacent to the bacterial membrane with an array of filaments (actinae, Steigen et al., 2013) penetrating the membrane on an adjacent or opposite side, indicative of a polarized bacterial cell with clearly defined functional regions.

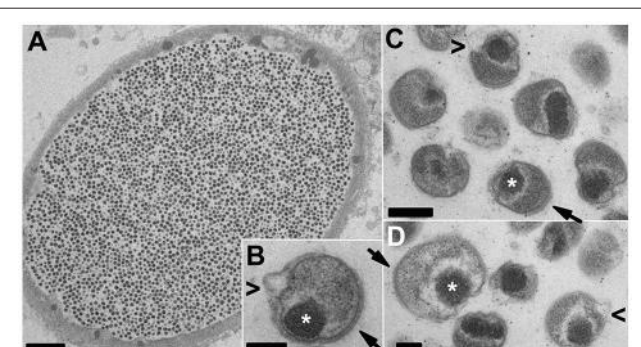


FIGURE 4 | TEM of putative late-stage *Ca. Similichlamydia* cysts containing uniform populations of EB-like forms. An overview of an entire cyst (**A**) together with a selection of higher magnification images of individual EBs (**B–D**) showing tightly condensed chromosomes (*) associated with the bacterial membrane in a polar location and adjacent or opposite, bacterial membrane spanning actinae (filaments, arrows) projecting away from the outer bacterial membrane. The EBs appear to reduce in size and become more compact by the pinching off of outer membrane vesicles (arrowheads < in **B–D**), although this may also be a shrinking artifact of the chemical fixation methods used. Scale bars (**A**) (5 μ m), (**B,C**) (0.2 μ m), (**D**) (0.1 μ m).

DISCUSSION

Investigation of the deepest rooting *Ca. Piscichlamydia* clade within the phylum *Chlamydiae* is attractive for exploring the origins of this large phylum (Lagkouvardos et al., 2013) and highly successful group of obligate intracellular bacteria. In particular, morphological and molecular features shared with the sister phyla of the *Planctomycetes* and *Verrumicrobiae* of the PVC superphylum may aid us in understanding how these bacteria evolved. The *Chlamydiae* are all thought to progress through a biphasic developmental cycle, initiated by infection of a susceptible host epithelial cell with the infectious particles or EBs, which are taken up and enclosed in a membrane bound inclusion, whereupon larger replicative forms of dividing bacteria (RBs) multiply to fill the inclusion before condensing to form EBs, which are released from the cell to initiate a fresh infectious cycle. Both the *Chlamydiae* and members of the *Planctomycetes* lack the tubulin homolog FtsZ which is involved in forming the septum regulating the binary fission of most bacterial cells, raising the question as to how this process is regulated. In FtsZ-less members of the *Planctomycetes* this occurs by a polar budding of bodies from a larger intermediate form (Fuerst, 1995; Lee et al., 2009; Santarella-Mellwig et al., 2013). Elements of these processes may be present in this deep rooted *Ca. Piscichlamydia/Similichlamydia* clade.

Several features stand out. During the replicative stage, the RBs are amorphous in form and size and can contain multiple nucleoids, with a new bacterium being generated via a single polar budding process. We only observed the budding of a bacterium with a single nucleoid and did not find evidence for cleavage of a multi-nucleoid containing RB into two RBs, each still with multiple nucleoids. This would indicate that the budding process is a tightly regulated one. We have previously described what appeared to be budding RBs in TEM images of *Ca. Piscichlamydia* from epitheliocystis lesions in brown trout (*Salmo trutta*, Schmidt-Posthaus et al., 2012), indicating that this mechanism may be common for the entire deep rooted clade comprising the four putative families (*Ca. Piscichlamydia*, *Similichlamydia*, *Parilichlamydia*, *Actinochlamydia*), all members of which have only been found as intracellular bacterial pathogens of marine or fresh water vertebrates, indicative of their early evolutionary origins and specialization for an aqueous environment (Draghi et al., 2004; Schmidt-Posthaus et al., 2012; Steigen et al., 2013, 2015; Stride et al., 2013a,b,c). Curiously, the large RBs with multiple nucleoids which we find commonly here (Figures 3C,D) are more reminiscent of the aberrant bodies generated by antibiotic treatment or nutrient restriction in the *Chlamydiaceae* (Polkinghorne et al., 2006). *Ca. Similichlamydia* RBs are also distributed throughout the inclusion and do not appear to be preferentially aligned along the inclusion membrane with attachment through filaments or projections, as has been observed for the *Chlamydiaceae* or for their immediate marine relatives, the *Clavichlamydiaceae* (Schmidt-Posthaus et al., 2012).

Another feature is the small (0.3–0.5 μm) densely packed particles (Figure 4), resembling the infectious particles or EBs of the *Chlamydiaceae*, (Taylor-Brown et al., 2015) albeit with

a polar form and clusters of membrane spanning filaments or actinae, first described in the *Ca. Actinochlamydia* (Steigen et al., 2013), which could temptingly be postulated to influence host recognition and uptake. A major caveat, indeed a caveat which applies to the majority of the EM studies with *Chlamydia*, is that the use of chemical fixation combined with classical dehydration procedures prior to embedding can lead to a range of artifacts and poor membrane preservation. However, due to the remoteness of the fish farms, we had no possibility of applying advanced cryo-EM techniques as used to excellent effect by others (i.e., Santarella-Mellwig et al., 2013) to the samples we collected, and which would have aided us greatly in the interpretation of morphological features. This is a possibility for the future, but would require setting up of aquarium facilities close to the EM facilities and stocking these with infected fish, not a trivial undertaking. Conversely, should we one day finally succeed in isolating and cultivating these bacteria, this will be one of the experimental priorities.

It was long thought that the *Chlamydiaceae* RBs undergo binary fission, as most other bacteria, prior to transformation into the infectious particles or EBs. This may not be the case. As we were preparing this manuscript, an elegant study was forthcoming, indicating that at least with *Chlamydia trachomatis*, EBs are generated by polar budding from RBs, possibly also containing multiple chromosomes (Abdelrahman et al., 2016), reminiscent of the structures we present here for *Ca. Similichlamydia* (Figure 3). This study relies strongly on excellent high resolution immuno-light microscopy imaging, and identifies a number of chlamydial proteins which may have a role in regulating this process. It would be intriguing to investigate whether homologs of these proteins are encoded by the similichlamydial genome, and if so, how these proteins might be regulated.

Indeed, a concerted effort to analyse the genomes of this deep-rooted chlamydial clade would provide an invaluable insight into the essence of what makes a *Chlamydia* and how the members of this phylum share their origins within the PVC superphylum. Detailed morphological studies are critical to these efforts (Draghi et al., 2004; Schmidt-Posthaus et al., 2012; Steigen et al., 2013, 2015), to complement genomic analyses, which have now come within reach (Katharios et al., 2015; Qi et al., 2016; Seth-Smith et al., 2016).

AUTHOR CONTRIBUTIONS

Conceived and designed the experiments: AF, HSS, JM, MR, ND, PK, and LV. Performed the experiments: AF, HSS, JM, LN, MS, MR, ND, PK, and LV. Analyzed the data: AF, HSS, JM, LN, MR, MS, PK, and LV. Contributed reagents/materials/analysis tools: HSS, JM, MS, ND, and PK. Contributed to writing the manuscript: HSS, JM, MR, PK, and LV.

FUNDING

This work was supported by the European Union through Marie Curie Intra-European Fellowship grant number 332058 to HSS and an FP7 Aquaxcel-TNA project 01-05-15-0004-B to LV and

PK. AF was partly supported by SNF project 310030_138533 to LV. The funders had no role in study design, data collection and analysis, decision to publish or preparation of the manuscript.

SUPPLEMENTARY MATERIAL

The Supplementary Material for this article can be found online at: <http://journal.frontiersin.org/article/10.3389/fmicb.2017.00508/full#supplementary-material>

Video S1 | Video of sequential Z-slices of a portion of a cyst taken with FIB-SEM showing the inclusion membrane (putative outermembrane). The

broad cell wall of smaller early stage cysts, detected in histology, revealed itself to be an intricate tubular, or vesicular network along the outer side of the inclusion membrane, often enmeshing mitochondria as well as darkly staining deposits, possibly lipid containing, and intimately connecting with the chlamydial inclusion membrane. The amorphous nature of the RBs and the variable number of electron dense nucleoids can readily be seen.

Video S2 | Video of a portion of a cyst taken with FIB-SEM showing a segmented reconstruction of a large amorphous RB containing multiple condensed chromosomes. In this orthogonal projection, the electron-dense material, bacterial chromatin, or nucleoids, is rendered in red and the outer surface of the bacteria in blue. The number of nucleoids per bacteria is variable, indicative that replicating bacteria at various stages of growth are present. The voxel size in both videos is 5 × 5 × 20 (XYZ).

REFERENCES

- Abdelrahman, Y., Ouellette, S. P., Belland, R. J., and Cox, J. V. (2016). Polarized cell division of *Chlamydia trachomatis*. *PLoS Pathog.* 12:e1005822. doi: 10.1371/journal.ppat.1005822
- Cardona, A., Saalfeld, S., Schindelin, J., Arganda-Carreras, I., Preibisch, S., Longair, M., et al. (2012). TrakEM2 software for neural circuit reconstruction. *PLoS ONE* 7:e38011. doi: 10.1371/journal.pone.0038011
- Contador, E., Methner, P., Ryerse, I., Huber, P., Lillie, B. N., Frasca, S. Jr., et al. (2016). Epitheliocystis in lake trout *Salvelinus namaycush* (Walbaum) is associated with a β-proteobacteria. *J. Fish Dis.* 39, 353–366. doi: 10.1111/jfd.12369
- Crespo, S., Zarzo, C., Padros, F., and de Mateo, M. M. (1999). Epitheliocystis agents in sea bream *Sparus aurata*: morphological evidence for two distinct chlamydialike developmental cycles. *Dis. Aquat. Org.* 37, 61–72. doi: 10.3354/dao037061
- Draghi, A., Popov, V. L., Kahl, M. M., Stanton, J. B., Brown, C. C., Tsongalis, G. J., et al. (2004). Characterization of “*Candidatus Piscichlamydia salmonis*” (Order Chlamydiales), a *Chlamydia*-like bacterium associated with epitheliocystis in farmed Atlantic Salmon (*Salmo salar*). *J. Clin. Microbiol.* 42, 5286–5297. doi: 10.1128/JCM.42.11.5286-5297.2004
- Everett, K. D. E., Hornung, L. J., and Andersen, A. A. (1999). Rapid detection of the Chlamydiateae and other families in the order Chlamydiales: three PCR tests. *J. Clin. Microbiol.* 37, 575–580.
- Fuerst, J. A. (1995). The Planctomyces: emerging models for microbial ecology, evolution and cell biology. *Microbiology* 141, 1493–1506. doi: 10.1099/13500872-141-7-1493
- Gouy, M., Guindon, S., and Gascuel, O. (2010). SeaView version 4: a multiplatform graphical user interface for sequence alignment and phylogenetic tree building. *Mol. Biol. Evol.* 27, 221–224. doi: 10.1093/molbev/msp259
- Guevara Soto, M., Vidondo, B., Vaughan, L., Seth-Smith, H. M. B., Nufer, L., Segner, H., et al. (2016). The emergence of epitheliocystis in the upper Rhone region: evidence for Chlamydiae in wild and farm salmonid populations. *Arch. Microbiol.* 198, 315–324. doi: 10.1007/s00203-016-1192
- Hoffman, G. L., Dunbar, C. E., Wolf, K., and Zwillingberg, L. O. (1969). Epitheliocystis, a new infectious disease of the bluegill (*Lepomis macrochirus*). *Antonie van Leeuwenhoek* 35, 146–158. doi: 10.1007/BF02219125
- Karslen, M., Nylund, A., Watanabe, K., Helvik, J. V., Nylund, S., and Plarre, H. (2008). Characterization of ‘*Candidatus Clavochlamydia salmonicola*’: an intracellular bacterium infecting salmonid fish. *Environ. Microbiol.* 10, 208–218. doi: 10.1111/j.1462-2920.2007.01445.x
- Katharios, P., Seth-Smith, H. M., Fehr, A., Mateos, J. M., Qi, W., Richter, D., et al. (2015). Environmental marine pathogen isolation using mesocosm culture of sharpsnout seabream: striking genomic and morphological features of novel *Endozoicomonas* sp. *Sci. Rep.* 5:17609. doi: 10.1038/srep17609
- Lagkouvardos, I., Weinmaier, T., Lauro, F. M., Cavicchioli, R., Rattei, T., and Horn, M. (2013). Integrating metagenomic and amplicon databases to resolve the phylogenetic and ecological diversity of the chlamydiae. *ISME J.* 8, 115–125. doi: 10.1038/ismej.2013.142
- Lee, K. C., Webb, R. I., and Fuerst, J. A. (2009). The cell cycle of the planctomycete *Gemmata obscuriglobus* with respect to cell compartmentalization. *BMC Cell Biol.* 10:4. doi: 10.1186/1471-2121-10-4
- Mendoza, M., Guiza, L., Martinez, X., Caraballo, X., Rojas, J., Aranguren, L. F., et al. (2013). A novel agent (*Endozoicomonas elysicola*) responsible for epitheliocystis in cobia *Rachycentrum canadum* larvae. *Dis. Aquat. Organ.* 106, 31–37. doi: 10.3354/dao02636
- Nowak, B. F., and LaPatra, S. E. (2006). Epitheliocystis in fish. *J. Fish. Dis.* 29, 573–588. doi: 10.1111/j.1365-2761.2006.00747.x
- Nylund, A., Kvænseth, A. M., and Isdal, E. (1998). A morphological study of the epitheliocystis agent in farmed Atlantic salmon. *J. Aquat. Anim. Health* 10, 43–55. doi: 10.1577/1548-8667(1998)010<0043:AMSOTE>2.0.CO;2
- Paperna, I. (1977). Epitheliocystis infection in wild and cultured sea bream (*Sparus aurata*, Sparidae) and grey mullets (*Liza Ramada*, Mugilidae). *Aquaculture* 10, 169–176. doi: 10.1016/0044-8486(77)90018-7
- Polkinghorne, A., Hogan, R. J., Vaughan, L., Summersgill, J. T., and Timms, P. (2006). Differential expression of chlamydial signal transduction genes in normal and interferon gamma-induced persistent *Chlamydophila pneumoniae* infections. *Microbes Infect.* 8, 61–72. doi: 10.1016/j.micinf.2005.05.018
- Ponti, A., Schwarb, P., Gulati, A., and Bäcker, V. (2007). A web interface for high-volume batch deconvolution. *Imaging Microsc.* 9, 57–58.
- Qi, W., Vaughan, L., Katharios, P., Schlapbach, R., and Seth-Smith, H. M. (2016). Host-associated genomic features of the novel uncultured intracellular pathogen *Ca. Ichthyocystis* revealed by direct sequencing of epitheliocysts. *Genome Biol. Evol.* 8, 1672–1689. doi: 10.1093/gbe/ewv111
- Santarella-Mellwig, R., Prugnaller, S., Roos, N., Mattaj, I. W., and Devos, D. P. (2013). Three-dimensional reconstruction of bacteria with a complex endomembrane system. *PLoS Biol.* 11:e1001565. doi: 10.1371/journal.pbio.1001565
- Schmidt-Posthaus, H., Polkinghorne, A., Nufer, L., Schifferli, A., Zimmermann, D. R., Segner, H., et al. (2012). A natural freshwater origin for two chlamydial species, *Candidatus Piscichlamydia salmonis* and *Candidatus Clavochlamydia salmonicola*, causing mixed infections in wild brown trout (*Salmo trutta*). *Environ. Microbiol.* 14, 2048–2057. doi: 10.1111/j.1462-2920.2011.02670.x
- Seth-Smith, H. M. B., Dourala, N., Fehr, A., Qi, W., Katharios, P., Ruettem, M., et al. (2016). Emerging pathogens of gilthead seabream: characterisation and genomic analysis of novel intracellular beta-proteobacteria. *ISME J.* 10, 1791–1803. doi: 10.1038/ismej.2015.223
- Sommer, C., Strähle, C., Köthe, U., and Hamprecht, F. A. (2011). “Ilastik: interactive learning and segmentation toolkit,” in *Eighth IEEE International Symposium on Biomedical Imaging (ISBI), Proceedings* (Chicago), 230–233.
- Steigen, A., Karlsbakk, E., Plarre, H., Watanabe, K., Øvergård, A. C., Brevik, Ø., et al. (2015). A new intracellular bacterium, *Candidatus Similichlamydia labri* sp. nov. (Chlamydiateae) producing epitheliocysts in ballan wrasse, *Labrus bergylta* (Pisces, Labridae). *Arch. Microbiol.* 197, 311–318. doi: 10.1007/s00203-014-1061-4
- Steigen, A., Nylund, A., Karlsbakk, E., Akoll, P., Fiksdal, I. U., Nyland, S., et al. (2013). ‘Cand. *Actinochlamydia clariae*’ gen. nov., sp. nov., a unique intracellular bacterium causing epitheliocystis in Catfish (*Clarias gariepinus*) in Uganda. *PLoS ONE* 8:e66840. doi: 10.1371/journal.pone.0066840
- Steinum, T., Kvellestad, A., Colquhoun, D. J., Heum, M., Mohammad, S., Grøntvedt, R. N., et al. (2010). Microbial and pathological findings in farmed Atlantic salmon *Salmo salar* with proliferative gill inflammation. *Dis. Aquat. Org.* 91, 201–211 doi: 10.3354/dao02266

- Stride, M. C., Polkinghorne, A., and Nowak, B. F. (2014). Chlamydial infections of fish: diverse pathogens and emerging causes of disease in aquaculture species. *Vet. Microbiol.* 170, 19–27. doi: 10.1016/j.vetmic.2014.01.022
- Stride, M. C., Polkinghorne, A., Miller, T. L., and Nowak, B. F. (2013b). Molecular characterization of “*Candidatus Similichlamydia latridicola*” gen. nov., sp. nov. (*Chlamydiales*: “*Candidatus Parilichlamydiaceae*”), a novel *Chlamydia*-like epitheliocystis agent in the striped trumpeter, *Lutjanus lineatus* (Forster). *Appl. Environ. Microbiol.* 79, 4914–4920 doi: 10.1128/AEM.00746-13
- Stride, M. C., Polkinghorne, A., Miller, T. L., Groff, J. M., LaPatra, S. E., and Nowak, B. F. (2013a). Molecular characterization of “*Candidatus Parilichlamydia carangidicola*”, a Novel *Chlamydia*-Like epitheliocystis agent in Yellowtail Kingfish, *Seriola lalandi* (Valenciennes), and the proposal of a new family, “*Candidatus Parilichlamydiaceae*” fam. nov. (Order *Chlamydiales*). *Appl. Environ. Microbiol.* 79, 1590–1597. doi: 10.1128/AEM.02899-12
- Stride, M. C., Polkinghorne, A., Powell, M. D., and Nowak, B. F. (2013c). “*Candidatus Similichlamydia laticola*”, a novel *Chlamydia*-like agent of epitheliocystis in seven consecutive cohorts of farmed Australian barramundi, *Lates calcarifer* (Bloch). *PLoS ONE* 8:e82889. doi: 10.1371/journal.pone.0082889
- Taylor-Brown, A., Vaughan, L., Greub, G., Timms, P., and Polkinghorne, A. (2015). Twenty years of research into *Chlamydia*-like organisms: a revolution in our understanding of the biology and pathogenicity of members of the phylum *Chlamydiae*. *Pathog. Dis.* 73, 1–15. doi: 10.1093/femspd/ftu009
- Toenshoff, E. R., Kvellestad, A., Mitchell, S. O., Steinum, T., Falk, K., Colquhoun, D. J., et al. (2012). A novel betaproteobacterial agent of gill epitheliocystis in seawater farmed Atlantic Salmon (*Salmo salar*). *PLoS ONE* 7:e32696 doi: 10.1371/journal.pone.0032696
- Yarza, P., Yilmaz, P., Pruesse, E., Glockner, F. O., Ludwig, W., Schleifer, K. H., et al. (2014). Uniting the classification of cultured and uncultured bacteria and archaea using 16S rRNA gene sequences. *Nat. Rev. Microbiol.* 12, 635–645. doi: 10.1038/nrmicro3330
- Conflict of Interest Statement:** The authors declare that the research was conducted in the absence of any commercial or financial relationships that could be construed as a potential conflict of interest.
- Copyright © 2017 Seth-Smith, Katharios, Dourala, Mateos, Fehr, Nufer, Ruettner, Guevara Soto and Vaughan. This is an open-access article distributed under the terms of the Creative Commons Attribution License (CC BY). The use, distribution or reproduction in other forums is permitted, provided the original author(s) or licensor are credited and that the original publication in this journal is cited, in accordance with accepted academic practice. No use, distribution or reproduction is permitted which does not comply with these terms.



Fuerstia marisgermaniae gen. nov., sp. nov., an Unusual Member of the Phylum Planctomycetes from the German Wadden Sea

Timo Kohn¹, Anja Heuer¹, Mareike Jogler¹, John Vollmers¹, Christian Boedeker¹, Boyke Bunk¹, Patrick Rast¹, Daniela Borchert¹, Ines Glöckner¹, Heike M. Freese¹, Hans-Peter Klenk², Jörg Overmann¹, Anne-Kristin Kaster¹, Manfred Rohde³, Sandra Wiegand¹ and Christian Jogler^{1*}

¹ Leibniz Institut Deutsche Sammlung Von Mikroorganismen und Zellkulturen, Braunschweig, Germany, ² School of Biology, Newcastle University, Newcastle, UK, ³ Helmholtz Centre for Infectious Disease, Braunschweig, Germany

OPEN ACCESS

Edited by:

Damien Paul Devos,
Pablo de Olavide University, Spain

Reviewed by:

Svetlana N. Dedysh,
Winogradsky Institute of Microbiology,
Russian Academy of Science, Russia
Johannes Gijsbrecht Kuenen,
Delft University of Technology,
Netherlands

*Correspondence:

Christian Jogler
christian@jogler.de

Specialty section:

This article was submitted to
Evolutionary and Genomic
Microbiology,
a section of the journal
Frontiers in Microbiology

Received: 30 September 2016

Accepted: 08 December 2016

Published: 22 December 2016

Citation:

Kohn T, Heuer A, Jogler M, Vollmers J, Boedeker C, Bunk B, Rast P, Borchert D, Glöckner I, Freese HM, Klenk H-P, Overmann J, Kaster A-K, Rohde M, Wiegand S and Jogler C (2016) *Fuerstia marisgermaniae* gen. nov., sp. nov., an Unusual Member of the Phylum Planctomycetes from the German Wadden Sea. *Front. Microbiol.* 7:2079.
doi: 10.3389/fmicb.2016.02079

Members of the phylum Planctomycetes are ubiquitous bacteria that dwell in aquatic and terrestrial habitats. While planctomycetal species are important players in the global carbon and nitrogen cycle, this phylum is still undersampled and only few genome sequences are available. Here we describe strain NH11^T, a novel planctomycete obtained from a crustacean shell (Wadden Sea, Germany). The phylogenetically closest related cultivated species is *Gimesia maris*, sharing only 87% 16S rRNA sequence identity. Previous isolation attempts have mostly yielded members of the genus *Rhodopirellula* from water of the German North Sea. On the other hand, only one axenic culture of the genus *Pirellula* was obtained from a crustacean thus far. However, the 16S rRNA gene sequence of strain NH11^T shares only 80% sequence identity with the closest relative of both genera, *Rhodopirellula* and *Pirellula*. Thus, strain NH11^T is unique in terms of origin and phylogeny. While the pear to ovoid shaped cells of strain NH11^T are typical planctomycetal, light-, and electron microscopic observations point toward an unusual variation of cell division through budding: during the division process daughter- and mother cells are connected by an unseen thin tubular-like structure. Furthermore, the periplasmic space of strain NH11^T was unusually enlarged and differed from previously known planctomycetes. The complete genome of strain NH11^T, with almost 9 Mb in size, is among the largest planctomycetal genomes sequenced thus far, but harbors only 6645 protein-coding genes. The acquisition of genomic components by horizontal gene transfer is indicated by the presence of numerous putative genomic islands. Strikingly, 45 "giant genes" were found within the genome of NH11^T. Subsequent analysis of all available planctomycetal genomes revealed that Planctomycetes as such are especially rich in "giant genes". Furthermore, Multilocus Sequence Analysis (MLSA) tree reconstruction support the phylogenetic distance of strain NH11^T from other cultivated Planctomycetes of the same phylogenetic cluster. Thus, based on our findings, we propose to classify strain NH11^T as *Fuerstia marisgermaniae* gen. nov., sp. nov., with the type strain NH11^T, within the phylum Planctomycetes.

Keywords: planctomycetes, *Fuerstia marisgermaniae*, giant genes, cell division, animal associated

INTRODUCTION

Planctomycetes are a phylum of ubiquitous, environmentally important bacteria that play key roles in global carbon and nitrogen cycles (Fuerst and Sagulenko, 2011; Kartal et al., 2013). Together with the Verrucomicrobia and the Chlamydia, planctomycetes belong to the PVC superphylum (Wagner and Horn, 2006). While Chlamydia are intracellular pathogens (Stephens et al., 1998), Verrucomicrobia (Petroni et al., 2000), and Planctomycetes (Fuerst et al., 1997; Lage and Bondoso, 2014) can be closely associated with eukaryotes as well. The Planctomycetes are divided into four distinct orders. While the orders Phycisphaerales, Tepidisphaerales, and Planctomycetales are based on axenic cultures, the order Brocadiales is formed by well described enrichment cultures, the so-called anammox-Planctomycetes. These organisms are capable of anaerobic ammonium oxidation, a trait extremely useful for wastewater treatment (Kartal et al., 2013). In particular, members of the order Planctomycetales were found to encode numerous secondary metabolite-related genes and gene clusters (Jeske et al., 2013), that were recently found to be active under conditions that chemically mimicked the interaction with eukaryotes (Jeske et al., 2016). Consequently, Planctomycetes were postulated to be “talented producers” of small molecules and they might represent a yet untapped resource of novel bioactive molecules (Jeske et al., 2016). Furthermore, the biotechnological application of planctomycetal enzymes such as sulfatases as biocatalysts was demonstrated (Wallner et al., 2005). Thus, Planctomycetes are environmentally important and of general biotechnological interest.

Planctomycetes were further proposed to comprise conspicuous cell biological features such as endocytosis-like uptake of proteins (Fuerst and Sagulenko, 2010) and compartmentalization of their cytosol (Fuerst, 2005). In addition, they were believed to lack peptidoglycan (PG) in their cell walls (König et al., 1984). Recently some of these unique features were questioned. For example, the presence of PG was demonstrated (Jeske et al., 2015; van Teeseling et al., 2015). However, in particular the unusual cell division of Planctomycetales through polar budding makes them unique among bacteria, as they lack the otherwise universal bacterial cell division protein FtsZ (van Niftrik et al., 2009; Jogler et al., 2012).

Despite their importance for environmental microbiology, biotechnology and cell biology, only 30 planctomycetal species were obtained as axenic cultures and only 10 completely closed genome sequences are available through NCBI GenBank. Thus, from a phylogenetic point of view, the phylum Planctomycetes is heavily undersampled and only few representatives of this phylum are taxonomically characterized in detail (Ward, 2010; Fuerst and Sagulenko, 2011).

In this study, we selectively target eukaryote-associated species from a marine habitat. We revisit the German North Sea, which is a well-known resource for the cultivation of Planctomycetes (Glöckner et al., 2003; Winkelmann and Harder, 2009). To focus on potentially eukaryote-associated species, we collected crab shells as the successful isolation of novel Planctomycetes from Crustacea was previously reported (Fuerst et al., 1997). As

planctomycetes are known to be resistant to multiple antibiotics such as carbenicillin (Cayrou et al., 2010; Aghnatiou et al., 2015), we employed a 96 well-based high-throughput cultivation procedure and subsequently screened hundreds of carbenicillin-resistant bacterial cultures with a PCR targeting the 16S rRNA gene. The obtained strain NH11^T was selected for further analysis and full-length 16S rRNA gene sequencing revealed its affiliation with the phylum Planctomycetes. Here we show how strain NH11^T differs from other planctomycetal species and therefore propose the new genus *Fuerstia* gen. nov., with the type species *Fuerstia marisgermanicae* sp. nov.

MATERIALS AND METHODS

Sampling Site

The strain was isolated from a crustacean shell (crab) which was collected on the 22nd May 2012 at low tide (8:30 a.m.) at 16°C ambient temperature in some residue water on the tidal mud flat of the German Wadden Sea, Neuharlingersiel (53°42'15.5" N, 7°42'15.9" E).

Isolation and Maintenance

In a first step the surface of a crustacean shell was scraped-off and the shell material was transferred to sterile artificial sea water (ASW) supplemented with 10-fold diluted HD medium, to serve as biofilm suspension. ASW was prepared modified after Levring (1946) consisting of (per liter distilled water): 23.6 g NaCl; 0.64 g KCl; 4.53 g MgCl₂ · 6 H₂O; 5.94 g MgSO₄ · 7 H₂O; 1.3 g CaCl₂ · 2 H₂O; 10 mg Na₂PO₄ · 2 H₂O; 2.1 mg NH₄NO₃. To avoid precipitation, the CaCl₂ solution was sterilized separately (Bruns et al., 2003). HD medium was composed of 0.25 g/l yeast extract, 0.1 g/l glucose, 0.5 g/l peptone and 2.38 g/l HEPES; the pH was adjusted to 7.3. The suspension of the bacterial biofilm was used to inoculate fifty 96 well plates employing a multidrop device as previously described (Jogler et al., 2013). Cultures were subsequently transferred to fresh 96 well plates with the same medium but supplemented with 2 mg/ml carbenicillin. Cultures that survived this treatment were screened employing a 16S rRNA gene targeting PCR, using the primer set 8f (5'-AGA GTT TGA TCM TGG CTC AG-3') and 1492r (5'-GGY TAC CTT GTT ACG ACT T-3') modified from Lane (1991). PCR amplifications were performed employing a Veriti 96-Well Thermal Cycler (Applied Biosystems) applying the following conditions: initial denaturation at 94°C for 5 min, followed by 10 cycles of denaturation at 94°C for 30 s, annealing at 59°C for 30 s and elongation at 72°C for 60 s. This first 10 cycles were followed by 20 cycles of denaturation at 94°C for 30 s, annealing at 54°C for 30 s, elongation at 72°C for 60 s and a final elongation at 72°C for 5 min. Amplification products were subject to 16S rRNA gene sequencing and NCBI database comparison to identify novel strains. Based on this analysis, strain NH11^T was selected for subsequent experiments. Further cultivation was performed employing a modified M2 culture broth (M2mod) previously used for *Rhodopirellula baltica* (Jeske et al., 2013) containing 0.5 g/l peptone, 0.25 g/l glucose, 250 ml/l artificial sea water (ASW), 5 ml/l vitamin solution (double concentrated) and 20 ml/l mineral salt solution. The medium was buffered with

2.38 g/l HEPES at pH 7.0. Artificial sea water was composed of 46.94 g/l NaCl, 7.84 g/l Na₂SO₄, 21.28 g/l MgCl₂ · 6 H₂O, 2.86 g/l CaCl₂ · 2 H₂O, 0.384 g/l NaHCO₃, 1.384 g/l KCl, 0.192 g/l KBr, 0.052 g/l H₃BO₃, 0.08 g/l SrCl₂ · 6 H₂O, and 0.006 g/l NaF. The vitamin solution was composed of 4 mg/l biotin, 4 mg/l folic acid, 20 mg/l pyridoxine-HCl, 10 mg/l riboflavin, 10 mg/l thiamine-HCl · 2 H₂O, 10 mg/l nicotinamide, 10 mg/l D-Capentothenate, 0.2 mg/l vitamin B₁₂, and 10 mg/l *p*-aminobenzoic acid. Mineral salt solution was composed of 10 g/l nitrilotriacetic acid (NTA), 29.70 g/l MgSO₄ · 7 H₂O, 3.34 g/l CaCl₂ · 2 H₂O, 12.67 mg/l Na₂MoO₄ · 2 H₂O, 99 mg/l FeSO₄ · 7 H₂O, and 50 ml/l metal salt sol. "44". Metal salt sol. "44" was composed of 250 mg/l Na-EDTA, 1.095 g/l ZnSO₄ · 7 H₂O, 0.5 g/l FeSO₄ · 7 H₂O, 154 mg/l MnSO₄ · H₂O, 39.20 mg/l CuSO₄ · 5 H₂O, 24.80 mg/l Co(NO₃)₂ · 6 H₂O, and 17.70 mg/l Na₂B₄O₇ · 10 H₂O. Solid medium was prepared by adding 15 g/l of three times prewashed agar (Becton, Dickinson and Company) to the medium.

Light Microscopy

Phase contrast (Phaco) and differential interference contrast (DIC) analysis were performed employing a Nikon Eclipse Ti inverted microscope with a Nikon N Plan Apochromat λ 100x/1.45 Oil objective and a Nikon DS-Ri2 camera. Specimens were immobilized in MatTek glass bottom dishes (35 mm, No. 1.5) employing a 1% agarose cushion. Images were analyzed using the Nikon NIS-Elements software (Version V4.3).

Electron Microscopy

For field emission scanning electron microscopy (FESEM) bacteria were fixed in 1% formaldehyde in HEPES buffer (3 mM HEPES, 0.3 mM CaCl₂, 0.3 mM MgCl₂, 2.7 mM sucrose, pH 6.9) for 1 h on ice and washed one time employing the same buffer. Cover slips with a diameter of 12 mm were coated with a poly-L-lysine solution (Sigma-Aldrich) for 10 min, washed in distilled water and air-dried. Fifty microliter of the fixed bacteria solution was placed on a cover slip and allowed to settle for 10 min. Cover slips were then fixed in 1% glutaraldehyde in TE buffer (20 mM TRIS, 1 mM EDTA, pH 6.9) for 5 min at room temperature and subsequently washed twice with TE-buffer before dehydrating in a graded series of acetone (10, 30, 50, 70, 90, and 100%) on ice for 10 min at each concentration. Samples from the 100% acetone step were brought to room temperature before placing them in fresh 100% acetone. Samples were then subjected to critical-point drying with liquid CO₂ (CPD 300, Leica). Dried samples were covered with a gold/palladium (80/20) film by sputter coating (SCD 500, Bal-Tec) before examination in a field emission scanning electron microscope (Zeiss Merlin) using the Everhart Thornley HESE2-detector and the inlens SE-detector in a 25:75 ratio at an acceleration voltage of 5 kV. TEM micrographs of NH11^T cells were taken after negative staining with aqueous 0.1–2% uranyl acetate, employing a Zeiss transmission electron microscope EM 910 at an acceleration voltage of 80 kV at calibrated magnification as previously described (Wittmann et al., 2014). Prior TEM analysis cells were fixated for 2 h with 3% glutaraldehyde in 3 mM EM-HEPES buffer.

Thin sections of strain NH11^T were prepared by high pressure freezing and freeze substitution as previously described (Jogler

et al., 2011). Sections were subsequently analyzed employing a JEOL 1200EX-80kV TEM microscope.

Physiological Tests

Physiological tests such as salinity, pH, and temperature tolerance were performed in liquid medium M2mod. To test the NaCl tolerance, medium M2mod was prepared employing ASW devoid of NaCl. The required NaCl concentrations were adjusted prior inoculation, using a 30% NaCl (w/v) solution. The ASW tolerance was tested using M2mod without ASW. Again, the required concentration of ASW was adjusted prior inoculation. Growth was detected by monitoring the optical density at 600 nm using a Photometer Ultrospec II (LKB Biochrom). Carbon source utilization was tested using the GN2 MicroPlate™ system (Biolog), while enzymatic activities were tested using the API® ZYM method (bioMérieux). The physical features of the cell wall were analyzed by Gram staining, KOH test and Bactident® Aminopeptidase test strips. Growth under anoxic conditions was investigated using the api® 20 NE system (bioMérieux) according to the manufacturer's instructions.

Phylogenetic Analysis and Tree Reconstruction

For phylogenetic analysis version 6.0.2 of the ARB software package (Ludwig et al., 2004) was used together with the SILVA database SSURef_NR99 (Version 119, released on 14.07.2014; Pruesse et al., 2007). The full length 16S rRNA gene sequence was imported into ARB and then aligned using the fast aligner tool of the ARB software package. The resulting alignment was further edited manually to improve alignment quality. During the phylogenetic tree reconstruction, different type strains of the phylum Planctomycetes were used as reference sequences, while type strains of the phylum Verrucomicrobia served as out-group. All sequences that were included are listed in Table S1. Tree reconstruction was performed with the ARB software package (Ludwig et al., 2004). The Maximum Likelihood RAxML module was used with the rate distribution model GTR GAMMA running the rapid bootstrap analysis algorithm. The Neighbor Joining tool was employed with Felsenstein correction, while the Maximum Parsimony analysis was achieved with the Phylip DNAPARS module. Bootstrap values for all three methods were calculated with 1000 resamplings including the *E. coli* 16S rRNA gene positions 101–1371.

To facilitate the taxonomic classification of strain NH11^T, a cluster analysis was performed employing version 6.0.6 of the ARB software package (Ludwig et al., 2004) together with the database SSURef_NR99 (Version 123.1, released on 03.03.16) using a 87.65% sequence identity cutoff (threshold for the minimal sequence identity within a taxonomic family after Yarza et al., 2014) and *E. coli* 16S rRNA gene positions 112–1393. This analysis included all sequences of the family *Planctomycetaceae* that were available in the database as well as sequences of uncultivated planctomycetes, while the three clusters obtained for *Rubinisphaera brasiliensis* DSM 5305^T, *Gimesia maris* 534-30^T and strain NH11^T were selected for further phylogenetic tree reconstruction. For the NH11^T containing cluster, the highest, lowest, average and median sequence identities were determined

by calculating a distance matrix based on the *E. coli* 16S rRNA position 112–1393.

Genome Sequencing

Genomic DNA of strain NH11^T was extracted using the Genomic-tip 20/G kit (Qiagen, Germany) and a >10 kb SMRTbell™ template library was prepared according to the manufacturer instructions (PacificBiosciences, USA). In brief, ~10 µg of genomic DNA was end-repaired and ligated to hairpin adapters overnight (DNA/Polymerase Binding Kit 2.0, Pacific Biosciences, USA). The SMRTbell™ template was exonuclease treated for removal of incompletely formed reaction products. Conditions for annealing of sequencing primers and binding of polymerase to purified SMRTbell™ template were assessed with the calculator in RS Remote (PacificBiosciences, USA). Five SMRT cells were sequenced on the PacBio RS/RSII (PacificBiosciences, USA), each covered with a 90-min movie. Eight additional SMRT cells were used applying the DNA/Polymerase Binding Kit P4 (PacificBiosciences, USA) in order to collect larger read lengths. For those cells, 180-min movies were taken and a sub read lengths up to 20 kb was observed.

In addition, 2 × 9,143,110 paired-end Illumina reads were obtained employing an Illumina HiSeq 2500 for 101 cycles in both directions using the TruSeq DNA Sample Prep Kit v2 according to the manufacturer's instructions (Illumina Inc., San Diego, CA, USA). The genome assembly was performed using the RS_HGAP_Assembly.2 protocol included in SMRT Portal version 2.2.0 utilizing 520,016 reads from all 13 SMRT cells applying standard parameters with exception of the genome size, which was set to 9,100,000. Thus, one final contig could be obtained, which afterwards was error-corrected using a subset of 2 × 4,000,000 Illumina reads using BWA (Li and Durbin, 2009) with subsequent variant and consensus calling employing the CLC Genomics Workbench 7.03 (<http://www.clcbio.com>). Visual inspection of 41 called variants has been performed using IGV (Thorvaldsdóttir et al., 2013) in addition to prediction of rRNAs using RNAmmer (Lagesen et al., 2007). Hereby, the error-corrected consensus was trimmed, circularized and adjusted to *dnaA* as the first gene. For the circular genome of *Fuerstia marisgermanicae* NH11^T the finishing quality is estimated to be at 99.9999% (QV 60) confirmed by final PacBio resequencing. Genome annotation has been performed using PROKKA 1.8 (Seemann, 2014).

Genome Analysis

Genomic islands and CRISPR regions were identified using IslandViewer3 (Dhillon et al., 2015) and CRT (Bland et al., 2007), respectively. The planctomycetal genomes for the gene content analysis were derived from NCBI and IMG (Markowitz et al., 2012) in April 2016 and had to match the following criteria upon CheckM analysis (Parks et al., 2015): completeness >90, contamination <5 and strain heterogeneity <20. Orthologs were detected with Proteinortho5 (Lechner et al., 2011), a tool that identifies the reciprocal best hits from the given protein sequences. The genome plot was then generated with BRIG (Alikhan et al., 2011). The G+C content of the DNA was

estimated by analyzing the genome data using the software Artemis (Rutherford et al., 2000).

The gene size was calculated from annotations and analyzed with R (R Core Team, 2015) using the packages ggplot2 (Wickham, 2009), reshape (Wickham, 2007), xlsx (Dragulescu, 2014). Threshold for large genes were set to 5 kb according to Reva and Tümmler (2008). The biggest giant genes of NH11^T with a size over 20 kb were further analyzed using the InterProScan web service (Jones et al., 2014; Mitchell et al., 2015). The genome of strain NH11^T was screened for putative secondary metabolite clusters using the tool antiSMASH 3.0 (Weber et al., 2015).

Multilocus Sequence Analysis (MLSA)

Orthologs were identified using Proteinortho5 (Lechner et al., 2011) with the “-selfblast” option (which enables paralog-detection) enabled. Only genes present exclusively in single copy in all compared genomes were selected for MLSA. Alignments of the respective gene product amino acid sequences were generated individually for each ortholog group using MUSCLE v3.8.31 (Edgar, 2004a,b) and subsequently concatenated. Unalignable regions, caused by e.g., unique N-terminal or C-terminal sequence overhangs, were filtered from the concatenated alignment using Gblocks v.0.91b (Castresana, 2000). Phylogenetic relationships were inferred from the remaining unambiguous alignment positions by Neighbor Joining clustering with 1000 bootstrap iterations, using ARB 6.0.5 (Ludwig et al., 2004) and by Maximum Likelihood calculation using RAxML v. 8.0.26 (Stamatakis, 2014).

Fatty Acid Analysis

For fatty acid analysis, biomass of the three compared strains (NH11^T, *R. brasiliensis* DSM 5305^T and *G. maris* 534-30^T) was obtained from liquid cultures, grown in M2mod culture broth, at 20°C and slight agitation in baffled flasks. The obtained biomasses were processed according to the standards of the Identification Service of the German Collection of Microorganisms and Cell Cultures (DSMZ) (Miller, 1982; Kuykendall et al., 1988; Kämpfer and Kroppenstedt, 1996).

Nucleotide Sequence Accession Numbers

The accession numbers of the nucleotide sequences used for giant gene analysis or phylogenetic reconstruction are shown in Table S1. The NCBI genome accession number is CP017641.

RESULTS

Phylogenetic Analysis

Based on 16S rRNA gene phylogeny (Figure 1), strain NH11^T clusters together with *G. maris* within the family *Planctomycetaceae* (bootstrap support values: 69% for Maximum Likelihood, 43% for Maximum Parsimony, 46% for Neighbor Joining). However, it shares only 87.1% 16S rRNA gene sequence identity with *G. maris* based on BLAST analysis. Its next closest relative besides *G. maris* is *R. brasiliensis* (84.5% 16S rRNA gene sequence identity). An overview of the identities, generated with the manually curated SILVA alignment of all species of the

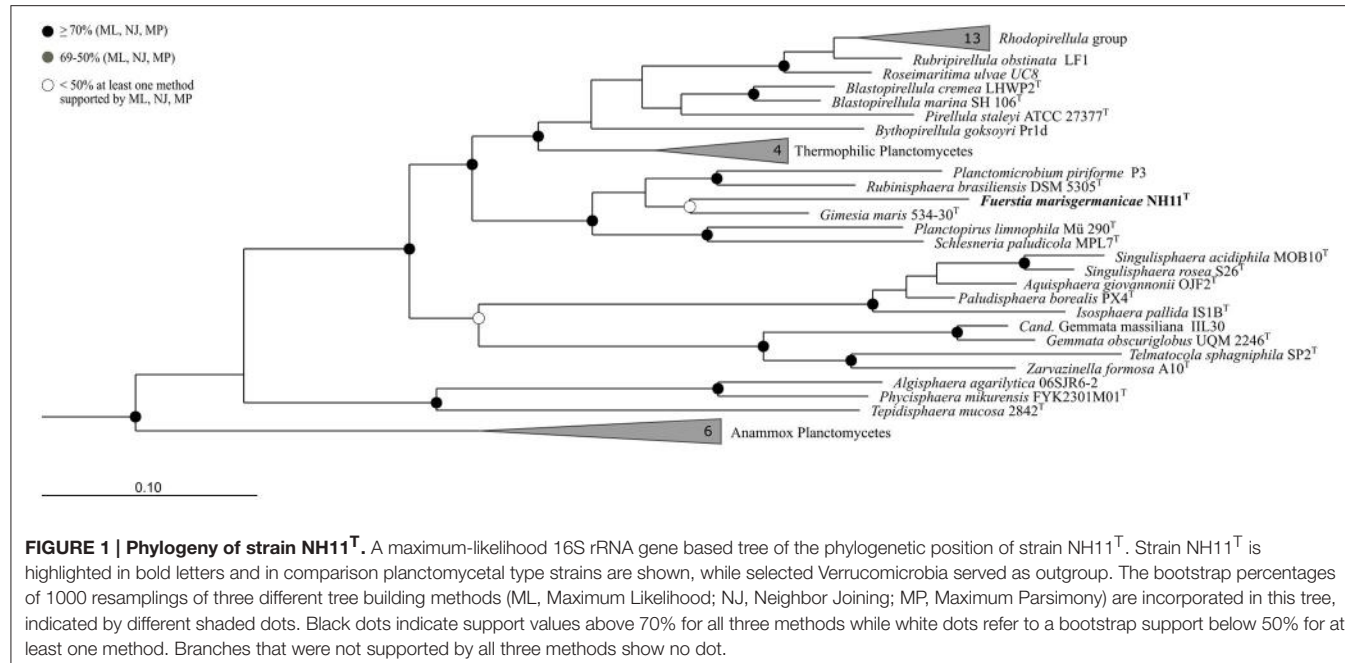


FIGURE 1 | Phylogeny of strain NH11^T. A maximum-likelihood 16S rRNA gene based tree of the phylogenetic position of strain NH11^T. Strain NH11^T is highlighted in bold letters and in comparison planctomycetal type strains are shown, while selected Verrucomicrobia served as outgroup. The bootstrap percentages of 1000 resamplings of three different tree building methods (ML, Maximum Likelihood; NJ, Neighbor Joining; MP, Maximum Parsimony) are incorporated in this tree, indicated by different shaded dots. Black dots indicate support values above 70% for all three methods while white dots refer to a bootstrap support below 50% for at least one method. Branches that were not supported by all three methods show no dot.

phylum Planctomycetes, based on the 1270 base pairs used for phylogenetic reconstruction, is given in Table S2. In this analysis the Felsenstein correction was used, to take evolutionary events that occurred during speciation into account. According to this analysis strain NH11^T shares 85.4% identity with *G. maris* and 84.1% with *R. brasiliensis*, differing from BLAST search results described above. The performed cluster analysis revealed, that NH11^T, *G. maris* and *R. brasiliensis* form three distinct clusters within the family *Planctomycetaceae* with an identity of at least 87.65% within each cluster, which is identical with the minimum sequence identity threshold for taxonomic families (Yarza et al., 2014; Figures S1–S3). In particular, within the cluster of strain NH11^T the minimal sequence identity is 88.3% and the maximal identity is 99.9%. The average identity in this cluster is 94.48% with a median of 94.4%, matching the threshold of 92.25% for median sequence identity for taxonomic families.

Morphological Characterization

Cells of strain NH11^T are pear to ovoid shaped (Figure 2) and form cream colored colonies on solid medium and motile swimmer cells in liquid culture. Cells are 1.2–2.5 × 0.9–1.7 μm in size. Its major phenotypic characteristics compared to those of *G. maris* and *R. brasiliensis* are listed in Table 1. No rosettes or stalks are formed in culture in contrast to the closest cultivated relatives *G. maris* and *R. brasiliensis* (Figures 2, 3). The surface of strain NH11^T is smooth and seems to lack crateriform structures except of polar regions where fiber-like structures seem to emerge from crateriform pits (Figure 3). Furthermore, the cell architecture of strain NH11^T and its mode of division seem to differ from all other planctomycetes described thus far (Figure 2). High pressure frozen and freeze substitution sections of strain NH11^T display a condensed nucleoid that was previously described in other planctomycetes, too (Figures 4A–C, white

arrow). However, some cells display exceptional patterns of cytoplasmic invaginations (Figures 4A,B), while others, except for the condensed nucleoid, comprise a cell envelope comparable to *E. coli* (Figure 4C). Despite of the degree of invaginations with characteristics different from other planctomycetes, ribosomes seem to localize frequently in close proximity to the cytoplasmic membrane in a rope-of-pearls-like pattern (Figures 4A–C, white arrowheads). Cells of strain NH11^T divide through budding and unlike all other planctomycetes described thus far, the mother- and daughter-cells seem to be connected via a tubular structure during cell division (Figures 4D–F). In particular, a dark structure at the division plane seems to parallel the cell division ring previously described for anammox Planctomycetes (van Niftrik et al., 2009; Figure 4D, black arrow).

Physiological Characterization

Strain NH11^T is able to grow between pH 6 and 10, with an optimal growth at pH 7 (Figure S4A). NH11^T tolerates up to 5% NaCl supplementation (Figure S4B) and requires at least 27.5% ASW for detectable growth (Figure S4C). In contrast, up to 230% ASW can be tolerated, while optimal growth conditions are in the range of 50–117.5% ASW. Temperature-wise, strain NH11^T can grow between 20 and 30°C, with optimal growth at 28°C (Figure S4D). Thus, strain NH11^T is a mesophilic organism. It is capable of utilizing a variety of carbon sources, listed in Table 2. In particular N-acetyl-D-galactosamine, N-acetyl-D-glucosamine, L-arabinose, D-cellobiose, D-galactose, gentiobiose, α-D-glucose, α-D-lactose, lactulose, maltose, D-mannose, D-melibiose, β-methyl-D-glucoside, sucrose, D-trehalose, turanose, succinic acid mono-methyl-ester, acetic acid, γ-hydroxybutyric acid, itaconic acid, propionic acid and glycerol were utilized. In contrast to the closest related *G. maris* and *R. brasiliensis*, strain NH11^T was not able to use

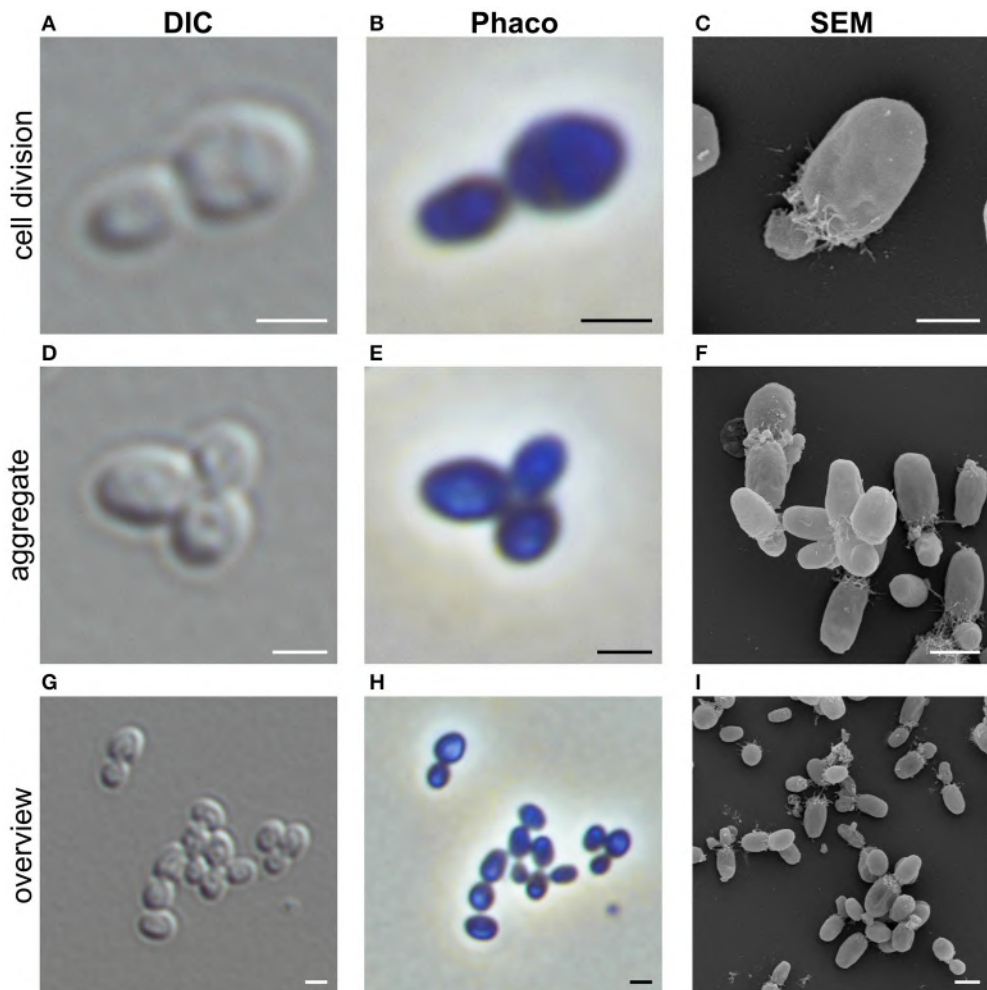


FIGURE 2 | Morphology of strain NH11^T. Representative differential interference contrast (DIC), Phase-contrast (Phaco) and scanning electron microscopic (SEM) micrographs of strain NH11. Shown are individual representative cells during division through polar budding (A–C) and -aggregate formation (D–F). In addition, an overview of multiple cells from a representative liquid culture is provided (G–I). Bar, 1 μ m.

L-rhamnose as carbon source. The enzymatic repertoire of strain NH11^T comprises alkaline phosphatase, esterase, esterase lipase, leucine arylamidase, valine arylamidase, cysteine arylamidase, trypsin, α -chymotrypsin, acid phosphatase, naphthol-AS-BI-phosphohydrolase, α -galactosidase, and α -glucosidase. All enzymatic features are listed in Table 3. No growth under anoxic conditions was observed.

Lipid Composition

The fatty acids of strain NH11^T and its closest relatives *G. maris* and *R. brasiliensis* were analyzed and compared. The major fatty acids of strain NH11^T consist of 59.16% C_{16:1} ω 6c/16:1 ω 7c (summed feature 3), 19.83% C_{18:1} ω 6c/18:1 ω 7c (summed feature 8) and 15.12% C_{16:0}. In comparison, *G. maris* comprised 26.63% of C_{16:1} ω 6c/16:1 ω 7c (summed feature 3), 23.50% of C_{16:0}, and 12.98% of C_{16:0} 10-methyl/Iso-C_{17:1} ω 6c (summed feature 9). The fatty acid profile of *R. brasiliensis* is composed of 47.10% C_{16:0} and 45.77% C_{16:1} ω 6c/16:1 ω 7c (summed feature 3). The

complete fatty acid profiles of strain NH11^T, *G. maris* and *R. brasiliensis* are listed in Table 4.

Taken together, the general fatty acid profile of strain NH11^T is similar, yet distinct compared to its closest relatives *G. maris* and *R. brasiliensis* and differs mainly in the components proportions.

Genome Analysis

The complete chromosome of strain NH11^T comprises 8,920,478 bp, with a GC content of 55.9%. Within the genome, 6732 genes were annotated, of which 6645 were identified as protein-coding genes. As known for other planctomycetes (Fuerst and Sagulenko, 2011), only for 54.3% of these genes a function could be predicted, while the remaining genes were annotated as hypothetical proteins or proteins with unknown function. Notable islands of unique gene content were found to especially comprise regions of predicted genomic islands and regions containing so-called “giant genes” (Reva and Tümler, 2008). The genomic features of strain NH11^T are summarized in

TABLE 1 | Morphological- and physiological features.

| Characteristic | NH11 ^T | G. maris | R. brasiliensis |
|-------------------------|----------------------|--------------------|--------------------|
| Cell shape | Pear shaped to ovoid | Spherical to ovoid | Spherical to ovoid |
| Cell size, µm | 1.2–2.5 × 0.9–1.7 | 0.4–1.5 | 0.7–1.8 |
| Flagellation | + | + | + |
| Rosette formation | – | + | + |
| Stalk formation | – | + | + |
| Colony color | Cream | Cream | Yellow to ochre |
| ASW tolerance (%) | 27.5–230 | 25–150 | 20–300 |
| ASW optimum (%) | 50–117.5 | n.d. | 40–180 |
| NaCl tolerance (%, w/v) | <5 | 1.5–4 | 0.6–10 |
| pH growth range | 6–10 | n.d. | n.d. |
| pH optimum | 7 | 7 | 7.5 |
| Temperature range, °C | 20–30 | 6–37 | <38 |
| Temperature optimum, °C | 28 | 30 | 27–35 |

Comparison of morphological- and physiological features of strain NH11^T with the two closest related type species *Gimesia maris* (Bauld and Staley, 1976) and *Rubinisphaera brasiliensis* (Schlesner, 1989).

Figure 5. In total, the genome of strain NH11^T comprises 45 giant genes, with a size greater than 5 kb (**Figure S5**). By the time of the first description of giant genes in the genome of *R. baltica* (Reva and Tümmeler, 2008) no other planctomycetal genome sequence was available. Thus, we analyzed the general distribution of giant genes amongst Planctomycetes and found all 29 available planctomycetal genomes to encode such genes (**Figure 6**). Fifteen strains encoded genes with a size >20 kb, two of which *Rhodopirellula* sp. K833 and NH11^T, even encode five >20 kb genes (**Figure S6**). Thus, genes >20 kb could be found in less than 50% of the available planctomycetal genomes. Furthermore, genes >30 kb were exclusively found in strain NH11^T and *G. maris*. Thus strain NH11^T is somewhat unique if gene-length is compared to other planctomycetes. Consequently, we analyzed the potential function of five NH11^T protein-coding genes >20 kb. The results, obtained from the InterProScan web service, points toward potential functions in cell adhesion, carbohydrate binding and partial location on the outer membrane of NH11^T.

Because TEM analysis pointed toward an anammox Planctomycetes-like cell division ring (van Niftrik et al., 2009; **Figure 4D**, black arrow), the genome was analyzed toward the presence of the putative cell division ring protein of *Candidatus “K. stuttgartiensis”* (locus tag kustd1438, NCBI Accession Number CAJ72183). The best match was a hypothetical protein with 36% sequence identity but only 19% query coverage (Fuma_00096), suggesting that this is presumably not a homolog of the putative protein found in *Candidatus “K. stuttgartiensis”*. However, with a size of 8699 bp, the gene that encodes for this hypothetical protein of strain NH11^T belongs to the identified giant genes. Analysis of this hypothetical protein, using the InterProScan web service, revealed the presence of Lamin Tail-(IPR001322), Ig-like- (IPR032812), and PapD-like domains (IPR008962), indicating putative involvement of this protein in cell shape maintenance or sub cellular organization.

Besides the giant genes, further analysis of the genome revealed the presence of a complete CRISPR type II system (cas9: Fuma_04885, cas1: Fuma_4887, cas2: Fuma_4888; Taylor et al., 2015). Only 2 other of the 35 analyzed planctomycetal genomes, corresponding to organisms *Blastopirellula marina* SH 106 and *Candidatus “Brocadia sinica* JPN1,” comprise such a system while the closest relative of strain NH11^T, *G. maris* lacks equivalent genes. This indicates that bacteriophages can infect strain NH11^T as the CRISPR type II system is primarily used for phage defense. Furthermore, absence in *G. maris* indicates differences in terms of phage susceptibility and/or defense strategy in comparison to strain NH11^T.

As Planctomycetes are a known source of potential bioactive compounds (Jeske et al., 2013), the genome of strain NH11^T was analyzed using antiSMASH 3.0 (Weber et al., 2015). In total, four secondary metabolite-associated gene clusters were found. In contrast, *G. maris*, as closest relative to NH11^T, encodes 9 putative secondary metabolite related genes and gene clusters. Thus, again, strain NH11^T differs from its peers.

However, the four identified genes and clusters might be related to bacteriocins (2), terpenes (1), and ectoines (1) based on the antiSMASH prediction. Ectoines are compatible solutes, playing a role in the salt stress response, e.g., in halophilic eubacteria (Peters et al., 1990; Bernard et al., 1993; Pastor et al., 2010). However, physiological tests gave no evidence for an increased salt tolerance [>5% NaCl (w/v)] of strain NH11^T (see **Table 1**).

The genome sequence of strain NH11^T was further used to verify the 16S rRNA gene sequence based phylogeny via Multi Locus Sequence Analysis (MLSA). This method enables to increase the phylogenetic resolution and to avoid the bias caused by single marker gene-based phylogenies. This was achieved by considering sequences of multiple independent single copy genes shared by the comparison organisms (Glaeser and Kämpfer, 2015). The MLSA-based phylogeny is shown in **Figure 7** and further supports our 16S rRNA gene based placement.

DISCUSSION

Strain NH11^T is in many ways an unusual planctomycete. Based on 16S rRNA gene sequence comparison, it branches within the former genus *Planctomyces* which was recently found to be polyphyletic. Consequently, it was further subdivided into the separate genera *Gimesia*, *Planctopirus*, *Rubinisphaera*, and *Planctomyces*, which all belong to the order Planctomycetales and the family *Planctomycetaceae* (Scheuner et al., 2014). Similar results were obtained by a MLSA phylogenetic analysis, while both approaches provided rather low bootstrap support. However, since both methods gave similar results, strain NH11^T is likely to cluster within the family *Planctomycetaceae*.

To allow a detailed taxonomic classification, we performed further 16S rRNA gene sequence comparison (**Table 1**). We found, if evolutionary events were considered, that strain NH11^T belongs to a novel family based on current thresholds (Yarza et al., 2014). In contrast, direct comparison, without acknowledging evolutionary events, led to 87.1% 16S rRNA gene sequence

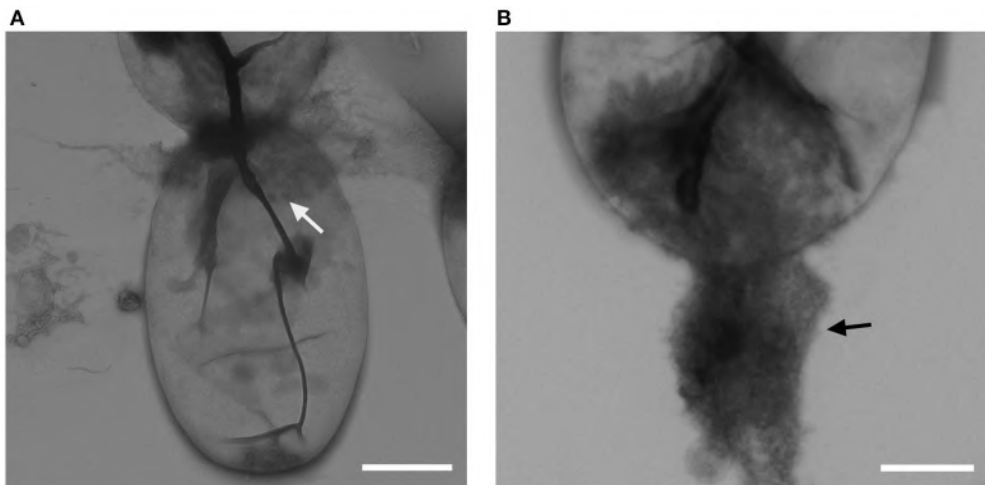


FIGURE 3 | Crateriform structures of strain NH11^T. TEM analysis of negative stained NH11^T cells revealed crateriform structures solely on the cell pole (**A**, white arrow) and fiber like structures seem to arise from such pits (**B**, black arrow). Bar, 0.5 μm.

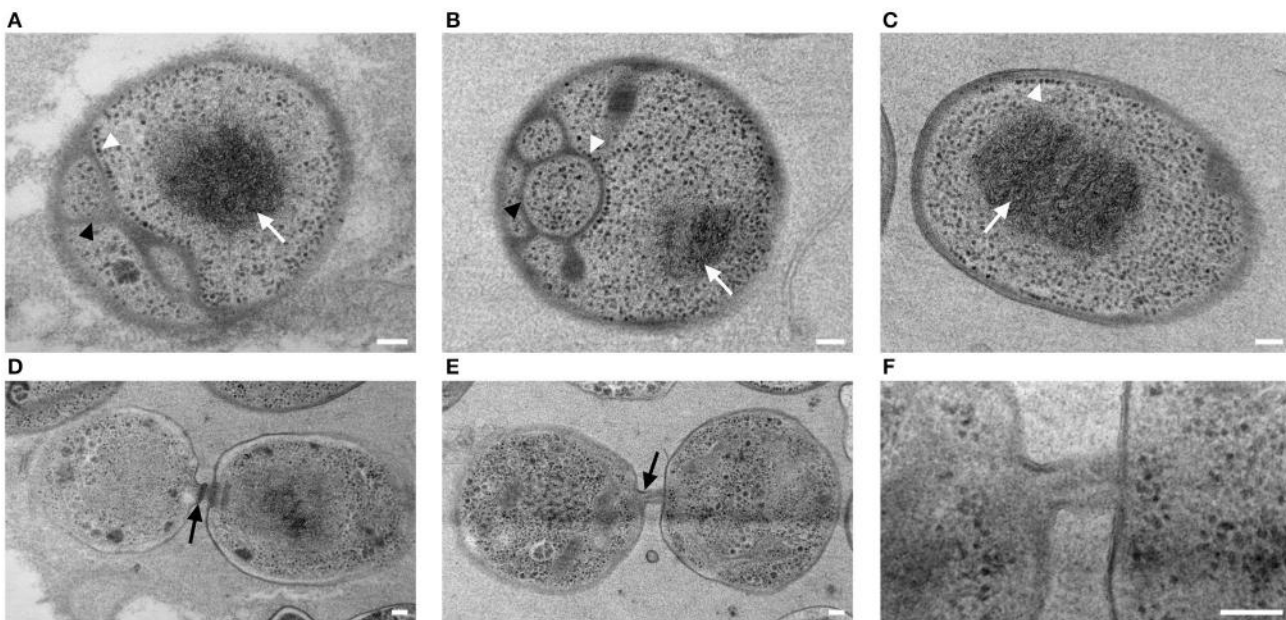


FIGURE 4 | Subcellular organization and cell division of strain NH11^T. High pressure frozen and freeze substituted cells of strain NH11^T were subject to thin-sectioning and TEM analysis. Three representative sections of individual cells correspond to differences in subcellular organization of strain NH11^T (**A–C**). Cells always comprise a condensed nucleoid which is visible as a black structure (white arrow), while their cytoplasmic membrane can show different degrees of invaginations (**A,B**, black arrowheads). Some cells even lack any invagination of the cytoplasmic membrane (**C**). Some ribosomes (white arrowheads) are always located at the cytoplasmic membrane despite its degree of invagination (**A–C**). Dividing cells are interconnected by a tubular like structure (**D–F**). Between mother and daughter cell, sometimes a black structure, potentially correlating with a division ring, became visible (**D**, black arrow). This structure could only be observed in some sections, while it was absent in others (**E–F**). Bar, 0.1 μm.

identity to its closest relative *G. maris*, while the current taxonomic thresholds of the bacterial family border is 86.5%. However, within a family, a minimum sequence identity of 87.65% should be given between the separate species (Yarza et al., 2014), while strain NH11^T and *G. maris* comprise only 87.1% sequence identity. Thus without taking evolutionary events into

account, strain NH11^T falls right in between both thresholds (Yarza et al., 2014). To solve this conflict, a 16S rRNA sequence alignment based cluster analysis was performed. The results (Figures S1–S3) clearly demonstrate that all available 16S rRNA gene sequences from cultivated and uncultivated members of the family *Planctomycetaceae* form multiple clusters, while strain

TABLE 2 | Carbon sources utilized by strain NH11^T.

| Carbon sources | |
|---------------------------------|---|
| N-Acetyl-D-Galactosamine | + |
| N-Acetyl-D-Glucosamine | + |
| L-Arabinose | + |
| D-Cellobiose | + |
| D-Galactose | + |
| Gentiobiose | + |
| α-D-Glucose | + |
| α-D-Lactose | + |
| Lactulose | + |
| Maltose | + |
| D-Mannose | + |
| D-Melibiose | + |
| β-Methyl-D-Glucoside | + |
| L-Rhamnose | - |
| Sucrose | + |
| D-Trehalose | + |
| Turanose | + |
| Succinic Acid Mono-Methyl-Ester | + |
| Acetic Acid | + |
| D-Glucuronic Acid | W |
| γ-Hydroxybutyric Acid | W |
| Itaconic Acid | W |
| Propionic Acid | W |
| Glycerol | + |

+, positive; -, negative; W, weakly positive.

NH11^T and the genera *Gimesia* and *Rubinispshaera* belong to three distinct clusters. Thus from a phylogenetic perspective strain NH11^T belongs to a novel family.

This conclusion is consistent with other types of evidence obtained in this study: the morphological features of strain NH11^T differ from those of its closest relatives. For example, *G. maris* is described to stain Gram negative (Bauld and Staley, 1976) whereas employing the same Gram staining method to strain NH11^T delivered no clear result. However, others and we recently demonstrated the presence of peptidoglycan in a phylogenetically representative set of planctomycetal model species (Jeske et al., 2015; van Teeseling et al., 2015). Consequently, we suggest to exclude this classical Gram staining test as a valid tool for future characterization of novel planctomycetal strains, as it is of limited explanatory power for Planctomycetes. Nevertheless, other aspects of strain NH11^T differ from its peers as well. Another aspect that differs between strain NH11^T and members of the family *Planctomycetaceae* such as *P. limnophila* is the localization of the crateriform structures. They are hardly visible (Figure 3) and seem to be associated with fiber-like structures. However, such fiber-like structures might be artifacts from EM fixation methods and thus require further investigation. If such structures are associated with cell attachment to surfaces remains as well enigmatic. While *G. maris* and *R. brasiliensis* form stalks and rosettes in culture, strain NH11^T lacks both features. In addition, strain NH11^T

TABLE 3 | Enzymatic activities of strain NH11^T, determined with the API ZYM test.

| Enzymatic activities | |
|---------------------------------|---|
| Alcaline phosphatase | + |
| Esterase (C 4) | + |
| Esterase lipase (C 8) | + |
| Lipase (C 14) | - |
| Leucinearylamidase | + |
| Valinearylamidase | + |
| Cysteine arylamidase | + |
| Trypsin | + |
| α-chymotrypsin | + |
| Acid phosphatase | + |
| Naphthol-AS-BI-phosphohydrolase | + |
| α-galactosidase | - |
| β-galactosidase | - |
| β-glucuronidase | - |
| α-glucosidase | + |
| β-glucosidase | - |
| N-acetyl-β-glucosaminidase | - |
| α-mannosidase | - |
| α-fucosidase | - |

+, positive; -, negative.

forms a tubular connection between daughter and mother cell (Figures 4D–F). Within this tubes in some sections a dark structure became visible that was previously identified as cell division ring in anammox Planctomycetes (van Niftrik et al., 2009). However, anammox bacteria divide, in contrast to budding members of the order Planctomyctales, through binary fission. While both types of organisms lack the otherwise universal cell division protein FtsZ, only for anammox Planctomycetes a potential substitute is known (locus tag kustd1438, NCBI Accession Number CAJ72183). While no homolog protein could be determined in the genome of strain NH11^T, the molecular mechanism of its unusual cell division remains enigmatic. One might speculate that Fuma_00096, a protein similar, yet distinct from kustd1438, might be involved in the formation of the unique tubular connection between mother and daughter cell and might correlate with the anecdotally observed structure (Figure 4D, black arrow). This idea is based on the Lamin Tail domain of Fuma_00096, which corresponds to an intermediate filament (IF). Such IFs are frequently found in eukaryotic cells to provide mechanical strength and support for fragile tubulin structures (Goldman et al., 1996). However, this is only a hypothesis at this stage, that requires experimental verification.

Besides morphological differences, the genome of strain NH11^T shows distinct features if compared to other Planctomycetes as well. First, it contains areas of unique genes, if compared against the available high quality planctomycetal genomes. Second, these areas were found to comprise both, genomic islands - likely acquired through horizontal gene transfer - and giant genes. In total, 19 giant genes with a size >10 kb were detected, which is the highest number amongst all analyzed planctomycetal genomes (Figure S7). Representatives

TABLE 4 | Cellular fatty acid contents (%) of NH11^T in comparison to *G. maris* and *R. brasiliensis*.

| Fatty acid | NH11 ^T | <i>G. maris</i> | <i>R. brasiliensis</i> |
|--|-------------------|-----------------|------------------------|
| SATURATED | | | |
| C _{14:0} | 0.18 | 0.32 | 0.27 |
| C _{16:0} | 15.12 | 23.50 | 45.77 |
| C _{17:0} | 0.44 | 7.11 | 0.53 |
| C _{17:0} 10-methyl | – | 1.03 | – |
| C _{18:0} | 0.61 | 1.41 | 0.56 |
| UNSATURATED | | | |
| C _{15:1} ω6c | 0.88 | 2.46 | 0.28 |
| C _{16:1} ω5c | 0.45 | 0.36 | 0.36 |
| C _{17:1} ω6c | 1.82 | 4.63 | – |
| C _{17:1} ω7c | 0.62 | – | – |
| C _{17:1} ω8c | – | 3.05 | 0.30 |
| C _{18:1} ω5c | 0.14 | – | – |
| C _{18:1} ω7c | – | 5.76 | – |
| C _{18:1} ω9c | – | 2.43 | 1.02 |
| C _{20:1} ω7c | – | 0.26 | 2.76 |
| BRANCHED | | | |
| Iso-C _{16:0} | 0.19 | 1.96 | – |
| 3-HYDROXY | | | |
| C _{12:0} 3-OH | – | 0.33 | – |
| SUMMED FEATURES | | | |
| 2: C _{14:0} 3-OH/Iso-C _{16:1} | 0.55 | – | – |
| 3: C _{16:1} ω6c/16:1 ω7c | 59.16 | 26.63 | 47.10 |
| 8: C _{18:1} ω6c/18:1 ω7c | 19.83 | 5.76 | 1.06 |
| 9: C _{16:0} 10-methyl/Iso-C _{17:1} ω6c | – | 12.98 | – |

Major fatty acids of the strain NH11^T are C_{16:1}ω6c/16:1 ω7c (Summed feature), C_{18:1}ω6c/18:1 ω7c (Summed feature) and C_{16:0}.

of the family *Planctomycetaceae* in contrast possess a maximum of 13 giant genes of this dimension. The protein products of giant genes, if synthetized, would represent a huge metabolic burden, suggesting that they have an important cellular function. Thus, 6–19 additional giant genes >10 kb compared to its peers suggests a huge difference in strain NH11^T's cell surface or secondary metabolism. This is because more than 90% of giant genes encode either surface proteins or polyketide/nonribosomal peptide synthetases (PKS/NRPS) (Reva and Tümmler, 2008). Surprisingly, our antiSMASH analysis revealed only four secondary metabolite-associated gene clusters. One of these gene clusters is predicted to encode the compatible solute ectoine, giving a hint toward an increased salt tolerance of the strain. However, since ASW is tolerated up to 230% (v/v) and NaCl up to 5% (w/v), it is rather adapted to moderate salt concentration. In contrast to the four clusters found in strain NH11^T's genome, its closest relatives *R. brasiliensis* and *G. maris* comprise 8 and 9 of such clusters (Jeske et al., 2013). Furthermore, a significant linear correlation between genome size and number of secondary metabolite related genes has been described (Jeske et al., 2013). With a genome size of almost 9 MB strain NH11^T is an exception to this observation. Two potential scenarios could be envisioned: either the giant

genes of strain NH11^T fulfill other, maybe structural functions, or they might be involved in the formation of yet unknown secondary metabolites. While the latter hypothesis fits to the recent observation of novel antibiotic small molecules from Planctomycetes (Jeske et al., 2016), at least some giant genes are predicted to encode proteins with structural function such as the discussed Fuma_00096. While resolving this issue is beyond the scope of this study, we conclude that the genome of strain NH11^T differs in important aspects from its peers.

Taken together, the 16S rRNA gene sequence identity, the unusual mode of cell division, its unique cell plan and its unusual planctomycetal genome require to place this novel and exceptional species in a new family. However, the family Planctomycetaceae would not be monophyletic anymore and based on our cluster analysis requires division into three distinct families. To prevent back- and forth renaming of species, genera and families, we describe strain NH11^T as novel genus and species for now. We soon will present multiple novel planctomycetal strains and only in the light of such isolates rewriting the planctomycetal taxonomy would make sense. Thus, rearrangements within the family *Planctomycetaceae* will be revisited in the future (Jogler C, personal communication).

Description of *Fuerstia* gen. nov.

Fuerstia (named in honor of John Fuerst, an Australian microbiologist from University of Queensland, who played a key role in planctomycetal research). The pear to ovoid shaped cells form aggregates in liquid culture, but no rosettes. Daughter cells are motile, while mother cells are non-motile and no stalk formation was observed. The surface is smooth, crateriform stuctures are limited to one pole and cells reproduce by polar budding while mother- and daughter cells are connected by a thin tubular-like structure. The lifestyle is heterotrophic, obligatory aerobic and mesophilic. The major fatty acids are C_{16:1}ω6c/16:1 ω7c (Summed feature), C_{18:1}ω6c/18:1 ω7c (Summed feature), and C_{16:0}. Member of the phylum Planctomycetes, class Planctomyces, order Planctomycetales, family *Planctomycetaceae*. The type species is *Fuerstia marisgermanicae*.

Description of *Fuerstia marisgermanicae* sp. nov.

Fuerstia marisgermanicae (ma'ris L. n. maris of the sea and ger.ma'ni.ca L. adj. German, pertaining to the German North Sea from which the type strain was isolated). In addition to the features described for the genus, the species exhibits the following properties. Colonies on solid medium are cream colored. Cells are 1.2–2.5 × 0.9–1.7 μm in size. Non motile mother cells spawn motile, swimming, daughter cells. Gram staining delivers no clear result. KOH test and aminopeptidase test are negative, while oxidase and catalase tests positive. The organism is able to degrade a wide range of carbon sources, in particular N-acetyl-D-galactosamine, N-acetyl-D-glucosamine, L-arabinose, D-cellobiose, D-galactose, gentiobiose, α-D-glucose, α-D-lactose, lactulose, maltose, D-mannose, D-melibiose, β-methyl-D-glucoside, sucrose, D-trehalose, turanose, succinic acid

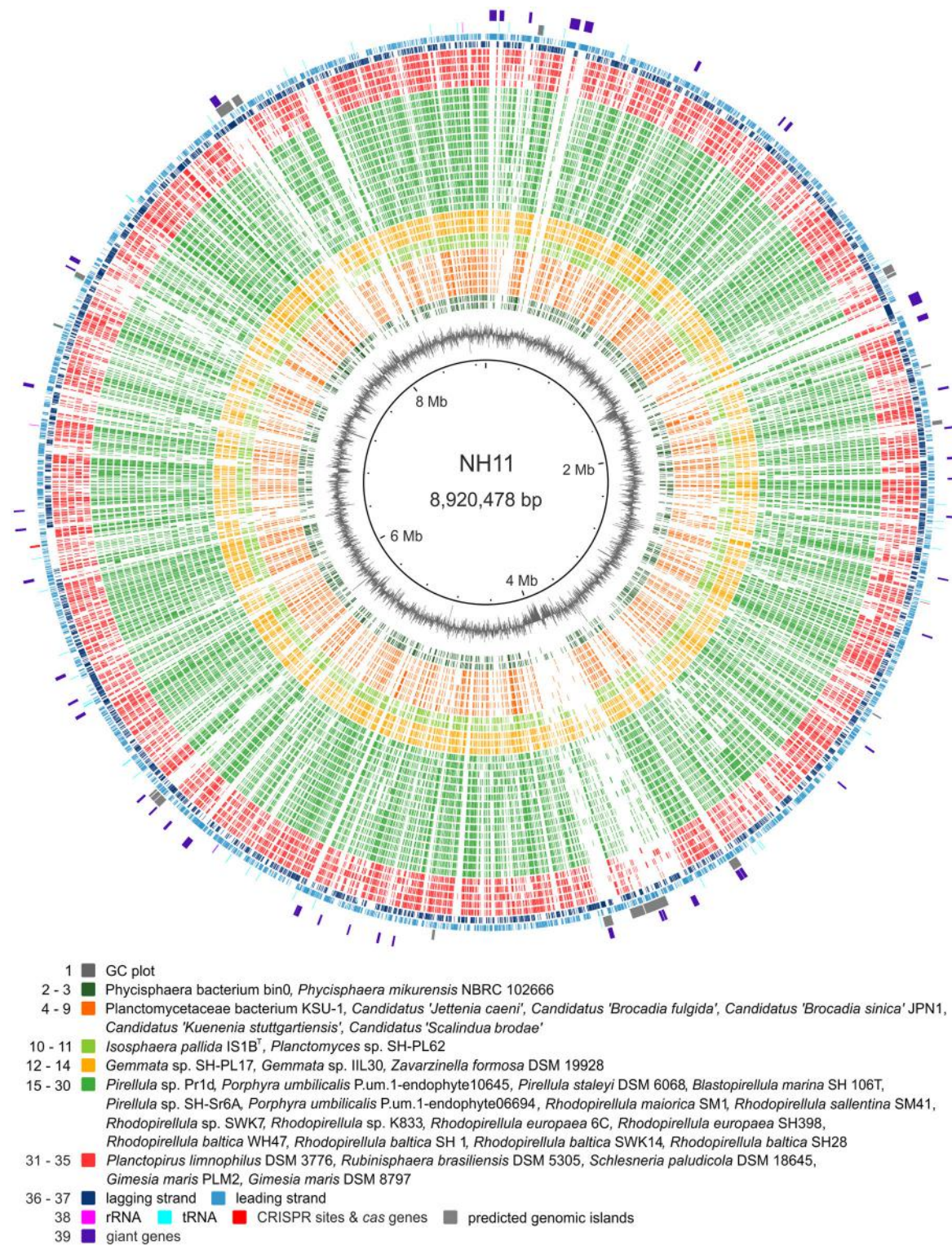


FIGURE 5 | Genomic features of strain NH11^T. The circular plot of strain NH11^T's 8.9 Mb chromosome summarizes multiple genomic features: the outer circles display protein (light and dark blue), tRNA (turquoise), and rRNA (pink) encoding genes as well as predicted genomic islands (gray) and giant genes (purple). The innermost circle shows the GC plot (gray). In between, ortholog genes from planctomycetal strains, for which high quality genomes were available, were identified by reciprocal BLAST and are depicted in green, yellow, and orange, according to the color scheme of Figure 7. Notable islands of unique gene content in NH11^T are visualized as gaps and they are found to in regions of predicted genomic islands and/or giant genes.

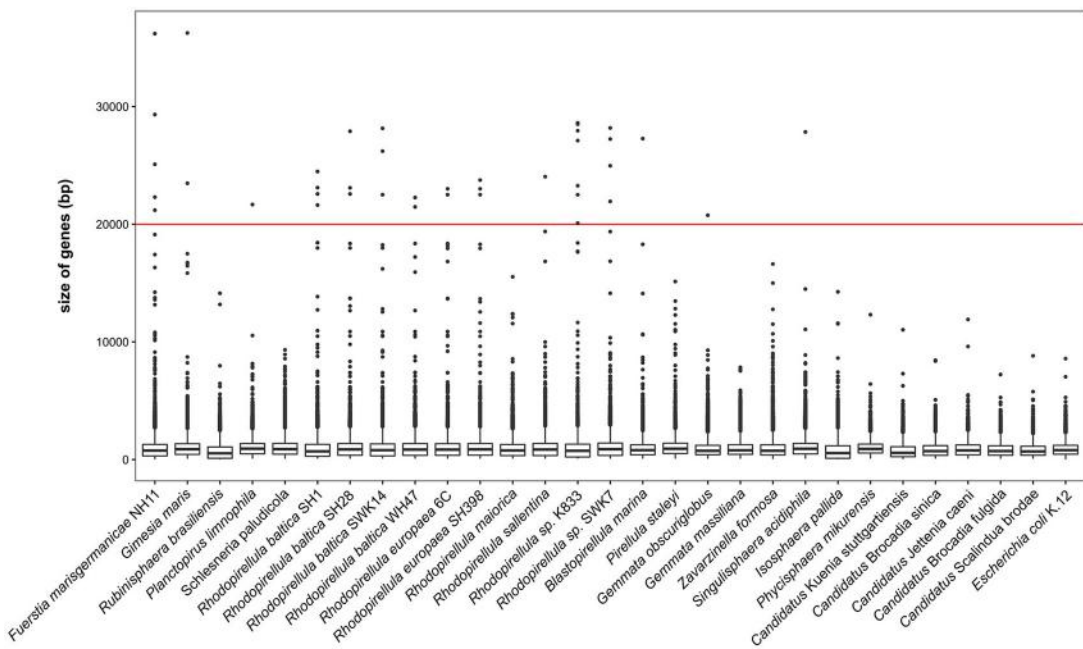


FIGURE 6 | Planctomycetal giant genes. The gene size distribution of different Planctomycetes with available genomes is ordered by declining phylogenetic relationship to NH11^T. Median size of genes, 25 and 75% percentiles are shown and whiskers represents the 1.5* interquartile range and dots outliers. *Fuerstia marisgermanicae* comprises 45 giant genes (>5 kb), the biggest gene is 36,239 bp in size.

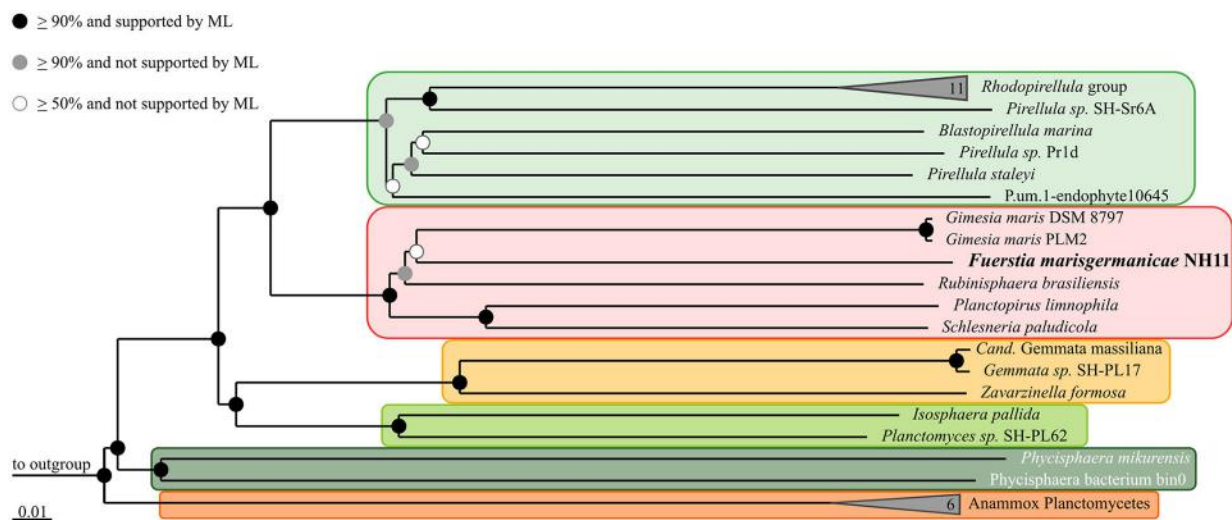


FIGURE 7 | Multilocus sequence analysis (MLSA) of strain NH11^T. The phylogenetic tree is based on Neighbor Joining analysis, with bootstrap values (presented by black, gray and white dots) based on 1000 permutations. Additionally, Maximum Likelihood (ML) analysis was performed and is also indicated by dots. The performed calculations were based on 68,695 unambiguous amino acid sequence alignment positions of 143 concatenated orthologous single-copy protein gene products shared by all 37 included genomes. The ortholog selection was based on bidirectional BLAST analysis as implemented in Proteinortho5 (Lechner et al., 2011). Sequences were aligned individually for each ortholog group and subsequently concatenated. Unalignable regions were filtered from the alignments using Gblocks (Castresana, 2000). The genomes of *Opitutus terrae* PB90-1 and *Verrucomicromyobium spinosum* DSM 4136 served as outgroup. To enhance clarity, several monophyletic groups of reference organisms are shown collapsed as others are indicated by orange and green boxes, according to the color scheme of Figure 5.

mono-methyl-ester, acetic acid, γ -hydroxybutyric acid, itaconic acid, propionic acid, and glycerol were utilized. The enzymatic repertoire of the species, tested with API ZYM, is listed in Table 3.

Growth occurs between pH 6 and 10 with an optimum at pH 7. At least 27.5% ASW is needed for growth. The optimal temperature for growth is 28°C (range between 20 and 30°C). The type

strain is NH11^T (= DSM 27554 = LMG 27831) isolated from a crustacean shell.

AUTHOR CONTRIBUTIONS

TK analyzed the data and wrote the manuscript. AH performed the physiological experiments and proofread the manuscript. MJ was involved in planning the project, aided in cultivation and helped writing and proofread the manuscript. JV, AK developed the pipeline for the genome analysis. CB prepared thin sections of the strain and performed TEM imaging, was involved in writing and proofreading the manuscript. JO, BB did the genome sequencing of the strain and were involved writing and proofreading the manuscript. PR accomplished phylogenetic analyses, helped writing and proofreading the manuscript. DB performed light-microscopic observations. IG performed the initial cultivation and isolated the stain. HF analyzed the genome for giant genes and proofread the manuscript. HK conducted the fatty acid analysis and proofread the manuscript. MR did the scanning electron microscopy of the strain, TEM imaging of negatively stained cells and proofread the manuscript. SW was involved in the genome analysis and did the multilocus sequence analysis and proofread the manuscript. CJ designed the project and wrote the manuscript.

ACKNOWLEDGMENTS

This work was funded by the Deutsche Forschungsgemeinschaft to CJ (JO 893/3-1) and to JO (TRR 51/2 TA07). We thank Dr. Cathrin Spröer for support and Simone Severitt, Nicole Heyer, and Gabriele Pötter for skilled technical assistance. We thank Elizabeth Benecci from the Harvard Medical School's EM Facility for technical assistance.

SUPPLEMENTARY MATERIAL

The Supplementary Material for this article can be found online at: <http://journal.frontiersin.org/article/10.3389/fmicb.2016.02079/full#supplementary-material>

REFERENCES

- Aghnatiros, R., Cayrou, C., Garibal, M., Robert, C., Azza, S., Raoult, D., et al. (2015). Draft genome of *Gemmata massiliiana* sp. nov, a water-borne *Planctomycetes* species exhibiting two variants. *Stand. Genomic Sci.* 10, 120. doi: 10.1186/s40793-015-0103-0
- Alikhan, N. F., Petty, N. K., Ben Zakour, N. L., and Beatson, S. A. (2011). BLAST Ring Image Generator (BRIG): simple prokaryote genome comparisons. *BMC Genomics* 12:402. doi: 10.1186/1471-2164-12-402
- Bauld, J., and Staley, J. T. (1976). *Planctomyces maris* sp. nov.: a Marine isolate of the Planctomyces-Blastocaulis group of Budding Bacteria. *Microbiology* 97, 45–55. doi: 10.1099/00221287-97-1-45
- Bernard, T., Jebbar, M., Rassouli, Y., Himdi-Kabbab, S., Hamelin, J., and Blanco, C. (1993). Ectoine accumulation and osmotic regulation in *Brevibacterium linens*. *Microbiology* 139, 129–136. doi: 10.1099/00221287-139-1-129
- Bland, C., Ramsey, T. L., Sabree, F., Lowe, M., Brown, K., Kyripides, N. C., et al. (2007). CRISPR recognition tool (CRT): a tool for automatic detection of clustered regularly interspaced palindromic repeats. *BMC Bioinformatics* 8:209. doi: 10.1186/1471-2105-8-209
- Bruns, A., Philipp, H., Cypionka, H., and Brinkhoff, T. (2003). Aeromicrobium marinum sp. nov., an abundant pelagic bacterium isolated from the German Wadden Sea. *Int. J. Syst. Evol. Microbiol.* 53, 1917–1923. doi: 10.1099/ijs.0.02735-0
- Castresana, J. (2000). Selection of conserved blocks from multiple alignments for their use in phylogenetic analysis. *Mol. Biol. Evol.* 17, 540–552. doi: 10.1093/oxfordjournals.molbev.a026334
- Cayrou, C., Raoult, D., and Drancourt, M. (2010). Broad-spectrum antibiotic resistance of Planctomyces organisms determined by Etest. *J. Antimicrob. Chemother.* 65, 2119–2122. doi: 10.1093/jac/dkq290
- Dhillon, B. K., Laird, M. R., Shay, J. A., Winsor, G. L., Lo, R., Nizam, F., et al. (2015). IslandViewer 3: more flexible, interactive genomic island

Figure S1 | Maximum likelihood tree of the detected clusters of NH11^T, *Gimesia maris*, and *Rubinispahrea brasiliensis* using a minimum sequence identity threshold of 87.65% within a cluster corresponding to phylogenetic families.

All three cultivated species form distinct clusters with sequences of uncultivated planctomycetes with at least 87.65% similarity within their cluster. The corresponding clusters are marked with brackets. The bootstrap percentages of 1000 resamplings are given for each node. *Anammox planctomycetes* served as outgroup.

Figure S2 | Maximum parsimony tree of the detected clusters of NH11^T, *Gimesia maris*, and *Rubinispahrea brasiliensis* using a minimum sequence identity threshold of 87.65% within a cluster corresponding to phylogenetic families.

All three cultivated species form distinct clusters with sequences of uncultivated planctomycetes with at least 87.65% similarity within their cluster. The corresponding clusters are marked with brackets. The bootstrap percentages of 1000 resamplings are given for each node. *Anammox planctomycetes* served as outgroup.

Figure S3 | Neighbor joining tree of the detected clusters of NH11^T, *Gimesia maris*, and *Rubinispahrea brasiliensis* using a minimum sequence identity threshold of 87.65% within a cluster corresponding to phylogenetic families.

All three cultivated species form distinct clusters with sequences of uncultivated planctomycetes with at least 87.65% similarity within their cluster. The corresponding clusters are marked with brackets. The bootstrap percentages of 1000 resamplings are given for each node. *Anammox planctomycetes* served as outgroup.

Figure S4 | Temperature, pH, ASW, and NaCl optimum of strain NH11^T.

To determine the pH (A), NaCl (B), and ASW (C) tolerance as well as the optimal growth temperature (D), the optical density was measured at 600 nm (OD 600 nm) and slope values, corresponding to change of OD 600 nm over time during exponential growth phase, were plotted against the corresponding pH, NaCl, ASW, or temperature value. Growth is best at pH 7, NaCl concentrations up to 5% are tolerated and ASW is tolerated from 27.5 to 230%. Growth is best at 28°C. Each dot represents the mean of triplicate measurements.

Figure S5 | Number of giant genes >5 kb amongst the analyzed strains ordered by declining phylogenetic relationship.

Strain NH11^T comprises 45 giant genes >5 kb, which is the second highest number after *Zavarzinella Formosa* with 60 giant genes above this size.

Figure S6 | Number of giant genes >20 kb amongst the analyzed strains ordered by declining phylogenetic relationship.

Strain NH11^T comprises five giant genes >20 kb, which is the second highest number after *Rhodopirellula* sp. K833 with seven giant genes above this threshold.

Figure S7 | Number of giant genes >10 kb amongst the analyzed strains ordered by declining phylogenetic relationship.

With 19 giant genes >10 kb, Strain NH11^T comprises the highest number above this threshold.

- discovery, visualization and analysis. *Nucleic Acids Res.* 43, W104–W108. doi: 10.1093/nar/gkv401
- Dragulescu, A. A. (2014). *Read, Write, Format Excel 2007 and Excel 97/2000/XP/2003 Files*. R package version 0.5.7 ed. Available online at: <https://cran.r-project.org/web/packages/xlsx/>
- Edgar, R. C. (2004a). MUSCLE: a multiple sequence alignment method with reduced time and space complexity. *BMC Bioinformatics* 5:113. doi: 10.1186/1471-2105-5-113
- Edgar, R. C. (2004b). MUSCLE: multiple sequence alignment with high accuracy and high throughput. *Nucleic Acids Res.* 32, 1792–1797. doi: 10.1093/nar/gkh340
- Fuerst, J. A. (2005). Intracellular compartmentation in *Planctomycetes*. *Annu. Rev. Microbiol.* 59, 299–328. doi: 10.1146/annurev.micro.59.030804.121258
- Fuerst, J. A., Gwilliam, H. G., Lindsay, M., Lichanska, A., Belcher, C., Vickers, J. E., et al. (1997). Isolation and molecular identification of planctomycete bacteria from postlarvae of the giant tiger prawn, *Penaeus monodon*. *Appl. Environ. Microbiol.* 63, 254–262.
- Fuerst, J. A., and Sagulenko, E. (2010). Protein uptake by bacteria: an endocytosis-like process in the planctomycete *Gemmata obscuriglobus*. *Commun. Integr. Biol.* 3, 572–575. doi: 10.4161/cib.3.6.13061
- Fuerst, J. A., and Sagulenko, E. (2011). Beyond the bacterium: *Planctomycetes* challenge our concepts of microbial structure and function. *Nat. Rev. Microbiol.* 9, 403–413. doi: 10.1038/nrmicro2578
- Glaeser, S. P., and Kämpfer, P. (2015). Multilocus sequence analysis (MLSA) in prokaryotic taxonomy. *Syst. Appl. Microbiol.* 38, 237–245. doi: 10.1016/j.syapm.2015.03.007
- Glöckner, F. O., Kube, M., Bauer, M., Teeling, H., Lombardot, T., Ludwig, W., et al. (2003). Complete genome sequence of the marine planctomycete *Pirellula* sp. strain 1. *Proc. Natl. Acad. Sci. U.S.A.* 100, 8298–8303. doi: 10.1073/pnas.1431443100
- Goldman, R. D., Khuon, S., Chou, Y. H., Opal, P., and Steinert, P. M. (1996). The function of intermediate filaments in cell shape and cytoskeletal integrity. *J. Cell. Biol.* 134, 971–983.
- Jeske, O., Jogler, M., Petersen, J., Sikorski, J., and Jogler, C. (2013). From genome mining to phenotypic microarrays: *Planctomycetes* as source for novel bioactive molecules. *Antonie Van Leeuwenhoek* 104, 551–567. doi: 10.1007/s10482-013-0007-1
- Jeske, O., Schüler, M., Schumann, P., Schneider, A., Boedeker, C., Jogler, M., et al. (2015). *Planctomycetes* do possess a peptidoglycan cell wall. *Nat. Commun.* 6, 7116. doi: 10.1038/ncomms8116
- Jeske, O., Surup, F., Ketteniß, M., Rast, P., Förster, B., Jogler, M., et al. (2016). Developing techniques for the utilization of *Planctomycetes* as producers of bioactive molecules. *Front. Microbiol.* 7:1242. doi: 10.3389/fmicb.2016.01242
- Jogler, C., Glöckner, F. O., and Kolter, R. (2011). Characterization of *Planctomyces limnophilus* and development of genetic tools for its manipulation establish it as a model species for the phylum *Planctomycetes*. *Appl. Environ. Microbiol.* 77, 5826–5829. doi: 10.1128/AEM.05132-11
- Jogler, C., Waldmann, J., Huang, X., Jogler, M., Glöckner, F. O., Mascher, T., et al. (2012). Identification of proteins likely to be involved in morphogenesis, cell division, and signal transduction in *Planctomycetes* by comparative genomics. *J. Bacteriol.* 194, 6419–6430. doi: 10.1128/JB.01325-12
- Jogler, M., Chen, H., Simon, J., Rohde, M., Busse, H. J., Klenk, H. P., et al. (2013). Description of *Sphingorhabdus planktonica* gen. nov., sp. nov. and reclassification of three related members of the genus *Sphingopyxis* in the genus *Sphingorhabdus* gen. nov. *Int. J. Syst. Evol. Microbiol.* 63, 1342–1349. doi: 10.1099/ijss.0.043133-0
- Jones, P., Binnns, D., Chang, H. Y., Fraser, M., Li, W., Mcanulla, C., et al. (2014). InterProScan 5: genome-scale protein function classification. *Bioinformatics* 30, 1236–1240. doi: 10.1093/bioinformatics/btu031
- Kämpfer, P., and Kroppenstedt, R. M. (1996). Numerical analysis of fatty acid patterns of coryneform bacteria and related taxa. *Can. J. Microbiol.* 42, 989–1005. doi: 10.1139/m96-128
- Kartal, B., de Almeida, N. M., Maalcke, W. J., Op den Camp, H. J., Jetten, M. S., and Keltjens, J. T. (2013). How to make a living from anaerobic ammonium oxidation. *FEMS Microbiol. Rev.* 37, 428–461. doi: 10.1111/1574-6976.12014
- König, E., Schlesner, H., and Hirsch, P. (1984). Cell-wall studies on budding bacteria of the *Planctomyces/Pasteuria* group and on a *Prosthecomicrobium* sp. *Arch. Microbiol.* 138, 200–205. doi: 10.1007/BF00402120
- Kuykendall, L. D., Roy, M. A., Apos Neill, J. J., and Devine, T. E. (1988). Fatty acids, antibiotic resistance, and deoxyribonucleic acid homology groups of *Bradyrhizobium japonicum*. *Int. J. Syst. Evol. Microbiol.* 38, 358–361. doi: 10.1099/00207713-38-4-358
- Lage, O. M., and Bondoso, J. (2014). Planctomycetes and macroalgae, a striking association. *Front. Microbiol.* 5:267. doi: 10.3389/fmicb.2014.00267
- Lagesen, K., Hallin, P., Rødland, E. A., Staerfeldt, H. H., Rognes, T., and Ussery, D. W. (2007). RNAmmer: consistent and rapid annotation of ribosomal RNA genes. *Nucleic Acids Res.* 35, 3100–3108. doi: 10.1093/nar/gkm160
- Lane, D. J. (ed.). (1991). *16S/23S rRNA Sequencing*. Chichester: Wiley.
- Lechner, M., Findeiss, S., Steiner, L., Marz, M., Stadler, P. F., and Prohaska, S. J. (2011). Proteinortho: detection of (co-)orthologs in large-scale analysis. *BMC Bioinformatics* 12:124. doi: 10.1186/1471-2105-12-124
- Levrings, T. (1946). Some culture experiments with *Ulva* and artificial sea water. *Fysiotr. Sällsk. Förhandl.* 16, 1–12.
- Li, H., and Durbin, R. (2009). Fast and accurate short read alignment with Burrows-Wheeler transform. *Bioinformatics* 25, 1754–1760. doi: 10.1093/bioinformatics/btp324
- Ludwig, W., Strunk, O., Westram, R., Richter, L., Meier, H., Yadukumar, et al. (2004). ARB: a software environment for sequence data. *Nucleic Acids Res.* 32, 1363–1371. doi: 10.1093/nar/gkh293
- Markowitz, V. M., Chen, I. M., Palaniappan, K., Chu, K., Szeto, E., Grechkin, Y., et al. (2012). IMG: the Integrated Microbial Genomes database and comparative analysis system. *Nucleic Acids Res.* 40, D115–D122. doi: 10.1093/nar/gkr1044
- Miller, L. T. (1982). Single derivatization method for routine analysis of bacterial whole-cell fatty acid methyl esters, including hydroxy acids. *J. Clin. Microbiol.* 16, 584–586.
- Mitchell, A., Chang, H. Y., Daugherty, L., Fraser, M., Hunter, S., Lopez, R., et al. (2015). The InterPro protein families database: the classification resource after 15 years. *Nucleic Acids Res.* 43, D213–D221. doi: 10.1093/nar/gku1243
- Parks, D. H., Imelfort, M., Skennerton, C. T., Hugenholtz, P., and Tyson, G. W. (2015). CheckM: assessing the quality of microbial genomes recovered from isolates, single cells, and metagenomes. *Genome Res.* 25, 1043–1055. doi: 10.1101/gr.186072.114
- Pastor, J. M., Salvador, M., Argandoña, M., Bernal, V., Reina-Bueno, M., Csonka, L. N., et al. (2010). Ectoines in cell stress protection: uses and biotechnological production. *Biotechnol. Adv.* 28, 782–801. doi: 10.1016/j.biotechadv.2010.06.005
- Peters, P., Galinski, E. A., and Trüper, H. G. (1990). The biosynthesis of ectoine. *FEMS Microbiol. Lett.* 71, 157–162. doi: 10.1111/j.1574-6968.1990.tb03815.x
- Petroni, G., Spring, S., Schleifer, K. H., Verni, F., and Rosati, G. (2000). Defensive extrusive ectosymbionts of *Euplotidium* (Ciliophora) that contain microtubule-like structures are bacteria related to *Verrucomicrobia*. *Proc. Natl. Acad. Sci. U.S.A.* 97, 1813–1817. doi: 10.1073/pnas.030438197
- Pruess, E., Quast, C., Knittel, K., Fuchs, B. M., Ludwig, W., Peplies, J., et al. (2007). SILVA: a comprehensive online resource for quality checked and aligned ribosomal RNA sequence data compatible with ARB. *Nucleic Acids Res.* 35, 7188–7196. doi: 10.1093/nar/gkm864
- R Core Team (2015). *R: A Language Environment for Statistical Computing*. Available online at: <https://www.r-project.org/>
- Reva, O., and Tümmeler, B. (2008). Think big – giant genes in bacteria. *Environ. Microbiol.* 10, 768–777. doi: 10.1111/j.1462-2920.2007.01500.x
- Rutherford, K., Parkhill, J., Crook, J., Horsnell, T., Rice, P., Rajandream, M. A., et al. (2000). Artemis: sequence visualization and annotation. *Bioinformatics* 16, 944–945. doi: 10.1093/bioinformatics/16.10.944
- Scheuner, C., Tindall, B. J., Lu, M., Nolan, M., Lapidus, A., Cheng, J. F., et al. (2014). Complete genome sequence of *Planctomyces brasiliensis* type strain (DSM 5305(T)), phylogenomic analysis and reclassification of *Planctomycetes* including the descriptions of *Gimesia* gen. nov., *Planctopirpus* gen. nov. and *Rubinospaera* gen. nov. and emended descriptions of the order *Planctomycetales* and the family *Planctomycetaceae*. *Stand. Genomic. Sci.* 9:10. doi: 10.1186/1944-3277-9-10
- Schlesner, H. (1989). *Planctomyces brasiliensis* sp. nov., a halotolerant bacterium from a salt pit. *Sys. Appl. Microbiol.* 12, 159–161.
- Seemann, T. (2014). Prokka: rapid prokaryotic genome annotation. *Bioinformatics* 30, 2068–2069. doi: 10.1093/bioinformatics/btu153

- Stamatakis, A. (2014). RAxML version 8: a tool for phylogenetic analysis and post-analysis of large phylogenies. *Bioinformatics* 30, 1312–1313. doi: 10.1093/bioinformatics/btu033
- Stephens, R. S., Kalman, S., Lammel, C., Fan, J., Marathe, R., Aravind, L., et al. (1998). Genome sequence of an obligate intracellular pathogen of humans: *Chlamydia trachomatis*. *Science* 282, 754–759.
- Taylor, D. W., Zhu, Y., Staals, R. H., Kornfeld, J. E., Shinkai, A., van der Oost, J., et al. (2015). Structures of the CRISPR-Cmr complex reveal mode of RNA target positioning. *Science* 348, 581–585. doi: 10.1126/science.aaa4535
- Thorvaldsdóttir, H., Robinson, J. T., and Mesirov, J. P. (2013). Integrative Genomics Viewer (IGV): high-performance genomics data visualization and exploration. *Brief Bioinform.* 14, 178–192. doi: 10.1093/bib/bbs017
- van Niftrik, L., Geerts, W. J., van Donselaar, E. G., Humbel, B. M., Webb, R. I., Harhangi, H. R., et al. (2009). Cell division ring, a new cell division protein and vertical inheritance of a bacterial organelle in anammox planctomycetes. *Mol. Microbiol.* 73, 1009–1019. doi: 10.1111/j.1365-2958.2009.06841.x
- van Teeseling, M. C., Mesman, R. J., Kuru, E., Espaillat, A., Cava, F., Brun, Y. V., et al. (2015). Anammox Planctomycetes have a peptidoglycan cell wall. *Nat. Commun.* 6, 6878. doi: 10.1038/ncomms7878
- Wagner, M., and Horn, M. (2006). The *Planctomycetes*, *Verrucomicrobia*, *Chlamydiae* and sister phyla comprise a superphylum with biotechnological and medical relevance. *Curr. Opin. Biotechnol.* 17, 241–249. doi: 10.1016/j.copbio.2006.05.005
- Wallner, S. R., Bauer, M., Würdemann, C., Wecker, P., Glöckner, F. O., and Faber, K. (2005). Highly enantioselective sec-alkyl sulfatase activity of the marine planctomycete *Rhodopirellula baltica* shows retention of configuration. *Angew. Chem. Int. Ed. Engl.* 44, 6381–6384. doi: 10.1002/anie.200501955
- Ward, N. L. (2010). “Phylum XXV. Planctomycetes Garrity and Holt 2001, 13 emend,” Ward (this Volume) in *Bergey’s Manual® of Systematic Bacteriology: Volume Four The Bacteroidetes, Spirochaetes, Tenericutes (Mollicutes), Acidobacteria, Fibrobacteres, Fusobacteriia, Dictyoglomi, Gemmatimonadetes, Lentisphaerae, Verrucomicrobia, Chlamydiae, and Planctomycetes*, eds N. R. Krieg, J. T. Staley, D. R. Brown, B. P. Hedlund, B. J. Paster, N. L. Ward, W. Ludwig, and W. B. Whitman (New York, NY: Springer), 879–925.
- Weber, T., Blin, K., Duddela, S., Krug, D., Kim, H. U., Brucolieri, R., et al. (2015). antiSMASH 3.0—a comprehensive resource for the genome mining of biosynthetic gene clusters. *Nucleic Acids Res.* 43, W237–W243. doi: 10.1093/nar/gkv437
- Wickham, H. (2007). Reshaping data with the reshape package. *J. Stat. Softw.* 21, 1–20. doi: 10.18637/jss.v021.i12
- Wickham, H. (2009). *ggplot2: Elegant Graphics for Data Analysis*. New York, NY: Springer.
- Winkelmann, N., and Harder, J. (2009). An improved isolation method for attached-living Planctomycetes of the genus *Rhodopirellula*. *J. Microbiol. Methods* 77, 276–284. doi: 10.1016/j.mimet.2009.03.002
- Wittmann, J., Dreiseikelmann, B., Rohde, C., Rohde, M., and Sikorski, J. (2014). Isolation and characterization of numerous novel phages targeting diverse strains of the ubiquitous and opportunistic pathogen *Achromobacter xylosoxidans*. *PLOS ONE* 9:e86935. doi: 10.1371/journal.pone.0086935
- Yarza, P., Yilmaz, P., Pruesse, E., Glöckner, F. O., Ludwig, W., Schleifer, K. H., et al. (2014). Uniting the classification of cultured and uncultured bacteria and archaea using 16S rRNA gene sequences. *Nat. Rev. Microbiol.* 12, 635–645. doi: 10.1038/nrmicro3330

Conflict of Interest Statement: The authors declare that the research was conducted in the absence of any commercial or financial relationships that could be construed as a potential conflict of interest.

Copyright © 2016 Kohn, Heuer, Jogler, Vollmers, Boedeker, Bunk, Rast, Borchert, Glöckner, Freese, Klenk, Overmann, Kaster, Rohde, Wiegand and Jogler. This is an open-access article distributed under the terms of the Creative Commons Attribution License (CC BY). The use, distribution or reproduction in other forums is permitted, provided the original author(s) or licensor are credited and that the original publication in this journal is cited, in accordance with accepted academic practice. No use, distribution or reproduction is permitted which does not comply with these terms.



Corrigendum: *Fuerstia marisgermanicae* gen. nov., sp. nov., an Unusual Member of the Phylum Planctomycetes From the German Wadden Sea

Timo Kohn¹, Anja Heuer¹, Mareike Jogler¹, John Vollmers¹, Christian Boedeker¹, Boyke Bunk¹, Patrick Rast¹, Daniela Borchert¹, Ines Glöckner¹, Heike M. Freese¹, Hans-Peter Klenk², Jörg Overmann¹, Anne-Kristin Kaster¹, Manfred Rohde³, Sandra Wiegand¹ and Christian Jogler^{1*}

¹ Leibniz Institut Deutsche Sammlung Von Mikroorganismen und Zellkulturen, Braunschweig, Germany, ² School of Biology, Newcastle University, Newcastle, United Kingdom, ³ Helmholtz Centre for Infectious Disease, Braunschweig, Germany

Keywords: planctomycetes, *Fuerstia marisgermanicae*, giant genes, cell division, animal associated

OPEN ACCESS

Edited and reviewed by:

Ludmila Chistoserdova,
University of Washington,
United States

*Correspondence:

Christian Jogler
christian@jogler.de

Specialty section:

This article was submitted to
Evolutionary and Genomic
Microbiology,
a section of the journal
Frontiers in Microbiology

Received: 09 April 2019

Accepted: 24 April 2019

Published: 15 May 2019

Citation:

Kohn T, Heuer A, Jogler M, Vollmers J, Boedeker C, Bunk B, Rast P, Borchert D, Glöckner I, Freese HM, Klenk H-P, Overmann J, Kaster A-K, Rohde M, Wiegand S and Jogler C (2019) Corrigendum: *Fuerstia marisgermanicae* gen. nov., sp. nov., an Unusual Member of the Phylum Planctomycetes From the German Wadden Sea. *Front. Microbiol.* 10:1029. doi: 10.3389/fmicb.2019.01029

A Corrigendum on

Fuerstia marisgermanicae gen. nov., sp. nov., an Unusual Member of the Phylum Planctomycetes from the German Wadden Sea

by Kohn, T., Heuer, A., Jogler, M., Vollmers, J., Boedeker, C., Bunk, B., et al. (2016). *Front. Microbiol.* 7:2079. doi: 10.3389/fmicb.2016.02079

In the original article, there was an error. In the Discussion of the article, we described the novel genus “*Fuerstia*,” named to honor John Fuerst, and “*Fuerstia marisgermanicae*,” the proposed type species of the genus. These names were effectively published in *Frontiers in Microbiology*, but they cannot be validly published based on the Rules of the International Code of Nomenclature of Prokaryotes. The proposed generic name cannot be used as a generic name for a new prokaryote as it is illegitimate based on Principle 2 of the Code. Moreover, the specific epithet is malformed. Therefore, we present corrected names that are here effectively published and will be submitted for validation according to the Rules of the Code.

A correction has been made to the Discussion, subsection Description of *Fuerstia* gen. nov.:

“*Fuerstiella* (Fuer.sti.el'la. N.L. dim. fem. n. *Fuerstiella*, named in honor of John Fuerst, an Australian microbiologist from University of Queensland, who played a key role in planctomycetal research). The pear to ovoid shaped cells form aggregates in liquid culture, but no rosettes. Daughter cells are motile, while mother cells are non-motile and no stalk formation was observed. The surface is smooth, crateriform structures are limited to one pole and cells reproduce by polar budding while mother- and daughter cells are connected by a thin tubular-like structure. The lifestyle is heterotrophic, obligatory aerobic and mesophilic. The major fatty acids are C₁₆:1 ω6c/16:1 ω7c (Summed feature), C₁₈:1 ω6c/18:1 ω7c (Summed feature), and C₁₆:0. Member of the phylum Planctomycetes, class Planctomyceae, order Planctomycetales, family *Planctomycetaceae*. The type species is *Fuerstiella marisgermanici*.”

Additionally, a correction has been made to the **Description**, subsection *Fuerstia marisgermanicae* sp. nov.:

“*Fuerstiella marisgermanici* (ma.ris.ger.ma’ni.ci. L. neut. n. mare the sea; L. masc. adj. *germanicus* German; N.L. gen. n. *marisgermanici* of the German sea, pertaining to the German North Sea from which the type strain was isolated). In addition to the features described for the genus, the species exhibits the following properties. Colonies on solid medium are cream colored. Cells are 1.2–2.5 × 0.9–1.7 µm in size. Non-motile mother cells spawn motile, swimming, daughter cells. Gram staining delivers no clear result. KOH test and aminopeptidase test are negative, while oxidase and catalase tests positive. The organism is able to degrade a wide range of carbon sources, in particular N-acetyl-D-galactosamine, N-acetyl-D-glucosamine, L-arabinose, D-cellobiose, D-galactose, gentiobiose, α-D-glucose, α-D-lactose, lactulose, maltose, D-mannose, D-melibiose, β-methyl-D-glucoside, sucrose, D-trehalose, turanose, succinic acid mono-methyl-ester, acetic acid, γ-hydroxybutyric acid, itaconic

acid, propionic acid, and glycerol were utilized. The enzymatic repertoire of the species, tested with API ZYM, is listed in Table 3 of the original publication. Growth occurs between pH 6 and 10 with an optimum at pH 7. At least 27.5% ASW is needed for growth, the optimal temperature for growth is 28°C (range between 20 and 30°C). The type strain is NH11^T (= DSM 27554 = LMG 27831) isolated from a crustacean shell.”

The authors apologize for this error and state that this does not change the scientific conclusions of the article in any way.

Copyright © 2019 Kohn, Heuer, Jogler, Vollmers, Boedeker, Bunk, Rast, Borchert, Glöckner, Freese, Klenk, Overmann, Kaster, Rohde, Wiegand and Jogler. This is an open-access article distributed under the terms of the Creative Commons Attribution License (CC BY). The use, distribution or reproduction in other forums is permitted, provided the original author(s) and the copyright owner(s) are credited and that the original publication in this journal is cited, in accordance with accepted academic practice. No use, distribution or reproduction is permitted which does not comply with these terms.



Development of Genetic Tools for the Manipulation of the Planctomycetes

Elena Rivas-Marín¹, Inés Canosa², Eduardo Santero² and Damien P. Devos^{1*}

¹ Laboratory of Evolutionary Innovations, Centro Andaluz de Biología del Desarrollo, Consejo Superior de Investigaciones Científicas, Universidad Pablo de Olavide, Seville, Spain, ² Microbiology Area, Centro Andaluz de Biología del Desarrollo, Consejo Superior de Investigaciones Científicas, Universidad Pablo de Olavide, Seville, Spain

Bacteria belonging to the Planctomycetes, Verrucomicrobia, Chlamydiae (PVC) superphylum are of interest for biotechnology, evolutionary cell biology, ecology, and human health. Some PVC species lack a number of typical bacterial features while others possess characteristics that are usually more associated to eukaryotes or archaea. For example, the Planctomycetes phylum is atypical for the absence of the FtsZ protein and for the presence of a developed endomembrane system. Studies of the cellular and molecular biology of these infrequent characteristics are currently limited due to the lack of genetic tools for most of the species. So far, genetic manipulation in Planctomycetes has been described in *Planctopirus limnophila* only. Here, we show a simple approach that allows mutagenesis by homologous recombination in three different planctomycetes species (*i.e.*, *Gemmata obscuriglobus*, *Gimesia maris*, and *Blastopirellula marina*), in addition to *P. limnophila*, thus extending the repertoire of genetically modifiable organisms in this superphylum. Although the Planctomycetes show high resistance to most antibiotics, we have used kanamycin resistance genes in *G. obscuriglobus*, *P. limnophila*, and *G. maris*, and tetracycline resistance genes in *B. marina*, as markers for mutant selection. In all cases, plasmids were introduced in the strains by mating or electroporation, and the genetic modification was verified by Southern Blotting analysis. In addition, we show that the green fluorescent protein (*gfp*) is expressed in all four backgrounds from an *Escherichia coli* promoter. The genetic manipulation achievement in four phylogenetically diverse planctomycetes will enable molecular studies in these strains, and opens the door to developing genetic approaches not only in other planctomycetes but also other species of the superphylum, such as the Lentisphaerae.

OPEN ACCESS

Edited by:

Frank T. Robb,
University of California, Riverside, USA

Reviewed by:

Marc Strous,
University of Calgary, Canada
Nils-Kaare Birkeland,
University of Bergen, Norway

*Correspondence:

Damien P. Devos
damienpdevos@gmail.com

Specialty section:

This article was submitted to
Evolutionary and Genomic
Microbiology,
a section of the journal
Frontiers in Microbiology

Received: 31 March 2016

Accepted: 27 May 2016

Published: 16 June 2016

Citation:

Rivas-Marín E, Canosa I, Santero E and Devos DP (2016) Development of Genetic Tools for the Manipulation of the Planctomycetes. *Front. Microbiol.* 7:914.
doi: 10.3389/fmicb.2016.00914

INTRODUCTION

The PVC superphylum comprises the Planctomycetes, Verrucomicrobia, Chlamydiae (PVC) superphylum comprises the Planctomycetes, the Verrucomicrobia and the Chlamydiae phyla, but also several others, including the Lentisphaerae (Wagner and Horn, 2006; Fuerst, 2013). Bacteria belonging to the Planctomycetes present peculiar features that are rare in bacteria (Devos, 2013; Fuerst, 2013; Devos and Ward, 2014), and some of which are more frequent in archaea or eukaryotes (Devos and Reynaud, 2010; Reynaud and Devos, 2011). Typical examples are the lack of the protein FtsZ and the division mode by budding

in some Planctomycetes, the synthesis of sterol (Pearson et al., 2003; Desmond and Gribaldo, 2009), or the presence of a complex endomembrane system (Devos, 2014). Also, the Planctomycetes represent an exceptional clade within the domain Bacteria because they are main players in the global nitrogen and carbon cycles (Strous et al., 1999; Lindsay et al., 2001; van Niftrik et al., 2004).

Despite the interest in the study of these and other peculiar features, their detailed characterization has so far been limited, mainly to computational genomes and proteomes analyses, and microscopy, due to the lack of genetic tools to manipulate the organisms.

Taking into account that those bacteria are fastidious, *i.e.*, their doubling times are in the order of a few hours (Jetten et al., 1998), they tend to aggregate into big clamps and they are naturally resistant to many antibiotics (Cayrou et al., 2010), it is not surprising that little is known about their genetic manipulation. So far, the only species that has been successfully genetically modified is *Planctopirus limnophila*, which shows one of the fastest growth rates among the cultured Planctomycetes (Jogler et al., 2011). Furthermore, endogenous plasmids and bacteriophage have been reported (Ward-Rainey et al., 1996; Ward et al., 2006; Labutti et al., 2010), and its genome sequence is available (Labutti et al., 2010). Genetic manipulation of *P. limnophila* by electroporation of circular or linear DNA, containing homologous sequence of the chromosome, has been achieved (Jogler et al., 2011; Erbilgin et al., 2014), and also by transposon mutagenesis using the EZ-Tn5 transposome (Epicenter) (Schreier et al., 2012).

To expand our knowledge about these peculiar bacteria, we have developed new strategies for genetic manipulation of other members of this group. We have selected the three following strains; *Gemmata obscuriglobus* UQM 2246 (Franzmann and Skerman, 1984), *Blastopirellula marina* DSM 3645 (Schlesner et al., 2004), and *Gimesia maris* DSM 8797 (Bauld and Staley, 1976), as they belong to the three main branches of the Planctomycetes phylum (Figure 1). *G. obscuriglobus* shows so far, some of the most interesting features of this phylum, which are the presence of membrane coat-like proteins, one of which has been located in tight interaction with the membranes of the periplasmic vesicles (Santarella-Mellwig et al., 2010), its ability to internalize whole proteins prior to their intracellular degradation (Lonhienne et al., 2010), or the presence of sterol embedded in their membranes (Pearson et al., 2003). *G. maris* was selected because it is susceptible to DNA acquisition by biparental mating with distantly related strains such as the Gram negative *Pseudomonas putida* (Dahlberg et al., 1997, 1998). Finally, *B. marina*, a phylogenetically distant strain to *G. obscuriglobus*, *G. maris*, and *P. limnophila* within the Planctomycetes clade was selected in an attempt to cover the diversity of the Planctomycetes phylum as broadly as possible.

In the present study, we developed an efficient targeted-gene disruption approach by homologous recombination in three strains, which have never been genetically modified, as well as *P. limnophila*. The gene encoding for a beta lactamase (*bla* gene) has been selected for mutagenesis since multiple

copies are found in the genomes and seems to be non-essential. Both interruption and deletion of the gene have been explored. This method represents an initial framework to develop new genetic tools in other Planctomycetes and opens up enormous fields of research amongst which the possibility to explore the cellular biology of those peculiar bacteria stands out.

MATERIALS AND METHODS

Bacterial Strains and Culture Conditions

The bacterial strains used in this work are summarized in Table 1. *Escherichia coli* was grown in Luria-Bertani medium (LB) at 37°C, *G. obscuriglobus* UQM 2246 in LB NaCl-free at pH 7.2, *G. maris* DSM 8797 in Maris broth (C. Jogler, DSMZ, Braunschweig, Germany, personal communication), *B. marina* DSM 3645 in M14 medium (DSMZ medium 600, M14) and *P. limnophila* DSM 3776 in a modified PYGV medium (DSMZ medium¹ 621: 0.1% yeast extract, 0.1% peptone, 0.1% glucose, 10 mM HEPES (pH 7.5), vitamin solution, and Hutmars basal salt solution from DSMZ 590 medium). All planctomycetes were grown at 28°C. 1.5% bacto-agar was added for solid medium. To avoid contamination of the planctomycetes cultures, cycloheximide 50 µg ml⁻¹ and ampicillin 100 µg ml⁻¹ were added. Cultures were grown aerobically in a shaker (180 rpm) using 125 or 250 ml baffled flasks closed with aluminum stopper filled with 25 or 50 ml of medium, respectively (one fifth of the volume of the flask). When required, antibiotics were used at the following concentrations (µg ml⁻¹): kanamycin (Km) 30 for *G. obscuriglobus*, 50 for *P. limnophila* and 60 for *G. maris* and, tetracycline (Tc) 2.5 for *B. marina*. All reagents were purchased from Sigma-Aldrich.

Plasmid Description

The oligonucleotides and plasmids used in this work are summarized in Tables 1 and 2, respectively. All DNA manipulations were made using standard protocols (Sambrook et al., 2001). Plasmid pMPO1012 was used as template for one-event homologous recombination insertion mutants. It is a ColE1- mobilizable plasmid, which bears the *mut3a-green fluorescent protein (gfp)* gene encoding for a gfp (Cormack et al., 1996) expressed under the *E. coli rrnb* promoter, and an *nptII* kanamycin resistance gene. In order to support homologous recombination, a 1000–1300 bp fragment of the corresponding *bla* genes for each strain was amplified using genomic DNA as a template, and were cloned into the pMPO1012 vector as a *HindIII* – directed fragment. If kanamycin was not suitable for selection of the recombinant strains, the tetracycline resistance gene from pUTminiTn5Tc (Herrero et al., 1990) was cloned into the *SmaI* restriction site. Plasmids used for gene deletion in a double event of homologous recombination were derived from pEX18Tc vector (Hoang et al., 1998), which is a suicide plasmid containing *sacB* gene from *Bacillus subtilis* used as counter-selectable marker, and a tetracycline resistance gene.

¹<http://www.dsmz.de>

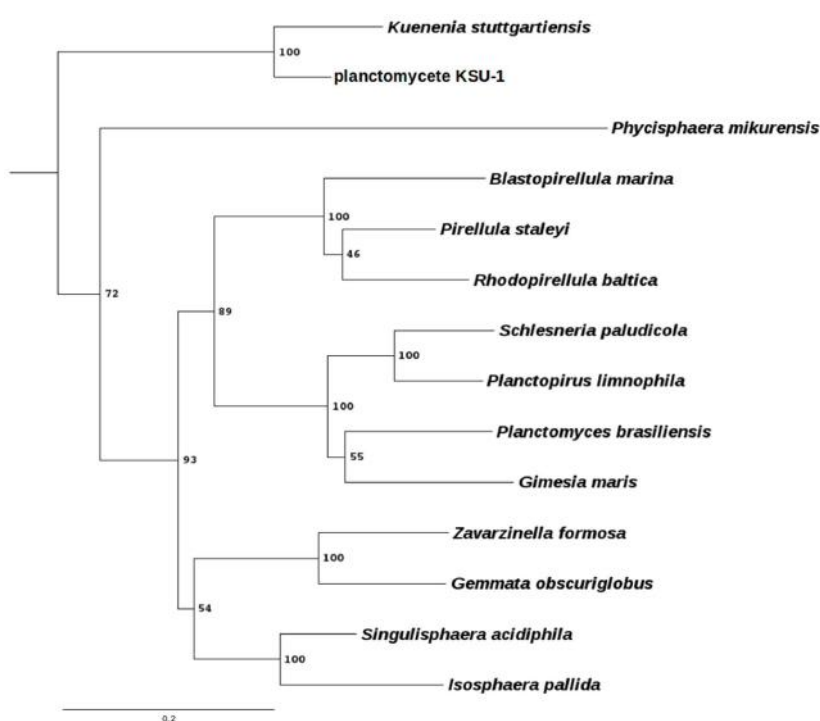


FIGURE 1 | Phylogenetic tree of some planctomycetes species. Phylogenetic profiling was done using the RNA-polymerase subunit β protein, encoded by the *rpoB* gene. Protein sequences were extracted using BLAST (Altschul and Lipman, 1990) with an e-value of $1e^{-5}$. The multiple sequence alignment was done using Clustal Omega (Sievers et al., 2011) with default parameters and manually curated. The tree was generated using PhyML 3.1 (Guindon, 2010) using the LG matrix, 100 bootstraps, tree and leaves refinement, SPR moves and amino acids substitution rates were determined empirically. Bootstrap values are indicated at the nodes. Scale bar indicates the amount of substitution per site. The chlamydial *Waddlia chondrophila* was used as an outgroup.

TABLE 1 | Strains used in this study.

| Strain name | Genotype | Reference |
|--|--|-----------------------------|
| <i>Escherichia coli</i> DH5 α | F $^-\phi 80$ lacZ Δ M15 Δ (lacZYA-argF)U169 recA1 endA1 hsdR17(rK $^+$ mK $^-$) supE44 thi-1 gyrA relA1 | Hanahan, 1983 |
| Gemmata obscuriglobus UQM 2246 | Wild type (WT) strain | Franzmann and Skerman, 1984 |
| <i>G. obscuriglobus</i> UQM 2246 DV001 | <i>bla'</i> ::pDV003 | This work |
| <i>Gimesia maris</i> DSM 8797 | WT strain | Bauld and Staley, 1976 |
| <i>G. maris</i> DSM 8797 DV005 | <i>bla'</i> ::pDV002 | This work |
| <i>Blastopirellula marina</i> DSM 3645 | WT strain | Schlesner et al., 2004 |
| <i>B. marina</i> DSM 3645 DV009 | <i>bla'</i> ::pDV017 | This work |
| <i>Planctopirus limnophila</i> DSM3776 | WT strain | Hirsch and Müller, 1985 |
| <i>P. limnophila</i> DSM3776 DV004 | <i>bla'</i> ::pDV004 | This work |
| <i>P. limnophila</i> DSM3776 DV007 | Δ <i>bla</i> | This work |

To construct knockout plasmids for *bla* gene, fragment *bla*-up containing 1000–1500 bp sequences upstream of *bla* was amplified by PCR from genomic DNA of the appropriate strain using the primer pairs listed in Supplementary Table S1. The fragment *bla*-down containing 1000–1500 bp sequences downstream of *bla* was amplified by PCR using primer cited in Supplementary Table S1. The *Eco*RI/*Bam*HI(*Bcl*I)-digested *bla*-up fragment and *Bam*HI(*Bcl*I)/*Hind*III(*Sma*I)-digested *bla*-down fragment were then cloned into *Eco*RI/*Hind*III(*Sma*I)-digested pEX18Tc by three-way ligation. Finally, the kanamycin resistance gene from the pUTminiTn5km plasmid (Herrero et al., 1990)

was subsequently cloned as a *Bam*HI (or *Bcl*I) fragment between the two flanking regions.

Genetic Modification: Triparental Mating

Genetic modification of *G. obscuriglobus*, *G. maris*, *B. marina*, and *P. limnophila* was performed by triparental mating using 200 μ l of an exponentially growing culture ($A_{600} \sim 0.4$) of the donor (see Table 2) and helper (pRK2013/*E. coli* DH5 α) strains in LB, with the cell pellet of a 15–20 ml culture of the receptor strain ($A_{600} \sim 0.4$). Each culture was previously individually washed in phosphate buffer and resuspended in a total volume of 100 μ l

TABLE 2 | Plasmid used in this work.

| Plasmid name | Main features | Source |
|--------------|--|--|
| pMPO1012 | Mobilizable, ColE1, Km ^R . Modified from pFPV25 (Valdivia and Falkow, 1996) | Lab collection. Beatriz Mesa, personal communication |
| pRK2013 | Helper plasmid. ColE1. Tra ⁺ , Km ^r | Figurski and Helinski, 1979 |
| pBF1 | Natural marine isolated conjugative plasmid, Hg ^r | Dahlberg et al., 1998 |
| pDV002 | 1090 bp fragment in pMPO1012, bearing a bla gene from <i>G. maris</i> . Km ^r | This work |
| pDV003 | 1078 bp fragment in pMPO1012, bearing a bla gene from <i>G. obscuriglobus</i> . Km ^r | This work |
| pDV004 | 1081 bp fragment in pMPO1012, bearing a bla gene from <i>P. limnophila</i> . Km ^r | This work |
| pDV012 | 1410 bp upstream and 1243 bp downstream of bla gene from <i>G. obscuriglobus</i> flanking a kanamycin resistance gene cloned into pEX18Tc. Km ^r , Tc ^r | This work |
| pDV013 | 1472 bp upstream and 1304 bp downstream of bla gene from <i>G. maris</i> flanking a kanamycin resistance gene cloned into pEX18Tc. Km ^r , Tc ^r | This work |
| pDV014 | 1498 bp upstream and 1443 bp downstream of bla gene from <i>P. limnophila</i> flanking a kanamycin resistance gene cloned into pEX18Tc. Km ^r , Tc ^r | This work |
| pDV017 | 1234 bp fragment in pMPO1012, bearing a bla gene from <i>B. marina</i> . Km ^r , Tc ^r | This work |
| pDV018 | pMPO1012 with a tetracycline resistance cloned | This work |

that was spotted onto the corresponding agar plates containing cycloheximide. The conjugation patches were incubated for 24 h at 28°C, and resuspended in 1 ml of phosphate buffer. Transconjugants and viable cells were plated with the appropriate antibiotics. Colonies appeared after 12–16 days of incubation at 28°C. Transconjugants were refreshed onto new selection plates with the appropriate antibiotics before they were used to inoculate liquid media. For double recombination events, the pEX18Tc derived- plasmid candidates containing the insertion of the whole plasmid (see Table 2) were grown in liquid cultures containing cycloheximide. After 10 days of growth, candidates were segregated onto selective plates containing kanamycin and different concentration of sucrose (0.1, 0.5, 1, 5, and 10%) to counterselect the second recombination event. Transconjugants were verified by PCR and Southern Blotting analysis.

Genetic Modification: Electroporation

Genetic transformation of *P. limnophila* was performed also by electroporation as described before (Jogler et al., 2011) with some modifications. Fresh electrocompetent cells were prepared from 400 ml of a culture at an A_{600} of 0.4 in modified PYGV. The cells were washed twice with 100 and 50 ml of ice-cold double distilled sterile water and once with 2 ml of ice-cold 10% glycerol. Then, the pellet was resuspended in 400 μ l of ice-cold 10% glycerol, and aliquots of 100 μ l were dispensed into 0.1-mm gapped electroporation cuvettes along with ~1 μ g of circular DNA (see Table 2) and 1 μ l of Type-One restriction inhibitor (Epicenter). Electroporation was performed with a Bio-Rad Micropulser (Ec3 pulse, voltage [V] 3.0 kV). Electroporated cells were immediately recovered in 1 ml of cold modified PYGV and incubated at 28°C for 1.5–2 h with shaking. The cells

were then plated onto modified PYGV plates supplemented with kanamycin 50 μ g ml⁻¹ and were incubated at 28°C until colony formation after 5 to 7 days. Colonies were segregated onto fresh selection plates and genotyped by PCR and Southern Blotting analysis.

Characterisation of Modified Strains by PCR and Southern Blotting

Strains harboring the mutation were genotyped by PCR analysis after fluorescent detection under the microscope. Candidates were checked by amplifying them with paired oligonucleotides located upstream and downstream of the disrupted genes in the genomic DNA (Supplementary Table S1). Once candidates were tested by PCR, Southern Blotting analysis with 2 μ g of genomic DNA was performed. Genomic DNA was extracted using Wizard Genomic DNA Purification Kit (Promega) with a previous lysozyme treatment (0.5 mg/ml, 1 h at 37°C). The digested DNA was resolved by agarose gel electrophoresis and the DNA transfer was performed as described previously (Brown, 2001). PCR amplicons used as probes were synthetized with the same primers used for genomic amplification for DNA cloning (Supplementary Table S1). Probes were labeled according to the manufacturer's instructions (DIG DNA Labeling Kit, Roche). DIG-labeled probes were detected with anti-Digoxigenin-AP, Fab fragments (Roche), and CSPD (Roche). Visualizations were performed using Chemidoc XRS, and images were analysed with ImageLab 5.0 software.

Fluorescence Microscopy

For confocal microscopy, cells were grown to an A_{600} ~0.4, and washed twice with phosphate buffer. After washing, microscopy was performed on a Leica TCS SP5 II microscope using a 63 \times

immersion objective. The fluorescence parameters were fixed for all the strains used in this work. The images were processed by Fiji (version 2.0.0-rc-43/1.50e).

RESULTS

Development of a Gene Transfer System and Directed Mutagenesis

Gemmata obscuriglobus

In the first place, the sensitivity of *G. obscuriglobus* to kanamycin was evaluated. Saturated cultures of *G. obscuriglobus* were spotted onto LB NaCl-free agar plates supplemented with different concentrations of the antibiotic (5, 10, 20, and 30 $\mu\text{g ml}^{-1}$). After incubation at 28°C for 8–12 days, kanamycin showed growth inhibition at 5 $\mu\text{g ml}^{-1}$ (data not shown), and a concentration of 30 $\mu\text{g ml}^{-1}$ was further used for selection of *G. obscuriglobus* transconjugants.

The pDV003 plasmid, containing a 1078 bp DNA fragment of *bla* gene from *G. obscuriglobus* genome (genbank identifier:163804324:4223-6571) cloned into the pMPO1012 vector, was conjugated into the receptor cells by triparental mating. After 12–16 days of incubation at 28°C isolated colonies were detected in the kanamycin selective medium. No colonies were observed on the selective plates in the mixtures without DNA or when transformed with the empty vector (pMPO1012). The transconjugants (DV001 candidates), which resulted from the integration of a plasmid into the chromosome due to a single event of homologous recombination, were tested by PCR and Southern Blotting analysis using genomic DNA. Southern Blotting assays confirmed the expected pattern of bands sizes after digestion with the appropriate restriction enzymes for the wild type (WT) strains and the insertion mutant (**Figure 2A**). The integration frequency of pDV003 was around 10^{-7} – 10^{-8} cfu per recipient. In addition, the DV001 transconjugants showed higher fluorescence at the fluorescence microscope as they expressed the *gfp* encoded in the vector, in comparison with the auto-fluorescent signal of the WT cells (**Figure 2B**).

Gimesia maris

The natural plasmid pBF1, which was isolated from marine bacterial communities, was tested for mating in *G. maris*. This plasmid had previously been reported to be transferred from *P. putida* to *G. maris* (Dahlberg et al., 1998). In this work only the transmission of this plasmid was tested, not its stability. To determine if, we could use this plasmid, or its elements, to develop a suitable vector to work with it in *G. maris*, a deeper study of this plasmid was performed. In the first place, the susceptibility of *G. maris* to mercury, the resistance marker of pBF1, was tested. Saturated cultures of the WT strain were spotted onto Maris broth agar plates supplemented with growing concentrations of mercury from a range of 5 to 160 $\mu\text{g ml}^{-1}$. After incubation at 28°C for 10–15 days, *G. maris* showed complete growth inhibition with the lowest mercury concentration tested (data not shown). Biparental mating using pBF1 as donor plasmid were performed as previously described (Dahlberg et al., 1998).

Once the cells were conjugated and plated onto Maris broth containing mercury 5 $\mu\text{g ml}^{-1}$, no colony was observed on the selective plates. This data suggest that even though pBF1 vector can be transmitted to *G. maris* by mating, it may not be stable, or the resistance markers are not properly expressed in this strain.

The construction of an insertion mutant in *G. maris* by a single step of homologous recombination was also assessed. The sensitivity assays for kanamycin resistance were performed by spotting saturated cultures of the WT *G. maris* onto Maris broth agar plates supplemented with several concentrations of this antibiotic (5, 10, 20, 30, 40, 50, and 60 $\mu\text{g ml}^{-1}$). Kanamycin showed a partial growth inhibition at a concentration of 50 $\mu\text{g ml}^{-1}$, so 60 $\mu\text{g ml}^{-1}$ was used for marker selection. For triparental matings in *G. maris*, the plasmid pDV002 containing 1090 bp of the *bla* gene (genbank identifier:149173661:342452-343846) cloned into the pMPO1012 vector, was used as donor. Kanamycin resistant transconjugants, named DV005, grew in Maris broth after incubation at 28°C for 10–15 days. Southern Blotting assays using genomic DNA of the DV005 transconjugants and the WT strains, showed the correct genomic organization as a result of one event of homologous recombination (**Figure 3A**). *G. maris* also displayed increased fluorescence compared to the auto-fluorescence signal, showing that the heterologous *gfp* gene encoded in the plasmid (**Figure 3B**) was expressed in *G. maris*.

Blastopirellula marina

Since, *B. marina* is naturally resistant to kanamycin, tetracycline was used as a selection marker (Cayrou et al., 2010). pDV017 plasmid is equivalent to the vectors used for mutagenesis of *G. obscuriglobus*, *P. limnophila*, or *G. maris* but it contains 1234 bp of the *bla* gene from *B. marina* genome (genbank identifier:211606473:c1147370-1146660) and a tetracycline resistance gene.

pDV017 plasmid was mated into *B. marina* for a single homologous recombination event. After incubation at 28°C for 12–16 days, isolated tetracycline resistant colonies appeared with a frequency of approximately 10^{-9} per recipient (DV009 candidates). No single colonies were obtained in the negative control, however, colonies were detected when the empty plasmid (pDV018) was mated. DV009 transconjugant candidates were tested by PCR analysis, which confirmed the insertion of the plasmid into the chromosome, while Southern Blotting analysis (**Figure 4A**) showed that pDV017 was replicative in *B. marina* and also integrated in the genome by homologous recombination of the *bla* gene at the same time. This was in concordance with the results obtained with the empty plasmid, which was successfully isolated from the transconjugant strains confirming that the pMPO1012-derived plasmids were replicative in *B. marina*. When checked by fluorescence microscopy the mutant strain was also fluorescent as a result of the *gfp* expression (**Figure 4B**).

Planctopirus limnophila

For genetic manipulation of *P. limnophila*, electroporation and conjugation were tested. The vector pDV004 containing 1081 bp

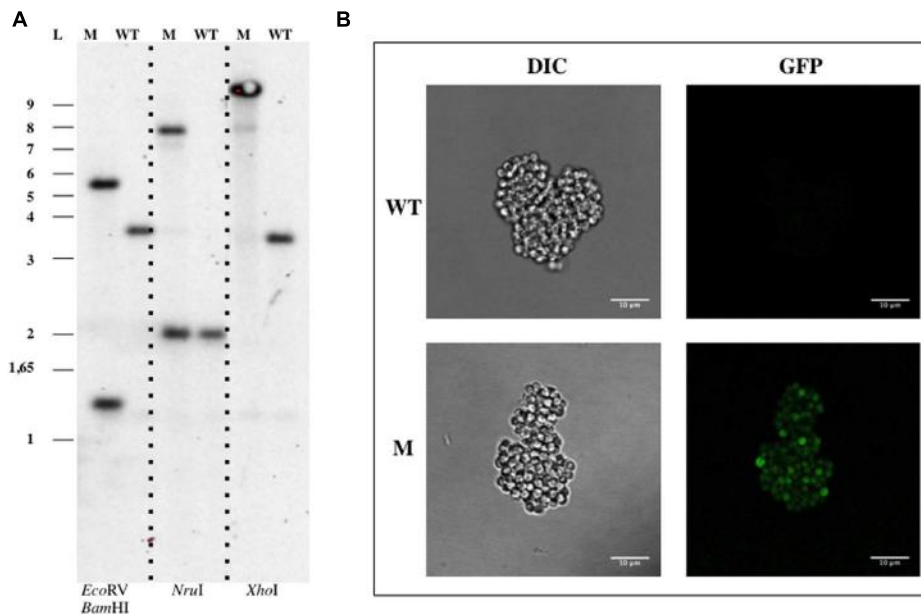


FIGURE 2 | Genetic manipulation of *Gemmata obscuriglobus* UQM 2246. (A) Southern Blotting analysis of *G. obscuriglobus* DV001. **(B)** Confocal imaging of *G. obscuriglobus*. Abbreviations: WT, wild type; M, mutant; L, ladder; DIC, Differential Interference Contrast.

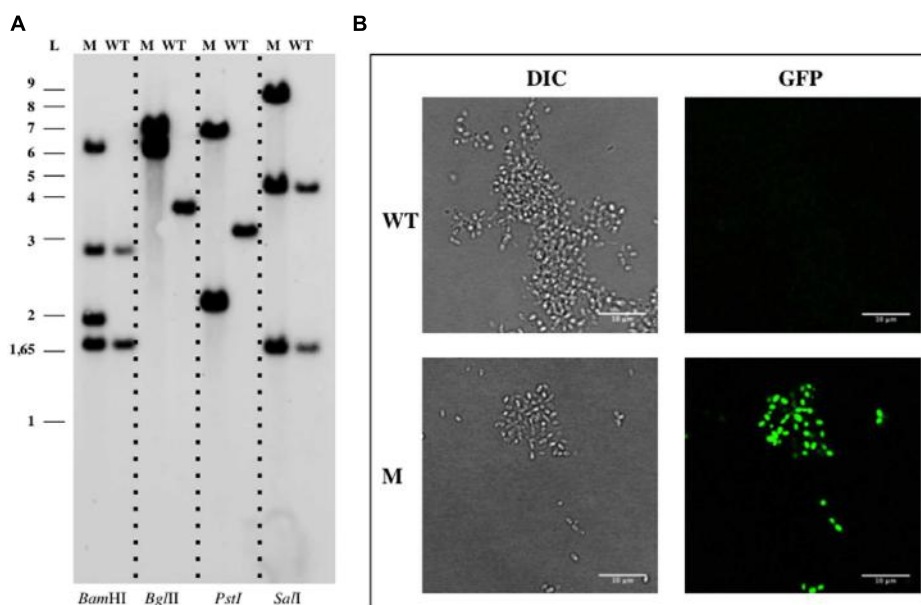


FIGURE 3 | Genetic manipulation of *Gimesia maris* DSM 8797. (A) Southern Blotting analysis of *G. maris* DV005. **(B)** Confocal imaging of *G. maris*. Abbreviations: WT, wild type; M, mutant; L, ladder; DIC, Differential Interference Contrast.

of the *bla* gene (genbank identifier: 296120274:807838-809091) was cloned into pMPO1012 vector to perform an insertion mutant by single homologous recombination. Modified strains obtained by electroporation or mating (DV004 candidates) were selected using kanamycin, as previously described (Jogler et al., 2011). No colonies were observed in the negative controls in the mixtures without DNA or with the empty

plasmid (pMPO1012). Plasmid integration was verified by PCR using genomic DNA of the DV004 candidates as template and, finally, their genomic arrangement were confirmed by Southern Blotting assays (Figure 5A). The integration frequency of the mating was estimated as approximately 10^{-6} – 10^{-7} cfu per recipient. The *gfp* reporter gene harbored in pDV004 was expressed in *P. limnophila* and non-endogenous

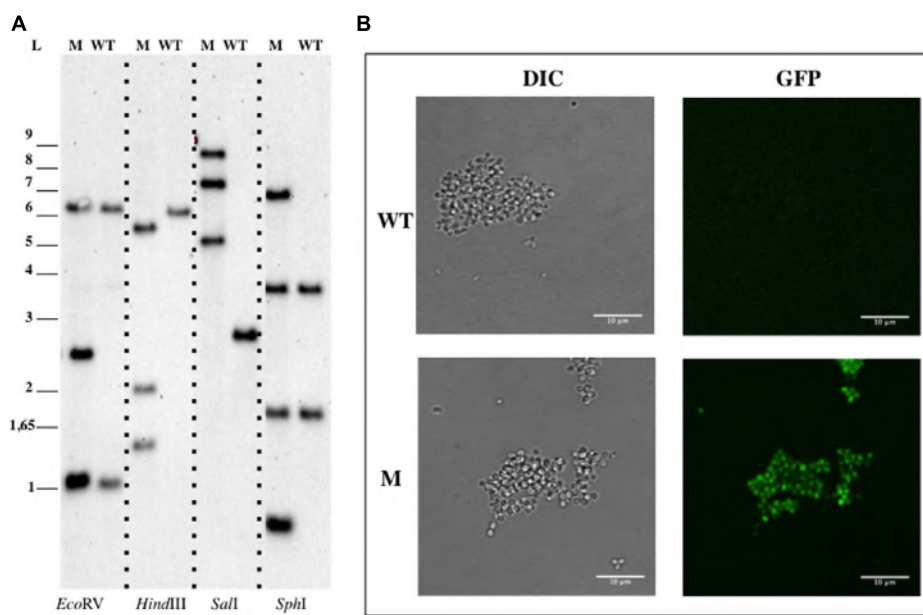


FIGURE 4 | Genetic manipulation of *Blastopirellula marina* DSM 3645. (A) Southern Blotting analysis of *B. pirellula* DV009. **(B)** Confocal imaging of *B. marina*. Abbreviations: WT, wild type; M, mutant; L, ladder; DIC, Differential Interference Contrast.

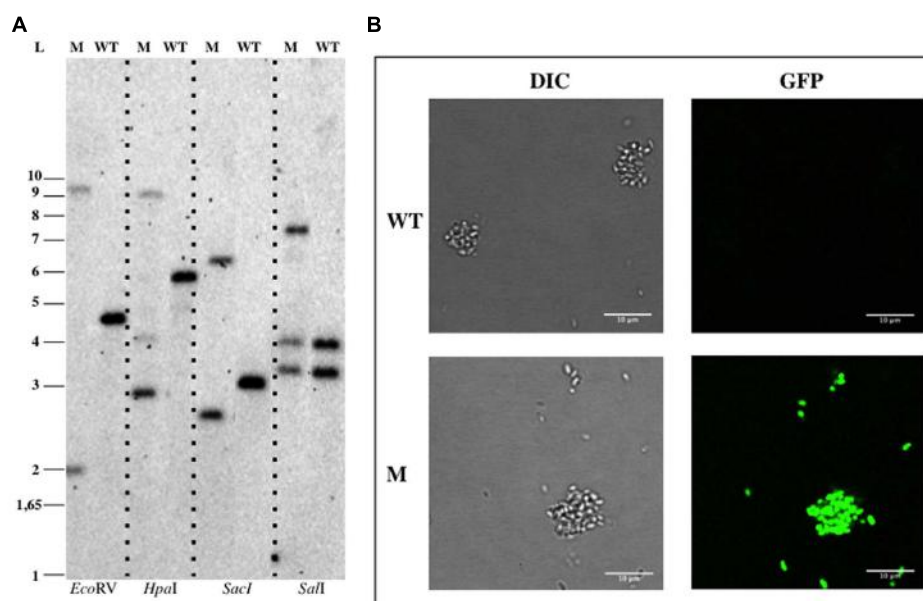


FIGURE 5 | Genetic manipulation of *Planctopirus limnophila* DSM 3776. (A) Southern Blotting analysis of *P. limnophila* DV004. **(B)** Confocal imaging of *B. marina*. Abbreviations: WT, wild type; M, mutant; L, ladder; DIC, Differential Interference Contrast.

fluorescence was clearly detected by fluorescence microscopy (**Figure 5B**).

In order to delete the target gene, cells were electroporated with pDV014, designed for double homologous recombination that contained the flanking regions of the *bla* gene, and plated in Km 50 $\mu\text{g ml}^{-1}$ or Km 50 $\mu\text{g ml}^{-1}$ Tc 5 $\mu\text{g ml}^{-1}$ dishes. No colonies were observed in the plates containing kanamycin

plus tetracycline, although colonies appeared in plates with just kanamycin with an estimated frequency of 2×10^{-5} cfu ug $^{-1}$ DNA. These candidates were verified by Southern Blotting analysis (**Figure 6**), and in all cases, a restriction pattern of a *bla* deletion mutant after a double event of homologous recombination was observed. The second recombination event resulted directly without the necessity to force it as described

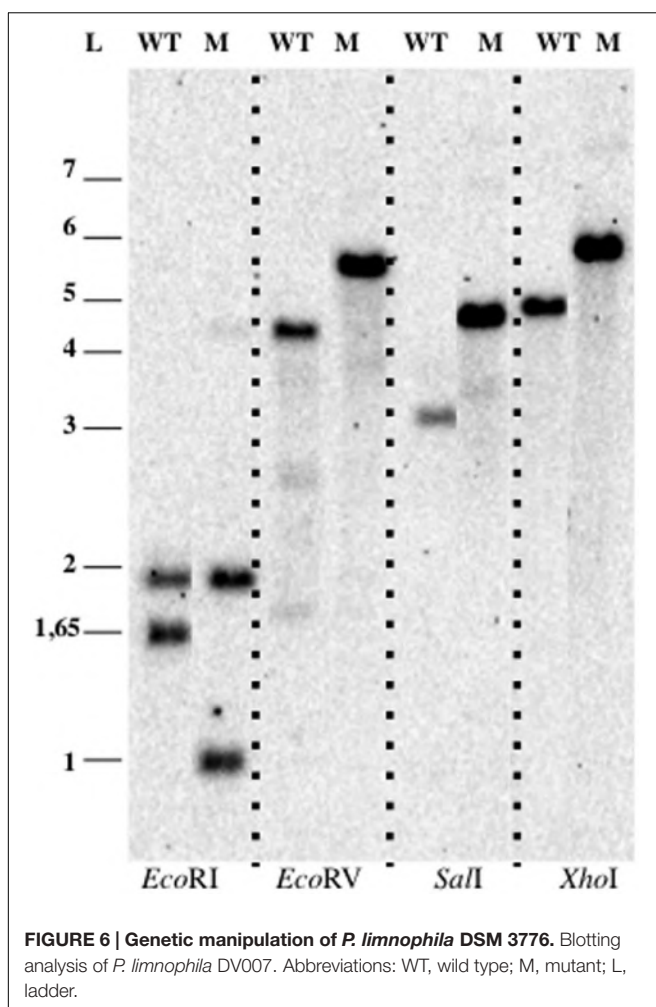


FIGURE 6 | Genetic manipulation of *P. limnophila* DSM 3776. Blotting analysis of *P. limnophila* DV007. Abbreviations: WT, wild type; M, mutant; L, ladder.

previously (Erbilgin et al., 2014). The tetracycline marker was not conferring resistance to the antibiotic in *P. limnophila*, explaining why no candidates were observed when plated on kanamycin and tetracycline.

DISCUSSION

Genetic modification combined with phenotypic study of mutants is a powerful tool for the study of gene function. Genetic tools for many bacterial species are available, however, genetic manipulation of non-model organisms, such as Planctomycetes, are frequently hampered by the lack of them. In this work, we describe a protocol for the construction of insertion mutants in *B. marina*, *G. obscuriglobus*, *G. maris*, and *P. limnophila* by a single event of homologous recombination. In addition, we further show the production of a deletion mutant in *P. limnophila* by a double event of recombination.

In order to construct insertion mutants, we use a ColE1-derived plasmid (pMPO102), which encodes an antibiotic resistance gene (kanamycin or/and tetracycline) and the gene coding for the *gfp*. pMPO102 is a high copy number plasmid in *E. coli*, which yields high amounts of plasmidic DNA

from small cultures. Moreover it can be transferred to the receptor cells by conjugation because it contains the origin of conjugal DNA transfer (*oriT*). Surprisingly, we found that the pMPO102-derived plasmid is replicative in *B. marina*, even though ColE1 replicon has been described as a narrow broad range plasmid, for its replication requires proteins from its host bacterium *E. coli* (Kues and Stahl, 1989). In our case, even though the plasmid is replicative, it is also able to integrate into the bacterial chromosome by homologous recombination of the cloned sequence. Nevertheless, in order to promote a single integration event, a non-replicative plasmid would be more suitable. On the other hand, the description of a replicative plasmid in the Planctomycetes opens up additional possibilities in the genetic manipulation of these organisms.

The *gfp* gene encoded by the pMPO102-derived plasmids, which is under the control of the *E. coli rrnb* promoter, is successfully expressed in all the strains assayed. The fluorescence of the insertion mutant strains is clearly higher than the one observed in the four WT strains. The *gfp* expression enables rapid identification of clones, originating from a single homologous recombination event, by fluorescence microscopy visualization or fluorescence-assisted cell sorting (FACS). The *gfp* expression is higher in *G. maris* and *P. limnophila* than in *G. obscuriglobus* and *B. marina*. A possible explanation for these differences is that the promoter sequence for the *E. coli* vegetative sigma factor could be more similar to the one of *G. maris* and *P. limnophila*, it is also possible that the codon usage is affecting the different patterns of expression. Thus, heterologous promoters can be functional in Planctomycetes and could be used to express products of interest inside these cells. Depending on the target strain, the promoter and the gene sequence could be optimized to maximize expression.

Although it has been possible to construct a deletion mutant by a double homologous recombination event in *P. limnophila* using pDV014 vector, the construction of deletion mutant in the other three species tested is limited by the number of available resistance gene cassettes and intrinsic resistance of target organisms (Cayrou et al., 2010). An attempt to promote a double homologous recombination event was also performed using plasmid pDV012 and pDV013 that contained the two flanking regions of *bla* gene of *G. obscuriglobus* and *G. maris*, respectively. Those strains were shown to be very sensitive to low concentrations of sucrose (0.1%) and this sugar can thus not be used to counterselect for the *sacB* gene marker in the pEX18Tc-derived plasmid. Also, the tetracycline resistance of the plasmid was not useful in those strains since the first- recombination event candidates were not able to grow on the lowest concentration of tetracycline tested ($2.5 \mu\text{g ml}^{-1}$). Those strains are known to be sensitive to tetracycline (Cayrou et al., 2010), however, it seems that the tetracycline resistance gene cloned into pDV012, pDV013 and also into pDV014, is not expressed or its product is not active in either *G. obscuriglobus*, *G. maris*, or *P. limnophila* since they are not able to grow in the presence of this antibiotic even when bearing the resistance gene. Therefore, the search of deletion mutants could not be checked by the loss of growth in the presence of tetracycline. Even in *B. marina*, where the tetracycline

marker allowed the mutant selection, this antibiotic is required in a very low concentration. New selective markers to combine with kanamycin in *G. maris*, *P. limnophila*, and *G. obscuriglobus* or with tetracycline in *B. marina* are needed to further develop the genetic tools applicable to Planctomycetes.

During the growth of a first cross-over mutant, second cross-over rarely occurs, resulting in a tedious manual screening through colony PCR. Thus, in order to promote a second event of homologous recombination, and excision of the integrated plasmid, a counterselection method would be convenient. In the Planctomycetes, the *sacB* selection method based on sucrose sensitivity (Hoang et al., 1998) is not suitable because sucrose is highly toxic for these organisms, other systems based on conditionally lethal genes, such as *pheS* (Kast, 1994) could be adapted. There are alternative methods to construct deletion mutant, such as the I-SceI endonuclease, the site-specific recombination *cre/loxP*-based systems- (Suzuki et al., 2005; Yu et al., 2008; Horzempa et al., 2010; Siegl et al., 2010), or the recent CRISPR (Clustered Regularly Interspaced Short Palindromic Repeats)-associated Cas9 endonucleases system genome-editing tools (Jiang et al., 2013). Nevertheless, they may have other limitations, such as the specificity or the requirements for additional components that should be provided in *trans*, which makes mandatory the finding of replicative plasmids in these organisms.

In this work, we presented the initial tools for genetic manipulation of several Planctomycetes strains, allowing the design of more complex genetic events. This opens up a new field in the characterization of features of these peculiar organisms that will magnify their relevance in the understanding of genome evolution.

CONCLUSION

We successfully developed a simple genetic modification approach by triparental mating for four genera of Planctomycetes. This work shows a targeted gene insertion method using gfp for identification and a resistance marker

REFERENCES

- Altschul, S. F., and Lipman, D. J. (1990). Protein database searches for multiple alignments. *Proc. Natl. Acad. Sci. U.S.A.* 87, 5509–5513. doi: 10.1073/pnas.87.14.5509
- Bauld, J., and Staley, J. T. (1976). *Planctomyces maris* sp. nov: a marine isolate of *Planctomyces-Blastocaulis* group of budding bacteria. *J. Gen. Microbiol.* 97, 45–55. doi: 10.1099/00221287-97-1-45
- Brown, T. (2001). Southern blotting. *Curr. Protoc. Immunol.* Chapter 10, Unit 10.6A. doi: 10.1002/0471142727.mb0209as21
- Cayrou, C., Raoult, D., and Drancourt, M. (2010). Broad-spectrum antibiotic resistance of Planctomycetes organisms determined by Etest. *J. Antimicrob. Chemother.* 65, 2119–2122. doi: 10.1093/jac/dkq290
- Cormack, B. P., Valdivia, R. H., and Falkow, S. (1996). FACS-optimized mutants of the green fluorescent protein (GFP). *Gene* 173, 33–38. doi: 10.1016/0378-1119(95)00685-0
- Dahlberg, C., Bergstrom, M., and Hermansson, M. (1998). In situ detection of high levels of horizontal plasmid transfer in marine bacterial communities. *Appl. Environ. Microbiol.* 64, 2670–2675.
- Dahlberg, C., Linberg, C., Torsvik, V. L., and Hermansson, M. (1997). Conjugative plasmids isolated from bacteria in marine environments show various degrees of homology to each other and are not closely related to well-characterized plasmids. *Appl. Environ. Microbiol.* 63, 4692–4697.
- Desmond, E., and Gribaldo, S. (2009). Phylogenomics of sterol synthesis: insights into the origin, evolution, and diversity of a key eukaryotic feature. *Genome Biol. Evol.* 1, 364–381. doi: 10.1093/gbe/evp036
- Devos, D. P. (2013). Gemmata obscuriglobus. *Curr. Biol.* 23, R705–R707. doi: 10.1016/j.cub.2013.07.013
- Devos, D. P. (2014). PVC bacteria: variation of, but not exception to, the Gram-negative cell plan. *Trends Microbiol.* 22, 14–20. doi: 10.1016/j.tim.2013.10.008
- Devos, D. P., and Reynaud, E. G. (2010). Evolution. Intermediate steps. *Science* 330, 1187–1188. doi: 10.1126/science.1196720
- Devos, D. P., and Ward, N. L. (2014). Mind the PVCs. *Environ. Microbiol.* 16, 1217–1221. doi: 10.1111/1462-2920.12349
- Erbilgin, O., McDonald, K. L., and Kerfeld, C. A. (2014). Characterization of a planctomycetal organelle: a novel bacterial microcompartment for the aerobic degradation of plant saccharides. *Appl. Environ. Microbiol.* 80, 2193–2205. doi: 10.1128/AEM.03887-13

as selection. This approach could be applied to other Planctomycetes strains in order to expand the knowledge of this unusual phylum, broadening the applicability of genetic manipulation in these bacteria, and raising the possibility to manipulate microorganisms of other phyla in the PVC superphylum.

AUTHOR CONTRIBUTIONS

ER-M designed and performed the experiments, analyzed the results and wrote the paper. IC and ES contributed to the discussion of the results, and DD designed the general strategy, supervised the work, analyzed data and wrote the paper. All authors reviewed the manuscript.

FUNDING

ER-M and DPD are supported by the Spanish Ministry of Economy and Competitiveness (Grant BFU2013-40866-P) and the Junta de Andalucía (CEIC Grant C2A program to DPD). IC and ES are supported by the Spanish Ministry of Economy and Competitiveness (Grant BIO2014-57545-R).

ACKNOWLEDGMENTS

We would like to thank Guadalupe Martín for technical help, all members of the Microbiology Area for their insights and suggestions, and Nicola Bordin for the tree construction. Thanks to C. Jogler (DSMZ, Braunschweig, DE) for strains and medium recipes sharing.

SUPPLEMENTARY MATERIAL

The Supplementary Material for this article can be found online at: <http://journal.frontiersin.org/article/10.3389/fmicb.2016.00914>

- Figurski, D. H., and Helinski, D. R. (1979). Replication of an origin-containing derivative of plasmid RK2 dependent on a plasmid function provided in trans. *Proc. Natl. Acad. Sci. U.S.A.* 76, 1648–1652. doi: 10.1073/pnas.76.4.1648
- Franzmann, P. D., and Skerman, V. B. (1984). *Gemmata obscuriglobus*, a new genus and species of the budding bacteria. *Antonie Van Leeuwenhoek* 50, 261–268. doi: 10.1007/BF02342136
- Fuerst, J. A. (2013). The PVC superphylum: exceptions to the bacterial definition? *Antonie Van Leeuwenhoek* 104, 451–466. doi: 10.1007/s10482-013-9986-1
- Guindon, S. (2010). Bayesian estimation of divergence times from large sequence alignments. *Mol. Biol. Evol.* 27, 1768–1781. doi: 10.1093/molbev/msq060
- Hanahan, D. (1983). Studies on transformation of *Escherichia coli* with plasmids. *J. Mol. Biol.* 166, 557–580. doi: 10.1016/S0022-2836(83)80284-8
- Herrero, M., de Lorenzo, V., and Timmis, K. N. (1990). Transposon vectors containing non-antibiotic resistance selection markers for cloning and stable chromosomal insertion of foreign genes in gram-negative bacteria. *J. Bacteriol.* 172, 6557–6567.
- Hirsch, P., and Müller, M. (1985). *Planctomyces limnophilus* sp. nov., a Stalked and Budding Bacterium from Freshwater. *Syst. Appl. Microbiol.* 6, 276–280. doi: 10.1016/S0723-2020(85)80031-X
- Hoang, T. T., Karkhoff-Schweizer, R. R., Kutchma, A. J., and Schweizer, H. P. (1998). A broad-host-range Flp-FRT recombination system for site-specific excision of chromosomally-located DNA sequences: application for isolation of unmarked *Pseudomonas aeruginosa* mutants. *Gene* 212, 77–86. doi: 10.1016/S0378-1119(98)00130-9
- Horzempa, J., Shanks, R. M., Brown, M. J., Russo, B. C., O'Dee, D. M., and Nau, G. J. (2010). Utilization of an unstable plasmid and the I-SceI endonuclease to generate routine markerless deletion mutants in *Francisella tularensis*. *J. Microbiol. Methods* 80, 106–108. doi: 10.1016/j.mimet.2009.10.013
- Jetten, M. S., Strous, M., van de Pas-Schoonen, K. T., Schalk, J., van Dongen, U. G., van de Graaf, A. A., et al. (1998). The anaerobic oxidation of ammonium. *FEMS Microbiol. Rev.* 22, 421–437. doi: 10.1111/j.1574-6976.1998.tb00379.x
- Jiang, W., Bikard, D., Cox, D., Zhang, F., and Marraffini, L. A. (2013). RNA-guided editing of bacterial genomes using CRISPR-Cas systems. *Nat. Biotechnol.* 31, 233–239. doi: 10.1038/nbt.2508
- Jogler, C., Glockner, F. O., and Kolter, R. (2011). Characterization of *Planctomyces limnophilus* and development of genetic tools for its manipulation establish it as a model species for the phylum Planctomycetes. *Appl. Environ. Microbiol.* 77, 5826–5829. doi: 10.1128/AEM.05132-11
- Kast, P. (1994). pKSS—a second-generation general purpose cloning vector for efficient positive selection of recombinant clones. *Gene* 138, 109–114. doi: 10.1016/0378-1119(94)90790-0
- Kues, U., and Stahl, U. (1989). Replication of plasmids in gram-negative bacteria. *Microbiol. Rev.* 53, 491–516.
- Labutti, K., Sikorski, J., Schneider, S., Nolan, M., Lucas, S., Glavina Del Rio, T., et al. (2010). Complete genome sequence of *Planctomyces limnophilus* type strain (Mu 290). *Stand. Genomic Sci.* 3, 47–56. doi: 10.4056/sigs.1052813
- Lindsay, M. R., Webb, R. I., Strous, M., Jetten, M. S., Butler, M. K., Forde, R. J., et al. (2001). Cell compartmentalisation in planctomycetes: novel types of structural organisation for the bacterial cell. *Arch. Microbiol.* 175, 413–429. doi: 10.1007/s002030100280
- Lonhienne, T. G., Sagulenko, E., Webb, R. I., Lee, K. C., Franke, J., Devos, D. P., et al. (2010). Endocytosis-like protein uptake in the bacterium *Gemmata obscuriglobus*. *Proc. Natl. Acad. Sci. U.S.A.* 107, 12883–12888. doi: 10.1073/pnas.1001085107
- Pearson, A., Budin, M., and Brocks, J. J. (2003). Phylogenetic and biochemical evidence for sterol synthesis in the bacterium *Gemmata obscuriglobus*. *Proc. Natl. Acad. Sci. U.S.A.* 100, 15352–15357. doi: 10.1073/pnas.2536559100
- Reynaud, E. G., and Devos, D. P. (2011). Transitional forms between the three domains of life and evolutionary implications. *Proc. Biol. Sci.* 278, 3321–3328. doi: 10.1098/rspb.2011.1581
- Sambrook, J., Fritsch, E. F., and Maniatis, T. (2001). *Molecular Cloning: A Laboratory Manual*. Cold Spring Harbor, NY: Cold Spring Harbor Laboratory Press.
- Santarella-Mellwig, R., Franke, J., Jaedicke, A., Gorjanacz, M., Bauer, U., Budd, A., et al. (2010). The compartmentalized bacteria of the planctomycetes-verrucomicrobia-chlamydias superphylum have membrane coat-like proteins. *PLoS Biol.* 8:e1000281. doi: 10.1371/journal.pbio.1000281
- Schlesner, H., Rensmann, C., Tindall, B. J., Gade, D., Rabus, R., Pfeiffer, S., et al. (2004). Taxonomic heterogeneity within the Planctomycetales as derived by DNA-DNA hybridization, description of *Rhodopirellula baltica* gen. nov., sp. nov., transfer of *Pirellula marina* to the genus *Blastopirellula* gen. nov. as *Blastopirellula marina* comb. nov. and emended description of the genus *Pirellula*. *Int. J. Syst. Evol. Microbiol.* 54, 1567–1580. doi: 10.1099/ijs.0.63113-0
- Schreier, H. J., Dejtsakdi, W., Escalante, J. O., and Brailo, M. (2012). Transposon mutagenesis of *Planctomyces limnophilus* and analysis of a pckA mutant. *Appl. Environ. Microbiol.* 78, 7120–7123. doi: 10.1128/AEM.01794-12
- Siegls, T., Petzke, L., Welle, E., and Luzhetskyy, A. (2010). I-SceI endonuclease: a new tool for DNA repair studies and genetic manipulations in streptomyces. *Appl. Microbiol. Biotechnol.* 87, 1525–1532. doi: 10.1007/s00253-010-2643-y
- Sievers, F., Wilm, A., Dineen, D., Gibson, T. J., Karplus, K., Li, W., et al. (2011). Fast, scalable generation of high-quality protein multiple sequence alignments using Clustal Omega. *Mol Syst Biol* 7:539. doi: 10.1038/msb.2011.75
- Strous, M., Fuerst, J. A., Kramer, E. H., Logemann, S., Muyzer, G., van de Pas-Schoonen, K. T., et al. (1999). Missing lithotroph identified as new planctomycete. *Nature* 400, 446–449. doi: 10.1038/22749
- Suzuki, N., Nonaka, H., Tsuge, Y., Okayama, S., Inui, M., and Yukawa, H. (2005). Multiple large segment deletion method for *Corynebacterium glutamicum*. *Appl. Microbiol. Biotechnol.* 69, 151–161. doi: 10.1007/s00253-005-1976-4
- Valdivia, R. H., and Falkow, S. (1996). Bacterial genetics by flow cytometry: rapid isolation of *Salmonella typhimurium* acid-inducible promoters by differential fluorescence induction. *Mol. Microbiol.* 22, 367–378. doi: 10.1046/j.1365-2958.1996.00120.x
- van Niftrik, L. A., Fuerst, J. A., Sinninghe Damsté, J. S., Kuenen, J. G., Jetten, M. S., and Strous, M. (2004). The anammoxosome: an intracytoplasmic compartment in anammox bacteria. *FEMS Microbiol. Lett.* 233, 7–13. doi: 10.1016/j.femsle.2004.01.044
- Wagner, M., and Horn, M. (2006). The Planctomycetes, Verrucomicrobia, Chlamydiae and sister phyla comprise a superphylum with biotechnological and medical relevance. *Curr. Opin. Biotechnol.* 17, 241–249. doi: 10.1016/j.copbio.2006.05.005
- Ward, N., Staley, J. T., Fuerst, J. A., Giovannoni, S., Schlesner, H., and Stackebrandt, E. (2006). “The order Planctomycetales, including the Genera *Planctomyces*, *Pirellula*, *Gemmata* and *Isosphaera* and the Candidatus Genera *Brocadia*, *Kuenenia* and *Scalindua*,” in *The Prokaryotes: Vol. 7: Proteobacteria: Delta, Epsilon Subclass*, eds M. Dworkin, S. Falkow, E. Rosenberg, K.-H. Schleifer, and E. Stackebrandt (New York, NY: Springer New York), 757–793.
- Ward-Rainey, N., Rainey, F. A., Wellington, E. M., and Stackebrandt, E. (1996). Physical map of the genome of *Planctomyces limnophilus*, a representative of the phylogenetically distinct planctomycete lineage. *J. Bacteriol.* 178, 1908–1913.
- Yu, B. J., Kang, K. H., Lee, J. H., Sung, B. H., Kim, M. S., and Kim, S. C. (2008). Rapid and efficient construction of markerless deletions in the *Escherichia coli* genome. *Nucleic Acids Res.* 36:e84. doi: 10.1093/nar/gkn359
- Conflict of Interest Statement:** The authors declare that the research was conducted in the absence of any commercial or financial relationships that could be construed as a potential conflict of interest.
- Copyright © 2016 Rivas-Marín, Canosa, Santero and Devos. This is an open-access article distributed under the terms of the Creative Commons Attribution License (CC BY). The use, distribution or reproduction in other forums is permitted, provided the original author(s) or licensor are credited and that the original publication in this journal is cited, in accordance with accepted academic practice. No use, distribution or reproduction is permitted which does not comply with these terms.

Advantages of publishing in Frontiers



OPEN ACCESS

Articles are free to read for greatest visibility and readership



FAST PUBLICATION

Around 90 days from submission to decision



HIGH QUALITY PEER-REVIEW

Rigorous, collaborative, and constructive peer-review



TRANSPARENT PEER-REVIEW

Editors and reviewers acknowledged by name on published articles



REPRODUCIBILITY OF RESEARCH

Support open data and methods to enhance research reproducibility



DIGITAL PUBLISHING

Articles designed for optimal readership across devices



FOLLOW US
@frontiersin



IMPACT METRICS

Advanced article metrics track visibility across digital media



EXTENSIVE PROMOTION

Marketing and promotion of impactful research



LOOP RESEARCH NETWORK

Our network increases your article's readership